Springer Series in Materials Science 246

Tian-You Fan

Mathematical Theory of Elasticity of Quasicrystals and Its Applications

Second Edition

Science Press Beijing

Springer

Springer Series in Materials Science

Volume 246

The Springer Series in Materials Science covers the complete spectrum of materials physics, including fundamental principles, physical properties, materials theory and design. Recognizing the increasing importance of materials science in future device technologies, the book titles in this series reflect the state-of-the-art in understanding and controlling the structure and properties of all important classes of materials.

More information about this series at http://www.springer.com/series/856

Tian-You Fan

Mathematical Theory of Elasticity of Quasicrystals and Its Applications

Second Edition

Science Press
Beijing

Springer

Tian-You Fan
Beijing Institute of Technology
Beijing
China

ISSN 0933-033X ISSN 2196-2812 (electronic)
Springer Series in Materials Science
ISBN 978-981-10-1982-1 ISBN 978-981-10-1984-5 (eBook)
DOI 10.1007/978-981-10-1984-5

Jointly published with Science Press, Beijing, China
ISBN: 978-7-03-047429-2 Science Press, Beijing, China

Library of Congress Control Number: 2016945944

Printed on acid-free paper

This Springer imprint is published by Springer Nature
The registered company is Springer Science+Business Media Singapore Pte Ltd.

Preface

The first edition of this book was published by Scienec Press, Beijing/ Springer-Verlag, Heidelberg, in 2010 mainly concerning a mathematical theory of elasticity of solid quasicrystals, in which the Landau symmetry breaking and elementary excitation principle plays a central role. Bak, Lubensky and other pioneering researchers introduced a new elementary excitation—phason drawn from theory of incommensurate phase apart from the phonon elemetary excitation well-known in condensed matter physics.

Since 2004, the soft-matter quasicrystals with 12-fold symmetry have been observed in liquid crystals, colloids and polymers; in particular, 18-fold symmetry quasicrystals were observed in 2011 in colloids; this symmetry in quasicrystals is discovered for the first time. These observations belong to an important event of chemistry in twenty-first century and have attracted a great deal of attention of researchers. Readers are interested in many topics of the new area of study. However, accumulated experimental data related with mechanical behaviour of the new phase are very limited, there is the lack of fundamental data, the mechanism of deformation and motion of the matter has not sufficiently been exploared after the discovery over one decade, and it leads to fundamental difficultis to the study. Due to these difficulties, an introduction to soft-matter qusicrystals is given in very brief in Major Appendix of this book.

Though the new edition increases some new contents, the title of the book has not been changed, because the main part of which is still concerned with elasticity of solid quasicrystals, and only new chapter—Chap. 16—on hydrodynamics of quasicrystals is added; the introduction on soft-matter quasicrystals is very limited and listed in the Major Appendix. The changes of the contents of the first 15 chapters are not too great; we add some examples with application significance and exclude ones of less practical meaning; a part of contents of Appendix A is moved into the Appendix of Chap. 11, and add a new appendix, i.e. Appendix C in the Major Appendix, in which some additional derivations of hydrodynamic equations of solid quasicrystals based on the Poisson bracket method are included, which may be referred by readers. Some type and typesetting errors and mistakes contained in

the first edition are removed, but some new errors and mistakes might appear in the new edition; any criticisms from readers are warmly welcome!

The author sincerely thanks the National Natural Science Foundation of China and the Alexander von Humbold Foundation of Germany for their support over the years. Due to the support of AvH Foundation, the author could visit the Max-Planck Institute for Microstructure Physics in Halle and the Institute for Theoretical Physics in University of Stuttgart in Germany; the cooperative work and discussions with Profs. U. Messerschmidt, H.-R. Trebin and Dr. C. Walz were helpful, especially cordial thanks due to Prof. U. Messerschmidt for his outstanding monograph "Dislocation Dynamics During Plastic Deformation" which helped the work of the present edition of the book. Thanks also to Profs T.C. Lubensky in University of Pennsylvania, Z.D. Stepen Cheng in University of Akron in USA and Xian-Fang Li of Central South University in China for beneficial discussions and kind helps. At last, the author thanks the readers, their downloading, view, review and citation are very active, and this encourages me to improve the work.

Beijing, China Tian-You Fan

Contents

Notations

$\mathbf{r}$	Radius vector
Ω	Domain
S	Boundary of domain
S_{u}	Boundary part at which the displacements are given
S_{t}	Boundary part at which the tractions are given (or S_σ at which the applied stresses are given)
ρ	Mass density (g/cm^3)
p	Fluid pressure (Pa = N/m^2)
$\mathbf{u}$	Phonon-type displacement field (cm)
$\mathbf{w}$	Phason-type displacement field (or second phason displacement field only for quasicrystals with 18-fold symmetry) (cm)
$\mathbf{V}$	Velocity field of solid viscosity (cm/s)
$\varepsilon_{ij} = \frac{1}{2}\left(\frac{\partial u_i}{\partial x_j} + \frac{\partial u_j}{\partial x_i}\right)$	Phonon strain tensor
$w_{ij} = \frac{\partial w_i}{\partial x_j}$	Phason strain tensor (or second phason strain tensor only for quasicrystals with 18-fold symmetry)
$\dot{\xi}_{ij} = \frac{1}{2}\left(\frac{\partial V_i}{\partial x_j} + \frac{\partial V_j}{\partial x_i}\right)$	Deformation velocity tensor of solid viscosity (1/s)
σ_{ij}	Phonon stress tensor (Pa)
H_{ij}	Phason stress tensor (or second phason stress tensor only for quasicrystals with 18-fold symmetry) (Pa)
σ'_{ij}	Viscosity stress tensor (Pa)
C_{ijkl}	Phonon elastic coefficient tensor (Pa)
K_{ijkl}	Phason elastic coefficient tensor (or second kind phason elastic coefficient tensor only for quasicrystals with 18-fold symmetry) (Pa)
R_{ijkl}	Phonon-phason coupling elastic coefficient tensor (u–w coupling elastic coefficient tensor) (Pa)
η	First viscosity coefficient of fluid (0.1 Pa $\cdot$ s = Poise)
η/ρ	First kinetic viscosity coefficient of fluid (cm^2/s)

ζ	Second viscosity coefficient of fluid ($0.1\,\mathrm{Pa}\cdot\mathrm{s}$ = Poise)
ζ/ρ	Second kinetic viscosity coefficient of fluid (cm^2/s)
Γ_u	Phonon dissipation coefficient ($\mathrm{m}^3\mathrm{s/kg}$)
Γ_w	Phason dissipation coefficient (or second kind phason dissipation coefficient tensor only for quasicrystals with 18-fold symmetry) ($\mathrm{m}^3\mathrm{s/kg}$)
$\mathbf{v}$	First phason-type displacement field (only for quasicrystals with 18-fold symmetry) (cm)
$v_{ij} = \frac{\partial v_i}{\partial x_j}$	First phason strain tensor (only for quasicrystals with 18-fold symmetry)
τ_{ij}	First phason stress tensor (only for quasicrystals with 18-fold symmetry) (Pa)
r_{ijkl}	Phonon-first phason coupling elastic coefficient tensor (or u–v coupling elastic coefficient tensor only for quasicrystals with 18-fold symmetry) (Pa)

Chapter 1
Crystals

This book discusses mainly elasticity and defects of quasicrystals in solid; however, quasicrystals have inherent connection with crystals. This chapter provides the basic knowledge on crystals which may be beneficial to study quasicrystals and relevant topics.

1.1 Periodicity of Crystal Structure, Crystal Cell

Based on X-ray diffraction patterns, it is known that a crystal consists of particles (i.e. collections of ions, atoms and molecules) which are arranged regularly in space. The arrangement is a repetition of the smallest unit, called a unit cell, resulting in the periodicity of a complete crystal. The frame of the periodic arrangement of centres of particles is called a lattice. Thus, the properties of corresponding points of different cells in a crystal will be the same. The positions of these points can be defined by radius vectors $\mathbf{r}$ and $\mathbf{r}'$ in a coordinate frame $\mathbf{e}_1, \mathbf{e}_2, \mathbf{e}_3$, and $\mathbf{a}, \mathbf{b}$ and $\mathbf{c}$ are three non-mutually co-linear vectors, respectively (the general concept on vector referring to Chap. 2). Hence, we have

$$\mathbf{r}' = \mathbf{r} + l\mathbf{a} + m\mathbf{b} + n\mathbf{c} \tag{1.1.1}$$

in which $\mathbf{a}, \mathbf{b}$ and $\mathbf{c}$ are the basic translational vectors describing the particle arrangement in the complete crystal, and l, m and n are arbitrary integers. If the physical properties are described by function $f(\mathbf{r})$, then the above-mentioned invariance may be expressed mathematically as

$$f(\mathbf{r}') = f(\mathbf{r} + l\mathbf{a} + m\mathbf{b} + n\mathbf{c}) = f(\mathbf{r}) \tag{1.1.2}$$

This is called the translational symmetry or long-range translational order of a crystal, because the symmetry is realized by the operation of translation.

T.-Y. Fan, *Mathematical Theory of Elasticity of Quasicrystals and Its Applications*,
Springer Series in Materials Science 246, DOI 10.1007/978-981-10-1984-5_1

Equation (1.1.1) represents a kind of translational transform, while (1.1.2) shows that the lattice is invariant under transformation (1.1.1). The collection of all translational transform remaining lattice invariant constitutes the translational group.

1.2 Three-Dimensional Lattice Types

Cells of lattice may be described by a parallel hexahedron having lengths of its three sides $\mathbf{a}, \mathbf{b}$ and $\mathbf{c}$ and angles α, β and γ between the sides. According to the relationship between the length of sides and angles, there are seven different forms observed for the cells, which form seven crystal systems given by Table 1.1.

Among each crystal system, there are some classes of crystals that are classified based on the configuration such that whether the face centred or body centred contains lattice point. For example, the cubic system can be classified as three classes: the simple cubic, body-centred cubic and face-centred cubic. According to this classification, the seven crystal systems contain 14 different lattice cells, which are called Bravais cells, as shown in Fig. 1.1.

Apart from the above-mentioned 14 Bravais cells with three-dimensional lattices, there are 5 Bravais cells of two-dimensional lattice, we do not give any further.

1.3 Symmetry and Point Groups

In Sect. 1.1, we have discussed the translational symmetry of crystals. Here, we point out that the symmetry reveals invariance of crystals under translational transformation

$$\mathbf{T} = l\mathbf{a} + m\mathbf{b} + n\mathbf{c} \tag{1.3.1}$$

Equation (1.3.1) is referred to as an operation of symmetry, which is a translational operation. Apart from this, there are rotation operation and reflection (or mapping)

Table 1.1 Crystals and the relationship of length of sides and angles

Crystal system	Characters of cell
Triclinic	$a \neq b \neq c, \alpha \neq \beta \neq \gamma$
Monoclinic	$a \neq b \neq c, \alpha = \gamma = 90^\circ \neq \beta$
Orthorhombic	$a \neq b \neq c, \alpha = \beta = \gamma = 90^\circ$
Rhombohedral	$a = b = c, \alpha = \beta = \gamma \neq 90^\circ$
Tetragonal	$a = b \neq c, \alpha = \beta = \gamma = 90^\circ$
Hexagonal	$a = b \neq c, \alpha = \beta = 90^\circ, \gamma = 120^\circ$
Cubic	$a = b = c, \alpha = \beta = \gamma = 90^\circ$

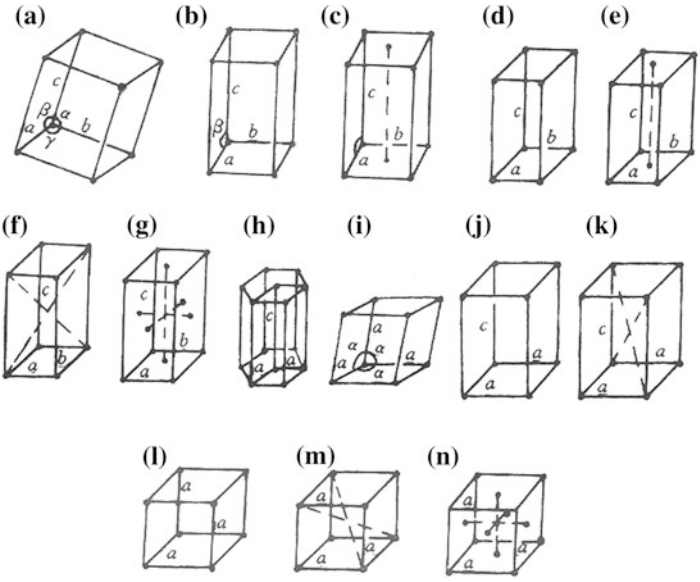

Fig. 1.1 The 14 crystal cells of three dimension **a** simple triclinic, **b** simple monoclinic, **c** button-centred monoclinic, **d** simple orthorhombic, **e** button-centred orthorhombic, **f** body-centred orthorhombic, **g** face-centred orthorhombic, **h** hexagonal, **i** rhombohedral, **j** simple tetragonal, **k** body-centred tetragonal, **l** simple cubic, **m** body-centred cubic, **n** face-centred cubic

operation, they belong to so-called point operation. A brief introduction on the rotation operation and orientational symmetry of crystals is given below.

By rotating about an axis through a lattice, the crystal can always return to the original state since the rotational angles are $2\pi/1, 2\pi/2, 2\pi/3, 2\pi/4$ and $2\pi/6$ or integer times of these values. This is the orientational symmetry or the long-range orientational order of a crystal. Because of the constraint of translational symmetry, the orientational symmetry holds for $n = 1, 2, 3, 4$ and 6 only, which is neither equal to 5 nor greater than 6 where n is the denominator of $2\pi/n$ (e.g. a molecule can have fivefold rotation symmetry, but a crystal cannot have this symmetry because the cells either overlap or have gaps between the cells when $n = 5$, Fig. 1.2 is an example). The fact constitutes the following fundamental law of crystallography:

Law of symmetry of crystals Under rotation operation, n-fold symmetry axis is marked by n. Due to the constraint of translational symmetry, axes $n = 1, 2, 3, 4$ and 6 exist only; neither 5 nor number greater than 6 exists.

In contrast to translational symmetry, rotation is a point symmetry. Other point symmetries are as follows: plane of symmetry, the corresponding operation is mapping, marked by m; centre of symmetry, the corresponding operation is inversion, marked by I; rotation-inversion axis, the corresponding operation is composition of rotation and inversion, when the inversion after rotation $2\pi/n$, marked by $\bar{n}$.

Fig. 1.2 There is no fivefold rotational symmetry in crystals

For crystals, the point operation consists of eight independent ones only, that is

$$1, 2, 3, 4, 6,\ I = (\bar{I}),\ m = \bar{2}, \bar{4} \tag{1.3.2}$$

which are basic symmetric elements of point symmetry.

The rotation operation is also denoted by $C_n, n = 1, 2, 3, 4, 6$.

The mapping operation can also be expressed by σ. The horizontal mapping by m_h and S_h, and vertical one by S_v.

The mapping-rotation is a composite operation, denoted by S_n, which can be understood as

$$S_n = C_n\sigma_h = \sigma_h C_n$$

The inversion mentioned previously can be understood as

$$I = S_2 = C_2\sigma_h = \sigma_h C_2$$

Another composite operation—rotation-inversion $\bar{n}$, is related to S_n, e.g. $\bar{1} = S_2 = I$, $\bar{2} = S_1 = \sigma, \bar{3} = S_6, \bar{4} = S_4, \bar{6} = S_3$.

So that (1.3.2) can also be redescribed as

$$C_1, C_2, C_3, C_4, C_6, I, \sigma, S_4 \tag{1.3.3}$$

The collection of each symmetric operation among these eight basic operations constitutes a point group, the collection of their composition forms 32 point groups listed in Table 1.2.

The concept and sign of point groups will be used in the subsequent chapters.

Table 1.2 32 point groups of crystals

Sign	Meaning of sign	Point group	Number
C_n	Having n-fold axis	C_1, C_2, C_3, C_4, C_6	5
I	Symmetry centre	$I(i)$	1
$\sigma(m)$	Mapping	$\sigma(m)$	1
C_{nh}	Having n-fold axis and horizontal symmetry plane	$C_{2h}, C_{3h}, C_{4h}, C_{6h}$	4
C_{nv}	Having n-fold axis and vertical symmetry plane	$C_{2v}, C_{3v}, C_{4v}, C_{6v}$	4
D_n	Having n-fold axis and n twofold axis, they are perpendicular to each other	D_2, D_3, D_4, D_6	4
D_{nh}	Meaning of h is the same as before	$D_{2h}, D_{3h}, D_{4h}, D_{6h}$	4
D_{nd}	d means in D_n there is a symmetry plane dividing the angle between two twofold axes	D_{2d}, D_{3d}	2
S_n	Having n-fold mapping-rotation axis	$S_4, S_6 = C_{3i}$	2
T	Having four threefold axes and three twofold axes	T	1
T_h	Meaning of h is the same as before	T_h	1
T_d	Meaning of d is the same as previous	T_d	1
O	Having three fourfold axes which perpendicular each other and six twofold axes and four threefold axes	O, O_h	2

Note
$T = C_{3'}D_2$ means the composition between operations $C_{3'}$ and D_2, where suffix $3'$ denotes a threefold axis
$O = C_{3'}C_4C_{2''}$ means the composition between operations $C_{3'}$, C_4 and $C_{2''}$ where $3'$ represents a threefold axis, $2''$ a twofold axis

1.4 Reciprocal Lattice

The concept of the reciprocal lattice will be concerned in the following chapters, here is a brief introduction.

Assume there is relation between base vectors $\mathbf{a_1}, \mathbf{a_2}$ and $\mathbf{a_3}$ of a lattice (L) and base vectors $\mathbf{b_1}, \mathbf{b_2}$ and $\mathbf{b_3}$ for another lattice (L_R)

$$\mathbf{b}_i \cdot \mathbf{a}_j = \delta_{ij} = \begin{cases} 1, & i = j \\ 0, & i \neq j \end{cases} \quad (i,j = 1,2,3) \tag{1.4.1}$$

that the lattice with base vectors $\mathbf{b_1}, \mathbf{b_2}, \mathbf{b_3}$ is the reciprocal lattice L_R of crystal lattice L which has base vectors $\mathbf{a_1}, \mathbf{a_2}, \mathbf{a_3}$. Between $\mathbf{b_i}$ and $\mathbf{a_j}$, there exist relationship

$$\mathbf{b}_1 = \frac{\mathbf{a}_2 \times \mathbf{a}_3}{\Omega}, \quad \mathbf{b}_2 = \frac{\mathbf{a}_3 \times \mathbf{a}_1}{\Omega}, \quad \mathbf{b}_3 = \frac{\mathbf{a}_1 \times \mathbf{a}_2}{\Omega} \tag{1.4.2}$$

where $\Omega = \mathbf{a_1} \cdot (\mathbf{a_2} \times \mathbf{a_3})$ is the volume of lattice cell.

Denote

$$\Omega^* = \mathbf{b_1} \cdot (\mathbf{b_2} \times \mathbf{b_3})$$

then

$$\Omega^* = \frac{1}{\Omega}$$

The position of any point in reciprocal lattice can be expressed by

$$\mathbf{G} = h_1\mathbf{b_1} + h_2\mathbf{b_2} + h_3\mathbf{b_3} \tag{1.4.3}$$

in which

$$h_1, h_2, h_3 = \pm 1, \pm 2, \ldots$$

Points in lattice can be described by $\mathbf{a_1}, \mathbf{a_2}, \mathbf{a_3}$ as well as by $\mathbf{b_1}, \mathbf{b_2}, \mathbf{b_3}$.

In similar version, the concept of reciprocal lattice can be extended to higher-dimensional space, e.g. six-dimensional space, which will be discussed in Chap. 4.

The brief introduction above provides a basic knowledge for reading the subsequent text of the book, the further information on crystals, diffraction theory and point group can be found from the book [1] and monograph [2]. We will recall the concepts in the following text.

1.5 Appendix of Chapter 1: Some Basic Concepts

Some basic concepts will be described in the following chapters, with which most of the physicists are familiar. For the readers of non-physicists, a simple introduction is provided as follows, the details can be found in the relevant references.

1.5.1 Concept of Phonon

In general, the course of crystallography does not contain the contents given in this section. Because the discussion here is dependent on quasicrystals, especially with the elasticity of quasicrystals, we have to introduce some of the simplest relevant arguments.

In 1900, Planck put forward the quantum theory. Soon after Einstein developed the theory and created the photon concept and explained the photoelectric effect, which leads to the photon concept. Einstein also studied the specific heat c_v of crystals arising from lattice vibration by using the Planck quantum theory. There are some unsatisfactory points in the work of Einstein on specific heat though his

formula successfully explained the phenomenon of $c_v = 0$ at $T = 0$, where T denotes the absolute temperature (or Kelvin temperature). To improve the Enistein's work, Debye [3] and Born et al. [4, 5] applied the quantum theory to study the specific heat in 1912 and 1913, respectively, and got a great success. The theoretical prediction is in excellent agreement to the experimental results, at least for specific heat of the atom crystals.

The propagation of the lattice vibration is called lattice wave. Under the long-wavelength approximation, the lattice vibration can be seen as continuum elastic vibration, i.e., the lattice wave can be approximately seen as continuum elastic wave. The motion is a mechanical motion, but Debye and Born assumed that the energy can be quantized based on the Planck's hypothesis. With the elastic wave approximation and quantization, Debye and Born successfully explained the specific heat of crystals at low temperature, and the theoretical prediction is consistent with experimental results in all range of temperature, at least for atom crystals. The quanta of the elastic vibration or the smallest unit of energy of the elastic wave is named phonon, because the elastic wave is one of acoustic waves. Unlike photon, the phonon is not an elementary particle, but in the sense of quantization, the phonon presents natural similarity to that of photon and other elementary particles, thus can be named quasiparticle. The concept created by Debye and Born opened the study on lattice dynamics, an important branch of solid-state physics. Yet according to the view point at present, the Debye and Born theory on solid belongs to a phenomenological theory, though they used the classical quantum theory. The quantum mechanics theory of the topic is referred to Born and Huang [5] and Landau and Lifshitz [6].

Landau [6] further developed the phenomenological theory and put forward the concept of elementary excitation. According to the concept, photon and phonon, etc., belong to elementary excitations. In general, one elementary excitation corresponds to a certain field, e.g., photon corresponds to electromagnetic wave and phonon corresponds to elastic wave. The phonon concept is further extended by Born [5] and other scientists, they pointed out the phonon theory given by Debye, in general, is not suitable for compounds. As atoms in a compound constitute a molecular collection in solid state, then the vibration of atoms can be approximately classified into two cases: one is vibration of whole body of molecule; another is relative vibration among atoms within a molecule. The first type of vibration is the same that described by Debye theory, called phonetic frequency vibration modes, or the phonetic branch of phonon. In this case, the physical quantity phonon (under long-wavelength approximation) describing displacement field deviated from the equilibrium position of particles at lattice is also called as phonon-type displacement, or phonon field, or briefly phonon. Macroscopically, it is the displacement vector $\mathbf{u}$ of elastic body (if the crystal is regarded as an elastic body). And the second type of vibration, i.e. the relative vibration among atoms within a molecule, is called photonic frequency vibration modes, or photonic branch of phonon. For this branch, the phonon cannot be simply understood as macroscopic displacement field. But our discussion in this book is confined to the framework of continuum

medium, with no concern with the photonic branch, so the phonon field is the macro-displacement field in the consideration.

In many physical systems (classical or quantum systems), the motion presents the discrete spectrum (the energy spectrum or frequency spectrum which corresponds to the discrete spectrum of an eigenvalue problem of a certain operator from the mathematical point of view). The lowest energy (frequency)-level state is called ground state and that beyond the ground state is named excited state. The so-called elementary excitation induces a transfer from the ground state to the state with the smallest nonzero energy (or frequency). Strictly speaking, it should be named lowest energy (or frequency) elementary excitation.

The solid-state physics was intensively developed in 1960–70s and then evolved into the condensed matter physics. The condensed matter physics is not only extending the scope of solid-state physics by considering liquid-state and micro-powder structure, but also developing basic concepts and principles. Modern condensed matter physics is established as a result of the construction of its paradigm, in which the symmetry-breaking is in a central place, which was contributed by Landau [6] and Anderson [7] and other scientists.

Considering the importance of the concept and principle of symmetry-breaking in the development of elasticity of quasicrystals, we give brief discussion here.

It is well-known that for a system with a constant volume, the equilibrium state thermodynamically requires the free energy of the system

$$F = E - TS \tag{1.5.1}$$

be minimum, in which E is the internal energy, S the entropy and T the absolute temperature, respectively.

Landau proposed the so-called second-order phase transition theory by introducing a macroscopic order-parameter η (to describe order–disorder) phase transition, i.e., assuming that the free energy can be expanded as a power series of η

$$F(\eta, T) = F_0(T) + A(T)\eta^2 + B(T)\eta^4 + \cdots \tag{1.5.2}$$

in which according to requirement of stability condition of phase transition (i.e. the variational condition $\delta F = 0$ or $\partial F/\partial \eta = 0$), the coefficients of odd terms should be taken to zero, and $B(T) > 0$. At high temperature, the system is in disorder state, so $A(T) > 0$, too; as temperature reduces, $A(T)$ will change its sign; at the critic temperature T_C, there exists $A(T_C) = 0$. The simplest choice in satisfying these conditions is

$$A(T) = \alpha(T - T_C), B(T) = B(T_C) \tag{1.5.3}$$

in which α is a constant. Without concerning concrete micro-mechanism, the Landau theory has the merits of simplicity and generality; it can be used to many systems and has achieved successes, especially for the study of superconductivity, liquid crystals, high-energy physics. (To the author's understanding, the

quasicrystals study is another area that has been achieved following of the line of the symmetry-breaking principle.) Applying the above principle to periodic crystals, we have [7]

$$F = \frac{1}{2}\alpha(|\mathbf{G}|)(T - T_C(\mathbf{G}))\eta^2 + \text{higher-order terms} \tag{1.5.4}$$

where the constant α is related to reciprocal vector $\mathbf{G}$ (for the concepts on the reciprocal vector and reciprocal lattice, refer to Sect. 1.4). Further, Anderson [7] proved for crystals if the density of periodic crystals can be expressed by Fourier series (the expansion exists due to the periodicity of the structure in three-dimensional lattice or reciprocal lattice)

$$\rho(\mathbf{r}) = \sum_{\mathbf{G}\in L_R} \rho_{\mathbf{G}} \exp\{\mathrm{i}\mathbf{G}\cdot\mathbf{r}\} = \sum_{\mathbf{G}\in L_R} |\rho_{\mathbf{G}}| \exp\{-\mathrm{i}\Phi_{\mathbf{G}} + \mathrm{i}\mathbf{G}\cdot\mathbf{r}\} \tag{1.5.5}$$

where $\mathbf{G}$ is a reciprocal vector just mentioned above, and L_R the reciprocal lattice in three-dimensional space, $\rho_{\mathbf{G}}$ is a complex number

$$\rho_{\mathbf{G}} = |\rho_{\mathbf{G}}|\mathrm{e}^{\mathrm{i}\Phi_{\mathbf{G}}} \tag{1.5.6}$$

with the amplitude $|\rho_{\mathbf{G}}|$ and phase angle $\Phi_{\mathbf{G}}$, due to $\rho(r)$ being real, $|\rho_{\mathbf{G}}| = |\rho_{-\mathbf{G}}|$ and $\Phi_{\mathbf{G}} = -\Phi_{-\mathbf{G}}$, then the order parameter is

$$\eta = |\rho_{\mathbf{G}}| \tag{1.5.7}$$

Anderson pointed further out that for crystals the phase angle $\Phi_{\mathbf{G}}$ contains the phonon $\mathbf{u}$, that is

$$\Phi_{\mathbf{G}} = \mathbf{G}\cdot\mathbf{u} \tag{1.5.8}$$

in which both $\mathbf{G}$ and $\mathbf{u}$ are in three-dimensional physical space. If we consider only the phonetic branch of phonon, then here $\mathbf{u}$ can be understood as phonon-type displacement field. So the displacement field in periodic crystals can be understood as phonon field from the Landau symmetry-breaking hypothesis, though it possesses an intuitive physical meaning under the approximation of long-wavelength (refer to Chap. 2). The description based on the symmetry-breaking, physical quantity $\mathbf{u}$ is connected with reciprocal vector $\mathbf{G}$ and reciprocal lattice L_R of crystals, so it presents more profound insight (a result of symmetry-breaking of the crystals) than that of the intuitive description of displacement field $\mathbf{u}$, though the explanation here is still phenomenological (because the Landau theory is a phenomenological theory), rather than that from the first principles.

The concept of phonon is originated from Debye [3] and Born et al. [4, 5], which describes the mechanical vibration of lattice mass points (atoms or ions or molecules) deviating from their equilibrium position; the propagation of the vibration leads to the lattice wave, and the motion can be quantized, the quanta is the phonon.

This is an elementary excitation in condensed matter. The symmetry-breaking leads to appearance of new ordered phase (e.g. crystals), new order parameter (e.g. $\eta = |\rho_{\mathbf{G}}|$, the wave amplitude of mass density wave), the new elementary excitation (e.g. phonon), and new conservation law (e.g. the crystal symmetry law given in Sect. 1.3). The above description on phonon from the symmetry-breaking point of view helps us to understand in-depth the physical nature of phonon.

Following this scheme, some elementary excitations (e.g. phason) temporarily without complete intuition meaning can also be explained by the Landau theory, and one can further find out their physical meaning from the point of view of symmetry rather than from the simple intuition point of view, because for some complex phenomena, the simple intuition cannot give complete and correct explanation.

We recall that the elementary excitations are related to broken symmetry or symmetry-breaking, e.g. a liquid behaves arbitrary translational symmetry and arbitrary orientational symmetry; then the periodicity of crystals (i.e. the lattice) breaks the translational symmetry and orientational symmetry of liquid, and the phonon is elementary excitation, resulting from the symmetry-breaking. We can say that the quasicrystal is a result of symmetry-breaking of crystal, which will be discussed in Chap. 4.

If it is not necessary to give description on phason concept in-depth, this section can be omitted. The reader is advised to jump over the section if who is not interested in.

More profound discussion on phonon concept can be found in Born and Huang's classical monograph on lattice dynamics [5] and vol V of Course of Theoretical Physics of Landau and Lifshitz [6], they give both phenomenological and quantum mechanics descriptions, and the previous introduction is only a phenomenological description.

1.5.2 Incommensurate Crystals

In this book, we do not discuss incommensurate phases, but quasicrystals are related to so-called incommensurate structure, we have to mention it in brief.

Since 60s of the last century, incommensurate crystals have been studied by many physicists, see e.g. [8]. The so-called incommensurate phase means that it is added an additional incommensurate modulate at the basic lattice, in which the modulated ones may be displacements or compounds of atoms or arrangement of spin, etc. As an example, if a modulated displacement λ is added to a lattice with period a, and if λ/a is a rational number, the crystal becomes a superstructure with long period (which is the integer times of a); and if λ/a is an irrational number, the crystal becomes an incommensurate structure. In this case along the modulate direction, the periodicity is lost. The modulation can be one-dimensional, e.g. Na_2CO_3, $NaNO_2$; or two-dimensional, e.g. $TaSe_2$, quartz; or three-dimensional, e.g. $Fe_{1-x}O$,. In incommensurate phases, the modulation is only a "perturbation" of

another period to the basic lattice, the diffraction pattern of the basic lattice holds, i.e., the crystallography symmetry holds still, so one calls the structure being incommensurate crystals. It is noticed that there is new degrees of freedom in the phases, named phasons. Here, the phason modes present long-wavelength propagation similar to that of phonon modes. In Chap. 4, we shall discuss that the phason modes in quasicrystals present quite different nature, i.e., the motion of atoms exhibits discontinuous jumps rather than the long-wavelength propagation. In addition, in quasicrystals there is non-crystallographic orientational symmetry, which is essentially different from that of general incommensurate crystals.

1.5.3 Glassy Structure

The crystals are solid with long-range order due to atom arrangement regularly. In contrast, there is a solid without order, but it has short-range order in scale within atom size. This material is the glassy structure, as a branch of the condensed matter physics.

1.5.4 Mathematical Aspect of Group

1.5.4.1 Mathematical Definition of Group

In previous sections, we introduced group concept through the symmetry operations, this is intuitive and easy understood. Under a transformation a system maintains invariance, we can call the transformation is a symmetry transformation. In succeeding take two transformations are defined as a product of the two transformations, it is evident, which is the symmetry transformation of the system, too. The product over three symmetry transformations satisfies the associate law. The identical transformation is also a symmetry transformation, the product between it and any symmetry transformation is the transformation. The inversion of a symmetry transformation is still a symmetry transformation. The connection of transformations of a system forms a transformation group. We have defined the concept of product, the mathematical definition on group can be given as below:

1. Closeness of connection—The product between any two elements g_i and g_j in a connection G belongs to the connection, i.e. $g_i \in G, g_j \in G, g_i g_j \in G$;
2. Associate law—If $g_i, g_j, g_k \in G$, then $g_i(g_j, g_k) = (g_i, g_j)g_k$;
3. There is identical element E—If $g_i \in G$, then $Eg_i = g_i$;
4. There is inversion element g_i^{-1}—If $g_i \in G$, then $g_i g_i^{-1} = E$.

The definition on group is also called axiom of group which is valid for all groups, including the point groups. In this book, we mainly concern the point

groups, but also Lie groups in Chap. 16 and Appendix C in main appendixes of the book.

1.5.4.2 The Linear Representation of Group

Assume element g_i belongs to group G, which corresponds to matrix A_i, and assume all matrixes have the same order, their determinates are not equal to zero, if product $g_i g_j$ corresponds to product $A_i A_j$, then say that matrix A_i is a linear representation of group G. Assume a linear expression of group G corresponds to a matrix A_i of n order, and a linear expression of the same group corresponds to matrix B_i of m order, which constitutes quasidiagonal matrix of $(n+m)$ order

$$[A_i, B_i] = \begin{bmatrix} A_i, & 0 \\ 0, & B_i \end{bmatrix} \equiv [C_i]$$

If assume transforming to the equivalent expression according to matrix XC_iX^{-1} , then in general, the character of quasidiagonal matrix will be lost. If this character can be maintained still, we say this expression is reducible; otherwise, it is irreducible.

References

1. Kittel C, 1976, Introduction to the Solid State Physics, New York : Wiley John & Sons, Inc..
2. Wybourne B G, 1974, Classical Group Theory for Physicists, New York :Wiley John & Sons, Inc..
3. Debye P, Die Eigentuemlichkeit der spezifischen Waermen bei tiefen Temperaturen, Arch de Genéve, **33**(4), 256–258, 1912.
4. Born M and von Kármán Th, Zur Theorie der spezifischen Waermen, Physikalische Zeitschrift, **14**(1), 15–19, 1913.
5. Born M and Huang K, 1954, Dynamic Theory of Crystal Lattices, Oxford :Clarendon Press.
6. Landau L D and Lifshitz M E, 1980, Theoretical Physics V: *Statistical Physics, 3rd Edition*, Oxford : Pergamon Press.
7. Anderson P W, 1984, Basic Notations of Condensed Matter Physics, Menlo Park : Benjamin-Cummings.
8. Blinc B and Lavanyuk A P, 1986, Incommensurate Phases in Dielectrics I, II, Amsterdam : North Holland.

Chapter 2
Framework of Crystal Elasticity

As the knowledge of crystals is a benefit for understanding quasicrystals, it is worthwhile having a concise review of the crystal elasticity or classical elasticity before learning elasticity of quaicrystals. Here is a brief description to the theory. The detailed material for this theory can be found in many monographs and textbooks, e.g. Landau and Lifshitz [1]. Though the discussion here is limited within the framework of continuum medium mechanics, there are still connections to physical nature of the elasticity of crystals reflected by phonon concept (discussed in Sect. 1.5). The readers are advised to refer to the relevant chapters and sections of monographs of Born and Huang [2] and Anderson [3] which would help us understanding the phonon concept so the phason concept and elasticity of quasicrystals, which will be presented in the following chapters. The practice shows that it would be hard to understand phason concept and the phason elasticity if we limited our knowledge only within the classical continuum medium and complete intuition.

For simplicity, the tensor algebra will be used in the text.

2.1 Review on Some Basic Concepts

2.1.1 Vector

A quantity with both magnitude and direction is named vector, denoted by $\mathbf{a}$, and $a = |\mathbf{a}|$ represents its magnitude. The scalar product $\mathbf{a} \cdot \mathbf{b} = ab\cos(\mathbf{a}, \mathbf{b})$ of two vectors $\mathbf{a}$ and $\mathbf{b}$. The vector product $\mathbf{a} \times \mathbf{b} = \mathbf{n}ab\sin(\mathbf{a}, \mathbf{b})$, in which $\mathbf{n}$ is the unit vector perpendicular to both $\mathbf{a}$ and $\mathbf{b}$, so $|\mathbf{n}| = 1$. A more general definition on vector is given later.

T.-Y. Fan, *Mathematical Theory of Elasticity of Quasicrystals and Its Applications*,
Springer Series in Materials Science 246, DOI 10.1007/978-981-10-1984-5_2

2.1.2 Coordinate Frame

To describe vector and tensor, it is convenient to introduce the coordinate frame. We will consider the orthogonal frame. Assume that $\mathbf{e_1}, \mathbf{e_2}$ and $\mathbf{e_3}$ are three unit vectors and mutually perpendicular, i.e. $\mathbf{e_1} \cdot \mathbf{e_2} = 0, \mathbf{e}_2 \cdot \mathbf{e}_3 = 0, \mathbf{e}_3 \cdot \mathbf{e}_1 = 0,$ and $\mathbf{e_3} = \mathbf{e_1} \times \mathbf{e_2}, \mathbf{e_2} = \mathbf{e_3} \times \mathbf{e_1}, \mathbf{e_1} = \mathbf{e_2} \times \mathbf{e_3}$, then they are base vectors of an orthogonal coordinate frame, and often called base vectors briefly.

In the orthogonal coordinate frame $\mathbf{e_1}, \mathbf{e_2}, \mathbf{e_3}$, any vector $\mathbf{a}$ can be expressed by

$$\mathbf{a} = a_1\mathbf{e_1} + a_2\mathbf{e_2} + a_3\mathbf{e}_3 \tag{2.1.1}$$

or

$$\mathbf{a} = (a_1, a_2, a_3)$$

2.1.3 Coordinate Transformation

Consider another orthogonal frame $\mathbf{e}'_1, \mathbf{e}'_2, \mathbf{e}'_3$ which can be expressed in terms of $\mathbf{e}_1, \mathbf{e}_2, \mathbf{e}_3$. From (2.1.1), there are

$$\begin{aligned}
\mathbf{e}'_1 &= c_{11}\mathbf{e_1} + c_{12}\mathbf{e_2} + c_{13}\mathbf{e_3} \\
\mathbf{e}'_2 &= c_{21}\mathbf{e_1} + c_{22}\mathbf{e_2} + c_{23}\mathbf{e_3} \\
\mathbf{e}'_3 &= c_{31}\mathbf{e_1} + c_{32}\mathbf{e_2} + c_{33}\mathbf{e_3}
\end{aligned} \tag{2.1.2}$$

where $c_{11}, c_{12}, \ldots, c_{33}$ are some scalar constants. The relation (2.1.2) is named coordinate transformation too, which can also be denoted by matrix

$$\begin{bmatrix} \mathbf{e}'_1 \\ \mathbf{e}'_2 \\ \mathbf{e}'_3 \end{bmatrix} = [C] \begin{bmatrix} \mathbf{e_1} \\ \mathbf{e_2} \\ \mathbf{e_3} \end{bmatrix} \tag{2.1.3}$$

where

$$[C] = \begin{bmatrix} c_{11} & c_{12} & c_{13} \\ c_{21} & c_{22} & c_{23} \\ c_{31} & c_{32} & c_{33} \end{bmatrix}$$

which is an orthogonal matrix, consequently

$$[C]^T = [C]^{-1} \tag{2.1.4}$$

here notation "T" marks transpose operation and "− 1" the inversion operation. It is natural that

$$\begin{bmatrix} \mathbf{e_1} \\ \mathbf{e_2} \\ \mathbf{e_3} \end{bmatrix} = [C]^T \begin{bmatrix} \mathbf{e'_1} \\ \mathbf{e'_2} \\ \mathbf{e'_3} \end{bmatrix} = [C]^{-1} \begin{bmatrix} \mathbf{e'_1} \\ \mathbf{e'_2} \\ \mathbf{e'_3} \end{bmatrix} \tag{2.1.5}$$

Based on (2.1.1), if in the frame $\mathbf{e'}_1, \mathbf{e'}_2, \mathbf{e'}_3$ then

$$\mathbf{a} = a'_1\mathbf{e}'_1 + a'_2\mathbf{e}'_2 + a'_3\mathbf{e}'_3 \tag{2.1.6}$$

Substituting (2.1.5) into (2.1.1) yields

$$\mathbf{a} = (c_{11}a_1 + c_{12}a_2 + c_{13}a_3)\mathbf{e}'_1 + (c_{21}a_1 + c_{22}a_2 + c_{23}a_3)\mathbf{e}'_2 + (c_{31}a_1 + c_{32}a_2 + c_{33}a_3)\mathbf{e}'_3 \tag{2.1.7}$$

It follows that by the comparison between (2.1.6) and (2.1.7)

$$\begin{aligned} a'_1 &= c_{11}a_1 + c_{12}a_2 + c_{13}a_3 \\ a'_2 &= c_{21}a_1 + c_{22}a_2 + c_{23}a_3 \\ a'_3 &= c_{31}a_1 + c_{32}a_2 + c_{33}a_3 \end{aligned} \tag{2.1.8}$$

or by the matrix expression, i.e.

$$\begin{bmatrix} a'_1 \\ a'_2 \\ a'_3 \end{bmatrix} = [C] \begin{bmatrix} a_1 \\ a_2 \\ a_3 \end{bmatrix} \tag{2.1.8'}$$

Whatever (2.1.8) or (2.1.8′), there is

$$a'_i = \sum_{j=1}^{3} c_{ij}a_j = c_{ij}a_j \tag{2.1.9}$$

The summation sign in the right-hand side of (2.1.9) is omitted, when the repeated indexes in $c_{ij}a_j$ represent summing. Henceforth, the summation convention will be used throughout.

A set of numbers (a_1, a_2, a_3) satisfying the relation (2.1.9) under linear transformation (2.1.2) will be called vector regardless its physical meaning. This is an algebraic definition of vector; it is more general than saying that the vector has both magnitude and direction.

2.1.4 Tensor

Let us define 9 numbers in the orthogonal frame $\mathbf{e}_1, \mathbf{e}_2, \mathbf{e}_3$ as $\mathbf{A}$:

$$\mathbf{A} = \begin{bmatrix} A_{11} & A_{12} & A_{13} \\ A_{21} & A_{22} & A_{23} \\ A_{31} & A_{32} & A_{33} \end{bmatrix} \tag{2.1.10}$$

in which the components satisfy the relation

$$A'_{kl} = \sum_{i,j=1}^{3} c_{ki} c_{lj} A_{ij} = c_{ki} c_{lj} A_{ij} \tag{2.1.11}$$

under the linear transformation, then $\mathbf{A}$ is a tensor of rank 2, where c_{ij} are given by (2.1.3) and the summing sign is omitted in the right-hand side of (2.1.11). It is evident that the concept of tensor is an extension of that of vector. According to the definition A_{ij} represents a tensor where $i = 1, 2, 3, j = 1, 2, 3$. It is understood that it represents a component with the indexes i and j of the tensor.

2.1.5 Algebraic Operation of Tensor

(i) Unit tensor

$$I = \delta_{ij} = \begin{cases} 0 & i \neq j \\ 1 & i = j \end{cases} \tag{2.1.12}$$

which is named the Kronecker sign conventionally.

(ii) Transpose of tensor

$$A^T = \begin{bmatrix} A_{11} & A_{21} & A_{31} \\ A_{12} & A_{22} & A_{32} \\ A_{13} & A_{23} & A_{33} \end{bmatrix} \tag{2.1.13}$$

(iii) Algebraic sum of tensors

$$A \pm B = A_{ij} \pm B_{ij} \tag{2.1.14}$$

(iv) Product of scalar and tensor

$$mA = mA_{ij} \tag{2.1.15}$$

(v) Product of tensors

$$AB = A_{ij}B_{kl} \tag{2.1.16}$$

Other operations about tensors will be provided in the description of the subsequent text.

2.2 Basic Assumptions of Theory of Elasticity

The theory of elasticity is a branch of continuum mechanics, it follows the basic assumptions thereof whereas there are:

(i) Continuity
In the theory one assumes that the medium fills the full space that it occupies, and this means the medium is continuous. Connected with this, the field variables concerning the medium are continuous and differentiable functions of coordinates.

(ii) Homogeneity
Physical constants describing the medium are independent from coordinates, so the medium is homogeneous.

(iii) Small deformation
Assume that displacements u_i are small and $\partial u_i/\partial x_j$ are less than unity. Due to small deformation, the boundary conditions are written at the boundaries before deformation though those boundaries have taken some deformation. This makes the problems linearized and simplifies the solution procedure.

2.3 Displacement and Deformation

That elastic body exhibiting deformation is connected to the relative displacement between points in it. So we first look for the displacement field.

Consider a region R in an elastic body, refer to Fig. 2.1, it becomes another region R' after deformation. The point O with radius vector $\mathbf{r}$,

before deformation, which becomes point O' with radius vector $\mathbf{r}'$ after deformation, and $\mathbf{u}$ is the displacement vector of point O during the deformation process (see Fig. 2.1), i.e.

$$\mathbf{r}' = \mathbf{r} + \mathbf{u} \tag{2.3.1}$$

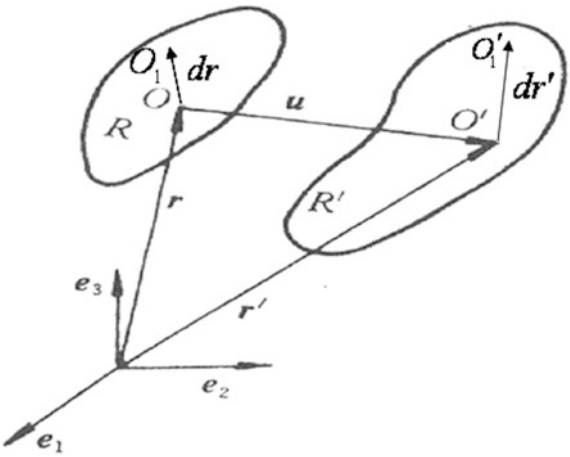

Fig. 2.1 Displacement of a point in an elastic body

or

$$\mathbf{u} = \mathbf{r}' - \mathbf{r} = x_i' - x_i \tag{2.3.1'}$$

In Fig. 2.1, frame $\mathbf{e_1}$, $\mathbf{e_2}$, $\mathbf{e_3}$ depicts any orthogonal coordinate system, especially we use the rectilinear coordinate system (x_1, x_2, x_3) or (x, y, z). Assume that O_1 in R is a point near the point O, the radius vector joining them is $\mathrm{d}\mathbf{r} = \mathrm{d}x_i$. The point O_1 becomes point O_1' in R' after deformation. The vector radius joining points O_1 and point O_1' is $\mathrm{d}\mathbf{r}' = \mathrm{d}x_i' = \mathrm{d}x_i + \mathrm{d}u_i$. The displacement of point O_1 is $\mathbf{u}'$, there is

$$\mathbf{u}' = \mathbf{u} + d\mathbf{u} \tag{2.3.2}$$

i.e.

$$\mathrm{d}u_i = u_i' - u_i \tag{2.3.3}$$

and

$$\mathrm{d}u_i = \frac{\partial u_i}{\partial x_j}\mathrm{d}x_j \tag{2.3.4}$$

Equation (2.3.4) expresses the Taylor expansion at point O and takes the first-order term only. Under the small deformation assumption, this reaches a very high accuracy. It denotes

$$\frac{\partial u_i}{\partial x_j} = \varepsilon_{ij} + \omega_{ij} \tag{2.3.5}$$

in which

$$\varepsilon_{ij} = \frac{1}{2}\left(\frac{\partial u_i}{\partial x_j} + \frac{\partial u_j}{\partial x_i}\right) \tag{2.3.6}$$

$$\omega_{ij} = \frac{1}{2}\left(\frac{\partial u_i}{\partial x_j} - \frac{\partial u_j}{\partial x_i}\right) \tag{2.3.7}$$

here ε_{ij} is a symmetric tensor

$$\varepsilon_{ij} = \varepsilon_{ji} \tag{2.3.8}$$

and called the strain tensor, while ω_{ij} an asymmetric tensor, which has only three independent components

$$\begin{aligned}
\Omega_x &= \omega_{yz} = \frac{1}{2}\left(\frac{\partial u_y}{\partial z} - \frac{\partial u_z}{\partial y}\right) \\
\Omega_y &= \omega_{zx} = \frac{1}{2}\left(\frac{\partial u_z}{\partial x} - \frac{\partial u_x}{\partial z}\right) \\
\Omega_z &= \omega_{xy} = \frac{1}{2}\left(\frac{\partial u_x}{\partial y} - \frac{\partial u_y}{\partial x}\right)
\end{aligned} \tag{2.3.9}$$

The physical meaning of ε_{ij} describes volume and shape changes of a cell, and that of ω_{ij} the rigid rotation, which is independent on deformation, so only ε_{ij} is considered afterwards.

The components $\varepsilon_{11}, \varepsilon_{22}$ and ε_{33} (if denote $x = x_1, y = x_2, z = x_3$, then we have $\varepsilon_{xx}, \varepsilon_{yy}$ and ε_{zz}) represent normal strains describing volume change of a cell, while $\varepsilon_{32} = \varepsilon_{23}, \varepsilon_{13} = \varepsilon_{31}$ and $\varepsilon_{12} = \varepsilon_{21}$ (or $\varepsilon_{yz} = \varepsilon_{zy}, \varepsilon_{zx} = \varepsilon_{xz}$ and $\varepsilon_{xy} = \varepsilon_{yx}$) represent shear strains describing shape change of a cell.

2.4 Stress Analysis

The internal forces per unit area due to deformation are called stresses, and denoted by σ_{ij}, which will be zero if there is no deformation for a body. When the body is in static equilibrium according to the law of momentum conservation, we have

$$\frac{\partial \sigma_{ij}}{\partial x_i} + f_j = 0 \tag{2.4.1}$$

in which the equation holds for any infinitesimal volume element of the body, and σ_{ij} represents the components of the stress tensor as mentioned above, and suffix j the acting direction of the component, i the direction of outward normal vector of the surface element that the component exerted and f_i the body force density vector. Amongst all, the components of σ_{ij}, σ_{xx}, σ_{yy} and σ_{zz} are normal to the surface

elements which they exerted, and $\sigma_{yz}, \sigma_{zy}, \sigma_{zx}, \sigma_{xz}, \sigma_{xy}$ and σ_{yx} are along the tangent directions of the surface elements, the former are called normal stresses, and the latter shear stresses.

According to the angular momentum conservation, one finds that

$$\sigma_{ij} = \sigma_{ji} \tag{2.4.2}$$

this means the stress tensor is a symmetric tensor and (2.4.2) is named as the shear stress mutual equal law.

External surface forces density (tractions) T_i subjected to the surface of a body should be balanced with the internal stresses, this leads to

$$\sigma_{ij} n_j = T_i \tag{2.4.3}$$

where n_j is the unit vector along the outward normal to the surface element. People also call T_i area force density.

Equation (2.4.3) describes the stress boundary conditions which play a very important role for elasticity.

2.5 Generalized Hooke's Law

Between stresses σ_{ij} and strains ε_{ij}, there exists a certain relationship depending upon the material behaviour of the body. Hereafter, we consider only the linear elastic behaviour of materials and the state without initial stresses. In the case, the classical experimental law–Hooke's law can be extended as

$$\sigma_{ij} = \frac{\partial U}{\partial \varepsilon_{ij}} = C_{ijkl}\varepsilon_{kl} \tag{2.5.1}$$

in which U denotes the free energy density, or the strain energy density, i.e.

$$U = F = \frac{1}{2} C_{ijkl}\varepsilon_{ij}\varepsilon_{kl} \tag{2.5.2}$$

and C_{ijkl} is the elastic constant tensor, consisting of 81 components. Due to the symmetry of σ_{ij} and ε_{ij}, each of them has independent 6 components only, such that the independent components of C_{ijkl} reduce to 36. Formula (2.5.2) shows that U is a homogenous quantity of ε_{ij} of rank two, considering the symmetry of ε_{ij}, then we have

$$C_{ijkl} = C_{klij} \tag{2.5.3}$$

so the independent components amongst 36 reduce to 21.

The relation (2.5.1) with 21 independent elastic constants is named as generalized Hooke's law.

The generalized Hooke's law describes anisotropic elastic bodies including crystals. Stress and strain tensors can also be expressed by corresponding vectors with 6 independent elements, then can be denoted by corresponding elastic constants matrix $\left[B_{ijkl}\right]$

$$\begin{bmatrix}\sigma_{11}\\ \sigma_{22}\\ \sigma_{33}\\ \sigma_{23}\\ \sigma_{31}\\ \sigma_{12}\end{bmatrix} = \begin{bmatrix} B_{1111} & B_{1122} & B_{1133} & B_{1123} & B_{1131} & B_{1112} \\ & B_{2222} & B_{2233} & B_{2223} & B_{2231} & B_{2212} \\ & & B_{3333} & B_{3323} & B_{3331} & B_{3312} \\ & & & B_{2323} & B_{2331} & B_{2312} \\ & (symmetry) & & & B_{3131} & B_{3112} \\ & & & & & B_{1212} \end{bmatrix} \begin{bmatrix}\varepsilon_{11}\\ \varepsilon_{22}\\ \varepsilon_{33}\\ \varepsilon_{23}\\ \varepsilon_{31}\\ \varepsilon_{12}\end{bmatrix} \tag{2.5.4}$$

Applying formula (2.5.4) to crystals, between the elements C_{ijkl} (or B_{ijkl}), there are some relations by considering certain symmetry of the crystals, so that the resulting number of the elastic constants for certain individual crystal systems may be less than 21. In the following, we give a brief discussion on the argument.

1. Triclinic system (classes 1 or C_1 and C_i)
   The triclinic symmetry does not add any restrictions to the components of tensor C_{ijkl} (or B_{ijkl} in (2.5.4)); however, appropriate choice of the coordinate system enables us to reduce the number of nonzero independent elastic constants. Because the orientation of the coordinate system is determined by three rotation angles, this provides three conditions to restrict some components in C_{ijkl} (or B_{ijkl} in (2.5.4)); for example, one can take three of them to be zero, such that, the triclinic crystal system has 18 components of elastic moduli.
2. Monoclinic system (classes C_s, C_2 and C_{2h})
   In the class C_s, there is a plane of symmetry, we take it as $x_3 = 0$ $(z = 0)$ in coordinate frame $\mathbf{e_1}$, $\mathbf{e_2}$, $\mathbf{e_3}$. Making a coordinate transformation with this plane of symmetry one can obtain a new coordinate frame $\mathbf{e'_1}, \mathbf{e'_2}, \mathbf{e'_3}$. Between these two coordinate frames, there are relations

$$\mathbf{e}'_1 = \mathbf{e}_1, \mathbf{e'_2} = \mathbf{e}_2, \mathbf{e'_3} = -\mathbf{e}_3 \tag{2.5.5}$$

   This operation is the reflection or mapping. In addition, we know that between σ'_{ij} in $\mathbf{e'_1}, \mathbf{e'_2}, \mathbf{e'_3}$ and σ_{ij} in $\mathbf{e_1}$, $\mathbf{e_2}$, $\mathbf{e_3}$, there are (refer to §2.1)

$$\sigma'_{kl} = \alpha_{kj}\alpha_{li}\sigma_{ji} \tag{2.5.6}$$

   in which α_{ij} are the coefficients of linear transformation, i.e.

$$\mathbf{e}'_i = \alpha_{ij}\mathbf{e}_j \tag{2.5.7}$$

Under the transformation (2.5.5), there are

$$\alpha_{11} = 1, \alpha_{22} = 1, \alpha_{33} = -1, \quad others = 0 \tag{2.5.8}$$

Therefore, under the transformation, for C_{ijkl} in (2.5.1) (or B_{ijkl} in (2.5.4)) whose suffixes containing 3 with an odd number of times (1 or 3) will change sign, while the others will remain invariant. Considering the symmetry of the crystal, however, the physical properties including C_{ijkl} (or B_{ijkl} in (2.5.4)) should remain unchanged under symmetric operation (including the reflection). So it is obvious that all components with an odd number of suffixes 3 must vanish, i.e.

$$B_{1123} = B_{1131} = B_{2223} = B_{2231} = B_{3323} = B_{3331} = B_{2312} = B_{3112} = 0 \tag{2.5.9}$$

Consequently, there are only 13 independent elastic constants.
A similar discussion can be done for the classes C_2 and C_{2h}.

3. Orthorhombic system (classes C_{2v}, D_2 and D_{2h})
This crystal system has a macroscopic corresponding, i.e. the orthotropic materials, in which there exist two planes of symmetry perpendicular to each other. Let us take $x_3 = 0$ and $x_1 = 0$ as the planes. If on reflection in plane $x_3 = 0$, it is just the case for monoclinic system mentioned above. Subsequently, considering the mapping in plane $x_1 = 0$, between the new and old coordinate systems, there is the relation such as

$$\begin{bmatrix} e_1' \\ e_2' \\ e_3' \end{bmatrix} = \begin{bmatrix} -1 & 0 & 0 \\ 0 & 1 & 0 \\ 0 & 0 & 1 \end{bmatrix} \begin{bmatrix} e_1 \\ e_2 \\ e_3 \end{bmatrix}$$

By a similar description to that for monoclinic system, one finds that

$$B_{1112} = B_{2212} = B_{3312} = B_{2331} = 0 \tag{2.5.10}$$

Collecting to (2.5.9), the system contains 9 independent elastic constants.

4. Tetragonal system (classes C_{4v}, D_{2d}, D_4 and D_{4h})
This crystal system has 4 axes of symmetry. Similar to previous discussion, those independent elastic moduli are

$$B_{1111}, B_{3333}, B_{1122}, B_{1212}, B_{1133}, B_{1313}$$

The total number of these is six.

5. Rhombohedral system (classes C_{3v}, 3 or C_3, D_3, D_{3d} and S_6)
In this system, there is a third-order axis of symmetry (or threefold symmetric axis). We can take axis of symmetry as the axis $\mathbf{e_3}$, after a lengthy description that six independent elastic constants are as follows:

$$B_{3333}, B_{\xi\eta\xi\eta}, B_{\xi\xi\eta\eta}, B_{\xi\eta 33}, B_{\xi 3\eta 3}, B_{\xi\xi\xi 3}$$

with

$$\xi = x_1 + ix_2, \eta = x_1 - ix_2$$

The moduli can also be written in conventional version as

$$B_{3333}, B_{1212}, B_{1122}, B_{1233}, B_{1323}, B_{1113}$$

6. Hexagonal system (class C_6)
   The crystal system has a macroscopic correspondence—the transverse isotropic material, whose elasticity presents fundamental importance to elasticity of one- and two-dimensional quasicrystals.
   There is a sixth-order axis of symmetry (or say sixfold symmetric axis) in the system. By taking this axis as x_3-axis and using the coordinate substitution $\xi = x_1 + ix_2, \eta = x_1 - ix_2$. In a rotation with angle $2\pi/6$ about the x_3-axis, the coordinates ξ and η are experienced a transformation $\xi \rightarrow \xi e^{i2\pi/6}$, $\eta \rightarrow \eta e^{-i2\pi/6}$. Then one can see that only those components C_{ijkl} do not vanish which have the same number of suffixes ξ and η. These are

$$B_{3333}, B_{\xi\eta\xi\eta}, B_{\xi\xi\eta\eta}, B_{\xi\eta 33}, B_{\xi 3\eta\xi}$$

   or in conventional expressions

$$C_{1111} = C_{2222}, C_{3333}, C_{2323} = C_{3131}, C_{1122},$$
$$C_{1133} = C_{2233}, C_{1212}$$

   in which $2C_{1212} = C_{1111} - C_{1122}$, so the number of independent elastic constants is five.
7. Cubic system
   For this system there are 3 fourfold symmetric axes, in which there is tetragonal symmetry. If taking the fourfold symmetric axis of the tetragonal symmetry in the x_3-direction, the number of independent components of C_{ijkl} (or B_{ijkl} in (2.5.4)) are $B_{1111}, B_{1122}, B_{1212}$
8. Isotropic body
   In this case there are two elastic moduli, e.g. the Young's modulus and Poisson's ratio

$$E, v$$

   respectively, or the Lamé constants

$$\lambda = \frac{vE}{(1+v)(1-2v)}, \mu = \frac{E}{2(1+v)} \tag{2.5.11}$$

or the bulk modulus of compression and shear modulus $K = \frac{E}{3(1-2v)}, \mu = \frac{E}{2(1+v)} = G$

In this case the generalized Hooke's law presents very simple form, i.e.

$$\sigma_{ij} = 2\mu\varepsilon_{ij} + \lambda\varepsilon_{kk}\delta_{ij} \tag{2.5.12}$$

where $\varepsilon_{kk} = \varepsilon_{11} + \varepsilon_{22} + \varepsilon_{33} = \varepsilon_{xx} + \varepsilon_{yy} + \varepsilon_{zz}$,$\delta_{ij}$ is the unit tensor. An equivalent form of (2.5.12) is

$$\varepsilon_{ij} = \frac{1+v}{E}\sigma_{ij} - \frac{v}{E}\sigma_{kk}\delta_{ij} \tag{2.5.13}$$

in which $\sigma_{kk} = \sigma_{11} + \sigma_{22} + \sigma_{33} = \sigma_{xx} + \sigma_{yy} + \sigma_{zz}$

2.6 Elastodynamics, Wave Motion

When the inertia effect is considered in (2.4.1), then it becomes

$$\frac{\partial\sigma_{ij}}{\partial x_j} + f_i = \rho\frac{\partial^2 u_i}{\partial t^2} \tag{2.6.1}$$

where ρ is the mass density of the material.

Considering isotropic medium and omitting body forces from (2.6.1), (2.3.6) and (2.5.12), the equations of wave motion are obtained as

$$(c_1^2 - c_2^2)\frac{\partial^2 u_i}{\partial x_i \partial x_j} + c_2^2\frac{\partial^2 u_j}{\partial x_i^2} = \frac{\partial^2 u_j}{\partial t^2} \tag{2.6.2}$$

where c_1 and c_2 defined by

$$c_1 = \left(\frac{\lambda+2\mu}{\rho}\right)^{\frac{1}{2}}, c_2 = \left(\frac{\mu}{\rho}\right)^{\frac{1}{2}} \tag{2.6.3}$$

which are speeds of elastic longitudinal and transverse waves, respectively. If put

$$\mathbf{u} = \nabla\phi + \nabla \times \boldsymbol{\psi} \tag{2.6.4}$$

then (2.6.2) can be reduced to

$$\nabla^2\phi = \frac{1}{c_1^2}\frac{\partial^2\phi}{\partial t^2}, \nabla^2\boldsymbol{\psi} = \frac{1}{c_2^2}\frac{\partial^2\boldsymbol{\psi}}{\partial t^2} \tag{2.6.5}$$

where ϕ is scalar potential, $\boldsymbol{\psi}$ the vector potential and $\nabla^2 = \frac{\partial^2}{\partial x^2} + \frac{\partial^2}{\partial y^2} + \frac{\partial^2}{\partial z^2}$, (2.6.5) are typical wave equations of mathematical physics. To solve the problem apart from the boundary conditions one needs initial conditions, i.e.

$$\begin{aligned} u_i(x_i, 0) &= u_{i0}(x_i) \\ & \qquad x_i \in \Omega \\ \dot{u}_i(x_i, 0) &= \dot{u}_{i0}(x_i). \end{aligned}$$

2.7 Summary

The classical theory of elasticity is concluded to solve the following initial-boundary value problem

$$\begin{aligned} &\varepsilon_{ij} = \frac{1}{2}\left(\frac{\partial u_i}{\partial x_j} + \frac{\partial u_j}{\partial x_i}\right) \\ &\frac{\partial \sigma_{ij}}{\partial x_i} = \rho\frac{\partial^2 u_j}{\partial t^2} - f_j, (t > 0, x_i \in \Omega) \\ &\sigma_{ij} = C_{ijkl}\varepsilon_{ijkl} \\ &u_i(x_i, 0) = u_{i0}(x_i) \\ &\dot{u}_i(x_i, 0) = \dot{u}_{i0}(x_i), (x_i \in \Omega) \\ &\sigma_{ij}n_j = T_i, t > 0, x_i \in S_t \\ &u_i = \bar{u}_i, t > 0, x_i \in S_u \end{aligned}$$

where $u_{i0}(x_i), \dot{u}_{i0}(x_i), T_i$ and $\bar{u}_i$ are known functions, Ω denotes the region of materials we studied, S_t and S_u are parts of boundary S on which the tractions and displacements are prescribed, respectively, and $S = S_t + S_u$. If $\frac{\partial^2 u_j}{\partial t^2} = 0$, the problem reduces to a static problem as pure-boundary value problem, there are no initial conditions at all.

References

1. Landau L D and Lifshitz E M, 1986, *Theoretical Physics V: Theory of Elasticity*, Pergamon Press, Oxford.
2. Born M and Huang K, 1954, *Dynamic Theory of Crystal Lattices*, Clarendon Press, Oxford.
3. Anderson P W, 1984, *Basic Notations of Condensed Matter Physics*, Benjamin-Cummings, Menlo Park.

Chapter 3
Quasicrystal and Its Properties

3.1 Discovery of Quasicrystal[1]

The first observation of quasicrystal was done in April 1982, while D. Shechtman as guest scholar was working in the Bureau of Standards in USA. He observed from electronic microscopy that a rapid cooled Al–Mn alloy exhibits fivefold orientational symmetry by the diffraction patterns with bright diffraction spots and sharp Bragg reflections, as shown in Fig. 3.1. Because the fivefold orientational symmetry is of contradiction with the basic law of symmetry of crystals (refer to Chap. 1), the result could not be understood within the first two years since the discovery. Colleague of Shechtman, I. Blech in Israel, gave him a powerful support and explained it might be an icosahedral glass. They drafted a paper concerning the experimental results and sent off to a journal, but which was rejected. Then, they submitted it to another journal, which could not be published too. J. W. Cahn, the hosting scientist in the Bureau of Standards, recommended streamlining the paper, leaving out details of the model and experiment, and limiting it solely the experimental findings. After consulting with D. Gratias, a mathematical crystallographer at the Centre National de la Recherche Scientifique in France, the group submitted an abbreviated article to *Physical Review Letters* (PRL) in October 1984, more than two years after Shechtman's initial experiment. The article was published several weeks later. This is the Ref. [1].

More recently, the natural quasicrystals, apart those from alloys, were observed by Bindi et al.[2]

After four weeks, Levine and Steinhardt [2] published their work by PRL to introduce ordered structure with quasiperiodicity and called the novel alloy as "quasicrystal" formally, in which their theoretical (computed) diffraction pattern is in excellent agreement with that of the experimental observation. Soon after, other

[1]This is referred to article PRL Top 10:#8 of APS.
[2]Bindi L, Steinhardt P J, Yao N and Lu P J, 2009, Natural quasicrystals, *Science*, **324**, 1306-1309.

T.-Y. Fan, *Mathematical Theory of Elasticity of Quasicrystals and Its Applications*,
Springer Series in Materials Science 246, DOI 10.1007/978-981-10-1984-5_3

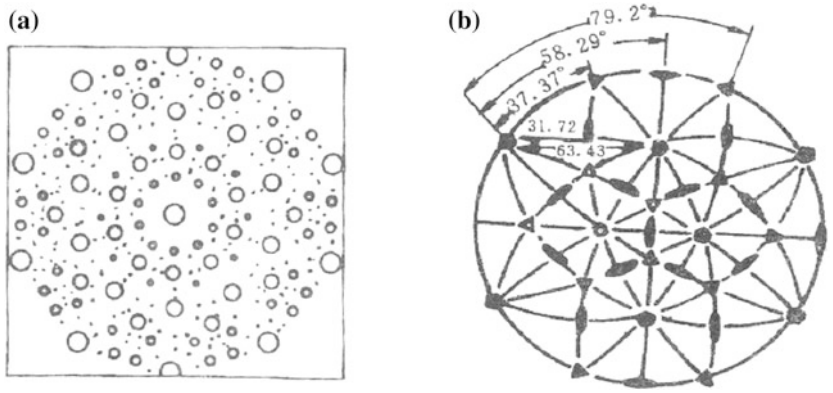

Fig. 3.1 The patterns of diffraction of icosahedral quasicrystal. **a** The fivefold symmetry and **b** the stereographic structure of the quasicrystal

groups, such as Ye et al. [3] and Zhang et al. [4], also found similar structure of fivefold symmetry and icosahedral quasicrystal in Ni–V and Ni–Ti alloys.

The icosahedral quasicrystals are one of the three-dimensional quasicrystals, in which atomic arrangement is quasiperiodic in three directions. Another kind of three-dimensional quasicrystal is cubic quasicrystal observed by Feng et al. [5] later.

Successively two-dimensional quasicrystals were observed. Here, the atomic arrangement is quasiperiodic along two directions and periodic along the third direction, which is just the directions of 5-, 8-, 10- and 12-fold symmetrical axes of the two-dimensional quasicrystals observed to date, such that one finds four kinds of two-dimensional quasicrystals with 5-, 8-, 10- and 12-fold rotation symmetries which are also called pentagonal, octagonal, decagonal and dodecagonal quasicrystals, respectively (see Bendersky [6], Chattopadhyay et al. [7], Fung et al. [8], Urban et al. [9], Wang et al. [10], Li et al. [11]).

There is another class of quasicrystals, the one-dimensional quasicrystals, in which the atomic arrangement is quasiperiodic along one axis and periodic along the plane perpendicular to the axis (see Merdin et al. [12], Hu et al. [13], Fung et al. [14], Terauchi et al. [15], Chen et al. [16] and Yang et al. [17]).

The discovery of this novel matter with long-range order and non-crystallographic symmetry changes the traditional concept of classifying solids into two classes, crystal and non-crystal, gives a strong impact on traditional crystallography and brings profound new physical idea into the matter structure and symmetry.

The unusual structure of quasicrystals leads to a series of properties different from that of crystals, which has created a great deal of attention by researchers in a range of fields, such as physics, crystallography and chemistry.

A decade before the discovery, mathematician Penrose [18] put forward a mathematical model of quasicrystals, afterward called Penrose tiling, in which a tiling without an overlap or a gap in two different rhombohedra can result in

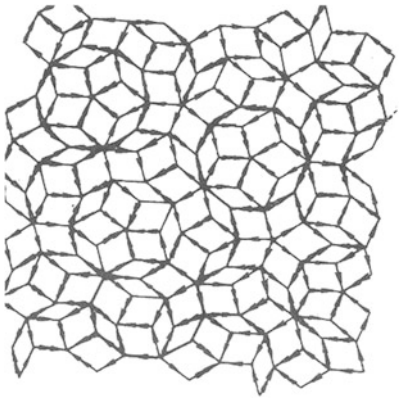

Fig. 3.2 Penrose tiling of two-dimensional quasicrystal with fivefold symmetry

quasiperiodic structure. After the discovery of quasicrystals, Penrose tiling has become a geometric tool of the new solid phase. As an example, a Penrose tiling for describing a two-dimensional fivefold symmetry is shown in Fig. 3.2, in which the local structure of the tiling is similar, and this is called local isomorphism (LI). The quasiperiodic symmetry and local isomorphism of the Penrose tiling present significance for describing the new solid-phase quasicrystals. The discovery of quasicrystal physically promotes the development of the Penrose geometry and the relevant discrete geometry. It promotes the development of ergodic theory, group theory, Fourier analysis, etc., too.

Quasicrystals with thermodynamical stability are becoming a new class of functional and structural materials, which have many prospective engineering applications. The study on physical and mechanical properties of the material is put forward. Among the mechanical behaviour of quasicrystals, the elasticity and defects are of important topics. These provide many new challenges as well as opportunities to the continuum mechanics.

However, there was a different point of view, e.g. L. Pauling[3] claimed that the icosahedral quasicrystal is a cubic crystal rather than quasicrystals, but various quasicrystals are observed experimentally, and the argument is ended.

3.2 Structure and Symmetry of Quasicrystals

Quasicrystals are different from periodic crystals, but with certain symmetry, it is one of the kinds of aperiodic crystals. The unusual characters of quasicrystals are originated from their special atomic constitution. The character of this structure is explored by diffraction patterns. Just through these diffraction patterns, people

[3]Pauling L, 1985, Apparent icosahedral symmetry is due to directed multiple twinning of cubic crystals, *Nature*, **317**, 512-514.

discovered differences between crystals and quasicrystals, so discovered the quasicrystals.

Similar to other aperiodic crystals, quasiperiodicity induces new degrees of freedom, which can be explained as follows. In crystallography and solid-state physics, the Miller indices (h, k, l) are often used to describe the structure of crystals. These indices can explain the spectra of diffraction patterns of all crystals. In Chap. 1, we mentioned that the number of base vectors for crystal N is identical to the number of the dimensions d of the crystal, i.e. $N = d$. However, because quasicrystals have quasiperiodic symmetry (including both or either quasiperiodic translational and orientational symmetries disallowed by the rule of crystallography), the Miller indices cannot be used, and instead, we need to employ six indices $(n_1, n_2, n_3, n_4, n_5, n_6)$. This feature implies to characterize the symmetry of quasicrystals that it is necessary to introduce higher dimensional (four- or five- or six-dimensional) spaces. This idea is identical to that of group theory, i.e. the quasiperiodic structure is periodic in higher dimensional (four- or five- or six-dimensional) spaces. Quasicrystals in real three-dimensional space (physical space) may be seen as a projection of a periodic lattice in higher dimensional (mathematical) space. The projection of periodic lattice at four-, five- and six-dimensional spaces to physical space generates one-, two- and three-dimensional quasicrystals, respectively. The six-dimensional space is denoted by E^6, which consists of two subspaces: One is physical space, called the parallel space and denoted by $E_{\parallel}^3$, and another is the complementary space also called vertical space and denoted by $E_{\perp}^3$ so that

$$E^6 = E_{\parallel}^3 \oplus E_{\perp}^3 \tag{3.2.1}$$

where $\oplus$ denotes the direct sum.

For one-, two- and three-dimensional quasicrystals, the number of the base vectors is $N = 4, 5, 6$ and the number of the realistic dimensions of the material (in physical space) is $d = 3$, so $N > d$, and this is different from that of crystals.

The method of group theory is the most appropriate method to describe the symmetry of quasicrystals.

The one-dimensional quasicrystals have 31 point groups and consist of 6 quasicrystal systems and 10 Laue classes, respectively, in which the all point groups are crystallographic point groups listed in Table 3.1.

The two-dimensional quasicrystals have 57 point groups, in which 31 are crystallographic point groups have been listed in Table 1.1, and other 26 are non-crystallographic point groups listed in Table 3.2, they belong to 4 quasicrystal systems and 8 Laue classes, respectively.

The three-dimensional quasicrystals have 60 point groups. They are as follows: (1) 32 crystallographic point groups and 28 non-crystallographic point groups, i.e. icosahedral point groups (235, $\frac{2}{m}\overline{3}\overline{5}$) and 26 point groups with 5-, 8-, 10- and 12-fold symmetries (5, $\overline{5}$, 52, $\overline{5}$ m, $5m$, and N, $\overline{N}$, N/m, $N22$, Nmm, $\overline{N}$ $m2$, N/mmm, N = 8, 10, 12), and the latter are listed in Table 3.2.

Table 3.1 The systems, Laue classes, and point groups of one-dimensional quasicrystals

System	Laue class	Point group
Triclinic	1	$1,\overline{1}$
Monoclinic	2 3	$2,\ m_h,\ 2/m_h$ $2_h,\ m,\ 2_h/m$
Orthorhombic	4	$2_h2_h2,\ mm2,\ 2_hmm_h,\ mmm_h$
Tetragonal	5 6	$4,\ \overline{4},\ 4/m_h$ $42_h2_h,\ 4mm,\ 4/m_h,\ mm$
Rhombohedral (trigonal)	7 8	$3,\ \overline{3}$ $32_h,\ 3m,\ \overline{3}m$
Hexagonal	9 10	$6,\ \overline{6},\ 6/m_h$ $62_h2_h,\ 6mm,\ \overline{6}m2_h,\ 6/m_hmm$

Table 3.2 The systems, Laue classes, and point groups of non-crystallography of two-dimensional quasicrystals

System	Laue class	Point group
Pentagonal	11 12	$5,\ \overline{5}$ $5m,\ 52,\ \overline{5}\ m$
Octagonal	13 14	$8,\ \overline{8},\ 8/m$ $8mm\ ,822,\ \overline{8}m2,\ 8/mmm$
Decagonal	15 16	$10,\ \overline{10},\ 10/m$ $10mm,\ 1022,\ \overline{10}m2,\ 10/mmm$
Dodecagonal	17 18	$12,\ \overline{12},12/m$ $12mm,1222,\overline{12}m2,12/mmm$

3.3 A Brief Introduction on Physical Properties of Quasicrystals

The unusual structure of quasicrystals leads to some new physical properties of the material.

The mechanical behaviour of quasicrystals, especially the distinguishing features of elasticity to those of crystals, has aroused a great deal of interests of researchers. These will be discussed starting from Chap. 4 in detail, so we do not talk about it any more here.

The thermal properties of quasicrystals are a field that attracts attention of many scientists [19–27]. The thermal conductivity of quasicrystals is lower than that of conventional metals.

Among the profound studied properties of quasicrystals, the first is the structural and elastic properties, and the second may be the properties of electricity of the material. The conductivity of electricity of quasicrystals is lower. And the Hall effect [28–32] was well studied. The absolute number of the Hall coefficient RH is greater, i.e. two orders of magnitude, than that of conventional metals. In addition, the pressure–resistance properties of quasicrystals are also discussed by some references (see, e.g. [33]).

The light conductivity rate of quasicrystals is quite different from that of conventional metals, and the people are interested in the singularity (see [34–36]). Recently, the quasicrystals photonic crystal study becomes a focus [37–39], there is a trend of further development of study [40–42].

The electronic structure of quasicrystals and relevant topics have also been concerned after the discovery [43–45]. Due to lack of periodicity, the Bloch theorem and Brillouin zone concept cannot be used. By some simple models and through numerical computations, one can obtain the results on electronic energy spectra. Some results on wave functions obtained exhibit behaviour neither in extending state nor in localization state. For some quasicrystalline materials, e.g. AlCuLi and AlFe, there are pseudogaps when energy is over the Fermi energy.

Many mathematicians developed several mathematical models to describe electronic energy spectrum, and readers who are interested can refer to Refs. [46–60].

Because the present book discusses the elasticity of quasicrystals only, the other properties will not be dealt with. The above introduction is very simple and brief.

3.4 One-, Two- and Three-Dimensional Quasicrystals

It is needed to recall the concept of one-, two- and three-dimensional quasicrystals. The one-dimensional quasicrystals are ones in which the atom arrangement is quasiperiodic in one direction and periodic in other two directions. The two-dimensional quasicrystals belong to ones in which the atom arrangement is quasiperiodic in two directions and periodic in another one. The three-dimensional quasicrystals behave in such a way that the arrangement represents quasiperiodicity in all three directions.

There exist over 200 quasicrystals observed to date, among which the halves are icosahedral and about 70 decagonal quasicrystals, respectively, so these two kinds of quasicrystal systems represent major importance of the material. Recently, the two-dimensional quasicrystals with 12- and 18-fold symmetries in soft matter are observed [61–64], these quasicrystals have just been studied.

3.5 Two-Dimensional Quasicrystals and Planar Quasicrystals

The two-dimensional quasicrystals and planar quasicrystals are different concepts. The two-dimensional quasicrystals are introduced in the previous section, which represent a three-dimensional structure with two-dimensional quasiperiodic planes

stacked along the third direction, and in this direction, the atom arrangement is periodic. While the planar quasicrystals belong to a two-dimensional structure within the plane, the atom arrangement is quasiperiodic, and there is no third dimension.

References

1. Shechtman D, Blech I, Gratias D and Cahn J W, 1984, Metallic phase with long-range orientational order and no translational symmetry, *Phys Rev Lett*, **53**(20), 1951-1953.
2. Levine D and Steinhardt P J, 1984, Quasicrystals: A new class of ordered structure. *Phys Rev Lett*, **53**(26), 2477-2480.
3. Ye H Q, Wang D and Kuo K H, 1985, Five-fold symmetry in real and reciprocal space, *Ultramicrossopy*, **16**(2), 273-277.
4. Zhang Z, Ye H Q and Kuo K H, 1985, A new icosahedral phase with m35 symmetry. *Phil Mag* A, **52**(6), L49-L52.
5. Feng Y C, Lu G and Witers R I, 1989, An incommensurate structure with cubic point group symmetry in rapidly solidified V-Vi-Si alloy. *J Phys Condens Matter*, **1**(23),3695-3700.
6. Bendersky L,1985, Quasicrystal with one-dimensional translational symmetry and a tenfold rotation axis, *Phys Rev Lett*, **55**(14), 1461-1463.
7. Chattopadhyay K, Lele S and Thangarai N et al, 1987,Vacancy ordered phases and one-dimensional quasiperiodicity, *Acta Metall,* **35**(3), 727-733.
8. Fung K K, Yang C Y and Zhou Y Q et al, 1986, Icosahedrally related decagonal quasicrystal in rapidly cooled Al-14-at.%-Fe alloy. *Phys Rev Lett*, **56**(19), 2060-2063.
9. Urban K, Mayer J, Rapp M, Wilkens M, Csanady, A, and Fidler J, 1986, Studies on aperiodic crystals in Al-Mn and Al-V alloys by means of transmission electron microscopy, *Journal de Physique Colloque*, **47C**(3), 465-475.
10. Wang N, Chen H and Kuo K H, 1987,Two-dimensional quasicrystal with eightfold rotational symmetry, *Phys Rev Lett*, **59**(9),1010-1013.
11. Li X Z and Guo K H, 1988, Decagonal quasicrystals with different periodicities along the tenfold axis in rapidly solidified AlNi alloys. *Phil Mag Lett*, **58**(3), 167-171.
12. Merdin R, Bajema K, Clarke R, Juang F-Y and Bhattacharya P K, 1985,Quasiperiodic GaAs-AlAs heterostructures, *Phys Rev Lett*, **55**(17), 1768-1770.
13. Hu A, Tien C and Li X et al, 1986, X-ray diffraction pattern of quasiperiodic (Fibonacci) Nb-Cu superlattices, *Phys Lett* A, **119**(6), 313-314.
14. Feng D, Hu A, Chen K J et al, 1987, Research on quasiperiodic superlattice, *Mater Sci Forum*, **22** (24), 489-498,.
15. Terauchi H, Noda Y, Kamigami K et al, 1988, X-Ray diffraction patterns of configuration Fibonacci lattices, *J Phys Jpn*, **57**(7), 2416-2424.
16. Chen K J, Mao G M and Fend D et al, 1987,Quasiperiodic a-Si: H/a-SiNx: H multilayer structures, *J Non-cryst Solids*, **97**(1), 341-344.
17. Yang W G, Wang R H and Gui J,1996, Some new stable one-dimensional quasicrystals in Al_{65} Cu_{20} Fe_{10} Mn_5 alloy, *Phil Mag Lett*, **74**(5), 357-366.
18. Penrose R.,1974, The role of aesthetics in pure and applied mathematical research. In: *Bulletin of the Institute of Mathematics and Its Applications* (*Bull. Inst. Math. Appl.*). Southend-on-Sea, **10**, ISSN 0146-3942, 266–271; Pentaplexity - A Class of non-periodic tilings of the plane. In: *The Mathematical Intelligencer*. Vol.2, No. 1, Springer, New York 1979, ISSN 0343-6993, pp. 32–37.
19. Biham O, Mukamel D and Shtrikman, 1986, Symmetry and stability of icosahedral and other quasicrystalline phases, *Phys. Rev. Lett*., **56**(20),2191-2194.

20. Scheater R J and Bendersky L A, 1988, *Introduction to Quasicrystals*, ed. By Jaric M. V., Boston, MA: Academic Press.
21. Widom M, Deng D P and Henleg C L, 1989,Transfer-matrix analysis of a two-dimensional quasicrystal, *Phys. Rev. Lett*., **63**(3), 310-313.
22. Yang W G, Ding D H, Wang R H and Hu C Z, Thermodynamics of equilibrium properties of quasicrystals. *Z Phys.* B, **100** (3), 447-454.
23. Hu C Z, Yang W G, Wang R H and Ding D H, 1997, Quasicrystal Symmetry and Physical Properties. *Progress in Phys.* (in Chinese), **17** (4). 345-367.
24. Fan T Y, 1999, A study on specific heat of one-dimensional hexagonal quasicrystal, *J. Phys.: Condens. Matter*, **11**(45), L513-517.
25. Fan T Y and Mai Y W, 2003, Partition function and state equation of point group 12 mm two-dimensional dodecagonal quasicrystals, *Euro. Phys. J.B,* **31**(2),17-21.
26. Li C Y and Liu Y Y, 2001, Phason-strain influence on low-temperature specific heat of the decagonal Al-Ni-Co quasicrystal, *Chin. Phys. Lett*., **18**(4), 570-573.
27. Li C Y and Liu Y Y, 2001,Low-temperature lattice excitation of icosahedral Al-Mn-Pd quasicrystals*, Phys. Rev.* B, **63**(6),064203-064211.
28. Biggs B D, Li Y and Poon S J, 1991, Electronic properties of icosahedral, approximant, and amorphous phases of an Al-Cu-Fe alloy, *Phys. Rev.* B, **43**(10), 8747-8750.
29. Lindqvist P, Berger C, Klein T et al, 1993, Role of Fe and sign reversal of the Hall coefficient in quasicrystalline Al-Cu-Fe, *Phys. Rev.* B, **48**(1), 630-633.
30. Klein T, Gozlen A, Berger C, Cyrot-Lackmann F, Calvayrac Y and Quivy A, 1990, Anomalous transport properties in pure AlCuFe icosahedral phases of high structural quality, *Europhys.Lett.*, **13**(2), 129-134.
31. Pierce F S, Guo Q and Poon S J, 1994, Enhanced insulatorlike electron transport behavior of thermally tuned quasicrystalline states of Al-Pd-Re alloys, *Phys. Rev. Lett*., **73**(16), 2220-2223.
32. Wang A J, Zhou X, Hu C Z and Miao L, 2005,Properties of nonlinear elasticity of quasicrystals with five-fold symmetry, Wuhan University Journal, Nat. Sci., 51(5), 536-566. (in Chinese).
33. Zhou X, Hu C Z, Gong P and Qiu S D, 2004, Piezoresistance properties of quasicrystals, *J. Phys.:Condens. Matter*, **16**(30), 5419-5425.
34. Homes C C,Timusk T, Wu X, Altounian Z, Sahnoune A and Ström-Olsen J O,1991,Optical conductivity of the stable icosahedral quasicrystal $Al_{63.5}Cu_{24.5}Fe_{12}$, *Phy. Rev. Lett*., **67**(19), 2694–2696.
35. Burkov S E, 1992, Optical conductivity of icosahedral quasi-crystals, *J. Phys.: Condens. Matter*, **4** (47), 9447–9458.
36. BasovD N, Timusk T, Barakat F, Greedan J and Grushko B, 1994,Anisotropic optical conductivity of decagonal quasicrystals, *Phys. Rev. Lett*., **72**(12), 1937–1940.
37. Villa D, Enoch S and Tayeb G et al, 2005, Band gap formation and multiple scattering in photonic quasicrystals with a Penrose-type lattice, *Phys. Rev. Lett.*, **94**(18), 183903-183907.
38. Didier Mayou, 2000,Generalized Drude Formula for the Optical Conductivity of Quasicrystals, *Phys. Rev. Lett.,* 85(6), 1290-1293.
39. Notomi M, Suzuk H and Tamamura T et al, 2004,**L**asing action due to the two-dimensional quasiperiodicity of photonic quasicrystals with a Penrose lattice, *Phys. Rev. Lett.*, 90(12), 123906-123910.
40. Feng Z F, Zhang X D and Wang Y Q, 2005,**N**egative refraction and imaging using 12-fold-symmetry quasicrystals, *Phys. Rev. Lett*., **94**(24), 247402-247406.
41. Lifshitz R, Arie A and Bahabad A, 2005, Photonic quasicrystals for nonlinear optical frequency conversion, *Phys. Rev. Lett.*, **95**(13), 13390.
42. Marn W and Megens M, 2005, Experimental measurement of the photonic properties of icosahedral quasicrystals. *Nature*, **436**(7053), 993–996.
43. Kohmoto M and Sutherland B, 1986, Electronic states on a Penrose lattice, *Phys Rev Lett*, **56** (25), 2740-2743.

44. Sutherland B, 1986,Simple system with quasiperiodic dynamics: a spin in a magnetic field, *Phys Rev* B, **34**(8), 5208-5211.
45. Fujiwara T and Yokokawa T, 1991,Universal pseudogap at Fermi energy in quasicrystals, *Phys. Rev. Lett.*, **66**(3),333-336.
46. Casdagli M, 1986, Symbolic dynamics for the renormalization map of a quasiperiodic Schroedinger equation, *Commun. Math. Phys*. 107(2), 295–318.
47. Sueto A, 1987, The spectrum of a quasiperiodic Schroedinger operator, Comm. Math. Phys, 111(3), 409–415.
48. Kotani S, 1989, Jacobi matrices with random potentials taking finitely many values, Rev. Math. Phys. 1(1), 129–133.
49. Bellissard J, Lochum B, Scoppola E, Testart D, 1989, Spectral properties of one dimensional quasi-crystals, Commun. Math. Phys. 125(3), 527–543.
50. Bovier A, Ghez J-M, 1993, Spectrum properties of one-dimensional Schroedinger operators with potentials generated by substitutions, Commun. Math. Phys. 158(1), 45-66.
51. Liu Q H, Tan B, Wen Z X, Wu J, 2002, Measure zero spectrum of a class of Schroedinger operators, J. Statist. Phys. 106(3-4), 681–691.
52. Lenz D, 2002, Singular spectrum of Lebesgue measure zero for one-dimensional quasicrystals, Comm. Math. Phys. 227(1), 119–130.
53. Furman A, 1997, On the multiplicative ergodic theorem for uniquely ergodic systems, Ann. Inst. H. Poincare Probab. Statist. 33 (6), 797–815.
54. Damanik D, Lenz D, 2006, A, condition of Boshernitzan and uniform convergence in the multiplicative ergodic theorem, Duke Math. J. 133(1), 95–123.
55. Liu Q H, Qu Y H, 2011, Uniform Convergence of Schroedinger Cocycles over Simple Toeplitz Subshift, Annales Henri Poincare, 12(1), 153–172.
56. Liu Q H, Qu Y H, 2012, Uniform Convergence of Schroedinger Cocycles over bounded Toeplitz Subshift, Annales Henri Poincare, 13(6), 1483-1550.
57. Liu Q H, Wen Z Y, 2004, Hausdorff dimension of spectrum of one-dimensional Schroedinger operator with Sturmian potentials, Potential Analysis, 20(1), 33–59.
58. Damanik D, Embree M, Gorodetski A, Tcheremchantsev S, 2008, the fractal dimension of the spectrum of the Fibonacci Hamiltonian, Commun. Math. Phys. 280(2), 499-516.
59. Liu Q H, Peyrière J, Wen Z Y, 2007, Dimension of the spectrum of one-dimensional discrete Schrodinger operators with Sturmian potentials, Comptes Randus Mathematique, 345(12), 667–672.
60. Fan S, Liu Q H, Wen Z Y, 2011, Gibbs-like measure for spectrum of a class of quasi-crystals, Ergodic Theory Dynam. Systems, 31(6), 1669-1695.
61. Fischer S, Exner A, Zielske K, Perlich J, Deloudi S, Steuer W, Linder P and Foestor S, 2011, Colloidal quasicrystals with 12-fold and 18-fold symmetry, Proc Nat Ac Sci, 108, 1810-1814.
62. Talapin V D, Shevechenko E V, Bodnarchuk M I, Ye X C, Chen J and Murray C B, 2009, Quasicrystalline order in self-assembled binary nanoparticle superlattices, Nature, 461, 964-967.
63. Zeng X ,Ungar G, Liu Y, Percec V, Dulcey A E,Hobbs J K, 2004, Supermolecular dentritic liquid quasicrystals, Nature, 428, 157-160.
64. Takano K, 2005, A mesoscopic Archimedian tiling having a complexity in polymeric stars, J Polym Sci Pol Phys, 43, 2427-2432.

Chapter 4
The Physical Basis of Elasticity of Solid Quasicrystals

The physical background on elasticity of solid quasicrystals is quite different from that of the crystal elasticity or classical elasticity; the discussion about this provides a basis of the subsequent contents of the book.

4.1 Physical Basis of Elasticity of Quasicrystals

Solid quasicrystal has become a type of functional and structural materials, having potential engineering applications. As a material, quasicrystal is deformed under applied forces, thermal loads and certain internal effects. The deformation of crystals has been discussed in Chap. 2. Questions arise as to what the characteristics in the deformation process of the quasicrystals are. How to describe mathematically the behaviour of the quasicrystal deformation and motion? To answer these questions, it is necessary to consider the physical background of elasticity of quasicrystals. The study in this regard was conducted soon after discovery of the new solid phase.

Because quasicrystals observed in binary and ternary alloys belong to a new structure of solid, theoretical physicists have proposed various descriptions of their elasticity. The majority agrees that the Landau density wave theory (refer to Refs. [1–25]) is the physical basis of elasticity of quasicrystals. We shall introduce the theory in Appendix of this chapter (i.e. the Sect. 4.9). In particular, the description suggested that there are two displacement fields $\mathbf{u}$ and $\mathbf{w}$ in a quasicrystal: the former is similar to that in crystals, named the phonon field according to the physical terminology, and its macro-mechanical behaviour is discussed in Chap. 2; the latter is new displacement field named phason field. The total displacement field in a quasicrystal is expressed by

$$\bar{\mathbf{u}} = \mathbf{u}^{\parallel} \oplus \mathbf{u}^{\perp} = \mathbf{u} \oplus \mathbf{w} \tag{4.1.1}$$

T.-Y. Fan, *Mathematical Theory of Elasticity of Quasicrystals and Its Applications*,
Springer Series in Materials Science 246, DOI 10.1007/978-981-10-1984-5_4

where $\oplus$ represents the direct sum. According to the explanation of physicists that $\mathbf{u}$ is in the physical space, or the parallel space $E_{\parallel}^{3}$; $\mathbf{w}$ in the complement space, or perpendicular space $E_{\perp}^{3}$, which is an internal space.

Furthermore, the two displacement vectors are dependent only upon the coordinate vector $\mathbf{r}^{\parallel}$ in physical space, i.e.

$$\mathbf{u} = \mathbf{u}(\mathbf{r}^{\parallel}), \quad \mathbf{w} = \mathbf{w}(\mathbf{r}^{\parallel}) \tag{4.1.2}$$

For simplicity, the superscript of $\mathbf{r}^{\parallel}$ will be removed hereafter. From the angle of mathematical theory of elasticity of quasicrystals and its technological applications, the formulas (4.1.1) and (4.1.2) are enough for understanding the following contents within Chaps. 1–15 of the book. If readers are interested in the further physical background on the phonon and phason fields in quasicrystals, we suggest that they could read the Appendix of this chapter (i.e. the Sect. 4.9).

With basic formulas (4.1.1) and (4.1.2) and some fundamental conservation laws well-known in physics, the macroscopic basis of the continuous medium model of elasticity of solid quasicrystals can be set up; in some extent, the discussion is an extension to that in Chap. 2, which will be done in the following sections.

4.2 Deformation Tensors

In Chap. 2, we introduced that the deformation of phonon field lies in the relative displacement (i.e. the rigid translation and rotation do not result in deformation), which can be expressed by

$$\mathrm{d}\mathbf{u} = \mathbf{u}' - \mathbf{u}$$

If we set up an orthogonal coordinate system (x_1, x_2, x_3) or (x, y, z), then we have $\mathbf{u} = (u_x, u_y, u_z) = (u_1, u_2, u_3)$ and

$$\mathrm{d}u_i = \frac{\partial u_i}{\partial x_j}\mathrm{d}x_j \tag{4.2.1}$$

in which $\partial u_i/\partial x_j$ has the meaning of the gradient of vector $\mathbf{u}$. In some publications, one denotes

$$\nabla\mathbf{u} = \frac{\partial u_i}{\partial x_j} = \begin{bmatrix} \frac{\partial u_x}{\partial x} & \frac{\partial u_x}{\partial y} & \frac{\partial u_x}{\partial z} \\ \frac{\partial u_y}{\partial x} & \frac{\partial u_y}{\partial y} & \frac{\partial u_y}{\partial z} \\ \frac{\partial u_z}{\partial x} & \frac{\partial u_y}{\partial y} & \frac{\partial u_y}{\partial z} \end{bmatrix} \tag{4.2.2}$$

and

$$\begin{bmatrix} \frac{\partial u_x}{\partial x} & \frac{\partial u_x}{\partial y} & \frac{\partial u_x}{\partial z} \\ \frac{\partial u_y}{\partial x} & \frac{\partial u_y}{\partial y} & \frac{\partial u_y}{\partial z} \\ \frac{\partial u_z}{\partial x} & \frac{\partial u_z}{\partial y} & \frac{\partial u_z}{\partial z} \end{bmatrix} = \begin{bmatrix} \frac{\partial u_x}{\partial x} & \frac{1}{2}\left(\frac{\partial u_x}{\partial y} + \frac{\partial u_y}{\partial x}\right) & \frac{1}{2}\left(\frac{\partial u_x}{\partial z} + \frac{\partial u_z}{\partial x}\right) \\ \frac{1}{2}\left(\frac{\partial u_x}{\partial y} + \frac{\partial u_y}{\partial x}\right) & \frac{\partial u_y}{\partial y} & \frac{1}{2}\left(\frac{\partial u_y}{\partial z} + \frac{\partial u_z}{\partial y}\right) \\ \frac{1}{2}\left(\frac{\partial u_x}{\partial z} + \frac{\partial u_z}{\partial x}\right) & \frac{1}{2}\left(\frac{\partial u_y}{\partial z} + \frac{\partial u_z}{\partial y}\right) & \frac{\partial u_z}{\partial z} \end{bmatrix}$$

$$+ \begin{bmatrix} 0 & -\frac{1}{2}\left(\frac{\partial u_y}{\partial x} - \frac{\partial u_x}{\partial y}\right) & -\frac{1}{2}\left(\frac{\partial u_z}{\partial x} - \frac{\partial u_x}{\partial z}\right) \\ -\frac{1}{2}\left(\frac{\partial u_x}{\partial y} - \frac{\partial u_y}{\partial x}\right) & 0 & -\frac{1}{2}\left(\frac{\partial u_z}{\partial y} - \frac{\partial u_y}{\partial z}\right) \\ -\frac{1}{2}\left(\frac{\partial u_x}{\partial z} - \frac{\partial u_z}{\partial x}\right) & -\frac{1}{2}\left(\frac{\partial u_y}{\partial z} - \frac{\partial u_z}{\partial y}\right) & 0 \end{bmatrix}$$

$$= \frac{1}{2}\left(\frac{\partial u_i}{\partial x_j} + \frac{\partial u_j}{\partial x_i}\right) - \frac{1}{2}\left(\frac{\partial u_j}{\partial x_i} - \frac{\partial u_i}{\partial x_j}\right) = \varepsilon_{ij} + \omega_{ij}$$

$$\varepsilon_{ij} = \frac{1}{2}\left(\frac{\partial u_i}{\partial x_j} + \frac{\partial u_j}{\partial x_i}\right) \tag{4.2.3}$$

$$\omega_{ij} = \frac{1}{2}\left(\frac{\partial u_i}{\partial x_j} - \frac{\partial u_j}{\partial x_i}\right) \tag{4.2.4}$$

which means the gradient of phonon vector $\mathbf{u}$ can be decomposed into two parts ε_{ij} and ω_{ij}, in which ε_{ij} has contribution to deformation energy, and ω_{ij} represents a kind of rigid rotations. We consider only ε_{ij}, which is phonon deformation tensor, called strain tensor, and a symmetric tensor: $\varepsilon_{ij} = \varepsilon_{ji}$.

Similarly for phason field, we have

$$\mathrm{d}w_i = \frac{\partial w_i}{\partial x_j}\mathrm{d}x_j \tag{4.2.5}$$

and

$$\nabla \mathbf{w} = \frac{\partial w_i}{\partial x_j} = \begin{bmatrix} \frac{\partial w_x}{\partial x} & \frac{\partial w_x}{\partial y} & \frac{\partial w_x}{\partial z} \\ \frac{\partial w_y}{\partial x} & \frac{\partial w_y}{\partial y} & \frac{\partial w_y}{\partial z} \\ \frac{\partial w_z}{\partial x} & \frac{\partial w_z}{\partial y} & \frac{\partial w_z}{\partial z} \end{bmatrix} \tag{4.2.6}$$

Though it can be decomposed into symmetric and asymmetric parts, all components $\frac{\partial w_i}{\partial x_j}$ contribute to the deformation of quasicrystals; the phason deformation tensor, or phason strain tensor, is defined by

$$w_{ij} = \frac{\partial w_i}{\partial x_j} \tag{4.2.7}$$

which describes the local rearrangement of atoms in a cell and is asymmetric tensor $w_{ij} \neq w_{ji}$.

The difference between ε_{ij} and w_{ij} given by (4.2.3) and (4.2.7) are originated from physical properties of phonon modes and phason modes. This can also be explained by group theory; i.e., they follow different irreducible representations for some symmetry transformations for most quasicrystal systems; except the three-dimensional cubic quasicrystal system, the detail about this is omitted here.

For the three-dimensional cubic quasicrystals, the phason modes exhibit the same behaviour like that of phonon modes, which will be particularly discussed in Chap. 9.

4.3 Stress Tensors and Equations of Motion

The gradient of displacement field **w** figures out the local rearrangement of atoms in a cell in quasicrystals. It needs external forces to drive the atoms through barriers when they make the local rearrangement in a cell. Such that, there are another kind of body forces and tractions apart from the conventional body forces **f** and tractions **T** for deformed quasicrystals, which are named the generalized body forces (density) **g** and generalized tractions (the generalized area forces density) **h**.

At first, we consider the static case.

Denoting the stress tensor corresponding to ε_{ij} by σ_{ij}, called the phonon stress tensor, and that to w_{ij} by H_{ij}, the phason stress tensor, we have the following equilibrium equations

$$\left.\begin{array}{l} \dfrac{\partial \sigma_{ij}}{\partial x_j} + f_i = 0 \\ \dfrac{\partial H_{ij}}{\partial x_j} + g_i = 0 \end{array}\right\} (x, y, z) \in \Omega \tag{4.3.1}$$

based on the momentum conservation law.

From the angular momentum conservation law to the phonon field

$$\frac{\mathrm{d}}{\mathrm{d}t}\int_{\Omega} \mathbf{r}^{\parallel} \times \rho \dot{\mathbf{u}} \mathrm{d}\Omega = \int_{\Omega} \mathbf{r}^{\parallel} \times \mathbf{f} \mathrm{d}\Omega + \int_{\Omega} \mathbf{r}^{\parallel} \times \mathbf{T} \mathrm{d}\Gamma \tag{4.3.2}$$

and by using the Gauss theorem, it follows that

$$\sigma_{ij} = \sigma_{ji} \tag{4.3.3}$$

This indicates that the phonon stress tensor is symmetric.

Since $\mathbf{r}^{\parallel}$ and $\mathbf{w}(\mathbf{g}, \mathbf{h})$ transform under different representations of the point groups, more precisely that, the former transform like a vector, but latter does not, the product representations: $\mathbf{r}^{\parallel} \times \mathbf{w}$, $\mathbf{r}^{\parallel} \times \mathbf{g}$ and $\mathbf{r}^{\parallel} \times \mathbf{h}$ do not contain any vector

representations. This implies that for the phason field, there is no equation analogous to (4.3.2), from which it follows that generally

$$H_{ij} \neq H_{ji} \tag{4.3.4}$$

The result holds for all quasicrystal systems except the case for three-dimensional cubic quasicrystals.

In dynamic case, the deformation process is quite complicated and there are different arguments. Lubensky et al. [5] claimed that phonon modes and phason modes are different based on their role in six-dimensional hydrodynamics; phonons are of wave propagation, while phasons are diffusive with very large diffusive time. Physically, the phason modes represent a relative motion of the constituent density waves. Dolinsek et al. [22, 23] further developed the point of view of Lubensky et al. and argued the atom flip or atom hopping concept for the phason dynamics. But according to Bak [1, 2], the phason describes particular structural disorders or structure fluctuations in quasicrystals, and it can be formulated based on a six-dimensional space description. Since there are six continuous symmetries, there exist six hydrodynamic vibration modes. In the following, we give a brief introduction on elastodynamics based on the Bak's argument as well as argument of Lubensky et al.

Ding et al. [26] and Hu et al. [16] derived that

$$\left.\begin{aligned} \frac{\partial \sigma_{ij}}{\partial x_j} + f_i &= \rho \frac{\partial^2 u_i}{\partial t^2} \\ \frac{\partial H_{ij}}{\partial x_j} + g_i &= \rho \frac{\partial^2 w_i}{\partial t^2} \end{aligned}\right\} (x, y, z) \in \Omega, \quad t > 0 \tag{4.3.5}$$

based on the momentum conservation law. We believe that the derivation is carried out by the Bak's argument, in which ρ is the mass density of quasicrystals.

In according to the argument of Lubensky et al., people cannot obtain (4.3.5), instead get

$$\left.\begin{aligned} \frac{\partial \sigma_{ij}}{\partial x_j} + f_i &= \rho \frac{\partial^2 u_i}{\partial t^2} \\ \frac{\partial H_{ij}}{\partial x_j} + g_i &= \kappa \frac{\partial w_i}{\partial t} \end{aligned}\right\} (x, y, z) \in \Omega, \quad t > 0 \tag{4.3.6}$$

in which $\kappa = 1/\Gamma_w$, and Γ_w is the kinetic coefficient of phason field. The equations are given by Fan et al. [27], and Rochal and Norman [28], which are identical to those given by Lubensky et al. [5] for linear case and omitting fluid velocity field. Lubensky et al. gave their hydrodynamics formulation based on Landau symmetry-breaking principle, so Eq. (4.3.6) may be seen as elasto-/hydrodynamic equation of quasicrystals. In particular, the second equation of (4.3.6) presents the dissipation

feature of motion of phason degrees in dynamic process, and it is irreversible thermodynamically.

The dynamics of quasicrystals faces a great challenge (see, e.g. [28–30]); we discuss it in Chaps. 10 and 16 in the text and Appendix C in the Major Appendix in detail.

4.4 Free Energy Density and Elastic Constants

Consider the free energy density or the strain energy density of a quasicrystal $F(\varepsilon_{ij}, w_{ij})$ whose general expression is difficult to obtain. We take a Taylor expansion in the neighbourhood of $\varepsilon_{ij} = 0$ and $w_{ij} = 0$ and remain up to the second-order term, then

$$\begin{aligned} F(\varepsilon_{ij}, w_{ij}) &= \frac{1}{2}\left[\frac{\partial^2 F}{\partial\varepsilon_{ij}\partial\varepsilon_{kl}}\right]_0 \varepsilon_{ij}\varepsilon_{kl} + \frac{1}{2}\left[\frac{\partial^2 F}{\partial\varepsilon_{ij}\partial w_{kl}}\right]_0 \varepsilon_{ij} w_{kl} + \frac{1}{2}\left[\frac{\partial^2 F}{\partial w_{ij}\partial w_{kl}}\right]_0 w_{ij} w_{kl} \\ &\quad + \frac{1}{2}\left[\frac{\partial^2 F}{\partial w_{ij}\partial\varepsilon_{kl}}\right]_0 w_{ij}\varepsilon_{kl} = \frac{1}{2}C_{ijkl}\varepsilon_{ij}\varepsilon_{kl} + \frac{1}{2}R_{ijkl}\varepsilon_{ij} w_{kl} + \frac{1}{2}K_{ijkl} w_{ij} w_{kl} + \frac{1}{2}R'_{ijkl} w_{ij}\varepsilon_{kl} \\ &= F_u + F_w + F_{uw} \end{aligned} \tag{4.4.1}$$

where F_u, F_w and F_{uw} denote the parts contributed by phonon, phason and phonon-phason coupling, respectively, and

$$C_{ijkl} = \left[\frac{\partial^2 F}{\partial\varepsilon_{ij}\partial\varepsilon_{kl}}\right]_0 \tag{4.4.2}$$

is the phonon elastic constant tensor, discussed in Chap. 2 already, and

$$C_{ijkl} = C_{klij} = C_{jikl} = C_{ijlk} \tag{4.4.3}$$

The tensor can be expressed by a symmetric matrix

$$[C]_{9\times 9}$$

In (4.4.1), another elastic constant tensor

$$K_{ijkl} = \left[\frac{\partial^2 F}{\partial w_{ij}\partial w_{kl}}\right]_0 \tag{4.4.4}$$

in which, the suffixes j, l belong to space $E_{\parallel}^3$, and i, k to space $E_{\perp}^3$, and

$$K_{ijkl} = K_{klij} \tag{4.4.5}$$

All components of K_{ijkl} can also be expressed by symmetric matrix

$$[K]_{9\times 9}$$

In addition,

$$R_{ijkl} = \left[\frac{\partial^2 F}{\partial \varepsilon_{ij}\partial w_{kl}}\right]_0 \tag{4.4.6}$$

$$R'_{ijkl} = \left[\frac{\partial^2 F}{\partial w_{ij}\partial \varepsilon_{kl}}\right]_0 \tag{4.4.7}$$

are the elastic constants of phonon-phason coupling, to be noted that the suffixes i, j, l belong to space $E_{\parallel}^3$ and k belongs to space $E_{\perp}^3$, and

$$R_{ijkl} = R_{jikl}, \quad R'_{ijkl} = R_{klij}, \quad R'_{klij} = R_{ijkl} \tag{4.4.8}$$

but

$$R_{ijkl} \neq R_{klij}, \quad R'_{ijkl} \neq R'_{klij} \tag{4.4.9}$$

all components of which can be expressed in symmetric matrixes

$$[R]_{9\times 9}, \quad [R']_{9\times 9}$$

and

$$[R]^{\mathrm{T}} = [R'] \tag{4.4.10}$$

where T denotes the transpose operator. The composition of four matrixes $[C], [K], [R]$ and $[R']$ forms a matrix with 18×18

$$[C, K, R] = \begin{bmatrix} [C] & [R] \\ [R'] & [K] \end{bmatrix} = \begin{bmatrix} [C] & [R] \\ [R]^T & [K] \end{bmatrix} \tag{4.4.11}$$

If the strain tensor is expressed by a row vector with 18 elements, i.e.

$$\left[\varepsilon_{ij}, w_{ij}\right] = \begin{bmatrix} \varepsilon_{11}, \varepsilon_{22}, \varepsilon_{33}, \varepsilon_{23}, \varepsilon_{31}, \varepsilon_{12}, \varepsilon_{32}, \varepsilon_{13}, \varepsilon_{21}, \\ w_{11}, w_{22}, w_{33}, w_{23}, w_{31}, w_{12}, w_{32}, w_{13}, w_{21} \end{bmatrix} \tag{4.4.12}$$

then the transpose of which denotes the array vector, then the free energy density (or strain energy density) may be expressed by

$$F = \frac{1}{2}\left[\varepsilon_{ij}, w_{ij}\right]\begin{bmatrix}[C] & [R]\\ [R]^{\mathrm{T}} & [K]\end{bmatrix}\left[\varepsilon_{ij}, w_{ij}\right]^{\mathrm{T}} \tag{4.4.13}$$

which is identical to that given by (4.4.1).

4.5 Generalized Hooke's Law

For application of theory of elasticity of quasicrytals to any science or engineering problem, one must determine the displacement field and stress field, this requires that we need to set up relationship between strains and stresses, the relations are called the generalized Hooke's law of quasicrystalline material. From the free energy density (4.4.1) or (4.4.13), we have

$$\begin{aligned}\sigma_{ij} &= \frac{\partial F}{\partial \varepsilon_{ij}} = C_{ijkl}\varepsilon_{kl} + R_{ijkl}w_{kl}\\ H_{ij} &= \frac{\partial F}{\partial w_{ij}} = K_{ijkl}w_{kl} + R_{klij}\varepsilon_{kl}\end{aligned} \tag{4.5.1}$$

or in the form of matrixes

$$\begin{bmatrix}\sigma_{ij}\\ H_{ij}\end{bmatrix} = \begin{bmatrix}[C] & [R]\\ [R]^{\mathrm{T}} & [K]\end{bmatrix}\begin{bmatrix}\varepsilon_{ij}\\ w_{ij}\end{bmatrix} \tag{4.5.2}$$

where

$$\begin{aligned}\begin{bmatrix}\sigma_{ij}\\ H_{ij}\end{bmatrix} &= \left[\sigma_{ij}, H_{ij}\right]^{\mathrm{T}}\\ \begin{bmatrix}\varepsilon_{ij}\\ w_{ij}\end{bmatrix} &= \left[\varepsilon_{ij}, w_{ij}\right]^{\mathrm{T}}\end{aligned} \tag{4.5.3}$$

4.6 Boundary Conditions and Initial Conditions

The above general formulas give a description of the basic law of elasticity of quasicrystals and provide a key to solve those problems in the application for academic research and engineering practice; the formulas hold in any interior of the body, i.e. $(x, y, z) \in \Omega$ where (x, y, z) denote the coordinates of any point of the

interior, and Ω the body. The formulas are concluded as some partial differential equations; to solve them, it is necessary to know the situation of the field variables at the boundary S of Ω; without appropriate information at the boundary, the solution has no any physical meaning. According to practical case, the boundary S consists of two parts S_t and S_u, i.e. $S = S_t + S_u$, at S_t, the tractions are given, and at S_u, the displacements are prescribed. For the former case

$$\left.\begin{aligned} \sigma_{ij} n_j &= T_i \\ H_{ij} n_j &= h_i \end{aligned}\right\} (x, y, z) \in S_t \tag{4.6.1}$$

where n_j represents the unit outward normal vector at any point at S, and T_i and h_i represent the traction and generalized traction vectors, which are given functions at the boundary. Formula (4.6.1) is called the stress boundary conditions. And for the latter case

$$\left.\begin{aligned} u_i &= \bar{u}_i \\ w_i &= \bar{w}_i \end{aligned}\right\} (x, y, z) \in S_u \tag{4.6.2}$$

where $\bar{u}_i$ and $\bar{w}_i$ are known functions at the boundary. Formula (4.6.2) is named the displacement boundary conditions.

If $S = S_t$ (i.e. $S_u = 0$), the problem for solving Eqs. (4.2.3), (4.2.7), (4.3.1) and (4.5.1) under boundary conditions (4.6.1) is called stress boundary value problem. While $S = S_u$ (i.e. $S_t = 0$), the problem for solving Eqs. (4.2.3), (4.2.7), (4.3.1) and (4.5.1) under boundary conditions (4.6.2) is called displacement boundary value problem.

If $S = S_u + S_t$ and both $S_t \neq 0, S_u \neq 0$, the problem for solving Eqs. (4.2.3), (4.2.7), (4.3.1) and (4.5.1) under boundary conditions (4.6.1) and (4.6.2) is called mixed boundary value problem.

For dynamic problem, if taking wave equations (4.3.5) together with (4.2.3), (4.2.7) and (4.5.1), besides boundary conditions (4.6.1) and (4.6.2), we must give relevant initial value conditions, i.e.

$$\left.\begin{aligned} u_i(x, y, z, 0) &= u_{i0}(x, y, z), \dot{u}_i(x, y, z, 0) = \dot{u}_{i0}(x, y, z) \\ w_i(x, y, z, 0) &= w_{i0}(x, y, z), \dot{w}_i(x, y, z, 0) = \dot{w}_{i0}(x, y, z) \end{aligned}\right\} (x, y, z) \in \Omega \tag{4.6.3}$$

in which $u_{i0}(x, y, z, 0)$, $\dot{u}_{i0}(x, y, z, 0)$,$w_{i0}(x, y, z, 0)$ and $\dot{w}_{i0}(x, y, z, 0)$ are known functions and $\dot{u}_i = \frac{\partial u_i}{\partial t}$. In this case, the problem is called initial-boundary value problem.

But if taking wave equations coupling diffusion equations (4.3.6) together with (4.2.3) and (4.5.1), then the initial value conditions will be

$$\left.\begin{array}{l} u_i(x,y,z,0) = u_{i0}(x,y,z), \dot{u}_i(x,y,z,0) = \dot{u}_{i0}(x,y,z) \\ w_i(x,y,z,0) = w_{i0}(x,y,z) \end{array}\right\} (x,y,z) \in \Omega \qquad (4.6.4)$$

This is also called initial-boundary value problem, but different from the previous one.

4.7 A Brief Introduction on Relevant Material Constants of Solid Quasicrystals

In above discussion, we find that the solid quasicrystals present different nature with those of crystals. Connection with this, the material constants of the solid should be different from those of crystals and other conventional structural materials, in which the constants appearing in the above basic equations are interesting at least. We here give a brief introduction to help readers in conceptional point of view. The detailed introduction will be given in Chaps. 6, 9 and 10.

The measurement of material constants of quasicrystals is difficult, but the experimental technique is progressed, especially in recent years. Due to the majority of icosahedral and decagonal quasicrystals in the material, the measured data are most for these two kinds of the solid phase.

For icosahedral quasicrystals, the independent nonzero components of phonon elastic constants C_{ij} are only λ and μ, phason elastic contants K_{ij} only K_1 and K_2 and phonon-phason coupling elastic constants R_{ij} only R. For the most important icosahedral Al–Pd–Mn quasicrystal, the measured data including the mass density and dissipation coefficient of phonon and phason are as follows [31, 32], respectively:

$$\begin{aligned} &\rho = 5.1\ \text{g/cm}^3, \quad \lambda = 74.9, \quad \mu = 72.4\ \text{GPa}, \quad K_1 = 72, \\ &K_2 = -37\ \text{MPa}, \quad R \approx 0.01\ \mu, \\ &\Gamma_u = 4.8 \times 10^{-17}\ \text{m}^3\ \text{s/kg} = 4.8 \times 10^{-8}\ \text{cm}^3\ \mu\text{s/g}, \\ &\Gamma_w = 4.8 \times 10^{-19}\ \text{m}^3\ \text{s/kg} = 4.8 \times 10^{-10}\ \text{cm}^3\ \mu\text{s/g}, \end{aligned}$$

and for two-dimensional quasicrystals, the independent nonzero components of the phonon elastic constants are only $C_{11}, C_{33}, C_{44}, C_{12}, C_{13}$ and $C_{66} = (C_{11} - C_{12})/2$, the phason ones only K_1, K_2, K_3 and the phonon-phason coupling ones only R_1, R_2. For decagonal Al–Ni–Co quasicrystal, the measured data are [31], respectively:

$$\begin{aligned} &\rho = 4.186\ \text{g/cm}^3, \quad C_{11} = 234.3, \quad C_{33} = 232.22, \quad C_{44} = 70.19, \\ &C_{12} = 57.41, \quad C_{13} = 66.63\ \text{GPa} \end{aligned}$$

$$R_1 = -1.1, |R_2| < 0.2\ \text{GPa}.$$

and there are no measured data for K_1, K_2 (but we can use those obtained by the Monte Carlo simulation), Γ_u and Γ_w can approximately be taken the value of icosahedral quasicrystal. In addition, the tensile strength $\sigma_c = 450$ MPa for decagonal Al–Cu–Co quasicrystals before annealing and $\sigma_c = 550$ MPa after annealing. The hardness for decagonal Al–Cu–Co quasicrystals is 4.10 GPa [33, 34], the fracture toughness of which is $1.0-1.2$ MPa$\sqrt{\text{m}}$ [33].

With these basic data, the computation for stress analysis for statics and dynamics can be undertaken.

4.8 Summary and Mathematical Solvability of Boundary Value or Initial-Boundary Value Problem

For static equilibrium problem, the mathematical formulation is

$$\frac{\partial \sigma_{ij}}{\partial x_j} + f_i = 0, \quad \frac{\partial H_{ij}}{\partial x_j} + h_i = 0, \quad x_i \in \Omega \tag{4.8.1}$$

$$\varepsilon_{ij} = \frac{1}{2}\left(\frac{\partial u_i}{\partial x_j} + \frac{\partial u_j}{\partial x_i}\right), \quad w_{ij} = \frac{\partial w_i}{\partial x_j}, \quad x_i \in \Omega \tag{4.8.2}$$

$$\left.\begin{aligned} \sigma_{ij} &= C_{ijkl}\varepsilon_{kl} + R_{ijkl}w_{kl} \\ H_{ij} &= K_{ijkl}w_{kl} + R_{klij}\varepsilon_{kl} \end{aligned}\right\}, \quad x_i \in \Omega \tag{4.8.3}$$

$$\sigma_{ij}n_j = T_i, \quad H_{ij}n_j = h_i, \quad x_i \in S_t \tag{4.8.4}$$

$$u_i = \bar{u}_i, \quad w_i = \bar{w}_i, \quad x_i \in S_u \tag{4.8.5}$$

For dynamic problem, based on the Bak's argument, the mathematical formulation is

$$\frac{\partial \sigma_{ij}}{\partial x_j} + f_i = \rho\frac{\partial^2 u_i}{\partial t^2}, \quad \frac{\partial H_{ij}}{\partial x_j} + g_i = \rho\frac{\partial^2 w_i}{\partial t^2}, \quad x_i \in \Omega, \quad t > 0 \tag{4.8.6}$$

$$\varepsilon_{ij} = \frac{1}{2}\left(\frac{\partial u_i}{\partial x_j} + \frac{\partial u_j}{\partial x_i}\right), \quad w_{ij} = \frac{\partial w_i}{\partial x_j}, \quad x_i \in \Omega, \quad t > 0 \tag{4.8.7}$$

$$\left.\begin{aligned} \sigma_{ij} &= C_{ijkl}\varepsilon_{kl} + R_{ijkl}w_{kl} \\ H_{ij} &= K_{ijkl}w_{kl} + R_{klij}\varepsilon_{kl} \end{aligned}\right\}, x_i \in \Omega, \quad t > 0 \tag{4.8.8}$$

$$\sigma_{ij}n_j = T_i, \quad H_{ij}n_j = h_i, \quad x_i \in S_t, \quad t > 0 \tag{4.8.9}$$

$$u_i = \bar{u}_i, \quad w_i = \bar{w}_i, \quad x_i \in S_u, \quad t > 0 \tag{4.8.10}$$

$$u_i|_{t=0} = u_{i0}, \quad \dot{u}_i|_{t=0} = \dot{u}_{i0}, \quad w_i|_{t=0} = w_{i0}, \quad \dot{w}_i|_{t=0} = \dot{w}_{i0}, \quad x_i \in \Omega \tag{4.8.11}$$

For dynamic problem, based on the argument of Lubensky et al., the mathematical formulation is

$$\frac{\partial \sigma_{ij}}{\partial x_j} + f_i = \rho \frac{\partial^2 u_i}{\partial t^2}, \quad \frac{\partial H_{ij}}{\partial x_j} + h_i = \kappa \frac{\partial w_i}{\partial t}, \quad \kappa = \frac{1}{\Gamma_w}, \quad x_i \in \Omega, \quad t > 0 \tag{4.8.12}$$

$$\varepsilon_{ij} = \frac{1}{2}\left(\frac{\partial u_i}{\partial x_j} + \frac{\partial u_j}{\partial x_i}\right), \quad w_{ij} = \frac{\partial w_i}{\partial x_j}, \quad x_i \in \Omega, \quad t > 0 \tag{4.8.13}$$

$$\left.\begin{aligned} \sigma_{ij} &= C_{ijkl}\varepsilon_{kl} + R_{ijkl}w_{kl} \\ H_{ij} &= K_{ijkl}w_{kl} + R_{klij}\varepsilon_{kl} \end{aligned}\right\}, x_i \in \Omega, \quad t > 0 \tag{4.8.14}$$

$$\sigma_{ij}n_j = T_i, \quad H_{ij}n_j = h_i, \quad x_i \in S_t, \quad t > 0 \tag{4.8.15}$$

$$u_i = \bar{u}_i, \quad w_i = \bar{w}_i, \quad x_i \in S_u, \quad t > 0 \tag{4.8.16}$$

$$u_i|_{t=0} = u_{i0}, \quad \dot{u}_i|_{t=0} = \dot{u}_{i0}, \quad w_i|_{t=0} = w_{i0}, \quad x_i \in \Omega \tag{4.8.17}$$

The solution satisfying all equations and corresponding initial conditions and boundary conditions is just the realistic solution of elasticity of quasicrystals mathematically and has physical meaning.

The existence and uniqueness of solutions of elasticity of quasicrystals will further be discussed in Chap. 13.

4.9 Appendix of Chapter 4: Description on Physical Basis of Elasticity of Quasicrystals Based on the Landau Density Wave Theory

In Sect. 4.1, we gave the formula (4.1.1) as the physical basis of elasticity of quasicrystals and did not discuss its profound physical source, because the discussion is concerned with quite complicated background, which is not the most necessary for a beginner before reading Sects. 4.2–4.8. At this point, it is advantageous to study physical background. The reader is advised to read Sect. 1.5 (the Appendix of Chap. 1) first.

Chapter 3 shows quasicrystals which belong to subject of condensed matter physics rather than traditional solid state physics, though the former is evolved from the latter. In the development, the symmetry-breaking (or broken symmetry) forms the core concept and principle of the condensed matter physics. According to the

understanding of physicists, the Landau density wave description on the elasticity of quasicrystals is a natural choice, though there are some other descriptions, e.g. the unit-cell description based on the Penrose tiling. Now, the difficulty lies in that the workers in other disciplines are not so familiar with the Landau theory and the relevant topics. For this reason, we have introduced the Landau theory in the Appendix of Chap. 1 (i.e. the Sect. 1.5, in which the concept on incommensurate crystals is also introduced in brief, which will be concerned though it is not related to Landau theory) and the Penrose tiling in Sect. 3.1. These important physical and mathematical results can help us to understand the elasticity of quasicrystals.

Immediately after the discovery of quasicrystals, Bak [1] published the theory of elasticity in which he used the three important results in physics and mathematics mentioned above, but the core is the Landau theory on elementary excitation and symmetry-breaking of condensed matter. Bak [1, 2] pointed out too, ideally, one would like to explain the structure from first-principle calculations taking into account the actual electronic properties of constituent atoms. Such a calculation is hardly possible to date. So he suggested that the Landau's phenomenological theory [3] on structural transition can be used; i.e., the condensed phase is described by a symmetry-breaking order parameter which transforms as an irreducible representation of the symmetry group of a liquid with full translational and rotational symmetry. According to the Landau theory, the order parameter of quasicrystals is the wave vector (more exactly speaking, the amplitude of the quantity) of expansion of density wave in reciprocal lattice. The density of the ordered, low-temperature, d-dimensional quasicrystal can be expressed as a Fourier series by extended formula (1.5.5) (the expansion exists due to the periodicity in lattice or reciprocal lattice of higher dimensional space)

$$\rho(\mathbf{r}) = \sum_{\mathbf{G}\in L_R} \rho_{\mathbf{G}} \exp\{i\mathbf{G}\cdot\mathbf{r}\} = \sum_{\mathbf{G}\in L_R} |\rho_{\mathbf{G}}| \exp\{-i\Phi_{\mathbf{G}} + i\mathbf{G}\cdot\mathbf{r}\} \tag{4.9.1}$$

where $\mathbf{G}$ is a reciprocal vector, and L_R is the reciprocal lattice (the concepts on the reciprocal vector and reciprocal lattice, referring to Chap. 1); $\rho_{\mathbf{G}}$ is a complex number

$$\rho_{\mathbf{G}} = |\rho_{\mathbf{G}}| \mathrm{e}^{-i\Phi_{\mathbf{G}}} \tag{4.9.2}$$

with an amplitude $|\rho_{\mathbf{G}}|$ and phase angle $\Phi_{\mathbf{G}}$, due to $\rho(r)$ being real, $|\rho_{\mathbf{G}}| = |\rho_{-\mathbf{G}}|$ and $\Phi_{\mathbf{G}} = -\Phi_{-\mathbf{G}}$.

There exists a set of N base vectors, $\{\mathbf{G}_n\}$, so that each $\mathbf{G} \in L_R$ can be written as $\sum m_n \mathbf{G}_n$ for integers m_n. Furthermore, $N = kd$, where k is the number of the mutually incommensurate vectors in the d-dimensional quasicrystal. In general, $k = 2$. A convenient parametrization of the phase angle is given by

$$\Phi_n = \mathbf{G}_n^{\parallel} \cdot \mathbf{u} + \mathbf{G}_n^{\perp} \cdot \mathbf{w} \tag{4.9.3}$$

in which $\mathbf{u}$ can be understood similar to the phonon like that in conventional crystals, while $\mathbf{w}$ can be understood as the phason degrees of freedom in quasicrystals, which describe the local rearrangement of unit-cell description based on the Penrose tiling. Both are functions of the position vector in the physical space only, where $\mathbf{G}_n^{\parallel}$ is the reciprocal vector in the physical space $E_{\parallel}^3$ just mentioned and $\mathbf{G}_n^{\perp}$ is the conjugate vector in the perpendicular space $E_{\perp}^3$. People can realize that the above-mentioned Bak's hypothesis is a natural development of Anderson's theory introduced in Sect. 1.5.

Almost in the same time, Levine et al. [4], Lubensky et al. [5–8], Kalugin et al. [9], Torian and Mermin [10], Jaric [11], Duneau and Katz [12], Socolar et al. [13] and Gahler and Phyner [14] carried out the study on elasticity of quasicrystals. Though the researchers studied the elasticity from different descriptions, the unit-cell description based on the Penrose tiling is adopted too, but the density wave description based on the Laudau phenomenological theory on symmetry-breaking of condensed matter has played the central role and been widely acknowledged. This means there are two elementary excitations of low energy, phonon $\mathbf{u}$ and phason $\mathbf{w}$ for quasicrystals, in which vector $\mathbf{u}$ is in the parallel space $E_{\parallel}^3$ and vector $\mathbf{w}$ is in the perpendicular space $E_{\perp}^3$, respectively. So that total displacement field for quasicrystals is

$$\bar{\mathbf{u}} = \mathbf{u}^{\parallel} \oplus \mathbf{u}^{\perp} = \mathbf{u} \oplus \mathbf{w}$$

which is the formula (4.1.1), where $\oplus$ represents the direct sum.

According to the argument of Bak et al.,

$$\mathbf{u} = \mathbf{u}(\mathbf{r}^{\parallel}), \quad \mathbf{w} = \mathbf{w}(\mathbf{r}^{\parallel})$$

i.e. $\mathbf{u}$ and $\mathbf{w}$ depend upon special radius vector $\mathbf{r}^{\parallel}$ in parallel space $E_{\parallel}^3$ only, that is formula (4.1.2). For simplicity, the superscript of $\mathbf{r}^{\parallel}$ is removed in the presentation in Sects. 4.2–4.8.

Even if introducing $\mathbf{u}$ and $\mathbf{w}$ by such a way, the concept of phason is hard to be accepted by some readers. We would like to give some additional explanation in terms of projection concept as below.

We previously said that the quasicrystal in three-dimensional space may be seen as a projection of periodic structure in higher dimensional space. For example, one-dimensional quasicrystals in physical space may be seen as a projection of "periodic crystals" in four-dimensional space, while in the one-dimensional quasicrystals, the atom arrangement is quasiperiodic only in one direction, say z-axis direction, and periodic in other two directions. The atom arrangement quasiperiodic axis may be seen as a projection of two-dimensional periodic crystal as shown in Fig. 4.1a, in which dots form the two-dimensional, e.g. right square crystal, and lines with slop of irrational numbers can correspond to quasiperiodic structures (by contrast, if the slope is rational number, it corresponds to the periodic structure). For

this purpose, we can use the so-called Fibonacci sequence formed by a longer segment L and a shorter segment S according to the recurrence (whose geometry depiction is shown in Fig. 4.1b)

$$F_{n+1} = F_n + F_{n-1}$$

and

$$\begin{aligned} F_0 &: S \\ F_1 &: L \\ F_2 &: LS \\ F_3 &: LSL \\ F_4 &: LSLLS \end{aligned}$$

The geometric expression of the sequence can be shown in the axis E_1 i.e.$E_{\|}$ in Fig. 4.1a, and $E_{\|}$ is the so-called parallel space and that perpendicular to which is

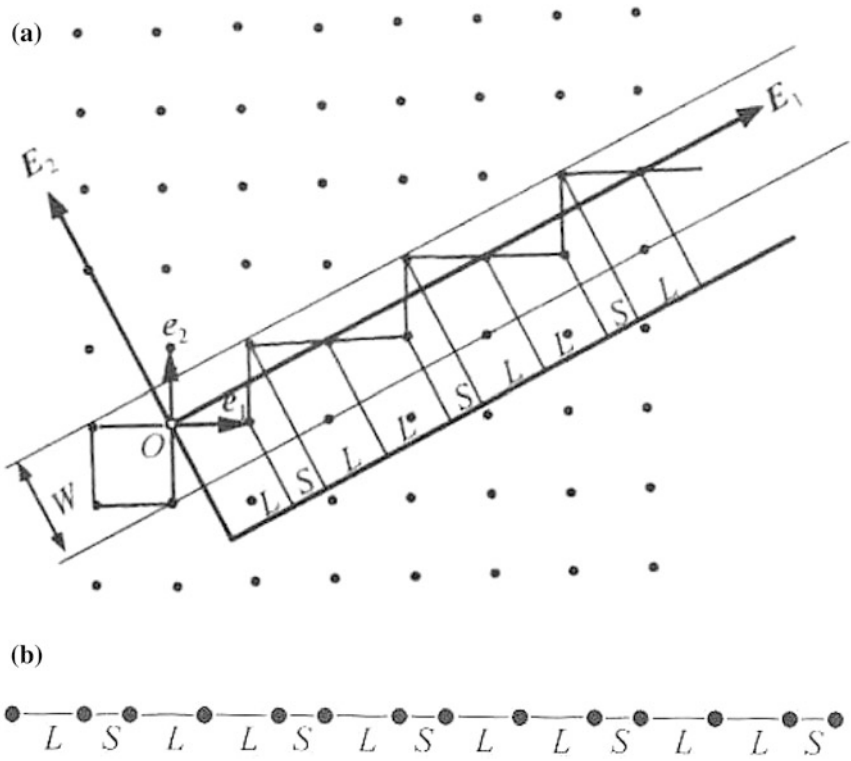

Fig. 4.1 A geometrical representation for one-dimensional quasiperiodic structure. **a** A projection of two-dimensional crystal can generate a one-dimensional quasiperiodic structure, **b** the Fibonacci sequence

the so-called vertical space E_2, i.e. $E_\perp$. The Fibonacci sequence is a useful tool to describe the geometry of one-dimensional quasiperiodic structure, like that the Penrose tiling to describe the geometry of two- and three-dimensional quasicrystals. Fig. 4.1 helps us to understand the internal space $E_\perp$. For one-dimensional quasicrystals, the figure can give an explicit description, while for two- and three-dimensional quasicrystals, there is no such an explicit graph.

Since quasicrystals belong to one of incommensurate phases, there are phason modes in the incommensurate crystals, denoted by $\mathbf{w}(\mathbf{r}^{\parallel})$, which may understood as the corresponding new displacement field; if people have knowledge on incommensurate phases, then they may easily understand the origin of phason modes in quasicrystal, though conventional incommensurate crystals are not certainly the actual quasicrystals.

The phonon variables $\mathbf{u}(\mathbf{r}^{\parallel})$ appears in the physical space $E_{\parallel}^3$, vector $\mathbf{u}$ represents the displacement of lattice point deviated from its equilibrium position due to the vibration of the lattice, and the propagation of this vibration is sound waves in solids. Though vibration is a mechanical motion, which can be quantized, the quanta of this motion are named phonon. So the $\mathbf{u}$ field is called phonon field in physical terminology. The gradient of the $\mathbf{u}$ field characterizes the changes in volume and in shape of cells—this is identical to that in the classical elasticity (see, e.g. Chap. 2, and previous sections of this chapter).

As mentioned before, the phason variables are substantively related with structural transitions of alloys, some among which can be observed from the characteristics of diffraction patterns. Lubensky et al. [5, 7] and Horn et al. [15] discussed the connection between the phenomena and phason strain. These profound observations could not be discussed here; readers can refer to the review given by Hu et al. [16]. This makes us know that the phason modes exist truly. The physical meaning of phason variables can be explained as a quantity to describe the local rearrangement of atoms in a cell. We know that the phase transition in crystalline materials is just arisen by the atomic local rearrangement. The unit-cell description on quasicrystals mentioned above predicts that $\mathbf{w}$ describes the local arrangement of Penrose titling. These findings may help us to understand the meaning of the unusual field variables. After the experimental investigations by neutron scattering [17–20], by Moessbauer spectroscopy [21], by NMR (Nuclear Magnetic Resonance) [22, 23] and by specific heat measurements [24, 25], the concept of thermal-induced phason flips is suggested, and this is identical to the diffusive essentiality of phasons, but note that the so-called diffusion here is quite different from that appeared in metallic periodic crystals (which mainly results from the presence of vacancies in the lattice, which is related with dissipation of phonons, and has been discussed by Lubensky et al. [5] in hydrodynamics of icosahedral quasicrystals), which will be concerned simply in Chaps. 10 and 16.

We must point out that vector $\mathbf{u}$ and vector $\mathbf{w}$ present different behaviour under some symmetry operations. This can be explained by group theory; the discussion is omitted here.

References

1. Bak P, 1985, Phenomenological theory of icosahedral incommensurate ("quaisiperiodic") order in Mn-Al alloys, *Phys. Rev. Lett*., **54**(8), 1517–1519.
2. Bak P, 1985, Symmetry, stability and elastic properties of icosahedral incommensurate crystals, *Phys. Rev*. B, **32**(9), 5764–5772.
3. Landau L D and Lifshitz E M, 1980, *Theoretical Physics V*: *Statistical Physics*, 3rd ed. Pregamen Press, New York.
4. Levine D, Lubensky T C, Ostlund S, Ramaswamy S, Steinhardt P J and Toner J, 1985, Elasticity and dislocations in pentagonal and icosahedral quasicrystals, *Phys. Rev. Lett*., **54**(8), 1520–1523.
5. Lubensky T C, Ramaswamy S and Toner J,1985, Hydrodynamics of icosahedral quasicrystals, *Phys. Rev*. B, **32**(11), 7444–7452.
6. Lubensky T C, Ramaswamy S and Toner J, 1986, Dislocation motion in quasicrystals and implications for macroscopic properties, *Phys. Rev*. B, **33**(11), 7715–7719.
7. Lubensky T C, Socolar J E S, Steinhardt P J, Bancel P A and Heiney P A, 1986, Distortion and peak broadening in quasicrystal diffraction patterns, *Phys. Rev. Lett*., **57**(12), 1440–1443.
8. Lubensky T C, 1988, *Introduction to Quasicrystals*, ed by Jaric M V, Boston: Academic Press
9. Kalugin P A, Kitaev A and Levitov L S, 1985, 6-dimensional properties of $Al_{0.86}Mn_{0.14}$alloy, *J. Phys. Lett*., **46**(13), 601–607.
10. Torian S M and Mermin D,1985, Mean-field theory of quasicrystalline order, *Phys. Rev. Lett*., **54**(14), 1524–1527.
11. Jaric M V, 1985, Long-range icosahedral orientational order and quasicrystals, *Phys.Rev. Lett.*, **55**(6), 607–610.
12. Duneau M and Katz A, 1985, Quasiperiodic patterns, *Phys. Rev. Lett.*, **54**(25), 2688–2691.
13. Socolar J E S, Lubensky T C and Steinhardt P J, 1986, Phonons, phasons, and dislocations in quasicrystals, *Phys. Rev*. B, **34**(5), 3345–3360.
14. Gahler F and Rhyner J, 1986, Equivalence of the generalised grid and projection methods for the construction of quasiperiodic tilings, *J. Phys. A: Math. Gen*. **19**(2), 267–277.
15. Horn P M, Melzfeldt W, Di Vincenzo D P, Toner J and Gambine R, 1986,Systematics of disorder in quasiperiodic material, *Phys. Rev. Lett*., **57**(12), 1444–1447.
16. Hu C Z, Wang R H and Ding D H, 2000, Symmetry groups, physical property tensors, elasticity and dislocations in quasicrystals, *Rep. Prog. Phys*., **63**(1), 1–39.
17. Coddens G, Bellissent R, Calvayrac Y et al, 1991, Evidence for phason hopping in icosahedral AlFeCu quasi-crystals, *Europhys. Lett*., **16**(3), 271–276.
18. Coddens G and Sturer W, 1999, Time-of-flight neutron-scattering study of phason hopping in decagonal Al-Co-Ni quasicrystals, *Phys. Rev.* **B, 60**(1), 270–276.
19. Coddens G, Lyonnard S, Hennion B et al, 2000, Triple-axis neutron-scattering study of phason dynamics in Al-Mn-Pd quasicrystals, *Phys. Rev.* B, **62**(10), 6268–6295.
20. Coddens G, Lyonnard S, Calvayrac Y et al, 1996, Atomic (phason) hopping in perfect icosahedral quasicrystals Al70.3Pd21.4Mn8.3 by time-of-flight quasielastic neutron scattering, *Phys. Rev.* B**, 53**(6), 3150–3160.
21. Coddens G, Lyonnard S, Sepilo B et al, 1995, **E**vidence for atomic hopping of Fe in perfectly icosahedral AlFeCu quasicrystals by^{57}Fe Moessbauer spectroscopy, *J. Phys.*, **5(7)**, 771–776.
22. Dolisek J, Ambrosini B, Vonlanthen P et al, 1998, Atomic motion in quasicrystalline $Al_{70}Re_{8.6}Pd_{21.4}$: A two-dimensional exchange NMR study, *Phys. Rev. Lett.*, **81**(17), 3671–3674.
23. Dolisek J, Apih T, Simsic M et al,1999, Self-diffusion in icosahedral $Al_{72.4}Pd_{20.5}Mn_{7.1}$ and phason percolation at low temperatures studied by ^{27}Al NMR, *Phys. Rev. Lett.,* **82**(3), 572–575.
24. Edagawa K and Kajiyama K, 2000, High temperature specific heat of Al-Pd-Mn and Al-Cu-Co quasicrystals, *Mater. Sci. and Eng.* **A**, **294–296**(5), 646-649.

25. Edagawa K, Kajiyama K and Tamura R et al, 2001, High-temperature specific heat of quasicrystals and a crystal approximant, *Mater. Sci. and Eng.* **A**, **312**(1–2), 293-298.
26. Ding D H, Yang W G, Hu C Z et al, 1993, Generalized elasticity theory of quasicrystals, *Phys. Rev*. B, **48**(10), 7003–7010.
27. Fan T Y, Wang X F, Li W and Zhu A Y, 2009, Elasto-hydrodynamics of quasicrystals, *Phil. Mag*. **89**(6), 501–512.
28. Rochal S B and Lorman V L, 2002, Minimal model of the phonon-phason dynamics on icosahedral quasicrystals and its application for the problem of internal friction in the i-AIPdMn alloys, *Phys. Rev*. B, **66** (14), 144204.
29. Francoual S, Levit F, de Boussieu M et al, 2003, Dynamics of phason fluctuations in the *i*–Al-Pd-Mn quasicrystals, *Phys. Rev. Lette*., **91**(22), 225501.
30. Coddens G, 2006, On the problem of the relation between phason elasticity and phason dynamics in quasicrystals, *Eur. Phys. J.* B, **54**(1), 37–65.
31. Edagawa K and Takeuchi S, Elasticity, dislocations and their motion in quasicrystals, *Dislocation in Solids*, Chpater 76, ed. by Nabarro E R N and Hirth J P, 367–417.
32. Edagawa K and Giso Y, 2007, Experimental evaluation of phonon-phason coupling in icosahedral quasicrystals, *Phil. Mag*., 87(1), 77–95.
33. Meng X M, Tong B Y and Wu Y K, 1994, Mechanical properties of quasicrystal $Al_{65}Cu_{20}Co_{15}$, Acta Metallurgica Sinica, 30(2), 61–64(in Chinese).
34. Takeuchi S, Iwanhaga H and Shibuya T, 1991, Hardness of quasicrystals, *Japanese J. Appl. Phys*., **30**(3), 561–562.

Chapter 5
Elasticity Theory of One-Dimensional Quasicrystals and Simplification

As mentioned in Chap. 4, there exist three one-, two- and three-dimensional quasicrystals. Each can be further divided into subclasses with respect to symmetry consideration.

In the class of one-dimensional quasicrystals, the atom arrangement is quasiperiodic only in one direction (say, the z-direction) and is periodic in the plane perpendicular to the direction (xy-plane). Although the quasicrystal is one-dimensional, the structure is three-dimensional; it is generated in a three-dimensional body. One-dimensional quasicrystals can be regarded as a projection of periodic crystals in four-dimensional space to physical space. There are 4 nonzero displacements, i.e. u_x, u_y, u_z and w_z (and $w_x = w_y = 0$). In this sense, the elasticity of one-dimensional quasicrystals is a four-dimensional problem.

We here briefly list the systems and Laue classes of one-dimensional quasicrystals, in which the concept of point group must be concerned, and we do not concern with the concept of space group.

In the following, we will discuss the elasticity of quasicrystals of certain types listed in Table 5.1.

5.1 Elasticity of Hexagonal Quasicrystals

As pointed out previously that for one-dimensional quasicrystals, there are phonon displacements u_x, u_y and u_z, and phason displacement w_z (and $w_x = w_y = 0$); the corresponding strains are as follows:

$$\varepsilon_{xx} = \frac{\partial u_x}{\partial x} \quad \varepsilon_{yy} = \frac{\partial u_y}{\partial y}, \quad \varepsilon_{zz} = \frac{\partial u_z}{\partial z} \tag{5.1.1}$$

T.-Y. Fan, *Mathematical Theory of Elasticity of Quasicrystals and Its Applications*,
Springer Series in Materials Science 246, DOI 10.1007/978-981-10-1984-5_5

Table 5.1 System, Laue classes and point groups of one-dimensional quasicrystals

Systems	Laue classes	Point groups
Triclinic	1	$1, \bar{1}$
Monoclinic	2 3	$2, m_h, 2/m_h$ $2_h, m, 2_h/m$
Orthorhombic	4	$2_h2_h2, 2mm, 2_hmm_h, m_hmm$
Tetragonal	5 6	$4\ \bar{4}\ 4/m_h$ $42_h2_h4mm, \bar{4}2_hm4/m_hmm$
Rhombohedral (or trigonal)	7 8	$3, \bar{3}$ $32_h, 3m, \bar{3}m$
Hexagonal	9 10	$6, \bar{6}, 6/m_h$ $62_h2_h, 6mm, \bar{6}2_hm, 6/m_hmm$

$$\begin{aligned}
\varepsilon_{yz} &= \varepsilon_{zy} = \frac{1}{2}\left(\frac{\partial u_z}{\partial y} + \frac{\partial u_y}{\partial z}\right), \\
\varepsilon_{zx} &= \varepsilon_{xz} = \frac{1}{2}\left(\frac{\partial u_z}{\partial x} + \frac{\partial u_x}{\partial z}\right), \\
\varepsilon_{xy} &= \varepsilon_{yx} = \frac{1}{2}\left(\frac{\partial u_x}{\partial y} + \frac{\partial u_y}{\partial x}\right) \\
w_{zx} &= \frac{\partial w_z}{\partial x}, \quad w_{zy} = \frac{\partial w_z}{\partial y}, \quad w_{zz} = \frac{\partial w_z}{\partial z}
\end{aligned} \tag{5.1.2}$$

and other $w_{ij} = 0$. Formulas (5.1.1) and (5.1.2) hold for all one-dimensional quasicrystals. In this section, we only discuss one-dimensional hexagonal quasicrystals.

Let the strains given by (5.1.1) and (5.1.2) be expressed by the vector with 9 components,

$$[\varepsilon_{11}, \varepsilon_{22}, \varepsilon_{33}, 2\varepsilon_{23}, 2\varepsilon_{31}, 2\varepsilon_{12}, w_{33}, w_{31}, w_{32}] \tag{5.1.3}$$

or

$$[\varepsilon_{xx}, \varepsilon_{yy}, \varepsilon_{zz}, 2\varepsilon_{yz}, 2\varepsilon_{zx}, 2\varepsilon_{xy}, w_{zz}, w_{zx}, w_{zy}] \tag{5.1.4}$$

The corresponding stresses are

$$[\sigma_{xx}, \sigma_{yy}, \sigma_{zz}, \sigma_{yz}, \sigma_{zx}, \sigma_{xy}, H_{zz}, H_{zx}, H_{zy}] \tag{5.1.5}$$

The elastic constant matrix is

$$[CKR] = \begin{bmatrix} C_{11} & C_{12} & C_{13} & 0 & 0 & 0 & R_1 & 0 & 0 \\ C_{12} & C_{11} & C_{13} & 0 & 0 & 0 & R_1 & 0 & 0 \\ C_{13} & C_{13} & C_{33} & 0 & 0 & 0 & R_2 & 0 & 0 \\ 0 & 0 & 0 & C_{44} & 0 & 0 & 0 & 0 & R_3 \\ 0 & 0 & 0 & 0 & C_{44} & 0 & 0 & R_3 & 0 \\ 0 & 0 & 0 & 0 & 0 & C_{66} & 0 & 0 & 0 \\ R_1 & R_1 & R_2 & 0 & 0 & 0 & K_1 & 0 & 0 \\ 0 & 0 & 0 & 0 & R_3 & 0 & 0 & K_2 & 0 \\ 0 & 0 & 0 & R_3 & 0 & 0 & 0 & 0 & K_2 \end{bmatrix}$$

where a short notation for the phonon elastic constant tensor is used, i.e. index $11 \to 1$, $22 \to 2$, $33 \to 3$, $23 \to 4$, $31 \to 5$, $12 \to 6$, and C_{ijkl} is denoted as C_{pq} accordingly as follows:

$$C_{11} = C_{1111} = C_{2222}, \quad C_{12} = C_{1122},$$
$$C_{33} = C_{3333}, \quad C_{44} = C_{2323} = C_{3131}$$

$$C_{13} = C_{1133} = C_{2233}, C_{66} = (C_{11} - C_{12})/2 = (C_{1111} - C_{1122})/2$$

There are five independent phonon elastic constants; in addition $K_1 = K_{3333}$ and $K_2 = K_{3131} = K_{3232}$, i.e. the two independent phason elastic constants, and $R_1 = R_{1133} = R_{2233}$, $R_2 = R_{3333}$ and $R_3 = R_{2332} = R_{3131}$, i.e. there are three phonon-phason coupling elastic constants.

The corresponding stress–strain relations (or so-called constitutive equations, or the generalized Hooke's law) are as follows:

$$\begin{aligned} \sigma_{xx} &= C_{11}\varepsilon_{xx} + C_{12}\varepsilon_{yy} + C_{13}\varepsilon_{zz} + R_1 w_{zz} \\ \sigma_{yy} &= C_{12}\varepsilon_{xx} + C_{11}\varepsilon_{yy} + C_{13}\varepsilon_{zz} + R_1 w_{zz} \\ \sigma_{zz} &= C_{13}\varepsilon_{xx} + C_{13}\varepsilon_{yy} + C_{33}\varepsilon_{zz} + R_2 w_{zz} \\ \sigma_{yz} &= \sigma_{zy} = 2C_{44}\varepsilon_{yz} + R_3 w_{zy} \\ \sigma_{zx} &= \sigma_{xz} = 2C_{44}\varepsilon_{zx} + R_3 w_{zx} \\ \sigma_{xy} &= \sigma_{yx} = 2C_{66}\varepsilon_{xy} \\ H_{zz} &= R_1(\varepsilon_{xx} + \varepsilon_{yy}) + R_2\varepsilon_{zz} + K_1 w_{zz} \\ H_{zx} &= 2R_3\varepsilon_{zx} + K_2 w_{zx} \\ H_{zy} &= 2R_3\varepsilon_{yz} + K_2 w_{zy} \end{aligned} \tag{5.1.6}$$

and other $H_{ij} = 0$.

The stresses satisfy the following equilibrium equations:

$$\begin{aligned}
\frac{\partial \sigma_{xx}}{\partial x}+\frac{\partial \sigma_{xy}}{\partial y}+\frac{\partial \sigma_{xz}}{\partial z}&=0\\
\frac{\partial \sigma_{yx}}{\partial x}+\frac{\partial \sigma_{yy}}{\partial y}+\frac{\partial \sigma_{yz}}{\partial z}&=0\\
\frac{\partial \sigma_{zx}}{\partial x}+\frac{\partial \sigma_{zy}}{\partial y}+\frac{\partial \sigma_{zz}}{\partial z}&=0\\
\frac{\partial H_{zx}}{\partial x}+\frac{\partial H_{zy}}{\partial y}+\frac{\partial H_{zz}}{\partial z}&=0
\end{aligned} \tag{5.1.7}$$

The above results are obtained by Wang et al. [1].

The elastic equilibrium problem of one-dimensional hexagonal quasicrystals is more complicated than that of three-dimensional classical elasticity. Here, there are 4 displacements, 9 strains and 9 stresses, which added up to get 22 field variables. The corresponding field equations are also 22, consisting of 4 for equilibrium equations, 9 equations of deformation geometry and 9 stress–strain relations. We will present a rigorous treatment of the problem later on. In the following, we give a simplified treatment.

5.2 Decomposition of the Elasticity into a Superposition of Plane and Anti-plane Elasticity

If there is a straight dislocation or a Griffith crack along the direction of atom's quasiperiodic arrangement, i.e. the deformation is independent from the direction, say

$$\frac{\partial}{\partial z}=0 \tag{5.2.1}$$

Then

$$\frac{\partial u_i}{\partial z}=0,\ (i=1,2,3),\quad \frac{\partial w_z}{\partial z}=0 \tag{5.2.2}$$

Hence,

$$\varepsilon_{zz}=w_{zz}=0,\quad \varepsilon_{yz}=\varepsilon_{zy}=\frac{1}{2}\frac{\partial u_z}{\partial y},\quad \varepsilon_{zx}=\varepsilon_{xz}=\frac{1}{2}\frac{\partial u_z}{\partial x} \tag{5.2.3}$$

$$\frac{\partial \sigma_{ij}}{\partial z}=0,\quad \frac{\partial H_{ij}}{\partial z}=0 \tag{5.2.4}$$

The generalized Hooke's law is simplified as

$$\begin{aligned}
\sigma_{xx} &= C_{11}\varepsilon_{xx} + C_{12}\varepsilon_{yy} \\
\sigma_{yy} &= C_{12}\varepsilon_{xx} + C_{11}\varepsilon_{yy} \\
\sigma_{xy} &= \sigma_{yx} = 2C_{66}\varepsilon_{xy} \\
\sigma_{zz} &= C_{13}(\varepsilon_{xx} + \varepsilon_{yy}) \\
\sigma_{yz} &= \sigma_{zy} = 2C_{44}\varepsilon_{yz} + R_3 w_{zy} \\
\sigma_{zx} &= \sigma_{xz} = 2C_{44}\varepsilon_{zx} + R_3 w_{zx} \\
H_{zz} &= R_1(\varepsilon_{xx} + \varepsilon_{yy}) \\
H_{zx} &= 2R_3\varepsilon_{zx} + K_2 w_{zx} \\
H_{zy} &= 2R_3\varepsilon_{yz} + K_2 w_{zy}
\end{aligned} \tag{5.2.5}$$

In the absence of the body force and generalized body force, the equilibrium equations are

$$\frac{\partial \sigma_{xx}}{\partial x} + \frac{\partial \sigma_{xy}}{\partial y} = 0, \quad \frac{\partial \sigma_{yx}}{\partial x} + \frac{\partial \sigma_{yy}}{\partial y} = 0, \quad \frac{\partial \sigma_{zx}}{\partial x} + \frac{\partial \sigma_{zy}}{\partial y} = 0 \tag{5.2.6}$$

$$\frac{\partial H_{zx}}{\partial x} + \frac{\partial H_{zy}}{\partial y} = 0 \tag{5.2.7}$$

Equations (5.1.2), (5.1.3), and (5.2.5)–(5.2.7) define two decoupled problems [2]; the first of them is

$$\begin{aligned}
&\sigma_{xx} = C_{11}\varepsilon_{xx} + C_{12}\varepsilon_{yy} \\
&\sigma_{yy} = C_{12}\varepsilon_{xx} + C_{11}\varepsilon_{yy} \\
&\sigma_{xy} = (C_{11} - C_{12})\varepsilon_{xy} \\
&\sigma_{zz} = C_{13}(\varepsilon_{xx} + \varepsilon_{yy}) \\
&H_{zz} = R_1(\varepsilon_{xx} + \varepsilon_{yy}) \\
&\frac{\partial \sigma_{xx}}{\partial x} + \frac{\partial \sigma_{xy}}{\partial y} = 0, \quad \frac{\partial \sigma_{yx}}{\partial x} + \frac{\partial \sigma_{yy}}{\partial y} = 0 \\
&\varepsilon_{xx} = \frac{\partial u_x}{\partial x}, \quad \varepsilon_{yy} = \frac{\partial u_y}{\partial y}, \quad \varepsilon_{xy} = \frac{1}{2}\left(\frac{\partial u_y}{\partial x} + \frac{\partial u_x}{\partial y}\right)
\end{aligned} \tag{5.2.8}$$

which is plane elasticity of conventional hexagonal crystals. The second is

$$\begin{aligned}
&\sigma_{yz} = \sigma_{zy} = 2C_{44}\varepsilon_{yz} + R_3 w_{zy} \\
&\sigma_{zx} = \sigma_{xz} = 2C_{44}\varepsilon_{zx} + R_3 w_{zx} \\
&H_{zx} = 2R_3\varepsilon_{zx} + K_2 w_{zx} \\
&H_{zy} = 2R_3\varepsilon_{yz} + K_2 w_{zy} \\
&\frac{\partial \sigma_{zx}}{\partial x} + \frac{\partial \sigma_{zy}}{\partial y} = 0, \quad \frac{\partial H_{zx}}{\partial x} + \frac{\partial \sigma_{zy}}{\partial y} = 0 \\
&\varepsilon_{zx} = \frac{1}{2}\frac{\partial u_z}{\partial x} = \varepsilon_{xz}, \quad \varepsilon_{zy} = \frac{1}{2}\frac{\partial u_z}{\partial y} = \varepsilon_{yz} \\
&w_{zx} = \frac{\partial w_z}{\partial x}, \quad w_{zy} = \frac{\partial w_z}{\partial y}
\end{aligned} \tag{5.2.9}$$

which is a phonon-phason coupling elasticity problem. But, there are only displacements u_z and w_z, and it is an anti-plane elasticity problem.

The plane elasticity described by (5.2.8) has well been studied, extensively using the stress function approach, e.g. it introduces

$$\sigma_{xx} = \frac{\partial^2 U}{\partial y^2}, \quad \sigma_{yy} = \frac{\partial^2 U}{\partial x^2}, \quad \sigma_{xy} = -\frac{\partial^2 U}{\partial x \partial y}$$

then Eq. (5.2.8) are reduced to solve

$$\nabla^2 \nabla^2 U = 0$$

The problem is considerably discussed in crystal (or classical) elasticity, and we do not consider it here.

We are interested in the phonon-phason coupling anti-plane elasticity described by (5.2.9), which may bring some new insight into the scope of elasticity of quasicrystals.

Substituting deformation geometry relations into the stress–strain relations and then into the equilibrium equations yields the final governing equations as follows:

$$\begin{aligned}
C_{44}\nabla^2 u_z + R_3 \nabla^2 w_z = 0 \\
R_3 \nabla^2 u_z + K_2 \nabla^2 w_z = 0
\end{aligned} \tag{5.2.10}$$

Because $C_{44}K_2 - R_3^2 \neq 0$, we have

$$\nabla^2 u_z = 0, \quad \nabla^2 w_z = 0 \tag{5.2.11}$$

where $\nabla^2 = \frac{\partial^2}{\partial x^2} + \frac{\partial^2}{\partial y^2}$, so u_z and w_z are harmonic functions.

It is well known that the two-dimensional harmonic functions u_z and w_z can be a real part or an imaginary part of any analytic functions $\phi(t)$ and $\psi(t)$ of complex variable $t = x + \mathrm{i}y, \mathrm{i} = \sqrt{-1}$, respectively, i.e.

$$\begin{aligned} u_z(x, y) &= \mathrm{Re}\phi(t) \\ w_z(x, y) &= \mathrm{Re}\psi(t) \end{aligned} \tag{5.2.12}$$

In this version, Eq. (5.2.11) should be automatically satisfied. The determination of $\phi(t)$ and $\psi(t)$ depends upon appropriate boundary conditions, which will be discussed in detail in Chaps. 7 and 8. The complex variable function method for solving elasticity of one-, two- and three-dimensional quasicrystals will be summarized fully in Chap. 11.

5.3 Elasticity of Monoclinic Quasicrystals

Decomposition and superposition procedure suggested by the author, see Refs. [2, 3] for example, is applicable not only for hexagonal quasicrystals but also for other one-dimensional quasicrystals. We here discuss monoclinic quasicrystals.

For this kind of one-dimensional quasicrystals, there are 25 nonzero elastic constants in total, namely $C_{1111}, C_{2222}, C_{3333}, C_{1122}, C_{1133}, C_{1112}, C_{2233}, C_{2212}, C_{3312}, C_{3232}, C_{3231}, C_{3131}, C_{1212}$ for phonon field, $K_{3333}, K_{3131}, K_{3232}, K_{3132}$ for phason field and $R_{1133}, R_{2233}, R_{3333}, R_{1233}, R_{2331}, R_{2332}, R_{3132}, R_{1233}$ for phonon-phason coupling.

The corresponding generalized Hooke's law for the case is given as follows [1]:

$$\begin{aligned} \sigma_{xx} &= C_{11}\varepsilon_{xx} + C_{12}\varepsilon_{yy} + C_{13}\varepsilon_{zz} + 2C_{16}\varepsilon_{xy} + R_1 w_{zz} \\ \sigma_{yy} &= C_{12}\varepsilon_{xx} + C_{22}\varepsilon_{yy} + C_{23}\varepsilon_{zz} + 2C_{26}\varepsilon_{xy} + R_2 w_{zz} \\ \sigma_{zz} &= C_{13}\varepsilon_{xx} + C_{23}\varepsilon_{yy} + C_{33}\varepsilon_{zz} + 2C_{36}\varepsilon_{xy} + R_3 w_{zz} \\ \sigma_{yz} &= \sigma_{zy} = 2C_{44}\varepsilon_{yz} + 2C_{45}\varepsilon_{zx} + R_4 w_{zx} + R_5 w_{zy} \\ \sigma_{zx} &= \sigma_{xz} = 2C_{45}\varepsilon_{yz} + 2C_{55}\varepsilon_{zx} + R_6 w_{zx} + R_7 w_{zy} \\ \sigma_{xy} &= \sigma_{yx} = C_{16}\varepsilon_{xx} + C_{26}\varepsilon_{yy} + C_{36}\varepsilon_{zz} + 2C_{66}\varepsilon_{xy} + R_8 w_{zz} \\ H_{zx} &= 2R_4\varepsilon_{yz} + 2R_6\varepsilon_{zx} + K_1 w_{zx} + K_4 w_{zy} \\ H_{zy} &= 2R_5\varepsilon_{yz} + 2R_7\varepsilon_{zx} + K_4 w_{zx} + K_2 w_{zy} \\ H_{zz} &= R_1\varepsilon_{xx} + R_2\varepsilon_{yy} + R_3\varepsilon_{zz} + 2R_8\varepsilon_{xy} + K_3 w_{zz} \end{aligned} \tag{5.3.1}$$

where recalling that for the phonon elastic constant tensor a brief notation is used, i.e. index $11 \to 1$, $22 \to 2$, $33 \to 3$, $23 \to 4$, $31 \to 5$, $12 \to 6$, and C_{ijkl} is denoted as C_{pq}, in addition, for the phason elastic constants $K_{3131} = K_1$, $K_{3232} = K_2$, $K_{3333} = K_3$ and $K_{3132} = K_4$, and for phonon-phason coupling elastic

constants $R_{1133} = R_1$, $R_{2233} = R_2$, $R_{3333} = R_3$, $R_{2331} = R_4$, $R_{2332} = R_5$, $R_{3131} = R_6$, $R_{3132} = R_7$ and $R_{1233} = R_8$.

Under the assumption (5.2.1), the problem will be decomposed into two separate problems as [4, 5]

$$\begin{aligned}
\sigma_{xx} &= C_{11}\varepsilon_{xx} + C_{12}\varepsilon_{yy} + 2C_{16}\varepsilon_{xy} \\
\sigma_{yy} &= C_{12}\varepsilon_{xx} + C_{22}\varepsilon_{yy} + 2C_{26}\varepsilon_{xy} \\
\sigma_{xy} &= \sigma_{yx} = C_{16}\varepsilon_{xx} + C_{26}\varepsilon_{yy} + 2C_{66}\varepsilon_{xy} \\
\sigma_{zz} &= C_{13}\varepsilon_{xx} + C_{23}\varepsilon_{yy} + 2C_{36}\varepsilon_{xy} \\
H_{zz} &= R_1\varepsilon_{xx} + R_2\varepsilon_{yy} + R_3\varepsilon_{zz} + 2R_8\varepsilon_{xy}
\end{aligned} \tag{5.3.2}$$

and

$$\begin{aligned}
\sigma_{yz} &= \sigma_{zy} = 2C_{44}\varepsilon_{yz} + 2C_{45}\varepsilon_{zx} + R_4 w_{zx} + R_5 w_{zy} \\
\sigma_{zx} &= \sigma_{xz} = 2C_{45}\varepsilon_{yz} + 2C_{55}\varepsilon_{zx} + R_6 w_{zx} + R_7 w_{zy} \\
H_{zx} &= 2R_4\varepsilon_{yz} + 2R_6\varepsilon_{zx} + K_1 w_{zx} + K_4 w_{zy} \\
H_{zy} &= 2R_5\varepsilon_{yz} + 2R_7\varepsilon_{zx} + K_4 w_{zx} + K_2 w_{zy}
\end{aligned} \tag{5.3.3}$$

in which problem described by Eq. (5.3.2) is plane elasticity of monocline crystals; by introducing displacement potential $G(x, y)$

$$\begin{aligned}
u_x &= \left[C_{16}\frac{\partial^2}{\partial x^2} + C_{26}\frac{\partial^2}{\partial y^2} + (C_{12} + C_{66})\frac{\partial^2}{\partial x \partial y}\right] G \\
u_y &= -\left[C_{11}\frac{\partial^2}{\partial x^2} + C_{66}\frac{\partial^2}{\partial y^2} + 2C_{16}\frac{\partial^2}{\partial x \partial y}\right] G
\end{aligned}$$

the elasticity equations are reduced at last to

$$\left(c_1\frac{\partial^4}{\partial x^4} + c_2\frac{\partial^4}{\partial x^3 \partial y} + c_3\frac{\partial^4}{\partial x^2 \partial y^2} + c_4\frac{\partial^4}{\partial x \partial y^3} + c_5\frac{\partial^4}{\partial y^4}\right) G = 0$$

with constants

$$\begin{aligned}
c_1 &= C_{16}^2 - C_{11}C_{66}, \quad c_2 = 2(C_{16}C_{12} - C_{11}C_{26}) \\
c_3 &= C_{12}^2 - 2C_{16}C_{26} + 2C_{12}C_{66} - C_{11}C_{22} \\
c_4 &= 2(C_{26}C_{12} - C_{16}C_{22}), \quad c_5 = C_{26}^2 - C_{22}C_{66}
\end{aligned}$$

Because this is classical elasticity and does not have direct connection to phason elasticity of one-dimensional quasicrystal, we do not further discuss it here.

We are interested in the problem described by Eq. (5.3.3), which is a phonon-phason coupling problem. Substituting the equations of deformation geometry into the stress–strain relations and then into the equilibrium equations, we obtain the final governing equation as

$$\left(a_1\frac{\partial^4}{\partial x^4}+a_2\frac{\partial^4}{\partial x^3\partial y}+a_3\frac{\partial^4}{\partial x^2\partial y^2}+a_4\frac{\partial^4}{\partial x\partial y^3}+a_5\frac{\partial^4}{\partial y^4}\right)F=0 \tag{5.3.4}$$

where

$$\left.\begin{aligned} u_z &= \left[R_6\tfrac{\partial^2}{\partial x^2}+R_5\tfrac{\partial^2}{\partial y^2}+(R_4+R_7)\tfrac{\partial^2}{\partial x\partial y}\right]F \\ w_z &= -\left[C_{55}\tfrac{\partial^2}{\partial x^2}+C_{44}\tfrac{\partial^2}{\partial y^2}+2C_{45}\tfrac{\partial^2}{\partial x\partial y}\right]F \end{aligned}\right\} \tag{5.3.5}$$

and

$$\begin{aligned} a_1 &= R_6^2-K_1C_{55}, \quad a_2=2(R_0(R_4+R_7)-K_1C_{45}-K_1C_{35}) \\ a_3 &= 2R_5R_6+(R_4+R_7)^2-K_1C_{44}-K_2C_{55}-4K_4C_{45} \\ a_4 &= 2[R_5(R_4+R_7)-K_2C_{45}-K_4C_{44}], \quad a_5=R_5^2-K_2C_{44} \end{aligned} \tag{5.3.6}$$

In the subsequent contents of the book, we discuss only the anti-plane elasticity of monocline quasicrystals, which has the complex representation of solution as

$$F(x,y)=2\mathrm{Re}\sum_{k=1}^{2}F_k(z_k), \quad z_k=x+\mu_k y \tag{5.3.7}$$

where $F_k(z_k)$ are analytic functions of z_k and

$$\mu_k=\alpha_k+i\beta_k \tag{5.3.8}$$

are the distinct complex parameters to be determined by the characteristic equation (or call the eigenvalue equation)

$$a_5\mu^4+a_4\mu^3+a_3\mu^2+a_2\mu+a_1=0 \tag{5.3.9}$$

and $\mu_1\neq\mu_2$.

If the roots of Eq. (5.3.9) are multi-roots, i.e. $\mu_1=\mu_2$,, then

$$F(x,y)=2\mathrm{Re}[F_1(z_1)+\bar{z}_1F_2(z_1)], \quad z_1=x+\mu_1 y \tag{5.3.10}$$

Substituting formula (5.3.7) into (5.3.5) and then into (5.3.3), we can get the complex representation of the displacements and stresses as follows:

$$
\begin{aligned}
u_z &= 2\mathrm{Re}\sum_{k=1}^{2}[R_6+(R_4+R_7)\mu_k+R_5\mu_k^2]f_k(z_k)\\
w_z &= -2\mathrm{Re}\sum_{k=1}^{2}(C_{55}+2C_{45}\mu_k+C_{44}\mu_k^2)f_k(z_k)\\
\sigma_{zy} &= \sigma_{yz} = 2\mathrm{Re}\sum_{k=1}^{2}[R_6C_{45}-R_4C_{55}+(R_6C_{44}-R_4C_{45}+R_7C_{45}-R_5C_{55})\mu_k\\
&\quad +(R_7C_{44}-R_5C_{45})\mu_k^2]f_k'(z_k)\\
\sigma_{zx} &= \sigma_{xz} = 2\mathrm{Re}\sum_{k=1}^{2}[R_4C_{55}-R_6C_{45}+(R_5C_{55}+R_4C_{45}-R_6C_{44}-R_5C_{55})\mu_k\\
&\quad +(R_3C_{45}-R_7C_{44})\mu_k^2]\mu_kf_k'(z_k)\\
H_{zx} &= 2\mathrm{Re}\sum_{k=1}^{2}\big[(R_7+R_5\mu_k)(R_6+R_4\mu_k+R_7\mu_k+R_5\mu_k^2)\\
&\quad -(K_4+K_2\mu_k)(C_{55}+2C_{45}\mu_k+C_{44}\mu_k^2)\big]f_k'(z_k)\\
H_{zy} &= 2\mathrm{Re}\sum_{k=1}^{2}\big[(R_6+R_4\mu_k)(R_6+R_4\mu_k+R_7\mu_k+R_5\mu_k^2)\\
&\quad -(K_4+K_2\mu_k)(C_{55}+2C_{45}\mu_k+C_{44}\mu_k^2)\big]f_k'(z_k)
\end{aligned}
\tag{5.3.11}
$$

where $f_k(z_k)\equiv\partial^2F_k(z_k)/\partial z_k^2=F_k''(z_k)$.

The determination of analytic functions $F_k(z_k)$ depends on the boundary conditions of concrete problems, which will be investigated later in Chaps. 7 and 8.

5.4 Elasticity of Orthorhombic Quasicrystals

In Table 5.1, we know that orthorhombic quasicrystals contain the points $2_h2_h2, 2mm, 2_hmm_h$ and mmm_h, which belong to Laue class 4. Due to the increase of symmetrical elements of this quasicrystal system in comparison with monocline quasicrystal system, one has

$$C_{16}=C_{26}=C_{36}=C_{45}=K_4=R_4=R_7=R_8=0 \tag{5.4.1}$$

Therefore, the total number of nonzero elastic constants in the case reduces to 17, i.e. $C_{11}, C_{22}, C_{33}, C_{12}, C_{13}, C_{23}, C_{44}, C_{55}, C_{66}$ for the phonon field, K_1, K_2, K_3 for the phason fields and R_1, R_2, R_3, R_5, R_6 for phonon-phason coupling field.

Considering results of (5.4.1), (5.3.6) can be simplified to

$$\begin{aligned} &a_2 = a_4 = 0, \quad a_1 = R_6^2 - K_1 C_{55}, \\ &a_3 = 2R_5R_6 - K_1C_{44} - K_2C_{55}, \quad a_5 = R_5^2 - K_2C_{66} \end{aligned} \tag{5.4.2}$$

and a_1 and a_5 no change from (5.3.6). So that Eq. (5.3.4) is reduced to

$$\left(a_1 \frac{\partial^4}{\partial x^4} + a_3 \frac{\partial^4}{\partial x^2 \partial y^2} + a_5 \frac{\partial^4}{\partial y^4}\right) F = 0 \tag{5.4.3}$$

We have the expression of solution as follows:

$$\begin{aligned} u_z &= 2\mathrm{Re} \sum_{k=1}^{2} [R_6 + R_5 \mu_k^2] f_k(z_k) \\ w_z &= -2\mathrm{Re} \sum_{k=1}^{2} (C_{55} + C_{44} \mu_k^2) f_k(z_k) \\ \sigma_{zy} &= \sigma_{yz} = 2\mathrm{Re} \sum_{k=1}^{2} (R_6 C_{44} - R_5 C_{55}) \mu_k f_k'(z_k) \\ \sigma_{zx} &= \sigma_{xz} = 2\mathrm{Re} \sum_{k=1}^{2} (R_5 C_{55} - R_6 C_{44}) \mu_k^2 f_k'(z_k) \\ H_{zy} &= 2\mathrm{Re} \sum_{k=1}^{2} [R_5 R_6 - K_2 C_{55} + (R_5^2 - K_2 C_{44}) \mu_k^2 - (K_4 + K_2 \mu_k)] \mu_k f_k'(z_k) \\ H_{zx} &= 2\mathrm{Re} \sum_{k=1}^{2} [R_6^2 - K_1 C_{55} + (R_5 R_6 - K_1 C_{44}) \mu_k^2] f_k'(z_k) \end{aligned} \tag{5.4.4}$$

in which, $f_k(z_k)$ represents analytic function of z_k.

5.5 Tetragonal Quasicrystals

From Table 5.1, we know that one-dimensional tetragonal quasicrystal has 7 point groups, in which groups $\bar{4}2_h m, 4mm, 42_h 2_h$ and $4/m_h mm$ belong to Laue class 6, and besides (5.4.1) we have also

$$C_{11} = C_{22}, C_{13} = C_{23}, C_{44} = C_{55}, K_1 = K_2, R_1 = R_2, R_5 = R_6 \tag{5.5.1}$$

Therefore, the total number of nonzero elastic constants reduces to 11.

With (5.5.1) and (5.4.2), one can find the complex representation of solution for the anti-plane elasticity of quasicrystals that belong to Laue class 6.

The point group 4, $\bar{4}$ and $4/m_h$, belongs to Laue class 5, in which solution of the anti-plane elasticity can also be expressed in a similar manner.

The final governing equation of anti-plane elasticity for this kind of quasicrystals is

$$\nabla^2\nabla^2 F = 0 \tag{5.5.2}$$

5.6 The Space Elasticity of Hexagonal Quasicrystals

The decomposition and superposition procedure proposed by Ref. [2] has been developed for simplifying the elasticity of various systems of one-dimensional quasicrystals in the previous sections. The main feature of the procedure lies in decomposition of a space (three-dimensional) elasticity into a superposition of a plane elasticity and an anti-plane elasticity for the studied quasicrystalline material, and this often simplifies the solution process, whose worth will be shown in Chaps. 7 and 8 and other chapters.

In some cases, when the procedure cannot be used, we have to solve space elasticity. In this section, taking an example, we discuss the solution of space elasticity of hexagonal quasicrystals, which has been studied by many authors, e.g. Peng and Fan [6], Chen et al. [9] and Wang [10]; here, the derivation of Ref. [6, 7] is listed.

Substituting (5.5.1) into (5.1.6) and then into (5.1.7) yields the equilibrium equations expressed by the displacements:

$$\begin{aligned}
&\left(C_{11}\frac{\partial^2}{\partial x^2}+C_{66}\frac{\partial^2}{\partial y^2}+C_{44}\frac{\partial^2}{\partial z^2}\right)u_x+(C_{11}-C_{66})\frac{\partial^2 u_y}{\partial x\partial y}+(C_{13}+C_{44})\frac{\partial^2 u_z}{\partial x\partial z}+(R_1+R_3)\frac{\partial^2 w_z}{\partial x\partial z}=0\\
&(C_{11}-C_{66})\frac{\partial^2 u_x}{\partial x\partial y}+\left(C_{66}\frac{\partial^2}{\partial x^2}+C_{11}\frac{\partial^2}{\partial y^2}+C_{44}\frac{\partial^2}{\partial z^2}\right)u_y+(C_{13}+C_{44})\frac{\partial^2 u_z}{\partial y\partial z}+(R_1+R_3)\frac{\partial^2 w_z}{\partial y\partial z}=0\\
&(C_{13}+C_{44})\left(\frac{\partial^2 u_x}{\partial x\partial z}+\frac{\partial^2 u_y}{\partial y\partial z}\right)+\left(C_{44}\frac{\partial^2}{\partial x^2}+C_{44}\frac{\partial^2}{\partial y^2}+C_{33}\frac{\partial^2}{\partial z^2}\right)u_z+\left[R_3\left(\frac{\partial^2}{\partial x^2}+\frac{\partial^2}{\partial y^2}\right)+R_2\frac{\partial^2}{\partial z^2}\right]w_z=0\\
&(R_1+R_3)\left(\frac{\partial^2 u_x}{\partial x\partial z}+\frac{\partial^2 u_y}{\partial y\partial z}\right)+\left[R_3\left(\frac{\partial^2}{\partial x^2}+\frac{\partial^2}{\partial y^2}\right)+R_2\frac{\partial^2}{\partial z^2}\right]u_z+\left[K_2\left(\frac{\partial^2}{\partial x^2}+\frac{\partial^2}{\partial y^2}\right)+K_1\frac{\partial^2}{\partial z^2}\right]w_z=0
\end{aligned} \tag{5.6.1}$$

If we introduce 4 displacement functions such as

$$\begin{aligned}
u_x &= \frac{\partial}{\partial x}(F_1+F_2+F_3)-\frac{\partial F_4}{\partial y}, \quad u_Y = \frac{\partial}{\partial y}(F_1+F_2+F_3)+\frac{\partial F_4}{\partial x}\\
u_z &= \frac{\partial}{\partial z}(m_1F_1+m_2F_2+m_3F_3), \quad w_z = \frac{\partial}{\partial z}(l_1F_1+l_2F_2+l_3F_3)
\end{aligned} \tag{5.6.2}$$

and

$$\nabla_i^2 F_i = 0 \quad (i = 1, 2, 3, 4) \tag{5.6.3}$$

$$\nabla_i^2 = \frac{\partial^2}{\partial x^2} + \frac{\partial^2}{\partial y^2} + \gamma_i^2 \frac{\partial^2}{\partial z^2} \quad i = 1, 2, 3, 4 \tag{5.6.4}$$

with m_i, l_i and γ_i defined by

$$\begin{aligned} &\frac{C_{44} + (C_{13} + C_{44})m_i + (R_1 + R_3)l_i}{C_{11}} = \frac{C_{33}m_i + R_2 l_i}{C_{13} + C_{44} + C_{44}m_i + R_3 l_i} = \frac{R_2 m_i + K_1 l_i}{R_1 + R_2 + R_3 m_i + K_2 l_i} = \gamma_i^2, \quad i = 1, 2, 3 \\ &C_{44}/C_{66} = \gamma_4^2 \end{aligned} \tag{5.6.5}$$

then Eq. (5.6.1) will be automatically satisfied.

It is obvious that the final governing equations (5.6.3) are three-dimensional harmonic equations, and this greatly simplifies the solution.

By substituting (5.6.2) into (5.1.1), then (5.1.2) into (5.1.6), one can find the stresses expressed in terms of F_1, F_2, F_3 and F_4 as follows:

$$\begin{aligned} \sigma_{xx} &= \left[C_{11}\frac{\partial^2}{\partial x^2} + (C_{11} - 2C_{66})\frac{\partial^2}{\partial y^2}\right](F_1 + F_2 + F_3) - 2C_{66}\frac{\partial^2 F_4}{\partial x \partial y} \\ &\quad + C_{13}\frac{\partial^2}{\partial z^2}(m_1 F_1 + m_2 F_2 + m_3 F_3) + R_1 \frac{\partial^2}{\partial z^2}(l_1 F_1 + l_2 F_2 + l_3 F_3) \\ \sigma_{yy} &= \left[(C_{11} - 2C_{66})\frac{\partial^2}{\partial x^2} + C_{11}\frac{\partial^2}{\partial y^2}\right](F_1 + F_2 + F_3) + 2C_{66}\frac{\partial^2 F_4}{\partial x \partial y} \\ &\quad + C_{13}\frac{\partial^2}{\partial z^2}(m_1 F_1 + m_2 F_2 + m_3 F_3) + R_1 \frac{\partial^2}{\partial z^2}(l_1 F_1 + l_2 F_2 + l_3 F_3) \\ \sigma_{zz} &= -C_{13}\frac{\partial^2}{\partial z^2}(\gamma_1^2 F_1 + \gamma_2^2 F_2 + \gamma_3^2 F_3) + C_{33}\frac{\partial^2}{\partial z^2}(m_1 F_1 + m_2 F_2 + m_3 F_3) \\ &\quad + R_2 \frac{\partial^2}{\partial z^2}(l_1 F_1 + l_2 F_2 + l_3 F_3) \\ \sigma_{xy} &= \sigma_{yx} = 2C_{66}\frac{\partial^2}{\partial x \partial y}(F_1 + F_2 + F_3) + C_{66}\left(\frac{\partial^2}{\partial x^2} - \frac{\partial^2}{\partial y^2}\right)F_4 \\ \sigma_{yz} &= \sigma_{zy} = C_{44}\frac{\partial^2}{\partial y \partial z}[(m_1 + 1)F_1 + (m_2 + 1)F_2 + (m_3 + 1)F_3] \\ &\quad + C_{44}\frac{\partial^2 F_4}{\partial x \partial z} + R_3 \frac{\partial^2}{\partial y \partial z}(l_1 F_1 + l_2 F_2 + l_3 F_3) \end{aligned}$$

$$\sigma_{zx} = \sigma_{xz} = C_{44}\frac{\partial^2}{\partial x \partial z}[(m_1+1)F_1 + (m_2+1)F_2 + (m_3+1)F_3] - C_{44}\frac{\partial^2 F_4}{\partial y \partial z} + R_3\frac{\partial^2}{\partial x \partial z}(l_1F_1 + l_2F_2 + l_3F_3)$$

$$H_{zz} = -R_1\frac{\partial^2}{\partial z^2}(\gamma_1^2F_1 + \gamma_2^2F_2 + \gamma_3^2F_3) + R_2\frac{\partial^2}{\partial z^2}(m_1F_1 + m_2F_2 + m_3F_3) + K_1\frac{\partial^2}{\partial z^2}(l_1F_1 + l_2F_2 + l_3F_3)$$

$$H_{zx} = R_3\frac{\partial^2}{\partial x \partial z}[(m_1+1)F_1 + (m_2+1)F_2 + (m_3+1)F_3] - R_3\frac{\partial^2 F_4}{\partial y \partial z} + K_2\frac{\partial^2}{\partial x \partial z}(l_1F_1 + l_2F_2 + l_3F_3)$$

$$H_{zy} = R_3\frac{\partial^2}{\partial y \partial z}[(m_1+1)F_1 + (m_2+1)F_2 + (m_3+1)F_3] + R_3\frac{\partial^2 F_4}{\partial y \partial z} + K_2\frac{\partial^2}{\partial y \partial z}(l_1F_1 + l_2F_2 + l_3F_3)$$

Harmonic equations (5.6.3) will be solved under appropriate boundary conditions, which will be mentioned in Chap. 8.

5.7 Other Results of Elasticity of One-Dimensional Quasicrystals

There are many other results of elasticity of one-dimensional quasicrystals, e.g. Fan et al. [8] on elasticity of one-dimensional crystal–crystal coexisting phase (a brief discussion referring to Chap. 7), and Chen et al. [9], Wang et al. [10], Gao et al. [11], Li et al. [12], etc., on the three-dimensional elasticity of hexagonal quasicrystals; they carried out considerable research in the area and have got a quite lot of achievements. Due to the limitation of the space, the details of their work could not be handled here and reader can refer to the original literature.

References

1. Wang R H,Yang W G, Hu C Z and Ding D H, 1997, Point and space groups and elastic behaviour of one-dimensional quasicrystals, J. *Phys.:Condens. Matter*, **9**(11), 2411-2422.
2. Fan T Y, 2000, Mathematical theory of elasticity and defects of quasicrystals, *Advances in Mechanics* (in Chinese), **30**(2),161-174.
3. Fan T Y and Mai Y W, 2004, Elasticity theory, fracture mechanics and some relevant thermal properties of quasicrystalline materials, *Appl. Mech. Rev*., **57**(5), 325-344.

4. Liu G T, Fan T Y and Guo R P, 2004,Governing equations and general solutions of plane elasticity of one-dimensional quasicrystals, *Int. J. Solid and Structures*, **41**(14), 3949-3959.
5. Liu G T, 2004,The complex variable function method of the elastic theory of quasicrystals and defects and auxiliary equation method for solving some nonlinear evolution equations,, Dissertation (in Chinese), Beijing Institute of Technology.
6. Peng Y Z and Fan T Y, 2000, Elastic theory of 1-D quasiperiodic stacking 2-D crystals, *J. Phys.:Condens. Matter*, **12**(45), 9381-9387.
7. Peng Y Z, 2001, Study on elastic three-dimensional problems of cracks for quasicrystals, Dissertation (in Chinese), Beijing Institute of Technology.
8. Fan T Y, Xie L Y, Fan L and Wang Q Z, 2011, Study on interface of quasicrystal-crystal, *Chin Phys B*, 20(7), 076102.
9. Chen W Q, Ma Y L and Ding H J, 2004, On three-dimensional elastic problems of one-dimensional hexagonal quasicrystal bodies, *Mech. Res. Commun*., **31**(5), 633-641.
10. Wang X, 2006, The general solution of one-dimensional hexagonal quasicrystal, *Appl. Math. Mech*., **33**(4), 576-580.
11. Gao Y, Zhao Y T and Zhao B S, 2007, Boundary value problems of holomorphic vector functions in one-dimensional hexagonal quasicrystals, Physica B, Vol.394(1), 56-61.
12. Li X Y, 2013, Fundamental solutions of a penny shaped embedded crack and half-infinite plane crack in infinite space of one-dimensional hexagonal quasicrystals under thermal loading, Proc Roy Soc A, 469, 20130023.

Chapter 6
Elasticity of Two-Dimensional Quasicrystals and Simplification

As has been shown in Chap. 5, in one-dimensional quasicrystals, elasticity can be decomposed into plane elasticity and anti-plane elasticity in case that the configuration is independent of the quasiperiodic axis. In this case, plane elasticity is a classical elasticity problem and its solutions are well known, whereas the anti-plane elasticity is a problem concerned with the quasiperiodic structure, which is our main concern. This decomposition leads to great simplifications for the solution.

We now consider elasticity of two-dimensional quasicrystals, which is mathematically much more complicated than that of one-dimensional quasicrystals. The decomposition procedure developed in Chap. 5 hints that the elasticity of two-dimensional quasicrystals may somehow also be made of a decomposition for a wide range of applications. In this way, the problem can be greatly simplified and it is helpful to solve the boundary value problems by analytic methods.

Two-dimensional quasicrystals so far observed cover four systems, i.e., those involving fivefold, eightfold, tenfold and twelvefold symmetries, named the pentagonal, octagonal, decagonal and dodecagonal, respectively, and among them there are the different Laue classes. The importance of two-dimensional quasicrystals is only less than that of the three-dimensional icosahedral quasicrystals. To date, among the over 200 quasicrystals, there are halves icosahedral quasicrystals, and over 70 decagonal quasicrystals. These two kinds of quasicrystals constitute the majority of the material. The elasticity of icosahedral quasicrystals will be discussed in Chap. 9.

We will, at first, give a brief description of the point groups and Laue classes of the two-dimensional quasicrystals. There are 31 kinds of crystallographic point groups and 26 kinds of non-crystallographic point groups of the quasicrystals, the former will not be discussed here and we focus on the latter, which is further divided into eight Laue classes and four quasicrystal systems observed so far, as listed in Table 6.1.

Like that in the one-dimensional quasicrystals, the phonon field of two-dimensional quasicrystals is transversally isotropic. If we take the *xy*-plane (or

T.-Y. Fan, *Mathematical Theory of Elasticity of Quasicrystals and Its Applications*,
Springer Series in Materials Science 246, DOI 10.1007/978-981-10-1984-5_6

Table 6.1 Systems, Laue classes and point groups of two-dimensional quasicrystal

Systems	Laue classes	Point groups
Pentagonal	11	$5,\ \bar{5}$
	12	$5m,\ 52,\ \bar{5}m$
Decagonal	13	$10,\ \overline{10}, 10/m$
	14	$10mm,\ 1022,\ \overline{10}m2,\ 10/mmm$
Octagonal	15	$8,\ \bar{8},\ 8/m$
	16	$8mm,\ 822,\ \bar{8}m2,\ 8/mmm$
Dodecagonal	17	$12,\ \overline{12},\ 12/m$
	18	$12mm,\ 1222,\ \overline{12}m2,\ 12/mmm$

x_1x_2-plane) as the quasiperiodic plane, and axis z (or x_3) as the periodic axis, then xy-plane is the elasticity isotropic plane, within which the elastic constants are

$$\begin{aligned} C_{1111} &= C_{2222} = C_{11} \\ C_{1122} &= C_{12} \\ C_{1212} &= C_{1111} - C_{1122} = C_{11} - C_{12} = 2C_{66} \end{aligned}$$

This shows that C_{66} is not independent. Other independent elastic constants are out of the plane, that is,

$$\begin{aligned} C_{2323} &= C_{3131} = C_{44} \\ C_{1133} &= C_{2233} = C_{13} \\ C_{3333} &= C_{33} \end{aligned}$$

which are listed in Table 6.2.

The relevant phason elastic constants and phonon-phason coupling elastic constants are listed in Tables 6.3, 6.4, 6.5 and 6.6.

For Laue class 12:

$$\begin{aligned} &\textbf{If } 2//x_1, m\perp x_1: && K_6 = R_2 = R_3 = R_6 = 0 \\ &\textbf{If } 2//x_2, m\perp x_2: && K_7 = R_2 = R_4 = R_6 = 0 \end{aligned}$$

Table 6.2 Phonon elastic constants in two-dimensional quasicrystals (C_{ijkl})

	11	22	33	23	31	12
11	C_{11}	C_{12}	C_{13}	0	0	0
22	C_{12}	C_{11}	C_{13}	0	0	0
33	C_{13}	C_{13}	C_{33}	0	0	0
23	0	0	0	C_{44}	0	0
31	0	0	0	0	C_{66}	0
12	0	0	0	0	0	C_{66}

Table 6.3 Phason elastic constants for Laue class 11 (K_{ijkl})

	11	22	23	12	13	21
11	K_1	K_2	K_7	0	K_6	0
22	K_2	K_1	K_7	0	K_6	0
23	K_7	K_7	K_4	K_6	0	$-K_6$
12	0	0	K_6	K_1	$-K_7$	$-K_2$
13	K_6	K_6	0	$-K_7$	K_4	K_7
21	0	0	$-K_6$	$-K_2$	K_7	K_1

Table 6.4 Phonon-phason coupling elastic constants for Laue class 11 (R_{ijkl})

$\varepsilon_{ij}\backslash w_{ij}$	11	22	23	12	13	21
11	R_1	R_1	R_6	R_2	R_5	$-R_2$
22	$-R_1$	$-R_1$	$-R_6$	$-R_2$	$-R_5$	R_2
33	0	0	0	0	0	0
23	R_4	$-R_4$	0	R_3	0	R_3
31	$-R_3$	R_3	0	R_4	0	R_4
12	R_2	R_2	$-R_5$	$-R_1$	R_6	R_1

Table 6.5 The phason elastic constants for Laue class 15 (K_{ijkl})

	11	22	23	12	13	21
11	K_1	K_2	0	K_5	0	K_5
22	K_2	K_1	0	$-K_5$	0	$-K_5$
23	0	0	K_4	0	0	0
12	K_5	$-K_5$	0	K	0	K_3
13	0	0	0	0	K_4	0
21	K_5	$-K_5$	0	K_3	0	K

Table 6.6 The phonon-phason coupling elastic constants for Laue class 15 (R_{ijkl})

$\varepsilon_{ij}\backslash w_{ij}$	11	22	23	12	13	21
11	R_1	R_1	0	R_2	0	$-R_2$
22	$-R_1$	$-R_1$	0	$-R_2$	0	R_2
33	0	0	0	0	0	0
23	0	0	0	0	0	0
31	0	0	0	0	0	0
12	R_2	R_2	0	$-R_2$	0	R_1

For Laure class 13:

$$K_6 = K_7 = R_3 = R_4 = R_5 = R_6 = 0$$

For Laue class 14:

$$K_6 = K_7 = R_2 = R_3 = R_4 = R_5 = R_6 = 0$$

For Laue class 16: $K_6 = R_2 = 0$
For Laue class 17: the constants K_{ijkl} are the same as Table 6.5; and $R_{ijkl} = 0$
For Laue class 18: the constants K_{ijkl} are the same as those of Laue 16; and $R_{ijkl} = 0$

The experimental measurement of the above data for different quasicrystals is essential in studying the elasticity. We here list some data for decagonal quasicrystals in Tables 6.7, 6.8 and 6.9 in which B is bulk modulus, G the shear modulus and v the Poisson's ratio, respectively.

The phason elastic constants, for a decagonal Al–Ni–Co quasicrystal, anisotropic diffuse scattering has been observed in synchrotron X-ray diffraction measurements [2]. It has been shown that the measurement can attributed the phason elastic constants, although no quantitative evaluation on K_1 and K_2. The Monte Carlo simulation was used to evaluate the phason elastic constants, e.g. given in Table 6.8 [3].

where $1\,\text{GPa} = 10^{10}\,\text{dyn/cm}^2$. But the accuracy of the values given by Monte Carlo simulation should be verified.

Recently, the experimental measurement for phonon-phason coupling elastic constants for decagonal quasicrystals has been achieved; the results are listed in Table 6.9.

Table 6.7 Phonon elastic constants of an decagonal quasicrystal (the unit of C_{ij}, B, G is GPa) by experimental measurement [1]

Alloy	C_{11}	C_{33}	C_{44}	C_{12}	C_{13}	B	G	v
Al–Ni–Co	234.33	232.22	70.19	57.41	66.63	120.25	79.98	0.228

Table 6.8 Phason elastic constants of an Al–Ni–Co decagonal quasicrystal by Monte Carlo simulation [3]

Alloy	$K_1(10^{12}\,\text{dyn/cm}^2)$	$K_2(10^{12}\,\text{dyn/cm}^2)$
Al–Ni–Co	1.22	0.24

Table 6.9 Coupling elastic constants for point group $10, \overline{10}$, Al–Ni–Co decagonal quasicrystals [4]

Alloy	R_1(GPa)	$\lvert R_2\rvert$(GPa)
Al–Ni–Co	0.1	<0.2

Tables 6.2, 6.3, 6.4, 6.5 and 6.6 indicate that the phonon elasticity of two-dimensional quasicrystals is three-dimensional and that the phason and phonon-phason coupling elasticity are also three-dimensional. In general, they cannot be reduced to two-dimensional problems. In this case, there are 29 field variables and 29 field equations, their solution is very hard to obtain.

In practice, there is often a case in which the configuration of a system is uniform along a periodic axis, say the axis z, both physically and geometrically, so that the field variables are free from the coordinate z, that is,

$$\frac{\partial}{\partial z} = 0 \tag{6.0.1}$$

Under this condition, the elasticity of two-dimensional quasicrystals can be decomposed into a plane elasticity of quasicrystal and an anti-plane elasticity of crystal, where the latter is a pure phonon or classical elasticity, whose governing equation and boundary conditions are decoupled with the plane elasticity of quasiperiodic structure, which can be treated separately.

Uniform configuration along the z-axis physically and geometrically represents several meaningful physical problems, e.g. a straight dislocation line or a Griffith crack along the direction. This shows that the decomposition procedure presents important physical meaning.

In what follows, we derive the final governing equations for the plane and anti-plane elasticity of the four different systems, by introducing some displacement or stress potential functions. We will see that the field equations are dramatically simplified; this is helpful to solve them by analytic methods. Furthermore, we use the Fourier analysis or complex analysis method to construct analytic solutions of some boundary value problems of the equations. But the mathematical methods and numerous exact solutions for different boundary value problems will be performed in Chaps. 7 and 8 in detail. They reveal the exact mathematical structure of dislocations and cracks in two-dimensional quasicrystalline materials. In addition, they develop further the potential theory of classical elasticity as well as the classical methods of solution in mathematical physics.

6.1 Basic Equations of Plane Elasticity of Two-Dimensional Quasicrystals: Point Groups 5*m* and 10*mm* in Five- and Tenfold Symmetries

Following the introduction given in Chap. 1, it is understood that the sign 10 in the symbol 10*mm* represents a tenfold rotation symmetry and that *m* where signifies a mirror symmetry. The sign 10*mm* therefore means a combined operation of one rotation symmetry and two mirror symmetries. For other signs, the explanation is similar.

The point groups 5*m* and 10*mm* quasicrystals are quasicrystals with fivefold and tenfold symmetries, respectively, whose plane elasticity has been studied earlier, see, e.g. in reviews given by Fan and Mai [5] or by Hu et al. [6] or by Bohsung et al. [7]. The first solution of dislocation of pentagonal quasicrystals was given by De and Pelcovis [8], according to our understand which is the solution for point group 5*m* two-dimensional quasicrystal. The formulation and the solution method developed here and hereafter are quite different from those given by Ref. [8].

The diffraction pattern and relevant Penrose tiling are shown in Figs. 6.1 and 6.2. The Penrose tiling of pentagonal quasicrystals was shown in Chap. 3.

Quasicrystals with these symmetries belong to two-dimensional quasicrystals, i.e., the atomic arrangement is quasiperiodic in a plane, and periodic in the third direction. For clarity, the quasicrystals can be defined as being generated by stacking from planar quasiperiodic structures of fivefold or tenfold symmetry along the third symmetry axis. Here, the quasiperiodic plane is the *xy*-plane, and the fivefold or tenfold rotational axis is the *z*-axis, which is the only axis of symmetry.

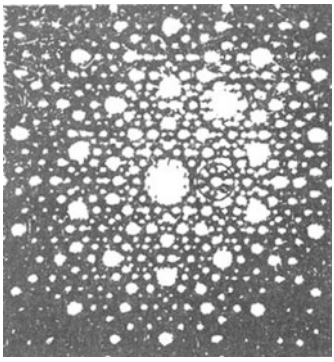

Fig. 6.1 Diffraction pattern of two-dimensional quasicrystal with tenfold symmetry

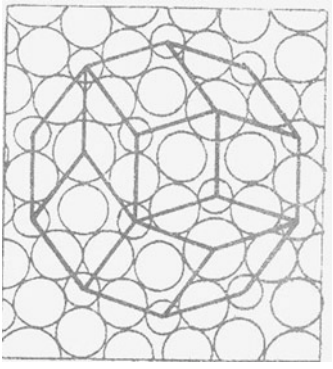

Fig. 6.2 Penrose tiling of point group 10*mm* of tenfold symmetry quasicrystals

Due to the presence of scaling of incommensurate length in the quasiperiodic plane, it leads to the additional degree of freedom that does not hold in conventional crystals, named the phason field **w**.

Although two-dimensional quasicrystal can be understood as a stacked planar quasiperiodic structure along the periodic symmetrical axis, it is three-dimensional in elasticity and is different from the plane problem in classical elasticity. And it can be decomposed into plane and anti-plane elasticity in special cases. We here consider only the plane elasticity, because the anti-plane elasticity is a classical one and independent of phason variables.

Tables 6.2, 6.3, 6.4, 6.5 and 6.6 listed all the elastic constants. Considering a plane in two-dimensional quasicrystals and assume that it is perpendicular to the periodic symmetrical axis (e.g. axis z). In this case,

$$\mathbf{u} = (u_x, u_y, u_z), \quad \mathbf{w} = (w_x, w_y, 0)$$

so the strains are $w_{zz} = w_{zx} = w_{xz} = w_{zy} = w_{yz} = 0$. Assumption (6.0.1) leads to $\varepsilon_{zz} = \varepsilon_{xz} = \varepsilon_{yz} = 0$, and Table 6.2 is simplified to the following Table 6.10 for phonon elastic constants for the plane elasticity.

The phonon elastic constants listed in Table 6.10 can be expressed in fourth-order tensor

$$C_{ijkl} = L\delta_{ij}\delta_{kl} + M(\delta_{jk}\delta_{jl} + \delta_{il}\delta_{jk}) \quad (i,j,k,l = 1,2) \tag{6.1.1}$$

$$L = C_{12}, \quad M = (C_{11} - C_{12})/2 = C_{66} \tag{6.1.2}$$

There are only two independent phonon elastic constants.

What data given in Table 6.10 and relation by Eqs. (6.1.1), (6.1.2) hold for all two-dimensional quasicrystals for the plane elasticity.

In the plane elasticity for two-dimensional quasicrystals with point groups $5m$, $52, \bar{5}m$, $10mm$, 1022, $\overline{10}m2$ and $10/mmm$, Table 6.3 is simplified to Table 6.11.

Table 6.10 Phonon elastic constants for plane elasticity of two-dimensional quasicrystals

	11	22	12	21
11	C_{11}	C_{12}	0	0
22	C_{12}	C_{11}	0	0
12	0	0	C_{66}	C_{66}
21	0	0	C_{66}	C_{66}

Table 6.11 Phason elastic constants for plane elasticity for point group 10*mm* quasicrystals

	11	22	12	21
11	K_1	K_2	0	0
22	K_2	K_1	0	0
12	0	0	K_1	$-K_2$
21	0	0	$-K_2$	K_1

Table 6.12 Phonon-phason coupling elastic constants for plane elasticity

$\varepsilon_{ij}\backslash w_{ij}$	11	22	12	21
11	R	R	0	0
22	$-R$	$-R$	0	0
12	0	0	$-R$	R
21	0	0	$-R$	R

This means

$$\begin{aligned} K_{1111} &= K_{2222} = K_{2121} = K_1 \\ K_{1122} &= K_{2211} = -K_{2112} = -K_{1221} = K_2 \end{aligned} \tag{6.1.3}$$

and other $K_{ijkl} = 0$, and the expression of them by tensor of four rank is

$$K_{ijkl} = K_1\delta_{ik}\delta_{jl} + K_2(\delta_{ij}\delta_{kl} - \delta_{il}\delta_{jk}) \quad (i,j,k,l = 1,2) \tag{6.1.4}$$

And Table 6.4 in the present case is simplified into Table 6.12 as follows. This shows that

$$R_{1111} = R_{1122} = -R_{2222} = R_{1221} = R_{2121} = -R_{1212} = -R_{2211} = -R_{2112} = R \tag{6.1.5}$$

or

$$R_{ijkl} = R(\delta_{i1} - \delta_{i2})(\delta_{ij}\delta_{kl} - \delta_{ik}\delta_{jl} + \delta_{il}\delta_{jk}) \quad (i,j,k,l = 1,2) \tag{6.1.6}$$

One can find that for plane elasticity point group 5*m* have the same elastic constants with point group 10*mm*, so they can be discussed in the same line.

The definition of strain tensor is as given in Chap. 4, that is,

$$\varepsilon_{ij} = \frac{1}{2}\left(\frac{\partial u_i}{\partial x_j} + \frac{\partial u_j}{\partial x_i}\right), \quad w_{ij} = \frac{\partial w_i}{\partial x_j} \tag{6.1.7}$$

In Chap. 4, it was seen that the stress, strain and elastic constant tensors can be expressed by matrices. The above-mentioned elastic constants may be denoted by matrix $[CKR]$. For the present case, the strain vector defined by (4.4.12) is simplified into

$$[\varepsilon_{ij}\ \ w_{ij}] = [\varepsilon_{11}\ \varepsilon_{22}\ \varepsilon_{12}\ \varepsilon_{21}\ w_{11}\ w_{22}\ w_{12}\ w_{21}] \tag{6.1.8}$$

and $[CKR]$ is

$$[CKR] = \begin{bmatrix} L+2M & L & 0 & 0 & R & R & 0 & 0 \\ L & L+2M & 0 & 0 & -R & -R & 0 & 0 \\ 0 & 0 & M & M & 0 & 0 & -R & R \\ 0 & 0 & M & M & 0 & 0 & -R & R \\ R & -R & 0 & 0 & K_1 & K_2 & 0 & 0 \\ R & -R & 0 & 0 & K_2 & K_1 & 0 & 0 \\ 0 & 0 & -R & -R & 0 & 0 & K_1 & -K_2 \\ 0 & 0 & R & R & 0 & 0 & -K_2 & K_1 \end{bmatrix}$$

$$= \begin{bmatrix} L+2M & L & 0 & 0 & R & R & 0 & 0 \\ & L+2M & 0 & 0 & -R & -R & 0 & 0 \\ & & M & M & 0 & 0 & -R & R \\ & & & M & 0 & 0 & -R & R \\ & & & & K_1 & K_2 & 0 & 0 \\ & \text{symmetry} & & & & K_1 & 0 & 0 \\ & & & & & & K_1 & -K_2 \\ & & & & & & & K_1 \end{bmatrix} \tag{6.1.9}$$

The free energy density (or strain energy density)

$$\begin{aligned} F = {} & \frac{1}{2}L\varepsilon_{ii}\varepsilon_{ii} + M\varepsilon_{ij}\varepsilon_{ij} + \frac{1}{2}K_1 w_{ij}w_{ij} + K_2(w_{xx}w_{yy} - w_{xy}w_{xy}) \\ & + R[(\varepsilon_{xx} - \varepsilon_{yy})(w_{xx} + w_{yy}) + 2\varepsilon_{xy}(w_{xy} - w_{yx})] \end{aligned} \tag{6.1.10}$$

From (6.1.9) and (4.5.3) of Chap. 4, or from (6.1.10) and (4.5.1) of Chap. 4, the generalized Hooke's law for plane elasticity of point group 10*mm* quasicrystals of tenfold symmetry is as

$$\left.\begin{aligned} \sigma_{xx} &= L(\varepsilon_{xx} + \varepsilon_{yy}) + 2M\varepsilon_{xx} + R(w_{xx} + w_{yy}) \\ \sigma_{yy} &= L(\varepsilon_{xx} + \varepsilon_{yy}) + 2M\varepsilon_{yy} - R(w_{xx} + w_{yy}) \\ \sigma_{xy} &= \sigma_{yx} = 2M\varepsilon_{xy} + R(w_{yx} - w_{xy}) \\ H_{xx} &= K_1 w_{xx} + K_2 w_{yy} + R(\varepsilon_{xx} - \varepsilon_{yy}) \\ H_{yy} &= K_1 w_{yy} + K_2 w_{xx} + R(\varepsilon_{xx} - \varepsilon_{yy}) \\ H_{xy} &= K_1 w_{xy} - K_2 w_{yx} - 2R\varepsilon_{xy} \\ H_{yx} &= K_1 w_{yx} - K_2 w_{xy} + 2R\varepsilon_{xy} \end{aligned}\right\} \tag{6.1.11}$$

In addition, for anti-plane elasticity there is

$$\left.\begin{aligned}\sigma_{xz} &= 2M\varepsilon_{xz}\\ \sigma_{yz} &= 2M\varepsilon_{yz}\end{aligned}\right\} \tag{6.1.12}$$

Monograph [9] pointed first out that (6.1.9)–(6.1.11) hold for the plane elasticity for both point group $5m$ and point group $10mm$, this identical to the argument of Ref. [6].

Equations (6.1.11) are the physical basis of elasticity of point groups $5m$ and $10mm$ quasicrystals. The geometry (or kinetics) basis of the subject is Eq. (6.1.7). Another necessary basis comes from statics, that is,

$$\left.\begin{aligned}\frac{\partial\sigma_{xx}}{\partial x}+\frac{\partial\sigma_{xy}}{\partial y}=0, \quad \frac{\partial\sigma_{yx}}{\partial x}+\frac{\partial\sigma_{yy}}{\partial y}=0\\ \frac{\partial H_{xx}}{\partial x}+\frac{\partial H_{xy}}{\partial y}=0, \quad \frac{\partial H_{yx}}{\partial x}+\frac{\partial H_{yy}}{\partial y}=0\end{aligned}\right\} \tag{6.1.13}$$

In addition, for the anti-plane elasticity there is

$$\frac{\partial\sigma_{zx}}{\partial x}+\frac{\partial\sigma_{zy}}{\partial y}=0 \tag{6.1.14}$$

Here, the body force density is omitted.

From (6.1.7), (6.1.11) and (6.1.13), we found that there are 18 field variables, i.e., four displacements u_x, u_y, w_x, w_y, seven strains $\varepsilon_{xx}, \varepsilon_{yy}$, $\varepsilon_{xy}=\varepsilon_{yx}, w_{xx}, w_{yy}$, w_{xy}, w_{yx} and seven stresses $\sigma_{xx}, \sigma_{yy}, \sigma_{xy}=\sigma_{yx}, H_{xx}, H_{yy}, H_{xy}, H_{yx}$. And the number of corresponding field equations is also 18, including four equations of statics, seven stress–strain relations and seven equations of deformation geometry. The number of field equations is equal to that of field variables. This means that the mathematical presentation of the problem is consistent and solvable under appropriate boundary conditions. In addition, (6.1.7), (6.1.12) and (6.1.14) give the description of anti-plane pure classical (phonon) elasticity. De and Pelcovits [10] solved the equations for dislocation problem by using the Green function method and iteration procedure. Ding et al. [11] solved the similar problem in terms of Fourier transforms and the Green function method. Taking different way from either De and Pelcovits or Ding et al., we at first reduce the 18 equations into a single partial differential of higher order by introducing some displacement potentials or stress potentials, which enable us to easily solve the problem by the Fourier transform method and complex analysis method. In the following, we derive the final governing equations and fundamental solutions for various quasicrystal systems. And the applications of the theory and methodology will be given in detail in Chaps. 7 and 8 for dislocation and crack problems of quasicrystals, respectively.

6.2 Simplification of the Basic Equation Set: Displacement Potential Function Method

The number of basic equations as given in the previous section is too large and it is very hard to solve them directly. In mathematical physics, a conventional procedure is to reduce the number of field equations. In the classical theory of elasticity, there is a way by introducing the so-called displacement or stress potential functions to realize the purpose, and the procedure is called the displacement potential method or stress potential method, respectively. In this section, we eliminate the stress and strain components in the basic equations and obtain some equilibrium equations expressed by displacement components; thus, the strain compatibility is automatically satisfied. Furthermore, by introducing a displacement potential function, the final governing equations become a single quadruple harmonic equation concerning the displacement potential function; thus, this is the so-called displacement potential method. In the next section, we will introduce the stress potential method, and there the governing equation becomes a single quadruple harmonic equation concerning the stress potential function that would be the so-called stress potential method. In this way, the huge number of equations involving elasticity can be simplified very much.

Substituting (6.1.7) into (6.1.11) and then into (6.1.12), we obtain

$$\left.\begin{aligned}
&M\nabla^2 u_x + (L+M)\tfrac{\partial}{\partial x}\nabla\cdot\mathbf{u} + R\left(\frac{\partial^2 w_x}{\partial x^2} + 2\frac{\partial^2 w_y}{\partial x\partial y} - \frac{\partial w_x}{\partial y^2}\right) = 0\\
&M\nabla^2 u_y + (L+M)\tfrac{\partial}{\partial y}\nabla\cdot\mathbf{u} + R\left(\frac{\partial^2 w_y}{\partial x^2} - 2\frac{\partial^2 w_x}{\partial x\partial y} - \frac{\partial^2 w_y}{\partial y^2}\right) = 0\\
&K_1\nabla^2 w_x + R\left(\frac{\partial^2 u_x}{\partial x^2} - 2\frac{\partial^2 u_y}{\partial x\partial y} - \frac{\partial^2 u_x}{\partial y^2}\right) = 0\\
&K_1\nabla^2 w_y + R\left(\frac{\partial^2 u_y}{\partial x^2} + 2\frac{\partial^2 u_x}{\partial x\partial y} - \frac{\partial^2 u_y}{\partial y^2}\right) = 0
\end{aligned}\right\} \tag{6.2.1}$$

in which

$$\nabla^2 = \frac{\partial^2}{\partial x^2} + \frac{\partial^2}{\partial y^2}, \quad \nabla\cdot\mathbf{u} = \frac{\partial u_x}{\partial x} + \frac{\partial u_y}{\partial y}$$

Equations (6.2.1) are actually the displacement equilibrium equations of the plane elasticity of point group $5m$ with fivefold symmetry or point group $10mm$ tenfold symmetry, as mentioned in the previous section. Here, there are only 4 displacement components u_x, u_y, w_x, w_y, i.e., the number of field variables are only 4, and the number of order of equations is 8.

Observation for the first two equations of (6.2.1) suggests that by introducing the unknown functions $\varphi(x, y)$ and $\psi(x, y)$ as follows:

$$\left.\begin{aligned} u_x &= (L+M)\frac{\partial^2\varphi}{\partial x\partial y} + M\frac{\partial^2\psi}{\partial x^2} + (L+2M)\frac{\partial^2\psi}{\partial y^2} \\ u_y &= -\left[(L+2M)\frac{\partial^2\varphi}{\partial x^2} + M\frac{\partial^2\varphi}{\partial y^2} + (L+M)\frac{\partial^2\psi}{\partial x\partial y}\right] \\ w_x &= -\frac{M(L+2M)}{R}\left[2\frac{\partial^2\varphi}{\partial x\partial y} + \frac{\partial^2\psi}{\partial x^2} - \frac{\partial^2\psi}{\partial y^2}\right] \\ w_y &= \frac{M(L+2M)}{R}\left[\frac{\partial^2\varphi}{\partial x^2} - \frac{\partial^2\varphi}{\partial y^2} - 2\frac{\partial^2\psi}{\partial x\partial y}\right] \end{aligned}\right\} \tag{6.2.2}$$

then the first two equations are automatically satisfied already. Substituting (6.2.2) into the last two equations in (6.2.1), there follows the equations

$$\left.\begin{aligned} (\alpha\Pi_1 + \beta\Pi_2)\tfrac{\partial^2\varphi}{\partial x\partial y} + \left(\alpha\Pi_1\tfrac{\partial^2}{\partial y^2} - \beta\Pi_2\tfrac{\partial^2}{\partial x^2}\right)\psi = 0 \\ \left(\alpha\Pi_2\tfrac{\partial^2}{\partial x^2} - \beta\Pi_1\tfrac{\partial^2}{\partial y^2}\right)\varphi + (\alpha\Pi_2 + \beta\Pi_1)\tfrac{\partial^2\psi}{\partial x\partial y} = 0 \end{aligned}\right\} \tag{6.2.3}$$

where

$$\Pi_1 = 3\frac{\partial^2}{\partial x^2} - \frac{\partial^2}{\partial y^2}, \quad \Pi_2 = 3\frac{\partial^2}{\partial y^2} - \frac{\partial^2}{\partial x^2} \tag{6.2.4}$$

$$\left.\begin{aligned} \alpha &= R(L+2M) - \omega K_1, \beta = RM - \omega K_1 \\ \delta &= RM - \omega K_1, \omega = M(L+2M)/R \end{aligned}\right\} \tag{6.2.5}$$

in which δ will be used in the following formula (6.2.6).

Equation (6.2.3) is much simpler compared with (6.2.1), still it can be simplest by letting

$$\varphi = \left(\beta\Pi_2\frac{\partial^2}{\partial x^2} - \alpha\Pi_1\frac{\partial^2}{\partial y^2}\right)F, \quad \psi = (\alpha\Pi_1 + \delta\Pi_2)\frac{\partial^2 F}{\partial x\partial y} \tag{6.2.6}$$

in which $F(x, y)$ is any function, and then, the first equation of (6.2.3) is satisfied. Substituting (6.2.6) into the second one of Eqs. (6.2.3), after manipulation, it reduces to

$$\nabla^2\nabla^2\nabla^2\nabla^2 F = 0 \tag{6.2.7}$$

This is the final governing equation of the plane elasticity of point groups $5m$ and $10mm$ quasicrystals. We call $F(x, y)$ as a displacement potential function, or simply displacement potential. Equation (6.2.7) is a quadruple harmonic equation, the order of which is much higher than that in the classical elasticity, where that is biharmonic equation.

All of displacement and stress components can be expressed by potential function $F(x, y)$ as follows:

$$\left.\begin{aligned} u_x &= [M\alpha\Pi_1 + (L+2M)\beta\Pi_2]\frac{\partial^2}{\partial x\partial y}\nabla^2 F \\ u_y &= [M\alpha\Pi_1\frac{\partial^2}{\partial y^2} - (L+2M)\beta\Pi_2\frac{\partial^2}{\partial x^2}]\nabla^2 F \end{aligned}\right\} \tag{6.2.8}$$

$$\left.\begin{aligned} w_x &= \omega(\alpha-\beta)\Pi_1\Pi_2\frac{\partial^2}{\partial x\partial y}F \\ w_y &= -\omega\left[\alpha\Pi_1^2\frac{\partial^2}{\partial y^2} + \beta\Pi_2^2\frac{\partial^2}{\partial x^2}\right]F \end{aligned}\right\} \tag{6.2.9}$$

$$\left.\begin{aligned} \sigma_{xx} &= 2M(L+M)\alpha\Pi_1\frac{\partial^3}{\partial y^3}\nabla^2 F \\ \sigma_{yy} &= 2M(L+M)\alpha\Pi_1\frac{\partial^3}{\partial x^2\partial y}\nabla^2 F \\ \sigma_{xy} &= \sigma_{yx} = -2M(L+M)\alpha\Pi_1\frac{\partial^3}{\partial x\partial y^2}\nabla^2 F \end{aligned}\right\} \tag{6.2.10}$$

$$\left.\begin{aligned} H_{xx} &= \alpha\beta\frac{\partial}{\partial y}\nabla^2\nabla^2\nabla^2 F + \omega(K_1-K_2)\frac{\partial}{\partial y}\left(\alpha\Pi_1^2\frac{\partial^2}{\partial y^2} + \beta\Pi_2^2\frac{\partial^2}{\partial x^2}\right)F \\ H_{yy} &= \alpha\beta\frac{\partial}{\partial y}\nabla^2\nabla^2\nabla^2 F - \omega(K_1-K_2)(\alpha-\beta)\Pi_1\Pi_2\frac{\partial^3}{\partial x^2\partial y}F \\ H_{xy} &= -\alpha\beta\frac{\partial}{\partial x}\nabla^2\nabla^2\nabla^2 F - \omega(K_1-K_2)\frac{\partial}{\partial x}\left(\alpha\Pi_1^2\frac{\partial^2}{\partial y^2} + \beta\Pi_2^2\frac{\partial^2}{\partial x^2}\right)F \\ H_{yx} &= \alpha\beta\frac{\partial}{\partial x}\nabla^2\nabla^2\nabla^2 F + \omega(K_1-K_2)(\alpha-\beta)\Pi_1\Pi_2\frac{\partial^3}{\partial x\partial y^2}F \end{aligned}\right\} \tag{6.2.11}$$

Li and Fan [12] have suggested the approach, and the practice shows that it is very effective. In the next two chapters, many applications of the approach will be given.

In addition, (6.1.12) and (6.1.14) yield the final governing equation for anti-plane elasticity

$$\nabla^2 u_z = 0 \tag{6.2.12}$$

It is obvious that the anti-plane problem is decoupled with the plane one.

6.3 Simplification of Basic Equations Set: Stress Potential Function Method

The stress potential method has widely been used in classical theory of elasticity. The author of the book and his students extended it to the study of elasticity of quasicrystals [13, 14].

From (6.1.7), the strain compatibility equations

$$\left.\begin{aligned} &\frac{\partial^2 \varepsilon_{xx}}{\partial y^2}+\frac{\partial^2 \varepsilon_{yy}}{\partial x^2}=2\frac{\partial^2 \varepsilon_{xy}}{\partial x \partial y} \\ &\frac{\partial w_{xy}}{\partial x}=\frac{\partial w_{xx}}{\partial y}, \frac{\partial w_{yx}}{\partial y}=\frac{\partial w_{yy}}{\partial x} \end{aligned}\right\} \tag{6.3.1}$$

The strain components ε_{ij} and w_{ij} can be expressed by the stress components σ_{ij} and H_{ij}, that is,

$$\left.\begin{aligned} \varepsilon_{xx} &= \tfrac{1}{4(L+M)}(\sigma_{xx}+\sigma_{yy})+\tfrac{1}{4C}[(K_1+K_2)(\sigma_{xx}+\sigma_{yy})-2R(H_{xx}+H_{yy})] \\ \varepsilon_{yy} &= \tfrac{1}{4(L+M)}(\sigma_{xx}+\sigma_{yy})-\tfrac{1}{4C}[(K_1+K_2)(\sigma_{xx}+\sigma_{yy})-2R(H_{xx}+H_{yy})] \\ \varepsilon_{xy} &= \varepsilon_{yx}=\tfrac{1}{C}[(K_1+K_2)\sigma_{xy}-R(H_{xy}+H_{yx})] \\ w_{xx} &= \tfrac{1}{2(K_1-K_2)}(H_{xx}-H_{yy})+\tfrac{1}{2C}[M(H_{xx}+H_{yy})-R(\sigma_{xx}-\sigma_{yy})] \\ w_{yy} &= -\tfrac{1}{2(K_1-K_2)}(H_{xx}-H_{yy})+\tfrac{1}{2C}[M(H_{xx}+H_{yy})-R(\sigma_{xx}-\sigma_{yy})] \\ w_{xy} &= \tfrac{1}{C}\left[R\sigma_{xy}-\tfrac{(R^2-MK_1)H_{xy}+(R^2-MK_2)H_{yx}}{K_1-K_2}\right] \\ w_{yx} &= \tfrac{1}{C}\left[-R\sigma_{xy}-\tfrac{(R^2-MK_1)H_{xy}+(R^2-MK_2)H_{yx}}{K_1-K_2}\right] \end{aligned}\right\} \tag{6.3.2}$$

with

$$C=M(K_1+K_2)-2R^2 \tag{6.3.3}$$

If substituting (6.3.2) into (6.3.1), one can find that the strain compatibility equations can be expressed by stress components (because they are too long to be listed, but we will give them in Sect. 6.7). In addition, there are equilibrium equations

$$\begin{aligned} &\frac{\partial \sigma_{xx}}{\partial x}+\frac{\partial \sigma_{xy}}{\partial y}=0, \quad \frac{\partial \sigma_{yx}}{\partial x}+\frac{\partial \sigma_{yy}}{\partial y}=0 \\ &\frac{\partial H_{xx}}{\partial x}+\frac{\partial H_{xy}}{\partial y}=0, \quad \frac{\partial H_{yx}}{\partial x}+\frac{\partial H_{yy}}{\partial y}=0 \end{aligned} \tag{6.3.4}$$

So that we have 7 equations in total in which there are 3 compatibility equations expressed by stress components and 4 equilibrium equations, and the number of the unknown functions is also 7, that is, $\sigma_{xx}, \sigma_{yy}, \sigma_{xy}=\sigma_{yx}$, $H_{xx}, H_{yy}, H_{xy}, H_{yx}$. The equation set is closed and is solvable.

If introducing the stress functions φ, ψ_1 and ψ_2 such as

$$\left.\begin{aligned}&\sigma_{xx}=\frac{\partial^2\varphi}{\partial y^2},\sigma_{yy}=\frac{\partial^2\varphi}{\partial x^2},\sigma_{xy}=\sigma_{yx}=-\frac{\partial^2\varphi}{\partial x\partial y}\\&H_{xx}=\frac{\partial\psi_1}{\partial y},H_{xy}=-\frac{\partial\psi_1}{\partial x},H_{yx}=-\frac{\partial\psi_2}{\partial y},H_{yy}=\frac{\partial\psi_2}{\partial x}\end{aligned}\right\}\tag{6.3.5}$$

then the equilibrium equations (6.3.4) are automatically satisfied. Substituting (6.3.5) into deformation compatibility equations expressed by stress components yields

$$\left.\begin{aligned}&\frac{1}{2C(L+M)}\nabla^2\nabla^2\varphi+\frac{K_1+K_2}{2C}\nabla^2\nabla^2\varphi+\frac{R}{C}\left(\frac{\partial}{\partial y}\Pi_1\psi_1-\frac{\partial}{\partial x}\Pi_2\psi_2\right)=0\\&\left(\frac{C}{K_1-K_2}+M\right)\nabla^2\psi_1+R\frac{\partial}{\partial y}\Pi_1\varphi=0\\&\left(\frac{C}{K_1-K_2}+M\right)\nabla^2\psi_2-R\frac{\partial}{\partial x}\Pi_2\varphi=0\end{aligned}\right\}\tag{6.3.6}$$

in which Π_1 and Π_2 defined by (6.2.4), and C is given by (6.3.3). By now, the numbers of equations and unknown functions are reduced to 3.

Now introducing a new unknown function $G(x,y)$ such as

$$\left.\begin{aligned}&\varphi=D\frac{\partial}{\partial y}\Pi_1\nabla^2G\\&\psi_1=-\frac{1}{R}(MK_1-R_2)[(L+2M)(K_1-K_2)-2R^2]\nabla^2\nabla^2\nabla^2G\\&\qquad+(L+M)(K_1-K_2)R\frac{\partial^2}{\partial x\partial y}\Pi_1\Pi_2G\\&\psi_2=(L+M)(K_1-K_2)R\frac{\partial^2}{\partial x\partial y}\Pi_1\Pi_2G\end{aligned}\right\}\tag{6.3.7}$$

If

$$\nabla^2\nabla^2\nabla^2\nabla^2G=0\tag{6.3.8}$$

then Eq. (6.3.6) are satisfied, in which

$$D=2(MK_1-R^2)(L+M)\tag{6.3.9}$$

At the same time, Eq. (6.2.12) holds too for anti-plane elasticity.

6.4 Plane Elasticity of Point Group 5, $\overline{5}$ and 10, $\overline{10}$ Pentagonal and Decagonal Quasicrystals

For plane elasticity, the fivefold and tenfold symmetries quasicrystals of point groups $5,\overline{5}$ and $10,\overline{10}$ are different in elasticity with that of point groups $5m$ and $10mm$, the difference lies in only the phonon-phason coupling elastic constants, in which the former has two coupling elastic constants R_1 and R_2 rather than one R. So that we have

$$R_{ijkl} = R_1(\delta_{i1} - \delta_{i2})(\delta_{ij}\delta_{kl} - \delta_{ik}\delta_{jl} + \delta_{il}\delta_{jk}) + R_2[(1 - \delta_{ij})\delta_{kl} + \delta_{ij}(\delta_{i1} - \delta_{i2})(\delta_{k1}\delta_{l2} - \delta_{k2}\delta_{l1})] \quad i,j,k,l = 1,2 \tag{6.4.1}$$

Apart from this, the phonon and phason elastic constants of point group $5, \overline{5}$ and point group $10, \overline{10}$ quasicrystals are the same as those of point groups $5m$ and $10mm$. The corresponding elastic constant matrix is

$$[CKR] = \begin{bmatrix} L+2M & L & 0 & 0 & R_1 & R_1 & R_2 & -R_2 \\ L & L+2M & 0 & 0 & -R_1 & -R_1 & -R_2 & R_2 \\ 0 & 0 & M & M & R_2 & R_2 & -R_1 & R_1 \\ 0 & 0 & M & M & R_2 & R_2 & -R_1 & R_1 \\ R_1 & -R_1 & R_2 & R_2 & K_1 & K_2 & 0 & 0 \\ R_1 & -R_1 & R_2 & R_2 & K_2 & K_1 & 0 & 0 \\ R_2 & -R_2 & -R_1 & -R_1 & 0 & 0 & K_1 & -K_2 \\ -R_2 & R_2 & R_1 & R_1 & 0 & 0 & -K_2 & K_1 \end{bmatrix}$$

$$= \begin{bmatrix} L+2M & L & 0 & 0 & R_1 & R_1 & R_2 & -R_2 \\ & L+2M & 0 & 0 & -R_1 & -R_1 & -R_2 & R_2 \\ & & M & M & R_2 & R_2 & -R_1 & R_1 \\ & & & M & R_2 & R_2 & -R_1 & R_1 \\ & \text{symmetry} & & & K_1 & K_2 & 0 & 0 \\ & & & & & K_1 & 0 & 0 \\ & & & & & & K_1 & -K_2 \\ & & & & & & & K_1 \end{bmatrix} \tag{6.4.2}$$

According to this elastic constant matrix, the stress–strain relation can be written as

$$\left.\begin{aligned} \sigma_{xx} &= L(\varepsilon_{xx} + \varepsilon_{yy}) + 2M\varepsilon_{xx} + R_1(w_{xx} + w_{yy}) + R_2(w_{xy} - w_{yx}) \\ \sigma_{yy} &= L(\varepsilon_{xx} + \varepsilon_{yy}) + 2M\varepsilon_{yy} - R_1(w_{xx} + w_{yy}) - R_2(w_{xy} - w_{yx}) \\ \sigma_{xy} &= \sigma_{yx} = 2M\varepsilon_{xy} + R_1(w_{yx} - w_{xy}) + R_2(w_{xx} + w_{yy}) \\ H_{xx} &= K_1 w_{xx} + K_2 w_{yy} + R_1(\varepsilon_{xx} - \varepsilon_{yy}) + 2R_2\varepsilon_{xy} \\ H_{yy} &= K_1 w_{yy} + K_2 w_{xx} + R_1(\varepsilon_{xx} - \varepsilon_{yy}) + 2R_2\varepsilon_{xy} \\ H_{xy} &= K_1 w_{xy} - K_2 w_{yx} - 2R_1\varepsilon_{xy} + R_2(\varepsilon_{xx} - \varepsilon_{yy}) \\ H_{yx} &= K_1 w_{yx} - K_2 w_{xy} + 2R_1\varepsilon_{xy} - R_2(\varepsilon_{xx} - \varepsilon_{yy}) \end{aligned}\right\} \tag{6.4.3}$$

In addition, the stresses σ_{ij} and H_{ij} satisfy the same equilibrium equations as (6.1.13).

Substituting (6.1.7) into (6.4.3) then into (6.1.12) leads to the equilibrium equations expressed by displacements such as

$$\begin{aligned}
M\nabla^2 u_x + (L+M)\frac{\partial}{\partial x}\nabla\cdot\mathbf{u} + R_1\left(\frac{\partial^2 w_x}{\partial x^2} + 2\frac{\partial^2 w_y}{\partial x\partial y} - \frac{\partial^2 w_x}{\partial y^2}\right) - R_2\left(\frac{\partial^2 w_y}{\partial x^2} - 2\frac{\partial^2 w_x}{\partial x\partial y} - \frac{\partial^2 w_y}{\partial y^2}\right) &= 0\\
M\nabla^2 u_y + (L+M)\frac{\partial}{\partial y}\nabla\cdot\mathbf{u} + R_1\left(\frac{\partial^2 w_y}{\partial x^2} - 2\frac{\partial^2 w_x}{\partial x\partial y} - \frac{\partial^2 w_y}{\partial y^2}\right) + R_2\left(\frac{\partial^2 w_x}{\partial x^2} + 2\frac{\partial^2 w_y}{\partial x\partial y} - \frac{\partial^2 w_x}{\partial y^2}\right) &= 0\\
K_1\nabla^2 w_x + R_1\left(\frac{\partial^2 u_x}{\partial x^2} - 2\frac{\partial^2 u_y}{\partial x\partial y} - \frac{\partial^2 u_x}{\partial y^2}\right) + R_2\left(\frac{\partial^2 u_y}{\partial x^2} + 2\frac{\partial^2 u_x}{\partial x\partial y} - \frac{\partial^2 u_y}{\partial y^2}\right) &= 0\\
K_1\nabla^2 w_y + R_1\left(\frac{\partial^2 u_y}{\partial x^2} + 2\frac{\partial^2 u_x}{\partial x\partial y} - \frac{\partial^2 u_y}{\partial y^2}\right) - R_2\left(\frac{\partial^2 u_x}{\partial x^2} - 2\frac{\partial^2 u_y}{\partial x\partial y} - \frac{\partial^2 u_x}{\partial y^2}\right) &= 0
\end{aligned} \tag{6.4.4}$$

The equations are similar to those of (6.2.1), the definitions on operators ∇^2 and $\nabla\cdot$ are the same there. It is obvious that Eq. (6.4.4) are more complex than those of (6.2.1). We now simplify the equations in terms of the displacement potential function method.

Introducing displacement potentials $\varphi(x,y)$ and $\psi(x,y)$ as below,

$$\left.\begin{aligned}
u_x &= (L+M)\frac{\partial^2\varphi}{\partial x\partial y} + M\frac{\partial^2\psi}{\partial x^2} + (L+2M)\frac{\partial^2\psi}{\partial y^2}\\
u_y &= -\left[(L+2M)\frac{\partial^2\varphi}{\partial x^2} + M\frac{\partial^2\varphi}{\partial y^2} + (L+M)\frac{\partial^2\psi}{\partial x\partial y}\right]\\
w_x &= -\omega\left\{\left[2R_1\frac{\partial^2}{\partial x\partial y} - R_2\left(\frac{\partial^2}{\partial x^2} - \frac{\partial^2}{\partial y^2}\right)\right]\varphi + \left[R_1\left(\frac{\partial^2}{\partial x^2} - \frac{\partial^2}{\partial y^2}\right) + 2R_2\frac{\partial^2}{\partial x\partial y}\right]\psi\right\}\\
w_y &= \omega\left\{\left[R_1\left(\frac{\partial^2}{\partial x^2} - \frac{\partial^2}{\partial y^2}\right) + 2R_2\frac{\partial^2}{\partial x\partial y}\right]\varphi - \left[2R_1\frac{\partial^2}{\partial x\partial y} - R_2\left(\frac{\partial^2}{\partial x^2} - \frac{\partial^2}{\partial y^2}\right)\right]\psi\right\}
\end{aligned}\right\} \tag{6.4.5}$$

in which

$$\omega = \frac{M(L+2M)}{R^2}, \quad R^2 = R_1^2 + R_2^2 \tag{6.4.6}$$

The functions $\varphi(x,y)$ and $\psi(x,y)$ defined by (6.4.5) automatically satisfy the first two of Eq. (6.4.4), and the substitution of formulas (6.4.6) into the second two of Eq. (6.4.4) results in

$$\left.\begin{aligned}
(L+2M)c_2\frac{\partial}{\partial x}\Lambda_1\varphi + Mc_1\frac{\partial}{\partial y}\Lambda_2\varphi + (L+2M)c_2\frac{\partial}{\partial y}\Lambda_1\psi - Mc_1\frac{\partial}{\partial x}\Lambda_2\psi &= 0\\
(L+2M)c_2\frac{\partial}{\partial x}\Lambda_2\varphi - Mc_1\frac{\partial}{\partial y}\Lambda_1\varphi + (L+2M)c_2\frac{\partial}{\partial y}\Lambda_2\psi + Mc_1\frac{\partial}{\partial x}\Lambda_1\psi &= 0
\end{aligned}\right\} \tag{6.4.7}$$

with

$$\left.\begin{aligned}\Lambda_1 &= R_1\frac{\partial}{\partial y}\Pi_1 + R_2\frac{\partial}{\partial x}\Pi_2\\ \Lambda_2 &= R_1\frac{\partial}{\partial x}\Pi_2 - R_2\frac{\partial}{\partial y}\Pi_1\end{aligned}\right\} \tag{6.4.8}$$

$$c_1 = (L+2M)K_1 - R^2, \quad c_2 = MK_1 - R^2 \tag{6.4.9}$$

If we introduce a new function $F(x,y)$ by means of

$$\left.\begin{aligned}\varphi &= -(L+2M)c_2R\frac{\partial}{\partial y}\Lambda_1 F + Mc_1R\frac{\partial}{\partial x}\Lambda_2 F\\ \psi &= (L+2M)c_2R\frac{\partial}{\partial x}\Lambda_1 F + Mc_1R\frac{\partial}{\partial y}\Lambda_2 F\end{aligned}\right\} \tag{6.4.10}$$

Then, the first one of Eq. (6.4.7) is automatically satisfied, and from the second one we find that

$$\nabla^2\nabla^2\nabla^2\nabla^2 F = 0 \tag{6.4.11}$$

The definitions of operators ∇^2 and $\nabla\cdot$ are the same as before.

All components of displacement vectors and stress tensors can be expressed by the potential function $F(x,y)$, for example,

$$u_x = R\left[c_2\frac{\partial}{\partial x}\Lambda_1 + c_1\frac{\partial}{\partial y}\Lambda_2\right]\nabla^2 F \tag{6.4.12a}$$

$$u_y = R\left[c_2\frac{\partial}{\partial y}\Lambda_1 - c_1\frac{\partial}{\partial x}\Lambda_2\right]\nabla^2 F \tag{6.4.12b}$$

$$w_x = -c_0\Lambda_1\Lambda_2 F \tag{6.4.12c}$$

$$w_y = -R^{-1}[c_2(L+2M)\Lambda_1^2 + c_1M\Lambda_2^2]F \tag{6.4.12d}$$

$$\sigma_{xx} = 2c_0c_2\frac{\partial^2}{\partial y^2}\Lambda_1\nabla^2 F \tag{6.4.12e}$$

$$\sigma_{yy} = 2c_0c_2\frac{\partial^2}{\partial x^2}\Lambda_1\nabla^2 F \tag{6.4.12f}$$

$$\sigma_{xy} = \sigma_{yx} = -2c_0c_2\frac{\partial^2}{\partial x\partial y}\Lambda_1\nabla^2 F \tag{6.4.12g}$$

$$H_{xx} = -c_1c_2R\frac{\partial}{\partial y}\nabla^2\nabla^2\nabla^2 F + R^{-1}K_0\frac{\partial}{\partial y}[c_2(L+2M)\Lambda_1^2 + c_1M\Lambda_2^2]F \tag{6.4.12h}$$

$$H_{xy} = c_1 c_2 R \frac{\partial}{\partial x} \nabla^2 \nabla^2 \nabla^2 F - R^{-1} K_0 \frac{\partial}{\partial x} [c_2 (L + 2M) \Lambda_1^2 + c_1 M \Lambda_2^2] F \tag{6.4.12i}$$

$$H_{yx} = -c_1 c_2 R \frac{\partial}{\partial x} \nabla^2 \nabla^2 \nabla^2 F - c_0 K_0 \frac{\partial}{\partial y} \Lambda_1 \Lambda_2 F \tag{6.4.12j}$$

$$H_{yy} = -c_1 c_2 R \frac{\partial}{\partial y} \nabla^2 \nabla^2 \nabla^2 F + c_0 K_0 \frac{\partial}{\partial x} \Lambda_1 \Lambda_2 F \tag{6.4.12k}$$

with

$$c_0 = R(L + M), \quad K_0 = K_1 - K_2 \tag{6.4.13}$$

The results were given by Li and Fan [15], Li et al. [16]. Recently, Li and Fan [14] have derived the final governing equation of elasticity of the same point groups through the stress potential method, the resulting equation is also quadruple harmonic equation; of course, the unknown function is the stress potential. Due to the limitation of the space, the derivation about this is omitted, but whose application will be shown in Chap. 8 for solving notch problem of point group $5, \overline{5}$ and point group $10, \overline{10}$ two-dimensional quasicrystals.

The frequent appearance of quadruple harmonic equations in (6.2.7), (6.3.8) and (6.4.11) shows that this kind of equations is very important in theory and practice.

6.5 Plane Elasticity of Point Group 12*mm* of Dodecagonal Quasicrystals

Point group 12*mm* dodecagonal quasicrystals belong to the two-dimensional; the Penrose tiling and the diffraction pattern are shown in Figs. 6.3 and 6.4, respectively. If taking z-axis as periodic arrangement direction, and supposing that the field variables independent from the coordinate z, then the elasticity problem can be decomposed into a plane elasticity and anti-plane elasticity.

As mentioned in previous sections, the quasiperiodic plane is taken as xy-plane, so the z-axis represents the 12-fold symmetry axis. Like that in other two-dimensional quasicrystals, the quasiperiodic plane is an elastic isotropic plane. There are two nonzero independent elastic constants in the plane, that is, L and M

$$L = C_{12}, \quad M = (C_{11} - C_{12})/2 = C_{66} \tag{6.5.1}$$

Here, we have nonzero K_{ijkl} as

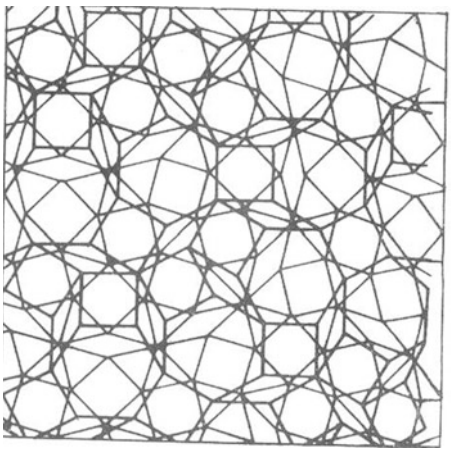

Fig. 6.3 Penrose tiling of dodecagonal quasicrystal

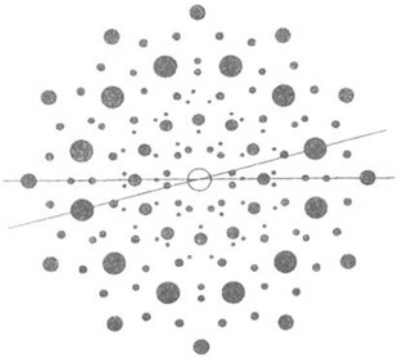

Fig. 6.4 Diffraction pattern of quasicrystal of 12-fold symmetry, in the condition of the phason strain field being uniformly

$$\left.\begin{aligned} K_{1111} = K_{2222} = K_1, K_{1122} = K_{2211} = K_2 \\ K_{1221} = K_{2112} = K_3, K_{2121} = K_{1212} = K_1 + K_2 + K_3 \end{aligned}\right\} \tag{6.5.2}$$

and others are zero. The results can also be expressed

$$\begin{aligned} K_{ijkl} = {} & (K_1 - K_2 - K_3)(\delta_{ik} - \delta_{il}) + K_2\delta_{ij}\delta_{kl} + K_3\delta_{il}\delta_{jk} \\ & + 2(K_2 + K_3)(\delta_{i1}\delta_{j2}\delta_{k1}\delta_{l2} + \delta_{i2}\delta_{j1}\delta_{k2}\delta_{l1}) \quad (i,j,k,l = 1,2) \end{aligned} \tag{6.5.3}$$

In addition, the phonon and phason are decoupled, that is,

$$R_{ijkl} = 0 \tag{6.5.4}$$

The elastic constant matrix is

$$[CKR] = \begin{bmatrix} L+2M & L & 0 & 0 & 0 & 0 & 0 & 0 \\ L & L+2M & 0 & 0 & 0 & 0 & 0 & 0 \\ 0 & 0 & M & M & 0 & 0 & 0 & 0 \\ 0 & 0 & M & M & 0 & 0 & 0 & 0 \\ 0 & 0 & 0 & 0 & K_1 & K_2 & 0 & 0 \\ 0 & 0 & 0 & 0 & K_2 & K_1 & 0 & 0 \\ 0 & 0 & 0 & 0 & 0 & 0 & K_1+K_2+K_3 & K_3 \\ 0 & 0 & 0 & 0 & 0 & 0 & K_3 & K_1+K_2+K_3 \end{bmatrix}$$

$$= \begin{bmatrix} L+2M & L & 0 & 0 & 0 & 0 & 0 & 0 \\ & L+2M & 0 & 0 & 0 & 0 & 0 & 0 \\ & & M & M & 0 & 0 & 0 & 0 \\ & & & M & 0 & 0 & 0 & 0 \\ & & & & K_1 & K_2 & 0 & 0 \\ & & \text{symmetry} & & & K_1 & 0 & 0 \\ & & & & & & K_1+K_2+K_3 & K_3 \\ & & & & & & & K_1+K_2+K_3 \end{bmatrix} \tag{6.5.5}$$

The relevant free energy density (or strain energy density)

$$\begin{aligned} F = {} & \frac{1}{2}L(\nabla \cdot u)^2 + M\varepsilon_{ij}\varepsilon_{ij} + \frac{1}{2}K_1 w_{ij}w_{ij} \\ & + \frac{1}{2}K_2(w_{yx}^2 + w_{xy}^2 + 2w_{xx}w_{yy}) + \frac{1}{2}K_3(w_{yx} + w_{xy})^2 \end{aligned} \tag{6.5.6}$$

where ε_{ij} and w_{ij} denote the strain tensors

$$\varepsilon_{ij} = \frac{1}{2}\left(\frac{\partial u_i}{\partial x_j} + \frac{\partial u_j}{\partial x_i}\right), \quad w_{ij} = \frac{\partial w_i}{\partial x_j} \tag{6.5.7}$$

From (4.5.1) of Chap. 4 and (6.5.5) or (6.5.6), one can find the generalized Hooke's law for plane elasticity of dodecagonal quasicrystals as follows:

$$\left.\begin{aligned} \sigma_{xx} &= L(\varepsilon_{xx} + \varepsilon_{yy}) + 2M\varepsilon_{xx} \\ \sigma_{yy} &= L(\varepsilon_{xx} + \varepsilon_{yy}) + 2M\varepsilon_{yy} \\ \sigma_{xy} &= \sigma_{yx} = 2M\varepsilon_{xy} \\ H_{xx} &= K_1 w_{xx} + K_2 w_{yy} \\ H_{yy} &= K_1 w_{yy} + K_2 w_{xx} \\ H_{xy} &= (K_1 + K_2 + K_3)w_{xy} + K_3 w_{yx} \\ H_{yx} &= (K_1 + K_2 + K_3)w_{yx} + K_3 w_{xy} \end{aligned}\right\} \tag{6.5.8}$$

and there are the equilibrium equations when the body force is ignored

$$\left.\begin{aligned} &\frac{\partial \sigma_{xx}}{\partial x}+\frac{\partial \sigma_{xy}}{\partial y}=0, \quad \frac{\partial \sigma_{yx}}{\partial x}+\frac{\partial \sigma_{yy}}{\partial y}=0 \\ &\frac{\partial H_{xx}}{\partial x}+\frac{\partial H_{xy}}{\partial y}=0, \quad \frac{\partial H_{yx}}{\partial x}+\frac{\partial H_{yy}}{\partial y}=0 \end{aligned}\right\} \tag{6.5.9}$$

Eliminating stress and strain components from (6.5.7), (6.5.8) and (6.5.9), we obtain the equilibrium equations expressed by displacement components as below:

$$\left.\begin{aligned} &M\nabla^2 u_x+(L+M)\frac{\partial}{\partial x}\nabla\cdot\mathbf{u}=0 \\ &M\nabla^2 u_y+(L+M)\frac{\partial}{\partial y}\nabla\cdot\mathbf{u}=0 \\ &K_1\nabla^2 w_x+(K_2+K_3)\frac{\partial}{\partial y}\left(\frac{\partial w_x}{\partial y}+\frac{\partial w_y}{\partial x}\right)=0 \\ &K_1\nabla^2 w_y+(K_2+K_3)\frac{\partial}{\partial x}\left(\frac{\partial w_x}{\partial y}+\frac{\partial w_y}{\partial x}\right)=0 \end{aligned}\right\} \tag{6.5.10}$$

If defining two displacement potentials $F(x,y)$ and $G(x,y)$ such as

$$\left.\begin{aligned} u_x &= (L+M)\frac{\partial^2 F}{\partial x\partial y} \\ u_y &= -(L+2M)\frac{\partial^2 F}{\partial x^2}-M\frac{\partial^2 F}{\partial y^2} \\ w_x &= (K_2+K_3)\frac{\partial^2 G}{\partial x\partial y} \\ w_y &= -K_1\frac{\partial^2 G}{\partial x^2}-(K_1+K_2+K_3)\frac{\partial^2 G}{\partial y^2} \end{aligned}\right\} \tag{6.5.11}$$

then Eq. (6.5.10) will be reduced to

$$\nabla^2\nabla^2 F=0, \quad \nabla^2\nabla^2 G=0 \tag{6.5.12}$$

which is found in Ref. [12] at first.

One can see that the problem is concluded to solve two biharmonic equations, and the theory and method studying this kind of equations are well developed in the theory of classical elasticity, which can be used in studying elasticity of quasicrystals. In this respect, the most systematic method is the complex variable function method. If assume $\phi_1(z), \psi_1(z), \pi_1(z)$ and $\chi_1(z)$ are analytic functions of complex variable $z=x+\mathrm{i}y$ $(\mathrm{i}=\sqrt{-1})$, then

$$\left.\begin{aligned} F(x,y) &= \mathrm{Re}[\bar{z}\varphi_1(z)+\int\psi_1(z)\mathrm{d}z] \\ G(x,y) &= \mathrm{Re}[\bar{z}\pi_1(z)+\int\chi_1(z)\mathrm{d}z] \end{aligned}\right\} \tag{6.5.13}$$

where $\bar{z}=x-\mathrm{i}y$ and Re denotes the real part of a complex number. Theory of analytic functions is a powerful tool to solve the boundary value problems of harmonic, biharmonic and multiple harmonic equations; the work on quadruple and sextuple harmonic equations is developed by the study of elasticity of quasicrystals,

and the details will be given in the successive chapters. As a complete description for the new development of the method, some detailed summarization will be displayed in Chap. 11.

Since 2004 the 12-fold quasicrystals observed in liquid crystals, colloids and polymers as pointed out in Chap. 3; this is very interesting and explores the importance of dodecagonal quasicrystals not only in solid but also in soft matter. Relevant discussion will be given in Appendix D in detail; of course, the scope of the discussion goes beyond elasticity.

6.6 Plane Elasticity of Point Group 8*mm* of Octagonal Quasicrystals, Displacement Potential

Octagonal quasicrystals belong to two-dimensional quasicrystals, the Penrose tiling of its quasiperiodic plane is shown in Fig. 6.5. The stowing of planes along the third direction perpendicular them will result the quasicrystals.

In the following considering only a simple case of elasticity of the material, i.e., all of the field variables are independent from the axis along which the atom arrangement is periodic. In the case, the elasticity can be decomposed into a plane elasticity and anti-plane elasticity. We focus on the solution for the plane elasticity. Within the quasiperiodic plane, the phonon elasticity is isotropic, so C_{ijkl} are the same of those discussed in previous sections. The phason elasticity here is anisotropic, but K_{ijkl} are the same with those of point group 12*mm* quasicrystals. Between phonon and phason fields there is coupling, the corresponding elastic constants R_{ijkl} are the same given by (6.1.6), that is,

$$R_{ijkl} = R(\delta_{i1} - \delta_{i2})(\delta_{ij}\delta_{kl} - \delta_{ik}\delta_{jl} + \delta_{il}\delta_{jk}) \quad (i,j,k,l = 1,2) \tag{6.6.1}$$

such that we have the elastic constants matrix

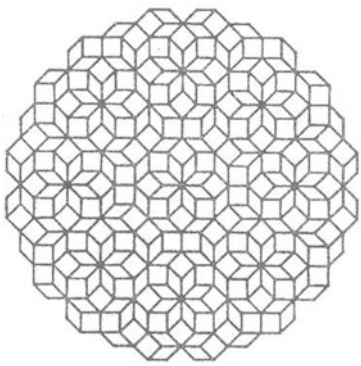

Fig. 6.5 Penrose tiling of eightfold symmetry quasicrystal

$$[CKR] = \begin{bmatrix} L+2M & L & 0 & 0 & R & R & 0 & 0 \\ L & L+2M & 0 & 0 & -R & -R & 0 & 0 \\ 0 & 0 & M & M & 0 & 0 & -R & R \\ 0 & 0 & M & M & 0 & 0 & -R & R \\ R & -R & 0 & 0 & K_1 & K_2 & 0 & 0 \\ R & -R & 0 & 0 & K_2 & K_1 & 0 & 0 \\ 0 & 0 & -R & -R & 0 & 0 & K_1+K_2+K_3 & K_3 \\ 0 & 0 & R & R & 0 & 0 & K_3 & K_1+K_2+K_3 \end{bmatrix}$$

$$= \begin{bmatrix} L+2M & L & 0 & 0 & R & R & 0 & 0 \\ & L+2M & 0 & 0 & -R & -R & 0 & 0 \\ & & M & M & 0 & 0 & -R & R \\ & & & M & 0 & 0 & -R & R \\ & & & & K_1 & K_2 & 0 & 0 \\ & & \text{symmetry} & & & K_1 & 0 & 0 \\ & & & & & & K_1+K_2+K_3 & K_3 \\ & & & & & & & K_1+K_2+K_3 \end{bmatrix} \tag{6.6.2}$$

The corresponding free energy density is

$$F = \frac{1}{2}L(\nabla \cdot \mathbf{u})^2 + M\varepsilon_{ij}\varepsilon_{ij} + \frac{1}{2}K_1 w_{ij}w_{ij} + \frac{1}{2}K_2(w_{xy}^2 + w_{yx}^2 + 2w_{xx}w_{yy}) + \frac{1}{2}K_3(w_{xy}+w_{yx})^2 + R[(\varepsilon_{xx}-\varepsilon_{yy})(w_{xx}+w_{yy}) + 2\varepsilon_{xy}(w_{yx}-w_{xy})] \tag{6.6.3}$$

where ε_{ij} and w_{ij} are defined as before, and it is not listed again.

From (6.6.3) and (4.5.1), the generalized Hooke's law can be expressed as

$$\left.\begin{aligned} \sigma_{xx} &= L(\varepsilon_{xx}+\varepsilon_{yy}) + 2M\varepsilon_{xx} + R(w_{xx}+w_{yy}) \\ \sigma_{yy} &= L(\varepsilon_{xx}+\varepsilon_{yy}) + 2M\varepsilon_{yy} - R(w_{xx}+w_{yy}) \\ \sigma_{xy} &= \sigma_{yx} = 2M\varepsilon_{xy} + R(w_{yx}-w_{xy}) \\ H_{xx} &= K_1 w_{xx} + K_2 w_{yy} + R(\varepsilon_{xx}-\varepsilon_{yy}) \\ H_{yy} &= K_1 w_{yy} + K_2 w_{xx} + R(\varepsilon_{xx}-\varepsilon_{yy}) \\ H_{xy} &= (K_1+K_2+K_3)w_{xy} + K_3 w_{yx} - 2R\varepsilon_{xy} \\ H_{yx} &= (K_1+K_2+K_3)w_{yx} + K_3 w_{xy} + 2R\varepsilon_{xy} \end{aligned}\right\} \tag{6.6.4}$$

For saving the space, similar discussion on stress equilibrium equations is omitted.

Through a similar procedure, equilibrium equations given by displacement components are as follows:

$$\left.\begin{aligned}
&M\nabla^2 u_x+(L+M)\frac{\partial}{\partial x}\nabla\cdot\mathbf{u}+R\left(\frac{\partial^2 w_x}{\partial x^2}+2\frac{\partial^2 w_y}{\partial x\partial y}-\frac{\partial^2 w_x}{\partial y^2}\right)=0\\
&M\nabla^2 u_y+(L+M)\frac{\partial}{\partial y}\nabla\cdot\mathbf{u}+R\left(\frac{\partial^2 w_y}{\partial x^2}-2\frac{\partial^2 w_x}{\partial x\partial y}-\frac{\partial^2 w_y}{\partial y^2}\right)=0\\
&K_1\nabla^2 w_x+(K_2+K_3)\left(\frac{\partial^2 w_x}{\partial y^2}+\frac{\partial^2 w_y}{\partial x\partial y}\right)+R\left(\frac{\partial^2 u_x}{\partial x^2}-2\frac{\partial^2 u_y}{\partial x\partial y}-\frac{\partial^2 u_x}{\partial y^2}\right)=0\\
&K_1\nabla^2 w_y+(K_2+K_3)\left(\frac{\partial^2 w_x}{\partial x\partial y}+\frac{\partial^2 w_y}{\partial x^2}\right)+R\left(\frac{\partial^2 u_y}{\partial x^2}+2\frac{\partial^2 u_x}{\partial x\partial y}-\frac{\partial^2 u_y}{\partial y^2}\right)=0
\end{aligned}\right\}\tag{6.6.5}$$

It is evident that, if $K_2+K_3=0$, the equations will be reduced to (6.2.1). In fact, $K_2+K_3\neq 0$, so the equations are more complex than those given in the previous sections. But the final governing equation for the present case presents more interesting in mathematical physics, we can see immediately.

At first, we introduce two auxiliary function φ and ψ in such a way

$$\left.\begin{aligned}
u_x&=(L+M)\frac{\partial^2\varphi}{\partial x\partial y}+M\frac{\partial^2\psi}{\partial x^2}+(L+2M)\frac{\partial^2\psi}{\partial y^2}\\
u_y&=-\left[(L+2M)\frac{\partial^2\varphi}{\partial x^2}+M\frac{\partial^2\varphi}{\partial y^2}+(L+M)\frac{\partial^2\psi}{\partial x\partial y}\right]\\
w_x&=-\omega\left(2\frac{\partial^2\varphi}{\partial x\partial y}+\frac{\partial^2\psi}{\partial x^2}-\frac{\partial^2\psi}{\partial y^2}\right)\\
w_y&=\omega\left(\frac{\partial^2\varphi}{\partial x^2}-\frac{\partial^2\varphi}{\partial y^2}-2\frac{\partial^2\psi}{\partial x\partial y}\right)
\end{aligned}\right\}\tag{6.6.6}$$

where $\omega=M(L+M)/R$, so that (6.6.5) is simplified as

$$\left.\begin{aligned}
&(\gamma\Pi_1+\delta\Pi_2)\frac{\partial^2\varphi}{\partial x\partial y}+\left(\alpha\Pi_1\frac{\partial^2}{\partial y^2}-\beta\Pi_2\frac{\partial^2}{\partial x^2}\right)\psi=0\\
&(\gamma\Pi_2+\delta\Pi_1)\frac{\partial^2\psi}{\partial x\partial y}+\left(\alpha\Pi_2\frac{\partial^2}{\partial y^2}-\beta\Pi_1\frac{\partial^2}{\partial x^2}\right)\varphi=0
\end{aligned}\right\}\tag{6.6.7}$$

in which

$$\left.\begin{aligned}
&\Pi_1=3\frac{\partial^2}{\partial x^2}-\frac{\partial^2}{\partial y^2},\Pi_2=3\frac{\partial^2}{\partial y^2}-\frac{\partial^2}{\partial x^2}\\
&\alpha=R(L+2M)-\omega(K_1+K_2+K_3)\\
&\beta=RM-\omega K_1,\delta=RM-\omega(K_1+K_2+K_3)\\
&\gamma=R(L+2M)-\omega K_1
\end{aligned}\right\}\tag{6.6.8}$$

and ω is given above. At last, the displacement potential $F(x,y)$ is introduced

$$\left.\begin{aligned}\varphi &= \left(\beta\Pi_2\tfrac{\partial^2}{\partial x^2} - \alpha\Pi_1\tfrac{\partial^2}{\partial y^2}\right)F \\ \psi &= (\gamma\Pi_1 + \delta\Pi_2)\tfrac{\partial^2 F}{\partial x\partial y}\end{aligned}\right\} \tag{6.6.9}$$

and (6.6.7) reduces to a single equation as below:

$$(\nabla^2\nabla^2\nabla^2\nabla^2 - 4\varepsilon\nabla^2\nabla^2\Lambda^2\Lambda^2 + 4\varepsilon\Lambda^2\Lambda^2\Lambda^2\Lambda^2)F = 0 \tag{6.6.10}$$

where

$$\left.\begin{aligned}&\nabla^2 = \tfrac{\partial^2}{\partial x^2} + \tfrac{\partial^2}{\partial y^2}, \Lambda^2 = \tfrac{\partial^2}{\partial x^2} - \tfrac{\partial^2}{\partial y^2} \\ &\varepsilon = \tfrac{R^2(L+M)(K_2+K_3)}{[M(K_1+K_2+K_3)-R^2][(L+2M)K_1-R^2]}\end{aligned}\right\} \tag{6.6.11}$$

It is obviously if $K_2 + K_3 = 0$, then $\varepsilon = 0$, and Eq. (6.6.10) will be reduced to (6.2.7).

If $F(x, y)$ is the solution of (6.6.10), substituting it into (6.6.9) and then into (6.6.6), one can obtain the displacement field

$$\left.\begin{aligned}u_x &= \tfrac{\partial^2}{\partial x\partial y}\{[M\alpha\Pi_1 + (L+2M)\beta\Pi_2] + 4\omega(K_2+K_3) \\ &\quad\times\left[M\tfrac{\partial^2}{\partial x^2} + (L+2M)\tfrac{\partial^2}{\partial y^2}\right]\Lambda^2\Big\}F \\ u_y &= \left[M\alpha\Pi_1\tfrac{\partial^2}{\partial y^2} - (L+2M)\beta\Pi_2\tfrac{\partial^2}{\partial x^2}\right]\nabla^2 F \\ &\quad -4\omega(K_2+K_3)(L+M)\tfrac{\partial^4}{\partial x^2\partial y^2}\Lambda^2 F \\ w_x &= \tfrac{\partial^2}{\partial x\partial y}[\omega(\alpha-\beta)\Pi_1\Pi_2 - 4\omega^2(K_2+K_3)\Lambda^2\Lambda^2]F \\ w_y &= -\omega\left[\alpha\Pi_1^2\tfrac{\partial^2}{\partial y^2} + \beta\Pi_2^2\tfrac{\partial^2}{\partial x^2}\right]F - 8\omega^2(K_2+K_3)\tfrac{\partial^4}{\partial x^2\partial y^2}\Lambda^2 F\end{aligned}\right\} \tag{6.6.12}$$

Similarly, the stress field has the following expressions:

$$\sigma_{xx} = 2M(L+M)\alpha\Pi_1\frac{\partial^3}{\partial y^3}\nabla^2 F + 8M\omega(L+M)(K_2+K_3)\frac{\partial^5}{\partial x^2\partial y^3}\Lambda^2 F$$

$$\sigma_{yy} = 2M(L+M)\alpha\Pi_1\frac{\partial^3}{\partial x^2\partial y}\nabla^2 F + 8M\omega(L+M)(K_2+K_3)\frac{\partial^5}{\partial x^4\partial y}\Lambda^2 F$$

$$\sigma_{xy} = \sigma_{yx} = -2M(L+M)\alpha\Pi_1\frac{\partial^3}{\partial x\partial y^2}\nabla^2 F - 8M\omega(L+M)(K_2+K_3)\frac{\partial^5}{\partial x^3\partial y^2}\Lambda^2 F$$

$$
\begin{aligned}
H_{xx} = \Bigg\{ & R\frac{\partial}{\partial y}\left[M\alpha\Pi_1\Lambda^2 + 2(L+2M)\beta\Pi_2\frac{\partial^2}{\partial x^2}\right]\nabla^2 \\
& + 4R\omega(K_2+K_3)\frac{\partial^3}{\partial x^2\partial y}\left[M\frac{\partial^2}{\partial x^2} + (2L+5M)\frac{\partial^2}{\partial y^2}\right]\Lambda^2 \\
& + K_1\omega\frac{\partial^3}{\partial x^2\partial y}[(\alpha-\beta)\Pi_1\Pi_2 - 4\omega(K_2+K_3)\Lambda^2\Lambda^2] \\
& - K_2\omega\left[\alpha\frac{\partial^3}{\partial y^3}\Pi_1^2 + \beta\frac{\partial^3}{\partial x^2\partial y}\Pi_2^2 + 8\omega(K_2+K_3)\frac{\partial^5}{\partial x^2\partial y^3}\Lambda^2\right]\Bigg\}F
\end{aligned}
$$

$$
\begin{aligned}
H_{yy} = \Bigg\{ & R\frac{\partial}{\partial y}\left[M\alpha\Pi_1\Lambda^2 + 2(L+2M)\beta\Pi_2\frac{\partial^2}{\partial x^2}\right]\nabla^2 \\
& + 4R\omega(K_2+K_3)\frac{\partial^3}{\partial x^2\partial y}\left[M\frac{\partial^2}{\partial x^2} + (2L+5M)\frac{\partial^2}{\partial y^2}\right]\Lambda^2 \\
& + K_2\omega\frac{\partial^3}{\partial x^2\partial y}[(\alpha-\beta)\Pi_1\Pi_2 - 4\omega(K_2+K_3)\Lambda^2\Lambda^2] \\
& - K_1\omega\left[\alpha\frac{\partial^3}{\partial y^3}\Pi_1^2 + \beta\frac{\partial^3}{\partial x^2\partial y}\Pi_2^2 + 8\omega(K_2+K_3)\frac{\partial^5}{\partial x^2\partial y^3}\Lambda^2\right]\Bigg\}F
\end{aligned}
$$

$$
\begin{aligned}
H_{xy} = \Bigg\{ & -R\frac{\partial}{\partial x}\left[2M\alpha\frac{\partial^2}{\partial y^2}\Pi_1 - (L+2M)\beta\Pi_2\Lambda^2\right]]\nabla^2 \\
& + 4R\omega(L+2M)(K_2+K_3)\frac{\partial^3}{\partial x\partial y^2}\Lambda^2\Lambda^2 \\
& + (K_1+K_2+K_3)\omega\frac{\partial^3}{\partial x\partial y^2}[(\alpha-\beta)\Pi_1\Pi_2 - 4\omega(K_2+K_3)\Lambda^2\Lambda^2] \\
& - K_3\omega\left[\alpha\frac{\partial^3}{\partial x\partial y^2}\Pi_1^2 + \beta\frac{\partial^3}{\partial x^3}\Pi_2^2 + 8\omega(K_2+K_3)\frac{\partial^5}{\partial x^3\partial y^2}\Lambda^2\right]\Bigg\}F
\end{aligned}
$$

$$
\begin{aligned}
H_{yx} = \Bigg\{ & R\frac{\partial}{\partial x}\left[2M\alpha\frac{\partial^2}{\partial y^2}\Pi_1 - (L+2M)\beta\Pi_2\Lambda^2\right]\nabla^2 \\
& - 4R\omega(L+2M)(K_2+K_3)\frac{\partial^3}{\partial x\partial y^2}\Lambda^2\Lambda^2 \\
& + K_3\omega\frac{\partial^3}{\partial x\partial y^2}[(\alpha-\beta)\Pi_1\Pi_2 - 4\omega(K_2+K_3)\Lambda^2\Lambda^2] \\
& - (K_1+K_2+K_3)\omega\left[\alpha\frac{\partial^3}{\partial x\partial y^2}\Pi_1^2 + \beta\frac{\partial^3}{\partial x^3}\Pi_2^2 + 8\omega(K_2+K_3)\frac{\partial^5}{\partial x^3\partial y^2}\Lambda^2\right]\Bigg\}F
\end{aligned}
\tag{6.6.13}
$$

A part of above results was reported by Refs. [12, 15, 17].

6.7 Stress Potential of Point Group $5, \overline{5}$ Pentagonal and Point Group $10, \overline{10}$ Decagonal Quasicrystals

In Sect. 6.4, we discussed the displacement potential of plane elasticity of point group $5, \overline{5}$ pentagonal and point group $10, \overline{10}$ decagonal quasicrystals. But the stress potential for the quasicrystals is also beneficial, which will be introduced in this section.

From the basic formulas listed in Sect. 6.4, if we exclude the displacements, then there are the deformation compatibility equations

$$\frac{\partial^2 \varepsilon_{xx}}{\partial y^2} + \frac{\partial^2 \varepsilon_{yy}}{\partial x^2} = 2\frac{\partial^2 \varepsilon_{xy}}{\partial x \partial y}, \quad \frac{\partial w_{xy}}{\partial x} = \frac{\partial w_{xx}}{\partial y}, \quad \frac{\partial w_{yx}}{\partial y} = \frac{\partial w_{yy}}{\partial x} \tag{6.7.1}$$

If introducing stress potential functions $\phi(x, y), \psi_1(x, y)$ and $\psi_2(x, y)$ such as

$$\begin{aligned} &\sigma_{xx} = \frac{\partial^2 \phi}{\partial y^2}, \quad \sigma_{yy} = \frac{\partial^2 \phi}{\partial x^2}, \quad \sigma_{xy} = \sigma_{yx} = -\frac{\partial^2 \phi}{\partial x \partial y} \\ &H_{xx} = \frac{\partial \psi_1}{\partial y}, \quad H_{xy} = -\frac{\partial \psi_1}{\partial x}, \quad H_{yx} = -\frac{\partial \psi_2}{\partial y}, \quad H_{yy} = \frac{\partial \psi_2}{\partial x} \end{aligned} \tag{6.7.2}$$

then equilibrium equations $\partial \sigma_{ij}/\partial x_j = 0$ and $\partial H_{ij}/\partial x_j = 0$ will be automatically satisfied.

Based on the generalized Hooke's law (6.4.3), all strain components can be expressed by relevant stress components:

$$\begin{aligned} \varepsilon_{xx} &= \frac{1}{4(L+M)}(\sigma_{xx} + \sigma_{yy}) + \frac{1}{4c}[(K_1 + K_2)(\sigma_{xx} - \sigma_{yy}) - 2R_1(H_{xx} + H_{yy}) - 2R_2(H_{xy} - H_{yx})] \\ \varepsilon_{yy} &= \frac{1}{4(L+M)}(\sigma_{xx} + \sigma_{yy}) - \frac{1}{4c}[(K_1 + K_2)(\sigma_{xx} - \sigma_{yy}) - 2R_1(H_{xx} + H_{yy}) - 2R_2(H_{xy} - H)] \\ \varepsilon_{xy} &= \varepsilon_{yx} = \frac{1}{2c}[(K_1 + K_2)\sigma_{xy} - R_2(H_{xx} + H_{yy}) + R_1(H_{xy} - H_{yx})] \\ w_{xx} &= \frac{1}{2(K_1 - K_2)}(H_{xx} - H_{yy}) + \frac{1}{2c}[M(H_{xx} + H_{yy}) - R_1(\sigma_{xx} - \sigma_{yy}) - 2R_2\sigma_{xy}] \\ w_{yy} &= -\frac{1}{2(K_1 - K_2)}(H_{xx} - H_{yy}) + \frac{1}{2c}[M(H_{xx} + H_{yy}) - R_1(\sigma_{xx} - \sigma_{yy}) - 2R_2\sigma_{xy}] \\ w_{xy} &= \frac{1}{2c}[-R_2(\sigma_{xx} - \sigma_{yy}) + 2R_1\sigma_{xy}] + \frac{1}{2(K_1 - K_2)}(H_{xy} + H_{yx}) + \frac{M}{2c}(H_{xy} - H_{yx}) \\ w_{yx} &= \frac{1}{2c}[R_2(\sigma_{xx} - \sigma_{yy}) - 2R_1\sigma_{xy}] + \frac{1}{2(K_1 - K_2)}(H_{xy} + H_{yx}) - \frac{M}{2c}(H_{xy} - H_{yx}) \end{aligned} \tag{6.7.3}$$

in which

$$c = M(K_1 + K_2) - 2(R_1^2 + R_2^2) \tag{6.7.4}$$

So the deformation compatibility equations (6.7.2) can be rewritten by the stresses σ_{ij}, H_{ij}, and then by employing (8.4.6), one has

$$\begin{aligned}
&\left(\frac{1}{2(L+M)} + \frac{K_1+K_2}{2c}\right)\nabla^2\nabla^2\phi + \frac{R_1}{c}\left(\frac{\partial}{\partial y}\Pi_1\psi_1 - \frac{\partial}{\partial x}\Pi_2\psi_2\right) \\
&\quad + \frac{R_2}{c}\left(\frac{\partial}{\partial x}\Pi_2\psi_1 + \frac{\partial}{\partial y}\Pi_1\psi_2\right) = 0 \\
&\left(\frac{c}{K_1 - K_2} + M\right)\nabla^2\psi_1 + R_1\frac{\partial}{\partial y}\Pi_1\phi + R_2\frac{\partial}{\partial x}\Pi_2\phi = 0 \\
&\left(\frac{c}{K_1 - K_2} + M\right)\nabla^2\psi_2 - R_1\frac{\partial}{\partial x}\Pi_2\phi + R_2\frac{\partial}{\partial y}\Pi_1\phi = 0
\end{aligned} \tag{6.7.5}$$

where

$$\nabla^2 = \frac{\partial^2}{\partial x^2} + \frac{\partial^2}{\partial y^2}, \quad \Pi_1 = 3\frac{\partial^2}{\partial x^2} - \frac{\partial^2}{\partial y^2}, \quad \Pi_2 = 3\frac{\partial^2}{\partial y^2} - \frac{\partial^2}{\partial x^2}$$

Equation (6.7.5) will be satisfied when we choose a new function G, which is called the stress function, such that

$$\begin{aligned}
\phi &= c_1\nabla^2\nabla^2 G, \\
\psi_1 &= -\left(R_1\frac{\partial}{\partial y}\Pi_1 + R_2\frac{\partial}{\partial x}\Pi_2\right)\nabla^2 G, \\
\psi_2 &= \left(R_1\frac{\partial}{\partial x}\Pi_2 - R_2\frac{\partial}{\partial y}\Pi_1\right)\nabla^2 G
\end{aligned} \tag{6.7.6}$$

in which

$$c_1 = \frac{c}{K_1 - K_2} + M \tag{6.7.7}$$

and

$$\nabla^2\nabla^2\nabla^2\nabla^2 G = 0 \tag{6.7.8}$$

So the final governing equation based on the stress potential is the same as that based on the displacement potential.

6.8 Stress Potential of Point Group 8*mm* Octagonal Quasicrystals

The final governing equation of plane elasticity of point group 8*mm* octagonal quasicrystals was given in Sect. 6.6 by displacement potential; similarly, we can also give a derivation by stress potential.

The strain compatibility equations and the definition on stress potentials are the same as those given by (6.7.1) and (6.7.2), and the strain–stress relations are as follows:

$$\varepsilon_{xx} = \frac{1}{(L+M)c}\left\{\frac{1}{4}\left[(K_1+K_2)(L+2M) - 2R^2\right]\sigma_{xx} - \frac{1}{4}\left[(K_1+K_2)L + 2R^2\right]\sigma_{yy} - \frac{1}{2}R(L+M)(H_{xx}+H_{yy})\right\} \tag{6.8.1a}$$

$$\varepsilon_{yy} = \frac{1}{(L+M)c}\left\{-\frac{1}{4}\left[(K_1+K_2)L + 2R^2\right]\sigma_{xx} + \frac{1}{4}\left[(K_1+K_2)(L+2M) - 2R^2\right]\sigma_{yy} + \frac{1}{2}R(L+M)(H_{xx}+H_{yy}\right\} \tag{6.8.1b}$$

$$\varepsilon_{xy} = \varepsilon_{yx} = \frac{1}{2c}\left[(K_1+K_2)\sigma_{xy} + R(H_{xy} - H_{yx})\right] \tag{6.8.1c}$$

$$w_{xx} = \frac{1}{(K_1-K_2)c}\left[\frac{1}{2}R(K_1-K_2)(\sigma_{yy}-\sigma_{xx}) + (K_1M - R^2)H_{xx} - (K_2M - R^2)H_{yy}\right] \tag{6.8.1d}$$

$$w_{yy} = \frac{1}{(K_1-K_2)c}\left[\frac{1}{2}R(K_1-K_2)(\sigma_{yy}-\sigma_{xx}) - (K_2M - R^2)H_{xx} + (K_1M - R^2)H_{yy}\right] \tag{6.8.1e}$$

$$w_{xy} = \frac{1}{(K_1+K_2+2K_3)c}\left\{R(K_1+K_2+2K_3)\sigma_{xy} + \left[(K_1+K_2+K_3)M - R^2\right]H_{xy} - (K_3M + R^2)H_{yx}\right\} \tag{6.8.1f}$$

$$w_{yx} = \frac{1}{(K_1+K_2+2K_3)c}\left\{-R(K_1+K_2+2K_3)\sigma_{xy} - (K_3M + R^2)H_{xy} + \left[(K_1+K_2+K_3)M - R^2\right]H_{yx}\right\} \tag{6.8.1g}$$

in which

$$c = M(K_1 + K_2) - 2R^2$$

If introducing stress potential functions $\phi(x,y), \psi_1(x,y)$ and $\psi_2(x,y)$ such as

$$\begin{aligned} &\sigma_{xx} = \frac{\partial^2 \phi}{\partial y^2}, \quad \sigma_{yy} = \frac{\partial^2 \phi}{\partial x^2}, \quad \sigma_{xy} = \sigma_{yx} = -\frac{\partial^2 \phi}{\partial x \partial y} \\ &H_{xx} = \frac{\partial \psi_1}{\partial y}, \quad H_{xy} = -\frac{\partial \psi_1}{\partial x}, \quad H_{yx} = -\frac{\partial \psi_2}{\partial y}, \quad H_{yy} = \frac{\partial \psi_2}{\partial x} \end{aligned} \tag{6.8.2}$$

then equilibrium equations (6.5.9) (or $\partial \sigma_{ij}/\partial x_j = 0, \partial H_{ij}/\partial x_j = 0$) will be automatically satisfied.

Substituting the stress formulas (6.8.2) into the strain–stress relation (6.8.1a) and then into the deformation compatibility equations (6.7.1), we have

$$\begin{aligned} c_1 \nabla^2 \nabla^2 \phi + 2R(L+M) \frac{\partial}{\partial y} \Pi_1 \psi_1 - 2R(L+M) \frac{\partial}{\partial x} \Pi_2 \psi_2 = 0 \\ -\frac{1}{2} R \frac{\partial}{\partial y} \Pi_1 \phi + c_2 \frac{\partial^2 \psi_2}{\partial x \partial y} - c_3 \frac{\partial^2 \psi_1}{\partial x^2} - c_4 \frac{\partial^2 \psi_1}{\partial y^2} = 0 \\ \frac{1}{2} R \frac{\partial}{\partial x} \Pi_2 \phi + c_2 \frac{\partial^2 \psi_1}{\partial x \partial y} - c_4 \frac{\partial^2 \psi_2}{\partial x^2} - c_3 \frac{\partial^2 \psi_2}{\partial y^2} = 0 \end{aligned} \tag{6.8.3}$$

where

$$\begin{aligned} &\nabla^2 = \frac{\partial^2}{\partial x^2} + \frac{\partial^2}{\partial y^2}, \quad \Pi_1 = 3\frac{\partial^2}{\partial x^2} - \frac{\partial^2}{\partial y^2}, \quad \Pi_2 = 3\frac{\partial^2}{\partial y^2} - \frac{\partial^2}{\partial x^2} \\ &c_1 = (K_1 + K_2)(L + 2M) - 2R^2, \quad c_2 = \frac{K_3 M + R^2}{K_1 + K_2 + 2K_3} + \frac{K_2 M + R^2}{K_1 - K_2} \\ &c_3 = \frac{(K_1 + K_2 + K_3)M - R^2}{K_1 + K_2 + 2K_3}, \quad c_4 = \frac{K_1 M + R^2}{K_1 - K_2} \end{aligned} \tag{6.8.4}$$

The manipulation of the second equation of (6.8.3) $\times \frac{\partial}{\partial x}\Pi_2 +$ the third equation of (6.8.3) $\times \frac{\partial}{\partial y}\Pi_1$ leads to

$$\begin{aligned} &\left(c_2 \frac{\partial^3}{\partial x \partial y^2} \Pi_1 - c_3 \frac{\partial^3}{\partial x^3} \Pi_2 - c_4 \frac{\partial^3}{\partial x \partial y^2} \Pi_2 \right) \psi_1 \\ &= \left(c_4 \frac{\partial^3}{\partial x^2 \partial y} \Pi_1 + c_3 \frac{\partial^3}{\partial y^3} \Pi_1 - c_2 \frac{\partial^3}{\partial x^2 \partial y} \Pi_2 \right) \psi_2 \end{aligned} \tag{6.8.5}$$

There exists a function $A(x,y)$ such that

$$\begin{aligned}\psi_1 &= \left(c_4\frac{\partial^3}{\partial x^2\partial y}\Pi_1 + c_3\frac{\partial^3}{\partial y^3}\Pi_1 - c_2\frac{\partial^3}{\partial x^2\partial y}\Pi_2\right)A\\ \psi_2 &= \left(c_2\frac{\partial^3}{\partial x\partial y^2}\Pi_1 - c_3\frac{\partial^3}{\partial x^3}\Pi_2 - c_4\frac{\partial^3}{\partial x\partial y^2}\Pi_2\right)A\end{aligned} \tag{6.8.6}$$

Substituting (6.8.6) into the third equation of (6.8.3), we arrive at the function $G(x,y)$ satisfying the relations such as

$$\begin{aligned}\phi &= -c_3c_4\nabla^2\nabla^2 G\\ A &= \frac{1}{2}RG\end{aligned} \tag{6.8.7}$$

In the derivation, the relation $c_2 = c_4 - c_3$ has been used. The stress potentials ϕ, ψ_1, ψ_2 can be expressed by the new function $G(x,y)$, that is,

$$\begin{aligned}\phi &= -c_3c_4\nabla^2\nabla^2 G\\ \psi_1 &= \frac{1}{2}R\left(c_4\frac{\partial^3}{\partial x^2\partial y}\Pi_1 + c_3\frac{\partial^3}{\partial y^3}\Pi_1 - c_2\frac{\partial^3}{\partial x^2\partial y}\Pi_2\right)G\\ \psi_2 &= \frac{1}{2}R\left(c_2\frac{\partial^3}{\partial x\partial y^2}\Pi_1 - c_3\frac{\partial^3}{\partial x^3}\Pi_2 - c_4\frac{\partial^3}{\partial x\partial y^2}\Pi_2\right)G\end{aligned} \tag{6.8.8}$$

Substituting (6.8.8) into the first equation of (6.8.3) yields

$$\begin{aligned}&-c_1c_3c_4\nabla^2\nabla^2\nabla^2\nabla^2 G + R^2(L+M)\\ &\left(c_4\frac{\partial^4}{\partial x^2\partial y^2}\Pi_1^2 + c_3\frac{\partial^4}{\partial y^4}\Pi_1^2 - 2c_2\frac{\partial^4}{\partial x^2\partial y^2}\Pi_1\Pi_2 + c_3\frac{\partial^4}{\partial y^4}\Pi_2^2 + c_4\frac{\partial^4}{\partial x^2\partial y^2}\Pi_2^2\right)G = 0\end{aligned} \tag{6.8.9}$$

Considering the following relations

$$\begin{aligned}&\frac{\partial^4}{\partial x^2\partial y^2} = \frac{1}{4}(\nabla^2\nabla^2 - \Lambda^2\Lambda^2), \quad \Pi_1\Pi_2 = \nabla^2\nabla^2 - 4\Lambda^2\Lambda^2, c_2 = c_4 - c_3\\ &\nabla^2 = \frac{\partial^2}{\partial x^2} + \frac{\partial^2}{\partial y^2}, \quad \Lambda^2 = \frac{\partial^2}{\partial x^2} - \frac{\partial^2}{\partial y^2}\end{aligned}$$

equation (6.8.9) can be simplified as

$$\nabla^2\nabla^2\nabla^2\nabla^2 G - 4\varepsilon\nabla^2\nabla^2\Lambda^2\Lambda^2 G + 4\varepsilon\Lambda^2\Lambda^2\Lambda^2\Lambda^2 G = 0 \tag{6.8.10}$$

with

$$\varepsilon = \frac{R^2(L+M)(c_3 - c_4)}{-c_1 c_3 + R^2(L+M)c_3} = \frac{R^2(L+M)(K_2 + K_3)}{[(K_1 + K_2 + K_3)M - R^2][K_1(L+2M) - R^2]} \tag{6.8.11}$$

The final governing equation in this case is exactly in agreement to that given by the displacement potential formulation, discussed in Sect. 6.6.

6.9 Engineering and Mathematical Elasticity of Quasicrystals

The complicated structure of quasicrystals leads to the tremendous complexity of their elasticity equations. Even though, the solution can also be carried out, and fruitful results are found. This formulation is effective not only for linear elasticity of the quasicrystals but also for nonlinear material response of the solids if coupling some physical models [18, 19]. Those studies belong to mathematical theory of elasticity of quasicrystals.

In the subsequent chapters, we can realize that the difficulty for analytic solutions does not only lie in the complexity of the equations but also the boundary conditions. In some cases, if one can simplify the boundary conditions, then some meaningful approximate solutions may be constructed even if it needs no difficult mathematical calculation. For this purpose, we consider an example.

From Sect. 6.3, we have deformation compatibility equations

$$\left.\begin{aligned} &\frac{\partial^2 \varepsilon_{xx}}{\partial y^2} + \frac{\partial^2 \varepsilon_{yy}}{\partial x^2} = 2\frac{\partial^2 \varepsilon_{xy}}{\partial x \partial y} \\ &\frac{\partial w_{xy}}{\partial x} = \frac{\partial w_{xx}}{\partial y}, \frac{\partial w_{yx}}{\partial y} = \frac{\partial w_{yy}}{\partial x} \end{aligned}\right\} \tag{6.9.1}$$

Then, the substitution of (6.3.2) into (6.9.1) yields the compatibility equations expressed by σ_{ij} and H_{ij}

$$\begin{aligned} &\nabla^2(\sigma_{xx} + \sigma_{yy}) - \frac{L+M}{C}\left(\frac{\partial^2}{\partial x^2} - \frac{\partial^2}{\partial y^2}\right) \times [(K_1 + K_2)(\sigma_{xx} - \sigma_{yy}) - 2R(H_{xx} + H_{yy})] \\ &= 8\frac{L+M}{C}\frac{\partial^2}{\partial x \partial y}[(K_1 + K_2)\sigma_{xy} - R(H_{xy} + H_{yx})] \end{aligned} \tag{6.9.2a}$$

$$\frac{1}{C}\frac{\partial}{\partial x}\left[R\sigma_{xy}-\frac{(R^2-MK_1)H_{xy}+(R^2-MK_2)H_{yx}}{K_1-K_2}\right]$$
$$=\frac{1}{2(K_1-K_2)}\frac{\partial}{\partial y}(H_{xx}-H_{yy})+\frac{1}{2C}\frac{\partial}{\partial y}[M(H_{xx}+H_{yy})-R(\sigma_{xx}-\sigma_{yy})] \tag{6.9.2b}$$

$$\frac{1}{C}\frac{\partial}{\partial y}\left[-R\sigma_{xy}-\frac{(R^2-MK_1)H_{xy}+(R^2-MK_2)H_{yx}}{K_1-K_2}\right]$$
$$=\frac{-1}{2(K_1-K_2)}\frac{\partial}{\partial x}(H_{xx}-H_{yy})+\frac{1}{2C}\frac{\partial}{\partial x}[M(H_{xx}+H_{yy})-R(\sigma_{xx}-\sigma_{yy})] \tag{6.9.2c}$$

in which C, M, L, K_1, K_2 and R are given in Sect. 6.3. These three equations are combined with the equilibrium equations

$$\left.\begin{aligned}\frac{\partial\sigma_{xx}}{\partial x}+\frac{\partial\sigma_{xy}}{\partial y}=0,\quad \frac{\partial\sigma_{yx}}{\partial x}+\frac{\partial\sigma_{yy}}{\partial y}=0\\ \frac{\partial H_{xx}}{\partial x}+\frac{\partial H_{xy}}{\partial y}=0,\quad \frac{\partial H_{yx}}{\partial x}+\frac{\partial H_{yy}}{\partial y}=0\end{aligned}\right\} \tag{6.9.3}$$

and this provides a basis for solving the problem.

A very meaningful example is pure bending of beam, shown in Fig. 6.6.

For this sample, at the upper and lower surfaces of the beam there are following boundary conditions

$$\left.\begin{aligned}\sigma_{yy}=0,\sigma_{xy}=0\\ H_{yy}=0,H_{xy}=0\end{aligned}\right\} \tag{6.9.4}$$

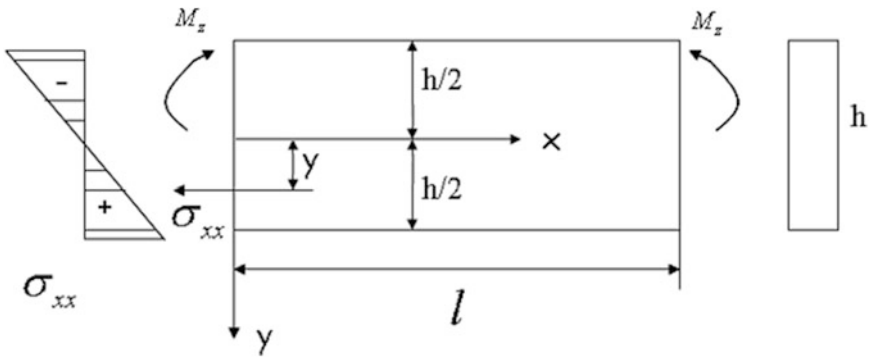

Fig. 6.6 Beam of quasicrystal of tenfold symmetry under pure bending

In addition, there are so-called St. Venant boundary conditions

$$\left.\begin{array}{ll} \int_{-h/2}^{h/2} \sigma_{xx}\mathrm{d}y = 0, & \int_{-h/2}^{h/2} y\sigma_{xx}\mathrm{d}y = M_z \\ \int_{-h/2}^{h/2} H_{xx}\mathrm{d}y = 0, & \int_{-h/2}^{h/2} yH_{xx}\mathrm{d}y = L_z \\ \int_{-h/2}^{h/2} \sigma_{xy}\mathrm{d}y = 0, & \int_{-h/2}^{h/2} H_{yx}\mathrm{d}y = 0 \end{array}\right\} \tag{6.9.5}$$

where M_z and L_z represent the resultant moments of σ_{xx} and H_{xx}. The direction of vector of the moments is z. Boundary conditions (6.9.5) are relaxation boundary conditions, and this gives some flexibility for solution.

At first, we assume that the value of L_z momentarily be undermined, and assume further

$$\sigma_{xx} = A_1 y, \quad \sigma_{yy} = \sigma_{xy} = \sigma_{yx} = 0, \quad H_{yy} = H_{xy} = H_{yx} = 0, \quad H_{xx} = f(y)$$

and A_1 and $f(y)$ to be determined. Substituting $\sigma_{xx} = A_1 y$ into (6.9.5), we find that

$$A_1 = \frac{12M_z}{h^3} \tag{6.9.6}$$

so that

$$\sigma_{xx} = \frac{M_z}{I} y \tag{6.9.7}$$

where $I = 1 \cdot h^3/12$ represents the inertia moment of the transverse section with height h and width 1.

It is seen that the above results have satisfied Eqs. (6.7.3), (6.9.2a) and (6.9.2c).

Substituting (6.9.7) into (6.9.2b) yields

$$H_{xx} = R\sigma_{xx} \Big/ \left[\frac{1}{2(K_1 - K_2)} + \frac{M}{2C}\right] = RM_z y \Big/ \left[\frac{1}{2(K_1 - K_2)} + \frac{M}{2C}\right] \tag{6.9.8}$$

so the equation is satisfied. So that we have the solution

$$\left.\begin{array}{l} \sigma_{xx} = \frac{M_z}{I} y, \sigma_{yy} = \sigma_{xy} = \sigma_{yx} = 0 \\ H_{xx} = \frac{RM_z y}{I[1/2(K_1 - K_2) + M/2C]}, H_{yy} = H_{xy} = H_{yx} = 0 \end{array}\right\} \tag{6.9.9}$$

At last, combining (6.9.9) and (6.9.5) determines the value of L_z.

Here, we utilize the physical character of the sample to solve the problem easily. This procedure presents quite effective for some practical problems and needs not

so hard mathematics. This treatment is similar to that in the engineering elasticity of conventional structural materials; namely, there is engineering elasticity of quasicrystals. But this monograph mainly discusses mathematical elasticity of quasicrystals, because the problems with topological or metric defects such as dislocations, cracks concerning stress singularities, or with local discontinuity of physical quantities such as in contact, shock wave problems, due to the complexity of boundary conditions the above engineering approximate treatment is ineffective, we must develop systematic and direct analysis methods. In the classical elasticity, such systematic and direct methods were developed by Muskhelishvili [20] in 1930s and Sneddon [21] in 1940s and present important effects promoting elasticity and relevant disciplines of science and engineering. By extending the methods in the classical elasticity to quasicrystal elasticity, we will display in detail the application in Chaps. 7, 8, for two-dimensional quasicrystals, and in Chap. 9 for three-dimensional quasicrystals, respectively.

References

1. Chernikov M A, Ott H R, Bianchi A et al, 1998, Elastic moduli of a single quasicrystal of decagonal Al-Ni-Co: evidence for transverse elastic isotropy, *Phys. Rev. Lett*., **80**(2), 321-324.
2. Abe H, Taruma N, Le Bolloc'h D et al, 2000, Anomalous-X-ray scattering associated with short-range order in an $Al_{70}Ni_{15}Co_{15}$ decagonal quasicrystal, *Mater. Sci. and Eng*. A, **294-296** (12), 299-302.
3. Jeong H C and Steinhardt P J, 1993, Finite-temperature elasticity phase transition in decagonal quasicrystals, *Phys. Rev*. B**,48**(13), 9394-9403.
4. Edagawa K,2007, Phonon-phason coupling in decagonal quasicrystals, *Phil. Mag*., **87**(18-21), 2789-2798.
5. Fan T Y and Mai Y W, 2004, Elasticity theory, fracture mechanics and relevant thermal properties of quasicrystalline materials, *Appl. Mech. Rev*., 57(5), 325-344.
6. Hu C Z, Yang W G, Wang R H and Ding D H, 1997, Symmetry and physical properties of quasicrystals, *Prog. Phys.*, **17**(4), 345-374. (in Chinese).
7. Bohsung J and Trebin H R, 1989,*Introduction to the Quasicrystal Mathematics*. ed by Jaric M. V., New York, Academic Press.
8. De P and Pelcovis R A, 1987, Disclinations in pentagonal quasicrystals, *Phys. Rev*. B, 35 (17), 9604-9607.
9. Yang S H and Ding D H, 1998, *Foundation of Dislocation Theory of Crystals,* Vol.2, Beijing, Science Press, (in Chinese).
10. De P and Pelcovits R A, 1987, Linear elasticity of pentagonal quasicrystals, *Phys. Rev.* B, **36** (13), 8609-8620.
11. Ding D H, Wang R H, Yang W G and Hu C Z, 1995, General expressions for the elastic displacement fields induced by dislocations in quasicrystals, *J. Phys. : Condens. Matter*, **7**(28), 5423-5426.
12. Li X F and Fan T Y, 1998, New method for solving elasticity problems of some planar quasicrystals and solutions, *Chin. Phys. Letter.*, **15**(4), 278-280.
13. Guo Y C and Fan T Y, 2001, ModeII Griffith crack in decagonal quasicrystals, *Appl. Math. Mech.* English Edition**, 22**(10)**,** 1311-1317.
14. Li L H and Fan T Y, 2006, Complex function method for solving notch problem of point 10 two-dimensional quasicrystal based on the stress potential function, *J. Phys.: Condens. Matter*, **18**(47)**,**10631-10641.

15. Li X F, Fan T Y and Sun Y F, 1999, A decagonal quasicrystal with a Griffith crack, *Phil.Mag*. A, **79**(7), 1943-1952.
16. Li X F, Duan X Y, Fan T.Y., et al, 1999, Elastic field for a straight dislocation in a decagonal quasicryatal, *J. Phys.: Condens. Matter,* **11**(3),703-711.
17. Zhou W.M. and Fan T.Y., 2001,Plane elasticity of octagonal quasicrystals and solutions, *Chin. Phys*., **10**(8),743-747.
18. Fan T Y, Trebin A R, Messerschmidt U and Mai Y W, 2004, Plastic flow coupled with a Griffith crack in some one- and two-dimensional quasicrystals, *J. Phys.: Condens. Matter.*, **16** (37), 5419-5429.
19. Fan T Y and Fan L, 2008, Plastic fracture of quasicrystals, *Phil. Mag*., **88**(4), 523-535.
20. N.I. Muskhelishvili, 1956, *Some Basic Problems in the Mathematical Theory of Elasticity*, English translation by Radok J R M, P. Noordhoff Ltd, Groringen.
21. Sneddon I N, 1951, *Fourier Transforms*, McGraw-Hill, New York.

Chapter 7
Application I—Some Dislocation and Interface Problems and Solutions in One- and Two-Dimensional Quasicrystals

In Chaps. 5 and 6, with the physical basis of quasicrystal elasticity based on the density wave model, we have performed some mathematical operations, by proper simplification, to reduce the original problems to the boundary value problems of high-order partial differential equations and to establish the standard solving procedure and the fundamental solution formulas. This work is the development of the boundary value problems in classical elasticity. Here, we need to pose a question: Do these mathematical operations contribute to solving the quasicrystal elasticity problems? This is answered only by practice. The following two chapters will provide the applications of these theories, including the solutions to some dislocation, crack and interface problems in one- and two-dimensional quasicrystals. The calculation results indicate that the mathematical operations in Chaps. 5 and 6 are powerful in solving these problems.

As we know, almost all monographs of classical elasticity do not place their main focus upon dislocation and crack problems. These problems have been investigated in monographs relating to dislocation theory and fracture theory, respectively. As a monograph on theories of elasticity of quasicrystals, the current work is not going to focus entirely on dislocations and cracks in quasicrystals. Therefore, as an attempt to examine the theories developed in Chaps. 5 and 6 and to show their applications in elasticity of quasicrystals, we present some calculation examples of certain realistic dislocation and crack problems in elasticity of quasicrystals. The methods developed in this work can be used for studying other problems in quasicrystals.

Historically, soon after the discovery of quasicrystals, scientists proposed the possibility of existing dislocations in quasicrystals. De and Pelcovits [1, 2] first studied elastic field around dislocations and disclinations in quasicrystals. Furthermore, Ding et al. [3, 4] conducted systematic investigations of this topic by using the Green function method.

T.-Y. Fan, *Mathematical Theory of Elasticity of Quasicrystals and Its Applications*,
Springer Series in Materials Science 246, DOI 10.1007/978-981-10-1984-5_7

Now, people have recognize that quasicrystal is a kind of ordered phase of quasiperiodic long-range. Similar to crystals with ordered phase of long-range, the breaking of long-range regularity takes place usually through topological defects, i.e. dislocations lead to the breaking of the long-range symmetry. As mentioned in Chap. 3, quasicrystals also possess the orientational symmetries incompatible with those permitted in crystal theory. In quasicrystals, another defect, disclinations, also exists simultaneously, which leads to breaking of the orientational symmetry in quasicrystals. In some cases, the crystalline phases often coexist with the quasicrystalline phases. So there is another kind of defects, the interface between quasicrystal and crystal. The existence of these defects including the stacking fault dramatically affects the mechanical properties of quasicrystals. Therefore, it is important to study the elastic properties of quasicrystals with dislocations, disclinations, interface and stacking faults.

As aforementioned, during the study of dislocations in quasicrystals, physicists have developed some mathematical methods, such as the Green function method. These important methods are available in the relevant literature. Hereafter, by using the elementary methods developed in Chaps. 5 and 6, complex analysis and Fourier transform, we study the displacement and stress fields around dislocations or interfaces in one-dimensional and two-dimensional quasicrystals quantitatively. The three-dimensional dislocation and dynamic dislocation problems will be discussed in Chaps. 9 and 10, respectively.

7.1 Dislocations in One-Dimensional Hexagonal Quasicrystals

Following the sequence from simplicity to complexity, we first study the dislocations in one-dimensional quasicrystals. A dislocation in an n-dimensional quasicrystal bears the Burgers vector $b^{\|} \oplus b^{\perp}$, where $b^{\|} = (b_1^{\|}, b_2^{\|}, \ldots, b_n^{\|})$ is its Burgers vector of phonon field and $b^{\perp} = (b_1^{\perp}, b_2^{\perp}, \ldots, b_n^{\perp})$ the Burgers vector of phase field. And $b^{\|}$ is located in the physical space $E_{\|}$, while $b^{\perp}$ in the supplementary space or the vertical space $E_{\perp}$. For a one-dimensional quasicrystals, $\mathrm{b}^{\|} = (b_1^{\|}, b_2^{\|}, b_3^{\|})$ and $b^{\perp} = (0, 0, b_3^{\perp})$ since $b_1^{\perp} = b_2^{\perp} = 0$. Therefore, $b^{\|} \oplus b^{\perp} = (b_1^{\|}, b_2^{\|}, b_3^{\|}, b_3^{\perp})$ here, which can be dealt with the superposition of $(b_1^{\|}, b_2^{\|}, 0, 0)$ and $(0, 0, b_3^{\|}, b_3^{\perp})$. The $(b_1^{\|}, b_2^{\|}, 0, 0)$ corresponds to the blade dislocation in regular hexagonal crystals, whose elastic solution is available in common metal physics or dislocation monographs, (e.g. Refs. [7, 8]). The one correspondence to the component $(0, 0, b_3^{\|}, b_3^{\perp})$ is the screw dislocation in one-dimensional quasicrystal. We solve the elastic field induced by this dislocation in the following.

In Sect. 5.2, we have obtained the governing equations for anti-plane strain problems in one-dimensional quasicrystal elasticity such as

$$\nabla^2 u_z = 0, \quad \nabla^2 w_z = 0. \tag{7.1.1}$$

The boundary conditions corresponding to the screw dislocation with Burgers vector $(0, 0, b_3^{\parallel}, b_3^{\perp})$ are

$$\left.\begin{aligned} u_z\big|_{y=0^+} - u_z\big|_{y=0^-} &= b_3^{\parallel} \\ w_z\big|_{y=0^+} - w_z\big|_{y=0^-} &= b_3^{\perp} \end{aligned}\right\} \tag{7.1.2a}$$

or

$$\int_{\Gamma} \mathrm{d}u_z = b_3^{\parallel}, \quad \int_{\Gamma} \mathrm{d}w_z = b_3^{\perp} \tag{7.1.2b}$$

where Γ indicates an arbitrary contour surrounding the dislocation core. The solution to the boundary value problem (7.1.1) and (7.1.2a) is:

$$u_z = \frac{b_3^{\parallel}}{2\pi}\arctan\frac{y}{x}, \quad w_z = \frac{b_3^{\perp}}{2\pi}\arctan\frac{y}{x}. \tag{7.1.3}$$

The stress components can be extracted according to the stress–stain relation (5.2.8) in Chap. 5 as:

$$\left.\begin{aligned} \sigma_{xz} = \sigma_{zx} &= -\frac{C_{44}b_3^{\parallel}}{2\pi}\left(\frac{y}{x^2+y^2}\right) - \frac{R_3 b_3^{\perp}}{2\pi}\left(\frac{y}{x^2+y^2}\right) \\ \sigma_{yz} = \sigma_{zy} &= -\frac{C_{44}b_3^{\parallel}}{2\pi}\left(\frac{x}{x^2+y^2}\right) + \frac{R_3 b_3^{\perp}}{2\pi}\left(\frac{x}{x^2+y^2}\right) \\ H_{zx} &= -\frac{K_2 b_3^{\perp}}{2\pi}\left(\frac{y}{x^2+y^2}\right) - \frac{R_3 b_3^{\parallel}}{2\pi}\left(\frac{y}{x^2+y^2}\right) \\ H_{zy} &= -\frac{K_2 b_3^{\perp}}{2\pi}\left(\frac{x}{x^2+y^2}\right) + \frac{R_3 b_3^{\parallel}}{2\pi}\left(\frac{x}{x^2+y^2}\right) \end{aligned}\right\}. \tag{7.1.4}$$

The displacement and stress field corresponding to the Burgers vector $b^{\parallel} \oplus b^{\perp} = (b_1^{\parallel}, b_2^{\parallel}, b_3^{\parallel}, b_3^{\perp})$ can be obtained by superposing the above elastic field on that of the regular hexagonal crystals.

The elastic strain energy induced by the screw dislocation is

$$\begin{aligned} W &= \tfrac{1}{2}\iint_{\Omega}\left(\sigma_{zj}\tfrac{\partial u_z}{\partial x_j} + H_{zj}\tfrac{\partial w_z}{\partial x_j}\right)\mathrm{d}x_1\mathrm{d}x_2 \\ &= \tfrac{1}{2}\int_{r_0}^{R_0}\int_{0}^{2\pi} r\left(\sigma_{zj}\tfrac{\partial u_z}{\partial x_j} + H_{zj}\tfrac{\partial w_z}{\partial x_j}\right)\mathrm{d}r\mathrm{d}\theta \\ &= \left(C_{44}b_3^{\parallel 2} + K_2 b_3^{\perp 2} + 2R_3 b_3^{\parallel} b_3^{\perp}\right)\tfrac{1}{4\pi}\ln\tfrac{R_0}{r_0} \end{aligned}, \tag{7.1.5}$$

where r_0 is the size of the dislocation core and R_0 is the size of the dislocation network or inclusion, which are available in theory of dislocations in regular crystals.

7.2 Dislocations in Quasicrystals with Point Groups 5*m* and 10*mm* Symmetries

Consider a dislocation in pentagonal point group 5*m* or decagonal point group 10*mm* quasicrystals with Burgers vector $b^{\|} \oplus b^{\perp} = (b_1^{\|}, b_2^{\|}, b_3^{\|}, b_1^{\perp}, b_2^{\perp})$, where $\mathrm{b}^{\|}$ is its Burgers vector of phonon field and $b^{\perp}$ is its Burgers vector of phase field. Here, $b_3^{\perp} = 0$ due to $w_z = 0$.

This dislocation problem can be dealt with the superposition of two dislocation problems of Burgers vectors $(b_1^{\|}, b_2^{\|}, 0, b_1^{\perp}, b_2^{\perp})$ and $(0, 0, b_3^{\|})$, respectively. On the dislocation line parallel to the direction of periodic arrangement (z-direction), the elastic field induced by the dislocation of Burgers vector $(b_1^{\|}, b_2^{\|}, 0, b_1^{\perp}, b_2^{\perp})$ can be simplified as an in-plane elastic field in quasicrystal elasticity, which can be analysed by the methods discussed in Sects. 6.1 and 6.2. The elastic field induced by $(0, 0, b_3^{\|})$ is governed by equation $\nabla^2 u_z = 0$, and its solution has been obtained in Sect. 7.1. Therefore, in the following two sections, we always assume the dislocation line parallel to the direction of atom periodic arrangement in quasicrystals, and we only study the elastic field induced by the dislocation with the Burgers vector $(b_1^{\|}, b_2^{\|}, 0, b_1^{\perp}, b_2^{\perp})$.

To demonstrate the methodology concisely, we first consider a special case of $(b_1^{\|}, 0, 0, b_1^{\perp}, 0)$. During this procedure, in order to further simplify the mathematical process, we first analyse the case of $b_1^{\|} \neq 0$ and $b_2^{\|} = b_1^{\perp} = b_2^{\perp} = 0$. In this case, we consider the problem in the upper half-space of $y \geq 0$, and the problem has the following boundary condition:

$$\left.\begin{aligned} &\sigma_{ij}(x,y) \to 0, H_{ij}(x,y) \to 0 (\sqrt{x^2+y^2} \to \infty) \\ &\sigma_{yy}(x,0) = 0 \\ &w_x(x,0) = w_y(x,0) = 0 \\ &u_x(x,0^+) - u_x(x,0^-) = b_1^{\|}, \quad x<0 \text{ or } \int_{\Gamma} \mathrm{d}u_x = b_1^{\|} \end{aligned}\right\}, \tag{7.2.1}$$

where Γ indicates an arbitrary contour surrounding the dislocation core.

To solve this dislocation problem under boundary condition (7.2.1), we need to solve the following Eq. (6.2.7), i.e.

$$\nabla^2\nabla^2\nabla^2\nabla^2 F = 0$$

By introducing the Fourier transform

$$\hat{F}(\xi, y) = \int_{-\infty}^{+\infty} F(x, y)\mathrm{e}^{\mathrm{i}\xi x}\mathrm{d}x \tag{7.2.2}$$

where ξ is the Fourier transform parameter, and the above equation can be reduced into:

$$\left(\frac{\mathrm{d}^2}{\mathrm{d}y^2} - \xi^2\right)^4 \hat{F}(\xi, y) = 0. \tag{7.2.3}$$

This is an ordinary partial differential equation with constant coefficients, and its general solution is

$$\begin{aligned}\hat{F}(\xi, y) = {} & [A_1 + B_1 y + C_1 y^2 + D_1 y^3]\mathrm{e}^{-|\xi|y} \\ & + [A_2 + B_2 y + C_2 y^2 + D_2 y^3]\mathrm{e}^{|\xi|y}\end{aligned} \tag{7.2.4}$$

where A_1, B_1, …, D_2 are functions with respect to ξ to be determined by boundary conditions.

We are going to use Fourier transform to search for problem solutions in Chaps. 7–10. For convenience, we only consider the problem in the upper half-space (or the lower half-space) based on the symmetry or anti-symmetry of the problems. It should be cautious that here the symmetry or anti-symmetry is in the view of macroscopic continuum media, namely the even and odd characteristics of the displacement function $F(x, y)$ or stress function $G(x, y)$ with respect to x, but not in the scale of crystalline structures. Furthermore, during the use of Fourier transform, we attempt to make the boundary condition homogeneous at infinity (zero boundary condition). For example, the boundary condition (7.2.1) is homogeneous at infinity. Therefore, we only consider the case in the upper half-space, and the formal solution (7.2.4) can be simplified as follows:

$$\hat{F}(\xi, y) = [A_1 + B_1 y + C_1 y^2 + D_1 y^3]\mathrm{e}^{-|\xi|y}. \tag{7.2.5}$$

In the evident reason, the suffix of A_1, B_1, C_1, D_1 can be removed in the following. For conciseness in writing, introduce the following indicator:

$$X = (A, B, C, D), \quad Y = (1, y, y^2, y^3)^{\mathrm{T}} \tag{7.2.6}$$

where the symbol T indicates the matrix transpose. Therefore, (7.2.5) can be rewritten as follows:

$$\hat{F}(\xi, y) = XY\mathrm{e}^{-|\xi|y} \tag{7.2.5'}$$

Since A, D, C, and D are arbitrary functions with respect to ξ, without the loss of generality, (7.2.5) can be rewritten as follows:

$$\hat{F}(\xi, y) = (4\xi^4)^{-1}XY\mathrm{e}^{-|\xi|y} \tag{7.2.7}$$

By performing Fourier transform on the displacement expressions (6.2.8) and (6.2.9) and stress expressions (6.2.10) and (6.2.11), and using the notation (7.2.7), we have

$$\hat{u}_x(\xi, y) = \mathrm{i}\xi^{-1}X[2n\xi^2Y' + (m-5n)|\xi|Y'' - (2m-5n)Y''']\mathrm{e}^{-|\xi|y} \tag{7.2.8a}$$

$$\hat{u}_y(\xi, y) = |\xi|^{-1}X[2n\xi^2Y' - (m+5n)|\xi|Y'' + (2m+5n)Y''']\mathrm{e}^{-|\xi|y} \tag{7.2.8b}$$

$$\hat{w}_x(\xi, y) = -\mathrm{i}\omega(\alpha-\beta)\xi^{-1}X[2n|\xi|^3Y - 12\xi^2Y' + 15|\xi|Y'' - 10Y''']\mathrm{e}^{-|\xi|y} \tag{7.2.9a}$$

$$\begin{aligned}\hat{w}_y(\xi, y) = -\omega(\alpha-\beta)|\xi|^{-1}X[4|\xi|^3Y - 12\xi^2Y' + 15|\xi|Y'' \\ - (10+e_0-e_1)Y''']\mathrm{e}^{-|\xi|y}\end{aligned} \tag{7.2.9b}$$

$$\hat{\sigma}_{xx}(\xi, y) = 2M\alpha(L+M)X(-2\xi^2Y' + 8|\xi|Y'' - 13Y''']\mathrm{e}^{-|\xi|y} \tag{7.2.10a}$$

$$\hat{\sigma}_{yy}(\xi, y) = 2M\alpha(L+M)X(2\xi^2Y' - 4|\xi|Y'' + 3Y''']\mathrm{e}^{-|\xi|y} \tag{7.2.10b}$$

$$\hat{\sigma}_{xy}(\xi, y) = \hat{\sigma}_{yx}(\xi, y) = \mathrm{i}2M\alpha(L+M)\xi^{-1}|\xi|X(2\xi^2Y' - 6|\xi|Y'' + \delta Y''']\mathrm{e}^{-|\xi|y} \tag{7.2.10c}$$

$$\begin{aligned}\hat{H}_{xx}(\xi, y) = -\omega(\alpha-\beta)(K_1-K_2)|\xi|^{-1}X[4|\xi|^3Y - 16\xi^2Y' + 27|\xi|Y'' \\ - (25+e_2)Y''']\mathrm{e}^{-|\xi|y}\end{aligned} \tag{7.2.11a}$$

$$\begin{aligned}\hat{H}_{yy}(\xi, y) = -\omega(\alpha-\beta)(K_1-K_2)X[-4|\xi|^3Y + 12\xi^2Y' - 15|\xi|Y'' \\ + (10-e_1)Y''']\mathrm{e}^{-|\xi|y}\end{aligned} \tag{7.2.11b}$$

$$\begin{aligned}\hat{H}_{xy}(\xi, y) = \mathrm{i}\omega(\alpha-\beta)(K_1-K_2)\xi^{-1}|\xi|X[-4|\xi|^3Y + 12\xi^2Y' \\ - 15|\xi|Y'' + (10+e_2)Y''']\mathrm{e}^{-|\xi|y}\end{aligned} \tag{7.2.11c}$$

$$\begin{aligned}\hat{H}_{yx}(\xi, y) = -\mathrm{i}\omega(\alpha-\beta)(K_1-K_2)\xi^{-1}|\xi|X[-4|\xi|^3Y \\ + 16\xi^2Y' - 27|\xi|Y'' + (25-e_1)Y''']\mathrm{e}^{-|\xi|y}\end{aligned} \tag{7.2.11d}$$

where

$$\left.\begin{aligned} &m = M\alpha + (L+2M)\beta, n = M\alpha - (L+2M)\beta \\ &e_1 = \frac{2\alpha\beta}{\omega(\alpha-\beta)(K_1-K_2)}, e_2 = \frac{2\alpha\beta}{\omega(\alpha-\beta)(K_1-K_2)} + \frac{(\alpha+\beta)}{(\alpha-\beta)} \end{aligned}\right\} \tag{7.2.12}$$

and α, β, δ and ω are given in (6.2.5).

The inverse of Fourier transform reads

$$F(x,y) = \frac{1}{2\pi}\int_{-\infty}^{+\infty} \hat{F}(\xi,y)\mathrm{e}^{-\mathrm{i}\xi x}\mathrm{d}\xi, \tag{7.2.13}$$

and similarly, the inverses of displacements and stresses are obtained as follows:

$$u_j(x,y) = \frac{1}{2\pi}\int_{-\infty}^{+\infty} \hat{u}_j(\xi,y)\mathrm{e}^{-\mathrm{i}\xi x}\mathrm{d}\xi \tag{7.2.14}$$

$$w_j(x,y) = \frac{1}{2\pi}\int_{-\infty}^{+\infty} \hat{w}_j(\xi,y)\mathrm{e}^{-\mathrm{i}\xi x}\mathrm{d}\xi \tag{7.2.15}$$

$$\sigma_{jk}(x,y) = \frac{1}{2\pi}\int_{-\infty}^{+\infty} \hat{\sigma}_{jk}(\xi,y)\mathrm{e}^{-\mathrm{i}\xi x}\mathrm{d}\xi \tag{7.2.16}$$

$$H_{jk}(x,y) = \frac{1}{2\pi}\int_{-\infty}^{+\infty} \hat{H}_{jk}(\xi,y)\mathrm{e}^{-\mathrm{i}\xi x}\mathrm{d}\xi \tag{7.2.17}$$

In the above dislocation problem, $u_x(x, y)$ is an odd function with respect to x; therefore, $F(x, y)$ must be an odd function with respect to x according to the first expression in (6.2.8). For an odd function, the Fourier transform (7.2.2) is rewritten as follows:

$$\hat{F}(\xi,y) = \int_0^{\infty} F(x,y)\sin(\xi x)\mathrm{d}x \tag{7.2.18}$$

and its inversion is:

$$F(x,y) = \frac{2}{\pi}\int_0^{\infty} \hat{F}(\xi,y)\sin(\xi x)\mathrm{d}\xi. \tag{7.2.19}$$

If $F(x, y)$ is an even function with respect to x, it has:

$$\hat{F}(\xi, y) = \int_0^\infty F(x, y)\cos(\xi x)\mathrm{d}x, \tag{7.2.20}$$

and its inversion is:

$$F(x, y) = \frac{2}{\pi}\int_0^\infty \hat{F}(\xi, y)\cos(\xi x)\mathrm{d}\xi. \tag{7.2.21}$$

Therefore, the corresponding integrals relating u_j, w_j, σ_{jk} and H_{jk} can be simplified.

So far, the displacement and stress components in the form of integrals have been obtained, which all include the unknown functions $A(\xi)$, $B(\xi)$, $C(\xi)$ and $D(\xi)$ to be determined by the second expressions in the boundary condition (7.2.1) such that

$$A = (9J\mathrm{sgn}\xi)/4\xi^2, \quad B = 2J\xi^2, \quad C = (J\mathrm{sgn}\xi)/2\xi^2, \quad D = 0, \tag{7.2.22}$$

where J is a constant to be determined. By using the last expression in (7.2.1), i.e. the dislocation condition, J can be expressed as follows:

$$J = \frac{b_1^{\|}}{8(n-m)}. \tag{7.2.23}$$

Substituting the above expressions into (7.2.8a)–(7.2.11a) and then into the inversion formulas (7.2.14)–(7.2.17) leads to the displacement and stress fields induced by the dislocation with Burgers vector $(b_1^{\|}, 0, 0, 0)$ in quasicrystals of point group $5m$ fivefold symmetry or *10mm* tenfold symmetry as given below:

$$u_x = \frac{b_1^{\|}}{2\pi}\left[\arctan\left(\frac{y}{x}\right) + \frac{(L+M)K_1}{(L+M)K_1 + (MK_1 - R^2)}\left(\frac{xy}{r^2}\right)\right] \tag{7.2.24a}$$

$$u_y = \frac{b_1^{\|}}{2\pi}\left[-\frac{(MK_1 - R^2)}{(L+M)K_1 + (MK_1 - R^2)}\left(\ln\frac{r}{a}\right) + \frac{(L+M)K_1}{(L+M)K_1 + (MK_1 - R^2)}\left(\frac{y^2}{r^2}\right)\right] \tag{7.2.24b}$$

$$w_x = \left(\frac{b_1^{\|}}{2\pi}\right)\frac{(L+M)K_1}{(L+M)K_1 + (MK_1 - R^2)}\left(\frac{2x^3y}{r^4}\right) \tag{7.2.25a}$$

$$w_y = \left(\frac{b_1^{\parallel}}{2\pi}\right)\frac{(L+M)K_1}{(L+M)K_1+(MK_1-R^2)}\left(\frac{2x^2y^2}{r^4}\right) \tag{7.2.25b}$$

$$\sigma_{xx} = -A\frac{y(3x^2+y^2)}{r^4} \tag{7.2.26a}$$

$$\sigma_{yy} = A\frac{y(x^2-y^2)}{r^4} \tag{7.2.26b}$$

$$\sigma_{xy} = \sigma_{yx} = A\frac{x(x^2-y^2)}{r^4} \tag{7.2.26c}$$

$$H_{xx} = -A\frac{R(K_1-K_2)}{MK_1-R^2}\left[\frac{x^2y(3x^2-y^2)}{r^6}\right] \tag{7.2.27a}$$

$$H_{yy} = -A\frac{R(K_1-K_2)}{MK_1-R^2}\left[\frac{x^2y(3y^2-x^2)}{r^6}\right] \tag{7.2.27b}$$

$$H_{xy} = A\frac{R(K_1-K_2)}{MK_1-R^2}\left[\frac{xy^2(3x^2-y^2)}{r^6}\right] \tag{7.2.27c}$$

$$H_{yx} = -A\frac{R(K_1-K_2)}{MK_1-R^2}\left[\frac{x^3(3y^2-x^2)}{r^6}\right] \tag{7.2.27d}$$

where $r = \sqrt{x^2+y^2}$, a is the size of dislocation core, and

$$A = \left(\frac{b_1^{\parallel}}{\pi}\right)\frac{(L-M)(MK_1-R^2)}{(L+M)K_1+(MK_1-R^2)}. \tag{7.2.28}$$

Considering $L = C_{12}$ and $M = (C_{11}-C_{12})/2 = C_{66}$ in (6.1.1) and substituting them into (7.2.24a) and (7.2.25a), we find that our solutions are exactly consistent with those given by Ding et al. [4, 7]. They used the Green function method. This examines the correction of our derivation.

In the case of $R = 0$, the above solution recovers the solution of dislocation in hexagonal crystals [8]. If the material is isotropic, therefore, $L = \lambda$ and $M = \mu$. Substitution of L and M into (7.2.28) yields

$$A = \frac{\mu b_1^{\parallel}}{2\pi(1-\nu)} \tag{7.2.29}$$

where λ and μ are the Lamé constants and ν is the Poisson's ratio of phonon field. In this case, u_i and σ_{ij} recover those in a regular isotropic crystal with an edge dislocation, while $w_i = 0$ and $H_{ij} = 0$.

Let us consider another special case of $b_1^{\perp} \neq 0$ and $b_1^{\parallel} = b_2^{\parallel} = b_2^{\perp} = 0$. In this case, the boundary condition can be described as follows:

$$\left.\begin{aligned} &\sigma_{ij}(x,y) \to 0, H_{ij}(x,y) \to 0, \sqrt{x^2+y^2} \to \infty \\ &H_{yy}(x,0) = 0 \\ &u_x(x,0) = u_y(x,0) = 0 \\ &w_x(x,0^+) - w_x(x,0^-) = b_1^{\perp}, \quad x<0 \text{ or } \int_{\Gamma} \mathrm{d}w_x = b_1^{\perp} \end{aligned}\right\} \tag{7.2.30}$$

where the meaning of Γ is aforementioned.

By using the similar procedure, the displacement and stress fields can be determined as follows:

$$u_x = \frac{b_1^{\perp} k_0}{2\pi c_2}\left[\frac{xy}{r^2} - \left(\frac{c_1 - c_2}{2c_1}\right)\frac{2xy^3}{r^4}\right] \tag{7.2.31a}$$

$$u_y = \frac{b_1^{\perp} k_0}{2\pi c_2}\left[-\frac{xy}{r^2} + \left(\frac{c_1 - c_2}{2c_1}\right)\frac{y^2(x^2-y^2)}{r^4}\right] \tag{7.2.31b}$$

$$w_x = \frac{b_1^{\perp}}{2\pi}\left[\arctan\left(\frac{y}{x}\right) + \left(\frac{c_0 k_0}{2c_1 c_2}\right)\frac{xy(3x^2-y^2)(3y^2-x^2)}{3r^6}\right] \tag{7.2.31c}$$

$$w_y = \frac{b_1^{\perp}}{2\pi}\left[\left(1 - \frac{L+2M}{2c_1} - \frac{M}{2c_2}\right)\ln\frac{r}{a} + \left(\frac{c_0 k_0}{2c_1 c_2}\right)\frac{y^2(3x^2-y^2)^2}{3r^6}\right] \tag{7.2.31d}$$

$$\sigma_{xx} = -\left(\frac{c_0 b_1^{\perp} k_0}{\pi c_1 R}\right)\frac{x^2 y(3x^2-y^2)}{r^6} \tag{7.2.32a}$$

$$\sigma_{yy} = -\left(\frac{c_0 b_1^{\perp} k_0}{\pi c_1 R}\right)\frac{y^3(3x^2-y^2)}{r^6} \tag{7.2.32b}$$

$$\sigma_{xy} = \sigma_{yx} = \left(\frac{c_0 b_1^{\perp} k_0}{\pi c_1 R}\right)\frac{2xy^2(y^2-x^2)}{r^6} \tag{7.2.32c}$$

$$H_{xx} = \frac{k_0 b_1^{\perp}}{2\pi e_1}\left[(e_1+e_2)\frac{y}{r^2} - \frac{2x^2 y(3x^2-y^2)(3y^2-x^2)}{r^8}\right] \tag{7.2.33a}$$

$$H_{yy} = -\left(\frac{k_0 b_1^{\perp} y}{2\pi e_1}\right)\left[\frac{2(x^2-y^2)}{r^4} + \frac{(x^2-y^2)(3x^2-y^2)(3y^2-x^2)}{r^8}\right] \tag{7.2.33b}$$

$$H_{xy} = \frac{k_0 b_1^{\perp}}{2\pi e_1}\left[(e_1+e_2)\frac{x}{r^2} + \frac{2xy^2(3x^2-y^2)(3y^2-x^2)}{r^8}\right] \tag{7.2.33c}$$

$$H_{yx} = -\left(\frac{k_0 b_1^{\perp} x}{2\pi e_1}\right)\frac{2(x^2-y^2)}{r^4} + \frac{(x^2-y^2)(3x^2-y^2)(3y^2-x^2)}{r^8} \tag{7.2.33d}$$

where $e_1 = \dfrac{2c_1c_2}{c_0k_0}$, $\quad e_2 = \dfrac{c_1c_2}{c_0k_0}\left(\dfrac{c_1'}{c_1} + \dfrac{c_2'}{c_2}\right)$

$$c_1' = (L+2M)K_2 - R^2, \quad c_2' = MK_2 - R^2$$

and c_0, c_1, c_2 and k_0 are given in Chap. 6, i.e.

$$c_0 = (L+2M)R, \quad c_1 = (L+2M)K_1 - R^2, \quad c_2 = MK_1 - R^2$$

$$k_0 = R(K_1 - K_2)$$

Superposition of the above two solutions yields the solution of dislocation $(b_1^{\parallel}, 0, b_1^{\perp}, 0)$. The solution of $(0, b_2^{\parallel}, 0, b_2^{\perp})$ can be determined similarly. Their superposition yields the solution of $(b_1^{\parallel}, b_2^{\parallel}, b_1^{\perp}, b_2^{\perp})$. The part of this work can be found in the paper given by Li and Fan [5]. Readers may examine that the present solutions are identical to those given by Ding et al. [4, 7] using the method of Green's functions (note that $L = C_{12}$, and $M = (C_{11}-C_{12})/2 = C_{66}$).

7.3 Dislocations in Quasicrystals with Point Groups $5, \bar{5}$ Fivefold and $10, \overline{10}$ Tenfold Symmetries

Similar to those discussed in the proceeding section, as two-dimensional quasicrystals, the Burgers vector of the dislocation is $b^{\parallel} \oplus b^{\perp} = (b_1^{\parallel}, b_2^{\parallel}, b_3^{\parallel}, b_1^{\perp}, b_2^{\perp})$. Due to $w_3 = 0$ and our assumption that dislocation line is parallel to the direction of periodic arrangement (z-direction), the above Burgers vector can be considered as the superposition of $(b_1^{\parallel}, b_2^{\parallel}, b_1^{\perp}, b_2^{\perp})$ and $(0, 0, b_3^{\perp})$. Under this assumption, the field variables do not vary with the change of the variable z. Therefore, the elastic field corresponding to $(b_1^{\parallel}, b_2^{\parallel}, b_1^{\perp}, b_2^{\perp})$ can be determined by using the theory of plane elasticity of two-dimensional quasicrystals discussed in Sect. 6.4. The anti-plane elastic field induced by $(0, 0, b_3^{\perp})$ is very simple and can be solved by using the method discussed in Sect. 7.1.

From Sect. 6.4, we have obtained the governing equation of plane elastic field of quasicrystals with point groups $5, \bar{5}$ fivefold and $10, \bar{10}$ tenfold symmetries:

$$\nabla^2\nabla^2\nabla^2\nabla^2 F = 0 \tag{7.3.1}$$

where $F(x, y)$ is the displacement potential function, defined in (6.4.10). By performing Fourier transform of (7.2.2) and considering the case of upper half-space $(y \geq 0)$, its Fourier transform $\hat{F}(\xi, y)$ has the form of

$$\hat{F}(\xi, y) = (4\xi^4 R^2)^{-1} XY \mathrm{e}^{-|\xi| y} \tag{7.3.2}$$

where X and Y have the same meanings as in Sect. 7.2 and ξ is the parameter of Fourier transform, and

$$R^2 = R_1^2 + R_2^2 \tag{7.3.3}$$

After some algebraic operations with (6.2.8)–(6.2.11), the displacement components in Fourier transform domain are:

$$\hat{u}_x(\xi, y) = \mathrm{i}\xi^{-1}\bar{R}_0 X[2n\xi^2 Y' + (m-5n)|\xi|Y'' - (2m-5n)Y''']\mathrm{e}^{-|\xi| y} \tag{7.3.4a}$$

$$\hat{u}_y(\xi, y) = |\xi|^{-1}\bar{R}_0 X[2n\xi^2 Y' - (m+5n)|\xi|Y'' + (2m+5n)Y''']\mathrm{e}^{-|\xi| y} \tag{7.3.4b}$$

$$\hat{w}_x(\xi, y) = \mathrm{i}c_0\xi^{-1}\bar{R}_0^2 X[4|\xi|^3 Y - 12\xi^2 Y' + 15|\xi|Y'' - 10Y''']\mathrm{e}^{-|\xi| y} \tag{7.3.4c}$$

$$\hat{w}_y(\xi, y) = c_0|\xi|^{-1}\bar{R}_0^2 X[4|\xi|^3 Y - 12\xi^2 Y' + 15|\xi|Y'' - (10 + e_0 R_0^2)Y''']\mathrm{e}^{-|\xi| y} \tag{7.3.4}$$

where

$$\left.\begin{array}{l} m = c_2 + c_1, n = c_2 - c_1, e_0 = -[C_{66}c_1 + C_{11}c_2]/(Rc_0) \\ R_0 = (R_1 + \mathrm{i}R_2\mathrm{sgn}\xi)/R, \bar{R}_0 = (R_1 - \mathrm{i}R_2\mathrm{sgn}\xi)/R \end{array}\right\} \tag{7.3.5}$$

Similarly, the stress components in Fourier transform domain are:

$$\hat{\sigma}_{xx}(\xi, y) = 2c_0c_2R^{-1}\bar{R}_0 X(-2\xi^2 Y' + 8|\xi|Y'' - 13Y''')\mathrm{e}^{-|\xi| y} \tag{7.3.6a}$$

$$\hat{\sigma}_{yy}(\xi, y) = 2c_0c_2R^{-1}\bar{R}_0 X(2\xi^2 Y' - 4|\xi|Y'' + 3Y''')\mathrm{e}^{-|\xi| y} \tag{7.3.6b}$$

$$\hat{\sigma}_{xy}(\xi, y) = \hat{\sigma}_{yx}(\xi, y) = \mathrm{i}2c_0c_2R^{-1}\bar{R}_0(\mathrm{sgn}\xi)X(2\xi^2 Y' - 6|\xi|Y'' + 7Y''']\mathrm{e}^{-|\xi| y} \tag{7.3.6c}$$

$$\hat{H}_{xx}(\xi, y) = c_0k_0\bar{R}_0^2 X[4|\xi|^3 Y - 16\xi^2 Y' + 27|\xi|Y'' - (25 + e_2 R_0^2)Y''']\mathrm{e}^{-|\xi| y} \tag{7.3.6d}$$

$$\hat{H}_{yy}(\xi, y) = c_0 k_0 \bar{R}_0^2 X[-4|\xi|^3 Y + 12\xi^2 Y' - 15|\xi|Y'' + (10 - e_1 R_0^2)Y''']\mathrm{e}^{-|\xi|y} \tag{7.3.6e}$$

$$\hat{H}_{xy}(\xi, y) = \mathrm{i}c_0 k_0 \bar{R}_0^2 (\mathrm{sgn}\xi) X[-4|\xi|^3 Y + 12\xi^2 Y' - 15|\xi|Y'' + (10 + e_2 R_0^2)Y''']\mathrm{e}^{-|\xi|y} \tag{7.3.6f}$$

$$\hat{H}_{yx}(\xi, y) = \mathrm{i}c_0 k_0 \bar{R}_0^2 (\mathrm{sgn}\xi) X[-4|\xi|^3 Y + 16\xi^2 Y' - 27|\xi|Y'' + (25 - e_1 R_0^2)Y''']\mathrm{e}^{-|\xi|y} \tag{7.3.6g}$$

$$\left.\begin{aligned} e_1 = \frac{2c_1 c_2}{c_0 k_0 R}, e_2 = \frac{c_1 c_2}{c_0 k_0 R}\left(\frac{c_1'}{c_1} + \frac{c_2'}{c_2}\right) \\ c_1' = C_{11}K_2 - R^2, c_2' = C_{66}K_2 - R^2 \end{aligned}\right\}, \tag{7.3.7}$$

where c_0 and K_0 are given in (6.4.13).

As introduced in the proceeding section, X includes four unknowns $A(\xi)$, $B(\xi)$, $C(\xi)$ and $D(\xi)$, which can be determined by boundary condition. Once $A(\xi)$, $B(\xi)$, $C(\xi)$ and $D(\xi)$ are determined, u_i, w_i, σ_{jk} and H_{jk} can be determined by the Fourier inverse.

In the case of dislocation problem $b^{\|} \oplus b^{\perp} = (b_1^{\|}, 0, b_1^{\perp}, 0)$, we try to determine these functions and their Fourier inverses in the following.

In order to simplify the calculation, we first consider the case of $b_1^{\|} \neq 0$ and $b_1^{\perp} = 0$. In this case, the boundary condition is

$$\left.\begin{aligned} &\sigma_{ij}(x, y) \to 0, H_{ij}(x, y) \to 0(\sqrt{x^2 + y^2} \to \infty) \\ &\sigma_{yy}(x, 0) = 0 \\ &w_x(x, 0) = w_y(x, 0) = 0 \\ &\int_\Gamma \mathrm{d}u_x = b_1^{\|}, \int_\Gamma \mathrm{d}u_y = 0 \end{aligned}\right\} \tag{7.3.8}$$

In Fourier transform domain, solutions (7.3.4), (7.3.6a) and the first three expressions in boundary condition (7.3.8) yield

$$A(\xi) = 9C(\xi)/4, \quad B(\xi) = 2C(\xi), \quad D(\xi) = 0, \tag{7.3.9}$$

and the dislocation condition leads to

$$\left.\begin{aligned} \int_\Gamma \mathrm{d}u_x = -4c_1 R^{-1}(R_1 \mathrm{Re}C + R_2 \mathrm{sgn}\xi \mathrm{Im}C) \\ \int_\Gamma \mathrm{d}u_y = 4c_1 R^{-1}(R_2 \mathrm{Re}C - R_1 \mathrm{sgn}\xi \mathrm{Im}C) \end{aligned}\right\} \tag{7.3.10}$$

where the indicators Re and Im stand for the real and imaginary parts of a complex number, respectively. Finally, expressions (7.3.10) and (7.3.8) define:

$$C(\xi) = \mathrm{Re}C + \mathrm{i}\mathrm{Im}C = -\frac{(R_1 + \mathrm{i}R_2\mathrm{sgn}\xi)b_1^{\parallel}}{4\pi R c_1} = -\frac{R_0 b_1^{\parallel}}{4\pi c_1} \tag{7.3.11}$$

where R_0 is given by (7.3.5) and c_1 is given by (6.4.9), i.e.

$$c_1 = (L+2M)K_1 - R^2, \quad R^2 = R_1^2 + R_2^2 \tag{7.3.12}$$

Therefore,

$$u_x = \frac{b_1^{\parallel}}{2\pi}\left[\arctan\left(\frac{y}{x}\right) + \frac{c_1 - c_2}{c_1}\left(\frac{xy}{r^2}\right)\right] \tag{7.3.13a}$$

$$u_y = \frac{b_1^{\parallel}}{2\pi}\left[-\ln\frac{r}{a} + \frac{c_1 - c_2}{c_1}\left(\ln\frac{r}{a} + \frac{y^2}{r^2}\right)\right] \tag{7.3.13b}$$

$$w_x = \frac{c_0 b_1^{\parallel}}{2\pi c_1}\left[\left(\frac{R_1}{R}\right)\frac{2x^3 y}{r^4} + \left(\frac{R_2}{R}\right)\frac{y^2(3x^2+y^2)}{r^4}\right] \tag{7.3.13c}$$

$$w_y = \frac{c_0 b_1^{\parallel}}{2\pi c_1}\left[\left(\frac{R_1}{R}\right)\frac{y^2(3x^2+y^2)}{r^4} + \left(\frac{R_2}{R}\right)\frac{2x^3 y}{r^4}\right] \tag{7.3.13d}$$

where c_0 is given by (6.4.13) and a indicates the radius of dislocation core.

The corresponding stress components can be determined by (7.3.13a) and generalized Hooke's law (6.4.3):

$$\sigma_{xx} = -\left(\frac{c_0 c_2 b_1^{\parallel}}{\pi c_1 R}\right)\frac{y(3x^2+y^2)}{r^4} \tag{7.3.14a}$$

$$\sigma_{yy} = \left(\frac{c_0 c_2 b_1^{\parallel}}{\pi c_1 R}\right)\frac{y(x^2-y^2)}{r^4} \tag{7.3.14b}$$

$$\sigma_{xy} = \sigma_{yx} = \left(\frac{c_0 c_2 b_1^{\parallel}}{\pi c_1 R}\right)\frac{x(x^2-y^2)}{r^4} \tag{7.3.14c}$$

$$H_{xx} = -\frac{c_0 k_0 b_1^{\parallel}}{\pi c_1}\left[\left(\frac{R_1}{R}\right)\frac{x^2 y(3x^2-y^2)}{r^6} + \left(\frac{R_2}{R}\right)\frac{x^3(3y^2-x^2)}{r^6}\right] \tag{7.3.14d}$$

$$H_{yy} = -\frac{c_0 k_0 b_1^{\parallel}}{\pi c_1}\left[\left(\frac{R_1}{R}\right)\frac{x^2 y(3x^2 - y^2)}{r^6} - \left(\frac{R_2}{R}\right)\frac{xy^2(3x^2 - y^2)}{r^6}\right] \tag{7.3.14e}$$

$$H_{xy} = -\frac{c_0 k_0 b_1^{\parallel}}{\pi c_1}\left[\left(\frac{R_1}{R}\right)\frac{xy^2(3x^2 - y^2)}{r^6} + \left(\frac{R_2}{R}\right)\frac{x^2 y(3y^2 - x^2)}{r^6}\right] \tag{7.3.14f}$$

$$H_{yx} = -\frac{c_0 k_0 b_1^{\parallel}}{\pi c_1}\left[-\left(\frac{R_1}{R}\right)\frac{x^3(3y^2 - x^2)}{r^6} + \left(\frac{R_2}{R}\right)\frac{x^2 y(3x^2 - y^2)}{r^6}\right] \tag{7.3.14g}$$

Now, let us consider the case of $b_1^{\parallel} = 0$ and $b_1^{\perp} \neq 0$. In this case, the corresponding boundary condition is:

$$\left.\begin{aligned} &\sigma_{ij}(x,y) \to 0, H_{ij}(x,y) \to 0 (\sqrt{x^2+y^2} \to \infty) \\ &H_{yy}(x,0) = 0 \\ &u_x(x,0) = u_y(x,0) = 0 \\ &\int_{\Gamma} \mathrm{d}w_x = b_1^{\perp}, \int_{\Gamma} \mathrm{d}w_y = 0 \end{aligned}\right\}. \tag{7.3.15}$$

By using the similar analysis, the corresponding displacement and stress fields can be determined as (7.3.16a) and (7.3.17a)

$$u_x = \frac{c_1 b_1^{\perp}}{\pi c_0 e_1}\left\{\frac{R_1}{R}\left[\frac{xy}{r^2} - \left(\frac{c_1 - c_2}{c_1}\right)\frac{2xy^3}{r^4}\right] + \frac{R_2}{R}\left[\frac{y^2}{r^2} + \left(\frac{c_1 - c_2}{c_1}\right)\frac{y^2(x^2 - y^2)}{r^4}\right]\right\} \tag{7.3.16a}$$

$$u_y = \frac{c_1 b_1^{\perp}}{\pi c_0 e_1}\left\{-\frac{R_1}{R}\left[\frac{y^2}{r^2} - \left(\frac{c_1 - c_2}{c_1}\right)\frac{y^2(x^2 - y^2)}{r^4}\right] + \frac{R_2}{R}\left[\frac{xy}{r^2} + \left(\frac{c_1 - c_2}{c_1}\right)\frac{2xy^3}{r^4}\right]\right\} \tag{7.3.16b}$$

$$w_x = \frac{b_1^{\perp}}{2\pi}\left[\arctan\left(\frac{y}{x}\right) + \left(\frac{R_1^2 - R_2^2}{e_1 R^2}\right)\frac{xy(3x^2 - y^2)(3y^2 - x^2)}{3r^6} + \left(\frac{2R_1 R_2}{e_1 R^2}\right)\frac{y^2(3x^2 - y^2)^2}{3r^6}\right] \tag{7.3.16c}$$

$$w_y = \frac{b_1^{\perp}}{2\pi e_1}\left[e_2 \ln\frac{r}{a} + \left(\frac{R_1^2 - R_2^2}{R^2}\right)\frac{y^2(3x^2 - y^2)^2}{3r^6} - \left(\frac{2R_1 R_2}{e_1 R^2}\right)\frac{xy(3x^2 - y^2)(3y^2 - x^2)}{3r^6}\right] \tag{7.3.16d}$$

$$\sigma_{xx} = -\frac{2c_2 b_1^{\perp}}{\pi e_1 R}\left[\frac{R_1}{R}\frac{x^2 y(3x^2 - y^2)}{r^6} + \frac{R_2}{R}\frac{x^3(3y^2 - x^2)}{r^6}\right] \tag{7.3.17a}$$

$$\sigma_{yy} = -\frac{2c_2 b_1^{\perp}}{\pi e_1 R}\left[\frac{R_1}{R}\frac{y^3(3x^2-y^2)}{r^6} + \frac{R_2}{R}\frac{xy^2(3y^2-x^2)}{r^6}\right] \tag{7.3.17b}$$

$$\sigma_{xy} = \sigma_{yx} = -\frac{2c_2 b_1^{\perp}}{\pi e_1 R}\left[\frac{R_1}{R}\frac{xy^2(3x^2-y^2)}{r^6} + \frac{R_2}{R}\frac{x^2(3y^2-x^2)}{r^6}\right] \tag{7.3.17c}$$

$$H_{xx} = \frac{K_0 b_1^{\perp}}{2\pi e_1}\left[-(e_1+e_2)\frac{y}{r^2} + x\left(\frac{R_1^2-R_2^2}{R^2}h_{21}(x,y) - \frac{2R_1R_2}{R^2}h_{22}(x,y)\right)\right] \tag{7.3.17d}$$

$$H_{yy} = -\frac{K_0 b_1^{\perp} y}{2\pi e_1}\left[\frac{R_1^2-R_2^2}{R^2}h_{22}(x,y) + \frac{2R_1R_2}{R^2}h_{21}(x,y)\right] \tag{7.3.17e}$$

$$H_{xy} = \frac{K_0 b_1^{\perp}}{2\pi e_1}\left[(e_1+e_2)\frac{x}{r^2} + y\left(\frac{R_1^2-R_2^2}{R^2}h_{21}(x,y) - \frac{2R_1R_2}{R^2}h_{22}(x,y)\right)\right] \tag{7.3.17f}$$

$$H_{yx} = -\frac{K_0 b_1^{\perp} x}{2\pi e_1}\left[\frac{R_1^2-R_2^2}{R^2}h_{22}(x,y) + \frac{2R_1R_2}{R^2}h_{21}(x,y)\right] \tag{7.3.17g}$$

in which

$$\begin{aligned} h_{21}(x,y) &= \frac{2xy(3x^2-y^2)(3y^2-x^2)}{r^8} \\ h_{22}(x,y) &= \frac{2(x^2-y^2)}{r^4} + \frac{(x^2-y^2)(3x^2-y^2)(3y^2-x^2)}{r^8} \end{aligned} \tag{7.3.18}$$

The solution to dislocation problem ($b_1^{\parallel}$, 0, $b_1^{\perp}$, 0) can be determined by superposing (7.3.13a) and (7.3.14a) onto (7.3.16a) and (7.3.17a). The solution to dislocation problem (0, $b_2^{\parallel}$, 0, $b_2^{\perp}$) can be determined in the similar way. As a result, the solution to dislocation problem with Burgers vector ($b_1^{\parallel}$, $b_2^{\parallel}$, $b_1^{\perp}$, $b_2^{\perp}$) can be determined completely.

The above work can be found in the literature [6].

7.4 Dislocations in Quasicrystals with Eightfold Symmetry

The final governing equation of elasticity of two-dimensional quasicrystals with eightfold symmetry can be expressed as follows:

$$(\nabla^2\nabla^2\nabla^2\nabla^2 - 4\varepsilon\nabla^2\nabla^2\Lambda^2\Lambda^2 + 4\varepsilon\Lambda^2\Lambda^2\Lambda^2\Lambda^2)F = 0 \tag{7.4.1}$$

in which

$$\left.\begin{aligned} \nabla^2 &= \frac{\partial^2}{\partial x^2} + \frac{\partial^2}{\partial y^2}, \quad \Lambda^2 = \frac{\partial^2}{\partial x^2} - \frac{\partial^2}{\partial y^2} \\ \varepsilon &= \frac{R^2(L+M)(K_2+K_3)}{[M(K_1+K_2+K_3) - R^2][(L+2M)K_1 - R^2]} \end{aligned}\right\} \tag{7.4.2}$$

(see (6.6.10), (6.6.11) for detail). Equation (7.4.1) is more complicated than that of (6.2.7) and (7.3.1), so the solution of which is also more complex than that discussed in the previous sections. Due to the limitation of space, we cannot list the whole procedure of the solution and only give some main results of which in the following, in which both Fourier transform and complex variable function methods are, respectively, used.

7.4.1 Fourier Transform Method

Considering dislocation problem $b^{\|} \oplus b^{\perp} = (b_1^{\|}, 0, b_1^{\perp}, 0, 0)$, we try to determine the displacement field under the action of the boundary conditions

$$\left.\begin{aligned} &\sigma_{ij}(x,y) \to 0, H_{ij}(x,y) \to 0 (\sqrt{x^2+y^2} \to \infty) \\ &\sigma_{yy}(x,0) = 0, H_{yy}(x,0) = 0 \\ &\int_\Gamma \mathrm{d}u_x = b_1^{\|}, \int_\Gamma \mathrm{d}w_x = b_1^{\perp} \end{aligned}\right\} \tag{7.4.3}$$

By performing Fourier transform of (7.4.1), it can be reduced to

$$\left[\left(\frac{\mathrm{d}^2}{\mathrm{d}y^2} - \xi^2\right)^4 - 4\varepsilon\left(\frac{\mathrm{d}^2}{\mathrm{d}y^2} - \xi^2\right)^2 + 4\varepsilon\left(\frac{\mathrm{d}^2}{\mathrm{d}y^2} + \xi^2\right)^4\right]\hat{F} = 0 \tag{7.4.4}$$

The eigen roots of Eq. (7.4.4) depend on the value of parameter ε, and Zhou [9] gave a detailed discussion for the solutions corresponding to case (1): $0 < \varepsilon < 1$ and case (2): $\varepsilon < 0$, but calculation is tremendously complex and lengthy which cannot be included here. For the case (1), the solution is

$$
\begin{aligned}
u_x(x,y) = &\frac{1}{2\pi}\left\{\frac{b_1^{\parallel}}{2}\left[\arctan\left(\frac{\lambda_1^2+\lambda_2^2}{\lambda_1}\frac{y}{x}+\frac{\lambda_2}{\lambda_1}\right)+\arctan\left(\frac{\lambda_1^2+\lambda_2^2}{\lambda_1}\frac{y}{x}-\frac{\lambda_2}{\lambda_1}\right)\right]\right.\\
&\left.+(F_3C+F_4D)\left[\arctan\frac{2\lambda_3 xy}{x^2-(\lambda_3^2+\lambda_4^2)y^2}-\arctan\frac{2\lambda_1 xy}{x^2-(\lambda_1^2+\lambda_2^2)y^2}\right]\right\}\\
&+\frac{1}{4\pi}\left[F_5\ln\frac{x^2+2\lambda_2 xy+(\lambda_1^2+\lambda_2^2)y^2}{x^2-2\lambda_2 xy+(\lambda_1^2+\lambda_2^2)y^2}+F_6\ln\frac{x^2+2\lambda_4 xy+(\lambda_3^2+\lambda_4^2)y^2}{x^2-2\lambda_4 xy+(\lambda_3^2+\lambda_4^2)y^2}\right]
\end{aligned}
$$

$$
\begin{aligned}
u_y = &\frac{1}{2\pi}\left\{H_1\left[\arctan\frac{2\lambda_1\lambda_2 y^2}{x^2+(\lambda_1^2-\lambda_2^2)y^2}-2\arctan\frac{\lambda_2}{\lambda_1}\right]\right.\\
&\left.+H_2\left[\arctan\frac{2\lambda_3\lambda_4 y^2}{x^2+(\lambda_3^2-\lambda_4^2)y^2}-2\arctan\frac{\lambda_4}{\lambda_3}\right]\right\}\\
&+\frac{1}{4\pi}\left\{H_3\ln\left[1+\frac{x^4+2(\lambda_1^2-\lambda_2^2)x^2y^2}{(\lambda_1^2+\lambda_2^2)^2y^4}\right]+H_4\ln\left[1+\frac{x^4+2(\lambda_3^2-\lambda_4^2)x^2y^2}{(\lambda_3^2+\lambda_4^2)^2y^4}\right]\right\}
\end{aligned}
$$

$$
\begin{aligned}
w_x(x,y) = &\frac{1}{2\pi}\left\{\frac{b_1^{\perp}}{2}\left[\arctan\left(\frac{\lambda_1^2+\lambda_2^2}{\lambda_1}\frac{y}{x}+\frac{\lambda_2}{\lambda_1}\right)+\arctan\left(\frac{\lambda_1^2+\lambda_2^2}{\lambda_1}\frac{y}{x}-\frac{\lambda_2}{\lambda_1}\right)\right]\right.\\
&\left.+(G_3C+G_4D)\times\left[\arctan\frac{2\lambda_3 xy}{x^2-(\lambda_3^2+\lambda_4^2)y^2}-\arctan\frac{2\lambda_1 xy}{x^2-(\lambda_1^2+\lambda_2^2)y^2}\right]\right\}\\
&+\frac{1}{4\pi}\left[G_5\ln\frac{x^2+2\lambda_2 xy+(\lambda_1^2+\lambda_2^2)y^2}{x^2-2\lambda_2 xy+(\lambda_1^2+\lambda_2^2)y^2}+G_6\ln\frac{x^2+2\lambda_4 xy+(\lambda_3^2+\lambda_4^2)y^2}{x^2-2\lambda_4 xy+(\lambda_3^2+\lambda_4^2)y^2}\right]
\end{aligned}
$$

$$
\begin{aligned}
w_y = &\frac{1}{2\pi}\left\{I_1\left[\arctan\frac{2\lambda_1\lambda_2 y^2}{x^2+(\lambda_1^2-\lambda_2^2)y^2}-2\arctan\frac{\lambda_2}{\lambda_1}\right]\right.\\
&\left.+I_2\left[\arctan\frac{2\lambda_3\lambda_4 y^2}{x^2+(\lambda_3^2-\lambda_4^2)y^2}-2\arctan\frac{\lambda_4}{\lambda_3}\right]\right\}\\
&+\frac{1}{4\pi}\left\{I_3\ln\left[1+\frac{x^4+2(\lambda_1^2-\lambda_2^2)x^2y^2}{(\lambda_1^2+\lambda_2^2)^2y^4}\right]+I_4\ln\left[1+\frac{x^4+2(\lambda_3^2-\lambda_4^2)x^2y^2}{(\lambda_3^2+\lambda_4^2)^2y^4}\right]\right\}
\end{aligned}
\tag{7.4.5}
$$

in which $F_1,\ldots,F_6, G_1,\ldots,G_6, H_1,\ldots,H_4$ and $I_1,\ldots,I_4$ are some functions of $\lambda_1,\lambda_2,\lambda_3$ and λ_4 which are constants constituted from the original material constants M, L, K_1, K_2, K_3 and R, and the expressions are very complicated and lengthy and hence omitted.

By using the similar procedure, the solution for the case (2) can also be obtained. But the solving procedure is very tedious due to the complexity of the final governing Eq. (7.4.1). We omit them for simplicity.

7.4.2 Complex Variable Function Method

The Eq. (7.4.1) can also be solved by complex variable function method. For this purpose, the equation can be rewritten as follows:

$$\left[\frac{\partial^8}{\partial x^8}+4(1-4\varepsilon)\frac{\partial^8}{\partial x^6\partial y^2}+2(3+16\varepsilon)\frac{\partial^8}{\partial x^4\partial y^4}+4(1-4\varepsilon)\frac{\partial^8}{\partial x^2\partial y^6}+\frac{\partial^8}{\partial y^8}\right]F=0 \tag{7.4.6}$$

The solution of Eq. (7.4.6) can be expressed in terms of 4 analytic functions $F_k(z_k)$ of complex variable z_k $(k=1,2,3,4)$, i.e.

$$F(x,y)=2\mathrm{Re}\sum_{k=1}^{4}F_k(z_k),\ z_k=x+\mu_k y \tag{7.4.7}$$

and $\mu_k=\alpha_k+i\beta_k$ $(i=1,2,3,4)$ are complex parameters and determined by the roots of the following eigenvalue equation

$$\mu^8+4(1-4\varepsilon)\mu^6+2(3+16\varepsilon)\mu^4+4(1-4\varepsilon)\mu^2+1=0 \tag{7.4.8}$$

Based on the displacement expressions (6.6.12) and the dislocation condition

$$\left.\int_\Gamma \mathrm{d}u_x=b_1^{\parallel},\quad \int_\Gamma \mathrm{d}u_y=b_2^{\parallel},\quad \int_\Gamma dw_x=b_1^{\perp},\quad \int_\Gamma dw_y=b_2^{\perp}\right\} \tag{7.4.9}$$

we can obtain the solution as follows:

$$u_x=2\mathrm{Re}\sum_{k=1}^{4}a_{1k}f_k(z_k),\quad u_y=2\mathrm{Re}\sum_{k=1}^{4}a_{2k}f_k(z_k)$$
$$w_x=2\mathrm{Re}\sum_{k=1}^{4}a_{3k}f_k(z_k),\quad w_y=2\mathrm{Re}\sum_{k=1}^{4}a_{4k}f_k(z_k)$$

where

$$f_k(z_k) = \frac{\partial^6 F_k(z_k)}{\partial z_k^6} \tag{7.4.9}$$

Some detail of this work can be found in Ref. [10].

7.5 Dislocations in Dodecagonal Quasicrystals

In monograph [7], Ding et al. give the solution in terms of the Green function method which has not been introduced in the present book, so the detail is omitted and only the results are listed, such as the phonon displacement field

$$\begin{aligned}
u_1 &= \frac{b_1^{\parallel}}{2\pi}\left(\arctan(x_2/x_1) + \frac{L+M}{L+2M}\frac{x_1x_2}{r^2}\right) \\
&\quad + \frac{b_2^{\parallel}}{2\pi}\left(\frac{M}{L+2M}\ln(r/r_0) + \frac{L+M}{L+2M}\frac{x_2^2}{r^2}\right), \\
u_2 &= -\frac{b_1^{\parallel}}{2\pi}\left(\frac{M}{L+2M}\ln(r/r_0) + \frac{L+M}{L+2M}\frac{x_1^2}{r^2}\right) \\
&\quad + \frac{b_2^{\parallel}}{2\pi}\left(\arctan(x_2/x_1) - \frac{L+M}{L+2M}\frac{x_1x_2}{r^2}\right), \\
u_3 &= 0.
\end{aligned} \tag{7.5.1}$$

and the phason displacement field

$$\begin{aligned}
w_1 &= \frac{b_1^{\perp}}{2\pi}\left(arc\tan(x_2/x_1) - \frac{(K_1+K_2)(K_2+K_3)}{2K_1(K_1+K_2+K_3)}\frac{x_1x_2}{r^2}\right) \\
&\quad + \frac{b_2^{\perp}}{4\pi}\left(-\frac{K_2(K_1+K_2+K_3)-K_1K_3}{K_1(K_1+K_2+K_3)}\ln(r/r_0)\right. \\
&\quad \left. + \frac{(K_1+K_2)(K_2+K_3)}{K_1(K_1+K_2+K_3)}\frac{x_2^2}{r^2})\right), \\
w_2 &= \frac{b_1^{\perp}}{4\pi}\left((\frac{K_2(K_1+K_2+K_3)-K_1K_3}{K_1(K_1+K_2+K_3)}\ln(r/r_0) - \frac{(K_1+K_2)(K_2+K_3)}{K_1(K_1+K_2+K_3)}\frac{x_1^2}{r^2})\right) \\
&\quad + \frac{b_2^{\perp}}{2\pi}\left(arc\tan(x_2/x_1) + \frac{(K_1+K_2)(K_2+K_3)}{2K_1(K_1+K_2+K_3)}\frac{x_1x_2}{r^2}\right).
\end{aligned} \tag{7.5.2}$$

and the signs L and M are phonon elastic constants and others are the same meaning as before. Because the phonons and phasons are decoupled for dodecagonal quasicrystals, the coupling constant $R = 0$.

7.6 Interface Between Quasicrystal and Crystal

In the previous sections, we discussed dislocation problems in one- and two-dimensional quasicrystals, and a series of analytic solutions are obtained. In Chap. 8, we will discuss the crack problems in the material. Apart from dislocations and cracks, interface is a kind of defects in quasicrystals too, which is of particular significance for some physical processes.

We know that all quasicrystals observed to date are alloys. This kind of alloys can be in crystalline phase, or in quasicrystalline phase or in crystal–quasicrystal coexisting phase. Li et al. [16, 17] observed the crystal–quasicrystal phase transition, which is continuous transition. During the process, there must be interface between crystal and quasicrystal, so the interface is an important problem. In this section, we give a phenomenological study on elastic behaviour of the interface for one-dimensional quasicrystal–isotropic crystal. Refs [15–17] pointed out that the phase transition is induced by the phason strains. However, this is a very complicated problem far unsolved. We focus only on the determination of the strains in this section, and further studies will be given in Chap. 9 for icosahedral quasicrystal–cubic crystal interface.

Consider an orthorhombic quasicrystal be laying at upper half-plane (i.e. $y > 0$) whose phonon-phason coupling problem is governed by (5.4.3), i.e.

$$\left(a_1 \frac{\partial^4}{\partial x^4} + a_3 \frac{\partial^4}{\partial x^2 \partial y^2} + a_5 \frac{\partial^4}{\partial y^4}\right) F = 0 \tag{7.6.1}$$

in which $F(x, y)$ denotes the displacement potential, a_1, a_3, a_5 the material constants composed from C_{ij}, K_i, and R_i defined by (5.3.6). We assume that the crystal coexisting with the quasicrystal be laying at the lower half-plane with thickness h (i.e. $-h < y < 0$), then the plane $y = 0$ is the interface between the quasicrystal and crystal, see Fig. 7.1. For simplicity, suppose the crystal be a isotropic material, characterized by elastic constants $C_{ij}^{(c)}(E^{(c)}, \mu^{(c)})$. At the interface, the following boundary conditions are as follows:

$$y = 0, \quad -\infty < x < \infty : \qquad \sigma_{zy} = \tau f(x) + k u(x), \quad H_{zy} = 0 \tag{7.6.2}$$

in which $f(x)$ is the distribution function of applied stress at the interface, $u(x) = u_z(x, 0)$ the value of displacement component of phonon field at the interface, τ a constant shear stress and k a material constant to be taken as follows:

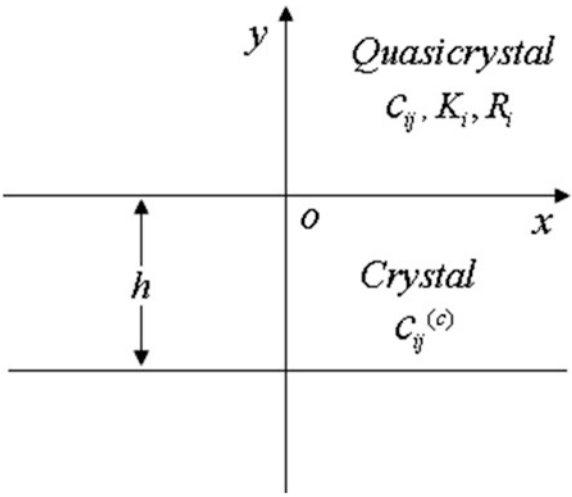

Fig. 7.1 Coexisting phase of quasicrystal–crystal

$$k = \frac{\mu^{(c)}}{h} \tag{7.6.3}$$

and where $\mu^{(c)}$ and h the shear modulus and thickness of the crystal. We further assume that at the outer boundaries, it is stress free.

Taking the Fourier transform

$$\hat{F}(\xi, y) = \int_{-\infty}^{\infty} F(x, y) \mathrm{e}^{i\xi x} \mathrm{d}x \tag{7.6.4}$$

to the Eq. (7.6.1) yields

$$\left(a_5 \frac{\mathrm{d}^4}{\mathrm{d}y^4} + a_3 \xi^2 \frac{\mathrm{d}^2}{\mathrm{d}y^2} + a_1 \xi^4 \right) \hat{F} = 0 \tag{7.6.5}$$

If assume solution of Eq. (7.6.5) be

$$\hat{F}(\xi, y) = \mathrm{e}^{-\lambda |\xi| y}$$

where $y > 0$ and λ is a parameter, and substituting it into (7.6.5) leads to

$$a_5 \lambda^4 - a_3 \lambda^2 + a_1 = 0 \tag{5.7.6}$$

with roots of which

$$\lambda_1, \lambda_2, \lambda_3, \lambda_4 = \sqrt{\frac{2a_3 \pm \sqrt{a_3^2 - 4a_1 a_5}}{2a_5}}, \quad -\sqrt{\frac{2a_3 \pm \sqrt{a_3^2 - 4a_1 a_5}}{2a_5}} \tag{7.6.7}$$

So that

$$\hat{F}(\xi, y) = A\mathrm{e}^{-\lambda_1|\xi|y} + B\mathrm{e}^{-\lambda_2|\xi|y} + B\mathrm{e}^{-\lambda_3|\xi|y} + D\mathrm{e}^{-\lambda_4|\xi|y}$$

By considering the condition of stress free at $y = \infty$, then $C = D = 0$, i.e.

$$\hat{F}(\xi, y) = A\mathrm{e}^{-\lambda_1|\xi|y} + B\mathrm{e}^{-\lambda_2|\xi|y} \tag{7.6.8}$$

According to Sect. 5.4, we have

$$\begin{aligned}
\sigma_{zy} &= (R_6 C_{44} - R_5 C_{55}) \frac{\partial^3 F}{\partial x^2 \partial y} \\
H_{zy} &= -\left(C_{55}\frac{\partial^2}{\partial x^2} + C_{44}\frac{\partial^2}{\partial y^2}\right)\left(K_1\frac{\partial}{\partial x} + K_2\frac{\partial}{\partial y}\right)F \\
u_z &= \left(R_6\frac{\partial^2}{\partial x^2} + R_5\frac{\partial^2}{\partial y^2}\right)F
\end{aligned} \tag{7.6.9}$$

The Fourier transforms of the stresses and displacement are, e.g.

$$\begin{aligned}
\hat{\sigma}_{zy} &= -(R_6 C_{44} - R_5 C_{55})\xi^2 \frac{\mathrm{d}\hat{F}}{\mathrm{d}y} \\
\hat{H}_{zy} &= -\mathrm{i}C_{55}K_1|\xi|\xi^2\hat{F} + C_{55}K_2\xi^2\frac{\mathrm{d}\hat{F}}{\mathrm{d}y} + iC_{44}K_1|\xi|\frac{\mathrm{d}^2\hat{F}}{\mathrm{d}y^2} - C_{44}K_2\frac{\mathrm{d}^3\hat{F}}{\mathrm{d}y^3}
\end{aligned}$$

$$\begin{aligned}
\hat{\sigma}_{zy} &= -(R_6 C_{44} - R_5 C_{55})\xi^2 \frac{\mathrm{d}\hat{F}}{\mathrm{d}y} \\
\hat{H}_{zy} &= -iC_{55}K_1|\xi|\xi^2\hat{F} + C_{55}K_2\xi^2\frac{\mathrm{d}\hat{F}}{\mathrm{d}y} + iC_{44}K_1|\xi|\frac{\mathrm{d}^2\hat{F}}{\mathrm{d}y^2} - C_{44}K_2\frac{\mathrm{d}^3\hat{F}}{\mathrm{d}y^3}
\end{aligned}$$

$$\hat{u}_z = \left(-\xi^2 R_6 + R_5\frac{\mathrm{d}^2}{\mathrm{d}y^2}\right)\hat{F} \tag{7.6.10}$$

Substituting (7.6.8) into the second one of (7.6.10) and then into the second one of (7.6.2) yields

$$B = \alpha A \tag{7.6.11}$$

where

$$\alpha = \frac{-\lambda_1 c_2 - \lambda_1^3 c_4 + i(c_1 + \lambda_1^2 c_3)}{\lambda_2 c_2 + \lambda_2^3 c_4 + i(-c_1 - \lambda_2^2 c_3)}$$

$$c_1 = C_{55}K_1, \quad c_2 = C_{55}K_2, \quad c_3 = C_{44}K_1, \quad c_4 = C_{44}K_2 \tag{7.6.12}$$

By applying the Fourier transform, the stress and displacement components are:

$$\hat{\sigma}_{zy}(\xi, 0) = A(\xi)|\xi|(\lambda_1 \mathrm{e}^{-\lambda_1|\xi|y} + \alpha\lambda_2 \mathrm{e}^{-\lambda_2|\xi|y})$$

$$\hat{u}_z(\xi, 0) = A(\xi)\xi^2[(-R_6 + \lambda_1^2 R_5)\mathrm{e}^{-\lambda_1|\xi|y} + \alpha(R_6 - \lambda_2^2 R_5)\mathrm{e}^{-\lambda_2|\xi|y}] \tag{7.6.13}$$

The Fourier transform of the first one of (7.6.2) is:

$$\hat{\sigma}_{zy}(\xi, 0) = \tau\hat{f}(\xi) + k\hat{u}(\xi, 0) \tag{7.6.14}$$

From (7.6.13) and (7.6.14), one determines the unknown function

$$A(\xi) = \frac{\tau\hat{f}(\xi)}{|\xi|(\lambda_1 + \alpha\lambda_2) - k\xi^2[-R_6 + \lambda_1^2 R_5 + \alpha(R_6 - \lambda_1^2 R_5)]} \tag{7.6.15}$$

So all stress and displacement components for phonon and phason fields can be evaluated, e.g.

$$\begin{aligned}
\sigma_{zy} &= \frac{1}{2\pi}\int_{-\infty}^{\infty} \hat{\sigma}_{zy}\mathrm{e}^{-i\xi x}d\xi = \frac{1}{2\pi}\int_{-\infty}^{\infty} A(\xi)|\xi|(\lambda_1 \mathrm{e}^{-\lambda_1|\xi|y} + \alpha\lambda_2 \mathrm{e}^{-\lambda_2|\xi|y})\mathrm{e}^{-\mathrm{i}\xi x}\mathrm{d}\xi \\
u_z &= \frac{1}{2\pi}\int_{-\infty}^{\infty} \hat{u}_z \mathrm{e}^{-\mathrm{i}\xi x}\mathrm{d}\xi \\
&= \frac{1}{2\pi}\int_{-\infty}^{\infty} A(\xi)\xi^2[(-R_6 + \lambda_1^2 R_5)\mathrm{e}^{-\lambda_1|\xi|y} + \alpha(R_6 - \lambda_2^2 R_5)\mathrm{e}^{-\lambda_2|\xi|y}]\mathrm{e}^{-\mathrm{i}\xi x}\mathrm{d}\xi
\end{aligned} \tag{7.6.16}$$

$$\begin{aligned}
w_z &= \frac{1}{2\pi}\int_{-\infty}^{\infty} \hat{w}_z \mathrm{e}^{-\mathrm{i}\xi x}\mathrm{d}\xi \\
&= -\frac{1}{2\pi}\int_{-\infty}^{\infty} A(\xi)\xi^2[(-C_{55} + \lambda_1^2 C_{66})\mathrm{e}^{-\lambda_1|\xi|y} + \alpha(C_{66} - \lambda_2^2 C_{55})\mathrm{e}^{-\lambda_2|\xi|y}]\mathrm{e}^{-\mathrm{i}\xi x}\mathrm{d}\xi
\end{aligned}$$

The phason strain field presents important effect in the phase transition of crystal–quasicrystal, which are determined from the above solution such as

$$w_{zx} = \frac{\partial w_z}{\partial x} = -\mathrm{i}\frac{1}{2\pi}\int_{-\infty}^{\infty} A(\xi)\xi^3[(-C_{55}+\lambda_1^2 C_{66})\mathrm{e}^{-\lambda_1|\xi|y}+\alpha(C_{66}-\lambda_2^2 C_{55})\mathrm{e}^{-\lambda_2|\xi|y}]\mathrm{e}^{-\mathrm{i}\xi x}\mathrm{d}\xi$$

$$w_{zy} = \frac{\partial w_z}{\partial y} = \frac{1}{2\pi}\int_{-\infty}^{\infty} A(\xi)\xi^2[\lambda_1|\xi|(-C_{55}+\lambda_1^2 C_{66})\mathrm{e}^{-\lambda_1|\xi|y} + \lambda_2|\xi|\alpha(C_{66}-\lambda_2^2 C_{55})\mathrm{e}^{-\lambda_2|\xi|y}]\mathrm{e}^{-\mathrm{i}\xi x}\mathrm{d}\xi \tag{7.6.17}$$

The calculation of integrals (7.6.17) depends upon the form of function $\hat{f}(\xi) = \int_{-\infty}^{\infty} f(x)\mathrm{e}^{\mathrm{i}\xi x}\mathrm{d}x$, in which $f(x)$ represents the stress distribution subjected at the interface. We can obtain the elementary form of the integrals by residual theorem for some cases, e.g. $f(x) = \delta(x)$, or

$$f(x) = \begin{cases} 1 & |x| \le a/2 \\ 0 & |x| \ge a/2 \end{cases}$$

The computed results vary from material constants C_{ij}, K_i, R_i of quasicrystals, and the material constant $\mu^{(c)}$ of crystals, applied stress τ and the size h of the crystals, so the results are very complicated.

Further discussion on interface and integral calculation will be given in Sect. 9.2 of Chap. 9.

7.7 Dislocation Pile up, Dislocation Group and Plastic Zone

Previous discussion gives some solutions of single dislocation in some one- and two-dimensional quasicrystals. The dislocations can pile up when they meet some obstacles and lead to dislocation group, and this is a plastic zone in the material. Dislocations and plastic zone influence the behaviour of materials evidently. There is a lack of theory of plasticity of quasicrystals so far. Observation on plasticity of quasicrystals from point of view of dislocation is a basic way at present. It provides not only the mechanism of plasticity of quasicrystals but also the tool for evaluating exactly some physical quantities concerning plastic deformation. This greatly helps the discussion in Chaps. 8 and 14, respectively.

The slow movement of dislocations includes forms of slip and clime, and they relate to plasticity of quasicrystals (refer to Messerschmidt [20]), which will be discussed in Chaps. 8 and 14.

7.8 Discussions and Conclusions

The main objective of this chapter lies in the demonstration on effect of our formulation in Chaps. 5 and 6, and it does not completely intend to explore the whole nature of dislocations and interfaces in quasicrystals. Other works, e.g. [11–15, 18, 19], can be referenced. But reader can find from the results listed above that dislocation leads to the appearance of singularity around the dislocation core, e.g. stresses $\sigma_{ij}, H_{ij} \sim 1/r \quad (r \to 0)$, which is the direct result of symmetry-breaking due to the appearance of the topological defect, where r is the distance measured from the dislocation core. This is similar to that of crystals, i.e. the symmetry-breaking also leads to the appearance of singularity in crystals. Physically, the high stress grade is called the stress concentration around dislocation core which results in plastic flow in crystals as well as in quasicrystals. So dislocation and other defects in quasicrystals affect evidently the mechanical and other physical properties of the material. The dislocation solutions present important application in studying plastic deformation and plastic fracture, and one can refer to [14] or Chap. 14 of this book. The discussion on interface here is in primary version, but it may be helpful for understanding crystal–quasicrystal phase transition. However, this is a very complicated problem, and the data in this respect are very limited so far. The dislocations and interfaces and the solutions in three-dimensional quasicrystals will be introduced in Chap. 9, and the dynamic dislocation problem can be referred in Chap. 10.

References

1. De P and Pelcovits R A, 1987, Linear elasticity theory of pentagonal quasicrystals. *Phys Rev* B, **35**(16), 8609-8620.
2. De P and Pelcovits R A, 1987, Disclination in pentagonal quasicrystals. *Phys Rev* B, **36**(17), 9304-9307.
3. Ding D H, Wang R H, Yang W G and Hu C Z, 1995, General expressions for the elastic displacement fields induced by dislocation in quasicrystals. *J. Phys. Condens. Matter*., 7(28), 5423-5436.
4. Ding D H, Wang R H, Yang W G, Hu C Z and Qin Y L, 1995, Elasticity theory of straight dislocation in quasicrystals, *Phil Mag Lett*, **72**(5), 353-359.
5. Li X F and Fan T Y, 1998, New method for solving elasticity problems of some planar quasicrystals and solutions. *Chin Phys Lett,* **15**(4), 278-280; Li X F, Defect problems and their analytic solutions in elasticity of quasicrystals, Dissertation, Beijing Institute of Technology, 1999.

6. Li X F, Duan X Y, Fan T Y et al, 1999, Elastic field for a straight dislocation in a decagonal quasicrystal, *J Phys.: Condens Matter*, **11**(3), 703-711.
7. Yang S H and Ding D H, 1998, *Fundamentals to Theory of Crystal Dislocations*, Vol II. (in Chinese), Beijing: Scientific Press.
8. Firth J P and Lothe J, 1982, *Theory of Dislocations*. John Wiley and Sons, New York.
9. Zhou W M, 2000, Dislocation, crack and contact problems in two- and three-dimensional quasicrystals, Dissertation (in Chinese), Beijing Institute of Technology.
10. Li L H, 2008, Study on complex variable function method and exact analytic solutions of elasticity of quasicrystals, Dissertation (in Chinese), Beijing Institute of Technology.
11. Fan T Y, Li X F and Sun Y F, 1999, A moving screw dislocation in an one-dimensional hexagonal quasicrystals. *Acta Physica Sinica* (Oversea Edition), **8**(3), 288-295.
12. Li X F and Fan T Y, 1999, A straight dislocation in one-dimensional hexagonal quasicrystals. *Phy Stat Sol* (b), **212**(1), 19-26.
13. Edagawa K, 2001, Dislocations in quasicrystals, *Mater Sci Eng A* **309-310**(2), 528-538.
14. Fan T Y, Trebin H R, Messeschmidt U and Mai Y W, 2004, Plastic flow coupled with a crack in some one- and two-dimensional quasicrystals, *J Phys.: Condens. Matter*, **16**(37), 5229-5240.
15. Hu C Z, Wang R H and Ding D H, 2000, Symmetry groups, physical property tensors, elasticity and dislocations in quasicrystals, *Rep. Prog. Phys*., **63**(1), 1-39.
16. Li F H, 1993, in *Crystal-Quasicrystal Transitions*, ed. by Jacaman M J and Torres M, Elsevier Sci Publ, 13-47.
17. Li F H, Teng C M, Huang Z R et al, 1988, In between crystalline and quasicrystalline states, *Phil. Mag. Lett*., **57** (1), 113-118.
18. Fan T Y, Xie L Y, Fan L and Wang Q Z, 2011, Study on interface of quasicrystal-crystal, *Chin. Phys*. B, 20(7), 076102.
19. Kordak M, Fluckider T, Kortan A R et al, 2004, Crystal-quasicrystal interface in Al-Pd-Mn, *Prog. Surface Sci*, **75**(3-8), 161-175.
20. Messerschmidt U, 2010, Dislocation Dynamics during Plastic Deformation, Chapter 10, Springer-Verlag, Heidelberg.

Chapter 8
Application II—Solutions of Notch and Crack Problems of One- and Two-Dimensional Quasicrystals

Quasicrystals are potential material to be developed for structural use, and their strength and toughness attract the attention of researchers. Experimental observations [1, 2] have shown that quasicrystals are brittle under low and middle temperature. With common experience of conventional structural materials, we know that the failure of brittle materials is related to the existence and growth of cracks. Chapter 7 indicated that dislocations have been observed in quasicrystals, and the accumulation of dislocations will eventually lead to cracking of the material. Now, let us study the crack problems in quasicrystals that have both theoretical and practical values in the view of application in the future.

Chapters 5–7 have discussed some elasticity and dislocation problems in one- and two-dimensional quasicrystals. It has shown that when the quasicrystal configuration is independent of one coordinate, e.g. variable z, its elasticity problem can be decoupled into a plane problem and an anti-plane problem. In the case of one-dimensional quasicrystals, if the z-direction accords to the quasiperiodic axis, the above plane problem belongs to classic elasticity problem, and the anti-plane problem is a coupling problem of phonon and phason fields. In the case of two-dimensional quasicrystals, if z-direction represents the periodic axis, the above plane problem is a coupling problem of phonon and phason fields, and the anti-plane problem belongs to a classical elasticity problem. Because of using decomposition procedure, the resulting problem can be dramatically simplified. Chapters 5 and 6 have given their corresponding fundamental solutions, and Chap. 7 conducted the solutions of dislocations in detail. The present chapter is going to focus on crack problems, and we continue using the above schemes, such as the fundamental solutions developed in Chaps. 5 and 6, and the Fourier transform and complex analysis used in Chap. 7. But it emphasizes the complex analysis method, which will be developed in Sects. 8.1, 8.2 and 8.4 and succeeded sections, and this approach is powerful. Problems displayed in Sects. 8.1 and 8.2 are relative simpler; the detailed introduction may help reader to understand and further handle

T.-Y. Fan, *Mathematical Theory of Elasticity of Quasicrystals and Its Applications*,
Springer Series in Materials Science 246, DOI 10.1007/978-981-10-1984-5_8

the principle and technique of the complex analysis method; though the representation is not beyond the classical Muskhelishvili [17] method, this is helpful to understand the solutions for more complicated problems displayed in Sects. 8.4–8.8 and in the next chapter. The further summary of the method will be introduced in Chap. 11, because the contents in Sects. 8.4–8.8 and Chap. 9 bring some new insights into the study and are beyond the classical Muskhelishvili method; the general discussion is necessary and may be beneficial.

Based on the common nature of exact solutions of different static and dynamic cracks in different quasicrystal systems in linear and nonlinear deformation (which are discussed in this chapter and Chaps. 9, 10 and 14), the fracture theory of quasicrystalline material is suggested in Chap. 15, which can be seen as a development of fracture mechanics of conventional structural materials.

8.1 Crack Problem and Solution of One-Dimensional Quasicrystals

8.1.1 Griffith Crack

As shown in Fig. 8.1, assume a Griffith crack along the quasiperiodic axis (z-direction) of a one-dimensional hexangular quasicrystal and under the action of external traction $\sigma_{yz}^{(\infty)} = \tau_1$ and/or $H_{zy}^{(\infty)} = \tau_2$. The deformation induced is often termed longitudinal shearing. Obviously, the geometry of the crack is independent of variable z. In this case, all field variables are independent of variable z. Therefore, based on the analysis in Chap. 5, this one-dimensional quasicrystal elasticity can be decomposed into a plane elasticity problem of regular crystal and an anti-plane

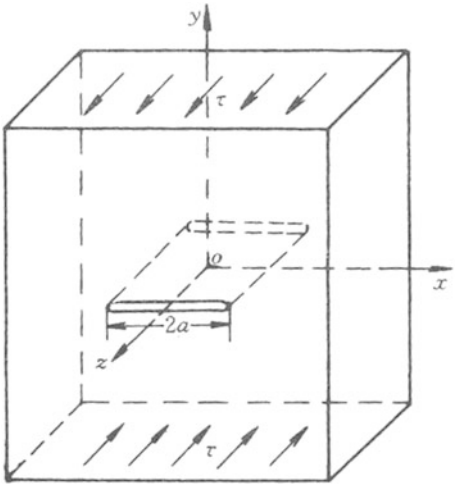

Fig. 8.1 A Griffith crack subjected to a longitudinal shear where $\tau = \tau_1$ corresponding to phonon field and $\tau = \tau_2$ corresponding to phason field of a Griffith crack

elasticity problem of phonon-phason coupling field. Plane elasticity problems of regular crystal have been studied extensively in classical elasticity, and its crack problems have also been studied in the classical fracture theory, such as in Ref. [3]. Therefore, we skip the discussion of crack problems in regular crystal. The anti-plane elasticity problem of the phonon-phason coupling field is described by using the following basic equations:

$$\left.\begin{aligned} \sigma_{yz} &= \sigma_{zy} = 2C_{44}\varepsilon_{yz} + R_3 w_{zy} \\ \sigma_{zx} &= \sigma_{xz} = 2C_{44}\varepsilon_{zx} + R_3 w_{zx} \\ H_{zy} &= K_2 w_{zy} + 2R_3 \varepsilon_{zy} \\ H_{zx} &= K_2 w_{zx} + 2R_3 \varepsilon_{zx} \end{aligned}\right\} \tag{8.1.1}$$

$$\left.\begin{aligned} \varepsilon_{yz} &= \varepsilon_{zy} = \tfrac{1}{2}\tfrac{\partial u_z}{\partial y}, \quad & \varepsilon_{zx} &= \varepsilon_{xz} = \tfrac{1}{2}\tfrac{\partial u_z}{\partial x} \\ w_{zy} &= \tfrac{\partial w_z}{\partial y}, & w_{zx} &= \tfrac{\partial w_z}{\partial x} \end{aligned}\right\} \tag{8.1.2}$$

$$\frac{\partial \sigma_{zx}}{\partial x} + \frac{\partial \sigma_{zy}}{\partial y} = 0, \quad \frac{\partial H_{zx}}{\partial x} + \frac{\partial H_{zy}}{\partial y} = 0 \tag{8.1.3}$$

The derivation in Chap. 5 shows that the above equations can be reduced to

$$\nabla^2 u_z = 0, \quad \nabla^2 w_z = 0 \tag{8.1.4}$$

where $\nabla^2 = \partial^2/\partial x^2 + \partial^2/\partial y^2$.

Figure 8.1 shows that the anti-plane deformation of a Griffith crack has the following boundary conditions:

$$\left.\begin{aligned} \sqrt{x^2+y^2} \to \infty: \quad & \sigma_{yz} = \tau_1, \quad H_{zy} = \tau_2, \sigma_{zx} = H_{zx} = 0 \\ y = 0, |x| < a: \quad & \sigma_{yz} = 0, \quad H_{zy} = 0 \end{aligned}\right\} \tag{8.1.5}$$

where a is the half-length of the crack.

Based on the results of linear elasticity analysis, if the quasicrystal is traction-free at infinity and instead there are a traction $\sigma_{yz} = -\tau_1$ and a generalized traction $H_{zy} = -\tau_2$ at the crack surface, then the boundary conditions stand for

$$\left.\begin{aligned} \sqrt{x^2+y^2} \to \infty: \quad & \sigma_{yz} = \sigma_{zx} = H_{zx} = H_{zy} = 0 \\ y = 0, |x| < a: \quad & \sigma_{yz} = -\tau_1, \quad H_{zy} = -\tau_2 \end{aligned}\right\} \tag{8.1.6}$$

Here, we give phason stress τ_2 at the crack surface from the physical point of view, though its measurement result has not been reported yet. For simplicity, we can assume $\tau_2 = 0$, sometimes.

In the following, we are going to solve the boundary value problem of (8.1.4) and (8.1.5) first. The complex analysis method will be used. To do so, we introduce the complex variable

$$t = x + iy = re^{i\theta}, \quad i = \sqrt{-1} \tag{8.1.7}$$

From Eq. (8.1.4), it is known that both $u_z(x, y)$ and $w_z(x, y)$ are harmonic functions that can be expressed in terms of the real part or the imaginary part of two arbitrary analytic functions $\phi_1(t)$ and $\psi_1(t)$ of complex variable t in a region occupied by the quasicrystal. For simplicity, we can call $\phi_1(t)$ and $\psi_1(t)$ as complex potentials. Here, assume

$$\left.\begin{aligned} u_z(x, y) &= \mathrm{Re}\phi_1(t) \\ w_z(x, y) &= \mathrm{Re}\psi_1(t) \end{aligned}\right\} \tag{8.1.8}$$

in which the symbol Re indicates the real part of a complex number.

It is well known that if a function $F(t)$ is analytic, then

$$\frac{\partial F}{\partial x} = \frac{dF}{dt}, \quad \frac{\partial F}{\partial y} = \frac{idF}{dt}. \tag{a}$$

Furthermore, assume

$$\begin{aligned} F(t) &= P(x, y) + iQ(x, y) \\ &= \mathrm{Re}F(t) + i\mathrm{Im}F(t), \end{aligned} \tag{b}$$

where symbol Im denotes the imaginary part of a complex, and $P(x, y)$ and $Q(x, y)$ represent the real and imaginary parts of $F(t)$, respectively. Therefore, the Cauchy–Riemann relation leads to

$$\frac{\partial P}{\partial x} = \frac{\partial Q}{\partial y}, \quad \frac{\partial P}{\partial y} = -\frac{\partial Q}{\partial x}. \tag{c}$$

With the aid of relation (a), formula (8.1.8) and Eqs. (8.1.1) and (8.1.2) lead to

$$\left.\begin{aligned} \sigma_{yz} = \sigma_{zy} &= C_{44}\frac{\partial}{\partial y}\mathrm{Re}\phi_1 + R_3\frac{\partial}{\partial y}\mathrm{Re}\psi_1 \\ \sigma_{zx} = \sigma_{xz} &= C_{44}\frac{\partial}{\partial x}\mathrm{Re}\phi_1 + R_3\frac{\partial}{\partial x}\mathrm{Re}\psi_1 \\ H_{zx} &= K_2\frac{\partial}{\partial x}\mathrm{Re}\psi_1 + R_3\frac{\partial}{\partial x}\mathrm{Re}\phi_1 \\ H_{zx} &= K_2\frac{\partial}{\partial y}\mathrm{Re}\psi_1 + R_3\frac{\partial}{\partial y}\mathrm{Re}\phi_1 \end{aligned}\right\} \tag{8.1.9}$$

Based on the Cauchy–Riemann relation (c), the above equation can be rewritten as

$$\left.\begin{aligned}\sigma_{zx} - i\sigma_{zy} &= C_{44}\phi_1' + R_3\psi_1' \\ H_{zx} - iH_{zy} &= K_2\psi_1' + R_3\phi_1'\end{aligned}\right\} \tag{8.1.10}$$

where $\phi_1' = \mathrm{d}\phi_1/\mathrm{d}t, \psi_1' = \mathrm{d}\psi_1/\mathrm{d}t$.

According to formula (8.1.10), we have

$$\left.\begin{aligned}\sigma_{yz} = \sigma_{zy} &= -\mathrm{Im}(C_{44}\phi_1' + R_3\psi_1') \\ H_{zy} &= -\mathrm{Im}(K_2\psi_1' + R_3\phi_1')\end{aligned}\right\} \tag{d}$$

Furthermore, for an arbitrary complex function $F(t)$, its imaginary part is

$$\mathrm{Im}F(t) = \frac{1}{2i}(F - \overline{F})$$

where $\overline{F}$ indicates the conjugate of F. Then, formula (d) can be expressed as follows:

$$\left.\begin{aligned}\sigma_{yz} = \sigma_{zy} &= -\frac{1}{2i}\left[C_{44}(\phi_1' - \overline{\phi_1'}) + R_3(\psi_1' - \overline{\psi_1'})\right] + \tau_1 \\ H_{zy} &= -\frac{1}{2i}\left[K_2(\psi_1' - \overline{\psi_1'}) + R_3(\phi_1' - \overline{\phi_1'})\right] + \tau_2\end{aligned}\right\} \tag{8.1.11}$$

The expression given by (8.1.11) ensures the solution constructed in the following to automatically satisfy the boundary condition at infinity, and the solution is:

$$\left.\begin{aligned}\phi_1(t) &= \frac{ia(K_2\tau_1 - R_3\tau_2)}{C_{44}K_2 - R_3^2}\left(\frac{t}{a} - \sqrt{\left(\frac{t}{a}\right)^2 - 1}\right) \\ \psi_1(t) &= \frac{ia(C_{44}\tau_2 - R_3\tau_1)}{C_{44}K_2 - R_3^2}\left(\frac{t}{a} - \sqrt{\left(\frac{t}{a}\right)^2 - 1}\right)\end{aligned}\right\} \tag{8.1.12}$$

whose derivation can be obtained in terms of the strict complex analysis method as well as the Fourier method given in Sect. 8.12—Appendix 1 of this chapter.

From (8.1.12),

$$\left.\begin{aligned}\phi_1'(t) &= \frac{i(K_2\tau_1 - R_3\tau_2)}{C_{44}K_2 - R_3^2}\left(1 - \frac{t}{\sqrt{t^2 - a^2}}\right) \\ \psi_1'(t) &= \frac{i(C_{44}\tau_2 - R_3\tau_1)}{C_{44}K_2 - R_3^2}\left(1 - \frac{t}{\sqrt{t^2 - a^2}}\right)\end{aligned}\right\} \tag{8.1.13}$$

and substitution of the above expressions into the first expression in (8.1.11) yields

$$\sigma_{zx} - i\sigma_{zy} = i\tau_1\left(-\frac{t}{\sqrt{t^2-a^2}}\right). \tag{8.1.14}$$

Separation of the real and imaginary parts of (8.1.14) leads to

$$\left.\begin{aligned}\sigma_{xz} = \sigma_{zx} &= \frac{\tau_1 r}{(r_1 r_2)^{1/2}}\sin\left(\theta - \frac{1}{2}\theta_1 - \frac{1}{2}\theta_2\right)\\ \sigma_{yz} = \sigma_{zy} &= \frac{\tau_1 r}{(r_1 r_2)^{1/2}}\cos\left(\theta - \frac{1}{2}\theta_1 - \frac{1}{2}\theta_2\right)\end{aligned}\right\} \tag{8.1.15}$$

where

$$t = re^{i\theta}, \quad t-a = r_1 2e^{i\theta_1}, \quad t+a = r_2 2e^{i\theta_2} \tag{8.1.16}$$

or

$$\left.\begin{aligned} r &= \sqrt{x^2+y^2}, \quad r_1 = \sqrt{(x-a)^2+y^2}, \quad r_2 = \sqrt{(x+a)^2+y^2}\\ \theta &= \arctan\left(\frac{y}{x}\right), \quad \theta_1 = \arctan\left(\frac{y}{x-a}\right), \quad \theta_2 = \arctan\left(\frac{y}{x+a}\right)\end{aligned}\right\} \tag{8.1.16'}$$

which is shown in Fig. 8.2.

Similarly,

$$H_{zx} - iH_{zy} = i\tau_2\left(-\frac{t}{\sqrt{t^2-a^2}}\right) \tag{8.1.17}$$

For these stress components, there are similar expressions like (8.1.15).

As a result,

$$\sigma_{zy}(x,0) = \begin{cases}\frac{\tau_1 x}{\sqrt{x^2-a^2}}, & |x| > a\\ 0 & |x| < a\end{cases} \tag{8.1.18}$$

$$H_{zy}(x,0) = \begin{cases}\frac{\tau_2 x}{\sqrt{x^2-a^2}} - \tau_2, & |x| > a\\ 0, & |x| < a\end{cases} \tag{8.1.19}$$

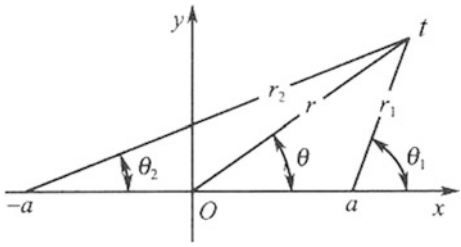

Fig. 8.2 The coordinate system of crack tip

The above two formulas indicate that at $y = 0$ and $|x| < 1$: $\sigma_{zy} = 0$, $H_{zy} = 0$. Therefore, the solution given above also satisfies the boundary condition at the crack surfaces.

Formulas (8.1.14) and (8.1.17) also show that when $\sqrt{x^2 + y^2} \to \infty$, $\sigma_{yz} = \tau_1$, $\sigma_{xz} = 0$ and $H_{zy} = \tau_2$, $H_{zx} = 0$, namely, the solution given above satisfies boundary condition at infinity.

8.1.2 Brittle Fracture Theory

The above formulas show that stresses have singular characteristics near crack tips, for example,

$$\begin{cases} \sigma_{zy}(x,0) = \dfrac{\tau_1 x}{\sqrt{x^2 - a^2}} \to \infty, & x \to a^+ \\ H_{zy}(x,0) = \dfrac{\tau_2 x}{\sqrt{x^2 - a^2}} \to \infty, & x \to a^+ \end{cases} \tag{8.1.20}$$

If defining the Mode III stress intensity factors of the phonon and phason fields such that:

$$K_{\mathrm{III}}^{\parallel} = \lim_{x \to a^+} \sqrt{2\pi(x-a)}\sigma_{zy}(x,0),$$
$$K_{\mathrm{III}}^{\perp} = \lim_{x \to a^+} \sqrt{2\pi(x-a)}H_{zy}(x,0),$$

we have

$$K_{\mathrm{III}}^{\parallel} = \sqrt{\pi a}\tau_1,\ K_{\mathrm{III}}^{\perp} = \sqrt{\pi a}\tau_2, \tag{8.1.21}$$

where subscript "III" stands for model III (longitudinal shearing mode) [3].

Now, let us calculate the crack strain energy:

$$\begin{aligned} W_{\mathrm{III}} &= 2\int_0^a \left(\sigma_{zy} \oplus H_{zy}\right)(u_z \oplus w_z)\mathrm{d}x \\ &= 2\int_0^a \left[\sigma_{zy}(x,0)u_z(x,0) + H_{zy}(x,0)w_z(x,0)\right]\mathrm{d}x \end{aligned} \tag{8.1.22}$$

From (8.1.8) and (8.1.12), we have

$$\left.\begin{aligned} u_z(x,0) &= \mathrm{Re}(\phi_1(t))_{t=x} = a\frac{K_2\tau_1 - R_3\tau_2}{C_{44}K_2 - R_3^2}\sqrt{1-\left(\frac{x}{a}\right)^2} \quad |x|<a \\ w_z(x,0) &= \mathrm{Re}(\psi_1(t))_{t=x} = a\frac{C_{44}\tau_2 - R_3\tau_1}{C_{44}K_2 - R_3^2}\sqrt{1-\left(\frac{x}{a}\right)^2} \quad |x|<a \end{aligned}\right\} \tag{8.1.23}$$

In addition, considering the equivalency of problems (8.1.5) and (8.1.6), we can take $\sigma_{yz}(x,0) = -\tau_1$ and $H_{zy} = -\tau_2$ as $|x|<a$, then the substitution of above results into (8.1.22) yields

$$W_{\mathrm{III}} = \frac{K_2\tau_1^2 + C_{44}\tau_2^2 - 2R_3\tau_1\tau_2}{C_{44}K_2 - R_3^2}\pi a^2 \tag{8.1.24}$$

From (8.1.24), we can determine the crack strain energy release rate (crack growth force) such that

$$\begin{aligned} G_{\mathrm{III}} &= \frac{1}{2}\frac{\partial W_{\mathrm{III}}}{\partial a} = \frac{K_2\tau_1^2 + C_{44}\tau_2^2 - 2R_3\tau_1\tau_2}{C_{44}K_2 - R_3^2}\pi a \\ &= \frac{K_2 K_{\mathrm{III}}^{\parallel\,2} + C_{44}K_{\mathrm{III}}^{\perp\,2} - 2R_3 K_{\mathrm{III}}^{\parallel}K_{\mathrm{III}}^{\perp}}{C_{44}K_2 - R_3^2} \end{aligned} \tag{8.1.25}$$

Clearly, the crack strain energy and energy release rate are related not only to phonon but also phason and phonon-phason coupling fields.

If $\tau_2 = 0$, then

$$G_{\mathrm{III}} = \frac{K_2 K_{\mathrm{III}}^{\parallel\,2}}{C_{44}K_2 - R_3^2} \tag{8.1.26}$$

Furthermore, if $R_3 = 0$, we have

$$G_{\mathrm{III}} = \frac{\pi a\tau_1^2}{C_{44}}, \text{ or } G_{\mathrm{III}} = \frac{(K_{\mathrm{III}}^{\parallel})^2}{C_{44}}. \tag{8.1.27}$$

Since G_{III} comprehensively describes the coupling effect of the phonon and phason fields and the stress status near crack tip, we recommend

$$G_{\mathrm{III}} = G_{\mathrm{IIIC}} \tag{8.1.28}$$

as the fracture criterion of quasicrystals under Mode III deformation, where G_{IIIC} is the critical (threshold) value of G_{III}, called Mode III fracture toughness to be determined by testing.

The stress intensity factor and strain energy release rate are fundamental physical parameters and constitute the basis of brittle fracture theory for both conventional crystalline as well as quasicrystalline materials.

8.2 Crack Problem in Finite-Sized One-Dimensional Quasicrystals

The preceding section discusses Griffith crack problems in one-dimensional quasicrystals and their exact solutions are obtained. In this section, we are going to discuss the solution of another kind of important crack problems, which go beyond the scope of the Griffith crack. In the previous section, we assumed that the size of quasicrystal is much more larger than that of the defect, while in this case we consider the quasicrystal as an infinite body. Therefore, this section is aimed at studying crack problems in quasicrystals of finite size.

8.2.1 Cracked Quasicrystal Strip with Finite Height

As shown in Fig. 8.3, a one-dimensional hexagonal quasicrystal strip of height $2H$ has a semi-infinite crack embedded at the mid-plane with crack tip corresponding to coordinate origin. Crack surfaces near the crack tip, i.e. $y = \pm 0$ and $-a < x < 0$, are assumed under the action of uniform shear traction $\sigma_{zy} = -\tau_1$, $H_{zy} = 0$, where a is a length used to simulate a finite-sized crack. The upper and lower strip surfaces are assumed to be traction-free; therefore, the boundary conditions are:

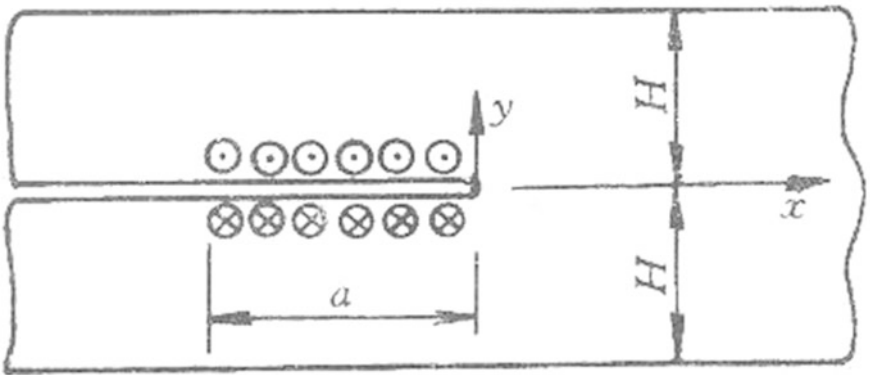

Fig. 8.3 Finite strip of hexagonal quasicrystal with a crack

$$\left.\begin{array}{l} y=\pm H,-\infty<x<\infty:\sigma_{zy}=0,H_{zy}=0 \\ x=\pm\infty,-H<y<H:\sigma_{zx}=0,H_{zx}=0 \\ y=\pm 0,-\infty<x<-a:\sigma_{zy}=0,H_{zy}=0;-a<x<0:\sigma_{zy}=-\tau_1,H_{zy}=-\tau_2 \end{array}\right\} \tag{8.2.1}$$

For simplicity, we assume that $\tau_2 = 0$ in (8.2.1).

Formulas (8.1.1)–(8.1.11) in the preceding section still hold in this section, and other notation and symbol are similar. Therefore, formula (8.1.12) should be modified as follows:

$$\left.\begin{array}{l} C_{44}\left(\phi_1'-\overline{\phi_1'}\right)+R_3\left(\psi_1'-\overline{\psi_1'}\right)=2i\tau_1 f(t) \\ K_2\left(\psi_1'-\overline{\psi_1'}\right)+R_3\left(\phi_1'-\overline{\phi_1'}\right)=0 \end{array}\right\} \tag{8.2.2}$$

where

$$f(x)=\begin{cases} 0, & x<-a, \\ 1, & -a<x<0 \end{cases} \tag{8.2.3}$$

By using the conformal mapping,

$$t=\omega(\zeta)=\frac{H}{\pi}\ln\left[1+\left(\frac{1+\zeta}{1-\zeta}\right)^2\right] \tag{8.2.4}$$

maps the domain in the t-plane onto the interior of the unit circle γ in the ζ-plane, $\zeta = \xi + i\eta$. Therefore, crack tip $t = 0$ corresponds to $\zeta = -1$, and $t = -a$ accords to two points on the unit circle in the ζ-plane such that:

$$\left.\begin{array}{l} \sigma_{-a}=\dfrac{-\mathrm{e}^{-\pi a/H}+2i\sqrt{1-\mathrm{e}^{-\pi a/H}}}{2-\mathrm{e}^{-\pi a/H}} \\ \overline{\sigma_{-a}}=\dfrac{-\mathrm{e}^{-\pi a/H}-2i\sqrt{1-\mathrm{e}^{-\pi a/H}}}{2-\mathrm{e}^{-\pi a/H}} \end{array}\right\} \tag{8.2.5}$$

where $\sigma = \mathrm{e}^{\mathrm{i}\theta} = \zeta|_{|\zeta|=1}$ denotes the value of ζ at the unit circle γ.

Equations in Sect. 8.1 and Appendix of this chapter (i.e. Sect. 8.7) are useful. Nevertheless, the first $2i\omega'(\sigma)\tau_1$ in (8.7.4) should be changed to $2if\omega'(\sigma)\tau$, and the first term in (8.7.5)

$$\frac{2i\tau_1}{C_{44}}\frac{1}{2\pi i}\int_\gamma \frac{\omega'(\sigma)}{\sigma-\zeta}\mathrm{d}\sigma$$

should be modified as follows:

$$\frac{2i\tau_1}{C_{44}}\frac{1}{2\pi i}\int_\gamma f\frac{\omega'(\sigma)}{\sigma-\zeta}\mathrm{d}\sigma.$$

Thus, Eq. (8.7.5) for the present problem becomes:

$$\left.\begin{aligned}\phi'(\zeta)+\frac{R_3}{C_{44}}\psi'(\zeta)&=\frac{2i\tau_1}{C_{44}}\frac{1}{2\pi i}\int_\gamma f\frac{\omega'(\sigma)}{\sigma-\zeta}\mathrm{d}\sigma\\ \psi'(\zeta)+\frac{R_3}{K_2}\phi'(\zeta)&=0\end{aligned}\right\} \tag{8.2.6}$$

where f is the function given by formula (8.2.3), which takes values between $\overline{\sigma_{-a}}$ and σ_{-a} in the ζ-plane.

Integration of the right-hand side of Eq. (8.2.6) leads to

$$\begin{aligned}\frac{1}{2\pi i}\int_\gamma f\frac{\omega'(\sigma)}{\sigma-\zeta}\mathrm{d}\sigma=\frac{1}{2\pi\tau}\Bigg[&\frac{1}{1-\zeta}\ln(\sigma-1)-\frac{1+\zeta}{(1-\zeta)(1+\zeta^2)}\ln(\sigma-\zeta)\\&-\frac{\zeta}{2(1+\zeta^2)}\ln(1+\sigma^2)+\frac{1}{2(1-\zeta^2)}\ln\frac{\sigma-i}{\sigma+i}\Bigg]_{\sigma=\sigma_a}^{\sigma=\overline{\sigma_{-a}}}\equiv F(\zeta)\end{aligned} \tag{8.2.7}$$

where $\overline{\sigma_{-a}}$ and σ_{-a} are given by formula (8.2.5). Based on the above relation, (8.2.6) is further reduced to

$$\phi'(\zeta)=\frac{K_2\tau_1}{C_{44}K_2-R_3^2}2iF(\zeta),\psi'(\zeta)=\frac{-R_3\tau_1}{C_{44}K_2-R_3^2}2iF(\zeta). \tag{8.2.8}$$

Now, let us calculate the stresses. During this process, the following relations will be used:

$$\begin{aligned}\phi_1'(t)&=\frac{\phi'(\zeta)}{\omega'(\zeta)}=\frac{2iK_2\tau_1}{C_{44}K_2-R_3^2}\cdot\frac{F'(\zeta)}{\omega'(\zeta)},\\ \psi_1'(t)&=\frac{\psi'(\zeta)}{\omega'(\zeta)}=-\frac{2iR_3\tau_1}{C_{44}K_2-R_3^2}\cdot\frac{F'(\zeta)}{\omega'(\zeta)}.\end{aligned}$$

Substitution of the above expressions into (8.1.10) leads to

$$\left.\begin{aligned}\sigma_{zx}-i\sigma_{zy}&=i\tau_1\frac{F'(\zeta)}{\omega'(\zeta)}\\ H_{zx}-iH_{zy}&=0\end{aligned}\right\} \tag{8.2.9}$$

which shows that the stress distribution is independent of material constants.

Substitution of (8.2.7) into (8.2.9) leads to the explicit expressions of stresses. The forms of $F(\zeta)$ and $F'(\zeta)$ are relatively complex, while the expressions of stress in terms of variable ζ $(=\xi+i\eta)$ are concise. In an attempt to invert them to the t-plane, inverse of transform (8.2.4) must be used:

$$\zeta=\omega^{-1}(t)=\frac{-(\mathrm{e}^{\pi t/H}-2)\pm 2i\sqrt{\mathrm{e}^{\pi t/H}-2}}{\mathrm{e}^{\pi t/H}-2} \tag{8.2.10}$$

Substitution of (8.2.10) into (8.2.9) yields the final expressions of σ_{zx}, σ_{zy}, H_{zx} and H_{zx} in the t-plane, which are very complex. Here, we skip this procedure.

Now, let us calculate the stress intensity factors. According to (8.3.15) and (8.1.16), it is known that at the region such that $r_1/a \ll 1$,

$$\sigma_{zx}=-\frac{K_{\mathrm{III}}^{\parallel}}{\sqrt{2\pi r_1}}\sin\frac{\theta_1}{2},\quad \sigma_{zy}=-\frac{K_{\mathrm{III}}^{\parallel}}{\sqrt{2\pi r_1}}\cos\frac{\theta_1}{2}$$

Therefore,

$$\sigma_{zx}-i\sigma_{zy}=-\frac{K_{\mathrm{III}}^{\parallel}}{\sqrt{2\pi r_1}}\left(\sin\frac{\theta_1}{2}-i\cos\frac{\theta_1}{2}\right)=-\frac{K_{\mathrm{III}}^{\parallel}}{\sqrt{2\pi t_1}} \tag{8.2.11}$$

where $t_1=r_1\mathrm{e}^{\mathrm{i}\theta_1}=x_1+iy_1$.

By using conformal mapping $t=\omega(\zeta)$, we have

$$t_1=\omega(\zeta_1), \tag{8.2.12}$$

where ζ_1 is the point in the ζ-plane corresponding to t_1. With relations (8.2.11) and (8.2.9), we define

$$K_{\mathrm{III}}^{\parallel}=\lim_{\zeta\to-1}\sqrt{\pi}\tau_1\frac{F''(\zeta)}{\sqrt{\omega'(\zeta)}},\quad K_{\mathrm{III}}^{\perp}=0 \tag{8.2.13}$$

and here $\zeta=-1$ is the point corresponding to the crack tip. Substitution of (8.2.4) and (8.2.7) into (8.2.13) yields

$$K_{\mathrm{III}}^{\parallel}=\frac{\sqrt{2H}\tau_1}{2\pi}\ln\frac{2\mathrm{e}^{\pi a/H}-1+2\mathrm{e}^{\pi a/H}\sqrt{1-\mathrm{e}^{-\pi a/H}}}{2\mathrm{e}^{\pi a/H}-1-2\mathrm{e}^{\pi a/H}\sqrt{1-\mathrm{e}^{-\pi a/H}}} \tag{8.2.14}$$

If we do not assume $\tau_2=0$ in (8.2.1), then the stress intensity factor $K_{\mathrm{III}}^{\perp}$ can be similarly evaluated, and the expression is similar to (8.2.14); this is the extension of work given by Ref. [4] for classical elasticity to quasicrystal elasticity.

8.2.2 Finite Strip with Two Cracks

The configuration is shown in Fig. 8.4, and these are the following boundary conditions:

$$\left.\begin{array}{l} y=\pm H,-\infty<x<\infty:\sigma_{zy}=0,H_{zy}=0 \\ x=\pm\infty,-H<y<H:\sigma_{zx}=0,H_{zx}=0 \\ y=\pm 0,-\infty<x<-a:\sigma_{zy}=0,H_{zy}=0;-a<x<0:\sigma_{zy}=-\tau_1,H_{zy}=-\tau_2; \\ L<x<\infty:\sigma_{zy}=0,H_{zy}=0 \end{array}\right\}. \tag{8.2.15}$$

For simplicity, we assume that $\tau_2=0$ in (8.2.15). The following conformal mapping

$$z=\omega(\zeta)=\frac{H}{\pi}\ln\frac{1+\alpha\left(\dfrac{1-\zeta}{1+\zeta}\right)^2}{1+\beta\alpha\left(\dfrac{1-\zeta}{1+\zeta}\right)^2} \tag{8.2.16}$$

transforms the region at z-plane onto the interior of the unit circle γ at ζ-plane, in which

$$\alpha=\frac{1-\mathrm{e}^{-\pi a/H}}{1-\mathrm{e}^{-\pi(a+L)/H}},\ \beta=\mathrm{e}^{-\pi L/H} \tag{8.2.17}$$

Then, substituting (8.2.16) into (8.2.6), we can find the solution $\phi'(\varsigma)$ and so the stress intensity factors such as

$$\begin{aligned} K_{\mathrm{III}}^{\|\,(0,0)} &= \lim_{\zeta\to 1+0}\left\{-2\sqrt{2\pi\omega(\zeta)}\tau_1\frac{F(\zeta)}{\omega'(\zeta)}\right\} \\ &= \frac{\sqrt{2H}\tau_1}{\pi\sqrt{1-\beta}}\left[\ln\frac{1+\sqrt{\alpha}}{1-\sqrt{\alpha}}-\sqrt{\beta}\ln\frac{1+\sqrt{\alpha\beta}}{1-\sqrt{\alpha\beta}}\right] \end{aligned}$$

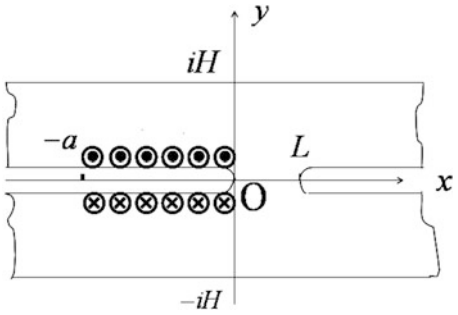

Fig. 8.4 Two cracks in a strip

$$\begin{aligned} K_{\mathrm{III}}^{\parallel\,(L,0)} &= \lim_{\zeta\to -1-0}\left\{-2\sqrt{2\pi(L-\omega(\zeta))}\tau_1\frac{F(\zeta)}{\omega'(\zeta)}\right\} \\ &= \frac{\sqrt{2H}\tau_1}{\pi\sqrt{1-\beta}}\left[\sqrt{\beta}\ln\frac{1+\sqrt{\alpha}}{1-\sqrt{\alpha}} - \ln\frac{1+\sqrt{\alpha\beta}}{1-\sqrt{\alpha\beta}}\right] \end{aligned} \tag{8.2.18}$$

in which

$$\begin{aligned} \phi'(\zeta) &= \frac{K_2\tau_1}{C_{44}K_2 - R_3^2}2iF(\zeta), \psi'(\zeta) = -\frac{R_3\tau_1}{C_{44}K_2 - R_3^2}2iF(\zeta) \\ F(\zeta) &= \frac{2H}{\pi^2}\left[\frac{\sqrt{\alpha}A}{(1+\zeta)^2+\alpha(1-\zeta)^2} - \frac{\sqrt{\alpha\beta}M}{(1+\zeta)^2+\alpha\beta(1-\zeta)^2}\right] \\ &\quad + \frac{2H}{\pi^2}\frac{i\alpha(1-\beta)(1-\zeta^2)}{[(1+\zeta)^2+\alpha(1-\zeta)^2][(1+\zeta)^2+\alpha\beta(1-\zeta)^2]}\ln\frac{i-\zeta}{1-i\zeta} \\ A &= \ln((1+\sqrt{\alpha})/(1-\sqrt{\alpha})),\ M = \ln((1+\sqrt{\alpha\beta})/(1-\sqrt{\alpha\beta})) \end{aligned} \tag{8.2.19}$$

If we do not assume $\tau_2 = 0$ in (8.2.15), then the stress intensity factor $K_{\mathrm{III}}^{\perp}$ can be similarly evaluated, and the expression is similar to (8.2.18), and this extends the study for the classical elasticity. The detail can be found in Refs. [5, 6], and for some calculations on the function $F(\zeta)$, refer to Sect. A.1 of Major Appendix of this book.

8.3 Griffith Crack Problems in Point Groups 5*m* and 10*mm* Quasicrystal Based on Displacement Potential Function Method

The literature [2] reported that Chinese materials scientists had started to characterize the fracture toughness of quasicrystals. Due to the lack of theoretical solutions to crack problems in quasicrystals, their experimental work was performed largely by indirectly measuring the fracture toughness. If the crack solution had been known then, the fracture toughness could have been determined by direct measurement, a much more simpler and accurate method.

This section aims to solve the Mode I Griffith crack in quasicrystal with a tenfold symmetry by using the method of displacement functions. Therefore, the fundamental formulas in Sect. 6.2 and formulas using Fourier transform in Sect. 7.2 are the basis for this section. To save space, we do not plan to list those formulas in detail here, and interested readers may refer to the previous two chapters. In the next section, we are going to solve this problem using method of stress functions. On the one hand, this demonstrates the problem-solving procedure based on the method of stress functions; on the other hand, this is targeted to examine the results obtained by the method of displacement functions. For a correct solution, it can be examined using any available method.

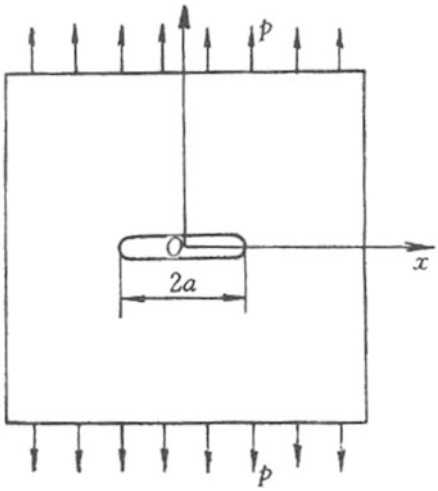

Fig. 8.5 Griffith crack along the periodic axis of quasicrystal and subjected to a tension

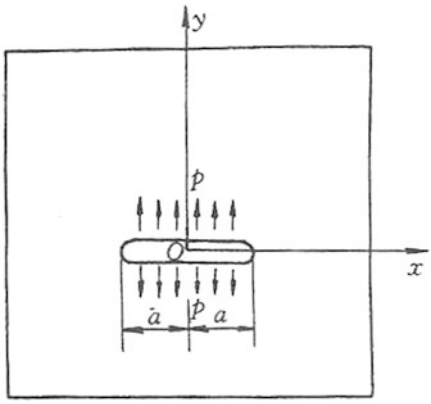

Fig. 8.6 The same Griffith crack as in Fig. 8.5 with external traction acting on crack surfaces

Consider a Griffith crack under the action of external traction, i.e. $\sigma_{yy}^{(\infty)} = p$, and the crack is assumed to penetrate the periodic axis (z-direction) of the quasicrystals, as shown in Fig. 8.5. Similar to the analysis in the preceding section, within the framework of Griffith's theory, this problem can be replaced by an equivalent crack problem shown in Fig. 8.6. Furthermore, assume the external traction being independent of z; therefore, the deformation of the quasicrystal is also independent of z, namely

$$\frac{\partial u_i}{\partial z} = 0, \quad \frac{\partial w_i}{\partial z} = 0 \quad (i = 1, 2, 3) \tag{8.3.1}$$

According to the analysis performed in Chap. 6, under this case, the two-dimensional quasicrystal elasticity problem can be decoupled into a plane

elasticity problem of phonon-phason coupling and an anti-plane pure elasticity problem. In this case, the latter only has a trivial solution under Mode I external traction, which can be neglected. The plane elasticity problem of phonon-phason coupling with point groups 5 m and 10 mm has been studied in Sect. 6.2, and its final governing equation is:

$$\nabla^2\nabla^2\nabla^2\nabla^2 F = 0 \tag{8.3.2}$$

and here $F(x, y)$ is the displacement potential function introduced in Sect. 6.2.

As shown in Fig. 8.6, the Griffith crack is under the action of uniform traction at crack surfaces, and without far-field traction, i.e. $\sigma_{yy}(x, 0) = -p,\ |x| < a$. We modify this problem into the semi-plane problem, i.e. we only study the case in the upper half-plane or the lower half-plane under the following conditions:

$$\left.\begin{array}{l} \sqrt{x^2+y^2} \to \infty : \sigma_{ij} = H_{ij} = 0 \\ y = 0, |x| < a : \sigma_{yy} = -p, \sigma_{yx} = 0 \\ H_{yy} = 0, \quad H_{yx} = 0 \\ y = 0, |x| > a : \sigma_{yx} = 0, H_{yx} = 0 \\ u_y = 0, \quad w_y = 0 \end{array}\right\}. \tag{8.3.3}$$

By performing Fourier transform on Eq. (8.3.2)

$$\hat{F}(\xi, y) = \int_{-\infty}^{\infty} F(x, y)\mathrm{e}^{\mathrm{i}\xi x}\mathrm{d}x \tag{8.3.4}$$

Equation (8.3.2) is therefore reduced to an ordinary differential equation such that:

$$\left(\frac{\mathrm{d}^2}{\mathrm{d}y^2} - \xi^2\right)^4 \hat{F}(\xi, y) = 0. \tag{8.3.5}$$

If we choose the upper half-plane $y > 0$ for our study, the solution of the above equation is:

$$\hat{F}(\xi, y) = (4\xi^4)^{-1} XY\mathrm{e}^{-|\xi|y} \tag{8.3.6}$$

where $X = (A, B, C, D)$, $Y = (1, y, y^2, y^3)^{\mathrm{T}}$ and A, B, C and D are arbitrary functions with respect to ξ to be determined according to the boundary condition; "T" stands for the transpose of a matrix. Fourier transforms of the displacement and stress components can be expressed in terms of $\hat{F}(\xi, y)$, i.e. X and Y as discussed in Sect. 7.2.

Solution (8.2.6) has satisfied the boundary condition (8.2.3) at infinity, and the left boundary condition in (8.2.3) results in

$$\left.\begin{aligned} A(\xi) &= [21C(\xi)|\xi| - 3(32 - e_2)D(\xi)]/2|\xi|^3 \\ B(\xi) &= [6C(\xi)|\xi| - 21D(\xi)]/\xi^2 \end{aligned}\right\} \tag{8.3.7}$$

and the following set of dual integral equations.

$$\left.\begin{aligned} &\tfrac{2}{d_{11}}\int_0^\infty [C(\xi)\xi - 6D(\xi)]\cos(\xi x)\mathrm{d}\xi = -p, \quad 0<x<a \\ &\int_0^\infty \xi^{-1}[C(\xi)\xi - 6D(\xi)]\cos(\xi x)\mathrm{d}\xi = 0, \quad x > a \\ &\tfrac{2}{d_{12}}\int_0^\infty D(\xi)\cos(\xi x)\mathrm{d}\xi = 0, \quad 0<x<a \\ &\int_0^\infty \xi^{-1}D(\xi)\cos(\xi x)\mathrm{d}\xi = 0, \quad x > a \end{aligned}\right\}. \tag{8.3.8}$$

Here, e_2 is given by the second relation in (7.2.12), i.e.

$$e_2 = \frac{2\alpha\beta}{\omega(\alpha-\beta)(K_1-K_2)} + \frac{\alpha-\beta}{\alpha+\beta},$$

α and β is given by the second relation in (6.2.5), i.e.

$$\alpha = R(L+2M) - \omega K_1, \beta = RM - \omega K_1, \omega = M(L+2M)/R$$

d_{11} and d_{22} are given as

$$\left.\begin{aligned} d_{11} &= nR/[(4M/L+M)(L+2M)(MK_1 - R^2)] \\ d_{12} &= nR^2/d_0M(L+2M) \\ d_0 &= -\big\{(MK_1 - R^2)[(L+2M)(K_1+K_2) - 2R^2] \\ &\quad -[(L+2M)K_1 - R^2][M(K_1+K_2) - 2R^2]\big\} \end{aligned}\right\} \tag{8.3.9}$$

and n is determined by (7.2.12), namely

$$n = M\alpha - (L+2M)\beta.$$

The theory of dual integral equations is listed in the Major Appendix of this monograph. Accordingly, solution to the set of Eq. (8.3.8) is:

$$2C(\xi)\xi = d_{11}p\alpha J_1(a\xi),\ D(\xi) = 0 \tag{8.3.10}$$

where $J_1(a\xi)$ is the first-order Bessel function of the first kind.

So far, the unknown functions $A(\xi)$, $B(\xi)$, $C(\xi)$ and $D(\xi)$ have been determined completely. In the view of mathematics, this problem has been solved. However, in the view of physics, we need to perform the Fourier inverse:

$$F(x,y)=\frac{1}{2\pi}\int_{-\infty}^{\infty}\hat{F}(\xi,y)\mathrm{e}^{-\mathrm{i}\xi x}\mathrm{d}\xi \tag{8.3.11}$$

in order to express the field variables in the physical space.

Obviously, once $F(x, y)$ is determined from the integral (8.3.11), u_j, σ_{jk} and H_{jk} can be determined by substituting $F(x, y)$ into (8.3.8)–(8.3.11). Alternatively, $\hat{u}_j(\xi,y)$, $\hat{w}_j(\xi,y)$, $\hat{\sigma}_{jk}(\xi,y)$, and $\hat{H}_{jk}(\xi,y)$ can be determined by substituting $X(\xi)$ and $Y(\xi)$ into (8.3.8)–(8.3.11), and then, their Fourier inverses finally lead to u_j, σ_{jk} and H_{jk}. Luckily, the above integrals with Bessel function can be expressed explicitly using elemental functions. Nevertheless, their final expressions in terms of variables x and y are extremely complex. However, the final expressions appear more concise if using (r, θ), (r_1, θ_1) and (r_2, θ_2) to stand for the three polar coordinate systems with the crack centre, left crack tip and right crack tip as origins, respectively, as shown in Fig. 8.2, similar to (8.1.16), i.e.

$$\left.\begin{aligned} x&=r\cos\theta=a+r_1\cos\theta_1=-a+r_2\cos\theta_2\\ y&=r\sin\theta=r_1\sin\theta_1=r_2\sin\theta_2\end{aligned}\right\} \tag{8.3.12}$$

The following infinite integrals involving Bessel functions are used for stress calculation:

$$\left.\begin{aligned}
&\int_0^{\infty}J_1(a\xi)\mathrm{e}^{-\xi z}\mathrm{d}\xi=\frac{1}{a}\left[1-\frac{z}{(a^2-z^2)^{1/2}}\right]\\
&\int_0^{\infty}\xi J_1(a\xi)\mathrm{e}^{-\xi z}\mathrm{d}\xi=\frac{a}{(a^2-z^2)^{3/2}}\\
&\int_0^{\infty}\xi^2 J_1(a\xi)\mathrm{e}^{-\xi z}\mathrm{d}\xi=\frac{3az}{(a^2-z^2)^{5/2}}\\
&\int_0^{\infty}\xi^3 J_1(a\xi)\mathrm{e}^{-\xi z}\mathrm{d}\xi=\frac{3a(4z^2-a^2)}{(a^2-z^2)^{7/2}}
\end{aligned}\right\} \tag{8.3.13}$$

where $z = x + iy$.

After proper calculation, we have

$$\left\{\begin{aligned}
\sigma_{xx}&=-p[1+\overline{r}(\overline{r_1r_2})^{-3/2}\cos(\theta-\overline{\theta})]-p\overline{r}(\overline{r_1r_2})^{-3/2}\sin\theta\sin3\overline{\theta}\\
\sigma_{yy}&=-p[1-\overline{r}(\overline{r_1r_2})^{-3/2}\cos(\theta-\overline{\theta})]+p\overline{r}(\overline{r_1r_2})^{-3/2}\sin\theta\sin3\overline{\theta}\\
\sigma_{xy}&=\sigma_{yx}=p\overline{r}(\overline{r_1r_2})^{-3/2}\sin\theta\cos3\overline{\theta}\\
H_{xx}&=-4d_{21}p\overline{r}(\overline{r_1r_2})^{-3/2}\sin\theta\cos3\overline{\theta}-6d_{21}p\overline{r}^3(\overline{r_1r_2})^{-5/2}\sin^2\theta\cos(\theta-5\overline{\theta})\\
H_{yy}&=-6d_{21}p\overline{r}^3(\overline{r_1r_2})^{-5/2}\sin^2\theta\cos(\theta-5\overline{\theta})\\
H_{xy}&=6d_{21}p\overline{r}^3(\overline{r_1r_2})^{-5/2}\sin^2\theta\sin(\theta-5\overline{\theta})\\
H_{yx}&=4d_{21}p\overline{r}(\overline{r_1r_2})^{-3/2}\sin\theta\cos3\overline{\theta}+6d_{21}p\overline{r}^3(\overline{r_1r_2})^{-5/2}\sin^2\theta\sin(\theta-5\overline{\theta})
\end{aligned}\right. \tag{8.3.14a}$$

in which $\overline{r} = r/a, \overline{r_1} = r_1/a, \overline{r_2} = r_2/a, \overline{\theta} = (\theta_1 + \theta_2)/2$

$$d_{21} = R(K_1 - K_2)/4(MK_1 - R^2) \tag{8.3.14b}$$

Similarly, displacement components u_j and w_j can be also expressed in terms of elemental functions. We list here only the component

$$u_y(x,0) = \begin{cases} 0 & |x| > a \\ \frac{p}{2}\left(\frac{K_1}{MK_1 - R^2} + \frac{1}{L+M}\right)\sqrt{a^2 - x^2} & |x| < a \end{cases} \tag{8.3.15}$$

From these results of (8.3.14a), we can find the stress intensity factor

$$K_{\mathrm{I}}^{\parallel} = \lim_{x \to a^+} \sqrt{2\pi(x-a)}\sigma_{yy}(x,0) = \sqrt{\pi a}p \tag{8.3.16}$$

and the crack strain energy as

$$\begin{aligned} W_{\mathrm{I}} &= 2\int_0^a (\sigma_{yy}(x,0) \oplus H_{yy}(x,0))(u_y(x,0) \oplus w_y(x,0))\mathrm{d}x \\ &= \frac{\pi a^2 p^2}{4}\left(\frac{1}{L+M} + \frac{K_1}{MK_1 - R^2}\right) \end{aligned} \tag{8.3.17}$$

So there is the crack energy release rate

$$G_I = \frac{1}{2}\frac{\partial W_1}{\partial a} = \frac{1}{4}\left(\frac{1}{L+M} + \frac{K_1}{MK_1 - R^2}\right)(K_{\mathrm{I}}^{\parallel})^2 \tag{8.3.18}$$

It is evident that the crack energy release rate depends on not only phonon elastic constants $L(= C_{12})$, $M(= (C_{11} - C_{12})/2)$, but also phason elastic constant K_1 and phonon-phason coupling elastic constant R. The further meaning and applications of these quantities will be discussed in detail in Chap. 15. This provides the basis for fracture theory of quasicrystalline materials.

This work has been published in Phil. Mag. A [7].

8.4 Stress Potential Function Formulation and Complex Analysis Method for Solving Notch/Crack Problem of Quasicrystals of Point Groups $5, \bar{5}$ and $10, \overline{10}$

The Fourier method cannot solve notch problems, while complex analysis method with conformal mapping can solve them. In this section, we develop complex potential method for notch/crack problems for plane elasticity of point groups $5, \bar{5}$

and $10, \overline{10}$ quasicrystals. We will use the stress potential formulation [9]; of course we can also use the displacement potential formulation for the plane elasticity introduced in Sect. 6.4.

8.4.1 Complex Analysis Method

From Sect. 6.7, we find that based on the stress potential method, the final governing equation of plane elasticity of point groups $5, \bar{5}$ and $10, \overline{10}$ decagonal quasicrystals is:

$$\nabla^2\nabla^2\nabla^2\nabla^2 G = 0 \tag{8.4.1}$$

The general solution of Eq. (8.4.1) is [8]:

$$G = 2\mathrm{Re}\left[g_1(z) + \bar{z}g_2(z) + \frac{1}{2}\bar{z}^2 g_3(z) + \frac{1}{6}\bar{z}^3 g_4(z)\right] \tag{8.4.2}$$

where $g_j(z), (j = 1, \ldots, 4)$ are four analytic functions of a single complex variable $z = x + iy = re^{i\theta}$. The bar over the quantity denotes the complex conjugate hereinafter, i.e. $\bar{z} = x - iy = re^{-i\theta}$. We can see that the complex analysis here will be more complicated than that of Muskhelishvili method for plane elasticity of classical elasticity.

8.4.2 The Complex Representation of Stresses and Displacements

Substituting expression (8.4.2) into Eq. (6.7.6) and then into Eq. (6.7.2) leads to

$$\begin{aligned}
\sigma_{xx} &= -32c_1\mathrm{Re}[\Omega(z) - 2g_4'''(z)] \\
\sigma_{yy} &= 32c_1\mathrm{Re}[\Omega(z) + 2g_4'''(z)] \\
\sigma_{xy} &= \sigma_{yx} = 32c_1\mathrm{Im}\Omega(z) \\
H_{xx} &= 32R_1\mathrm{Re}[\Theta'(z) - \Omega(z)) - 32R_2\mathrm{Im}(\Theta'(z) - \Omega(z)] \\
H_{xy} &= -32R_1\mathrm{Im}[\Theta'(z) + \Omega(z)) - 32R_2\mathrm{Re}(\Theta'(z) + \Omega(z)] \\
H_{yx} &= -32R_1\mathrm{Im}[\Theta'(z) - \Omega(z)) - 32R_2\mathrm{Re}(\Theta'(z) - \Omega(z)] \\
H_{yy} &= -32R_1\mathrm{Re}[\Theta'(z) + \Omega(z)) + 32R_2\mathrm{Im}(\Theta'(z) + \Omega]
\end{aligned} \tag{8.4.3}$$

where

$$\begin{aligned}\Theta(z) &= g_2^{(\mathrm{IV})}(z) + \bar{z}g_3^{(\mathrm{IV})}(z) + \frac{1}{2}\bar{z}^2 g_4^{(\mathrm{IV})}(z)\\ \Omega(z) &= g_3^{(\mathrm{IV})}(z) + \bar{z}g_4^{(\mathrm{IV})}(z)\end{aligned} \tag{8.4.4}$$

in which the prime, two prime, three prime and superscript (IV) denote the first- to fourth-order differentiation of $g_i(z)$ to variable z, in addition $\Theta'(z) = \mathrm{d}\Theta(z)/\mathrm{d}z$.

We further derive the complex representations of displacement components of phonon and phason fields. The first two equations of Eq. (6.7.3) can be rewritten as follows:

$$\begin{aligned}\varepsilon_{xx} &= c_2(\sigma_{xx}+\sigma_{yy}) - \frac{K_1+K_2}{2c}\sigma_{yy} - \frac{1}{2c}[R_1(H_{xx}+H_{yy}) + R_2(H_{xy}-H_{yx})]\\ \varepsilon_{yy} &= c_2(\sigma_{xx}+\sigma_{yy}) - \frac{K_1+K_2}{2c}\sigma_{xx} + \frac{1}{2c}[R_1(H_{xx}+H_{yy}) + R_2(H_{xy}-H_{yx})]\end{aligned} \tag{8.4.5}$$

where

$$c_2 = \frac{c+(L+M)(K_1+K_2)}{4(L+M)c} \tag{8.4.6}$$

and c refer to (6.7.4). Substituting Eq. (8.4.3) into (8.4.5) and integrating yield

$$\begin{aligned}u_x &= 128c_1c_2\mathrm{Re}g_4''(z) - \frac{K_1+K_2}{2c}\frac{\partial}{\partial x}\phi\\ &\quad + \frac{32(R_1^2+R_2^2)}{c}\mathrm{Re}\left[g_3'''(z) + \bar{z}g_4'''(z) - g_4''(z)\right] + f_1(y)\\ u_y &= 128c_1c_2\mathrm{Im}g_4''(z) - \frac{K_1+K_2}{2c}\frac{\partial}{\partial y}\phi\\ &\quad - \frac{32(R_1^2+R_2^2)}{c}\mathrm{Im}\left[g_3'''(z) + \bar{z}g_4'''(z) + g_4''(z)\right] + f_2(x)\end{aligned}$$

With these results and other equations of Eq. (6.7.3), one finds that

$$-\frac{\mathrm{d}f_1(y)}{\mathrm{d}y} = \frac{\mathrm{d}f_2(x)}{\mathrm{d}x}$$

This means these two functions must be constants which only give rigid body displacements. Omitting the trial functions $f_1(y)$, $f_2(x)$, one obtains

$$u_x + iu_y = 32(4c_1c_2 - c_3 - c_1c_4)g_4''(z) - 32(c_1c_4 - c_3)[\overline{g_3'''(z)} + z\overline{g_4'''(z)}] \tag{8.4.7}$$

where c_1 refer to (6.7.7) and

$$c_3 = \frac{R_1^2 + R_2^2}{c}, \quad c_4 = \frac{K_1 + K_2}{c} \tag{8.4.8}$$

Similarly, the complex representations of displacement components of phason fields can be expressed as follows:

$$w_x + iw_y = \frac{32(R_1 - iR_2)}{K_1 - K_2}\overline{\Theta(z)} \tag{8.4.9}$$

8.4.3 Elliptic Notch Problem

To illustrate the effect of the stress potential and complex analysis method to the complicated stress boundary value problems of eight order partial differential equations given above, we here calculate the stress and displacement fields induced by an elliptic notch $L : \frac{x^2}{a^2} + \frac{y^2}{b^2} = 1$, see Fig. 8.7a, the edge of which is subjected to a uniform pressure p, this problem is equivalent to the case that the body is subjected to a tension at infinity and the surface of the notch is stress-free shown in Fig. 8.7a if $\alpha = \pi/2$. The equivalency is proved in Sect. 11.3.9 in Chap. 11.

For the problem shown in Fig. 8.7a, the boundary conditions can be expressed as follows:

$$\begin{aligned} &\sigma_{xx}\cos(\mathbf{n}, x) + \sigma_{xy}\cos(\mathbf{n}, y) = T_x, \\ &\sigma_{xy}\cos(\mathbf{n}, x) + \sigma_{yy}\cos(\mathbf{n}, y) = T_y, (x, y) \in L \end{aligned} \tag{8.4.10}$$

$$\begin{aligned} &H_{xx}\cos(\mathbf{n}, x) + H_{xy}\cos(\mathbf{n}, y) = h_x, \\ &H_{yx}\cos(\mathbf{n}, x) + H_{yy}\cos(\mathbf{n}, y) = h_y, (x, y) \in L \end{aligned} \tag{8.4.11}$$

where $T_x = -p\cos(\mathbf{n}, x)$,$T_y = -p\cos(\mathbf{n}, y)$ denote the components of surface traction, p is the magnitude of the pressure, h_x and h_y are generalized surface tractions and $\mathbf{n}$ represents the outward unit normal vector of any point of the boundary. But the measurement of generalized tractions has not been reported so far, and for simplicity, we assume that $h_x = 0$, $h_y = 0$.

From Eqs. (8.4.3), (8.4.4) and (8.4.10), one has

$$g_4''(z) + \overline{g_3'''(z)} + z\overline{g_4'''(z)} = \frac{i}{32c_1}\int (T_x + iT_y)\mathrm{d}s = -\frac{1}{32c_1}pz \quad z \in L \tag{8.4.12}$$

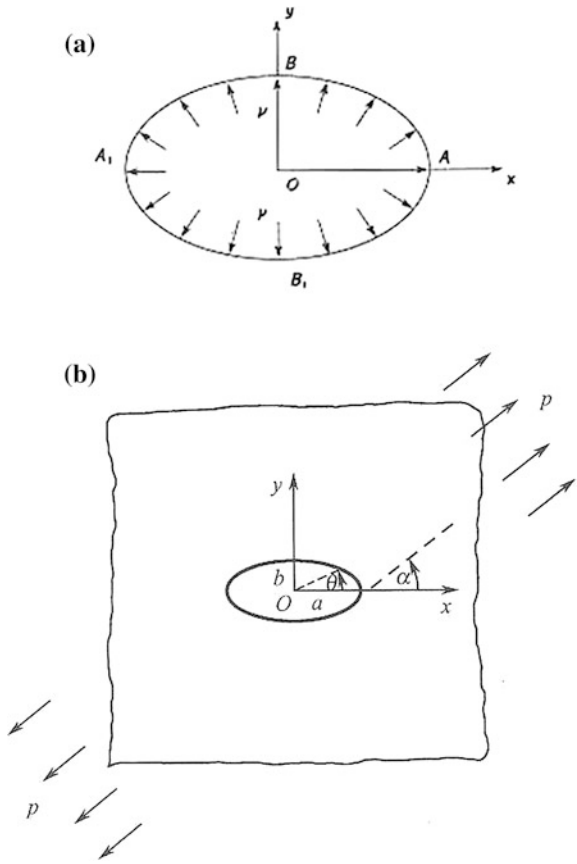

Fig. 8.7 **a** An infinite decagonal quasicrystal with an elliptic notch subjected to a uniform pressure and stress-free at infinity. **b** The elliptic notch subjected to an external tension and the surface of notch is stress-free

Taking the conjugate on both sides of Eq. (8.4.12) yields

$$\overline{g_4''(z)} + g_3'''z) + \bar{z}g_4'''z) = -\frac{1}{32c_1}p\bar{z} \quad z \in L \tag{8.4.13}$$

From Eqs. (8.4.3), (8.4.4) and (8.4.11), we have

$$\begin{aligned} &R_1 \mathrm{Im}\Theta(z) + R_2 \mathrm{Re}\Theta(z) = 0 \\ &-R_1 \mathrm{Re}\Theta(z) + R_2 \mathrm{Im}\Theta(z) = 0 \end{aligned} \quad z \in L \tag{8.4.14}$$

Multiplying the second formula of (8.4.14) by i and adding it to the first, one obtains

$$\Theta(z) = 0 \quad z \in L \tag{8.4.15}$$

Because the function $g_1(z)$ does not appear in the displacement and stress formulas, boundary Eqs. (8.4.12), (8.4.13) and (8.4.15) are enough for determining the

unknown functions $g_2(z), g_3(z)$ and $g_4(z)$. However, the calculation cannot be completed at the z-plane due to the complexity of the evaluation, and we must use the conformal mapping

$$z = \omega(\zeta) = R_0\left(\frac{1}{\zeta} + m\zeta\right) \tag{8.4.16}$$

to transform the region with ellipse at the z-plane onto the interior of the unit circle γ at the ζ-plane (refer to Fig. 8.8), where $\zeta = \xi + i\eta = \rho e^{i\varphi}$ and $R_0 = \frac{a+b}{2}$, $m = \frac{a-b}{a+b}$.For simplicity, we introduce the following new symbols:

$$g_2^{(\mathrm{IV})}(z) = F_2(z), g_3'''(z) = F_3(z),\ g_4''(z) = F_4(z). \tag{8.4.17}$$

And we have

$$F_j(z) = F_j(\omega(\zeta)) = \Phi_j(\zeta), F_j'(z) = \frac{\Phi_j'(\zeta)}{\omega'(\zeta)} \quad (j = 1, \ldots, 4) \tag{8.4.18}$$

Substituting (8.4.17) into (8.4.12), (8.4.13) and (8.4.15), then multiplying both sides of equations by $\frac{1}{2\pi i}\frac{\mathrm{d}\sigma}{\sigma-\zeta}$ and integrating along the unit circle, we have

$$\begin{aligned}
&\frac{1}{2\pi i}\int_\gamma \frac{\Phi_4(\sigma)\mathrm{d}\sigma}{\sigma-\zeta} + \frac{1}{2\pi i}\int_\gamma \frac{\overline{\Phi_3(\sigma)}\mathrm{d}\sigma}{\sigma-\zeta} + \frac{1}{2\pi i}\int_\gamma \frac{\omega(\sigma)}{\overline{\omega(\sigma)}}\frac{\overline{\Phi_4'(\sigma)}\mathrm{d}\sigma}{\sigma-\zeta} = -\frac{p}{32c_1}\frac{1}{2\pi i}\int_\gamma \frac{\omega(\sigma)\mathrm{d}\sigma}{\sigma-\zeta} \\
&\frac{1}{2\pi i}\int_\gamma \frac{\overline{\Phi_4(\sigma)}\mathrm{d}\sigma}{\sigma-\zeta} + \frac{1}{2\pi i}\int_\gamma \frac{\Phi_3(\sigma)\mathrm{d}\sigma}{\sigma-\zeta} + \frac{1}{2\pi i}\int_\gamma \frac{\overline{\omega(\sigma)}}{\omega(\sigma)}\frac{\Phi_4'(\sigma)\mathrm{d}\sigma}{\sigma-\zeta} = -\frac{p}{32c_1}\frac{1}{2\pi i}\int_\gamma \frac{\overline{\omega(\sigma)}\mathrm{d}\sigma}{\sigma-\zeta} \\
&\frac{1}{2\pi i}\int_\gamma \frac{\Phi_2(\sigma)\mathrm{d}\sigma}{\sigma-\zeta} + \frac{1}{2\pi i}\int_\gamma \frac{\overline{\omega(\sigma)}}{\omega'(\sigma)}\frac{\Phi_3'(\sigma)\mathrm{d}\sigma}{\sigma-\zeta} + \frac{1}{2\pi i}\left[\int_\gamma \frac{\overline{\omega(\sigma)}^2}{[\omega'(\sigma)]^2}\frac{\Phi_4''(\sigma)\mathrm{d}\sigma}{\sigma-\zeta}\right. \\
&\qquad\left. - \int_\gamma \frac{\overline{\omega(\sigma)}^2\omega''(\sigma)}{[\omega'(\sigma)]^3}\frac{\Phi_4'(\sigma)\mathrm{d}\sigma}{\sigma-\zeta}\right] = 0
\end{aligned} \tag{8.4.19}$$

where $\sigma = e^{i\varphi}(\rho = 1)$ represents the value of ζ at the unit circle.

According to Cauchy integral formula and analytic extension of the complex analysis theory, similar to the calculations at Sects. 8.1 and 8.2, from the first and the second equations of (8.4.19), one obtains

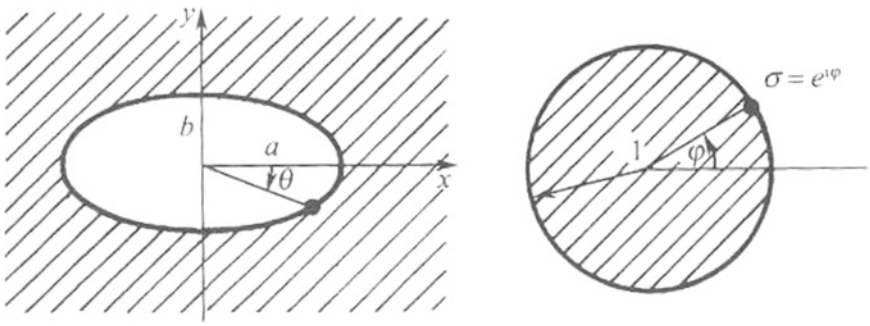

Fig. 8.8 Conformal mapping and boundary correspondence

$$\begin{aligned}\Phi_3(\zeta) &= \frac{pR_0}{32c_1}\frac{(1+m^2)\zeta}{m\zeta^2-1}\\ \Phi_4(\zeta) &= -\frac{pR_0}{32c_1}m\zeta\end{aligned} \tag{8.4.20}$$

Substitution of

$$\frac{\overline{\omega(\sigma)}}{\omega'(\sigma)} = \sigma\frac{\sigma^2+m}{m\sigma^2-1}, \frac{\overline{\omega(\sigma)}^2\omega''(\sigma)}{\omega'(\sigma)^3} = -\frac{2\sigma(\sigma^2+m)^2}{(m\sigma^2-1)^3}$$

and (8.4.20) into the third equation of (8.4.19) yields

$$\frac{1}{2\pi i}\int_\gamma \frac{\Phi_2(\sigma)\mathrm{d}\sigma}{\sigma-\zeta} + \frac{1}{2\pi i}\int_\gamma \sigma\frac{\sigma^2+m}{m\sigma^2-1}\frac{\Phi_3'(\sigma)\mathrm{d}\sigma}{\sigma-\zeta} + \frac{1}{2\pi i}\int_\gamma \frac{\sigma(\sigma^2+m)^2}{(m\sigma^2-1)^3}\frac{\Phi_4'(\sigma)\mathrm{d}\sigma}{\sigma-\zeta} = 0$$

By Cauchy integral formula, we have

$$\begin{aligned}\frac{1}{2\pi i}\int_\gamma \frac{\Phi_2(\sigma)\mathrm{d}\sigma}{\sigma-\zeta} &= \Phi_2(\zeta)\\ \frac{1}{2\pi i}\int_\gamma \sigma\frac{\sigma^2+m}{m\sigma^2-1}\frac{\Phi_3'(\sigma)\mathrm{d}\sigma}{\sigma-\zeta} &= \zeta\frac{\zeta^2+m}{m\zeta^2-1}\Phi_3'(\zeta)\\ \frac{1}{2\pi i}\int_\gamma \frac{\sigma(\sigma^2+m)^2}{(m\sigma^2-1)^3}\frac{\Phi_4'(\sigma)\mathrm{d}\sigma}{\sigma-\zeta} &= \frac{\zeta(\zeta^2+m)^2}{(m\zeta^2-1)^3}\Phi_4'(\zeta)\end{aligned}$$

Substituting these equations into (8.4.19), one finds that at last

$$\Phi_2(\zeta) = \frac{pR_0}{32c_1}\frac{\zeta(\zeta^2+m)[(1+m^2)(1+m\zeta^2)-(\zeta^2+m)]}{(m\zeta^2-1)^3} \tag{8.4.21}$$

Utilizing the above-mentioned results, the phonon and phason stresses can be determined at the ζ-plane. We here only give a simple example, i.e. along the edge of the notch ($\rho = 1$), there are the phonon stress components such as

$$\sigma_{\varphi\varphi} = p\frac{1-3m^2+2m\cos 2\varphi}{1+m^2-2m\cos 2\varphi}, \quad \sigma_{\rho\rho} = -p, \quad \sigma_{\rho\varphi} = \sigma_{\varphi\rho} = 0$$

which are identical to the well-known results of the classical elasticity theory.

8.4.4 Elastic Field Caused by a Griffith Crack

The solution of the Griffith crack subjected to a uniform pressure has been observed by Li et al. [7] in terms of the Fourier transform method, which can also be obtained by the notch solution in corresponding to the case $m = 1, R_0 = \frac{a}{2}$ of the present work. For explicitness, we express the solution in z-plane. The inversion of transformation (8.4.16) is as $m = 1$

$$\zeta = \frac{1}{a}\left(z - \sqrt{z^2-a^2}\right) \tag{8.4.22}$$

From Eqs. (8.4.20) and (8.4.22), we have

$$\begin{aligned} g_2^{(\mathrm{IV})}(z) &= -\frac{pa^2}{128c_1}\frac{z^2}{\sqrt{(z^2-a^2)^3}} \\ g_3'''(z) &= -\frac{p}{64c_1}\frac{a^2}{\sqrt{z^2-a^2}}, \\ g_4''(z) &= \frac{p}{64c_1}(\sqrt{z^2-a^2}-z) \end{aligned} \tag{8.4.23}$$

So the stresses and the displacements can be expressed with complex variable z.

Similar to (8.1.16), we introduce three pairs of the polar coordinates (r,θ), (r_1,θ_1) and (r_2,θ_2) with the origin at the crack centre, at the right crack tip and at the left crack tip, i.e. $z = re^{i\theta}, z-a = r_1e^{i\theta_1}, z+a = r_2e^{i\theta_2}$, respectively, and the analytic expressions for the stress and displacement fields can be obtained.

Moreover, the stress intensity factor and free energy of the crack and so on can be evaluated as the direct results of the solution. We here only list the stress intensity factor and energy release rate as below:

$$
\begin{aligned}
K_{\mathrm{I}}^{\|} &= \lim_{x\to a^+}\sqrt{2\pi(x-a)}\sigma_{yy}(x,0)=\sqrt{\pi a}p,\\
G_{\mathrm{I}} &= \frac{1}{2}\frac{\partial}{\partial a}\left\{2\int_0^a[(\sigma_{yy}(x,0)\oplus H_{yy}(x,0))((u_y(x,0)\oplus w_y(x,0))]\mathrm{d}x\right\}\\
&= \frac{L(K_1+K_2)+2(R_1^2+R_2^2)}{8(L+M)c}(K_{\mathrm{I}}^{\|})^2.
\end{aligned}
\tag{8.4.24}
$$

where $c=M(K_1+K_2)-2(R_1^2+R_2^2)$ and $L=C_{12}, M=(C_{11}-C_{12})/2=C_{66}$. The crack energy release rate G_{I} is dependent upon not only phonon elastic constants $L(=C_{12}), M(=(C_{11}-C_{12})/2)$, but also phason elastic constants K_1, K_2 and phonon-phason coupling elastic constants R_1, R_2, though we have assumed the generalized tractions $h_x=h_y=0$. The results are the same with those given by the Fourier analysis [10].

It is evident that the present solution covers the solution for point groups 5 m, 10 mm quasicrystals, or say the solution of the latter is a special case of the present problem.

The detail for some further principle of the complex analysis method will be discussed in-depth in Chap. 11. For the further implications and applications of the results to fracture theory of quasicrystals, refer to Chap. 15.

8.5 Solutions of Crack/Notch Problems of Two-Dimensional Octagonal Quasicrystals

Zhou and Fan [11] and Zhou [12] obtained the solution of a Griffith crack in octagonal quasicrystals in terms of the Fourier transform and dual integral equations, and the calculation is very complex and lengthy, which cannot be listed here.

Li [13] gave solutions for a notch/Griffith crack problem in terms of complex analysis method based on the stress potential formulation, and an outline of the algorithm was listed in Sect. 6.8.

The final governing equation of plane elasticity of octagonal quasicrystals of point group 8 mm based on the stress potential formulation is the same as that of (6.6.12), but we here rewrite as

$$
\left[\frac{\partial^8}{\partial x^8}+4(1-4\varepsilon)\frac{\partial^8}{\partial x^6\partial y^2}+2(3+16\varepsilon)\frac{\partial^8}{\partial x^4\partial y^4}+4(1-4\varepsilon)\frac{\partial^8}{\partial x^2\partial y^6}+\frac{\partial^8}{\partial y^8}\right]G=0 \tag{8.5.1}
$$

in which $G(x,y)$ is the stress potential function, and the material constant ε is the same as that given in Chaps. 6 and 7. The complex representation of Eq. (8.5.1) is:

$$G(x,y) = 2\mathrm{Re}\sum_{k=1}^{4} G_k(z_k), z_k = x + \mu_k y \tag{8.5.2}$$

in which unknown functions $G_k(z_k)$ are analytic functions of complex variable z_k $(k = 1, 2, 3, 4)$, to be determined, and $\mu_k = \alpha_k + i\beta_k$ $(k = 1, 2, 3, 4)$ are complex parameters and determined by the roots of the following eigenvalue equation:

$$\mu^8 + 4(1 - 4\varepsilon)\mu^6 + 2(3 + 16\varepsilon)\mu^4 + 4(1 - 4\varepsilon)\mu^2 + 1 = 0 \tag{8.5.3}$$

The stresses can be expressed by functions $G_k(z_k)$ such as

$$\sigma_{xx} = -2c_3c_4\ \mathrm{Re}\sum_{k=1}^{4} (\mu_k^2 + 2\mu_k^4 + \mu_k^6)g_k'(z_k) \tag{8.5.4a}$$

$$\sigma_{yy} = -2c_3c_4\mathrm{Re}\sum_{k=1}^{4} (1 + 2\mu_k^2 + \mu_k^4)g_k'(z_k) \tag{8.5.4b}$$

$$\sigma_{xy} = \sigma_{yx} = 2c_3c_4\mathrm{Re}\sum_{k=1}^{4} (\mu_k + 2\mu_k^3 + \mu_k^5)g_k'(z_k) \tag{8.5.4c}$$

$$H_{xx} = R\mathrm{Re}\sum_{k=1} [(4c_4 - c_3)\mu_k^2 + 2(3c_3 - 2c_4)\mu_k^4 - c_3\mu_k^6)]g_k'(z_k) \tag{8.5.4d}$$

$$H_{xy} = -R\mathrm{Re}\sum_{k=1}^{4} [(4c_4 - c_3)\mu_k + 2(3c_3 - 2c_4)\mu_k^3 - c_3\mu_k^5)]g_k'(z_k) \tag{8.5.4e}$$

$$H_{yx} = -R\mathrm{Re}\sum_{k=1}^{4} [c_3\mu_k + 2(c_4 - 2c_3)\mu_k^3 - (4c_4 - c_3)\mu_k^5)]g_k'(z_k) \tag{8.5.4f}$$

$$H_{yy} = R\mathrm{Re}\sum_{k=1}^{4} [c_3 + 2(c_4 - 2c_3)\mu_k^2 - (4c_4 - c_3)\mu_k^4)]g_k'(z_k) \tag{8.5.4g}$$

in which

$$g_k(z_k) = \frac{\partial^6 G_k(z_k)}{\partial z_k^6}, \quad g_k'(z_k) = \frac{\mathrm{d}g_k(z_k)}{\mathrm{d}z_k}$$

$$c_3 = \frac{(K_1 + K_2 + K_3)M - R^2}{K_1 + K_2 + 2K_3}, \quad c_4 = \frac{K_1 M - R^2}{K_1 - K_2}$$

We now consider an elliptic hole $L: x^2/a^2 + y^2/b^2 = 1$, at which there are the boundary conditions:

$$\begin{aligned}
&\sigma_{xx}\cos(\mathbf{n},x) + \sigma_{xy}\cos(\mathbf{n},y) = T_x,\\
&\sigma_{xy}\cos(\mathbf{n},x) + \sigma_{yy}\cos(\mathbf{n},y) = T_y, (x,y) \in L\\
&H_{xx}\cos(\mathbf{n},x) + H_{xy}\cos(\mathbf{n},y) = h_x,\\
&H_{yx}\cos(\mathbf{n},x) + H_{yy}\cos(\mathbf{n},y) = h_y, (x,y) \in L
\end{aligned} \tag{8.5.5}$$

The complex variable z_k can be rewritten as follows:

$$\begin{aligned}
&z_k = x_k + iy_k\\
&x_k = x + \alpha_k y, y_k = \beta_k y
\end{aligned} \tag{8.5.6}$$

The second formula of Eq. (8.5.6) represents a coordinate transformation.

8.6 Approximate Analytic Solutions of Notch/Crack of Two-Dimensional Quasicrystals with 5- and 10-Fold Symmetries

Fan and Tang [14] solved finite bending specimens with elliptic notch/crack of two-dimensional quasicrystal (refer to Fig. 8.9), in which (a) is the model of Muskhelishvili to calculate conventional structural materials, and our model is shown in (b).

According to the assumption of Muskhelishvili, the width is very larger than that of size of the elliptic notch, so that conformal mapping (8.4.16) can still be used. The problem has the following boundary conditions:

$$\begin{cases}
y \to \pm\infty, |x| < W/2 : B\int\limits_{-W/2}^{W/2} \sigma_{yy} x\mathrm{d}x = M, \sigma_{yx} = 0, H_{yy} = 0, H_{yx} = 0;\\
y = 0, |x| < a : \sigma_{yy} = 0, \sigma_{yx} = 0, H_{yy} = 0, H_{yx} = 0;\\
x = \pm W/2, -\infty < y < \infty : \sigma_{xx} = 0, \sigma_{xy} = 0, H_{xx} = 0, H_{xy} = 0
\end{cases} \tag{8.6.1}$$

The solution of Muskhelishvili [15, p. 344] for conventional structural materials is given for model (a) in Fig. 8.9, and he used conformal mapping

$$z = \omega(\zeta) = R_0\left(\frac{1}{\zeta} + m\zeta\right) \tag{8.6.2}$$

whose results are not suitable for model (b) in Fig. 8.9. The configuration of solution of Lokchine [16] for conventional structural materials is identical to that of ours, but he used elliptic coordinate in deriving solution, which is quite different

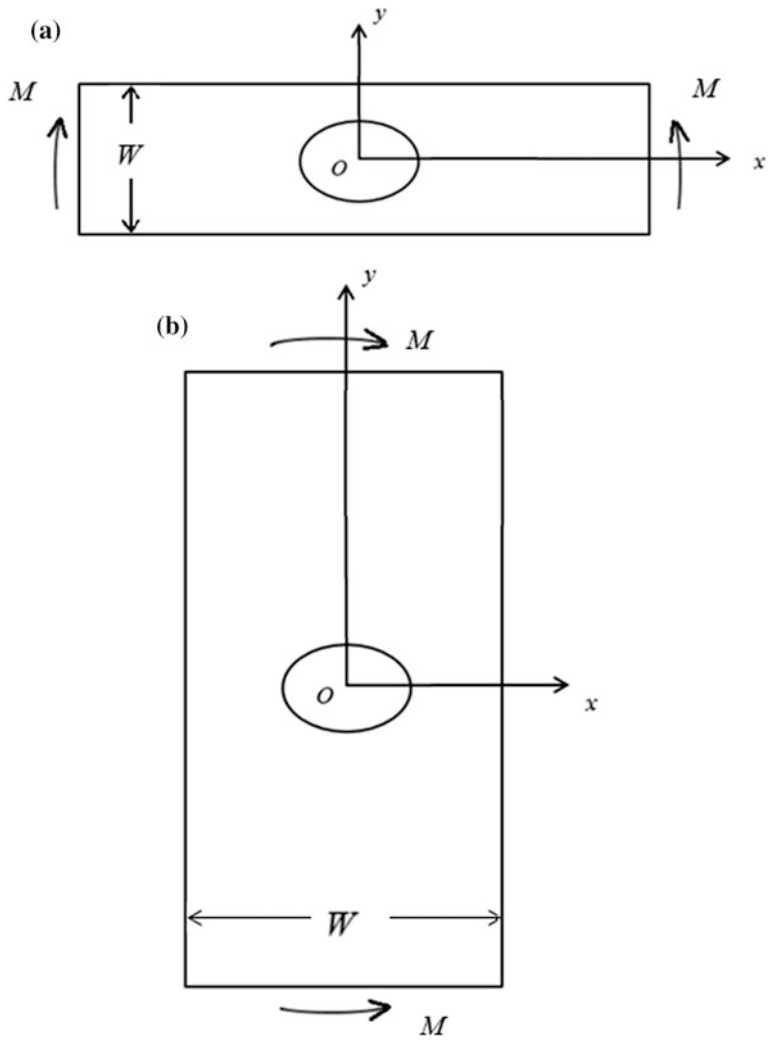

Fig. 8.9 Specimen with elliptical notch and finite width of two-dimensional quasicrystals. **a** Model of Muskhelishvili (for conventional structural materials) and **b** Fan and Tang's model [14] (for quasicrystals)

from complex analysis. Our interest aims to develop the complex analysis here. From the discussion of Chap. 6 referring to solution (6.9.7) of bending specimen without notch

$$\sigma_{yy} = \frac{M}{I}x,\ I = \frac{BW^3}{12} \tag{8.6.3}$$

In addition to the following, we take $B = 1$. In the further calculation, for simplicity, we remove the boundary conditions at upper and lower surfaces of the specimen listed in (8.6.1); instead, add equivalent boundary conditions at the notch surface. That is at the surface of notch/crack, there is the applied stress (8.6.3), and other stress components are zero. If we consider only the crack problem, then $m = 1, R_0 = a/2$ in (8.6.2).

As we have known from 8.4 that the key equation in system (8.4.19) concerning the crack stress intensity factor is:

$$\frac{1}{2\pi i}\int_{\gamma}\frac{\Phi_4(\sigma)\mathrm{d}\sigma}{\sigma-\zeta}+\frac{1}{2\pi i}\int_{\gamma}\frac{\overline{\Phi_3(\sigma)}\mathrm{d}\sigma}{\sigma-\zeta}+\frac{1}{2\pi i}\int_{\gamma}\frac{\omega(\sigma)}{\overline{\omega'(\sigma)}}\frac{\overline{\Phi_4'(\sigma)}\mathrm{d}\sigma}{\sigma-\zeta}=\frac{1}{32c_1}\frac{1}{2\pi i}\int_{\gamma}\frac{\mathbf{t}\mathrm{d}\sigma}{\sigma-\zeta} \tag{8.6.4}$$

where $\mathbf{t} = i\int(T_x + iT_y)\mathrm{d}s$. Substituting conformal mapping (8.6.2) and the boundary condition of crack surface (8.6.3) into Eq. (8.6.4) yields the solution

$$\Phi_4(\zeta) = \frac{Aa^2}{8}\frac{1}{\zeta^2} + \frac{Aa^2}{4} \tag{8.6.5}$$

where

$$A = 12\frac{M}{BW^3} \tag{8.6.6}$$

Bearing in mind the well-known results around the crack tip

$$\sigma_{xx} + \sigma_{yy} = (2/\pi r_1)^{1/2} K_{\mathrm{I}}^{\|}\cos(\theta_1/2)$$

and

$$\sigma_{xx} + \sigma_{yy} = -(2/\pi r_1)^{1/2} K_{\mathrm{II}}^{\|}\sin(\theta_1/2)$$

and define the complex stress intensity factor

$$K = K_{\mathrm{I}}^{\|} - iK_{\mathrm{II}}^{\|}$$

Note that $z - z_1 = r_1 \mathrm{e}^{\mathrm{i}\theta_1}$, where z_1 represents the location of the crack tip; then, we have

$$\sigma_{xx} + \sigma_{yy} = 2\mathrm{Re}\left(K/\sqrt{2\pi(z-z_1)}\right)$$

and find again

$$\sigma_{xx} + \sigma_{yy} = 128c_1 \mathrm{Re} g_4'''(z) = 128c_1 \mathrm{Re}\Phi_4(\zeta)$$

and the expression of complex stress intensity factor

$$\mathbf{K} = K_{\mathrm{I}}^{\parallel} - iK_{\mathrm{II}}^{\parallel} = 32c_1 \left(2\sqrt{\pi} \lim_{\zeta \to -1} \frac{\Phi_4'(\zeta)}{\sqrt{\omega_4''(\zeta)}} \right)$$

Substituting (8.6.2) into the above formula yields

$$K_{\mathrm{I}}^{\parallel} = \sqrt{\pi a}\sigma_N \tag{8.6.7}$$

in which

$$\sigma_N = 6\frac{Ma}{BW^3}$$

here $B = 1$, so further the energy release rate

$$G_{\mathrm{I}} = \frac{1}{4}\left(\frac{1}{L+M} + \frac{K_1}{MK_1 - R^2} \right) \left(K_{\mathrm{I}}^{\parallel} \right)^2 = \frac{1}{4}\left(\frac{1}{L+M} + \frac{K_1}{MK_1 - R^2} \right) \pi a (\sigma_N)^2 \tag{8.6.8}$$

The solution obtained here is approximate, and it presents enough accuracy provided

$$2a/W \leq 1/3. \tag{8.6.9}$$

8.7 Cracked Strip with Finite Height of Two-Dimensional Quasicrystals with 5- and 10-Fold Symmetries and Exact Analytic Solution

The power of complex analysis lies in the application of conformal mapping to some extent. To demonstrate further the effect of conformal mapping, we give another example for quasicrystals of point group 5 m and 10 mm, which is given by Fan and Tang [17] (refer to (8.7.1)):

The boundary conditions are as follows:

$$\left.\begin{array}{l} y=\pm H, -\infty<x<\infty : \sigma_{yy}=0, \sigma_{yx}=0, H_{yy}=0, H_{yx}=0 \\ x=\pm\infty, -H<y<H : \sigma_{xx}=0, \sigma_{xy}=0, H_{xx}=0, H_{xy}=0 \\ y=\pm 0, -\infty<x<-a : \sigma_{yy}=0, \sigma_{yx}=0, H_{yx}=0, H_{yx}=0; \\ -a<x<0 : \sigma_{yy}=-p, \sigma_{yx}=-\tau, H_{yx}=0, H_{yx}=0 \end{array}\right\} \tag{8.7.1}$$

So the problem is quite complicated, and solving is very difficult if taking other approaches. The complex analysis is effective for the solution. The conformal mapping here used is

$$z=\omega(\zeta)=\frac{H}{\pi}\ln\left[1+\left(\frac{1+\zeta}{1-\zeta}\right)^2\right] \tag{8.7.2}$$

which maps the region at physical plane shown in Fig. 8.10a onto the interior of the unit circle γ. This conformal mapping was used in solving problem of one-dimensional quasicrystals (refer to Sect. 8.2). Fan and Tang [17] developed approach given by [4]. The application of the mapping yields the function equations along the unit circle γ due to the boundary conditions:

$$\left\{\begin{array}{l} \dfrac{1}{2\pi i}\displaystyle\int_\gamma \frac{\Phi_4(\sigma)d\sigma}{\sigma-\zeta}+\frac{1}{2\pi i}\int_\gamma \frac{\overline{\Phi_3(\sigma)}\mathrm{d}\sigma}{\sigma-\zeta}+\frac{1}{2\pi i}\int_\gamma \frac{\omega(\sigma)}{\overline{\omega'(\sigma)}}\frac{\overline{\Phi_4'(\sigma)}\mathrm{d}\sigma}{\sigma-\zeta}=\frac{1}{32c_1}\frac{1}{2\pi i}\int_\gamma \frac{\mathbf{t}\mathrm{d}\sigma}{\sigma-\zeta} \\ \dfrac{1}{2\pi i}\displaystyle\int_\gamma \frac{\overline{\Phi_4(\sigma)}\mathrm{d}\sigma}{\sigma-\zeta}+\frac{1}{2\pi i}\int_\gamma \frac{\Phi_3(\sigma)\mathrm{d}\sigma}{\sigma-\zeta}+\frac{1}{2\pi i}\int_\gamma \frac{\overline{\omega(\sigma)}}{\omega'(\sigma)}\frac{\Phi_4'(\sigma)\mathrm{d}\sigma}{\sigma-\zeta}=\frac{1}{32c_1}\frac{1}{2\pi i}\int_\gamma \frac{\bar{\mathbf{t}}\mathrm{d}\sigma}{\sigma-\zeta} \\ \dfrac{1}{2\pi i}\displaystyle\int_\gamma \frac{\Phi_2(\sigma)\mathrm{d}\sigma}{\sigma-\zeta}+\frac{1}{2\pi i}\int_\gamma \frac{\overline{\omega(\sigma)}}{\omega'(\sigma)}\frac{\Phi_3'(\sigma)\mathrm{d}\sigma}{\sigma-\zeta}+\frac{1}{2\pi i}\Big[\int_\gamma \frac{\overline{\omega(\sigma)}^2}{[\omega'(\sigma)]^2}\frac{\Phi_4''(\sigma)\mathrm{d}\sigma}{\sigma-\zeta} \\ \quad -\displaystyle\int_\gamma \frac{\overline{\omega(\sigma)}^2\omega''(\sigma)}{[\omega'(\sigma)]^3}\frac{\Phi_4'(\sigma)\mathrm{d}\sigma}{\sigma-\zeta}\Big]=\frac{1}{R_1-iR_2}\frac{1}{2\pi i}\int_\gamma \frac{\mathbf{h}\mathrm{d}\sigma}{\sigma-\zeta} \end{array}\right. \tag{8.7.3}$$

The solution of these function equations will determine the complex stress potentials, in which $\mathbf{t}=i\int(T_x+iT_y)\mathrm{d}s, \bar{\mathbf{t}}=-i\int(T_x-iT_y)\mathrm{d}s, \mathbf{h}=i\int(h_1+ih_2)\mathrm{d}s$, and

$$\left\{\begin{array}{l} g_2^{(\mathrm{IV})}(z)=h_2(z), g_3'''(z)=h_3(z), g_4''(z)=h_4(z) \\ h_2(z)=h_2(\omega(z))=\Phi_2(\zeta), h_3(z)=h_3(\omega(z))=\Phi_3(\zeta) \\ h_4(z)=h_4(\omega(z))=\Phi_4(\zeta), h_1(z)=h_1(\omega(z))=\Phi_1(\zeta)=0 \end{array}\right. \tag{8.7.4}$$

The inversion of conformal mapping (8.7.1) is:

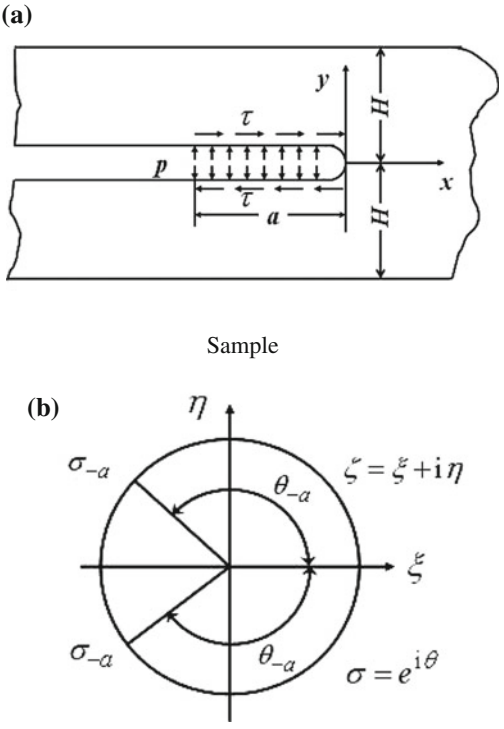

Fig. 8.10 Finite height specimen of quasicrystals (**a**) and conformal mapping onto the unit circle at ζ-plane (**b**)

Conformal mapping onto the unit circle at ζ-plane

$$\zeta = \omega^{-1}(z) = \frac{-\mathrm{e}^{-\pi z/H} \pm 2i\sqrt{1-\mathrm{e}^{-\pi z/H}}}{2-\mathrm{e}^{-\pi z/H}} \tag{8.7.5}$$

The points at γ in mapping plane corresponding to $z = (-a, 0^+)$ and $z = (-a, 0^-)$ in physical plane are:

$$\begin{cases} \sigma_{-a} = \dfrac{-\mathrm{e}^{-\pi a/H} + 2i\sqrt{1-\mathrm{e}^{-\pi a/H}}}{2-\mathrm{e}^{-\pi a/H}} \\ \overline{\sigma_{-a}} = \dfrac{-\mathrm{e}^{-\pi a/H} - 2i\sqrt{1-\mathrm{e}^{-\pi a/H}}}{2-\mathrm{e}^{-\pi a/H}} \end{cases} \tag{8.7.6}$$

In addition, the crack tip is mapped to $\zeta = -1$ Substituting the mapping into the equation

$$\Phi_4(\zeta) + \frac{1}{2\pi i}\int_{\gamma} \overline{G(\sigma)}\frac{\overline{\Phi_4'(\sigma)}}{\sigma-\zeta}\mathrm{d}\sigma + \overline{\Phi_3(0)} = \frac{1}{32c_1}\int_{\sigma_{-a}}^{\overline{\sigma_{-a}}} \frac{i\int(T_x+iT_y)\mathrm{d}s}{\sigma-\zeta}\mathrm{d}\sigma \tag{8.7.7}$$

in which

$$G(\zeta) = \overline{\frac{\omega\left(1/\overline{\zeta}\right)}{\omega'(\zeta)}} \tag{8.7.8}$$

then leads to

$$\Phi_4(\zeta) + \overline{G(0)\Phi_4'(0)} + \overline{\Phi_3(0)} = \frac{1}{32c_1}\int\limits_{\sigma_{-a}}^{\overline{\sigma_{-a}}} \left\{\frac{i\int(T_x + iT_y)\mathrm{d}s}{\sigma - \zeta}\right\}\mathrm{d}\sigma \tag{8.7.9}$$

and the solution at last

$$\begin{aligned}\Phi_4'(\zeta) = \frac{1}{32c_1}\cdot\frac{1}{2\pi i}\Bigg[&\frac{1}{1-\zeta}\ln(\sigma - 1) - \frac{1+\zeta}{(1-\zeta)(1+\zeta^2)}\ln(\sigma - \zeta) \\ &- \frac{\zeta}{2(1+\zeta^2)}\ln(1+\sigma^2) + \frac{1}{2(1-\zeta^2)}\ln\frac{\sigma - i}{\sigma + i}\Bigg]_{\sigma=\sigma_a}^{\sigma=\overline{\sigma_{-a}}}\end{aligned} \tag{8.7.10}$$

Similarly, $\Phi_2(\zeta)$ and $\Phi_3(\zeta)$ can also be determined. If it is calculating stress intensity factor the information on $\Phi_4'(\zeta)$ is enough, because of

$$\mathbf{K} = K_{\mathrm{I}}^{\parallel} - iK_{\mathrm{II}}^{\parallel} = 32c_1\left(2\sqrt{\pi}\lim_{\zeta\to -1}\frac{\Phi_4'(\zeta)}{\sqrt{\omega''(\zeta)}}\right) \tag{8.7.11}$$

Substituting the above results into this formula (note that $T_x = 0$, $T_y = -p, h_x = h_y = 0$) yields

$$K_{\mathrm{I}}^{\parallel} = \frac{\sqrt{2}p\sqrt{H}}{2\pi}F(a/H), \quad K_{\mathrm{II}}^{\parallel} = 0 \tag{8.7.12}$$

in which the configuration factor is:

$$F(a/H) = \ln\frac{2\mathrm{e}^{\pi a/H} - 1 + 2\mathrm{e}^{\pi a/H}\sqrt{1 - \mathrm{e}^{-\pi a/H}}}{2\mathrm{e}^{\pi a/H} - 1 - 2\mathrm{e}^{\pi a/H}\sqrt{1 - \mathrm{e}^{-\pi a/H}}} \tag{8.7.13}$$

Further, we have the crack energy release rate

$$G_I = \frac{1}{4}\left(\frac{1}{L+M} + \frac{K_1}{MK_1 - R^2}\right)\left(K_{\mathrm{I}}^{\parallel}\right)^2 \tag{8.7.14}$$

If the applied stress at the crack surface is pure shear stress, then

$$K_{\mathrm{II}}^{\parallel} = \frac{\sqrt{2}\tau\sqrt{H}}{2\pi} F(a/H), K_{\mathrm{I}}^{\parallel} = 0 \tag{8.7.15}$$

and

$$G_{\mathrm{II}} = \frac{1}{4}\left(\frac{1}{L+M} + \frac{K_1}{MK_1 - R^2}\right)\left(K_{\mathrm{II}}^{\parallel}\right)^2 \tag{8.7.16}$$

8.8 Exact Analytic Solution of Single Edge Crack in a Finite Width Specimen of a Two-Dimensional Quasicrystal of 10-Fold Symmetry

We have mentioned the power of complex analysis lies in the application of conformal mapping to some extent. To further demonstrate the powerful approach, let us consider another example of a cracked specimen of quasicrystal of point group 5 m and 10 mm and shown in Fig. 8.11, the exact solution of which is difficult due to finite width of the specimen.

The applied stresses are tensile at the top and bottom surfaces of the specimen (which is equivalent to inner pressure along the crack surface), or shear at the external surface of the sample (which is equivalent to shearing along the crack

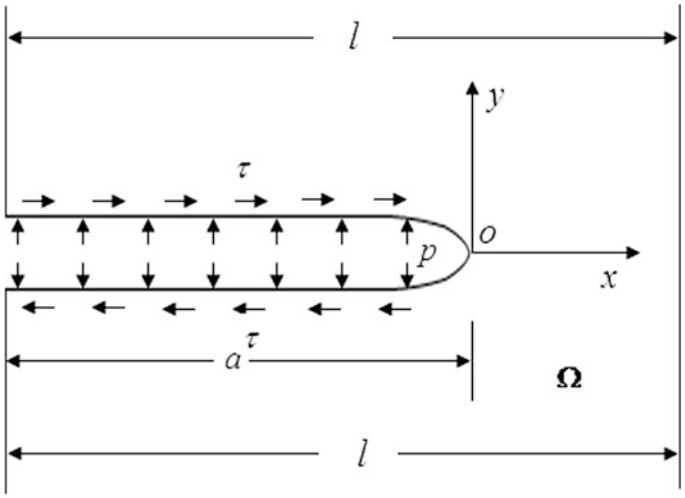

Fig. 8.11 Single edge-cracked specimen subjected to tension (or inner pressure along the crack surface) or shearing (or shearing along the crack surface)

surface). For simplicity, we consider the case of action of inner pressure along the crack surface or of shear along the crack surface only (this ensures stress-free at region faraway from the interior of the specimen), so we have boundary conditions for the case of action of inner pressure

$$\begin{cases} \sigma_{yy} = \sigma_{xy} = 0, H_{yy} = H_{yx} = 0, & y \pm \infty, -a < x < l - a; \\ \sigma_{xx} = \sigma_{xy} = 0, H_{xx} = H_{xy} = 0, & -\infty < y < +\infty, x = -a, x = l - a; \\ \sigma_{yy} = -p, \sigma_{xy} = 0, H_{yy} = H_{yx} = 0, & y = \pm 0, -a < x < 0. \end{cases} \tag{8.8.1}$$

The formulations are Eqs. (8.4.1)–(8.4.9), in which the key equation for boundary value problem is:

$$F_4(z) + \overline{F_3(z)} + z\overline{F_4'(z)} = f_0(z), \quad (x, y) \in S_t \ (or \ z \in S_t) \tag{8.8.2}$$

where

$$\begin{aligned} f_0(z) &= \frac{i}{32c_1} \int_{-a}^{z} \left(T_x + iT_y\right) \mathrm{d}s \\ &= -\frac{1}{32c_1} \int_{-a}^{z} p \mathrm{d}z = \begin{cases} -\frac{1}{32c_1} p(z + a), & -a < x < 0, \\ 0, & x \notin (-a, 0) \end{cases} \end{aligned} \tag{8.8.3}$$

For solving specimen shown by (8.8.1), we need to use the conformal mapping

$$z = \omega(\zeta) = \left(\frac{2l}{\pi}\right) \arctan\left[\sqrt{1 - \zeta^2} \cdot \tan\left(\frac{\pi a}{2l}\right)\right] - a \tag{8.8.4}$$

This mapping function is originated from Ref. [18], which is devoted to solve the crack problem of traditional materials. The conformal mapping maps the region at physical plane onto the upper half-plane (or lower half-plane) at ζ-plane. The complex potentials, e.g. $\Phi_3(\zeta)$ and $\Phi_4(\zeta)$ (refer to Sect. 8.4) transformed from $F_3(z)$ and $F_4(z)$ after the mapping respectively, and satisfy the boundary equations (transformed from (8.8.2) after the mapping)

$$\Phi_4(\zeta) + \frac{1}{2\pi i} \int_{\gamma} \frac{\omega(\sigma)}{\overline{\omega'(\sigma)}} \frac{\overline{\Phi_4'(\sigma)}}{\sigma - \zeta} \mathrm{d}\sigma + \overline{\Phi_3(0)} = \frac{1}{2\pi i} \int_{\gamma} \frac{f_0}{\sigma - \zeta} \mathrm{d}\sigma \tag{8.8.5a}$$

$$\overline{\Phi_4(0)} + \frac{1}{2\pi i} \int_{\gamma} \frac{\overline{\omega(\sigma)}}{\omega'(\sigma)} \frac{\Phi_4'(\sigma)}{\sigma - \zeta} \mathrm{d}\sigma + \Phi_3(\zeta) = \frac{1}{2\pi i} \int_{\gamma} \frac{\overline{f_0}}{\sigma - \zeta} \mathrm{d}\sigma \tag{8.8.5b}$$

where σ represents the value of ζ along γ at ζ-plane. We know that function $\frac{\omega(\zeta)}{\overline{\omega'(\zeta)}}\overline{\Phi_4'(\zeta)}$ is analytic in lower half-plane $\eta<0$, and according to the condition of stress-free in region faraway from the interior of the specimen,

$$\lim_{z\to\infty} z\overline{F_4'(z)} = 0. \tag{8.8.6}$$

so that $\lim\limits_{\zeta\to\infty}\frac{\omega(\zeta)}{\omega'(\zeta)}\overline{\Phi_4'(\zeta)} = \lim\limits_{z\to\infty} z\overline{F_4'(z)} = 0$. By applying the Cauchy integral theory, there is

$$\frac{1}{2\pi i}\int_{\gamma}\frac{\omega(\sigma)}{\overline{\omega'(\sigma)}}\frac{\overline{\Phi_4'(\sigma)}}{\sigma-\zeta}\mathrm{d}\sigma = 0 \tag{8.8.7}$$

From (8.8.7), (8.8.5a) and (8.8.3),

$$\Phi_4(\zeta) = -\frac{1}{32c_1}\frac{1}{2\pi i}\int_{-1}^{1}\frac{p[\omega(\sigma)+a]}{\sigma-\zeta}\mathrm{d}\sigma \tag{8.8.8}$$

Further, integrating by part after derivation to (8.8.8) with respect to ζ, we have

$$\Phi_4'(\zeta) = -\frac{1}{32c_1}\frac{1}{2\pi i}\int_{-1}^{1}\frac{p\omega'(\sigma)}{\sigma-\zeta}\mathrm{d}\sigma \tag{8.8.9}$$

By the way from (8.8.4), there is

$$\omega''(0) = -\frac{2l}{\pi}\tan\left(\frac{\pi a}{2l}\right)\cos^2\left(\frac{\pi a}{2l}\right) \tag{8.8.10}$$

According to the definition of complex stress intensity factor, for the crack under the action of inner pressure, one has

$$K_{\mathrm{I}}^{\|} = \frac{2}{\sqrt{\pi}}\sqrt{\frac{2l}{\pi a}\tan\frac{\pi a}{2l}}\sqrt{\pi a}p, \quad K_{\mathrm{II}}^{\|} = 0 \tag{8.8.11}$$

Similarly, for the case of action of inner shear, there is

$$K_{\mathrm{I}}^{\|} = 0, \quad K_{\mathrm{II}}^{\|} = \frac{2}{\sqrt{\pi}}\sqrt{\frac{2l}{\pi a}\tan\frac{\pi a}{2l}}\sqrt{\pi a}\tau \tag{8.8.12}$$

The work can be found in Ref. [19], and the detail is given by Appendix A.4 in Major Appendix of the book.

8.9 Perturbation Solution of Three-Dimensional Elliptic Disk Crack in One-Dimensional Hexagonal Quasicrystals

Elasticity for all quasicrystals is three-dimensional in fact, even if for one-dimensional quasicrystals, we have mentioned previously this point. To simplify solving procedure in previous and succeeded descriptions, we often decompose a complex three-dimensional problem into a plane and anti-plane elasticity to solve, and this helps us to construct some solutions. When the so-called decomposition is not available, one must to solve three-dimensional problem indeed. We here consider an example in one-dimensional hexagonal quasicrystals, in which there is a three-dimensional elliptic disk crack with major and minor semi-axes a and b, respectively, shown in Fig. 8.12, and the crack is located in the centre, subjected to a tension at region faraway from the crack.

For simplicity, assume that the external applied stress is removed and instead at the crack surface is subjected to a uniform pressure, and this results in the following boundary conditions:

$$\begin{aligned} &\sqrt{x^2+y^2+z^2} \to \infty : && \sigma_{ii} = 0, H_{ii} = 0 \\ &z = 0, (x, y) \in \Omega : && \sigma_{zz} = -p, H_{zz} = -q, \sigma_{xz} = \sigma_{yz} = 0 \\ &z = 0, (x, y) \notin \Omega : && \sigma_{xz} = \sigma_{yz} = 0, u_z = 0, w_z = 0 \end{aligned} \tag{8.9.1}$$

where Ω denotes the crack surface.

The governing equations of this problem are introduced in Chap. 5, which are not needed to be listed again.

Due to coupling between phonon and phason fields, the problem is very complicated, and a strict analysis is difficult. In the following, an approximate solution based on perturbation is discussed.

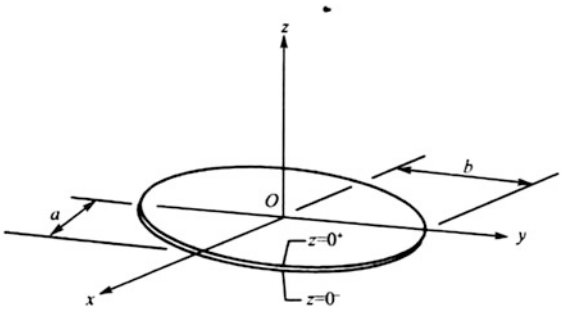

Fig. 8.12 Elliptic disc-shaped crack

Assume that the coupling elastic constants are very much smaller than those of phonon and phason, i.e.

$$\frac{R_i}{C_{jk}}, \frac{R_i}{K_j} \sim \varepsilon \ll 1 \tag{8.9.2}$$

Take perturbation expansions such as

$$u_i = \sum_{n=0}^{\infty} \varepsilon^n u_i^{(n)} \quad (i = x, y, z), \quad w_z = \sum_{n=0}^{\infty} \varepsilon^n w_z^{(n)} \tag{8.9.3}$$

Substituting (8.9.3) into the governing equations and considering condition (8.9.2), the zero-order solution expressed by displacements is as follows:

$$\begin{aligned} u_x^{(0)} &= \frac{\partial}{\partial x}(F_1 + F_2) - \frac{\partial}{\partial y} F_3, \quad u_y^{(0)} = \frac{\partial}{\partial y}(F_1 + F_2) + \frac{\partial}{\partial x} F_3 \\ u_z^{(0)} &= \frac{\partial}{\partial z}(m_1 F_1 + m_2 F_2), \qquad u_z^{(0)} = F_4 \end{aligned} \tag{8.9.4}$$

in which the displacement potentials satisfy the generalized harmonic equations

$$\nabla_i^2 F_i = 0 \quad (i = 1, 2, 3, 4) \tag{8.9.5}$$

where

$$\nabla_i^2 = \frac{\partial^2}{\partial x^2} + \frac{\partial^2}{\partial y^2} + \gamma_i^2 \frac{\partial^2}{\partial z^2} \tag{8.9.6}$$

$$\begin{aligned} \gamma_i^2 &= \frac{C_{44} + (C_{13} + C_{44}) m_i}{C_{11}} = \frac{C_{33} m_i}{C_{13} + C_{44} + C_{44} m_i} \, (i = 1, 2), \\ \gamma_3^2 &= \frac{C_{44}}{C_{66}}, \quad \gamma_4^2 = \frac{K_1}{K_2} \end{aligned} \tag{8.9.7}$$

Without losing generality, we can take

$$F_2 = F_3 = 0 \tag{8.9.8}$$

so that

$$u_z^{(0)} = m_1 \frac{\partial F_1}{\partial z}, \qquad w_z^{(0)} = F_4 \tag{8.9.9}$$

From the basic formulas of Chap. 5, it stands for the zero-order perturbation solution

$$\begin{aligned}
\sigma_{zz}^{(0)} &= -C_{13}\gamma_1^2\frac{\partial^2}{\partial z^2}F_1 + R_2\frac{\partial}{\partial z}F_4 \\
\sigma_{zx}^{(0)} &= C_{44}(m_1+1)\frac{\partial^2}{\partial x\partial z}F_1 + R_3\frac{\partial}{\partial x}F_4 \\
\sigma_{zy}^{(0)} &= C_{44}(m_1+1)\frac{\partial^2}{\partial y\partial z}F_1 + R_2\frac{\partial}{\partial y}F_4 \\
H_{zz}^{(0)} &= -R_1\gamma_1^2\frac{\partial^2}{\partial z^2}F_1 + K_1\frac{\partial}{\partial z}F_4
\end{aligned} \tag{8.9.10}$$

the stresses $\sigma_{xx}^{(0)}, \sigma_{yy}^{(0)}, \sigma_{xy}^{(0)}$ are not listed, because they have no direct connection with the following calculation. Thus, the zero-order perturbation solution on relevant stress components are expressed by

$$\begin{aligned}
\sigma_{zz}^{(0)} &\approx -C_{13}\gamma_1^2\frac{\partial^2}{\partial z^2}F_1^{(0)} \\
\sigma_{zx}^{(0)} &\approx C_{44}(m_1+1)\frac{\partial^2 F_1^{(0)}}{\partial x\partial z} \\
\sigma_{zy}^{(0)} &\approx C_{44}(m_1+1)\frac{\partial^2 F_1^{(0)}}{\partial y\partial z} \\
H_{zz}^{(0)} &\approx K_1\frac{\partial F_4^{(0)}}{\partial z}
\end{aligned} \tag{8.9.11}$$

in which the zero-order perturbations of $F_1^{(0)}$ and $F_4^{(0)}$ satisfy

$$\nabla_1^2 F_1^{(0)} = 0, \qquad \nabla_4^2 F_4^{(0)} = 0 \tag{8.9.12}$$

Due to the above treatment, the boundary conditions reduce to

$$\begin{aligned}
&\sqrt{x^2+y^2+z^2} \to \infty: \quad f = 0, \quad g = 0 \\
&z = 0, (x,y) \in \Omega: \qquad 2C_{13}\gamma_1^2\frac{\partial^2 F_1^{(0)}}{\partial z^2} = -p, K_1\frac{\partial F_4^{(0)}}{\partial z} = -q \\
&z = 0, (x,y) \notin \Omega: \qquad \frac{\partial F_1^{(0)}}{\partial z} = 0, \qquad F_4^{(0)} = 0
\end{aligned} \tag{8.9.13}$$

The boundary value problem of (8.9.12), (8.9.13) is the generalized Lamb problem originated from fluid dynamics [21, 22], and the solution is known (the well-known Green-Sneddon solution) as follows:

$$
\begin{aligned}
F_1^{(0)}(x,y,z) &= \frac{A}{2}\int_{\xi}^{\infty}\left[\frac{x^2}{a^2+s}+\frac{y^2}{b^2+s}+\frac{z^2}{s}\right]\frac{\mathrm{d}s}{\sqrt{Q(s)}} \\
F_4^{(0)}(x,y,z) &= \frac{B}{2}\int_{\xi}^{\infty}\left[\frac{x^2}{a^2+s}+\frac{y^2}{b^2+s}+\frac{z^2}{s}-1\right]\frac{\mathrm{d}s}{\sqrt{Q(s)}}
\end{aligned}
\tag{8.9.14}
$$

where

$$
Q(s) = s(a^2+s)(b^2+s) \tag{8.9.15}
$$

and A and B are unknown constants to be determined and ξ denotes ellipsoid coordinate. After lengthy calculation (see, e.g. [3] or Appendix 2 of this chapter), the unknown constants are determined as follows:

$$
A = \frac{-ab^2p}{4C_{13}\gamma_1^2E(k)}, \quad B = \frac{-ab^2q}{2K_1E(k)} \tag{8.9.16}
$$

where $E(k)$ is the complete elliptic integral of second kind, and $k^2 = (a^2-b^2)/a^2$. So far, the problem in the sense of the zero-order perturbation is solved already. The stress intensity factors of zero-order approximation are:

$$
\begin{aligned}
K_{\mathrm{I}}^{\parallel} &= \lim_{r_1\to 0}\sqrt{2\pi r_1}\sigma_{zz}(x,y,0) = \frac{p\sqrt{\pi}}{E(k)}\left(\frac{b}{a}\right)^{1/2}(a^2\sin^2\phi + b^2\cos^2\phi)^{1/4} \\
K_{\mathrm{I}}^{\perp} &= \lim_{r_1\to 0}\sqrt{2\pi r_1}H_{zz}(x,y,0) = \frac{q\sqrt{\pi}}{E(k)}\left(\frac{b}{a}\right)^{1/2}(a^2\sin^2\phi + b^2\cos^2\phi)^{1/4}
\end{aligned}
\tag{8.9.17}
$$

and $\phi = \arctan(y/x)$. For the detail of derivation, please refer to Appendix 2 of this chapter.

A modification to the zero-order approximation can be done. Substituting the zero-order approximate solution into the original equations that have not been approximated yields the one-order approximate solution, e.g.

$$
\sigma_{zz}^{(1)} = -C_{13}\gamma_1^2\frac{\partial^2}{\partial z^2}F_1^{(0)} + R_2\frac{\partial}{\partial z}F_4^{(0)}, \quad H_{zz}^{(1)} = K_1\frac{\partial}{\partial z}F_4^{(0)} - R_1\gamma_1^2\frac{\partial^2}{\partial z^2}F_1^{(0)} \tag{8.9.18}
$$

In this case, the stress components are in phonon-phason coupling already; furthermore, the stress intensity factors of one-order approximation and other quantities can be evaluated.

8.10 Other Crack Problems in One- and Two-Dimensional Quasicrystals

Peng and Fan [23] reported the study on circular disk-shaped crack, which is the special case of work of Fan and Guo [20].

Liu and Liu et al. gave some solutions of crack problems in terms of complex analysis; in particular, the discussion on those of one-dimensional quasicrystals is comparatively comprehensive, which are summarized in thesis [24].

Li et al. [25] studied the crack solution of one-dimensional hexagonal quasicrystals under the action of thermal stress.

The exact analytic solutions of quasicrystals provide a basis for fracture theory of the material, which will be summarized in Chap. 15.

8.11 Plastic Zone Around Crack Tip

Previous discussion lets us understanding the fact that there is highly stress concentration near the crack tip, and the maximum value of some stress components is beyond yielding limit of material and leads to plastic deformation of the material. That is a plastic zone appears around crack tip. How can we estimate the size of plastic zone and its effects? In classical fracture theory concerning structural materials (or engineering materials), the relevant analysis can be carried out by the theory of plasticity. However, there is no theory for quasicrystalline material so far. In principle, the analysis for plastic deformation of quasicrystals is not available at present.

In Chap. 7, we studied the solutions of dislocations of quasicrystals. Formation of dislocation means the starting of plastic deformation [26]. Movement of dislocations meets an obstacle, the dislocations will be piled up, the pile-up forms dislocation group, and this is a plastic zone macroscopically. By using a continuous distribution model of dislocations, the size of the plastic zone can be evaluated. The size of plastic zone around crack tip may be big or small. If the size can be compared with the crack size, this case is called large-scale plastic zone, and the fracture behaviour is dominated by plastic deformation. If the size is small in comparison with the crack size, this case is called small-scale plastic zone, and the fracture behaviour is still controlled by elastic deformation. In Chap. 14, we will give some analyses about this.

8.12 Appendix 1 of Chapter 8: Some Derivations in Sect. 8.1

Due to similarity to that of Sect. 8.4, some mathematical details of 8.1 are omitted. However, the complex analysis is very important, which is also the basis of 8.2, and we here give some additional details of the derivation.

For simplicity, consider boundary value problem (8.1.5) as an example. From (8.1.11), it is known

$$\left.\begin{aligned}\sigma_{yz}=\sigma_{zy}&=-\tfrac{1}{2i}\left[C_{44}(\phi_1'-\overline{\phi_1'})+R_3(\psi_1'-\overline{\psi_1'})\right]+\tau_1\\ H_{zy}&=-\tfrac{1}{2i}\left[K_2(\psi_1'-\overline{\psi_1'})+R_3(\phi_1'-\overline{\phi_1'})\right]+\tau_2\end{aligned}\right\}\tag{8.12.1}$$

In the following, denote L as crack surface, and then, the second formula of boundary conditions (8.1.5) can be rewritten as follows:

$$\left.\begin{aligned}C_{44}(\phi_1'-\overline{\phi_1'})+R_3(\psi_1'-\overline{\psi_1'})-2i\tau_1=0\quad t\in L\\ K_2(\psi_1'-\overline{\psi_1'})+R_3(\phi_1'-\overline{\phi_1'})-2i\tau_2=0\quad t\in L\end{aligned}\right\}\tag{8.12.2}$$

By applying conformal mapping,

$$t=\omega(\zeta)=\frac{a}{2}\left(\zeta+\frac{1}{\zeta}\right)\tag{8.12.3}$$

to transform domain with Griffith crack at t-plane onto the interior of the unit circle γ at ζ-plane ($\zeta=\xi+i\eta=\rho e^{i\varphi}$), and then, L 则 corresponds to the unit circle γ (similar to Fig. 8.8).

At the unit circle, γ, $\zeta=\sigma\equiv e^{i\varphi}$, $\rho=1$ Under the mapping (8.12.3), unknown functions $\phi_1(t)$ and $\psi_1(t)$ and their derivatives are expressed as follows:

$$\left.\begin{aligned}&\phi_1(t)=\phi_1[\omega(\zeta)]=\phi(\zeta),\ \psi_1(t)=\psi_1[\omega(\zeta)]=\psi(\zeta)\\ &\phi_1'(t)=\phi'(\zeta)/\omega'(\zeta),\qquad\qquad \psi_1'(t)=\psi'(\zeta)/\omega'(\zeta)\end{aligned}\right\}\tag{8.12.4}$$

Similar to 8.4, the boundary conditions are reduced to

$$\left.\begin{aligned}&\tfrac{1}{2\pi i}\int_\gamma\tfrac{\phi'(\sigma)}{\sigma-\zeta}\mathrm{d}\sigma-\tfrac{1}{2\pi i}\int_\gamma\tfrac{\omega'(\sigma)}{\overline{\omega'(\sigma)}}\overline{\phi'(\sigma)}\tfrac{\mathrm{d}\sigma}{\sigma-\zeta}+\tfrac{R_3}{C_{44}}\tfrac{1}{2\pi i}\int_\gamma\tfrac{\psi'(\sigma)}{\sigma-\zeta}\mathrm{d}\sigma\\ &-\tfrac{R_3}{C_{44}}\tfrac{1}{2\pi i}\int_\gamma\tfrac{\omega'(\sigma)}{\overline{\omega'(\sigma)}}\overline{\psi'(\sigma)}\tfrac{\mathrm{d}\sigma}{\sigma-\zeta}=\tfrac{2i\tau_1}{C_{44}}\tfrac{1}{2\pi i}\int_\gamma\tfrac{\omega'(\sigma)}{\sigma-\zeta}\mathrm{d}\sigma\\ &\tfrac{1}{2\pi i}\int_\gamma\tfrac{\psi'(\sigma)}{\sigma-\zeta}\mathrm{d}\sigma-\tfrac{1}{2\pi i}\int_\gamma\tfrac{\omega'(\sigma)}{\overline{\omega'(\sigma)}}\overline{\psi'(\sigma)}\tfrac{\mathrm{d}\sigma}{\sigma-\zeta}+\tfrac{R_3}{K_2}\tfrac{1}{2\pi i}\int_\gamma\tfrac{\phi'(\sigma)}{\sigma-\zeta}\mathrm{d}\sigma-\\ &\tfrac{R_3}{K_2}\tfrac{1}{2\pi i}\int_\gamma\tfrac{\omega'(\sigma)}{\overline{\omega'(\sigma)}}\overline{\phi'(\sigma)}\tfrac{\mathrm{d}\sigma}{\sigma-\zeta}=\tfrac{2i\tau_2}{K_2}\tfrac{1}{2\pi i}\int_\gamma\tfrac{\omega'(\sigma)}{\sigma-\zeta}\mathrm{d}\sigma\end{aligned}\right\}\tag{8.10.5}$$

It is analogous to Sect. 8.4, and there are

$$\left.\begin{aligned}
&\frac{1}{2\pi i}\int_{\gamma}\frac{\phi'(\sigma)}{\sigma-\zeta}\mathrm{d}\sigma=\phi'(\zeta),\frac{1}{2\pi i}\int_{\gamma}\frac{\omega'(\sigma)}{\overline{\omega'(\sigma)}}\overline{\phi'(\sigma)}\frac{\mathrm{d}\sigma}{\sigma-\zeta}=0\\
&\frac{1}{2\pi i}\int_{\gamma}\frac{\psi'(\sigma)}{\sigma-\zeta}\mathrm{d}\sigma=\psi'(\zeta),-\frac{1}{2\pi i}\int_{\gamma}\frac{\omega'(\sigma)}{\overline{\omega'(\sigma)}}\overline{\psi'(\sigma)}\frac{\mathrm{d}\sigma}{\sigma-\zeta}=0\\
&\frac{1}{2\pi i}\int_{\gamma}\frac{\omega'(\sigma)}{\sigma-\zeta}\mathrm{d}\sigma=\frac{a}{2}
\end{aligned}\right\}\qquad(a)$$

So that the solution of Eq. (8.10.5) is

$$\phi'(\zeta)=ia\frac{K_2\tau_1-R_3\tau_2}{C_{44}K_2-R_3^2},\quad \psi'(\zeta)=ia\frac{C_{44}\tau_2-R_3\tau_1}{C_{44}K_2-R_3^2}\qquad(8.12.6)$$

Integrating (8.12.6) yields

$$\phi(\zeta)=ia\frac{K_2\tau_1-R_3\tau_2}{C_{44}K_2-R_3^2}\zeta,\quad \psi(\zeta)=ia\frac{C_{44}\tau_2-R_3\tau_1}{C_{44}K_2-R_3^2}\zeta\qquad(8.12.7)$$

The single-valued inversion of conformal mapping (8.12.3) is

$$\zeta=\omega^{-1}(t)=\frac{t}{a}-\sqrt{\left(\frac{t}{a}\right)^2-1}\qquad(8.12.8)$$

due to $|t|=\infty$ corresponding to $\zeta=0$, and substituting this into, we obtain

$$\phi(\zeta)=\phi(\omega^{-1}(t))=\phi_1(t)=ia\frac{K_2\tau_1-R_3\tau_2}{C_{44}K_2-R_3^2}\zeta=ia\frac{K_2\tau_1-R_3\tau_2}{C_{44}K_2-R_3^2}\left(\frac{t}{a}-\sqrt{\left(\frac{t}{a}\right)^2-1}\right)$$

$$\psi(\zeta)=\psi(\omega^{-1}(t))=\psi_1(t)=ia\frac{C_{44}\tau_2-R_3\tau_1}{C_{44}K_2-R_3^2}\zeta=ia\frac{C_{44}\tau_2-R_3\tau_1}{C_{44}K_2-R_3^2}\left(\frac{t}{a}-\sqrt{\left(\frac{t}{a}\right)^2-1}\right)$$

These are the complex potentials of (8.1.12).

8.13 Appendix 2 of Chapter 8: Some Further Derivation of Solution in Sect. 8.9

To determine the unknown constants A, B, it must do some complex calculations and need to introduce ellipsoid coordinates and elliptic functions.

The region Ω is defined by ellipse, and outside which it is region marked by $(Z-\Omega)$, they can also be defined in terms of the ellipsoid coordinates ξ, η, ζ, which are of some roots s of the ellipsoid equation

$$\frac{x^2}{a^2+s}+\frac{y^2}{b^2+s}+\frac{z^2}{s}-1=0$$

in which

$$-a^2\leqslant\zeta\leqslant-b^2\leqslant\eta\leqslant 0\leqslant\xi<\infty.$$

The relations between ellipsoid coordinates ξ, η, ζ and rectilinear coordinates x, y, z

$$\left.\begin{aligned}a^2(a^2-b^2)x^2&=(a^2+\xi)(a^2+\eta)(a^2+\zeta)\\ b^2(b^2-a^2)y^2&=(b^2+\xi)(b^2+\eta)(b^2+\zeta)\\ a^2b^2z^2&=\xi\eta\zeta\end{aligned}\right\}\tag{8.13.1}$$

As $\xi=0$, corresponding to $z=0$, $(x,y)\in\Omega$, while $\eta=0$, corresponding to $z=0$, $(x,y)\in(Z-\Omega)$. So that the boundary conditions (8.9.1) can be rewritten in a more explicit version if using the ellipsoid coordinates:

$$\xi=0:\quad \sigma_{zz}=-p_0,\ \sigma_{xy}=\sigma_{yz}=0\tag{8.9.1$'$}$$

$$\eta=0:\quad u_z=0,\ \sigma_{xz}=\sigma_{yz}=0\tag{8.9.2$'$}$$

The derivatives of ellipsoid coordinate ξ with respect to rectilinear coordinates

$$\frac{\partial\xi}{\partial x}=\frac{x}{2h_1^2(a^2+\xi)},\frac{\partial\xi}{\partial y}=\frac{y}{2h_1^2(b^2+\xi)},\frac{\partial\xi}{\partial z}=\frac{z}{2\xi h_1^2}\tag{8.13.2}$$

where

$$4h_1^2Q(\xi)=(\xi-\eta)(\xi-\zeta)\tag{8.13.3}$$

and $Q(\xi)$ is defined by (8.9.15).

The derivative of the first formula of (8.9.14) with respect to z is:

$$\frac{\partial F_1^{(0)}}{\partial z}=Az\int_\xi^\infty\frac{\mathrm{d}s}{\sqrt{Q(s)}}\tag{8.13.4}$$

For the convenience of calculations afterwards, the right-hand side of the above equation can be changed as follows:

$$\frac{\partial F_1^{(0)}}{\partial z}=Az\left[\frac{2}{\sqrt{Q(s)}}-\int_\xi^\infty\frac{(2s+a^2+b^2)\mathrm{d}s}{(a^2+s)(b^2+s)\sqrt{Q(s)}}\right]$$

Putting a substitution

$$\xi = \frac{a^2 \mathrm{cn}^2 u}{\mathrm{sn}^2 u} = a^2(\mathrm{sn}^{-2}u - 1) \tag{8.13.5}$$

where $u, \mathrm{cn}u, \mathrm{sn}u, \mathrm{sn}^{-2}u$ are elliptic functions and their definitions and manipulations refer to the introduction hereafter. Inserting (8.13.5) into the above equation, then the partial derivative $\partial F_1^{(0)}/\partial z$ is expressed by elliptic functions:

$$\frac{\partial F_1^{(0)}}{\partial z} = \frac{2Az}{ab^2}\left[\frac{\mathrm{sn}u\mathrm{dn}u}{\mathrm{cn}u} - E(u)\right] \tag{8.13.4'}$$

in which $E(u)$ denotes the complete elliptic integral of second kind (see the following introduction), which can also be expressed by the integral of elliptic function $\mathrm{dn}^2 u$, i.e.

$$E(u) = \int_0^u \mathrm{dn}^2 \beta \mathrm{d}\beta \tag{8.13.6}$$

Taking the derivative of (8.13.4′) with respect to z and applying the formula (8.13.2), one finds that

$$\frac{\partial^2 F_1^{(0)}}{\partial z^2} = A\left\{\frac{2\xi^{1/2}[\xi(a^2b^2 - \eta\zeta) - a^2b^2(\eta + \zeta) - (a^2 + b^2)\eta\zeta]}{a^2b^2(\xi - \eta)(\xi - \zeta)(a^2 + \xi)^{1/2}(b^2 + \xi)^{1/2}} - \frac{2}{ab^2}\left[E(u) - \frac{\mathrm{sn}u\mathrm{cn}u}{\mathrm{dn}u}\right]\right\} \tag{8.13.7}$$

From (8.13.5), as $\xi = 0$, then $u = \pi/2$; from the succeeded formulas, there is $E(u) = E(k)$, $\mathrm{sn}u\mathrm{cn}u/\mathrm{dn}u = 0$. Comparison between (8.13.7) and the second formula of (8.9.1) determines the unknown constant A. Similarly, constant B can be determined.

After determination of constants A, B, function (8.9.14) is determined at all. Naturally, the stress and displacement fields are completely solved. Of course some calculations are still complicated.

Substituting (8.9.14) into the expression of normal stress of phonon field and for $\eta = 0$, there is

$$\begin{cases} \sigma_{zz}(x, y, 0) = \frac{p_0}{E(k)}\left\{\frac{ab^2}{\sqrt{Q(\zeta)}} - \left[E(u) - \frac{\mathrm{sn}_u\mathrm{cn}_u}{\mathrm{dn}_u}\right]\right\} \\ (x, y) \in (\mathrm{Z}-\Omega) \end{cases} \tag{8.13.8}$$

This is the normal stress of phonon field at plane $z = 0$ and outside the crack surface.

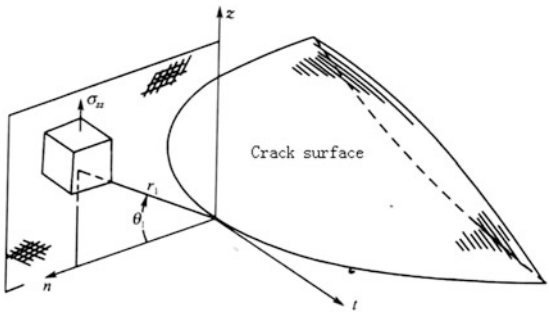

Fig. 8.13 The coordinate system of crack tip

We now calculate the stress intensity factor $K_{\mathrm{I}}^{\|}$, and according to the definition

$$K_{\mathrm{I}}^{\|} = \lim_{r_1 \to 0} \sqrt{2\pi r_1}\sigma_{zz}(x, y, 0)\Big|_{(x,y)\in(Z-\Omega)} \tag{8.13.9}$$

where r_1 characterizes a geometrical parameter of crack tip and $r_1 \ll a$, $r_1 \ll b$ (Fig. 8.13).

The limit process in (8.13.9) can also be expressed through the ellipsoid coordinate $\xi \to 0$. In Fig. 8.13, the location near the crack tip can be described by (8.13.10)

$$\left.\begin{aligned} z &= r_1 \sin\theta_1 \\ \xi &= \frac{2ab}{(\Pi_0)^{1/2}} r_1 \cos^2\frac{\theta_1}{2} \end{aligned}\right\} \tag{8.13.10}$$

and r_1, θ_1 are depicted in the figure, in addition

$$\Pi_0 = a^2 \sin^2\phi + b^2\cos^2\phi$$

ϕ is the polar angle at any point of contour of ellipse (3.11.1) (Fig. 8.14).

As previously pointed out, as $\xi \to 0$, $E(u)$ in (8.13.8) reduces to the complete elliptic integral of second kind, and $(\mathrm{sn}u/\mathrm{cn}u)/\mathrm{dn}u$ tends to zero, the first term presents singularity with order $(2r_1)^{-1/2}$, the coefficient containing the singular term is:

$$\frac{p_0}{E(k)}\Pi_0^{1/4}\left(\frac{b}{a}\right)^{1/2}$$

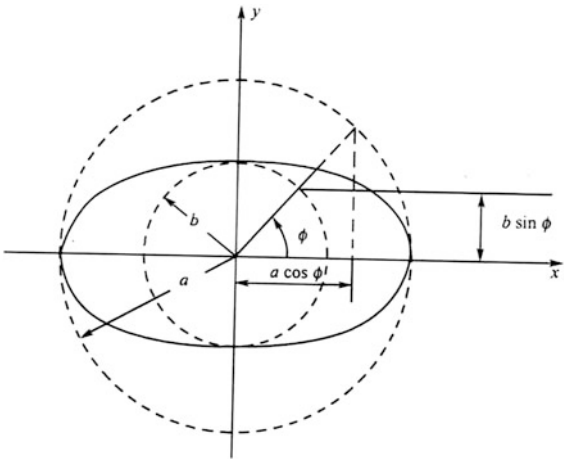

Fig. 8.14 The geometry relation concerning major and minor semi-axis of the elliptic crack

it follows that according to (8.13.9)

$$K_{\mathrm{I}}^{\parallel} = \frac{p\sqrt{\pi}}{E(k)}\left(\frac{b}{a}\right)^{1/2}\left(a^2\sin^2\phi + b^2\cos^2\phi\right)^{1/4} \tag{8.13.11}$$

which is the first formula of (8.9.17) and the second one is similarly obtained, this is the well-known Green-Sneddon solution [22].

In the above derivations, some elliptic functions are used and listed as below.

Denoting

$$u = \int_0^{\phi}\left(1 - k^2\sin^2 t\right)^{-1/2}\mathrm{d}t = F(\phi, k). \tag{a}$$

which is defined u to be function (multi-valued function) of $x = \sin\phi$; in contrast, equation (a) defines ϕ or $\sin\phi$ as a function of u (maybe a multi-valued function). Putting notation

$$\phi = \mathrm{am}u = \mathrm{am}(u, k) \tag{b}$$

means it to be a function of modulus k and argument u. These are the following basic functions:

$$\mathrm{sn}u = \mathrm{sn}(u, k) = \sin(\mathrm{am}u) \tag{c}$$

$$\mathrm{cn}u = \mathrm{cn}(u, k) = \cos(\mathrm{am}u) \tag{d}$$

$$\mathrm{dn}u = \mathrm{dn}(u,k) = \Delta(\mathrm{am}u,k) = [1 - k^2\sin^2(\mathrm{am}u)]^{1/2} \tag{e}$$

The ranges of variation of these functions are:

$$-1 \le \mathrm{sn}u \le 1, -1 \le \mathrm{cn}u \le 1, k' \le \mathrm{dn}u \le 1 \tag{f}$$

Apart from this, these are the following functions:

$$\left.\begin{array}{l} \mathrm{ns}u = 1/\mathrm{sn}u, \ \ \mathrm{nc}u = 1/\mathrm{cn}u \\ \mathrm{nd}u = 1/\mathrm{dn}u \\ \mathrm{cs}u = \mathrm{cn}u/\mathrm{sn}u, \ \ \mathrm{sc}u = \mathrm{sn}u/\mathrm{cn}u \\ \mathrm{sd}u = \mathrm{sn}u/\mathrm{dn}u \\ \mathrm{ds}u = \mathrm{dn}u/\mathrm{sn}u, \ \ \mathrm{dcu} = \mathrm{dn}u/\mathrm{cn}u \\ \mathrm{cd}u = \mathrm{cn}u/\mathrm{dn}u \end{array}\right\} \tag{g}$$

The above functions are named Jacobi elliptic functions.
At $u = 0$, put

$$\mathrm{sn}0 = 0, \ \mathrm{cn}0 = \mathrm{dn}0 = 1 \tag{h}$$

Besides, there is

$$\mathrm{cn}K = 0. \tag{i}$$

Periods of elliptic function $\mathrm{sn}(u,k)$ are $4K$, $i2K'$; periods of $\mathrm{cn}(u,k)$ are $4K$, $2K + i2K'$; periods of $\mathrm{dn}(u,k)$ are $2K$, $i4K'$.

Other properties of elliptic functions are listed a part which are concerned in the previous derivations, e.g.

$$\mathrm{sn}^2u + \mathrm{cn}^2u = 1 \tag{j}$$

$$k^2\mathrm{sn}^2u + \mathrm{dn}^2u = 1 \tag{k}$$

$$\mathrm{dn}^2u - k^2\mathrm{cn}^2u = k'^2 \tag{l}$$

$$k'^2\mathrm{sn}^2u + \mathrm{cn}^2u = \mathrm{dn}^2u \tag{m}$$

References

1. Hu C Z, Yang W H,Wang R H and Ding D H, 1997, Symmetry and physical properties of quasicrystals, Advances of Physics, **17**(4), 345-376 (in Chinese).
2. Meng X M, Tong B Y and Wu Y Q, 1994, Mechanical properties of quasicrystals $Al_{65}Cu_{20}Co_{15}$,Acta Metal Sinica, **30**(2), 61-64 (in Chinese).

3. Fan T Y, 2014, Foundation of Defect and Fracture Theory of Solid and Soft Matter, Beijing, Science Press (in Chinese).
4. Fan T Y, 1991, Exact analytic solutions of stationary and fast propagating cracks in a strip. *Science in China*, A. **34**(5), 560-569; Fan T Y, Mathematical Theory of Elasticity of Quasicrystals, Beijing, Beijing Institute of Technology Press, 1999 (in Chinese).
5. Li L H and Fan T Y, 2008, Exact solutions of two semi-infinite collinear cracks in a strip of one-dimensional hexagonal quasicrystal, *Applied Mathematics and Computation*, **196**(1), 1-5.
6. Shen D W and Fan T Y, 2003, Exact solutions of two semi-infinite collinear cracks in a strip, *Eng. Fracture Mech*., 70(8), 813-822.
7. Li X F, Fan T Y, and Sun Y F, 1999, A decagonal quasicrystal with a Griffith crack. *Phil Mag* A, **79**(8), 1943-1952.
8. Li L H and Fan T Y, 2007, Complex function method for solving notch problem of point group 10, 10 two-dimensional quasicrystals based on the stress potential function, *J. Phys.: Condens. Matter*, **18**(47)**,** 10631-10641.
9. Liu G T and Fan T Y, 2003,The complex method of the plane elasticity in 2D quasicrystals point group 10 *mm* ten-fold rotation symmetry notch problems, *Science in China*, E, **46**(3), 326-336.
10. Li X F, 1999, Elastic fields of dislocations and cracks in one- and two-dimensional quasicrystals, Dissertation, Beijing Institute of Technology, in Chinese.
11. Zhou W M and Fan T Y, 2001, Plane elasticity problem of two-dimensional octagonal quasicrystal and crack problem, *Chin. Phys*., **10**(8), 743-747.
12. Zhou W M, 2000, Mathematical analysis of elasticity and defects of two- and three-dimensional quasicrystals, Dissertation, Beijing Institute of Technology, in Chinese.
13. Li L H, 2008, Study on complex function method and analytic solutions of elasticity of quasicrystals,Dissertation, Beijing Institute of Technology, in Chinese.
14. Fan T Y and Tang Z Y, 2015, Bending problem for a two-dimensional quasicrystal with an elliptic notch and nonlinear analysis, submitted.
15. Muskhelishvili N I, 1953, *Some Basic Problems of the Mathematical Theory of Elasticity*, Noordhoff Ltd, Groningen.
16. Lokchine M A, Sur l'influence d'un trou elliptique dans la poutre qui eprouve une flexion. *C.R.Paris*, 1930, **190**, 1178-1179.
17. Fan T Y and Tang Z Y, 2016, Crack solution of a strip in a two-dimensional quasicrystal, submitted.
18. Fan T Y, Yang X C , Li H X, 1998, Exact analytic solution for a finite width strip with a single crack, Chin Phys Lett, 18(1), 18-21.
19. Li W, 2011, Analytic solutions of a finite width strip with a single edge crack of two-dimensional quasicrystals, Chin Phys B Vol. 20(11), 116201.
20. FanTY, Guo R P, 2013, Three-dimensional elliptic crack in one-dimensional hexagonal quasicrystals, unpublished work.
21. Lamb H, Hydrodynamics, 1933, Dover, New York.
22. Green A E, Sneddon I N, 1950, The distribution of stress in the neighbourhood of a at elliptic crack in an elastic solid, Proc. Ca mb. Phil. Soc., 46(2), 159-163.
23. Peng Y Z, Fan T Y, 2000, Elastic theory of 1D quasiperiodic stacking of 2D crystals, *J. Phys.: Condens. Matte*r, **12**(45), 9381-9387.
24. Liu G T,2004, Elasticity and defects of quasicrystals and auxiliary function method of nonlinear evolution equations, Dissertation, Beijing Institute of Technology, in Chinese.
25. Li X Y, Fundamental solutions of a penny shaped embedded crack and half-infinite plane crack in infinite space of one-dimensional hexagonal quasicrystals under thermal loading, Proc Roy Soc A, 469, 20130023, 2013.
26. Messerschmidt U, 2010, Dislocation Dynamics during Plastic Deformation, Chapter 10, Springer-Verlag, Heidelberg.

Chapter 9
Theory of Elasticity of Three-Dimensional Quasicrystals and Its Applications

In Chaps. 5–8, we discussed the theories of elasticity of one- and two-dimensional quasicrystals and their applications. In this chapter, the theory and applications of elasticity of three-dimensional quasicrystals will be dealt with. The three-dimensional quasicrystals include icosahedral quasicrystals and cubic quasicrystals. In all over 200 individual quasicrystals observed to date, there are almost half icosahedral quasicrystals, so they play the central role in this kind of solids. This suggests the major importance of elasticity of icosahedral quasicrystals in the study of mechanical behaviour of quasicrystalline materials.

There are some polyhedrons with the icosahedral symmetry; one of them is shown in Fig. 9.1, which consists of 20 right triangles and contains 12 fivefold symmetric axes $A5$, 20 threefold symmetric axes $A3$ and 30 twofold symmetric axes $A2$. One of the diffraction patterns is shown in Sect. 3.1.1, and the stereographic structure of one of icosahedral point groups is also depicted in Sect. 3.1.1.

The elasticity of icosahedral quasicrystals was studied immediately after the discovery of the structure, which is the pioneering work of the field, and promoted the development of the disciplinary of the research. The outlook about this was figured out in the Chap. 4, in which the contribution of pioneers such as P. Bak et al. was introduced. After Ding et al. [1] set up the physical framework of elasticity of icosahedral quasicrystals, they [2] also summarized the basic relationship of elasticity of cubic quasicrystals. In terms of the Green function method, Yang et al. [3] gave an approximate solution on dislocation for a special case, i.e. the phonon-phason decoupled plane elasticity of icosahedral quasicrystal. In this chapter, we mainly discuss the general theory of elasticity of icosahedral quasicrystals and the application; in addition, those for cubic quasicrystals are also concerned. We focus on the mathematical theory of the elasticity and the analytic solutions. Because of the large number of field variables and field equations involving elasticity of these two kinds of three-dimensional quasicrystals, the solution presents tremendous difficulty. We continue to develop the decomposition and superposition procedures adopted in the previous chapters; this can reduce the number of the field variables and field equations, and three-dimensional elasticity

T.-Y. Fan, *Mathematical Theory of Elasticity of Quasicrystals and Its Applications*,
Springer Series in Materials Science 246, DOI 10.1007/978-981-10-1984-5_9

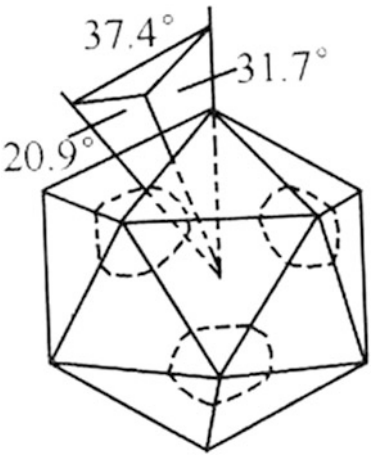

Fig. 9.1 Icosahedral

can be simplified to two-dimensional elasticity to solve cases with important practical applications. The introduction of displacement potentials or stress potentials [4, 5] can further simplify the problems. In the work, some systematic and direct methods of mathematical physics and functional theory have been developed, and a series of analytic solutions are constructed, which will be included in the chapter. Because the calculations are very complex, we would like to introduce them in as much detail as possible in order to facilitate comprehension of the text.

9.1 Basic Equations of Elasticity of Icosahedral Quasicrystals

The equations of deformation geometry are

$$\varepsilon_{ij} = \frac{1}{2}\left(\frac{\partial u_i}{\partial x_j} + \frac{\partial u_j}{\partial x_i}\right), \quad w_{ij} = \frac{\partial w_i}{\partial x_j} \tag{9.1.1}$$

which are similar in form to those given in previous chapters, but here u_i and w_i have 6 components, and ε_{ij} and w_{ij} have 15 components in total.

The equilibrium equations are as follows

$$\frac{\partial \sigma_{ij}}{\partial x_j} = 0, \quad \frac{\partial H_{ij}}{\partial x_j} = 0 \tag{9.1.2}$$

which are also similar in form to those listed in previous chapters; however, here adding σ_{ij} and H_{ij} gives 15 stress components.

Between the stresses and strains, there is the generalized Hooke's law such as

$$\sigma_{ij} = C_{ijkl}\varepsilon_{kl} + R_{ijkl}w_{kl} \quad H_{ij} = R_{klij}\varepsilon_{kl} + K_{ijkl}w_{kl} \tag{9.1.3}$$

in which the phonon elastic constants are described by

$$C_{ijkl} = \lambda\delta_{ij}\delta_{kl} + \mu\left(\delta_{ik}\delta_{jl} + \delta_{il}\delta_{jk}\right) \tag{9.1.4}$$

where λ and μ (=G in some references) are the Lamé constants.

If the strain components are arranged as a vector according to the order

$$[\varepsilon_{ij}, w_{ij}] = [\varepsilon_{11}\varepsilon_{22}\varepsilon_{33}\varepsilon_{23}\varepsilon_{31}\varepsilon_{12}w_{11}w_{22}w_{33}w_{23}w_{32}w_{12}w_{32}w_{13}w_{21}] \tag{9.1.5'}$$

and the stress components are also arranged according to the same order, i.e.

$$[\sigma_{ij}, H_{ij}] = [\sigma_{11}\sigma_{22}\sigma_{33}\sigma_{23}\sigma_{31}\sigma_{12}H_{11}H_{22}H_{33}H_{23}H_{32}H_{12}H_{32}H_{13}H_{21}] \tag{9.1.5"}$$

then phason and phonon-phason coupling elastic constants can be expressed by matrixes of $[K]$ and $[R]$

$$[K] = \begin{bmatrix} K_1 & 0 & 0 & 0 & K_2 & 0 & 0 & K_2 & 0 \\ 0 & K_1 & 0 & 0 & -K_2 & 0 & 0 & K_2 & 0 \\ 0 & 0 & K_2+K_1 & 0 & 0 & 0 & 0 & 0 & 0 \\ 0 & 0 & 0 & K_1-K_2 & 0 & K_2 & 0 & 0 & -K_2 \\ K_2 & -K_2 & 0 & 0 & K_1-K_2 & 0 & 0 & 0 & 0 \\ 0 & 0 & 0 & K_2 & 0 & K_1 & -K_2 & 0 & 0 \\ 0 & 0 & 0 & 0 & 0 & -K_2 & K_1-K_2 & 0 & -K_2 \\ K_2 & K_2 & 0 & 0 & 0 & 0 & 0 & K_1-K_2 & 0 \\ 0 & 0 & 0 & -K_2 & 0 & 0 & -K_2 & 0 & K_1 \end{bmatrix}$$

$$[R] = R\begin{bmatrix} 1 & 1 & 1 & 0 & 0 & 0 & 0 & 1 & 0 \\ -1 & -1 & 1 & 0 & 0 & 0 & 0 & -1 & 0 \\ 0 & 0 & -2 & 0 & 0 & 0 & 0 & 0 & 0 \\ 0 & 0 & 0 & 0 & 0 & -1 & 1 & 0 & -1 \\ 1 & -1 & 0 & 0 & 1 & 0 & 0 & 0 & 0 \\ 0 & 0 & 0 & -1 & 0 & -1 & 0 & 0 & 1 \\ 0 & 0 & 0 & 0 & 0 & -1 & 1 & 0 & -1 \\ 1 & -1 & 0 & 0 & 1 & 0 & 0 & 0 & 0 \\ 0 & 0 & 0 & -1 & 0 & -1 & 0 & 0 & 1 \end{bmatrix}$$

Equations (9.1.1)–(9.1.3) are basic equations of elasticity of icosahedral quasicrystals; there are 36 field equations in total, and the number of the field variables is also 36. It is consistent and solvable mathematically.

Due to the huge number of the field variables and field equations, the mathematical solution is highly complex. One way to solve the elasticity problem is to reduce the number of the field variables and field equations mentioned above. For this purpose, we can utilize the eliminating element method in classical mathematical physics.

Based on the matrix expression of the generalized Hooke's law of (4.5.3) in Chap. 4, i.e.

$$\begin{bmatrix} \sigma_{ij} \\ H_{ij} \end{bmatrix} = \begin{bmatrix} [C] & [R] \\ [R]^{\mathrm{T}} & [K] \end{bmatrix} \begin{bmatrix} \varepsilon_{ij} \\ w_{ij} \end{bmatrix}$$

where

$$\begin{bmatrix} \sigma_{ij} \\ H_{ij} \end{bmatrix} = \left[\sigma_{ij}, H_{ij}\right]^{\mathrm{T}}$$
$$\begin{bmatrix} \varepsilon_{ij} \\ w_{ij} \end{bmatrix} = \left[\varepsilon_{ij}, w_{ij}\right]^{\mathrm{T}}$$

then one has the explicit relationship between stresses and strains as below

$$\begin{aligned}
\sigma_{xx} &= \lambda\theta + 2\mu\varepsilon_{xx} + R(w_{xx} + w_{yy} + w_{zz} + w_{xz}) \\
\sigma_{yy} &= \lambda\theta + 2\mu\varepsilon_{yy} - R(w_{xx} + w_{yy} - w_{zz} + w_{xz}) \\
\sigma_{zz} &= \lambda\theta + 2\mu\varepsilon_{zz} - 2Rw_{zz} \\
\sigma_{yz} &= 2\mu\varepsilon_{yz} + R(w_{zy} - w_{xy} - w_{yx}) = \sigma_{zy} \\
\sigma_{zx} &= 2\mu\varepsilon_{zx} + R(w_{xx} - w_{yy} - w_{zx}) = \sigma_{xz} \\
\sigma_{xy} &= 2\mu\varepsilon_{xy} + R(w_{yx} - w_{yz} - w_{xy}) = \sigma_{yx}
\end{aligned}$$

$$\begin{aligned}
H_{xx} &= R(\varepsilon_{xx} - \varepsilon_{yy} + 2\varepsilon_{zx}) + K_1 w_{xx} + K_2(w_{zx} + w_{xz}) \\
H_{yy} &= R(\varepsilon_{xx} - \varepsilon_{yy} - 2\varepsilon_{zx}) + K_1 w_{yy} + K_2(w_{xz} - w_{zx}) \\
H_{zz} &= R(\varepsilon_{xx} + \varepsilon_{yy} - 2\varepsilon_{zz}) + (K_1 + K_2) w_{zz} \\
H_{yz} &= -2R\varepsilon_{xy} + (K_1 - K_2) w_{yz} + K_2(w_{xy} - w_{yx}) \\
H_{zx} &= 2R\varepsilon_{zx} + (K_1 - K_2) w_{zx} + K_2(w_{xx} - w_{yy}) \\
H_{xy} &= -2R(\varepsilon_{yz} + \varepsilon_{xy}) + K_1 w_{xy} + K_2(w_{yz} - w_{zy}) \\
H_{zy} &= 2R\varepsilon_{yz} + (K_1 - K_2) w_{zy} - K_2(w_{xy} + w_{yx}) \\
H_{xz} &= R(\varepsilon_{xx} - \varepsilon_{yy}) + K_2(w_{xx} + w_{yy}) + (K_1 - K_2) w_{xz} \\
H_{yx} &= 2R(\varepsilon_{xy} - \varepsilon_{yz}) + K_1 w_{yx} - K_2(w_{yz} + w_{zy})
\end{aligned} \tag{9.1.7}$$

where $\theta = \varepsilon_{xx} + \varepsilon_{yy} + \varepsilon_{zz}$ denotes the volume strain, and ε_{ij} and w_{ij} are defined by (9.1.1). This explicit expression was first given by Ding et al. [1].

Substituting (9.1.7) into (9.1.2) yields one of the forms of the final governing equations—the equilibrium equations in terms of displacements are as follows

$$\mu\nabla^2 u_x+(\lambda+\mu)\frac{\partial}{\partial x}\nabla\cdot\mathrm{u}+R\left(\frac{\partial^2 w_x}{\partial x^2}+\frac{\partial^2 w_x}{\partial x\partial z}-\frac{\partial^2 w_x}{\partial y^2}+2\frac{\partial^2 w_y}{\partial x\partial y}-2\frac{\partial^2 w_y}{\partial y\partial z}+2\frac{\partial^2 w_z}{\partial x\partial z}\right)=0$$
$$\mu\nabla^2 u_y+(\lambda+\mu)\frac{\partial}{\partial y}\nabla\cdot\mathrm{u}+R\left(-2\frac{\partial^2 w_x}{\partial x\partial y}-2\frac{\partial^2 w_x}{\partial y\partial z}+\frac{\partial^2 w_y}{\partial x^2}-2\frac{\partial^2 w_y}{\partial x\partial z}-\frac{\partial^2 w_y}{\partial y^2}+2\frac{\partial^2 w_z}{\partial y\partial z}\right)=0$$
$$\mu\nabla^2 u_z+(\lambda+\mu)\frac{\partial}{\partial z}\nabla\cdot\mathrm{u}+R\left(\frac{\partial^2 w_x}{\partial x^2}-2\frac{\partial^2 w_x}{\partial x\partial y}-\frac{\partial^2 w_x}{\partial y^2}+\frac{\partial^2 w_z}{\partial x^2}+\frac{\partial^2 w_z}{\partial y^2}-2\frac{\partial^2 w_z}{\partial z^2}\right)=0$$

$$\begin{aligned}
&K_1\nabla^2 w_x+K_2\left(2\frac{\partial^2 w_x}{\partial x\partial z}-\frac{\partial^2 w_x}{\partial z^2}+2\frac{\partial^2 w_y}{\partial y\partial z}+\frac{\partial^2 w_z}{\partial x^2}-\frac{\partial^2 w_z}{\partial y^2}\right)\\
&+R\left(\frac{\partial^2 u_x}{\partial x^2}+2\frac{\partial^2 u_x}{\partial x\partial z}-\frac{\partial^2 u_x}{\partial y^2}-2\frac{\partial^2 u_y}{\partial x\partial y}-2\frac{\partial^2 u_y}{\partial y\partial z}+\frac{\partial^2 u_z}{\partial x^2}-\frac{\partial^2 u_z}{\partial y^2}\right)=0\\
&K_1\nabla^2 w_y+K_2\left(2\frac{\partial^2 w_x}{\partial y\partial z}-2\frac{\partial^2 w_y}{\partial x\partial z}-2\frac{\partial^2 w_z}{\partial x\partial y}-\frac{\partial^2 w_y}{\partial z^2}\right)\\
&+R\left(\frac{\partial^2 u_y}{\partial x^2}-2\frac{\partial^2 u_x}{\partial y\partial z}+\frac{\partial^2 u_y}{\partial y^2}+2\frac{\partial^2 u_x}{\partial x\partial y}-2\frac{\partial^2 u_y}{\partial x\partial z}-2\frac{\partial^2 u_z}{\partial x\partial y}\right)=0\\
&(K_1-K_2)\nabla^2 w_z+K_2\left(\frac{\partial^2 w_x}{\partial x^2}-\frac{\partial^2 w_x}{\partial y^2}-2\frac{\partial^2 w_y}{\partial y\partial x}+2\frac{\partial^2 w_z}{\partial z^2}\right)\\
&+R\left(2\frac{\partial^2 u_x}{\partial x\partial z}+2\frac{\partial^2 u_x}{\partial x\partial z}+\frac{\partial^2 u_z}{\partial x^2}+\frac{\partial^2 u_z}{\partial y^2}-2\frac{\partial^2 u_z}{\partial z^2}\right)=0
\end{aligned}\tag{9.1.8}$$

where $\nabla^2=\frac{\partial^2}{\partial x^2}+\frac{\partial^2}{\partial y^2}+\frac{\partial^2}{\partial z^2}$, $\quad\nabla\cdot u=\frac{\partial u_x}{\partial x}+\frac{\partial u_y}{\partial y}+\frac{\partial u_z}{\partial z}$.

Equations (9.1.8) are 6 partial differential equations of second-order on displacements u_i and w_i. So the number of the field variables and field equations is reduced already. But obtaining solution is still very difficult; one of the reasons is the boundary conditions for quasicrystals which are much more complicated than those of the classical theory of elasticity. In the subsequent sections, we will make a great effort to solve some complex boundary value problems through different approaches.

It is obvious that the material constants of λ, μ, K_1, K_2 and R are very important for stress analysis for different icosahedral quasicrystals, which are experimentally measured through various methods (e.g. X-ray diffraction and neutron scattering) and listed in Tables 9.1, 9.2 and 9.3, respectively, as follows.

In this table, the measurement unit of λ, μ and B is GPa, and $B=(3\lambda+2\mu)/3$ represents the bulk modulus, and $\nu=\lambda/2(\lambda+\mu)$ represents the Poisson's ratio, respectively.

It is needed to point out that Eqs. (9.1.8) are not only a form of final governing equation of elasticity of icosahedral quasicrystals, but also there are other forms which will be discussed in Sect. 9.5.

Table 9.1 Phonon elastic constants of various icosahedral quasicrystals

Alloys	λ	$\mu(G)$	B	v	Refs.
Al–Li–Cu	30	35	53	0.23	[6]
Al–Li–Cu	30.4	40.9	57.7	0.213	[7]
Al–Cu–Fe	59.1	68.1	104	0.213	[8]
Al–Cu–Fe–Ru	48.4	57.9	87.0	0.228	[8]
Al–Pd–Mn	74.9	72.4	123	0.254	[8]
Al–Pd–Mn	74.2	70.4	121	0.256	[9]
Ti–Zr–Ni	85.5	38.3	111	0.345	[10]
Cu–Yh	35.28	25.28	52.13	0.2913	[11]
Zn–Mg–Y	33.0	46.5	64.0	0.208	[12]

Table 9.2 Phason elastic constants of various icosahedral quasicrystals

Alloys	Source	Meas. Temp.	K_1 (MPa)	K_2 (MPa)	Refs.
Al–Pd–Mn	X-ray	R.T.	43	−22	[13]
Al–Pd–Mn	Neutron	R.T.	72	−37	[13]
Al–Pd–Mn	Neutron	1043 K	125	−50	[13]
Zn–Mg–Sc	X-ray	R.T.	300	−45	[14]

Table 9.3 Phonon-phason coupling elastic constant of various icosahedral quasicrystals

Alloys	Source	R	Refs.
Mg–Ga–Al–Zn	X-ray	−0.04 μ	[15]
Al–Cu–Fe	X-ray	0.004 μ	[15]

9.2 Anti-plane Elasticity of Icosahedral Quasicrystals and Problem of Interface of Quasicrystal–Crystal

People can find Eqs. (9.1.8) is very complex, but they can be simplified for some meaningful cases physically. One of them is the so-called anti-plane case where the nonzero displacements are only u_z and w_z, and the other displacements vanish. In particular, these two displacements and relevant strains and stresses are independent from the coordinate x_3 (or z). If there is a Griffith crack along the axis z (see Fig. 9.2) or a straight dislocation line along the direction, in addition, the applied external fields are independent from variable z, so the field variables and field equations are free from the coordinate z for the configuration:

$$\frac{\partial}{\partial x_3}\left(=\frac{\partial}{\partial z}\right)=0 \tag{9.2.1}$$

Because there are only two components u_z and w_z, and others have vanished, the corresponding strains are only

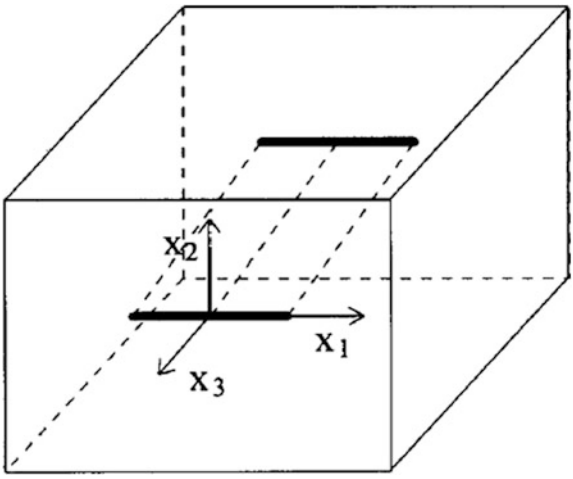

Fig. 9.2 One of configuration of plane or anti-plane elasticity

$$\varepsilon_{yz} = \varepsilon_{zy} = \frac{1}{2}\frac{\partial u_z}{\partial y}, \quad \varepsilon_{xz} = \varepsilon_{zx} = \frac{1}{2}\frac{\partial u_z}{\partial x}, \quad w_{zy} = \frac{\partial w_z}{\partial y}, \quad w_{zx} = \frac{\partial w_z}{\partial x} \tag{9.2.2}$$

From the formulas listed in Sect. 9.1, the nonzero stress components are

$$\begin{aligned}
\sigma_{xz} &= \sigma_{zx} = 2\mu\varepsilon_{xz} + Rw_{zx} \\
\sigma_{yz} &= \sigma_{zy} = 2\mu\varepsilon_{yz} + Rw_{zy} \\
H_{zx} &= (K_1 - K_2)w_{zx} + 2R\varepsilon_{xz} \\
H_{zy} &= (K_1 - K_2)w_{zy} + 2R\varepsilon_{yz} \\
H_{xx} &= 2R\varepsilon_{xz} + K_2 w_{zx} \\
H_{yy} &= -2R\varepsilon_{xz} - K_2 w_{zx} \\
H_{xy} &= -2R\varepsilon_{yz} - K_2 w_{zy} \\
H_{yx} &= -2R\varepsilon_{yz} - K_2 w_{zy}
\end{aligned} \tag{9.2.3}$$

and the equilibrium equations stand for

$$\left.\begin{aligned}
\frac{\partial \sigma_{zx}}{\partial x} + \frac{\partial \sigma_{zy}}{\partial y} = 0, \quad \frac{\partial H_{zx}}{\partial x} + \frac{\partial H_{zy}}{\partial y} = 0 \\
\frac{\partial H_{xx}}{\partial x} + \frac{\partial H_{xy}}{\partial y} = 0, \quad \frac{\partial H_{yx}}{\partial x} + \frac{\partial H_{yy}}{\partial y} = 0
\end{aligned}\right\} \tag{9.2.4}$$

The problem described by Eqs. (9.2.2)–(9.2.4) is anti-plane elasticity problem; we have the final governing equations

$$\nabla_1^2 u_z = 0, \quad \nabla_1^2 w_z = 0 \tag{9.2.5}$$

where $\nabla_1^2 = \frac{\partial^2}{\partial x^2} + \frac{\partial^2}{\partial y^2}$.

One can see that Eqs. (9.2.5) are similar to (5.2.11), which can be solved in a procedure similar to that adopted in Chaps. 5, 7 and 8.

As an example of solution of anti-plane elasticity of icosahedral quasicrystals, we discuss the interface problem between centre-body cubic crystals and icosahedral quasicrystals.

The physical model is similar to that proposed in Sect. 7.6, i.e. the icosahedral quasicrystal is located in upper half-space $y > 0$, whose governing equations are listed above, while the centre-body cubic crystal lies in lower space $y < 0$ with finite thickness h (refer to Sect. 7.6.1 in Chap. 7) and is governed by the following equation

$$\nabla^2 u_z^{(c)} = 0 \tag{9.2.6}$$

with the following stress–strain relations

$$\sigma_{zy}^{(c)} = \sigma_{yz}^{(c)} = 2\mu^{(c)}\varepsilon_{yz}^{(c)}, \quad \sigma_{zx}^{(c)} = \sigma_{xz}^{(c)} = 2\mu^{(c)}\varepsilon_{xz}^{(c)}$$

for crystals, in which $\varepsilon_{ij}^{(c)} = (\partial u_i^{(c)}/\partial x_j + \partial u_j^{(c)}/\partial x_i)/2$, $\mu^{(c)} = C_{44}^{(c)}$.

After Fourier transform, the solution of (9.2.6) is very easy to obtain such that

$$u_z(x,y) = \frac{1}{2\pi}\int_{-\infty}^{\infty} A(\xi)e^{-|\xi|y-i\xi x}\mathrm{d}\xi, \quad w_z(x,y) = \frac{1}{2\pi}\int_{-\infty}^{\infty} B(\xi)e^{-|\xi|y-i\xi x}\mathrm{d}\xi \tag{9.2.7}$$

and the relevant stresses, e.g.

$$\begin{aligned}
\sigma_{zy} &= -\mu\frac{1}{2\pi}\int_{-\infty}^{\infty} |\xi|A(\xi)e^{-|\xi|y-i\xi x}\mathrm{d}\xi - R\frac{1}{2\pi}\int_{-\infty}^{\infty} |\xi|B(\xi)e^{-|\xi|y-i\xi x}\mathrm{d}\xi \\
H_{zy} &= -R\frac{1}{2\pi}\int_{-\infty}^{\infty} |\xi|A(\xi)e^{-|\xi|y-i\xi x}\mathrm{d}\xi - (K_1 - K_2)\frac{1}{2\pi}\int_{-\infty}^{\infty} |\xi|B(\xi)e^{-|\xi|y-i\xi x}\mathrm{d}\xi
\end{aligned} \tag{9.2.8}$$

in which $y > 0$ and $A(\xi)$ and $B(\xi)$ are arbitrary functions of ξ to be determined.

According to the second boundary condition at the interface,

$$y = 0, \quad -\infty < x < \infty: \quad \sigma_{zy} = \tau f(x) + ku(x), \quad H_{zy} = 0 \tag{9.2.9}$$

where

$$k = \frac{\mu^{(c)}}{h} \tag{9.2.10}$$

and the relation between the two unknown functions is

$$B(\xi) = -\frac{R}{K_1 - K_2} A(\xi) \tag{9.2.11}$$

From (9.2.7) and (9.2.8), we have

$$\hat{\sigma}_{zy} = -\left(2\mu + \frac{R^2}{K_1 - K_2}\right) A(\xi)|\xi|$$

and from the first one of condition (9.2.9), one determines the unknown function

$$A(\xi) = -\frac{\tau \hat{f}(\xi)}{\left(\frac{R^2}{K_1 - K_2} + \mu\right)|\xi| + k} \tag{9.2.12}$$

So that

$$B(\xi) = \frac{R\tau \hat{f}(\xi)}{(K_1 - K_2)\left[\left(\frac{R^2}{K_1 - K_2} + \mu\right)|\xi| + k\right]} \tag{9.2.13}$$

in which τ and k are defined by (9.2.9) and (9.2.10), respectively. Thus the problem is solved. The phason strain field can be determined as

$$w_{zy}(x, y) = -R\tau \frac{1}{2\pi} \int_{-\infty}^{\infty} \frac{|\xi| \hat{f}(\xi)}{(R^2 - \mu(K_1 - K_2))|\xi| + k(K_1 - K_2)} e^{-|\xi| y - i\xi x} \mathrm{d}\xi$$

$$w_{zx}(x, y) = iR\tau \frac{1}{2\pi} \int_{-\infty}^{\infty} \frac{\xi \hat{f}(\xi)}{(R^2 - \mu(K_1 - K_2))|\xi| + k(K_1 - K_2)} e^{-|\xi| y - i\xi x} \mathrm{d}\xi \tag{9.2.14}$$

Note that $y > 0$. The integrals in (9.2.14) for some cases can be evaluated through the residual theorem introduced in the Major Appendix of this book.

As the first example, assume that $f(x) = 1$, as $-a/2 < x < a/2$, and $f(x) = 0$, as $x < -a/2$, and $x > a/2$, so $\hat{f}(\xi) = \frac{2}{\xi} \sin\left(\frac{a}{2}\xi\right)$; then from solution (9.2.14), we obtain

$$
\begin{aligned}
w_{zy}(x,y) &= \frac{a}{h}\frac{\mu^{(c)}R(K_1-K_2)\tau}{\left[\mu(K_1-K_2)-R^2\right]^2}\sin\left(\frac{1}{2}\frac{\mu^{(c)}(K_1-K_2)}{\mu(K_1-K_2)-R^2}\frac{a}{h}\right)\\
&\quad\times\exp\left(-\frac{\mu^{(c)}(K_1-K_2)}{\mu(K_1-K_2)-R^2}\frac{y}{h}\right)\cos\left[\frac{\mu^{(c)}(K_1-K_2)}{\mu(K_1-K_2)-R^2}\frac{x}{h}\right]\\
w_{zx}(x,y) &= \frac{a}{h}\frac{\mu^{(c)}R(K_1-K_2)\tau}{\left[\mu(K_1-K_2)-R^2\right]^2}\sin\left(\frac{1}{2}\frac{\mu^{(c)}(K_1-K_2)}{\mu(K_1-K_2)-R^2}\frac{a}{h}\right)\\
&\quad\times\exp\left(-\frac{\mu^{(c)}(K_1-K_2)}{\mu(K_1-K_2)-R^2}\frac{y}{h}\right)\sin\left[\frac{\mu^{(c)}(K_1-K_2)}{\mu(K_1-K_2)-R^2}\frac{x}{h}\right]
\end{aligned}
\tag{9.2.15}
$$

in which we have $k=\mu^{(c)}/h$ and have used the normalized expression, i.e. $x/h, y/h$. Then consider second example $f(x)=\delta(x)$, and then, the integrals (9.2.14) will be

$$
\begin{aligned}
w_{zy}(x,y) &= \frac{\mu^{(c)}R(K_1-K_2)\tau}{\left[\mu(K_1-K_2)-R^2\right]^2}\\
&\quad\times\exp\left(-\frac{\mu^{(c)}(K_1-K_2)}{\mu(K_1-K_2)-R^2}\frac{y}{h}\right)\sin\left[\frac{\mu^{(c)}(K_1-K_2)}{\mu(K_1-K_2)-R^2}\frac{x}{h}\right]\\
w_{zx}(x,y) &= \frac{\mu^{(c)}R(K_1-K_2)\tau}{\left[\mu(K_1-K_2)-R^2\right]^2}\\
&\quad\times\exp\left(-\frac{\mu^{(c)}(K_1-K_2)}{\mu(K_1-K_2)-R^2}\frac{y}{h}\right)\cos\left[\frac{\mu^{(c)}(K_1-K_2)}{\mu(K_1-K_2)-R^2}\frac{x}{h}\right]
\end{aligned}
\tag{9.2.16}
$$

The detail of the evaluation is given in the Major Appendix of the book.

The results are quite interesting. In the first example, the phason strain field is dominated by the elastic constants μ, K_1, K_2, R and $\mu^{(c)}$ of quasicrystal and crystal and applied stress τ and geometry parameters a and h, while in the second example, the geometry parameter is only h. For different $\tau/\mu, \mu^{(c)}/\mu, a/h$ and given values of μ, K_1, K_2 and R, one can find a rich set of numerical results. The computation used the measured values of these quantities for Al–Pd–Mn icosahedral quasicrystals which are provided in Tables 9.1, 9.2 and 9.3:

$$\mu = 72.4\,\text{GPa}, \quad K_1 = 125\,\text{MPa}, \quad K_2 = -50\,\text{MPa}, \quad R = 0.04\,\mu$$

In the first example, strain field of phason is dependent upon elastic constants μ, K_1, K_2, R of quasicrystal, elastic constant $\mu^{(c)}$ of crystal, and applied stress τ and geometry parameters a and h; in the second example, the geometry parameter is only h. For different values of $\tau/\mu, \mu^{(c)}/\mu, a/h$ under given values of μ, K_1, K_2 and R, some significant results are found and shown in Figs. 9.3, 9.4, 9.5 and 9.6,

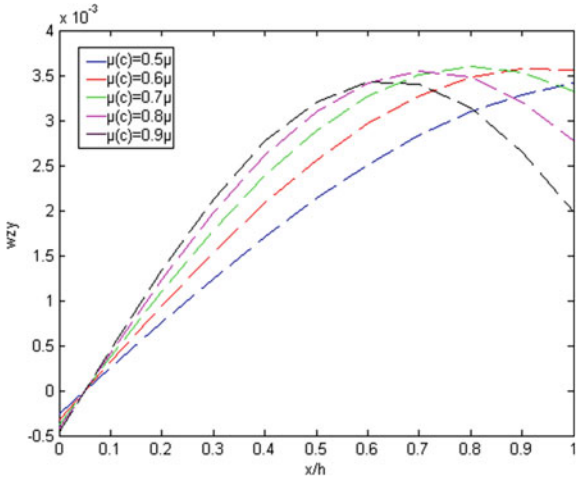

Fig. 9.3 Variation of w_{zy} versus x

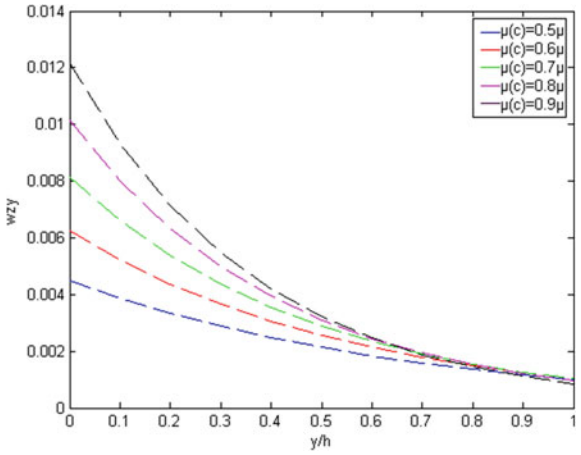

Fig. 9.4 Variation of w_{zy} versus y

respectively. The quasicrystalline material constants are taken from Tables 9.1, 9.2 and 9.3, i.e.

$$\mu = 72.4\,\text{GPa}, \quad K_1 = 125\,\text{MPa}, \quad K_2 = -50\,\text{MPa}, \quad R = 0.04\,\mu$$

The numerical results show that the influence of the ratio $\mu^{(c)}/\mu$ of shear modulus of crystal and quasicrystal is very evident. In addition, the influence of the applied stress τ/μ is also very important. Besides, the influence of a/h is not evident for the first example.

Another feature of solution here is quite different from that in Sect. 7.6 due to the reason of difference of quasicrystalline systems.

This work is reported in Ref. [24].

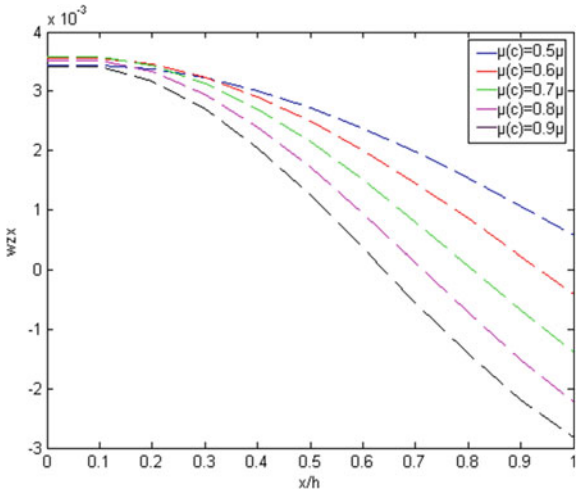

Fig. 9.5 Variation of w_{zx} versus x

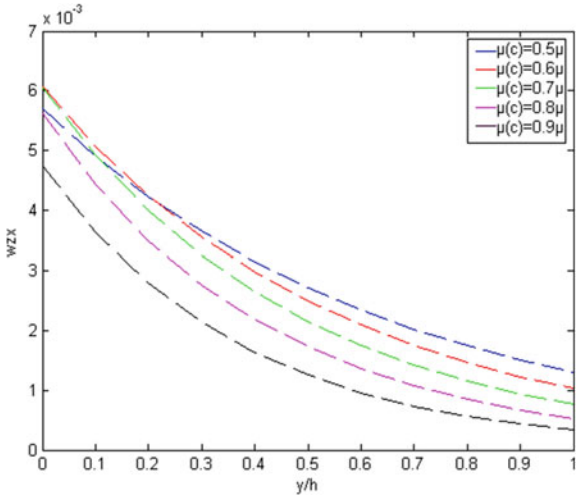

Fig. 9.6 Variation of w_{zx} versus y

9.3 Phonon-Phason Decoupled Plane Elasticity of Icosahedral Quasicrystals

Yang et al. [3] presented an approximate solution of a straight dislocation in icosahedral quasicrystals under assumptions

$$\frac{\partial}{\partial z} = 0 \tag{9.3.1}$$

and

$$R = 0 \tag{9.3.2}$$

The conditions (9.3.1) and (9.3.2) result a phonon-phason decoupled plane elasticity, which leads to

$$\varepsilon_{zz} = 0, \quad w_{zz} = w_{yz} = w_{xz} = 0 \tag{9.3.3}$$

Based on conditions (9.3.1) and (9.3.2), the final governing Eq. (9.1.8) reduces to

$$\begin{gathered}
\mu\nabla_1^2 u_x + (\lambda+\mu)\frac{\partial}{\partial x}\nabla_1 \cdot \mathbf{u_1} = 0 \\
\mu\nabla_1^2 u_y + (\lambda+\mu)\frac{\partial}{\partial y}\nabla_1 \cdot \mathbf{u_1} = 0 \\
\mu\nabla_1^2 u_z = 0 \\
K_1\nabla_1^2 w_x + K_2\left(\frac{\partial^2 w_z}{\partial x^2} - \frac{\partial^2 w_z}{\partial y^2}\right) = 0 \\
K_1\nabla_1^2 w_y - 2K_2\frac{\partial^2 w_z}{\partial x \partial y} = 0 \\
(K_1 - K_2)\nabla_1^2 w_z + K_2\left(\frac{\partial^2 w_x}{\partial x^2} - 2\frac{\partial^2 w_y}{\partial x \partial y} - \frac{\partial^2 w_y}{\partial y^2}\right) = 0
\end{gathered} \tag{9.3.4}$$

where

$$\nabla_1^2 = \frac{\partial^2}{\partial x^2} + \frac{\partial^2}{\partial y^2}, \quad \mathbf{u_1} = (u_x, u_y), \quad \nabla_1 \cdot \mathbf{u_1} = \frac{\partial u_x}{\partial x} + \frac{\partial u_y}{\partial y}$$

Because the phonons and phasons are decoupled, the first three equations of (9.3.4) are pure phonon equilibrium equations; in addition, u_z is independent from u_x and u_y, and the second three equations in (9.3.4) are pure phason equilibrium equations.

Yang et al. [3] solved the equations under the dislocation conditions

$$\int_\Gamma du_i = b_i^{\parallel}, \quad \int_\Gamma dw_i = b_i^{\perp} \tag{9.3.5}$$

where Γ represents a path enclosing the dislocation core. The authors used the Green function method to calculate. The results are

$$
\begin{aligned}
u_x &= \frac{b_1^{\parallel}}{2\pi}\left(\arctan\frac{y}{x}+\frac{\lambda+\mu}{\lambda+2\mu}\frac{xy}{r^2}\right)+\frac{b_2^{\parallel}}{2\pi}\left(\frac{\mu}{\lambda+2\mu}\ln\frac{r}{r_0}+\frac{\lambda+\mu}{\lambda+2\mu}\frac{x^2}{r^2}\right)\\
u_y &= -\frac{b_1^{\parallel}}{2\pi}\left(\frac{\mu}{\lambda+2\mu}\ln\frac{r}{r_0}+\frac{\lambda+\mu}{\lambda+2\mu}\frac{y^2}{r^2}\right)+\frac{b_2^{\parallel}}{2\pi}\left(\arctan\frac{y}{x}-\frac{\lambda+\mu}{\lambda+2\mu}\frac{xy}{r^2}\right)\\
u_z &= \frac{b_3^{\parallel}}{2\pi}\arctan\frac{y}{x}\\
w_x &= \frac{b_1^{\perp}}{2\pi}\left[\arctan\frac{y}{x}+\frac{K_2^2}{2K_5}\left(\frac{2xy^3}{r^4}-\frac{xy}{r^2}\right)\right]-\frac{b_2^{\perp}}{4\pi}\frac{K_2^2}{K_5}\left(\ln\frac{r}{r_0}+\frac{2x^2y^2}{r^4}\right)+\frac{b_3^{\perp}}{2\pi}\frac{K_2}{K_1}\frac{xy}{r^2}\\
w_y &= \frac{b_1^{\perp}}{4\pi}\frac{K_2^2}{K_5}\left(\ln\frac{r}{r_0}-\frac{2x^2y^2}{r^4}\right)+\frac{b_2^{\perp}}{2\pi}\left[\arctan\frac{y}{x}+\frac{K_2^2}{2K_5}\left(\frac{xy^3-x^3y}{r^4}\right)\right]-\frac{b_3^{\perp}}{2\pi}\frac{K_2}{K_1}\frac{y^2}{r^2}\\
w_z &= \frac{b_1^{\perp}}{2\pi}\frac{K_1K_2}{K_5}\frac{xy}{r^2}-\frac{b_2^{\perp}}{2\pi}\frac{K_1K_2}{K_5}\frac{y^2}{r^2}+\frac{b_3^{\perp}}{2\pi}\arctan\frac{y}{x}
\end{aligned}
\tag{9.3.6}
$$

in which

$$
r=\sqrt{x^2+y^2},\quad K_5=K_1^2-K_1K_2-K_2^2 \tag{9.3.7}
$$

The first three of (9.3.6) are well-known solutions of pure phonon field in classical theory of dislocation; the second three of (9.3.6) are new results for pure phason field. Due to lack of coupling terms, the interaction between phonons and phasons could not be revealed.

9.4 Phonon-Phason Coupled Plane Elasticity of Icosahedral Quasicrystals—Displacement Potential Formulation

In the previous section, Yang et al. [3] introduced the assumption (9.3.2), which is not valid and leads to loss a lot of information coming from phonon-phason coupling. In studies of Fan and Guo [4], Zhu and Fan [16] and Zhu et al. [17], they considered the coupling effects, i.e.

$$
R\neq 0
$$

and obtained the complete theory for the plane elasticity of quasicrystals. In the study, the assumption (9.2.1) or (9.3.1) still maintains, i.e.

$$\frac{\partial}{\partial z} = 0 \tag{9.4.1}$$

In this case, the three-dimensional elasticity can be reduced into a plane elasticity. From condition (9.3.1) directly, we have

$$\varepsilon_{zz} = w_{zz} = w_{xz} = w_{yz} = 0 \tag{9.4.2}$$

Thus the number of the field variables and field equations from 36 is reduced to 32. Though the reduction of the total number is not so much, the resulting equation system has been greatly simplified and with the following form

$$\begin{aligned}
&\mu\nabla_1^2 u_x + (\lambda+\mu)\frac{\partial}{\partial x}\nabla_1 \cdot \mathbf{u_1} + R\left(\frac{\partial^2 w_x}{\partial x^2} + 2\frac{\partial^2 w_y}{\partial x \partial y} - \frac{\partial^2 w_y}{\partial y^2}\right) = 0 \\
&\mu\nabla_1^2 u_y + (\lambda+\mu)\frac{\partial}{\partial y}\nabla_1 \cdot \mathbf{u_1} + R\left(\frac{\partial^2 w_y}{\partial x^2} - 2\frac{\partial^2 w_x}{\partial x \partial y} - \frac{\partial^2 w_y}{\partial y^2}\right) = 0 \\
&\mu\nabla_1^2 u_z + R\left(\frac{\partial^2 w_x}{\partial x^2} - 2\frac{\partial^2 w_y}{\partial x \partial y} - \frac{\partial^2 w_x}{\partial y^2} + \nabla_1^2 w_z\right) = 0 \\
&K_1\nabla_1^2 w_x + K_2\left(\frac{\partial^2 w_z}{\partial x^2} - \frac{\partial^2 w_z}{\partial y^2}\right) + R\left(\frac{\partial^2 u_x}{\partial x^2} - 2\frac{\partial^2 u_y}{\partial x \partial y} - \frac{\partial^2 u_x}{\partial y^2} + \frac{\partial^2 u_z}{\partial x^2} - \frac{\partial^2 u_z}{\partial y^2}\right) = 0 \\
&K_1\nabla_1^2 w_y - 2K_2\frac{\partial^2 w_z}{\partial x \partial y} + R\left(\frac{\partial^2 u_y}{\partial x^2} + 2\frac{\partial^2 u_x}{\partial x \partial y} - \frac{\partial^2 u_y}{\partial y^2} - 2\frac{\partial^2 u_z}{\partial x \partial y}\right) = 0 \\
&(K_1 - K_2)\nabla_1^2 w_z + K_2\left(\frac{\partial^2 w_x}{\partial x^2} - 2\frac{\partial^2 w_y}{\partial x \partial y} - \frac{\partial^2 w_y}{\partial y^2}\right) + R\nabla_1^2 u_z = 0
\end{aligned} \tag{9.4.3}$$

where ∇_1^2 and $\nabla_1 \cdot \mathbf{u_1}$ are the same of those in Sect. 9.3, but the suffix 1 of the two-dimensional Laplace operator will be omitted in the following for simplicity.

The equation set is much simpler than that of (9.1.8) but still quite complicated, too. If we introduce a displacement potential $F(x, y)$ such as

$$
\begin{aligned}
u_x &= R\frac{\partial^2}{\partial x\partial y}\nabla^2\nabla^2[\mu\alpha\Pi_1+\beta(\lambda+2\mu)\Pi_2]F \\
&\quad + c_0R\frac{\partial^2}{\partial x\partial y}\Lambda\left[(3\mu-\lambda)\frac{\partial^4}{\partial x^4}+10(\lambda+\mu)\frac{\partial^4}{\partial x^2\partial y^2}-(5\lambda+9\mu)\frac{\partial^4}{\partial y^4}\right]F \\
u_y &= R\nabla^2\nabla^2\left[\mu\alpha\frac{\partial^2}{\partial y^2}\Pi_1-\beta(\lambda+2\mu)\frac{\partial^2}{\partial x^2}\Pi_2\right]F \\
&\quad + c_0R\Lambda^2\left[(\lambda+2\mu)\frac{\partial^6}{\partial x^6}-5(2\lambda+3\mu)\frac{\partial^6}{\partial x^4\partial y^2}+5\lambda\frac{\partial^6}{\partial x^2\partial y^4}+\mu\frac{\partial^6}{\partial y^6}\right]F \\
u_z &= c_1\frac{\partial^2}{\partial x\partial y}\left[(\alpha-\beta)\Lambda^2\Pi_1\Pi_2+\alpha\frac{\partial^2}{\partial y^2}\Pi_1^2+\beta\frac{\partial^2}{\partial x^2}\Pi_2^2\right]F \\
w_x &= -\omega\frac{\partial^2}{\partial x\partial y}\nabla^2\left[2c_0\Lambda^2\nabla^2-(\alpha-\beta)\Pi_1\Pi_2\right]F \\
w_y &= -\omega\nabla^2\left[c_0\Lambda^2\Lambda^2\nabla^2+\alpha\frac{\partial^2}{\partial y^2}\Pi_1^2+\beta\frac{\partial^2}{\partial x^2}\Pi_2^2\right]F \\
w_z &= c_2\frac{\partial^2}{\partial x\partial y}\left[(\alpha-\beta)\Lambda^2\Pi_1\Pi_2+\alpha\frac{\partial^2}{\partial y^2}\Pi_1^2+\beta\frac{\partial^2}{\partial x^2}\Pi_2^2\right]F
\end{aligned}
\tag{9.4.4}
$$

then the field equations mentioned above will be satisfied if

$$
\nabla^2\nabla^2\nabla^2\nabla^2\nabla^2\nabla^2F(x,y)+\nabla^2LF(x,y)=0 \tag{9.4.5}
$$

where

$$
\begin{aligned}
&\alpha=(\lambda+2\mu)R^2-\omega K_1 \quad \beta=\mu R^2-\omega K_1 \quad \omega=\mu(\lambda+2\mu) \\
&c_0=\omega\frac{\mu K_2^2+(K_1-3K_2)R^2}{\mu(K_1-K_2)-R^2} \quad c_1=\frac{(K_1-2K_2)R\omega}{\mu(K_1-K_2)-R^2} \quad c_2=\frac{(K_2\mu-R^2)\omega}{\mu(K_1-K_2)-R^2} \\
&\Pi_1=3\frac{\partial^2}{\partial x^2}-\frac{\partial^2}{\partial y^2}, \quad \Pi_2=3\frac{\partial^2}{\partial y^2}-\frac{\partial^2}{\partial x^2}, \quad \nabla^2=\frac{\partial^2}{\partial x^2}+\frac{\partial^2}{\partial y^2}, \quad \Lambda^2=\frac{\partial^2}{\partial x^2}-\frac{\partial^2}{\partial y^2}
\end{aligned}
\tag{9.4.6}
$$

in which the suffix 1 of the two-dimensional Laplace operator is omitted and

$$
\begin{aligned}
L=\frac{c_0}{\beta}[&-\frac{\partial^{10}}{\partial x^{10}}+5\left(4-5\frac{\alpha}{\beta}\right)\frac{\partial^{10}}{\partial x^8\partial y^2}-10\left(11-10\frac{\alpha}{\beta}\right)\frac{\partial^{10}}{\partial x^6\partial y^4}+10\left(10-11\frac{\alpha}{\beta}\right)\frac{\partial^{10}}{\partial x^4\partial y^6} \\
&-5\left(5-4\frac{\alpha}{\beta}\right)\frac{\partial^{10}}{\partial x^2\partial y^8}-\frac{\alpha}{\beta}\frac{\partial^{10}}{\partial y^{10}}
\end{aligned}
\tag{9.4.7}
$$

Assuming

$$R^2/(\mu K_1) \ll 1, \tag{9.4.8}$$

(this is understandable, because the coupling effect is weaker than that of phonon), then from Eqs. (9.4.6) and (9.4.7)

$$\beta/\alpha \to 1, \quad \nabla^2 L = \frac{c_0}{\beta}\nabla^2\nabla^2\nabla^2\nabla^2\nabla^2\nabla^2 \tag{9.4.9}$$

substituting (9.4.9) into (9.4.5), we find that

$$\nabla^2\nabla^2\nabla^2\nabla^2\nabla^2\nabla^2 F(x,y) = 0 \tag{9.4.10}$$

This is our final governing equation for plane elasticity of quasicrystals based on the displacement potential formulation. With the aid of the generalized Hooke's law, the phonon and phason stress components can also be expressed in terms of potential function $F(x,y)$ and these expressions are omitted here due to the limitation of the space.

In other words, equation set (9.4.4) gives a fundamental solution in terms of $F(x,y)$ for the plane elasticity problem of an icosahedral quasicrystal. Once function $F(x,y)$ satisfying Eq. (9.4.10) is determined for prescribed boundary conditions, the entire elastic field of an icosahedral quasicrystal can be found from (9.4.4). This formulation is reported briefly by Fan and Guo [4] in some extent which is a development of Li and Fan [18] for elasticity of two-dimensional quasicrystals. The application of the formulation and relevant solution will be given in Sect. 9.6.

9.5 Phonon-Phason Coupled Plane Elasticity of Icosahedral Quasicrystals—Stress Potential Formulation

In the previous section, the displacement formulation exhibits its effect, which reduces a very complicated partial differential equation set into a single partial differential equation with higher order (12th order), and the latter will be easily to solve. At the meantime, the stress potential formulation is effective too. In this section, we will introduce the formulation.

To contrast the displacement potential formulation, we here maintain the stress components and exclude the displacement components. From the deformation geometry Eq. (9.1.1) and considering (9.3.1) and (9.3.2), we obtain the deformation compatibility equations as follows

$$\begin{aligned}
&\frac{\partial^2 \varepsilon_{xx}}{\partial y^2}+\frac{\partial^2 \varepsilon_{yy}}{\partial x^2}=2\frac{\partial^2 \varepsilon_{xy}}{\partial x \partial y}, \quad \frac{\partial \varepsilon_{yz}}{\partial x}=\frac{\partial \varepsilon_{zx}}{\partial y} \\
&\frac{\partial w_{xy}}{\partial x}=\frac{\partial w_{xx}}{\partial y}, \quad \frac{\partial w_{yy}}{\partial x}=\frac{\partial w_{yx}}{\partial y}, \quad \frac{\partial w_{zy}}{\partial x}=\frac{\partial w_{zx}}{\partial y}
\end{aligned} \tag{9.5.1}$$

Thus the displacements are excluded already.

By getting the expressions of strains through stresses from the inversion of equation set (9.1.7) and substituting them into (9.5.1), we obtain the deformation compatibility equations expressed by stress components, so that the strain components have been excluded up to now (those equations are too lengthy and we here do not list them).

So far one has the deformation compatibility equations expressed by stresses and equilibrium equations only.

If we introduce stress potential functions

$$\varphi_1(x,y), \quad \varphi_2(x,y), \quad \psi_1(x,y), \quad \psi_2(x,y), \quad \psi_3(x,y)$$

such as

$$\begin{aligned}
&\sigma_{xx}=\frac{\partial^2 \varphi_1}{\partial y^2}, \quad \sigma_{xy}=-\frac{\partial^2 \varphi_1}{\partial x \partial y}, \quad \sigma_{yy}=\frac{\partial^2 \varphi_1}{\partial x^2} \\
&\sigma_{zx}=\frac{\partial \varphi_2}{\partial y}, \quad \sigma_{zy}=-\frac{\partial \varphi_2}{\partial x} \\
&H_{xx}=\frac{\partial \psi_1}{\partial y}, \quad H_{xy}=-\frac{\partial \psi_1}{\partial x}, \quad H_{yx}=\frac{\partial \psi_2}{\partial y} \\
&H_{yy}=-\frac{\partial \psi_2}{\partial x}, \quad H_{zx}=\frac{\partial \psi_3}{\partial y}, \quad H_{zy}=-\frac{\partial \psi_3}{\partial x}
\end{aligned} \tag{9.5.2}$$

with

$$\begin{aligned}
\varphi_1 &= c_2 c_3 R \frac{\partial}{\partial y}\left[2\frac{\partial^2}{\partial x^2}\Pi_2-\Lambda^2\Pi_1\right]\nabla^2\nabla^2 G \\
\varphi_2 &= -c_3 c_4 \nabla^2\nabla^2\nabla^2\nabla^2\nabla^2 G \\
\psi_1 &= c_1 c_2 R \frac{\partial^2}{\partial y^2}\left[2\frac{\partial^2}{\partial x^2}\Pi_1\Pi_2-\Lambda^2\Pi_1^2\right]\nabla^2 G \\
&\quad + c_2 c_4 \Lambda^2 \nabla^2\nabla^2\nabla^2\nabla^2\nabla^2 G \\
\psi_2 &= c_1 c_2 R \frac{\partial^2}{\partial x \partial y}\left[2\frac{\partial^2}{\partial x^2}\Pi_2^2-\Lambda^2\Pi_1\Pi_2\right]\nabla^2 G \\
&\quad - 2c_2 c_4 \frac{\partial^2}{\partial x \partial y}\nabla^2\nabla^2\nabla^2\nabla^2\nabla^2 G \\
\psi_3 &= -\frac{1}{R}K_2 c_3 c_4 \nabla^2\nabla^2\nabla^2\nabla^2\nabla^2\nabla^2 G
\end{aligned} \tag{9.5.3}$$

then equilibrium equations and the deformation compatibility equations will be automatically satisfied if

$$\nabla^2\nabla^2\nabla^2\nabla^2\nabla^2\nabla^2\nabla^2 G = 0 \tag{9.5.4}$$

Under the approximation $R^2/K_1\mu \ll 1$, which is the final governing equation of plane elasticity of icosahedral quasicrystals, function $G(x, y)$ is named the stress potential in which

$$\begin{aligned} c_1 &= \frac{R(2K_2 - K_1)(\mu K_1 + \mu K_2 - 3R^2)}{2(\mu K_1 - 2R^2)} \\ c_2 &= \frac{1}{R}K_2(\mu K_2 - R^2) - R(2K_2 - K_1) \\ c_3 &= \mu(K_1 - K_2) - R^2 - \frac{(\mu K_2 - R^2)^2}{\mu K_1 - 2R^2} \\ c_4 &= c_1 R + \frac{1}{2}c_3\left(K_1 + \frac{\mu K_1 - 2R^2}{\lambda + \mu}\right) \end{aligned} \tag{9.5.5}$$

$$\Pi_1 = 3\frac{\partial^2}{\partial x^2} - \frac{\partial^2}{\partial y^2}, \quad \Pi_2 = 3\frac{\partial^2}{\partial y^2} - \frac{\partial^2}{\partial x^2}$$

$$\nabla^2 = \frac{\partial^2}{\partial x^2} + \frac{\partial^2}{\partial y^2}, \quad \Lambda^2 = \frac{\partial^2}{\partial x^2} - \frac{\partial^2}{\partial y^2}$$

In derivation of (9.5.4), the approximation (9.4.8) is used in the last step.

This work is given in Ref. [5], which may be seen as a development of the study for two-dimensional quasicrystals given by Guo and Fan (see, e.g. Fan [19] or Guo and Fan [20]).

9.6 A Straight Dislocation in an Icosahedral Quasicrystal

The formulations exhibited in the previous sections are meaningful, which have greatly simplified the complicated equations involving elasticity. Their applications will be addressed in this and subsequent sections, in which the Fourier analysis and complex variable function method play an important role.

We introduced the dislocation solution of Yang et al. [3] in an icosahedral quasicrystal. The authors of Ref. [3] assumed that the coupling effect between phonons and phasons is omitted, i.e. $R = 0$. In this case, the phonon solution of the dislocation is the same to that of the classical isotropic elastic solution of an edge dislocation. And the phason solution of the problem is newly found, which is independent from the phonon field. In this section, we try to give a complete

analysis of the problem in which the phonon-phason coupling effect is taken into account.

For a dislocation along x_3-axis (or z-axis) in icosahedral quasicrystal with the core at the origin, the Burgers vector is denoted as $b = b^{\parallel} \oplus b^{\perp} = (b_1^{\parallel}, b_2^{\parallel}, b_3^{\parallel}, b_1^{\perp}, b_2^{\perp}, b_3^{\perp})$ where the dislocation conditions are as

$$\int_{\Gamma} du_j = b_j^{\parallel} \quad \int_{\Gamma} dw_j = b_j^{\perp} \tag{9.6.1}$$

in which $x_1 = x, x_2 = y, x_3 = z$, and the integrals in (9.6.1) should be taken along the Burgers circuit surrounding the dislocation core in space $E_{\parallel}$. By using the superposition principle, we here calculate first the elastic field for a special case, i.e. which corresponds to $b_1^{\parallel} \neq 0, b_1^{\perp} \neq 0,$ and $b_2^{\parallel} = b_3^{\parallel} = 0, b_2^{\perp} = b_3^{\perp} = 0$.

For simplicity, we can solve a half-plane problem, by considering symmetry and anti-symmetry of relevant field variables, so the following boundary conditions include the dislocation condition:

$$\sigma_{yy}(x,0) = \sigma_{zy}(x,0) = 0 \tag{9.6.2a, b}$$

$$H_{yy}(x,0) = H_{zy}(x,0) = 0 \tag{9.6.2c, d}$$

$$\int_{\Gamma} du_x = b_1^{\parallel} \quad \int_{\Gamma} dw_x = b_1^{\perp} \tag{9.6.2e, f}$$

In addition, there are boundary conditions at infinity:

$$\sigma_{ij}(x,y) \to 0 \quad H_{ij}(x,y) \to 0 \quad \sqrt{x^2+y^2} \to \infty \tag{9.6.3}$$

In the following, we use the formulation of Sect. 9.4 to solve the above boundary value problem. Performing the Fourier transform to Eq. (9.4.10) and the above boundary conditions, we obtain the solution at the transformed domain, and then, taking inversion of the Fourier transform, we obtain the solution as follows

$$u_x = \frac{1}{2\pi}\left(b_1^{\parallel} \arctan\frac{y}{x} + c_{12}\frac{xy}{r^2} + c_{13}\frac{xy^3}{r^4}\right)$$

$$u_y = \frac{1}{2\pi}\left(-c_{21}\ln\frac{r}{r_0} + c_{22}\frac{y^2}{r^2} + c_{23}\frac{y^2(y^2-x^2)}{2r^4}\right)$$

$$u_z = \frac{1}{2\pi}\left(-c_{31}\arctan\frac{y}{x} + c_{32}\frac{xy}{r^2} + c_{33}\frac{xy^3}{r^4}\right)$$

$$w_x = \frac{1}{2\pi}\left(b_1^{\perp}\arctan\frac{y}{x} + c_{42}\frac{xy}{r^2} + c_{43}\frac{xy^3}{r^4}\right)$$

$$w_y = \frac{1}{2\pi}\left(-c_{51}\ln\frac{r}{r_0} + c_{52}\frac{y^2}{r^2} + c_{53}\frac{y^2(y^2-x^2)}{2r^4}\right) \tag{9.6.4}$$

$$w_z = \frac{1}{2\pi}\left(-c_{61}\arctan\frac{y}{x} + c_{62}\frac{xy}{r^2} + c_{63}\frac{xy^3}{r^4}\right)$$

in which $r^2 = x^2 + y^2$ and r_0, the radius of the dislocation core, and c_{ij} are constants shown as follows:

$$c_{12} = \frac{2c_0[\mu(2R^2 + c_0\mu)(\lambda^2 + 3\lambda\mu + 2\mu^2)b_1^{\parallel} + R[-e(\lambda+\mu) + 2\mu c_0(\lambda+2\mu)^2]b_1^{\perp}}{-e[2e + \mu c_0(\lambda+2\mu)] + \mu c_0(\lambda+2\mu)[e + 2\mu c_0(\lambda+2\mu)]}$$

$$c_{13} = \frac{2c_0R(\lambda+\mu)[2R\mu(\lambda+\mu)b_1^{\parallel} + 2\mu c_0(\lambda+2\mu)b_1^{\perp}]}{-e[2e + \mu c_0(\lambda+2\mu)] + \mu c_0(\lambda+2\mu)[e + 2\mu c_0(\lambda+2\mu)]}$$

$$c_{21} = \frac{[2c_0^2\mu^3(\lambda+2\mu) - 2e^2]b_1^{\parallel} + 2c_0R(\lambda+3\mu)eb_1^{\perp}}{-e[2e + \mu c_0(\lambda+2\mu)] + \mu c_0(\lambda+2\mu)[e + 2\mu c_0(\lambda+2\mu)]}$$

$$c_{22} = \frac{2c_0[-\mu^2(\lambda+\mu)(-2R^2 + c_0(\lambda+2\mu)]b_1^{\parallel} + R[-(\lambda+\mu)e + 2c_0\mu^2)b_1^{\perp}]}{-e[2e + \mu c_0(\lambda+2\mu)] + \mu c_0(\lambda+2\mu)[e + 2\mu c_0(\lambda+2\mu)]}$$

$$c_{23} = \frac{2c_0R(\lambda+\mu)[2R\mu(\lambda+\mu)b_1^{\parallel} + 2c_0\mu^2b_1^{\perp}]}{-e[2e + \mu c_0(\lambda+2\mu)] + \mu c_0(\lambda+2\mu)[e + 2\mu c_0(\lambda+2\mu)]}$$

$$c_{31} = \frac{-3c_1e\left\{\begin{array}{l} 2(c_0\mu + 7e)\mu c_0(\lambda+2\mu)b_1^{\parallel} + R[54c_0^2(\lambda^2 + 3\lambda\mu + \mu^2) \\ -2(\alpha-\beta)(e + \mu c_0(\lambda+2\mu))]b_1^{\perp} \end{array}\right\}}{4c_0R[-e(2e + \mu c_0(\lambda+2\mu)] + \mu c_0(\lambda+2\mu)[e + 2\mu c_0(\lambda+2\mu)]}$$

$$c_{32} = \frac{3c_1e\left\{2\mu[-e + \mu c_0(\lambda+2\mu)]b_1^{\parallel} + R[-2e + 2\mu c_0(\lambda+2\mu)]b_1^{\perp}\right\}}{-e[2e + \mu c_0(\lambda+2\mu)] + \mu c_0(\lambda+2\mu)[e + 2\mu c_0(\lambda+2\mu)]}$$

$$c_{33} = \frac{-3ec_1[2R\mu(\lambda+\mu)b_1^{\parallel} + 2\mu c_0(\lambda+2\mu)b_1^{\perp}]}{-e[2e + \mu c_0(\lambda+2\mu)] + \mu c_0(\lambda+2\mu)[e + 2\mu c_0(\lambda+2\mu)]}$$

$$c_{42} = \frac{-2e[2R\mu(\lambda+\mu)b_1^{\parallel} + 2\mu c_0(\lambda+2\mu)b_1^{\perp}]}{-e[2e + \mu c_0(\lambda+2\mu)] + \mu c_0(\lambda+2\mu)[e + 2\mu c_0(\lambda+2\mu)]}$$

$$c_{43} = 0$$

$$c_{51} = -\frac{\left\{\begin{array}{l} -4e\mu^2 c_0(\lambda+2\mu)b_1^{\parallel} + R[2(\lambda+2\mu)(e+0.5\mu c_0) \\ +\mu(2\beta^2\mu + 2c_0^2(\lambda+2\mu)^2 + c_0(\lambda+2\mu)(-\beta\mu + R^2(\lambda+\mu))]b_1^{\perp} \end{array}\right\}}{R(-e(2e+\mu c_0(\lambda+2\mu)) + \mu c_0(\lambda+2\mu)(e+2\mu c_0(\lambda+2\mu)))}$$

$$c_{52} = -\frac{2e[2R\mu(\lambda+\mu)b_1^{\parallel} + 2\mu c_0(\lambda+2\mu)b_1^{\perp}]}{-e[2e+\mu c_0(\lambda+2\mu)] + \mu c_0(\lambda+2\mu)[e+2\mu c_0(\lambda+2\mu)]} \tag{9.6.5}$$

$$c_{53} = 0$$

$$c_{61} = -\frac{3c_2 e\left\{\begin{array}{l} 2(c_0\mu+7e)\mu c_0(\lambda+2\mu)b_1^{\parallel} \\ +R[54c_0^2(\lambda^2+3\lambda\mu+\mu^2) - 2(\alpha-\beta)(e+\mu c_0(\lambda+2\mu))]b_1^{\perp} \end{array}\right\}}{4c_0R[-e(2e+\mu c_0(\lambda+2\mu)] + \mu c_0(\lambda+2\mu)[e+2\mu c_0(\lambda+2\mu)]}$$

$$c_{62} = \frac{3ec_2[2\mu(-e+\mu c_0(\lambda+2\mu))b_1^{\parallel} + R(-2e+2\mu c_0(\lambda+2\mu))b_1^{\perp}]}{-e[2e+\mu c_0(\lambda+2\mu)] + \mu c_0(\lambda+2\mu)[e+2\mu c_0(\lambda+2\mu)]}$$

$$c_{63} = \frac{-3ec_2[2R\mu(\lambda+\mu)b_1^{\parallel} + 2\mu c_0(\lambda+2\mu)b_1^{\perp}]}{-e[2e+\mu c_0(\lambda+2\mu)] + \mu c_0(\lambda+2\mu)[e+2\mu c_0(\lambda+2\mu)]}$$

with $e = -(\lambda+\mu)R^2$.

For the other two typical problems, in which the Burgers vector of a dislocation is denoted by $(0, b_2^{\parallel}, 0, 0, b_2^{\perp}, 0)$ and $(0, 0, b_3^{\parallel}, 0, 0, b_3^{\perp})$, respectively, a complete similar consideration will yield similar results, which are omitted here. Alternatively, the expressions are denoted as $u_j^{(2)}, w_j^{(2)}$ and $u_j^{(3)}, w_j^{(3)}$.

Analytic expressions for the elastic field of a dislocation $(b_1^{\parallel}, b_2^{\parallel}, b_3^{\parallel}, b_1^{\perp}, b_2^{\perp}, b_3^{\perp})$ in an icosahedral quasicrystal can be obtained by the superposition of the corresponding expressions for the elastic fields for $(b_1^{\parallel}, 0, 0, b_1^{\perp}, 0, 0)$, $(0, b_2^{\parallel}, 0, 0, b_2^{\perp}, 0)$ and $(0, 0, b_3^{\parallel}, 0, 0, b_3^{\perp})$, namely

$$u_j = u_j^{(1)} + u_j^{(2)} + u_j^{(3)} \quad w_j = w_j^{(1)} + w_j^{(2)} + w_j^{(3)} \quad i,j = 1,2,3 \tag{9.6.6}$$

We can see that the interaction between phonon-phonon, phason-phason and phonon-phason is very evident, so the solution (9.6.4) is quite different from the solution given by Yang et al. [3] [whose solution for phonon displacement field is given by the first three formulas of Eq. (9.3.6) and will be quoted again in the following (see formula (9.6.7))], where they took $R = 0$, i.e. they assumed the phonon and phason are decoupled, so the solution for phonon is the same as the classical solution for crystals. It is obvious that our solution given by (9.6.4) explores the realistic case for quasicrystals which is quite different from that of crystal. To illustrate the coupling effect, we give some numerical results in Figs. 9.7 and 9.8 for the normalized displacement $u_1/b_1^{\parallel}$ versus x and y, respectively, in

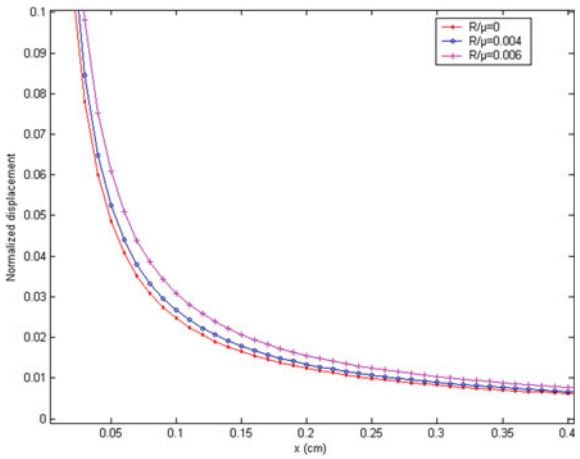

Fig. 9.7 The displacement $u_1/b_1^{\parallel}$ versus x for different coupling elastic constants

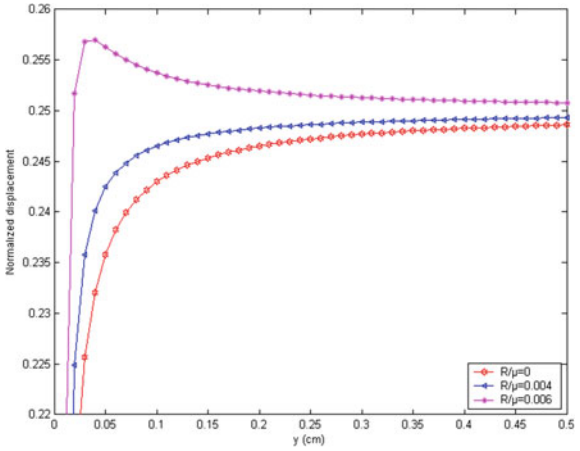

Fig. 9.8 The displacement $u_1/b_1^{\parallel}$ versus y for different coupling constants

which the results exhibit the influence of the coupling constant R that is significant. In the calculation, we take the data of elastic moduli as

$$\lambda = 74.9, \quad \mu = 72.4\,(\text{GPa}), \quad K_1 = 72, \quad K_2 = -73\,(\text{MPa})$$

and the phonon-phason coupling elastic constant for three different cases: i.e. $R/\mu = 0, R/\mu = 0.004$ and $R/\mu = 0.006$, in which the first one corresponds to decoupled case. The results are depicted in Fig. 9.7 for $u_1/b_1^{\parallel}$ versus x and in Fig. 9.8 for $u_1/b_1^{\parallel}$ versus y, respectively, as follows.

Figures show that the coupling effect is very important, and the displacement is increasing with the growth of value of R.

For icosahedral quasicrystals with the presence of a dislocation, there are five independent elastic constants. If $R = 0, w_i = 0$, our solution is exactly reduced to the solution of dislocation of crystals, i.e.

$$\begin{aligned} u_x &= \frac{b_1^{\parallel}}{2\pi}\left(\arctan\frac{y}{x} + \frac{\lambda+\mu}{\lambda+2\mu}\frac{xy}{r^2}\right) + \frac{b_2^{\parallel}}{2\pi}\left(\frac{\mu}{\lambda+2\mu}\ln\frac{r}{r_0} + \frac{\lambda+\mu}{\lambda+2\mu}\frac{x^2}{r^2}\right) \\ u_y &= -\frac{b_1^{\parallel}}{2\pi}\left(\frac{\mu}{\lambda+2\mu}\ln\frac{r}{r_0} + \frac{\lambda+\mu}{\lambda+2\mu}\frac{x^2}{r^2}\right) + \frac{b_2^{\parallel}}{2\pi}\left(\arctan\frac{y}{x} - \frac{\lambda+\mu}{\lambda+2\mu}\frac{xy}{r^2}\right) \\ u_z &= \frac{b_3^{\parallel}}{2\pi}\arctan\frac{y}{x} \end{aligned} \tag{9.6.7}$$

The present solution reveals the interactions between phonon-phonon, phason-phason and phonon-phason for a dislocation in icosahedral quasicrystals.

The displacement potential function formulation establishes the basis for solving defects in icosahedral quasicrystals. The formulation greatly simplifies the solution process. In the subsequent steps, a systematic Fourier analysis is developed, which provides a constructive procedure to find the analytic solution; it is effective not only for dislocation problem, but also for more complicated mixed boundary value problems (e.g. crack problems refer to the following section or Ref. [18]). The solution is explicit and with closed form. As a complete solution of dislocation of icosahedral quasicrystals, this is the first-time observation.

The present solution can be used as a fundamental solution for a dislocation in an icosahedral quasicrystal. Therefore, many elasticity problems in an icosahedral quasicrystal can be directly solved with the aid of this fundamental solution by superposition.

This work has been published in Ref. [17].

9.7 Application of Displacement Potential to Crack Problem of Icosahedral Quasicrystal

In the previous section, application of displacement potential to dislocation problem of icosahedral quasicrystal is given; we now discuss an application of the potential method to crack problem of the matter; with the help of the Fourier analysis and dual integral equation theory, an analytic solution is obtained, which is presented as below.

The cracked specimen is shown in Fig. 9.9; it is sufficient to consider a half of the sample, so it has the following boundary conditions:

$$\begin{array}{ll} \sigma_{yy}(x,0) = -p, \quad H_{yy}(x,0) = 0 & |x| \le a \\ u_y(x,0) = 0, \quad w_y(x,0) = 0 & |x| > a \\ \sigma_{xy}(x,0) = \sigma_{zy}(x,0) = 0, \quad H_{xy}(x,0) = H_{zy}(x,0) = 0 & -\infty < x < \infty \end{array} \tag{9.7.1}$$

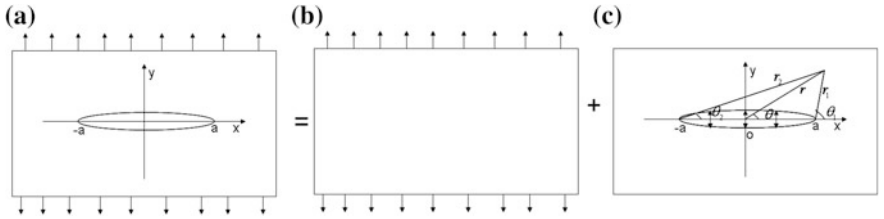

Fig. 9.9 A Griffith crack in an icosahedral quasicrystal

and

$$\sigma_{ij} \to 0, \quad H_{ij} \to 0 \quad \sqrt{x^2+y^2} \to \infty \tag{9.7.2}$$

After Fourier transform to Eq. (9.4.10), and by considering boundary condition at infinity, the formal solution in Fourier transform domain is

$$\tilde{F} = XYe^{-|\xi|y} \tag{9.7.3}$$

where $X = (A, B, C, D, E, F), Y = (1, y, y^2, y^3, y^4, y^5)^{\mathrm{T}}$, and A, B, C, D, E and F are unknown functions of ξ to be determined; superscript T denotes the transpose operator of matrix.

To determine unknown functions in (9.7.3), with the Fourier transforms of displacements and stresses and boundary conditions, the problem is reduced to solve the following dual integral equations

$$\begin{cases} \int_0^\infty \xi A_j \cos(\xi x)\mathrm{d}x = p\pi b_j & 0 < x \le a \\ \int_0^\infty A_j \cos(\xi x)\mathrm{d}x = 0 & x \ge a \end{cases} \tag{9.7.4}$$

where

$$A_1 = \xi^8 A, \quad A_2 = \left|\xi^7\right| B, \quad A_3 = 2\xi^6 C, \quad A_4 = 6\left|\xi^5\right| D, \quad A_5 = 24\xi^4 E, \quad A_6 = 120\left|\xi^3\right| F \tag{9.7.5}$$

$$b_j = (-1)^j \frac{\Delta_j}{\Delta} \quad j = 1, \ldots, 6 \tag{9.7.6}$$

$$\Delta = \begin{vmatrix} b_{11} & b_{12} & b_{13} & b_{14} & b_{15} & b_{16} \\ b_{21} & b_{22} & b_{23} & b_{24} & b_{25} & b_{26} \\ b_{31} & b_{32} & b_{33} & b_{34} & b_{35} & b_{36} \\ b_{41} & b_{42} & b_{43} & b_{44} & b_{45} & b_{46} \\ b_{51} & b_{52} & b_{53} & b_{54} & b_{55} & b_{56} \\ b_{61} & b_{62} & b_{63} & b_{64} & b_{65} & b_{66} \end{vmatrix}$$

$$\Delta_j = \begin{vmatrix} b_{21} & \cdots & b_{2,j-1} & b_{2,j+1} & \cdots & b_{26} \\ b_{31} & \cdots & b_{3,j-1} & b_{3,j+1} & \cdots & b_{36} \\ b_{41} & \cdots & b_{4,j-1} & b_{4,j+1} & \cdots & b_{46} \\ b_{51} & \cdots & b_{5,j-1} & b_{5,j+1} & \cdots & b_{56} \\ b_{61} & \cdots & b_{6,j-1} & b_{6,j+1} & \cdots & b_{66} \end{vmatrix} \tag{9.7.7}$$

b_{ij} are constants composed from basic elastic constants, given subsequently.

Equation (9.7.4) belongs to Titchmarsh–Busbridge dual integral equations; by using the standard solving procedure (refer to Major Appendix II of this book), we find the solution

$$A_j = ap\pi b_j J_1(\xi a)/\xi \tag{9.7.8}$$

where $J_1(x)$ is the first kind Bessel function of first order (see the Major Appendix). After the determination of these functions, the problem is solved mathematically, and then, taking inversion of Fourier transform, all field variables can be evaluated through a series of integrations. It is fortunate all integrals here can be expressed by elementary functions. We list only the displacements as below

$$\begin{aligned} u_x/p = {} & c_{11}[(r_1r_2)^{1/2}\cos\bar{\theta} - r\cos\theta] + c_{12}r^2(r_1r_2)^{-1/2}\sin\theta\sin(\theta-\bar{\theta}) + 1/2c_{13}r^2(r_1r_2)^{-3/2}a^2\sin^2\theta\cos 3\bar{\theta} \\ & - 1/2c_{14}r^4(r_1r_2)^{-5/2}a^2\sin^3\theta\sin(\theta-5\bar{\theta}) - 1/8c_{15}r^4(r_1r_2)^{-7/2}a^2\sin^4\theta h_{21} + 1/8c_{16}r^6(r_1r_2)^{-9/2}a^2\sin^5\theta h_{22} \end{aligned}$$

$$\begin{aligned} u_y/p = {} & c_{21}[(r_1r_2)^{1/2}\sin\bar{\theta} - r\sin\theta] + c_{22}r[1 - r(r_1r_2)^{-1/2}\cos(\theta-\bar{\theta})]\sin\theta - 1/2c_{23}r^2(r_1r_2)^{-3/2}a^2\sin^2\theta\sin 3\bar{\theta} \\ & + 1/2c_{24}r^4(r_1r_2)^{-5/2}a^2\sin^3\theta\cos(\theta-5\bar{\theta}) + 1/8c_{25}r^4(r_1r_2)^{-7/2}a^2\sin^4\theta h_{11} - 1/8c_{26}r^6(r_1r_2)^{-9/2}a^2\sin^5\theta h_{12} \end{aligned}$$

$$\begin{aligned} u_z/p = {} & c_{31}[(r_1r_2)^{1/2}\cos\bar{\theta} - r\cos\theta] + c_{32}r^2(r_1r_2)^{-1/2}\sin\theta\sin(\theta-\bar{\theta}) + 1/2c_{33}r^2(r_1r_2)^{-3/2}a^2\sin^2\theta\cos 3\bar{\theta} \\ & - 1/2c_{34}r^4(r_1r_2)^{-5/2}a^2\sin^3\theta\sin(\theta-5\bar{\theta}) - 1/8c_{35}r^4(r_1r_2)^{-7/2}a^2\sin^4\theta h_{21} + 1/8c_{36}r^6(r_1r_2)^{-9/2}a^2\sin^5\theta h_{22} \end{aligned}$$

$$\begin{aligned} w_x/p = {} & c_{41}[(r_1r_2)^{1/2}\cos\bar{\theta} - r\cos\theta] + c_{42}r^2(r_1r_2)^{-1/2}\sin\theta\sin(\theta-\bar{\theta}) + 1/2c_{43}r^2(r_1r_2)^{-3/2}a^2\sin^2\theta\cos 3\bar{\theta} \\ & - 1/2c_{44}r^4(r_1r_2)^{-5/2}a^2\sin^3\theta\sin(\theta-5\bar{\theta}) - 1/8c_{45}r^4(r_1r_2)^{-7/2}a^2\sin^4\theta h_{21} + 1/8c_{46}r^6(r_1r_2)^{-9/2}a^2\sin^5\theta h_{22} \end{aligned}$$

$$\begin{aligned} w_y/p = {} & c_{51}[(r_1r_2)^{1/2}\sin\bar{\theta} - r\sin\theta] + c_{52}r[1 - r(r_1r_2)^{-1/2}\cos(\theta-\bar{\theta})]\sin\theta - 1/2c_{53}r^2(r_1r_2)^{-3/2}a^2\sin^2\theta\sin 3\bar{\theta} \\ & + 1/2c_{54}r^4(r_1r_2)^{-5/2}a^2\sin^3\theta\cos(\theta-5\bar{\theta}) + 1/8c_{55}r^4(r_1r_2)^{-7/2}a^2\sin^4\theta h_{11} - 1/8c_{56}r^6(r_1r_2)^{-9/2}a^2\sin^5\theta h_{12} \end{aligned}$$

$$w_z/p = c_{61}[(r_1r_2)^{1/2}\cos\bar{\theta} - r\cos\theta] + c_{62}r^2(r_1r_2)^{-1/2}\sin\theta\sin(\theta-\bar{\theta}) + 1/2c_{63}r^2(r_1r_2)^{-3/2}a^2\sin^2\theta\cos 3\bar{\theta} - 1/2c_{64}r^4(r_1r_2)^{-5/2}a^2\sin^3\theta\sin(\theta-5\bar{\theta}) - 1/8c_{65}r^4(r_1r_2)^{-7/2}a^2\sin^4\theta h_{21} + 1/8c_{66}r^6(r_1r_2)^{-9/2}a^2\sin^5\theta h_{22} \tag{9.7.9}$$

where

$$h_{11} = a^2\sin 7\bar{\theta} - 4r^2\sin(2\theta - 7\bar{\theta}), \quad h_{12} = 3a^2\cos(\theta - 9\bar{\theta}) + 4r^2\cos(3\theta - 9\bar{\theta}),$$
$$h_{21} = a^2\cos 7\bar{\theta} + 4r^2\cos(2\theta - 7\bar{\theta}), \quad h_{22} = 3a^2\sin(\theta - 9\bar{\theta}) + 4r^2\sin(3\theta - 9\bar{\theta}) \tag{9.7.10}$$

with constants c_{ij}

$$c_{i1} = \sum_{j=1}^{6} a_{j1}b_j, \quad c_{i2} = \sum_{j=1}^{5} a_{j1}b_{j+1}, \quad c_{i3} = \sum_{j=1}^{4} a_{j1}b_{j+2}, \quad c_{i4} = \sum_{j=1}^{3} a_{j1}b_{j+3},$$
$$c_{i5} = \sum_{j=1}^{2} a_{j1}b_{j+4}, \quad c_{i6} = \sum_{j=1}^{1} a_{j1}b_{j+5}, \quad i = 1, 2, \ldots, 6 \tag{9.7.11}$$

$\theta = (\theta_1 + \theta_2)/2$, which are defined by Fig. 9.9c, and constants a_{ij} are listed below:

$a_{11} = R(2c_0(5\lambda + 9\mu) - \alpha\mu)$
$a_{12} = R(\alpha\mu - 2c_0(39\lambda + 67\alpha\mu))$
$a_{13} = 2R(-6\alpha\mu + 8\beta(\lambda + 2\mu) + c_0(111\lambda + 179\mu))$
$a_{14} = -2R(157c_0\lambda + 28\beta\lambda + 249c_0\mu - 16\alpha\mu + 56\beta\mu)$
$a_{15} = 5R(-7\alpha\mu + 16\beta(\lambda + 2\mu) + c_0(50\lambda + 82\mu))$
$a_{16} = R(21\alpha\mu - 58\beta(\lambda + 2\mu) - 8c_0(15\lambda + 26\mu))$
$a_{21} = c_0R(32\lambda + 27\mu)$
$a_{22} = -14c_0R(8\lambda + 5\mu)$
$a_{23} = R(c_0(176\lambda + 59\mu) + 16(\beta\lambda - \alpha\mu + 2\beta\mu))$
$a_{24} = -8(c_0(20\lambda - 2\mu) - 7\alpha\mu + 5\beta(\lambda + 2\mu))$
$a_{25} = 10R(c_0(9\lambda - 7\mu) + 4(-2\alpha\mu + \beta(\lambda + 2\mu)))$
$a_{26} = R(62\alpha\mu - 18\beta(\lambda + 2\mu) + c_0(-30\lambda + 62\mu))$
$a_{31} = 2c_1(24\alpha - 5\beta)$
$a_{32} = c_1(-192\alpha + 78\beta)$
$a_{33} = c_1(340\alpha - 226\beta)$
$a_{34} = c_1(-352\alpha + 306\beta)$
$a_{35} = 5c_1(47\alpha - 43\beta)$
$a_{36} = c_1(-103\alpha + 85\beta)$

$a_{41} = 0$
$a_{43} = -16\omega c_0$
$a_{43} = -16\omega c_0$
$a_{44} = -24\omega(2c_0 - \alpha + \beta)$
$a_{45} = 60\omega(c_0 - \alpha + \beta)$
$a_{46} = -2\omega(20c_0 - 27(\alpha - \beta))$
$a_{51} = 0$
$a_{52} = 32\omega(\alpha - \beta)$
$a_{53} = -16\omega(c_0 + 7\alpha - 7\beta)$
$a_{54} = 24\omega(2c_0 + 7\alpha - 7\beta)$
$a_{55} = -4\omega(17c_0 + 37\alpha - 33\beta)$
$a_{56} = 2\omega(28c_0 + 43\alpha - 27\beta)$
$a_{61} = 2c_2(24\alpha - 5\beta)$
$a_{62} = c_2(-192\alpha + 78\beta)$
$a_{63} = c_2(340\alpha - 226\beta)$
$a_{64} = c_2(-352\alpha + 306\beta)$
$a_{65} = 5c_2(47\alpha - 43\beta)$
$a_{66} = c_2(-103\alpha + 85\beta)$

$$
\begin{aligned}
a_{11} &= R(2c_0(5\lambda+9\mu)-\alpha\mu) & a_{41} &= 0\\
a_{12} &= R(\alpha\mu-2c_0(39\lambda+67\alpha\mu)) & a_{43} &= -16\omega c_0\\
a_{13} &= 2R(-6\alpha\mu+8\beta(\lambda+2\mu)+c_0(111\lambda+179\mu)) & a_{43} &= -16\omega c_0\\
a_{14} &= -2R(157c_0\lambda+28\beta\lambda+249c_0\mu-16\alpha\mu+56\beta\mu) & a_{44} &= -24\omega(2c_0-\alpha+\beta)\\
a_{15} &= 5R(-7\alpha\mu+16\beta(\lambda+2\mu)+c_0(50\lambda+82\mu)) & a_{45} &= 60\omega(c_0-\alpha+\beta)\\
a_{16} &= R(21\alpha\mu-58\beta(\lambda+2\mu)-8c_0(15\lambda+26\mu)) & a_{46} &= -2\omega(20c_0-27(\alpha-\beta))\\
a_{21} &= c_0R(32\lambda+27\mu) & a_{51} &= 0\\
a_{22} &= -14c_0R(8\lambda+5\mu) & a_{52} &= 32\omega(\alpha-\beta)\\
a_{23} &= R(c_0(176\lambda+59\mu)+16(\beta\lambda-\alpha\mu+2\beta\mu)) & a_{53} &= -16\omega(c_0+7\alpha-7\beta)\\
a_{24} &= -8(c_0(20\lambda-2\mu)-7\alpha\mu+5\beta(\lambda+2\mu)) & a_{54} &= 24\omega(2c_0+7\alpha-7\beta)\\
a_{25} &= 10R(c_0(9\lambda-7\mu)+4(-2\alpha\mu+\beta(\lambda+2\mu))) & a_{55} &= -4\omega(17c_0+37\alpha-33\beta)\\
a_{26} &= R(62\alpha\mu-18\beta(\lambda+2\mu)+c_0(-30\lambda+62\mu)) & a_{56} &= 2\omega(28c_0+43\alpha-27\beta)\\
a_{31} &= 2c_1(24\alpha-5\beta) & a_{61} &= 2c_2(24\alpha-5\beta)\\
a_{32} &= c_1(-192\alpha+78\beta) & a_{62} &= c_2(-192\alpha+78\beta)\\
a_{33} &= c_1(340\alpha-226\beta) & a_{63} &= c_2(340\alpha-226\beta)\\
a_{34} &= c_1(-352\alpha+306\beta) & a_{64} &= c_2(-352\alpha+306\beta)\\
a_{35} &= 5c_1(47\alpha-43\beta) & a_{65} &= 5c_2(47\alpha-43\beta)\\
a_{36} &= c_1(-103\alpha+85\beta) & a_{66} &= c_2(-103\alpha+85\beta)
\end{aligned}
$$

$$
\begin{aligned}
a_{11} &= R(2c_0(5\lambda+9\mu)-\alpha\mu) & a_{41} &= 0\\
a_{12} &= R(\alpha\mu-2c_0(39\lambda+67\alpha\mu)) & a_{43} &= -16\omega c_0\\
a_{13} &= 2R(-6\alpha\mu+8\beta(\lambda+2\mu)+c_0(111\lambda+179\mu)) & a_{43} &= -16\omega c_0\\
a_{14} &= -2R(157c_0\lambda+28\beta\lambda+249c_0\mu-16\alpha\mu+56\beta\mu) & a_{44} &= -24\omega(2c_0-\alpha+\beta)\\
a_{15} &= 5R(-7\alpha\mu+16\beta(\lambda+2\mu)+c_0(50\lambda+82\mu)) & a_{45} &= 60\omega(c_0-\alpha+\beta)\\
a_{16} &= R(21\alpha\mu-58\beta(\lambda+2\mu)-8c_0(15\lambda+26\mu)) & a_{46} &= -2\omega(20c_0-27(\alpha-\beta))\\
a_{21} &= c_0R(32\lambda+27\mu) & a_{51} &= 0\\
a_{22} &= -14c_0R(8\lambda+5\mu) & a_{52} &= 32\omega(\alpha-\beta)\\
a_{23} &= R(c_0(176\lambda+59\mu)+16(\beta\lambda-\alpha\mu+2\beta\mu)) & a_{53} &= -16\omega(c_0+7\alpha-7\beta)\\
a_{24} &= -8(c_0(20\lambda-2\mu)-7\alpha\mu+5\beta(\lambda+2\mu)) & a_{54} &= 24\omega(2c_0+7\alpha-7\beta)\\
a_{25} &= 10R(c_0(9\lambda-7\mu)+4(-2\alpha\mu+\beta(\lambda+2\mu))) & a_{55} &= -4\omega(17c_0+37\alpha-33\beta)\\
a_{26} &= R(62\alpha\mu-18\beta(\lambda+2\mu)+c_0(-30\lambda+62\mu)) & a_{56} &= 2\omega(28c_0+43\alpha-27\beta)\\
a_{31} &= 2c_1(24\alpha-5\beta) & a_{61} &= 2c_2(24\alpha-5\beta)\\
a_{32} &= c_1(-192\alpha+78\beta) & a_{62} &= c_2(-192\alpha+78\beta)\\
a_{33} &= c_1(340\alpha-226\beta) & a_{63} &= c_2(340\alpha-226\beta)\\
a_{34} &= c_1(-352\alpha+306\beta) & a_{64} &= c_2(-352\alpha+306\beta)\\
a_{35} &= 5c_1(47\alpha-43\beta) & a_{65} &= 5c_2(47\alpha-43\beta)\\
a_{36} &= c_1(-103\alpha+85\beta) & a_{66} &= c_2(-103\alpha+85\beta)
\end{aligned}
$$

(9.7.12)

Besides, b_j are defined by matrix calculation:

$$b_j = (-1)^j \frac{\Delta_j}{\Delta} \quad j = 1, \ldots, 6 \tag{9.7.13}$$

$$\Delta = \begin{vmatrix} b_{11} & b_{12} & b_{13} & b_{14} & b_{15} & b_{16} \\ b_{21} & b_{22} & b_{23} & b_{24} & b_{25} & b_{26} \\ b_{31} & b_{32} & b_{33} & b_{34} & b_{35} & b_{36} \\ b_{41} & b_{42} & b_{43} & b_{44} & b_{45} & b_{46} \\ b_{51} & b_{52} & b_{53} & b_{54} & b_{55} & b_{56} \\ b_{61} & b_{62} & b_{63} & b_{64} & b_{65} & b_{66} \end{vmatrix}$$

$$\Delta_j = \begin{vmatrix} b_{21} & \cdots & b_{2,j-1} & b_{2,j+1} & \cdots & b_{26} \\ b_{31} & \cdots & b_{3,j-1} & b_{3,j+1} & \cdots & b_{36} \\ b_{41} & \cdots & b_{4,j-1} & b_{4,j+1} & \cdots & b_{46} \\ b_{51} & \cdots & b_{5,j-1} & b_{5,j+1} & \cdots & b_{56} \\ b_{61} & \cdots & b_{6,j-1} & b_{6,j+1} & \cdots & b_{66} \end{vmatrix} \tag{9.7.14}$$

with matrix elements b_{ij}

$$\begin{aligned}
b_{11} &= -R(\alpha\lambda\mu + c_0(22\lambda^2 + 73\lambda\mu + 54\mu^2)) \\
b_{12} &= R(32\omega(\alpha-\beta) + \alpha\lambda\mu + c_0(66\lambda^2 + 215\lambda\mu + 194\mu^2)) \\
b_{13} &= -R(c_0(32\omega + 66\lambda^2 + 347\lambda\mu + 258\mu^2) + 4(36\omega(\alpha-\beta) + \mu(8\beta(\lambda+2\mu) - \alpha(\lambda+8\mu)))) \\
b_{14} &= R(c_0(112\omega + 22\lambda^2 + 217\lambda\mu + 86\mu^2) + 8(32\omega(\alpha-\beta) + \mu(14\beta(\lambda+2\mu) - \alpha(5\lambda+18\mu)))) \\
b_{15} &= R(-4c_0(44\omega + (\lambda - 43\mu)\mu) + 16\omega(16\beta - 15\alpha) + \mu(-160\beta(\lambda+2\mu) + \alpha(101\lambda + 272\mu))) \\
b_{16} &= R(4c_0(41\omega - (25\lambda + 66\mu)\mu) - 12\omega(11\beta - 15\alpha) + \mu(116\beta(\lambda+2\mu) - \alpha(121\lambda + 284\mu)))
\end{aligned}$$

$$\begin{aligned}
b_{21} &= 2(c_2K_2 + c_1R)(24\alpha - 5\beta) + R^2(-c_0(21\lambda + 8\mu) + \beta(\lambda + 2\mu) - 2\alpha\mu) \\
b_{22} &= (c_2K_2 - c_1R)(-288\alpha + 98\beta) + R^2(c_0(109\lambda - 10\mu) - \beta(\lambda + 2\mu) + 14\alpha\mu) \\
b_{23} &= 4(c_2K_2 + c_1R)(193\alpha - 98\beta) - 54\alpha\mu R^2 - c_0(16K_1\omega + R^2(220\lambda - 239\mu)) \\
b_{24} &= 2(-(c_2K_2 - c_1R)(612\alpha - 418\beta) - 12K_1\omega(\alpha - \beta) + 59\alpha\mu R^2) \\
&\quad + 5c_0(16K_1\omega + R^2(44\lambda - 157\mu)) \\
b_{25} &= (c_2K_2 - c_1R)(1279\alpha - 1053\beta) + 108K_1\omega(\alpha - \beta) - 145\alpha\mu R^2 \\
&\quad + c_0(-172K_1\omega - 5R^2(22\lambda - 216\mu)) \\
b_{26} &= -(c_2K_2 - c_1R)(925\alpha - 821\beta) - 198K_1\omega(\alpha - \beta) + 99\alpha\mu R^2 \\
&\quad + c_0(208K_1\omega + R^2(22\lambda - 1325\mu))
\end{aligned}$$

$$\begin{aligned}
b_{31} &= -2(c_2(K_1 - K_2) + c_1R)(24\alpha - 5\beta) + RK_2(c_0(42\lambda + 45\mu) - \alpha\mu) \\
b_{32} &= 2(c_2(K_1 - K_2) + c_1R)(144\alpha - 49\beta) - RK_2(c_0(242\lambda + 267\mu) - 3\alpha\mu) \\
b_{33} &= -4(c_2(K_1 - K_2) + c_1R)(193\alpha - 98\beta) + RK_2(c_0(676\lambda + 773\mu) - 31\alpha\mu + 32\beta(\lambda + 2\mu) \\
b_{34} &= 4(c_2(K_1 - K_2) + c_1R)(306\alpha - 209\beta) - RK_2(c_0(1172\lambda + 1391\mu) - 129\alpha\mu + 144\beta(\lambda + 2\mu) \\
b_{35} &= -(c_2(K_1 - K_2) + c_1R)(1279\alpha - 1053\beta) + RK_2(2c_0(675\lambda + 839\mu) - 247\alpha\mu + 288\beta(\lambda + 2\mu) \\
b_{36} &= (c_2(K_1 - K_2) + c_1R)(925\alpha - 821\beta) + RK_2(34c_0(31\lambda + 41\mu) - 265\alpha\mu + 332\beta(\lambda + 2\mu)
\end{aligned}$$

$$
\begin{aligned}
b_{41} &= -2(c_2R + c_1\mu)(24\alpha - 5\beta)\\
b_{42} &= -4((c_2R + c_1\mu)(96\alpha - 39\beta) + R\omega(20\alpha - 16\beta + 2c_0))\\
b_{43} &= -4(19(c_2R + c_1\mu)(7\alpha - 4\beta) + 28R\omega(\alpha - \beta))\\
b_{44} &= 4((c_2R + c_1\mu)(61\alpha - 49\beta) - R\omega(64\alpha - 36\beta - 24c_0))\\
b_{45} &= (c_2R + c_1\mu)(587\alpha - 521\beta) - R\omega(232\alpha - 216\beta - 40c_0)\\
b_{46} &= (c_2R + c_1\mu)(338\alpha - 300\beta) + R\omega(200\alpha - 168\beta - 44c_0)
\end{aligned}
$$

$$
\begin{aligned}
b_{51} &= R\mu(-c_0(42\lambda + 45\mu) + \alpha\mu)\\
b_{52} &= -2R(-4\omega(7\alpha - 5\beta) + \mu(11\alpha\mu - 4\beta(\lambda + 2\mu)) + c_0(4\omega + \mu(76\lambda + 93\mu)))\\
b_{53} &= R(112\omega(\alpha - \beta) + \mu(29\alpha\mu - 32\beta(\lambda + 2\mu)) + c_0(32\omega - \mu(476\lambda + 551\mu)))\\
b_{54} &= 4R(-\omega(92\alpha - 120\beta) + \mu(31\alpha\mu - 56\beta(\lambda + 2\mu)) + 2c_0(28\omega + \mu(17\lambda - 7\mu)))\\
b_{55} &= R(16\omega(4\alpha - 3\beta) + \mu(147\alpha\mu - 176\beta(\lambda + 2\mu)) + 2c_0(88\omega - \mu(327\lambda + 419\mu)))\\
b_{56} &= 2R(2\omega(7\alpha - 15\beta) - \mu(59\alpha\mu - 78\beta(\lambda + 2\mu)) - c_0(78\omega - \mu(200\lambda + 278\mu)))
\end{aligned}
$$

$$
\begin{aligned}
b_{61} &= -2(c_2K_2 + c_1R)(24\alpha - 5\beta) - \omega(\alpha + c_0)(K_1 + R) + Rc_0(42\lambda + 46\mu)\\
b_{62} &= 6(c_2K_2 + c_1R)(32\alpha - 13\beta) + \omega(9R\alpha - 23K_1\alpha + 32K_1\beta) - 8R^2\alpha\mu\\
&\quad + 3c_0(3K_1\omega + R(3\omega - 74R\lambda - 80R\mu))\\
b_{63} &= -2(c_2K_2 + c_1R)(170\alpha - 113\beta) + \omega(-36R\alpha + 108K_1\alpha + 144K_1\beta)\\
&\quad + 8R^2(\alpha\mu + \beta\lambda) + c_0(-20K_1\omega + R(-36\omega + 510R\lambda + 523R\mu))\\
b_{64} &= 2(c_2K_2 + c_1R)(176\alpha - 153\beta) + 2\omega(42R\alpha - 98K_1\alpha + 140K_1\beta)\\
&\quad + 4R^2(5\alpha\mu - 56\beta\lambda - 112\beta\mu) + c_0(20K_1\omega + R(84\omega - 650R\lambda - 625R\mu))\\
b_{65} &= -5(c_2K_2 + c_1R)(47\alpha - 43\beta) + 2\omega(-63R\alpha + 95K_1\alpha + 150K_1\beta)\\
&\quad + 5R^2(-9\alpha\mu + 32\beta\lambda + 64\beta\mu) - 2c_0(5K_1\omega + R(63\omega - 25R(10\lambda + 9\mu)))\\
b_{66} &= (c_2K_2 + c_1R)(103\alpha - 85\beta) + 6\omega(21R\alpha - 18K_1\alpha + 31K_1\beta)\\
&\quad + R^2(37\alpha\mu - 116\beta\lambda - 232\beta\mu) + 2c_0(K_1\omega + R(63\omega - 120R\lambda - 101R\mu))
\end{aligned}
\tag{9.7.15}
$$

With these data, any information concerning field variables in any point can be found.

In the practical applications, people are interested in the stress field near crack tip, i.e. the zone $r_1/a \ll 1$. Therefore, we consider the normal phonon stress around right crack tip, for example. In the obtained results, maintaining the term $(r_1/a)^{-1/2}$ in stress expressions is sufficient, and the others are higher small quantities. According to the definition, in the phonon stress intensity factor of Mode I, we find that

$$
K_{\mathrm{I}}^{\parallel} = \lim_{x \to a^+} \{[2\pi(x - a)]^{1/2}\sigma_{yy}(x, 0)\} = \sqrt{\pi a}p \tag{9.7.16}
$$

This is identical to that of conventional structural materials.

A more important quantity is crack energy release rate, which is correlated with not only stress field but also displacement field. Near the crack tip

$$u_y(y,0) = \begin{cases} pM\sqrt{a^2 - x^2} & |x| \le a \\ 0 & |x| > a \end{cases} \tag{9.7.17}$$

$$\sigma_{yy}(x,0) = \begin{cases} -p & |x| \le a \\ p\left(\frac{|x|}{\sqrt{x^2 - a^2}} - 1\right) & |x| > a \end{cases} \tag{9.7.18}$$

where

$$M = \sum_{j=1}^{6} a_{2j} b_j \tag{9.7.19}$$

a_{2j} see (9.7.12), b_j refer to (9.7.13).

The crack strain energy and energy release rate are as follows, respectively,

$$W = 2\int_0^a \sigma_{yy}(x,0) u_y(x,0) \mathrm{d}x = M\pi a^2 p^2/2 \tag{9.7.20}$$

$$G_I = \frac{1}{2}\frac{\partial W}{\partial a} = M(K_{\mathrm{I}}^{\|})^2/2$$

which is shown in Fig. 9.10. In addition, the crack opening displamentdisplacement is depicted in Fig. 9.11.

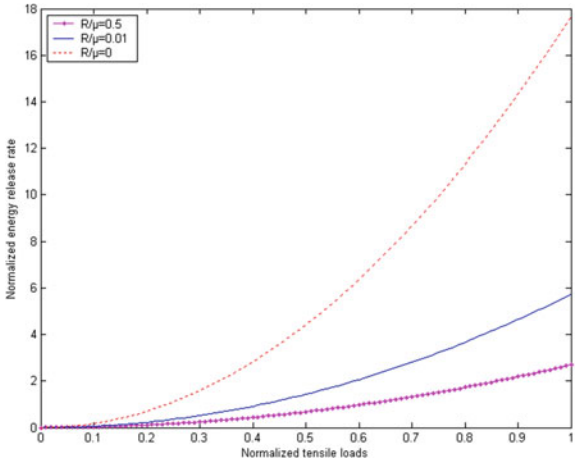

Fig. 9.10 Crack energy release rate versus applied stress, effect of coupling between phonons and phasons

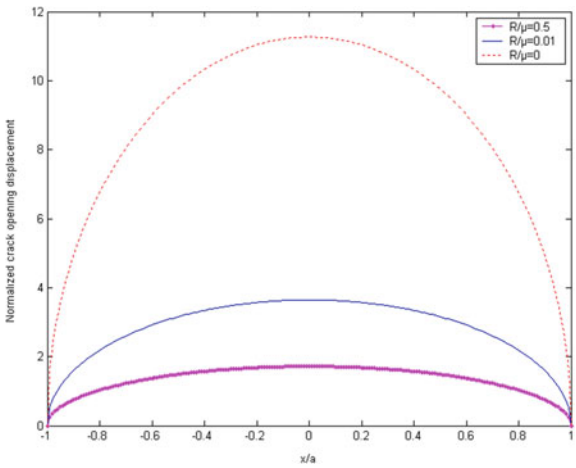

Fig. 9.11 Crack opening displacement and influence due to phonon-phason coupling

9.8 An Elliptic Notch/Griffith Crack in an Icosahedral Quasicrystal

The notch problem for icosahedral quasicrystals has no solution before 2006, the difficulty lies in which cannot be solved by the Fourier transform method. We must develop other methods, in which the complex variable function-conformal mapping method has particular effect, and some analytic solutions are constructed by the method. The results are given by Ref. [21], which may be seen as a development of the same authors in Ref. [22].

In the present section, we consider an icosahedral quasicrystal with an elliptic notch along the z-axis. On the basis of the general solution introduced in Sect. 9.5, explicit expressions of stress and displacement components of phonon and phason fields in the quasicrystals are given. With the help of conformal mapping, analytic solution for elliptic notch problem of the quasicrystals is presented. The solution of the Griffith crack problem can be observed as a special case of the results, which will be reduced to the well-known results in a conventional material if the phason field is absent. The stress intensity factor and energy of release rate are also obtained.

9.8.1 The Complex Representation of Stresses and Displacements

The solution of (9.5.4) can be expressed as

$$G(x,y) = \mathrm{Re}[g_1(z) + \bar{z}g_2(z) + \bar{z}^2 g_3(z) + \bar{z}^3 g_4(z) + \bar{z}^4 g_5(z) + \bar{z}^5 g_6(z)] \qquad (9.8.1)$$

where $g_i(z)$ are arbitrary analytic functions of $z = x+iy$, and the bar over complex variable or complex function denotes the complex conjugate.

By Eqs. (9.5.2)–(9.5.4) and (9.8.1), the stresses can be expressed as follows

$$\begin{gathered}
\sigma_{xx}+\sigma_{yy}=48c_2c_3R\mathrm{Im}\Gamma'(z)\quad \sigma_{yy}-\sigma_{xx}+2i\sigma_{xy}=8ic_2c_3R(12\overline{\Psi'(z)}-\Omega'(z))\\
\sigma_{zy}-i\sigma_{zx}=-960c_3c_4f_6'(z)\quad \sigma_{zz}=\frac{24\lambda R}{(\mu+\lambda)}c_2c_3\mathrm{Im}\Gamma'(z)\\
H_{xy}-H_{yx}-i(H_{xx}+H_{yy})=-96c_2c_5\overline{\Psi'(z)}-8c_1c_2R\Omega'(z)\\
H_{yx}-H_{xy}+i(H_{xx}-H_{yy})=-480c_2c_5\overline{f_6'(z)}-4c_1c_2R\Theta'(z)\\
H_{yz}+iH_{xz}=48c_2c_6\Gamma'(z)-4c_2R^2(2K_2-K_1)\overline{\Omega'(z)}\\
H_{zz}=\frac{24R^2}{(\mu+\lambda)}c_2c_3\mathrm{Im}\Gamma'(z)
\end{gathered}\tag{9.8.2}$$

where

$$\begin{aligned}
c_1&=\frac{R(2K_2-K_1)(\mu K_1+\mu K_2-3R^2)}{2(\mu K_1-2R^2)}\\
c_2&=\frac{1}{R}K_2(\mu K_2-R^2)-R(2K_2-K_1)\\
c_3&=\mu(K_1-K_2)-R^2-\frac{(\mu K_2-R^2)^2}{\mu K_1-2R^2}\\
c_4&=c_1R+\frac{1}{2}c_3\left(K_1+\frac{\mu K_1-2R^2}{\lambda+\mu}\right)
\end{aligned}$$

and

$$\begin{aligned}
&\Psi(z)=f_5(z)+5\bar{z}f_6'(z)\\
&\Gamma(z)=f_4(z)+4\bar{z}f_5'(z)+10\bar{z}^2f_6''(z)\\
&\Omega(z)=f_3(z)+3\bar{z}f_4'(z)+6\bar{z}^2f_5''(z)+10\bar{z}^3f_6'''(z)\\
&\Theta(z)=f_2(z)+2\bar{z}f_3'(z)+3\bar{z}^2f_4''(z)+4\bar{z}^3f_5'''(z)+5\bar{z}^4f_6^{(IV)}(z)\\
&c_5=2c_4-c_1R,\quad c_6=(2K_2-K_1)R^2-4c_4\frac{\mu K_2-R^2}{\mu K_1-2R^2}
\end{aligned}\tag{9.8.3}$$

In the above expressions, the function $g_1(z)$ does not appear; this implies that for stress boundary value problem in this formalism, only five complex potentials $g_2(z), g_3(z), g_4(z), g_5(z)$ and $g_6(z)$ are needed and can take $g_1(z) = 0$. For simplicity, we have introduced the following new symbols

$$\begin{aligned} &g_2^{(9)}(z) = f_2(z), \quad g_3^{(8)}(z) = f_3(z), \quad g_4^{(7)}(z) = f_4(z), \\ &g_5^{(6)}(z) = f_5(z), \quad g_6^{(5)}(z) = f_6(z) \end{aligned} \tag{9.8.4}$$

where $g_i^{(n)}$ denotes the nth differentiation with the argument z, accordingly $f_1(z) = 0$. Similar to the formalism in Chap. 8, the complex representations of displacement components can be written as follows (here we have omitted the rigid body displacements)

$$\begin{aligned} &u_y + iu_x = -6c_2R\left(\frac{2c_3}{\mu+\lambda} + c_7\right) - 2c_2c_7R\Omega(z) \\ &u_z = \frac{4}{\mu(K_1+K_2) - 3R^2}(240c_{10}\mathrm{Im}f_6(z)) + c_1c_2R^2\mathrm{Im}(\Theta(z) - 2\Omega(z) + 6\Gamma(z) - 24\Psi(z))) \\ &w_y + iw_x = -\frac{R}{c_1(\mu K_1 - 2R^2)}(24c_9\overline{\Psi(z)} - c_8\Theta(z)) \\ &w_z = \frac{4(\mu K_2 - R^2)}{(K_1 - 2K_2)R(\mu(K_1+K_2) - 3R^2)}(240c_{10}\mathrm{Im}f_6(z)) + c_1c_2R^2\mathrm{Im}(\Theta(z) - 2\Omega(z) + 6\Gamma(z) - 24\Psi(z))) \end{aligned} \tag{9.8.5}$$

in which

$$\begin{aligned} &c_7 = \frac{c_3K_1 + 2c_1R}{\mu K_1 - 2R^2}, \quad c_8 = c_1c_2R(\mu(K_1 - K_2) - R^2) \\ &c_9 = c_8 + 2c_2c_4\left(c_3 - \frac{(\mu K_2 - R^2)^2}{\mu K_1 - 2R^2}\right), \quad c_{10} = c_1c_2R^2 - c_4(c_2R - c_3K_1) \end{aligned} \tag{9.8.6}$$

9.8.2 *Elliptic Notch Problem*

We consider an icosahedral quasicrystal solid with an elliptic notch, which penetrates through the medium along the z-axis direction, the edge of the elliptic notch subject to the uniform pressure p, see Fig. 9.9.

The boundary conditions of this problem can be expressed as follows (Fig. 9.12)

$$\sigma_{xx}\cos(\mathbf{n}, x) + \sigma_{xy}\cos(\mathbf{n}, y) = T_x, \quad \sigma_{xy}\cos(\mathbf{n}, x) + \sigma_{yy}\cos(\mathbf{n}, y) = T_y, \quad (x, y) \in L \tag{9.8.7}$$

$$H_{xx}\cos(\mathbf{n}, x) + H_{xy}\cos(\mathbf{n}, y) = h_x, \quad H_{yx}\cos(\mathbf{n}, x) + H_{yy}\cos(\mathbf{n}, y) = h_y, \quad (x, y) \in L \tag{9.8.8}$$

$$\sigma_{zx}\cos(\mathbf{n}, x) + \sigma_{zy}\cos(\mathbf{n}, y) = 0, \quad H_{zx}\cos(\mathbf{n}, x) + H_{zy}\cos(\mathbf{n}, y) = 0, \quad (x, y) \in L \tag{9.8.9}$$

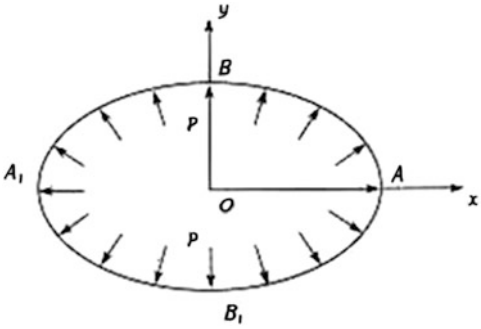

Fig. 9.12 An elliptic notch subject to an inner pressure in icosahedral quasicrystal

where

$$\cos(\mathbf{n},x)=\frac{\mathrm{d}y}{\mathrm{d}s},\quad \cos(\mathbf{n},y)=-\frac{\mathrm{d}x}{\mathrm{d}s},\quad T_x=-p\cos(\mathbf{n},x),\quad T_y=-p\cos(\mathbf{n},y)$$

T_x, T_y denote the components of surface traction, p is the magnitude of the pressure, h_x, h_y are components of the generalized surface traction, $\mathbf{n}$ is the outward unit normal vector of any point on the boundary and $L:\frac{x^2}{a^2}+\frac{y^2}{b^2}=1$ is the edge of the elliptic notch. Since the measurement of generalized traction has not been reported so far, for simplicity, we assume that

$$h_x=0,\quad h_y=0$$

Utilizing Eqs. (9.8.2), (9.8.3) and (9.8.7), we obtain

$$\begin{aligned}&-4c_2c_3R[3(f_4(z)+4\bar{z}f_5'(z)+10\bar{z}^2f_6''(z))-(\overline{f_3(z)}+3z\overline{f_4'(z)}+6z^2\overline{f_5''(z)}+10z^3\overline{f_6'''(z)})]\\&=\int(T_x+iT_y)\mathrm{d}s=ipz\end{aligned}\tag{9.8.10}$$

Taking complex conjugate on both sides of Eq. (9.7.10) yields

$$\begin{aligned}&-4c_2c_3R[3(\overline{f_4(z)}+4z\overline{f_5'(z)}+10z^2\overline{f_6''(z)})-(f_3(z)+3\bar{z}f_4'(z)+6z^2f_5'(z)+10\bar{z}^3f_6'''(z)\\&=-ip\bar{z}\end{aligned}\tag{9.8.11}$$

From Eqs. (9.8.2), (9.8.3) and (9.8.8), we have

$$\begin{aligned}&48c_2(2c_4-c_1R)\mathrm{Re}\overline{\Psi(z)}+2c_1c_2R\mathrm{Re}\Theta(z)=0\\&-48c_2(2c_4-c_1R)\mathrm{Im}\overline{\Psi(z)}-2c_1c_2R\mathrm{Im}\Theta(z)=0\end{aligned}\tag{9.8.12}$$

Multiplying the second formula of (9.8.12) by $-i$ and adding it to the first, one obtains

$$48c_2(2c_4 - c_1R)\overline{\Psi(z)} + 2c_1c_2R\Theta(z) = 0 \tag{9.8.13}$$

By Eqs. (9.8.2), (9.8.3) and (9.8.9), one has

$$\begin{aligned} &f_6(z) + \overline{f_6(z)} = 0 \\ &4c_{11}\mathrm{Re}[f_5(z) + 5\bar{z}f_6'(z)] + (2K_2 - K_1)R\mathrm{Re}[f_4(z) + 4\bar{z}f_5'(z) + 10\bar{z}^2f_6''(z) + 20f_6(z)] = 0 \end{aligned} \tag{9.8.14}$$

in which

$$c_{11} = (2K_2 - K_1)R - \frac{4c_4(\mu K_2 - R^2)}{(\mu K_1 - 2R^2)R} \tag{9.8.15}$$

However, the further calculation will be very difficult at the z-plane owing to the complicity of the manipulation; we must employ the conformal mapping

$$z = \omega(\zeta) = R_0\left(\frac{1}{\zeta} + m\zeta\right) \tag{9.8.16}$$

to transform the region with the ellipse at the z-plane onto the interior of the unit circle γ at ζ-plane, referring to Sect. 8.4.2, in which

$$R_0 = (a+b)/2, \quad m = (a-b)/(a+b)$$

Let

$$f_j(z) = f_j[\omega(\zeta)] = \Phi_j(\zeta) \quad (j = 2, \ldots, 6) \tag{9.8.17}$$

Substituting (9.8.16) into (9.8.10), (9.8.11), (9.8.13) and (9.8.14), then multiplying both sides of equations by $\mathrm{d}\sigma/[2\pi i(\sigma - \zeta)]$ (σ represents the value of ζ at the unit circle) and integrating around the unit circle γ, by means of Cauchy integral formula and analytic extension of the complex variable function theory, we obtain (the detail will be given in Appendix of Chap. 11)

$$\begin{aligned}
\Phi_2(\zeta) &= \frac{R_0}{2c_2c_3R}\frac{ip\zeta(\zeta^2+m)(m^3\zeta^2+1)}{(m\zeta^2-1)^3} \\
&\quad + \frac{(2K_2-K_1)R_0}{2c_2c_3C_{11}}\frac{pm\zeta^3(\zeta^2+m)[m^2\zeta^6-(m^3+4m)\zeta^4+(2m^4+4m^2+5)\zeta^2+m]}{(m\zeta^2-1)^5} \\
\Phi_3(\zeta) &= \frac{R_0}{4c_2c_3R}\frac{ip\zeta(m^2+1)}{(m\zeta^2-1)} - \frac{(2K_2-K_1)R_0}{12c_2c_3C_{11}}\frac{pm\zeta^3(\zeta^2+m)(m\zeta^2-m^2-2)}{(m\zeta^2-1)^3} \\
\Phi_4(\zeta) &= -\frac{R_0}{12c_2c_3R}ipm\zeta - \frac{(2K_2-K_1)R_0}{2c_2c_3C_{11}}\frac{pm\zeta(\zeta^2+m)}{(m\zeta^2-1)} \\
\Phi_5(\zeta) &= -\frac{(2K_2-K_1)R_0}{48c_2c_3C_{11}}pm\zeta, \quad \Phi_6(\zeta)=0
\end{aligned} \tag{9.8.18}$$

The elliptic notch problem has been solved.

The solution of the Griffith crack subjected to a uniform pressure can be obtained if put $m=1, R_0=a/2$ in the above notch solution. The solution of crack can be expressed explicitly on the z-plane, for example

$$\begin{aligned}
\sigma_{yy} = \mathrm{Im}\Bigg[& ip\left(\frac{z}{\sqrt{z^2-a^2}} + \frac{ia^2y}{(\sqrt{z^2-a^2})^3} - 1\right) + \frac{3(2K_2-K_1)R}{2c_{11}}\frac{ipa^2y}{\sqrt{(z^2-a^2)^3}} \\
& + \frac{(2K_2-K_1)R}{2c_{11}}\frac{ipy(2a^4-3z\bar{z})}{\sqrt{(z^2-a^2)^5}} - \frac{(2K_2-K_1)R}{4c_{11}}\frac{a^2pz(z\bar{z}-a^2)}{\sqrt{(z^2-a^2)^5}} + \frac{(2K_2-K_1)R}{4c_{11}}\frac{a^2p\bar{z}}{\sqrt{(z^2-a^2)^3}}\Bigg]
\end{aligned} \tag{9.8.19}$$

$$\begin{aligned}
u_y = & -6c_2R\left(\frac{2c_3}{\mu+\lambda}+c_7\right)\mathrm{Re}\left[\frac{ip}{24c_2c_3R}\overline{(z-\sqrt{z^2-a^2})} + \frac{2K_2-K_1}{24c_2c_3c_{11}}p\left(\frac{z\bar{z}}{\sqrt{z^2-a^2}} - \frac{a^2}{\sqrt{z^2-a^2}} - \sqrt{z^2-a^2}\right)\right] \\
& -2c_2c_7\mathrm{Re}\left[\frac{ip}{8c_2c_3R}\left(\frac{z\bar{z}}{\sqrt{z^2-a^2}} - \frac{a^2}{\sqrt{z^2-a^2}} - \bar{z}\right) - \frac{2K_2-K_1}{4c_2c_3c_{11}}ipy\right. \\
& \left. + \frac{2K_2-K_1}{16c_2c_3c_{11}}p\left(\frac{a^2[(z\bar{z}-a^2)+2iy\bar{z}]}{\sqrt{(z^2-a^2)^3}}\right) + \frac{2K_2-K_1}{16c_2c_3c_{11}}p\left(\frac{a^2}{\sqrt{z^2-a^2}} - \frac{2z\bar{z}}{\sqrt{z^2-a^2}} + 2\sqrt{z^2-a^2}\right)\right]
\end{aligned} \tag{9.8.20}$$

From Eqs. (9.7.19) and (9.7.20), the stress intensity factor and energy release rate can be evaluated as follows

$$K_I^{\parallel} = \sqrt{\pi a}p$$

$$G_I = \frac{1}{2}\frac{\partial}{\partial a}\left[2\int_{-a}^{a}(\sigma_{yy}(x,0)\oplus H(x,0))(u_y(x,0)\oplus w_y(x,0))\mathrm{d}x\right]$$
$$= \frac{1}{2}\left(\frac{1}{\lambda+\mu}+\frac{c_7}{c_3}\right)(K_I^{\parallel})^2 \tag{9.8.21}$$

in which material constant c_3 is given by (9.5.5) and c_7 by (9.8.6); it is evident that the crack energy release depends upon not only phonon elastic constants λ, μ but also phason elastic constants K_1, K_2 and phono-phason coupling elastic constant R though we assume phason tractions $h_x = h_y = 0$.

9.8.3 *Brief Summary*

The notch problem can be solved only by complex variable function method, and the solution includes that of Griffith crack problem naturally. Though the Fourier transform can solve the Griffith crack problem, referring to Zhu and Fan [25], it cannot solve the notch problem. Whatever solution for notch or crack here reveals the effects of not only phonon but also phason and phonon-phason coupling. The numerical examples on crack opening displacement $\delta(x) = u_y(x, +0) - u_y(x, -0)$ and energy release rate G_I for different values of R/μ are identical to those given in Figs. 9.10 and 9.11, respectively.

Both solutions given by the complex variable function method and the Fourier transform reduce to that of the classical theory when the phason is absent; this is helpful to examine the present result.

This study developed the previous work for the elasticity of two-dimensional quasicrystals given by Fan and co-workers. The work is helpful to understand quantitatively the influence of elliptic notch and crack on the mechanical behaviour of icosahedral quasicrystals. The stress intensity factor and energy release rate are also obtained as the direct results of the solution, which are all important criteria of fracture mechanics.

The strict theory on the complex potential method will be summarized in-depth in Chap. 11, which can also be referred to paper [26].

9.9 Elasticity of Cubic Quasicrystals—The Anti-plane and Axisymmetric Deformation

Cubic quasicrystal is one of important three-dimensional quasicrystals. Due to the complexity of the basic equations of the elasticity of the quasicrystal, there are few analytic solutions. Developing a systematic and direct method for solving complicated boundary value problem of elasticity of quasicrystal is a fundamental task. Because the phasons in this case have the same irreducible representation with the

phonons, the stress and strain tensors are symmetry. With this feature, we can discuss two cases, one for anti-plane and another for axisymmetric elastic theory of cubic quasicrystal, and the latter can reveal the three-dimensional effect of the elasticity; this may be the only three-dimensional elastic analytic solution for quasicrystals so far. In addition, a penny-shaped crack problem under tensile loading in the material is investigated, and the exact analytic solution is obtained by using Hankel transform and dual integral equation theory, and the stress intensity factor and the strain energy release rate are determined, which provide some useful information for studying deformation and fracture of the quasicrystalline material.

From the physical basis provided by Hu et al. [2], we first discuss the anti-plane elasticity such as the stress–stain relation

$$\begin{aligned}\sigma_{23} &= 2C_{44}\varepsilon_{23} + R_{44}w_{23}\\ \sigma_{31} &= 2C_{44}\varepsilon_{31} + R_{44}w_{31}\\ H_{23} &= 2R_{44}\varepsilon_{23} + K_{44}w_{23}\\ H_{31} &= 2R_{44}\varepsilon_{31} + K_{44}w_{31}\end{aligned}$$

the equations of deformation geometry

$$\varepsilon_{23} = \frac{1}{2}\frac{\partial u_3}{\partial x_2}, \quad \varepsilon_{31} = \frac{1}{2}\frac{\partial u_3}{\partial x_1}, \quad w_{23} = \frac{\partial w_3}{\partial x_2}, \quad w_{31} = \frac{\partial w_3}{\partial x_1}$$

and the equilibrium equations

$$\frac{\partial \sigma_{31}}{\partial x_1} + \frac{\partial \sigma_{32}}{\partial x_2} = 0, \quad \frac{\partial H_{31}}{\partial x_1} + \frac{\partial H_{32}}{\partial x_2} = 0.$$

These equations are exactly similar to those of anti-plane elasticity of one-dimensional and icosahedral quasicrystals, so that result in the final governing equations

$$\nabla^2 u_3 = 0, \quad \nabla^2 w_3 = 0$$

The solution can be derived from the relevant discussion in Chaps. 5, 7 and 8 and Sect. 9.2 of this chapter, so it need not be mentioned again.

For the axisymmetric case, Zhou an Fan [23] developed a displacement potential theory to reduce basic equations to a single partial differential equation with high order in circular cylindrical coordinate system (r, θ, z), i.e. assume

$$\frac{\partial}{\partial \theta} = 0 \tag{9.9.1}$$

and by the generalized Hooke's law

$$\begin{aligned}
\sigma_{rr} &= C_{11}\varepsilon_{rr} + C_{12}(\varepsilon_{\theta\theta} + \varepsilon_{zz}) + R_{11}w_{rr} + R_{12}(w_{\theta\theta} + w_{zz}) \\
\sigma_{\theta\theta} &= C_{11}\varepsilon_{\theta\theta} + C_{12}(\varepsilon_{rr} + \varepsilon_{zz}) + R_{11}w_{\theta\theta} + R_{12}(w_{rr} + w_{zz}) \\
\sigma_{zz} &= C_{11}\varepsilon_{zz} + C_{12}(\varepsilon_{rr} + \varepsilon_{\theta\theta}) + R_{11}w_{zz} + R_{12}(w_{\theta\theta} + w_{rr}) \\
\sigma_{zr} &= \sigma_{rz} = 2C_{44}\varepsilon_{rz} + 2R_{44}w_{rz} \\
H_{rr} &= R_{11}\varepsilon_{rr} + R_{12}(\varepsilon_{\theta\theta} + \varepsilon_{zz}) + K_{11}w_{rr} + K_{12}(w_{\theta\theta} + w_{zz}) \\
H_{\theta\theta} &= R_{11}\varepsilon_{\theta\theta} + R_{12}(\varepsilon_{rr} + \varepsilon_{zz}) + K_{11}w_{\theta\theta} + K_{12}(w_{rr} + w_{zz}) \\
H_{zz} &= R_{11}\varepsilon_{zz} + R_{12}(\varepsilon_{rr} + \varepsilon_{\theta\theta}) + K_{11}w_{zz} + K_{12}(w_{rr} + w_{\theta\theta}) \\
H_{zr} &= H_{rz} = 2R_{44}\varepsilon_{rz} + 2K_{44}w_{rz}
\end{aligned} \tag{9.9.2}$$

and the equations of deformation geometry

$$\varepsilon_{ij} = \frac{1}{2}\left(\frac{\partial u_i}{\partial x_j} + \frac{\partial u_j}{\partial x_i}\right), \quad w_{ij} = \frac{1}{2}\left(\frac{\partial w_i}{\partial x_j} + \frac{\partial w_j}{\partial x_i}\right)$$

which are

$$\begin{aligned}
&\varepsilon_{rr} = \frac{\partial u_r}{\partial r}, \quad \varepsilon_{\theta\theta} = \frac{u_r}{r}, \quad \varepsilon_{zz} = \frac{\partial u_z}{\partial z} \\
&\varepsilon_{rz} = \varepsilon_{zr} = \frac{1}{2}\left(\frac{\partial u_r}{\partial z} + \frac{\partial u_z}{\partial r}\right) \\
&w_{rr} = \frac{\partial w_r}{\partial r}, \quad w_{\theta\theta} = \frac{w_r}{r}, \quad \varepsilon_{zz} = \frac{\partial w_z}{\partial z} \\
&w_{rz} = w_{zr} = \frac{1}{2}\left(\frac{\partial w_r}{\partial z} + \frac{\partial w_z}{\partial r}\right)
\end{aligned} \tag{9.9.3}$$

and the equations of equilibrium

$$\begin{aligned}
&\frac{\partial \sigma_{rr}}{\partial r} + \frac{\partial \sigma_{rz}}{\partial z} + \frac{\sigma_{rr} - \sigma_{\theta\theta}}{r} = 0 \\
&\frac{\partial \sigma_{zr}}{\partial r} + \frac{\partial \sigma_{zz}}{\partial z} + \frac{\sigma_{zr}}{r} = 0 \\
&\frac{\partial H_{rr}}{\partial r}\frac{\partial \sigma_{zr}}{\partial r} + \frac{\partial \sigma_{zz}}{\partial z} + \frac{\sigma_{zr}}{r} = 0 \\
&\frac{\partial H_{zr}}{\partial r} + \frac{\partial H_{zz}}{\partial z} + \frac{H_{zr}}{r} = 0
\end{aligned} \tag{9.9.4}$$

If all displacements and stresses can be expressed by the potential $F(r, z)$, and which satisfies

$$\left[\frac{\partial^8}{\partial z^8} - b\left(\frac{\partial^2}{\partial r^2} + \frac{1}{r}\frac{\partial}{\partial r}\right)\frac{\partial^6}{\partial z^6} + c\left(\frac{\partial^2}{\partial r^2} + \frac{1}{r}\frac{\partial}{\partial r}\right)^2\frac{\partial^4}{\partial z^4} - d\left(\frac{\partial^2}{\partial r^2} + \frac{1}{r}\frac{\partial}{\partial r}\right)^3\frac{\partial^2}{\partial z^2} + e\left(\frac{\partial^2}{\partial r^2} + \frac{1}{r}\frac{\partial}{\partial r}\right)^4\right]F = 0 \tag{9.9.5}$$

then the Eqs. (9.9.2)–(9.9.4) have been automatically satisfied.

Due to the lengthiness of these expression which are not listed here.

As an application of above theory and method, the solutions of the elastic field of cubic quasicrystal with a penny-shaped crack are discussed in the following.

Assuming a penny-shaped crack with radius a in the centre of the cubic quasicrystal material, the size of the crack is much smaller than the solid, so that the size of the material can be considered as infinite; at the infinity, the quasicrystal material is subjected to a tension p in z-direction. The origin of coordinate system is at the centre of the crack (as shown in Fig. 9.13).

From the symmetry of the problem, it is enough to study the upper half-space $z > 0$ or lower half-space $z < 0$. In this case, for studying the upper half-space, the boundary conditions of the problem are described by

$$\begin{aligned}
&\sqrt{r^2+z^2} \to \infty: \quad \sigma_{zz} = p, \quad H_{zz} = 0, \quad \sigma_{rz} = 0, \quad H_{rz} = 0 \\
&z = 0, \quad 0 \le r \le a, \quad \sigma_{zz} = \sigma_{rz} = 0; \quad H_{zz} = H_{rz} = 0 \\
&z = 0, \quad r > a: \quad \sigma_{rz} = 0, \quad u_z = 0; \quad H_{rz} = 0, \quad w_z = 0
\end{aligned} \tag{9.9.6}$$

But boundary conditions can be replaced by

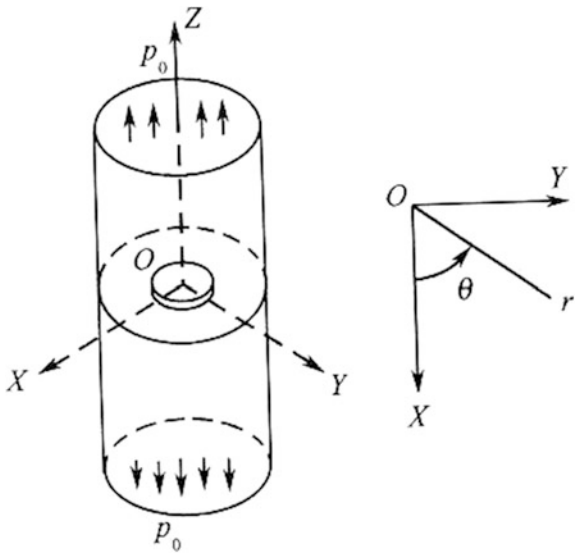

Fig. 9.13 Penny-shaped crack subject to a tension in a cubic quasicrystal

$$\begin{aligned}
&\sqrt{r^2+z^2}\to\infty: \quad \sigma_{ij}=0, \quad H_{ij}=0\\
&z=0, \quad 0\le r\le a, \quad \sigma_{zz}=-p_0, \quad \sigma_{rz}=0; \quad H_{zz}=H_{rz}=0\\
&z=0, \quad r>a: \quad \sigma_{rz}=0, \quad u_z=0; \quad H_{rz}=0, \quad w_z=0
\end{aligned} \tag{9.9.6'}$$

which are equivalent to (9.9.6) in the sense of fracture mechanics, if $p=p_0$.

By taking the Hankel transform to Eq. (9.9.1) and boundary conditions to (9.8.5), the solution at the transformed space is

$$\bar{F}(\xi,z)=A_1e^{-\lambda_1\xi z}+A_2e^{-\lambda_2\xi z}+A_3e^{-\lambda_3\xi z}+A_4e^{-\lambda_4\xi z} \tag{9.9.7}$$

where $A_i\,(i=1,2,3,4)$ are unknown functions of ξ to be determined, and $\lambda_i\,(i=1,2,3,4)$ are eigen roots obtained from the ordinary differential equation of $\bar{F}(\xi,r)$. According to the boundary conditions, $A_i(\xi)$ can be determined by solving the following dual integral equations

$$\begin{aligned}
&\int_0^\infty \xi A_i(\xi)J_0(\xi r)\mathrm{d}\xi=M_ip_0, \quad 0<r<a\\
&\int_0^\infty A_i(\xi)J_0(\xi r)\mathrm{d}\xi=0, \quad r>a
\end{aligned} \tag{9.9.8}$$

and $i=1,2,3,4$, in which M_i are some constants consisting elastic moduli, $J_0(\xi r)$, the first kind Bessel function of zero order.

According to the theory of dual integral equations (refer to Major Appendix), obtaining the solution of dual integral Eq. (9.9.8) is as follows

$$A_i(\xi)=2a^2M_ip(2\pi a\xi)^{-1/2}\xi^{-7}J_{3/2}(a\xi) \tag{9.9.9}$$

in which $J_{3/2}(a\xi)$ is the first kind Bessel function with 3/2 order (refer to the Major Appendix for the detailed calculation).

After some calculation, stress intensity factor K_I, strain energy W_I and strain energy release rate G_I can be obtained as follows

$$K_I=\frac{2}{\pi}\sqrt{\pi a}p, \quad W_I=Mp^2a^3, \quad G_I=\frac{1}{2\pi a}\frac{\partial W_I}{\partial a}=\frac{3Mp^2a}{2\pi} \tag{9.9.10}$$

where M is the constant composed of the elastic constants but which is quite lengthy so has not been included here.

From the applications of the Fourier transform, Hankel transform and dual integral equations in Sects. 7.6, 8.3, 9.2, 9.7 and 9.9 are developed the work of Sneddon in the classical elasticity [27]; this shows the Fourier analysis is a powerful tool in solving not only classical but also modern elasticity.

References

1. Ding D H, Yang W G, Hu C Z and Wang R H, 1993, Generalized theory of elasticity of quasicrystals, *Phys. Rev*. B, **48**(10), 7003-7010.
2. Hu C Z, Wang R H and Ding D H et al, 1996, Point groups and elastic properties of two-dimensional quasicrystals, *Acta Crystallog* A, **52**(2), 251-256.
3. Yang W G, Ding D H et al, 1998, Atomic model of dislocation in icosahedral quasicrystals, *Phil. Mag*. A, **77**(6), 1481-1497.
4. Fan T Y and Guo L H, 2005, Final governing equation of plane elasticity of icosahedral quasicrystals, *Phys. Lett*. A, **341**(5), 235-239.
5. Li L H and Fan T Y, 2006, Final governing equation of plane elasticity of icosahedral quasicrystals–stress potential method, *Chin. Phys. Lett*., **24**(9), 2519-2521.
6. Reynolds G A M, Golding B, Kortan A R et al, 1990, Isotropic elasticity of the Al-Cu-Li quasicrystal, *Phys. Rev*. B, **41** (2), 1194-1195.
7. Spoor P S, Maynard J D and Kortan A R, 1995, Elastic isotropy and anisotropy in quasicrystalline and cubic AlCuLi, *Phys. Rev. Lett.*, **75** (19), 3462-3465.
8. Tanaka K, Mitarai and Koiwa M, 1996, Elastic constants of Al-based icosahedral quasicrystals, *Phil. Mag*. **A**, 1715-1723.
9. Duquesne J-Y and Perrin B, 2002, Elastic wave interaction in icosahedral AlPdMn, *Physics* B, **316**-**317**, 317-320.
10. Foster K, Leisure R G, Shaklee A et al, 1999, Elastic moduli of a Ti-Zr-Ni icosahedral quasicrystal and a 1/1 bcc crystal approximant, *Phys. Rev*. B, 59(17), 11132-11135.
11. Schreuer J, Steurer W, Lograsso T A et al, 2004, Elastic properties of icosahedral i-$Cd_{84}Yb_{16}$ and hexagonal h-$Cd_{51}Yb_{14}$, *Phil. Mag. Lett*., **84**(10),643-653.
12. Sterzel R, Hinkel C, Haas A et al, 2000, Ultrasonic measurements on FCI Zn-Mg-Y single crystals, *Europhys. Lett*., **49**(6), 742-747.
13. Letoublon A, de Boissieu M, Boudard M et al, 2001, Phason elastic constants of the icosahedral Al-Pd-Mn phase derived from diffuse scattering measurements, *Phil. Mag. Lett.*, **81**(4), 273-283.
14. de Boissieu M, Francoual S, Kaneko Y et al, 2005, Diffuse scattering and phason fluctuations in the Zn-Mg-Sc icosahedral quasicrystal and its Zn-Sc periodic approximant, *Phys. Rev. Lett.*, **95**(10), 105503/1-4.
15. Edagawa K and So GI Y, 2007, Experimental evaluation of phonon-phason coupling in icosahedral quasicrystals, *Phil. Mag*., **87**(1), 77-95.
16. Zhu A Y and Fan T Y, 2007, Elastic field of a mode II Griffith crack in icosahedral quasicrystals, *Chinese Physics*, **16**(4), 1111-1118.
17. Zhu A Y , Fan T Y and Guo L H, 2007, A straight dislocation in an icosahedral quasicrystal, *J. Phys.: Condens. Matter*, **19**(23), 236216.
18. Li X F and Fan T Y, 1998, New method for solving elasticity problems of some planar quasicrystals, *Chin. Phys. Lett*., **15**(4), 278-280.
19. Fan T Y, 1999, *Mathematical Theory of Elasticity of Quasicrystals and Its Applications* (in Chinese), Beijing Institute of Technology Press, Beijing.
20. Guo Y C and Fan T Y, 2001, A mode-II Griffith crack in decagonal quasicrystals, *Appl. Math. Mech*., **22**(11), 1311-1317.
21. Li L H and Fan T Y, 2008, Complex variable function method for solving Griffith crack in an icosahedral quasicrystal, *Science in China*, G, **51**(6), 723-780.
22. Li L H and Fan T Y, 2006, Complex function method for solving notch problem of point 10 two-dimensional quasicrystal based on the stress potential function, *J. Phys.: Condens. Matter*, **18**(47)**,** 10631-10641.
23. Zhou W M and Fan T Y, 2000, Axisymmetric elasticity problem of cubic quasicrystal, *Chinese Physics,* **9**(4), 294-303.
24. Fan T Y, Xie L Y, Fan L and Wang Q Z, 2011, Study on interface of quasicrystal-crystal, *Chin. Phys*. B, 20(7), 076102.

25. Zhu A Y and Fan T Y, 2009, Elastic analysis of a Griffith crack in icosahedral Al-Pd-Mn quasicrystal, *Int. J. Mod. Phys. B*, 23(10), 1-16.
26. Fan T Y, Tang Z Y, Li L H and Li W, 2010, The strict theory of complex variable function method of sextuple harmonic equation and applications, J. Math. Phys., 51(5), 053519.
27. Sneddon I N, 1950, Fourier Transforms, New York, McGraw-Hill.

Chapter 10
Phonon-Phason Dynamics and Defect Dynamics of Solid Quasicrystals

Elastodynamics or phonon-phason dynamics of quasicrystals is a topic with different points of view. The focus of contradictions between different scholar circles lies in the role of phason variables in the dynamic process.

Lubensky et al. [1] and Socolar et al. [2] pointed out that phonon field **u** and phason field **w** play very different roles in the hydrodynamics of quasicrystals, because **w** is insensitive to spatial translations, and the phason modes represent the relative motion of the constituent density waves. They claimed that phasons are diffusive, not oscillatory, and with very large diffusion times. On the other hand, according to Bak [3, 4], the phason describes particular structure disorders or structure fluctuations in quasicrystals, and it can be formulated based on a six-dimensional space description, as has been displayed in the previous chapters. Since there are six continuous symmetries, there exist six hydrodynamic vibration modes. Following this point of view, **u** and **w** play similar roles in the dynamics. It is evident that the difference between the arguments of Lubensky et al. and Bak lies only in the dynamics. There is no difference between their arguments in statics (i.e. static equilibrium). Based on this reason in the discussions of the previous chapters, we need not distinguish the arguments of either Lubensky et al. or Bak.

Probably due to simpler mathematical formulation, many authors followed the Bak's argument, e.g. [5–12], in dynamic study. In this chapter, we will present some results given in the references. These Sects. 10.1–10.4 constitute the part one of this chapter. In the meantime, we introduce some other results [13, 14, 27] which are carried out by following the argument of Lubensky et al., and in this line of thinking, it appears that elastodynamics and hydrodynamics are combined in some extent so it can be called as elasto-/hydrodynamics of quasicrystals, or named phonon-phason dynamics by Rochal and Lorman [16]; they also call this model as minimal model of phonon-phason dynamics. The discussions given in Sects. 10.5–10.7 constitute the part two of this chapter. However, the hydrodynamics of solid quasicrystals created by Lubensky et al. will not be discussed in this chapter, because it is beyond the scope that we here studied. Their theory will be

T.-Y. Fan, *Mathematical Theory of Elasticity of Quasicrystals and Its Applications*,
Springer Series in Materials Science 246, DOI 10.1007/978-981-10-1984-5_10

partly concerned in Chap. 16 and introduced from angle of additional derivation in Major Appendix of the book.

The results based on different hypothesis are presented to provide readers for their consideration and comparison. Though some researchers believe that the hydrodynamics based on the argument of Lubensky et al. is more fundamentally sound, the major shortcoming so far is lack of proper experimental data for confirmation. Recently, research interest in this respect is growing up [13–16], but the most important accomplishment shall still be the quantitative results.

Recently, Coddens [31] et al. put forward some different points of view to the work given by Lubensky et al., which could not be discussed in this and other chapters of our book.

10.1 Elastodynamics of Quasicrystals Followed Bak's Argument

Ding et al. [5] first discussed the elastodynamics of quasicrystals. The basic equations in deformation geometry and generalized Hooke's law are the same as those of elastostatics, i.e.

$$\varepsilon_{ij} = \frac{1}{2}\left(\frac{\partial u_i}{\partial x_j} + \frac{\partial u_j}{\partial x_i}\right), \quad w_{ij} = \frac{\partial w_i}{\partial x_j} \tag{10.1.1}$$

$$\sigma_{ij} = C_{ijkl}\varepsilon_{kl} + R_{ijkl}w_{kl}$$

$$H_{ij} = K_{ijkl}w_{kl} + R_{klij}\varepsilon_{kl} \tag{10.1.2}$$

They claimed that law of the momentum conservation holds for both phonons and phasons; that is, for linear and small deformation cases, the equations of motion are as follows:

$$\frac{\partial \sigma_{ij}}{\partial x_j} = \rho \frac{\partial^2 u_i}{\partial t^2}, \quad \frac{\partial H_{ij}}{\partial x_j} = \rho \frac{\partial^2 w_i}{\partial t^2} \tag{10.1.3}$$

where ρ denotes the average mass density of the material.

This implies that they follow the Bak's argument. After seven years, Hu et al. [6] confirmed the point of view again. In fact the final elastodynamic equations can be deduced by substituting (10.1.1) and (10.1.2) into (10.1.3). The mathematical structure of this theory is relatively simpler, and the formulations are similar to that of classical elastodynamics, so many authors take this formulation to develop the elastodynamics of quasicrystals and give applications in defect dynamics and thermodynamics. In the subsequent sections, we will present some examples of applications of the theory.

10.2 Elastodynamics of Anti-plane Elasticity for Some Quasicrystals

For three-dimensional icosahedral or cubic or one-dimensional hexagonal quasicrystals, in the anti-plane elasticity the basic equations have similar form. First we consider icosahedral quasicrystals

$$\begin{aligned}
\sigma_{zy} &= \sigma_{yz} = \mu\frac{\partial u_z}{\partial y} + R\frac{\partial w_z}{\partial y} \\
\sigma_{xz} &= \sigma_{zx} = \mu\frac{\partial u_z}{\partial x} + R\frac{\partial w_z}{\partial x} \\
H_{zy} &= (K_1 - K_2)\frac{\partial w_z}{\partial y} + R\frac{\partial u_z}{\partial y} \\
H_{zx} &= (K_1 - K_2)\frac{\partial w_z}{\partial x} + R\frac{\partial u_z}{\partial x}
\end{aligned} \tag{10.2.1}$$

Substituting (10.2.1) into equations of motion of (10.1.3) yields

$$\begin{aligned}
\mu\nabla^2 u_z + R\nabla^2 w_z &= \rho\frac{\partial^2 u_z}{\partial t^2} \\
R\nabla^2 u_z + (K_1 - K_2)\nabla^2 w_z &= \rho\frac{\partial^2 w_z}{\partial t^2}
\end{aligned} \tag{10.2.2}$$

If displacement functions ϕ and ψ are defined such as

$$u_z = \alpha\phi - R\psi, \quad w_z = R\phi + \alpha\psi \tag{10.2.3}$$

then Eq. (10.2.2) is reduced to the standard wave equations

$$\nabla^2\phi = \frac{1}{s_1^2}\frac{\partial^2\phi}{\partial t^2}, \quad \nabla^2\psi = \frac{1}{s_2^2}\frac{\partial^2\psi}{\partial t^2} \tag{10.2.4}$$

where

$$\alpha = \frac{1}{2}\left[\mu - (K_1 - K_2) + \sqrt{(\mu - (K_1 - K_2))^2 + 4R^2}\right] \tag{10.2.5}$$

and

$$s_j = \sqrt{\frac{\varepsilon_j}{\rho}}, \quad j = 1, 2 \tag{10.2.6}$$

$$\varepsilon_{1,2} = \frac{1}{2}\left[\mu + (K_1 - K_2) \pm \sqrt{(\mu - (K_1 - K_2))^2 + 4R^2}\right]$$

s_j can be understood as the speeds of wave propagation in anti-plane deformation of the material. It is obvious that the wave speeds are the results of phonon-phason coupling. If there is no coupling, i.e. $R \to 0$, then

$$s_1 \to \sqrt{\frac{\mu}{\rho}}, \quad s_2 \to \sqrt{\frac{(K_1 - K_2)}{\rho}} \tag{10.2.7}$$

and $\sqrt{\frac{\mu}{\rho}}$ represents the speed of transverse wave of phonon field and $\sqrt{\frac{K_1-K_2}{\rho}}$ the speed of pure phason elastic wave, requiring $K_1 - K_2 > 0$.

Substituting (10.2.3) into (10.2.1) yields

$$\begin{aligned}
\sigma_{yz} &= \sigma_{zy} = (\alpha\mu + R^2)\frac{\partial \phi}{\partial y} + R(\alpha - \mu)\frac{\partial \psi}{\partial y} \\
\sigma_{xz} &= \sigma_{zx} = (\alpha\mu + R^2)\frac{\partial \phi}{\partial x} + R(\alpha - \mu)\frac{\partial \psi}{\partial x} \\
H_{zy} &= R(\alpha + (K_1 - K_2))\frac{\partial \phi}{\partial y} + \left(\alpha(K_1 - K_2) - R^2\right)\frac{\partial \psi}{\partial y} \\
H_{zx} &= R_3(\alpha + (K_1 - K_2))\frac{\partial \phi}{\partial x} + \left(\alpha(K_1 - K_2) - R^2\right)\frac{\partial \psi}{\partial x}
\end{aligned} \tag{10.2.8}$$

Formulas (10.2.3) and (10.2.8) give the expressions for displacements and stresses in terms of displacement functions ϕ and ψ, which satisfy the standard wave equations (10.2.4) for elastodynamics of anti-plane elasticity of three-dimensional icosahedral quasicrystals.

The above discussion is valid for anti-plane elasticity of three-dimensional cubic quasicrystals or one-dimensional quasicrystals too, the difference between these quasicrystals is only the material constants. If $\mu, K_1 - K_2$ and R are replaced by C_{44}, K_{44} and R_{44} (see Sect. 9.8) for cubic quasicrystals, or by C_{44}, K_2 and R_3 for one-dimensional hexagonal quasicrystals with the Laue classes $6/m_{\mathrm{h}}$ and $6/m_{\mathrm{h}}mm$ (see Sects. 7.1 or 8.1), one can find the similar equations.

The solution of (10.2.4) can be done by using method for solving pure wave equations in classical mathematical physics.

10.3 Moving Screw Dislocation in Anti-plane Elasticity

Assume a straight screw dislocation line parallel to the quasiperiodic axis which moves along one of periodic axes, say the x-axis in the periodic plane. For simplicity, consider the dislocation moves with constant velocity V.

For the problem, a dislocation condition is assumed

$$\int_{\Gamma} \mathrm{d}u_z = b_3^{\parallel}, \qquad \int_{Roman\Gamma} \mathrm{d}w_z = b_3^{\perp} \tag{10.3.1}$$

i.e. we assume that the dislocation has the Burgers vector $(0, 0, b_3^{\parallel}, 0, b_3^{\perp})$, and Γ denotes the Burgers circuit surrounding the core of the moving dislocation.

Starting now we denote the fixed coordinates as (x_1, x_2, t) and moving ones as (x, y).

By introducing Galilean transformation

$$x = x_1 - Vt, \quad y = x_2 \tag{10.3.2}$$

wave, Eq. (10.2.4) is reduced to the Laplace equations (i.e. $\left(\nabla^2 - \frac{1}{s_1^2}\frac{\partial^2}{\partial t^2}\right) \to \nabla_1^2$, $\left(\nabla^2 - \frac{1}{s_2^2}\frac{\partial^2}{\partial t^2}\right) \to \nabla_2^2, \nabla^2 = \frac{\partial^2}{\partial x_1^2} + \frac{\partial^2}{\partial x_2^2}$)

$$\nabla_1^2 \phi = 0, \quad \nabla_2^2 \psi = 0 \tag{10.3.3}$$

where

$$\nabla_1^2 = \frac{\partial^2}{\partial x^2} + \frac{\partial^2}{\partial y_1^2}, \quad \nabla_1^2 = \frac{\partial^2}{\partial x^2} + \frac{\partial^2}{\partial y_2^2} \tag{10.3.4a}$$

$$y_j = \beta_j y, \quad \beta_j = \sqrt{1 - V^2/c_j^2}, \quad j = 1, 2 \tag{10.3.4b}$$

Let complex variables z_j be

$$z_j = x + \mathrm{i} y_j \ (\mathrm{i} = \sqrt{-1}) \tag{10.3.5}$$

solution of Eq. (10.3.3) is

$$\phi = \mathrm{Im}\, F_1(z_1), \quad \psi = \mathrm{Im}\, F_2(z_2) \tag{10.3.6}$$

where $F_1(z_1)$ and $F_2(z_2)$ are analytic functions of z_1 and z_2, respectively, and Im marks the imaginary part of a complex function.

The boundary condition (10.3.1) determines the analytic functions as

$$\phi(x, y_1) = \frac{A_1}{2\pi} \arctan \frac{y_1}{x}, \quad \psi(x, y_2) = \frac{A_2}{2\pi} \arctan \frac{y_2}{x} \tag{10.3.7a}$$

with constants

$$A_1 = \frac{\alpha\, b_3^{\parallel} + R b_3^{\perp}}{\alpha^2 + R^2}, \quad A_2 = \frac{\alpha\, b_3^{\parallel} - R b_3^{\perp}}{\alpha^2 + R^2} \tag{10.3.7b}$$

and the displacement field is determined in the fixed coordinate system as

$$\begin{aligned} u_z(x,y,t) = \frac{1}{2\pi(\alpha^2+R^2)} \Bigg[& \left(\alpha^2 \arctan\frac{\beta_1 y}{x-Vt} + R^2 \arctan\frac{\beta_2 y}{x-Vt}\right) b_3^{\parallel} \\ & + \left(\arctan\frac{\beta_1 y}{x-Vt} - \arctan\frac{\beta_2 y}{x-Vt}\right) \alpha R b_3^{\perp} \Bigg] \end{aligned} \tag{10.3.8a}$$

$$\begin{aligned} w_z(x,y,t) = \frac{1}{2\pi(\alpha^2+R^2)} \Bigg[& \left(R^2 \arctan\frac{\beta_1 y}{x-Vt} + \alpha_3^2 \arctan\frac{\beta_2 y}{x-Vt}\right) b_3^{\perp} \\ & + \left(\arctan\frac{\beta_1 y}{x-Vt} - \arctan\frac{\beta_2 y}{x-Vt}\right) \alpha R b_3^{\parallel} \Bigg] \end{aligned} \tag{10.3.8b}$$

The expressions for strains and stresses are omitted here due to limitation of space.

We give the evaluation on the energy of the moving dislocation. Denote energy W per unit length on the moving dislocation which consists of the kinetic energy W_{k} and potential energy W_{p} defined by the integrals as

$$W_{\mathrm{k}} = \frac{1}{2}\rho \iint_{\Omega} \left[\left(\frac{\partial u_z}{\partial t}\right)^2 + \left(\frac{\partial w_z}{\partial t}\right)^2\right] \mathrm{d}x_1 \mathrm{d}x_2, \quad W_{\mathrm{p}} = \frac{1}{2} \iint_{\Omega} \left[\sigma_{ij}\frac{\partial u_z}{\partial t} + H_{ij}\frac{\partial w_z}{\partial t}\right] \mathrm{d}x_1 \mathrm{d}x_2 \tag{10.3.9}$$

respectively, where the integration should be taken over a ring $r_0 < r < R_0$, r_0 denotes the size of the dislocation core, and R_0 is the size of so-called dislocation net similar to those in conventional crystals. In general $r_0 \sim 10^{-8}$ cm, and $R_0 \sim 10^4 r_0$. Substituting displacement formulas and corresponding stress formulas into (10.3.9), we obtain $W_{\mathrm{k}} = \frac{k_{\mathrm{k}}}{4\pi} \ln \frac{R_0}{r_0}$,

$$W_{\mathrm{p}} = \frac{k_{\mathrm{p}}}{4\pi} \ln \frac{R_0}{r_0} \tag{10.3.10}$$

with

$$\begin{aligned} k_{\mathrm{k}} &= \frac{\rho V^2(\alpha^2+R^2)}{2}\left(\frac{A_1^2}{\beta_1} + \frac{A_2^2}{\beta_2}\right) \\ k_{\mathrm{p}} &= \frac{A_1^2}{2}\left(\mu\alpha^2 + (K_1 - K_2)\right)R^2 + 2\alpha R^2\Big)\left(\beta_1 + \frac{1}{\beta_1}\right) \\ &\quad + \frac{A_2^2}{2}\left(\mu R^2 + (K_1 - K_2)\alpha^2 - 2\alpha R^2\right)\left(\beta_2 + \frac{1}{\beta_2}\right) \end{aligned} \tag{10.3.11}$$

and A_1, A_2 given by (10.3.7). Therefore, the total energy is

$$W = \frac{k_{\mathrm{k}} + k_{\mathrm{p}}}{4\pi} \ln \frac{R_0}{r_0} \tag{10.3.12}$$

It is concluded that when $V \to s_2$, i.e. $\beta_2 \to 0$,, this leads to the infinity of the energy and is invalid; thus, s_2 is the limit of the velocity of a moving dislocation. Additionally, if $V \ll s_2$, the total energy can be written in the following simple form

$$W \approx W_0 + \frac{1}{2}\rho V^2 \left[(b_3^{\parallel})^2 + (b_3^{\perp})^2 \right] \frac{1}{4\pi} \ln \frac{R_0}{r_0} = W_0 + \frac{1}{2} m_0 V^2 \tag{10.3.13}$$

where W_0 is the elastic energy per unit length of a rest screw dislocation, i.e.

$$W_0 = \left[\mu (b_3^{\parallel})^2 + R (b_3^{\perp})^2 + 2 b_3^{\parallel} b_3^{\perp} R \right] \frac{1}{4\pi} \ln \frac{R_0}{r_0} \tag{10.3.14}$$

and m_0, the so-called apparent mass of the dislocation per unit length in the case considered

$$m_0 = \left[\mu (b_3^{\parallel})^2 + R (b_3^{\perp})^2 + 2 b_3^{\parallel} b_3^{\perp} R \right] \frac{1}{4\pi} \ln \frac{R_0}{r_0} \tag{10.3.15}$$

It is evident that if $V = 0$, the solution reduces to that of static dislocation, which is given in 7.1.

Furthermore, if $b_3^{\perp} = 0, R = 0$, then $\varepsilon_1 = \mu$, $\beta_1 = \sqrt{1 - V^2/c_2^2}$, and $s_1 = c_2 = \sqrt{\mu/\rho}$ is the speed of transverse wave of conventional crystal; the above solution reduces to

$$\begin{aligned} u_z(x - Vt, y) &= \frac{b}{2\pi} \arctan \frac{\beta_1 y}{x - Vt} \\ \sigma_{yz} = \sigma_{zy} &= \frac{b}{2\pi} \frac{\mu \beta_1 (x - Vt)}{(x - Vt)^2 + \beta_1^2 y^2} \\ \sigma_{xz} = \sigma_{zx} &= -\frac{b}{2\pi} \frac{\mu \beta_1 y}{(x - Vt)^2 + \beta_1^2 y^2} \\ W &\approx (\mu b^2 + \frac{1}{2}\rho V^2 b^2) \frac{1}{4\pi} \ln \frac{R_0}{r_0} \\ m_0 &= \frac{\rho b^2}{4\pi} \ln \frac{R_0}{r_0} \end{aligned} \tag{10.3.16}$$

This is identical to the well-known Eshelby solution for crystals [17].

The above discussion is valid for anti-plane elasticity of three-dimensional cubic or one-dimensional hexagonal quasicrystals; only the material constants $\mu, K_1 - K_2$ and R need to be replaced by C_{44}, K_{44} and R_{44}, or by C_{44}, K_2, and R_3, respectively.

10.4 Mode III Moving Griffith Crack in Anti-plane Elasticity

As another application of above elastodynamic theory, we study a moving Griffith crack of Mode III, which moves with constant speed V along x_1 (see Fig. 10.1).

Here we also take the fixed coordinates (x_1, x_2, t) and moving coordinates (x, y).

In the moving coordinates, the boundary conditions are

$$\sqrt{x^2+y^2} \to \infty : \sigma_{ij} = 0, \quad H_{ij} = 0$$

$$y = 0, \quad |x| < a : \sigma_{yz} = -\tau, \quad H_{yz} = 0 \tag{10.4.1}$$

Assume that the Laplace equations have the solution

$$\phi(x_1, y_1) = \text{Re}\, F_1(z_1), \psi(x_1, y_2) = \text{Re}\, F_2(z_2). \tag{10.4.2}$$

Here $F_1(z_1)$ and $F_2(z_2)$ are any analytic functions of z_1 and z_2.

Because the boundary conditions (10.4.1) are more complicated than those given by (10.3.1), we must use conformal mapping

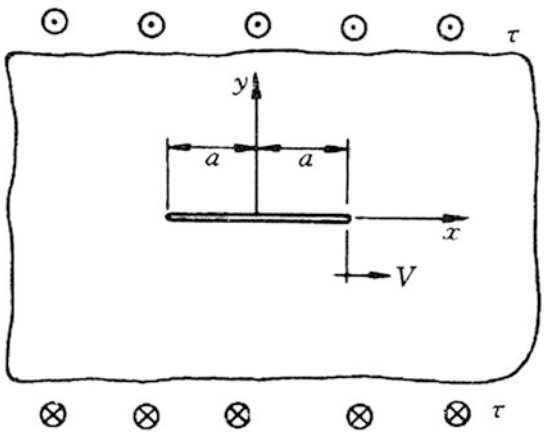

Fig. 10.1 Moving Griffith crack of Mode III

$$z_1, z_2 = \omega(\zeta) = \frac{a}{2}\left(\zeta + \zeta^{-1}\right) \tag{10.4.3}$$

to solve the problem at $\zeta(= \xi + \mathrm{i}\eta)$-plane.

After some calculations, we find the solution

$$F_1(z_1) = F_1[\omega(\zeta)] = G_1(\zeta) = \frac{i\Delta_1}{\Delta}\zeta, \quad F_2(z_2) = F_2[\omega(\zeta)] = G_2(\zeta) = \frac{i\Delta_2}{\Delta}\zeta \tag{10.4.4}$$

in which

$$\begin{aligned}
\Delta &= \beta_1\beta_2\left[(\alpha\mu + R^2)(\alpha(K_1 - K_2) - R^2) - R^2(\alpha + (K_1 - K_2))(\alpha - \mu)\right] \\
\Delta_1 &= \tau\alpha\beta_2\left(\alpha(K_1 - K_2) - R^2\right), \quad \Delta_2 = \tau\alpha\beta_1 R(\alpha + (K_1 - K_2))
\end{aligned} \tag{10.4.5}$$

Because there is the inverse mapping as

$$\zeta = \omega^{-1}(z_1) = \frac{z_1}{a} - \sqrt{\left(\frac{z_1}{a}\right)^2 - 1} = \omega^{-1}(z_2) = \frac{z_2}{a} - \sqrt{\left(\frac{z_2}{a}\right)^2 - 1}, \tag{10.4.6}$$

the manipulation afterwards can also be done in z_1-plane/z_2-plane.

The corresponding stresses are

$$\begin{aligned}
\sigma_{yz} &= \sigma_{zy} = (\alpha\mu + R^2)\beta_1 \frac{\partial}{\partial y_1}\mathrm{Re}\, F_1(z_1) + R(\alpha - \mu)\beta_2 \frac{\partial}{\partial y_2}\mathrm{Re}\, F_2(z_2) \\
\sigma_{xz} &= \sigma_{zx} = (\alpha\mu + R^2)\frac{\partial}{\partial x}\mathrm{Re}\, F_1(z_1) + R_3(\alpha - \mu)\beta_2 \frac{\partial}{\partial x}\mathrm{Re}\, F_2(z_2) \\
H_{zy} &= R_3(\alpha + (K_1 - K_2))\beta_1 \frac{\partial}{\partial y_1}\mathrm{Re}\, F_1(z_1) + (\alpha(K_1 - K_2) - R^2)\frac{\partial}{\partial y_2}\mathrm{Re}\, F_2(z_2) \\
H_{zx} &= R_3(\alpha + (K_1 - K_2))\beta_1 \frac{\partial}{\partial x}\mathrm{Re}\, F_1(z_1) + (\alpha(K_1 - K_2) - R^2)\frac{\partial}{\partial x}\mathrm{Re}\, F_2(z_2)
\end{aligned} \tag{10.4.7}$$

Substituting (10.4.6) into (10.4.4) then into (10.4.7), the stresses can be evaluated in explicit version, e.g.

$$\begin{aligned}
\sigma_{yz} = \sigma_{zy} = &-\frac{\tau}{\Delta}\left(\alpha\mu + R^2\right)\beta_1\beta_2\left(\alpha(K_1 - K_2) - R^2\right)\left[1 - \frac{d}{(d_1 d_2)^{\frac{1}{2}}}\cos\left(\theta - \frac{1}{2}\theta_1 - \frac{1}{2}\theta_2\right)\right] \\
&+ \frac{\tau}{\Delta}\beta_1\beta_2 R^2(\alpha + (K_1 - K_2))(\alpha - \mu)\left[1 - \frac{D}{(D_1 D_2)^{\frac{1}{2}}}\cos\left(\Theta - \frac{1}{2}\Theta_1 - \frac{1}{2}\Theta_2\right)\right]
\end{aligned} \tag{10.4.8}$$

with

$$\begin{aligned} d &= \sqrt{x^2+y_1^2}, \quad d_1 = \sqrt{(x-a)^2+y_1^2}, \quad d_2 = \sqrt{(x+a)^2+y_1^2}, \\ D &= \sqrt{x^2+y_2^2}, \quad D_1 = \sqrt{(x-a)^2+y_2^2}, \quad D_2 = \sqrt{(x+a)^2+y_2^2}, \\ \theta &= \arctan\left(\frac{y_1}{x}\right), \quad \theta_1 = \arctan\left(\frac{y_1}{x-a}\right), \quad \theta_2 = \arctan\left(\frac{y_1}{x+a}\right) \\ \Theta &= \arctan\left(\frac{y_2}{x}\right), \quad \Theta_1 = \arctan\left(\frac{y_2}{x-a}\right), \quad \Theta_2 = \arctan\left(\frac{y_2}{x+a}\right) \end{aligned} \tag{10.4.9}$$

It is easy to prove that (10.4.8) satisfies the relevant boundary conditions and is the exact solution.

Similarly, $\sigma_{xz} = \sigma_{zx}$, H_{zx} and H_{zy} can also be expressed explicitly.

From (10.4.8), as $y = 0$, it yields

$$\sigma_{yz}(x,0) = \begin{cases} \frac{x\tau}{\sqrt{x^2-a^2}} - \tau, & |x| > a \\ -\tau, & |x<a| \end{cases} \tag{10.4.10}$$

The stress presents singularity of order $(x-a)^{-1/2}$ as $x \to a$.

The stress intensity factor for Mode III for phonon field is

$$K_I^{||} = \lim_{x \to a^+} \sqrt{\pi(x-a)}\sigma_{yz}(x,0) = \sqrt{\pi a}\tau \tag{10.4.11}$$

This is identical to the classical Yoffe solution [18], and the stress intensity factor is also independent from crack moving speed V.

Now we calculate energy of the moving crack, which is defined by

$$W = 2\int_0^a \left[\sigma_{zy}(x,0) \oplus H_{zy}(x,0)\right]\left[u_z(x,0) \oplus w_z(x,0)\right]\mathrm{d}x$$

$$\begin{aligned} W &= 2\int_0^a \left[\sigma_{zy}(x,0) \oplus H_{zy}(x,0)\right]\left[u_z(x,0) \oplus w_z(x,0)\right]\mathrm{d}x \\ &= \frac{1}{\Delta}(\Delta_1\alpha - \Delta_2 R)\tau\pi a = \frac{1}{\Delta}\left[\alpha\beta_2(\alpha(K_1-K_2)-R^2) - \beta_1 R^2(\alpha+(K_1-K_2))\right]\pi a^2\tau \end{aligned} \tag{10.4.12}$$

The crack energy release rate is

$$G = \frac{1}{2}\frac{\partial W}{\partial a} = \frac{1}{2\Delta}\left[\alpha\beta_2(\alpha(K_1-K_2)-R^2) - \beta_1 R^2(\alpha+(K_1-K_2)\right](K_I^{||})^2 \tag{10.4.13}$$

The above discussion, results, and conclusions are hold too for anti-plane elasticity of three-dimensional cubic or one-dimensional hexagonal quasicrystals, and only the material constants μ, $K_1 - K_2$ and R need to be replaced by C_{44}, K_{44}, and R_{44} or by C_{44}, K_2 and R_3, respectively.

10.5 Two-Dimensional Phonon-Phason Dynamics, Fundamental Solution

In contrast to Eq. (10.1.3) based on Bak's argument, we here use formulas of phonon-phason dynamics which is originated from hydrodynamics of Lubensky et al. (the detail can refer to Fan et al. [13])

$$\rho \frac{\partial^2 u_i}{\partial t^2} = \frac{\partial \sigma_{ij}}{\partial x_j}, \quad \kappa \frac{\partial w_i}{\partial t} = \frac{\partial H_{ij}}{\partial x_j} \tag{10.5.1}$$

where $\kappa = 1/\Gamma_w$, Γ_w is dissipation coefficient of phason field. The first equation is phonon elastodynamic equation (wave equation), the second equation is the equation of motion of phasons, and a diffusion equation comes from hydrodynamics of solid quasicrystals but after simplification. For coupling phonon-phason systems of quasicrystals, these two equations are coupled with each other. The detailed hydrodynamics of solid quasicrystals can be found in Major Appendix of this book, and we here do not concern the aspect, which is beyond the scope discussed in this chapter.

Li [19] studies the phonon-phason dynamics for two-dimensional decagonal quasicrystals starting from Eq. (10.5.1) and obtains the following wave equations in plane deformation case

$$M\nabla^2 u_x + (L+M)\frac{\partial}{\partial x}\left(\frac{\partial u_x}{\partial x} + \frac{\partial u_y}{\partial y}\right) + R\left[\left(\frac{\partial^2}{\partial x^2} - \frac{\partial^2}{\partial y^2}\right) w_x + 2\frac{\partial^2 w_y}{\partial x \partial y}\right] = \rho \frac{\partial^2 u_x}{\partial t^2}, \tag{10.5.2}$$

$$M\nabla^2 u_y + (L+M)\frac{\partial}{\partial y}\left(\frac{\partial u_x}{\partial x} + \frac{\partial u_y}{\partial y}\right) + R\left[\left(\frac{\partial^2}{\partial x^2} - \frac{\partial^2}{\partial y^2}\right) w_y - 2\frac{\partial^2 w_x}{\partial x \partial y}\right] = \rho \frac{\partial^2 u_y}{\partial t^2}, \tag{10.5.3}$$

$$K_1 \nabla^2 w_x + R\left[\left(\frac{\partial^2}{\partial x^2} - \frac{\partial^2}{\partial y^2}\right) u_x - 2\frac{\partial^2 u_y}{\partial x^2}\right] = \kappa \frac{\partial w_x}{\partial t}, \tag{10.5.4}$$

$$K_1 \nabla^2 w_y + R\left[\left(\frac{\partial^2}{\partial x^2} - \frac{\partial^2}{\partial y^2}\right) u_y + 2\frac{\partial^2 u_x}{\partial x \partial y}\right] = \kappa \frac{\partial w_y}{\partial t}, \tag{10.5.5}$$

where $\nabla^2 = \partial_1^2 + \partial_2^2$. If introduce a function Y

$$u_1 = L_1 Y, \qquad u_2 = L_2 Y, \tag{10.5.6}$$

in which $L_j (j = 1, 2)$ are two unknown linear operators, will be determined as below.

In order to find the explicit expressions of $L_j (j = 1, 2)$, substituting (10.5.6) into (10.5.4) and (10.5.5) yields

$$K_1 \nabla^2 w_1 + R\left[\left(\frac{\partial^2}{\partial x^2} - \frac{\partial^2}{\partial y^2}\right) L_1 Y - 2\frac{\partial^2}{\partial x \partial y} L_2 Y\right] = \kappa \dot{w}_1, \tag{10.5.7}$$

$$K_1 \nabla^2 w_2 + R\left[\left(\frac{\partial^2}{\partial x^2} - \frac{\partial^2}{\partial y^2}\right) L_2 Y + 2\frac{\partial^2}{\partial x \partial y} L_1 Y\right] = \kappa \dot{w}_2, \tag{10.5.8}$$

Thus, there are

$$w_1 = -R\left[\left(\frac{\partial^2}{\partial x^2} - \frac{\partial^2}{\partial y^2}\right) L_1 - 2\frac{\partial^2 L_2}{\partial x \partial y}\right] Z, \tag{10.5.9}$$

$$w_2 = -R\left[\left(\frac{\partial^2}{\partial x^2} - \frac{\partial^2}{\partial y^2}\right) L_2 + 2\frac{\partial^2 L_1}{\partial x \partial y}\right] Z, \tag{10.5.10}$$

$$Y = K_1 \nabla^2 Z - \kappa \dot{Z}, \tag{10.5.11}$$

Then (10.5.7) and (10.5.8) will be satisfied automatically, where Z represents a new unknown function. Substituting (10.5.9)–(10.5.11) and (10.5.6) into (10.5.2) and (10.5.3), respectively, leads to

$$\begin{aligned} &\left\{\left(K_1 \nabla^2 - \kappa \frac{\partial}{\partial t}\right)\left[(L+M)\frac{\partial^2}{\partial x^2} + M\nabla^2 - \rho \frac{\partial^2}{\partial t^2}\right] - R^2 \nabla^2 \nabla^2 \nabla^2\right\} L_1 Z \\ &+ (L+M)\left(K_1 \nabla^2 - \kappa \frac{\partial}{\partial t}\right) \frac{\partial^2}{\partial x \partial y} L_2 Z = 0, \end{aligned} \tag{10.5.12}$$

$$\begin{aligned} &\left\{\left(K_1 \nabla^2 - \kappa \frac{\partial}{\partial t}\right)\left[(L+M)\frac{\partial^2}{\partial y^2} + M\nabla^2 - \rho \frac{\partial^2}{\partial t^2}\right] - R^2 \nabla^2 \nabla^2 \nabla^2\right\} L_2 Z \\ &+ (L+M)\left(K_1 \nabla^2 - \kappa \frac{\partial}{\partial t}\right) \frac{\partial^2}{\partial x \partial y} L_1 Z = 0, \end{aligned} \tag{10.5.13}$$

Putting

$$L_1 Z = -\left(K_1\nabla^2 - \kappa\frac{\partial}{\partial t}\right)\frac{\partial^2}{\partial x\partial y}F, \tag{10.5.14}$$

$$L_2 Z = \frac{1}{L+M}\left\{\left(K_1\nabla^2 - \kappa\frac{\partial}{\partial t}\right)\left[(L+M)\frac{\partial^2}{\partial x^2} + M\nabla^2 - \rho\frac{\partial^2}{\partial t^2}\right] - R^2\nabla^2\nabla^2\nabla^2\right\}F, \tag{10.5.15}$$

Hence, one can find that (10.5.12) has been automatically satisfied, while (10.5.13) reduces to

$$\begin{aligned}&\left\{\left(K_1\nabla^2 - \kappa\frac{\partial}{\partial t}\right)\left[(2M+L)\nabla^2 - \rho\frac{\partial^2}{\partial t^2}\right] - R^2\nabla^2\nabla^2\nabla^2\right\}\\&\left[\left(K_1\nabla^2 - \kappa\frac{\partial}{\partial t}\right)\left(M\nabla^2 - \rho\frac{\partial^2}{\partial t^2}\right) - R^2\nabla^2\nabla^2\nabla^2\right]F = 0.\end{aligned} \tag{10.5.16}$$

In (10.5.13) and (10.5.14), L_1, L_2 denote operators. Similarly, if taking $L_1 Z$ and $L_2 Z$ in the following version

$$L_1 Z = \frac{1}{L+M}\left\{\left(K_1\nabla^2 - \kappa\frac{\partial}{\partial t}\right)\left[(L+M)\frac{\partial^2}{\partial y^2} + M\nabla^2 - \rho\frac{\partial^2}{\partial t^2}\right] - R^2\nabla^2\nabla^2\nabla^2\right\}F, \tag{10.5.17}$$

$$L_2 Z = -\left(K_1\nabla^2 - \kappa\frac{\partial}{\partial t}\right)\frac{\partial^2}{\partial x\partial y}F. \tag{10.5.18}$$

then it reduces to the final governing Eq. (10.5.16). As a check, in the static case, (10.5.15) reduces to

$$\nabla^2\nabla^2\nabla^2\nabla^2 F = 0; \tag{10.5.19}$$

this is Eq. (6.2.7) in Chap. 6, and the correctness of above derivation is proved.

The equations obtained above can be simplified further. Function F is decomposed into $F = F_1 + F_2$ so that $F_j (j = 1, 2)$ satisfies, respectively,

$$\left(K_1\nabla^2 - \kappa\frac{\partial}{\partial t}\right)\left[(2M+L)\nabla^2 - \rho\frac{\partial^2}{\partial t^2}\right]F_1 - R^2\nabla^2\nabla^2\nabla^2 F_1 = 0, \tag{10.5.20}$$

$$\left(K_1\nabla^2 - \kappa\frac{\partial}{\partial t}\right)\left(M\nabla^2 - \rho\frac{\partial^2}{\partial t^2}\right)F_2 - R^2\nabla^2\nabla^2\nabla^2 F_2 = 0, \tag{10.5.21}$$

or

$$\left[K_1(2M+L)-R^2\right]\nabla^2\nabla^2 F_1-\kappa(2M+L)\nabla^2\frac{\partial}{\partial t}F_1-\rho K_1\nabla^2\frac{\partial^2}{\partial t^2}F_1+\kappa\rho\frac{\partial^3}{\partial t^3}F_1 = 0, \tag{10.5.22}$$

$$\left(K_1M-R^2\right)\nabla^2\nabla^2 F_2-\kappa M\nabla^2\frac{\partial}{\partial t}F_2-\rho K_1\nabla^2\frac{\partial^2}{\partial t^2}F_2+\kappa\rho\frac{\partial^3}{\partial t^3}F_2=0. \tag{10.5.23}$$

These two equations are the final governing equations, which are "conjugated" through phonon-phason coupling constant R, and describe the interaction between wave propagation and diffusion. Otherwise, if $R=0$, then

$$F_1=\xi+\zeta, \tag{10.5.24}$$

$$F_2=\eta+\zeta, \tag{10.5.25}$$

and ξ and η satisfy

$$(2M+L)\nabla^2\xi=\rho\frac{\partial^2}{\partial t^2}\xi, \tag{10.5.26}$$

$$M\nabla^2\eta=\rho\frac{\partial^2}{\partial t^2}\eta, \tag{10.5.27}$$

This is entirely identical to the wave equations of the Lamé potentials. If the material is isotropic, then $L=\lambda$ and $M=\mu$; λ and μ are the Lamé constants. In this case, ζ satisfies

$$K_1\nabla^2\zeta=\kappa\partial_t\zeta, \tag{10.5.28}$$

which is classical diffusion equation.

Once potentials $F_j(j=1,2)$ are determined, displacement field can be evaluated. For example, as denoting

$$\varphi=-\left(K_1\nabla^2-\kappa\partial_t\right)(\partial_1+\partial_2)F_1,\quad \psi=-\left(K_1\nabla^2-\kappa\partial_t\right)(\partial_1-\partial_2)F_2, \tag{10.5.29}$$

then

$$u_x=\left(K_1\nabla^2-\kappa\frac{\partial}{\partial t}\right)\left(\frac{\partial}{\partial x}\varphi+\frac{\partial}{\partial y}\psi\right), \tag{10.5.30}$$

$$u_y=\left(K_1\nabla^2-\kappa\frac{\partial}{\partial t}\right)\left(\frac{\partial}{\partial y}\varphi-\frac{\partial}{\partial x}\psi\right), \tag{10.5.31}$$

$$w_x = R\left(\Pi_2 \frac{\partial}{\partial x}\varphi - \Pi_1 \frac{\partial}{\partial y}\psi\right), \tag{10.5.32}$$

$$w_y = -R\left(\Pi_1 \frac{\partial}{\partial y}\varphi + \Pi_2 \frac{\partial}{\partial x}\psi\right), \tag{10.5.33}$$

where

$$\Pi_1 = 3\frac{\partial^2}{\partial x^2} - \frac{\partial^2}{\partial y^2}, \quad \Pi_2 = 3\frac{\partial^2}{\partial y^2} - \frac{\partial^2}{\partial x^2}$$

Furthermore, the stresses are

$$\begin{aligned}\sigma_{xx} = &\left[\left(K_1\nabla^2 - \kappa\frac{\partial}{\partial t}\right)\left(L\nabla^2 + 2M\frac{\partial^2}{\partial x^2}\right) - R^2\nabla^2\left(\frac{\partial^2}{\partial x^2} - \frac{\partial^2}{\partial y^2}\right)\right]\varphi \\ &+ 2\frac{\partial^2}{\partial x\partial y}\left[M\left(K_1\nabla^2 - \kappa\frac{\partial}{\partial t}\right) - R^2\nabla^2\right]\psi,\end{aligned} \tag{10.5.34}$$

$$\begin{aligned}\sigma_{yy} = &\left[\left(K_1\nabla^2 - \kappa\frac{\partial}{\partial t}\right)\left(L\nabla^2 + 2M\frac{\partial^2}{\partial y^2}\right) + R^2\nabla^2\left(\frac{\partial^2}{\partial x^2} - \frac{\partial^2}{\partial y^2}\right)\right]\varphi \\ &- 2\frac{\partial^2}{\partial x\partial y}\left[M\left(K_1\nabla^2 - \kappa\frac{\partial}{\partial t}\right) - R^2\nabla^2\right]\psi,\end{aligned} \tag{10.5.35}$$

$$\begin{aligned}\sigma_{xy} = &2\frac{\partial^2}{\partial x\partial y}\left[M\left(K_1\nabla^2 - \kappa\frac{\partial}{\partial t}\right) - R^2\nabla^2\right]\varphi \\ &- \left(\frac{\partial^2}{\partial x^2} - \frac{\partial^2}{\partial y^2}\right)\left[M\left(K_1\nabla^2 - \kappa\frac{\partial}{\partial t}\right) - R^2\nabla^2\right]\psi,\end{aligned} \tag{10.5.36}$$

$$\begin{aligned}H_{xx} = &R\left[K_1\frac{\partial^2}{\partial x^2}\Pi_2 - K_2\frac{\partial^2}{\partial y^2}\Pi_1 + \left(K_1\nabla^2 - \kappa\frac{\partial}{\partial t}\right)\left(\frac{\partial^2}{\partial x^2} - \frac{\partial^2}{\partial y^2}\right)\right]\varphi \\ &- R\frac{\partial^2}{\partial x\partial y}\left[K_1\Pi_1 + K_2\Pi_2 - 2\left(K_1\nabla^2 - \kappa\frac{\partial}{\partial t}\right)\right]\psi,\end{aligned} \tag{10.5.37}$$

$$\begin{aligned}H_{yy} = &-R\left[K_1\frac{\partial^2}{\partial y^2}\Pi_1 - K_2\frac{\partial^2}{\partial x^2}\Pi_2 - \left(K_1\nabla^2 - \kappa\frac{\partial}{\partial t}\right)\left(\frac{\partial^2}{\partial x^2} - \frac{\partial^2}{\partial y^2}\right)\right]\varphi \\ &- R\frac{\partial^2}{\partial x\partial y}\left[K_1\Pi_2 + K_2\Pi_1 - 2\left(K_1\nabla^2 - \kappa\frac{\partial}{\partial t}\right)\right]\psi,\end{aligned} \tag{10.5.38}$$

$$H_{xy} = R\frac{\partial^2}{\partial x \partial y}\left[K_1\Pi_2 + K_2\Pi_1 - 2\left(K_1\nabla^2 - \kappa\frac{\partial}{\partial t}\right)\right]\varphi - R\left[K_1\frac{\partial^2}{\partial y^2}\Pi_1 - K_2\frac{\partial^2}{\partial x^2}\Pi_2 - \left(K_1\nabla^2 - \kappa\frac{\partial}{\partial t}\right)\left(\frac{\partial^2}{\partial x^2} - \frac{\partial^2}{\partial y^2}\right)\right]\psi, \tag{10.5.39}$$

$$H_{yx} = -R\frac{\partial^2}{\partial x \partial y}\left[K_1\Pi_1 + K_2\Pi_2 - 2\left(K_1\nabla^2 - \kappa\frac{\partial}{\partial t}\right)\right]\varphi - R\left[K_1\frac{\partial^2}{\partial x^2}\Pi_2 - K_2\frac{\partial^2}{\partial y^2}\Pi_1 + \left(K_1\nabla^2 - \kappa\frac{\partial}{\partial t}\right)\left(\frac{\partial^2}{\partial x^2} - \frac{\partial^2}{\partial y^2}\right)\right]\psi, \tag{10.5.40}$$

It can be verified all equations in phonon-phason dynamics are satisfied for plane field of two-dimensional quasicrystals with point group 10 mm; the further work is solving these equations under prescribed boundary conditions.

Li [20] develops the work introduced above, extends it into the dynamics of decagonal quasicrystals of point groups $10, \overline{10}$ and $10/m$, determines relevant wave speeds, and analyses the wave propagation. Figures 10.2 and 10.3 show his calculating results partly.

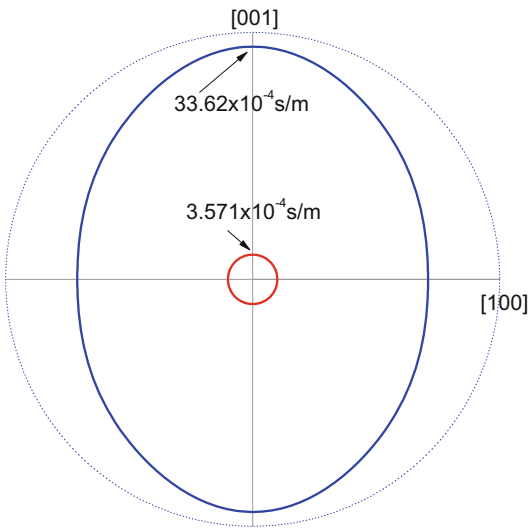

Fig. 10.2 A section of slow surface of acoustic wave propagation in xz-plane; material constants are $L = 30$ GPa, $M = 40$ GPa, $K_1 = 300$ MPa, $R = -0.05\mu$, $K_2 = -0.52K_1$ and $K_3 = 0.5K_1$

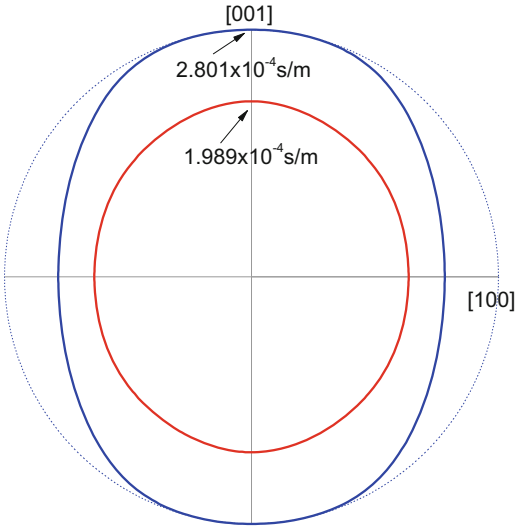

Fig. 10.3 A section of slow surface of acoustic wave propagation in xz-plane; material constants are $L = 75$ GPa, $M = 65$ GPa, $K_1 = 81$ GPa, $R = 0.4K_1$, $K_2 = -0.52K_1$ and $K_3 = 0.5K_1$

10.6 Phonon-Phason Dynamics and Solutions of Two-Dimensional Decagonal Quasicrystals

In this section, we would like to give a detailed description on the solution of two-dimensional quasicrystals based on the phonon-phason dynamics formulation.

The equations of deformation geometry and the generalized Hooke's law are the same as before which are not listed again here.

By using the dynamic equations (10.5.1) in Sect. 10.5, i.e. the so-called phonon-phason equations for quasicrystals, we can create the formalism for two-dimensional quasicrystals for the new dynamics. As an application of the formulation, some dynamic crack solutions are given in this section.

10.6.1 The Mathematical Formalism of Dynamic Crack Problems of Decagonal Quasicrystals

Over 200 quasicrystals observed to date, there are over 70 two-dimensional decagonal quasicrystals; so these kinds of solid phases play an important role in the material. For simplicity, here only point group 10-mm two-dimensional decagonal quasicrystal will be considered herein. We denote the periodic direction as the z-axis and the quasiperiodic plane as the xy-plane. Assume that a Griffith crack in the solid along the periodic direction, i.e. the z-axis. It is obvious that elastic field induced by a uniform tensile stress at upper and lower surfaces of the specimen is independent of z, so $\partial/\partial z = 0$. In this case, the stress–strain relations are reduced to

$$
\begin{aligned}
\sigma_{xx} &= L(\varepsilon_{xx}+\varepsilon_{yy})+2M\varepsilon_{xx}+R(w_{xx}+w_{yy})\\
\sigma_{yy} &= L(\varepsilon_{xx}+\varepsilon_{yy})+2M\varepsilon_{yy}-R(w_{xx}+w_{yy})\\
\sigma_{xy} &= \sigma_{yx}=2M\varepsilon_{xy}+R(w_{yx}-w_{xy})\\
H_{xx} &= K_1 w_{xx}+K_2 w_{yy}+R(\varepsilon_{xx}-\varepsilon_{yy})\\
H_{yy} &= K_1 w_{yy}+K_2 w_{xx}+R(\varepsilon_{xx}-\varepsilon_{yy})\\
H_{xy} &= K_1 w_{xy}-K_2 w_{yx}-2R\varepsilon_{xy}\\
H_{yx} &= K_1 w_{yx}-K_2 w_{xy}+2R\varepsilon_{xy}
\end{aligned}
\tag{10.6.1}
$$

where $L=C_{12}, M=(C_{11}-C_{12})/2$ are the phonon elastic constants, K_1 and K_2 are the phason elastic constants, and R the phonon-phason coupling elastic constant.

Substituting (10.6.1) into (10.5.1), we obtain the equations of motion of decagonal quasicrystals as follows:

$$
\begin{aligned}
\frac{\partial^2 u_x}{\partial t^2} &= c_1^2\frac{\partial^2 u_x}{\partial x^2}+(c_1^2-c_2^2)\frac{\partial^2 u_y}{\partial x\partial y}+c_2^2\frac{\partial^2 u_x}{\partial y^2}+c_3^2\left(\frac{\partial^2 w_x}{\partial x^2}+2\frac{\partial^2 w_y}{\partial x\partial y}-\frac{\partial^2 w_x}{\partial y^2}\right)\\
\frac{\partial^2 u_y}{\partial t^2} &= c_2^2\frac{\partial^2 u_y}{\partial x^2}+(c_1^2-c_2^2)\frac{\partial^2 u_x}{\partial x\partial y}+c_1^2\frac{\partial^2 u_y}{\partial y^2}+c_3^2\left(\frac{\partial^2 w_y}{\partial x^2}-2\frac{\partial^2 w_x}{\partial x\partial y}-\frac{\partial^2 w_y}{\partial y^2}\right)\\
\frac{\partial w_x}{\partial t} &= d_1^2\left(\frac{\partial^2 w_x}{\partial x^2}+\frac{\partial^2 w_x}{\partial y^2}\right)+d_2^2\left(\frac{\partial^2 u_x}{\partial x^2}-2\frac{\partial^2 u_y}{\partial x\partial y}-\frac{\partial^2 u_x}{\partial y^2}\right)\\
\frac{\partial w_y}{\partial t} &= d_1^2\left(\frac{\partial^2 w_y}{\partial x^2}+\frac{\partial^2 w_y}{\partial y^2}\right)+d_2^2\left(\frac{\partial^2 u_y}{\partial x^2}+2\frac{\partial^2 u_x}{\partial x\partial y}-\frac{\partial^2 u_y}{\partial y^2}\right)
\end{aligned}
\tag{10.6.2}
$$

where

$$
c_1=\sqrt{\frac{L+2M}{\rho}},\quad c_2=\sqrt{\frac{M}{\rho}},\quad c_3=\sqrt{\frac{R}{\rho}},\quad d_1=\sqrt{\frac{K_1}{\kappa}}\quad\text{and}\quad d_2=\sqrt{\frac{R}{\kappa}},
$$
$$
d_3=\sqrt{\frac{K_2}{\kappa}}
\tag{10.6.3}
$$

Note that constants c_1, c_2 and c_3 have the meaning of elastic wave speeds, while d_1^2, d_2^2 and d_3^2 do not represent wave speed; they are diffusive coefficients.

The decagonal quasicrystal with a crack is shown in Fig. 10.4. It is a rectangular specimen with a central crack of length $2a(t)$ subjected to a dynamic or static tensile stress at its ends ED and FC, in which $a(t)$ represents the crack length being a function of time, and for dynamic initiation of crack growth, the crack is stable, so $a(t)=a_0=$ constant, for fast crack propagation, $a(t)$ varies with time. At first we consider dynamic initiation of crack growth, then study fast crack propagation. Due to the symmetry of the specimen, only the upper right quarter is considered.

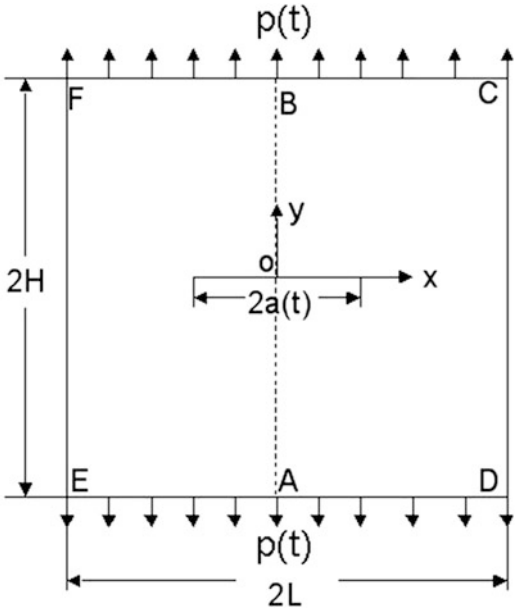

Fig. 10.4 Specimen with a central crack

Referring to the upper right part and considering a fix grips case, the following boundary conditions should be satisfied:

$$\begin{array}{llll}
u_x = 0,\ \sigma_{yx} = 0, w_x = 0, H_{yx} = 0 & \text{on } x = 0 & \text{for } 0 \le y \le H & \\
\sigma_{xx} = 0,\ \sigma_{yx} = 0, H_{xx} = 0, H_{yx} = 0 & \text{on } x = L & \text{for } 0 \le y \le H & \\
\sigma_{yy} = p(t),\ \sigma_{xy} = 0, H_{yy} = 0, H_{xy} = 0 & \text{on } y = H & \text{for } 0 \le x \le H & (10.6.4) \\
\sigma_{yy} = 0,\ \sigma_{xy} = 0, H_{yy} = 0, H_{xy} = 0 & \text{on } y = 0 & \text{for } 0 \le x \le a(t) & \\
u_y = 0,\ \sigma_{xy} = 0, w_y = 0, H_{xy} = 0 & \text{on } y = 0 & \text{for } a(t) \le x \le L &
\end{array}$$

in which $p(t) = p_0 f(t)$ is a dynamic load if $f(t)$ varies with time; otherwise, it is a static load (i.e. if $f(t) = \text{const}$), and $p_0 = \text{const}$ with the stress dimension.

The initial conditions are

$$\begin{array}{ll}
u_x(x, y, t)|_{t=0} = 0 & u_y(x, y, t)|_{t=0} = 0 \\
w_x(x, y, t)|_{t=0} = 0 & w_y(x, y, t)|_{t=0} = 0 \\
\frac{\partial u_x(x,y,t)}{\partial t}|_{t=0} = 0 & \frac{\partial u_y(x,y,t)}{\partial t}|_{t=0} = 0
\end{array} \qquad (10.6.5)$$

For implementation of finite difference, all field variables in governing Eq. (10.6.2) and boundary-initial conditions (10.6.4) and (10.6.5) must be expressed by displacements and their derivatives. This can be done through the constitutive equations (10.6.1). The detail of the finite difference scheme is given in Appendix of this chapter.

For the related parameters in this section, the experimentally determined mass density for decagonal Al–Ni–Co quasicrystal $\rho = 4.186 \times 10^{-3}$ g mm^{-3} is used

and phonon elastic moduli are $C_{11} = 2.3433, C_{12} = 0.5741 (10^{12}\ \text{dyn/cm}^2 = 10^2\ \text{GPa})$ which are obtained by resonant ultrasound spectroscopy [21], we have also chosen phason elastic constants $K_1 = 1.22$ and $K_2 = 0.24 (10^{12}\ \text{dyn/cm}^2 = 10^2\ \text{GPa})$ estimated by Monte Carlo simulation [22] and $\Gamma_w = 1/\kappa = 4.8 \times 10^{-19}\ \text{m}^3\ \text{s/kg} = 4.8 \times 10^{-10}\ \text{cm}^3\ \mu\text{s/g}$ [23]. The coupling constant R has been measured for some special cases recently, see Chaps. 6 and 9, respectively. In computation, we take $R/M = 0.01$ for coupling case corresponding to quasicrystals, and $R/M = 0$ for decoupled case in which the latter corresponds to crystals.

10.6.2 Examination on the Physical Model

In order to verify the correctness of the suggested model and the numerical simulation, we first explore the specimen without a crack. We know that there are the fundamental solutions characterizing time variation natures based on wave propagation of phonon field and on motion of diffusion according to mathematical physics

$$\begin{cases} u \sim \mathrm{e}^{\mathrm{i}\omega(t-x/c)} \\ w \sim \frac{1}{\sqrt{t-t_0}} \mathrm{e}^{-(x-x_0)^2/\Gamma_w(t-t_0)} \end{cases} \tag{10.6.6}$$

where ω is a frequency; c, a speed of the wave; t, the time; t_0, a special value of t, x, a distance; x_0, a special value of x; and Γ_w, the kinetic coefficient of phason defined previously.

Comparison results are shown in Figs. 10.5, 10.6 and 10.7, in which the solid line represents the numerical solution of quasicrystals, and the dotted line represents

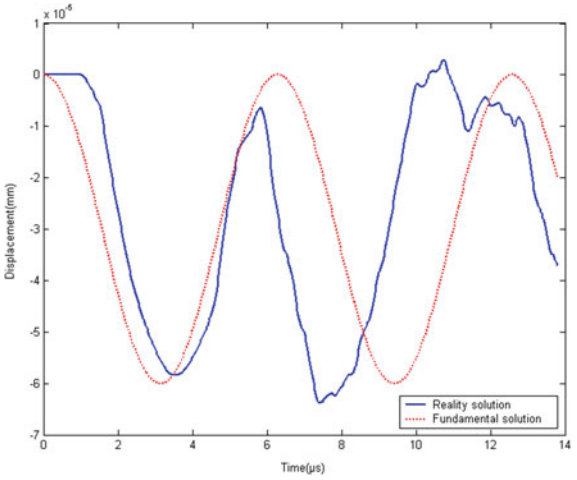

Fig. 10.5 Displacement component of phonon field u_x versus time

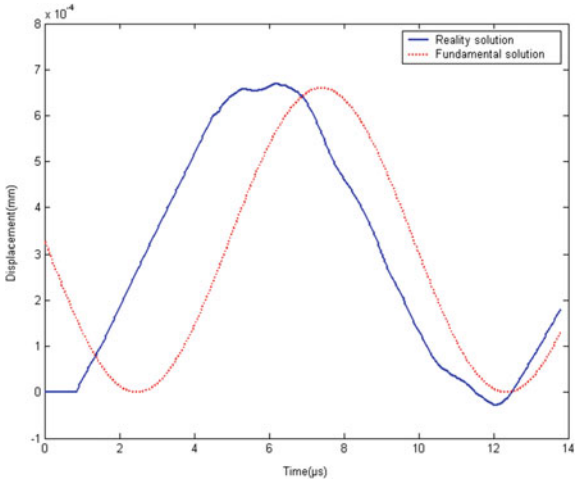

Fig. 10.6 Displacement component of phonon field u_y versus time

fundamental solution of Eq. (10.6.6). From Figs. 10.5 and 10.6 we can see that both displacement components of phonon field are excellent agreement to the fundamental solutions. However, there are some differences because the phonon field is influenced by phason field and the phonon-phason coupling effect. From Fig. 10.7, in the phason field we find that the phason mode presents diffusive nature in the overall tendency, but because of influence of the phonon and phonon-phason coupling, it can also have some character of fluctuation. So the model describes the dynamic behaviour of phonon field and phason field indeed. This also shows that the mathematical modelling of the present work is valid.

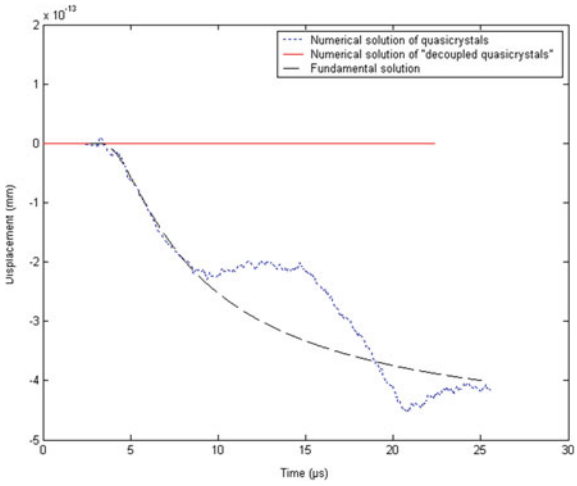

Fig. 10.7 Displacement component of phason field w_x versus time

10.6.3 Testing the Scheme and the Computer Programme

10.6.3.1 Stability of the Scheme

The stability of the scheme is the core problem of finite difference method which depends upon the choice of parameter $\alpha = c_1\tau/h$, which is the ratio between time step and space step substantively. The choice is related to the ratio c_1/c_2, i.e. the ratio between speeds of elastic longitudinal and transverse waves of the phonon field. To determine the upper bound for the ration to guarantee the stability, according to our computational practice and considering the experiences of computations for conventional materials, we choose $\alpha = 0.8$ in all cases and results are stable.

10.6.3.2 Accuracy Test

The stability is only a necessary condition for successful computation. We must check the accuracy of the numerical solution. This can be realized through some comparison with some well-known classical solutions (analytic as well as numerical solutions). For this purpose, the material constants in the computation are chosen as $c_1 = 7.34, c_2 = 3.92$ (mm/ μs) and $\rho = 5 \times 10^3 \mathrm{kg}/m^3$, $p_0 = 1\mathrm{MPa}$ which are the same with those in Refs. [24–26] (but are different from those listed in Sect. 10.6.1). At first the comparison of the classical exact analytic solution is carried out; in this case we put $w_x = w_y = 0$ (i.e. $K_1 = K_2 = R = 0$) for the numerical solution. The comparison has been done with the key physical quantity—dynamic stress intensity factor, which is defined by

$$K_{\mathrm{I}}(t) = \lim_{x \to a_0^+} \sqrt{\pi(x - a_0)}\sigma_{yy}(x, 0, t) \tag{10.6.7}$$

The normalized dynamic stress intensity factor can be denoted as $K_I(t)/K_I^{\mathrm{static}}$, in which K_I^{static} is the corresponding static stress intensity factor, whose value here is taken as $\sqrt{\pi a_0}p_0$ (the reason for this refers to Sect. 10.6.3.3). For the dynamic initiation of crack growth in classical fracture dynamics, there is the only exact analytic solution—the Maue's solution [24], but the configuration of whose specimen is quite different from that of our specimen. Maue studied a semi-infinite crack in an infinite body and subjected to a Heaviside impact loading at the crack surface. While our specimen is a finite size rectangular plate with a central crack, the applied stress is around the external boundary of the specimen. Generally, the Maue model cannot describe the interaction between wave and external boundaries. However, consider a very short time interval, i.e. during the period between the stress wave from the external boundary arriving at the crack tip (this time is denoted by t_1) and before the reflecting by external boundary stress wave emanating from the crack tip in the finite size specimen (the time is marked as t_2). During this special very short

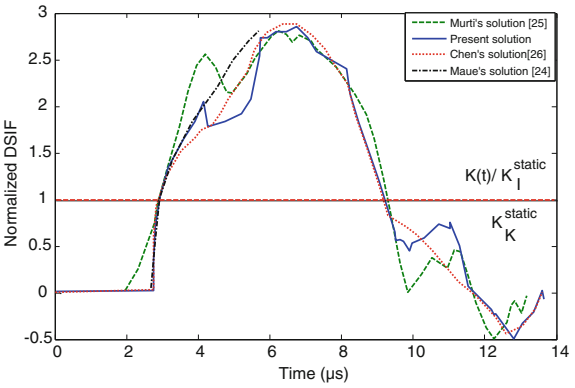

Fig. 10.8 Comparison of the present solution with analytic solution and other numerical solution for conventional structural materials given by other authors

time interval, our specimen can be seen as an "infinite specimen". Comparison given by Fig. 10.8 shows the numerical results are in excellent agreement with those of Maue's solution within the short interval in which the solution is valid.

Our solution corresponding to the case of $w_x = w_y = 0$ is also compared with numerical solutions of conventional crystals, e.g. Murti's solution [25] and Chen's solutions [26], which are also shown in Fig. 10.8; it is evident, and our solution presents very high precise.

10.6.3.3 Influence of Mesh Size (Space Step)

The mesh size or the space step of the algorithm can influence the computational accuracy too. To check the accuracy of the algorithm, we take different space steps shown in Table 10.1, which indicates if $h = a_0/40$ the accuracy is good enough. The check is carried out through static solution, because the static crack problem in infinite body of decagonal quasicrystals has exact solution, given by Li and Fan in Sect. 8.3 of Chap. 8; the normalized static intensity factor is equal to unit. In the static case, there is no wave propagation effect, $L/a_0 \geq 3, H/a_0 \geq 3$; the effect of boundary to solution is very weak, and for our present specimen $L/a_0 \geq 4$, $H/a_0 \geq 8$, which may seen as an infinite specimen, the normalized static stress intensity factor is approximately but with highly precise equal to unit. The table shows that the algorithm is with a quite highly accuracy when $h = a_0/40$.

Table 10.1 Normalized static S.I.F. of quasicrystals for different space steps

H	$a_0/10$	$a_0/15$	$a_0/20$	$a_0/30$	$a_0/40$
$\bar{K}$	0.9259	0.94829	0.96229	0.97723	0.99516
Errors (%)	7.410	5.171	3.771	2.277	0.484

10.6.4 Results of Dynamic Initiation of Crack Growth

The dynamic crack problem presents two "phases" in the process: the dynamic initiation of crack growth and fast crack propagation. In the phase of dynamic initiation of crack growth, the length of the crack is constant, assuming $a(t) = a_0$. The specimen with stationary crack that is subjected to a rapidly varying applied load $p(t) = p_0 f(t)$, where p_0 is a constant with stress dimension and $f(t)$ is taken as the Heaviside function. It is well known the coupling effect between phonon and phason is very important, which reveals the distinctive physical properties including mechanical properties, and makes quasicrystals distinguish the periodic crystals. So studying the coupling effect is significant.

The dynamic stress intensity factor $K_1(t)$ for quasicrystals has the same definition given by (10.6.7), whose numerical results are plotted in Fig. 10.8, where the normalized dynamics stress intensity factor $K_1(t)/\sqrt{\pi a_0} p_0$ is used. There are two curves in the figure; one represents quasicrystal, i.e. $R/M = 0.01$ and the other describes periodic crystals corresponding to $R/M = 0$; the two curves of the figure are apparently different, though they are similar to some extends. Because of the phonon-phason coupling effect, the mechanical properties of the quasicrystals are obviously different from the classical crystals. Thus, the coupling effect plays an important role.

In Fig. 10.9, t_0 represents the time that the wave from the external boundary propagates to the crack surface, in which $t_0 = 2.6735$ μs. So the velocity of the wave propagation is $v_0 = H/t_0 = 7.4807$ km/s, which is just equal to the longitudinal wave speed $c_1 = \sqrt{(L+2M)/\rho}$. This indicates that for the complex system of wave propagation-motion of diffusion coupling, the phonon wave propagation presents dominating role.

There are many oscillations in the figure, especially the stress intensity factor. These oscillations characterize the reflection and diffraction between waves coming from the crack surface and the specimen boundary surfaces. The oscillations are

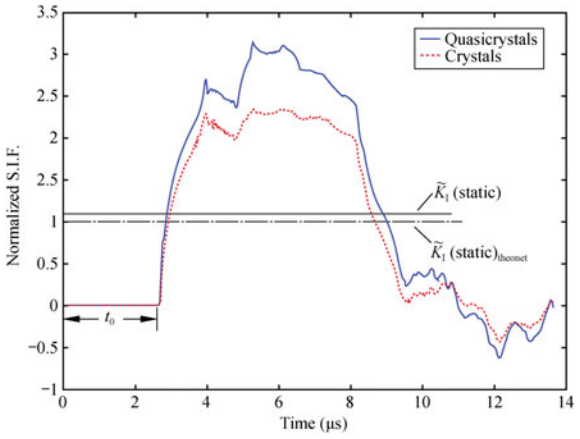

Fig. 10.9 Normalized dynamics stress intensity factor (DSIF) versus time

influenced by the material constants and specimen geometry including the shape and size very much.

10.6.5 Results of the Fast Crack Propagation

In this section, we focus on the discussion for the "phase" of fast crack propagation. To explore the inertia effect caused by the fast crack propagation, the specimen is designed under the action of constant load $P(t) = p$ rather than time-varying load, but the crack grows with high speed in this case. The problem for fast crack propagation is a nonlinear problem because of one part of the boundaries—crack is with unknown length beforehand. For this moving boundary problem, we must give additional condition for solution to be definite. That is, we must give a criterion checking crack propagation or crack arrest at the growing crack tip. This criterion can be imposed in different ways, e.g. the critical stress criterion or critical energy criterion. The stress criterion used in this paper $\sigma_{yy} < \sigma_c$ represents crack arrest, $\sigma_{yy} = \sigma_c$ represents critical state, and $\sigma_{yy} > \sigma_c$ represents crack propagation. Here we take $\sigma_c = 450$ MPa for decagonal Al–Ni–Co quasicrystals, which was obtained by referring measured value by Meng et al. for decagonal Al–Cu–Co quasicrystals, refer to Ref. [2] in Chap. 8, and the modification by referring the hardness of alloys Al–Ni–Co and Al–Cu–Co, and the hardness on decagonal Al–Ni–Co can be found in paper given by Takeuchi et al. [28]. The simulation of a fracturing process runs as follows:

Given the specimen geometry and its material constants, we first solve the initial dynamic problem in the way previously described. When the stress σ_{yy} reaches a prescribed critical value σ_c, the crack is extended by one grid interval. The crack now continues to grow, by one grid interval at a time, as long as the σ_{yy} stress level ahead of the propagating crack tip reaches the value of σ_c. During the propagation stage, the time that elapses between two sequential extensions is recorded and the corresponding velocity is evaluated.

The crack velocity for quasicrystals and periodic crystals is constructed in Fig. 10.10, from which we observe that the velocity in quasicrystals is lower than that of the periodic crystals; the phonon-phason coupling makes the quasicrystals being different from periodic crystals. The reason for this is not so clear.

We find that the fast crack propagating velocity is obviously different in quasicrystals compared to the crystalline and conventional engineering materials. Next we will explore the velocity under different loads in quasicrystal. The above-described procedure was conducted, keeping the same geometry and material constants. With various loads, the relation between velocity and crack growth is constructed in Fig. 10.10. The crack velocity increases smoothly with increasing applied load. It is understandable that as the load increases, the time to reach the critical stress is less, so the velocity increases (Fig. 10.11).

As shown in Fig. 10.12, the calculated crack propagation results show some roughness as the load increases. Currently, there is no experimental observation for

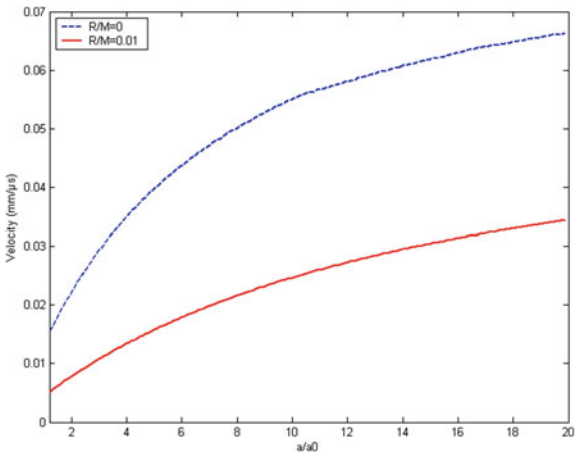

Fig. 10.10 Crack velocity versus normalized crack size with different phonon-phason coupling elastic constants

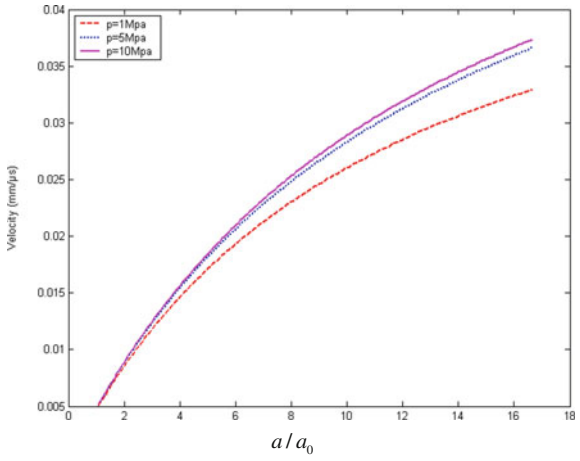

Fig. 10.11 Variation of crack velocity versus normalized crack size for different load levels

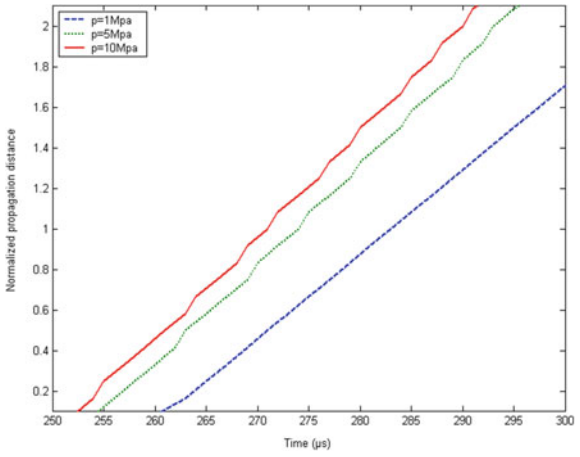

Fig. 10.12 Normalized crack growth size $(a - a_0)/a_0$ of crack tip versus time for different load levels

fast crack propagation, though Ebert et al. [27] made some observation by scanning tunnelling microscopy for quasistatic crack growth. Because the fast crack propagation and quasistatic crack growth belong to two different regimes, the comparison cannot be easily made.

10.7 Phonon-Phason Dynamics and Applications to Fracture Dynamics of Icosahedral Quasicrystals

10.7.1 Basic Equations, Boundary and Initial Conditions

The elasto-/hydrodynamics of icosahedral Al–Pd–Mn quasicrystals is more interesting topic than that of decagonal Al–Ni–Co quasicrystals, especially a rich set of experimental data for elastic constants can be used for the computation described here. From the previous section, we know there is a lack of measured data for phason elastic constants, which are obtained by Monte Carlo simulation; this makes some undetermined factors for computational results for decagonal quasicrystals. This shows that the discussion on icosahedral quasicrystals is more necessary, and the formalism and numerical results are presented in this section.

If considering only the plane problem, especially for the crack problems, there are much of similarities with those discussed in the previous section. We present herein only the parts that are different.

For the plane problem, i.e.

$$\frac{\partial}{\partial z} = 0 \tag{10.7.1}$$

the linearized elasto-/hydrodynamics of icosahedral quasicrystals have non-zero displacements u_z, w_z apart from u_x, u_y, w_x, w_y, so in the strain tensors

$$\varepsilon_{ij} = \frac{1}{2}\left(\frac{\partial u_i}{\partial x_j} + \frac{\partial u_j}{\partial x_i}\right) \quad w_{ij} = \frac{\partial w_i}{\partial x_j}$$

It increases some non-zero components compared with those in two-dimensional quasicrystals. In connecting with this, in the stress tensors, the non-zero components increase too relatively to two-dimensional ones. With these reasons, the stress–strain relation presents different nature with that of decagonal quasicrystals though the generalized Hooke's law has the same form with that in one- and two-dimensional quasicrystals, i.e.

$$\sigma_{ij} = C_{ijkl}\varepsilon_{kl} + R_{ijkl}w_{kl} \quad H_{ij} = R_{klij}\varepsilon_{kl} + K_{ijkl}w_{kl}$$

In particular, the elastic constants are quite different from those discussed in the previous sections, in which the phonon elastic constants can be expressed such as

$$C_{ijkl} = \lambda\delta_{ij}\delta_{kl} + \mu(\delta_{ik}\delta_{jl} + \delta_{il}\delta_{jk}) \tag{10.7.2}$$

and the phason elastic constant matrix [K] and phonon-phason coupling elastic one [R] are defined by formula (9.1.6) in Chap. 9, which are not listed here again.

Substituting these non-zero stress components into the equations of motion

$$\rho\frac{\partial^2 u_i}{\partial t^2} = \frac{\partial \sigma_{ij}}{\partial x_j}, \quad \kappa\frac{\partial w_i}{\partial t} = \frac{\partial H_{ij}}{\partial x_j} \tag{10.7.3}$$

and through the generalized Hooke's law and strain–displacement relation, we obtain the final dynamic equations as follows:

$$\begin{aligned}
&\frac{\partial^2 u_x}{\partial t^2} + \theta\frac{\partial u_x}{\partial t} = c_1^2\frac{\partial^2 u_x}{\partial x^2} + (c_1^2 - c_2^2)\frac{\partial^2 u_y}{\partial x\partial y} + c_2^2\frac{\partial^2 u_x}{\partial y^2} + c_3^2\left(\frac{\partial^2 w_x}{\partial x^2} + 2\frac{\partial^2 w_y}{\partial x\partial y} - \frac{\partial^2 w_x}{\partial y^2}\right)\\
&\frac{\partial^2 u_y}{\partial t^2} + \theta\frac{\partial u_y}{\partial t} = c_2^2\frac{\partial^2 u_y}{\partial x^2} + (c_1^2 - c_2^2)\frac{\partial^2 u_x}{\partial x\partial y} + c_1^2\frac{\partial^2 u_y}{\partial y^2} + c_3^2\left(\frac{\partial^2 w_y}{\partial x^2} - 2\frac{\partial^2 w_x}{\partial x\partial y} - \frac{\partial^2 w_y}{\partial y^2}\right)\\
&\frac{\partial^2 u_z}{\partial t^2} + \theta\frac{\partial u_z}{\partial t} = c_2^2\left(\frac{\partial^2}{\partial x^2} + \frac{\partial^2}{\partial y^2}\right)u_z + c_3^2\left(\frac{\partial^2 w_x}{\partial x^2} - \frac{\partial^2 w_x}{\partial y^2} - 2\frac{\partial^2 w_y}{\partial x\partial y} + \frac{\partial^2 w_z}{\partial x^2} + \frac{\partial^2 w_z}{\partial y^2}\right)\\
&\frac{\partial w_x}{\partial t} + \theta w_x = d_1\left(\frac{\partial^2}{\partial x^2} + \frac{\partial^2}{\partial y^2}\right)w_x + d_2\left(\frac{\partial^2}{\partial x^2} - \frac{\partial^2}{\partial y^2}\right)w_z\\
&\qquad\qquad + d_3\left(\frac{\partial^2 u_x}{\partial x^2} - 2\frac{\partial^2 u_y}{\partial x\partial y} - \frac{\partial^2 u_x}{\partial y^2} + \frac{\partial^2 u_z}{\partial x^2} - \frac{\partial^2 u_z}{\partial y^2}\right)\\
&\frac{\partial w_y}{\partial t} + \theta w_y = d_1\left(\frac{\partial^2}{\partial x^2} + \frac{\partial^2}{\partial y^2}\right)w_y - d_2\frac{\partial^2 w_z}{\partial x\partial y} + d_3\left(\frac{\partial^2 u_y}{\partial x^2} + 2\frac{\partial^2 u_x}{\partial x\partial y} - \frac{\partial^2 u_y}{\partial y^2} - 2\frac{\partial^2 u_z}{\partial x\partial y}\right)\\
&\frac{\partial w_z}{\partial t} + \theta w_z = (d_1 - d_2)\left(\frac{\partial^2}{\partial x^2} + \frac{\partial^2}{\partial y^2}\right)w_z + d_2\left(\frac{\partial^2 w_x}{\partial x^2} - \frac{\partial^2 w_x}{\partial y^2} - 2\frac{\partial^2 w_y}{\partial x\partial y}\right) + d_3\left(\frac{\partial^2}{\partial x^2} + \frac{\partial^2}{\partial y^2}\right)u_z
\end{aligned} \tag{10.7.4}$$

in which

$$c_1 = \sqrt{\frac{\lambda + 2\mu}{\rho}}, \quad c_2 = \sqrt{\frac{\mu}{\rho}}, \quad c_3 = \sqrt{\frac{R}{\rho}}, \quad d_1 = \frac{K_1}{\kappa}, \quad d_2 = \frac{K_2}{\kappa}, \quad d_3 = \frac{R}{\kappa}, \tag{10.7.5}$$

Note that constants c_1, c_2 and c_3 have the meaning of elastic wave speeds, while d_1, d_2 and d_3 do not represent wave speed, but are diffusive coefficients, and parameter θ may be understood as a man-made damping coefficient as in the previous section.

Consider an icosahedral quasicrystal specimen with a Griffith crack shown in Fig. 10.4; all parameters of geometry and loading are the same with those given in the previous, but in the boundary conditions there are some different points, which are given as below

$$
\begin{aligned}
&u_x = 0, \sigma_{yx} = 0, \sigma_{zx} = 0, w_x = 0, H_{yx} = 0, H_{zx} = 0 \quad \text{on} \quad x = 0 \quad \text{for} \quad 0 \le y \le H \\
&\sigma_{xx} = 0, \sigma_{yx} = 0, \sigma_{zx} = 0, H_{xx} = 0, H_{yx} = 0, H_{zx} = 0 \quad \text{on} \quad x = L \quad \text{for} \quad 0 \le y \le H \\
&\sigma_{yy} = p(t), \sigma_{xy} = 0, \sigma_{zy} = 0, H_{yy} = 0, H_{xy} = 0, H_{zy} = 0 \quad \text{on} \quad y = H \quad \text{for} \quad 0 \le x \le L \\
&\sigma_{yy} = 0, \sigma_{xy} = 0, \sigma_{zy} = 0, H_{yy} = 0, H_{xy} = 0, H_{zy} = 0 \quad \text{on} \quad y = 04 \quad \text{for} \quad 0 \le x \le a(t) \\
&u_y = 0, \sigma_{xy} = 0, \sigma_{zy} = 0, w_y = 0, H_{xy} = 0, H_{zy} = 0 \quad \text{on} \quad y = 0 \quad \text{for} \quad a(t) < x \le L
\end{aligned}
\tag{10.7.6}
$$

The initial conditions are

$$
\begin{aligned}
&u_x(x,y,t)|_{t=0} = 0 \quad u_y(x,y,t)|_{t=0} = 0 \quad u_z(x,y,t)|_{t=0} = 0 \\
&w_x(x,y,t)|_{t=0} = 0 \quad w_y(x,y,t)|_{t=0} = 0 \quad w_z(x,y,t)|_{t=0} = 0 \\
&\frac{\partial u_x(x,y,t)}{\partial t}|_{t=0} = 0 \quad \frac{\partial u_y(x,y,t)}{\partial t}|_{t=0} = 0 \quad \frac{\partial u_z(x,y,t)}{\partial t}|_{t=0} = 0
\end{aligned}
\tag{10.7.7}
$$

10.7.2 Some Results

We now concentrate on investigating the phonon and phason fields in the icosahedral Al–Pd–Mn quasicrystal, in which we take $\rho = 5.1$ g/cm^3 and $\lambda = 74.2, \mu = 70.4$ (GPa) of the phonon elastic moduli, for phason ones $K_1 = 72, K_2 = -37$(MPa) (refer to Chap. 9) and the constant relevant to diffusion coefficient of phason is $\Gamma_w = 1/\kappa = 4.8 \times 10^{-19}$ m^3 s/kg $= 4.8 \times 10^{-10}$ cm^3 μs/g [23]. On the phonon-phason coupling constant, there is no measured result for icosahedral quasicrystals so far; we take $R/\mu = 0.01$ for quasicrystals and $R/\mu = 0$ for "decoupled quasicrystals" or crystals.

The problem is solved by the finite difference method; the principle, scheme and algorithm are illustrated as those in the previous section and shall not be repeated here. The testing for the physical model, scheme, algorithm and computer programme is similar to that given in Sect. 10.6.

The numerical results for dynamic initiation of crack growth problem, the phonon and phason displacements are shown in Fig. 10.13.

The dynamic stress intensity factor $K_{\mathrm{I}}(t)$ is defined by

$$
K_{\mathrm{I}}(t) = \lim_{x \to a_0^+} \sqrt{\pi(x - a_0)}\sigma_{yy}(x, 0, t)
$$

and the normalized dynamics stress intensity factor (S.I.F.) $\tilde{K}_{\mathrm{I}}(t) = K_{\mathrm{I}}(t)/\sqrt{\pi a_0}p_0$ is used; the results are illustrated in Fig. 10.14 in which the comparison with those of crystals is shown; one can see the effects of phason and phonon-phason coupling are evident very much.

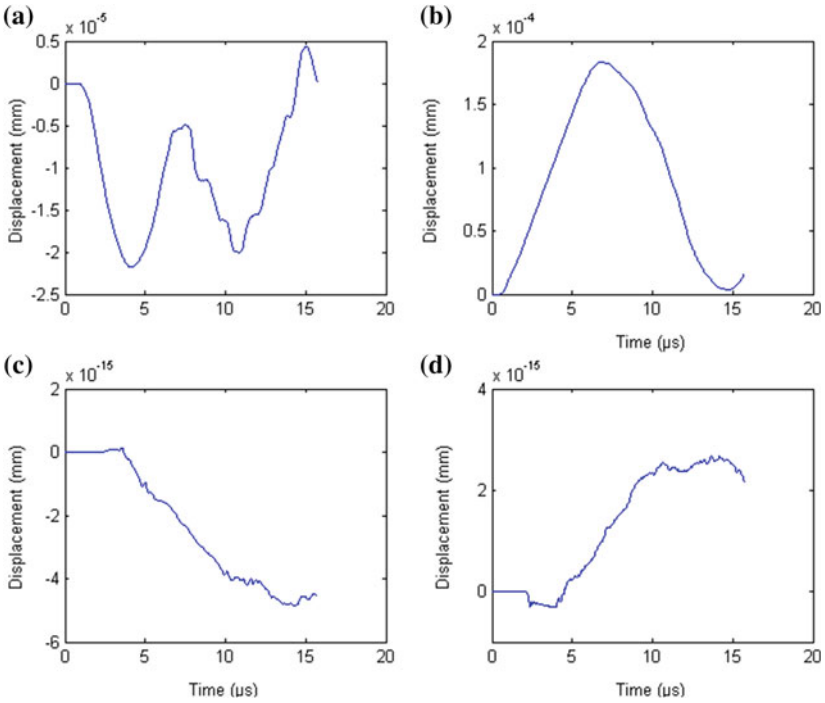

Fig. 10.13 Displacement components of quasicrystals versus time. **a** displacement component u_x; **b** displacement component u_y; **c** displacement component w_x; **d** displacement component w_y

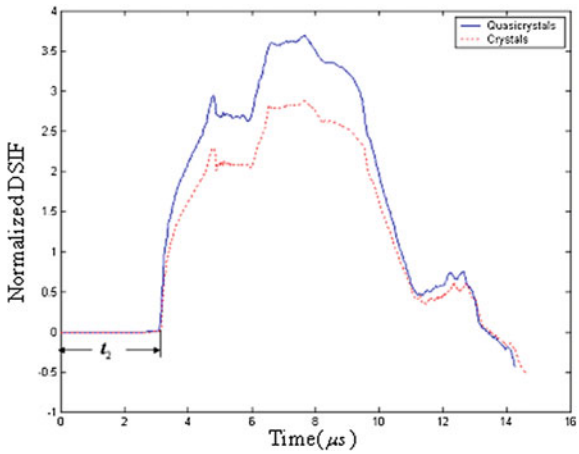

Fig. 10.14 Normalized dynamic stress intensity factor of central crack specimen under impact loading versus time

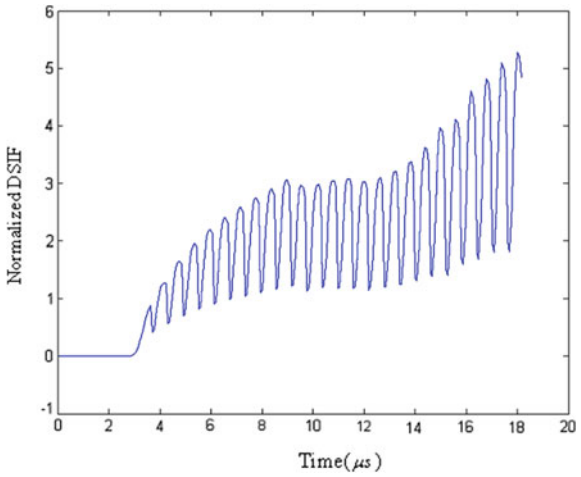

Fig. 10.15 Normalized stress intensity factor of propagating crack with constant crack speed versus time

For the fast crack propagation problem, the primary results are listed only the dynamic stress intensity factor versus time as given in Fig. 10.15.

Details of this work can are reported in Ref. [29].

10.7.3 Conclusion and Discussion

In Sects. 10.7.1 and 10.7.2, a new model on dynamic response of quasicrystals based on argument of Bak and argument of Lubensky et al. are formulated. This model regarded as an elasto-/hydrodynamics model for the material, or as a collaborating model of wave propagation and diffusion. This model is more complex than pure wave propagation model for conventional crystals, and the analytic solution is very difficult to obtain, except maybe for a few simple examples. Numerical procedure based on finite difference algorithm is developed. Computed results confirm the validity of wave propagation behaviour of phonon field and behaviour of diffusion of phason field. The interaction between phonons and phasons is also recorded.

The finite difference formalism is applied to analyse dynamic initiation of crack growth and fast crack propagation for two-dimensional decagonal Al–Ni–Co and three-dimensional icosahedral Al–Pd–Mn quasicrystals, and the displacement and stress fields around the tip of stationary and propagating cracks are revealed; the stress presents singularity with order $r^{-1/2}$, in which r denotes the distance measured from the crack tip. For the fast crack propagation, which is a nonlinear problem—moving boundary problem, one must provide additional condition for

determining solution. For this purpose, we give a criterion for checking crack propagation/crack arrest based on the critical stress criterion. Application of this additional condition for determining solution has helped us achieve the numerical simulation of the moving boundary value problem and reveal crack length-time evolution. However, more important and difficult problems are left open for further study.

10.8 Appendix of Chapter 10: The Detail of Finite Difference Scheme

Equations (10.6.2) subjected to conditions (10.6.4) and (10.6.5) are very complicated, and analytic solution for the boundary-initial value problem is not available at present, which have to be solved by numerical method. Here we extend the method of finite difference of Shmuely and Alterman [30] scheme for analysing crack problem for conventional engineering materials to quasicrystalline materials.

A grid is imposed on the upper right of the specimen shown in Fig. 10.16. For convenience, the mesh size h is taken to be the same in both x- and y-directions. The grid is extended beyond the half step by adding four special grid lines $x = -h/2, x = L + h/2, y = -h/2$, $y = H + h/2$ which form the grid boundaries.

Denoting the time step by τ and using central difference approximations, the finite difference formulation of Eq. (10.6.2), valid at the inner part of the grids, is

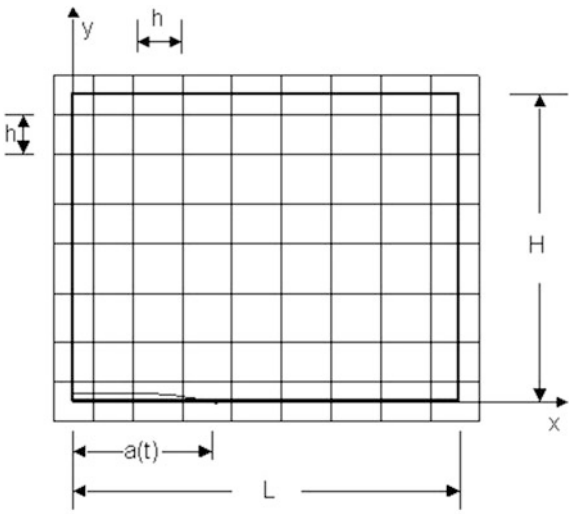

Fig. 10.16 Scheme of grid used

$$
\begin{aligned}
u_x(x,y,t+\tau) &= 2u_x(x,y,t) - u_x(x,y,t-\tau) + (\frac{\tau}{h}c_1)^2[u_x(x+h,y,t) - 2u_x(x,y,t) + u_x(x-h,y,t)] \\
&+ \left(\frac{\tau}{h}\right)^2(c_1^2 - c_2^2)[u_y(x+h,y+h,t) - u_y(x+h,y-h,t) \\
&- u_y(x-h,y+h,t) + u_y(x-h,y-h,t)] \\
&+ \left(\frac{\tau}{h}c_2\right)^2[u_x(x,y+h,t) - 2u_x(x,y,t) + u_x(x,y-h,t)] \\
&+ (\frac{\tau}{h}c_3)^2[w_x(x+h,y,t) - 2w_x(x,y,t) \\
&+ w_x(x-h,y,t)] + 2\left(\frac{\tau}{h}\right)^2 c_3^2[w_y(x+h,y+h,t) - w_y(x+h,y-h,t) - w_y(x-h,y+h,t) \\
&+ w_y(x-h,y-h,t)] - \left(\frac{\tau}{h}c_3\right)^2[w_x(x,y+h,t) - 2w_x(x,y,t) + w_x(x,y-h,t)]
\end{aligned}
$$

$$
\begin{aligned}
u_y(x,y,t+\tau) &= 2u_y(x,y,t) - u_y(x,y,t-\tau) + \left(\frac{\tau}{h}c_2\right)^2[u_y(x+h,y,t) \\
&- 2u_y(x,y,t) + u_y(x-h,y,t)] \quad + \left(\frac{\tau}{2h}\right)^2(c_1^2 - c_2^2)[u_x(x+h,y+h,t) \\
&- u_x(x+h,y-h,t) - u_x(x-h,y+h,t) + u_x(x-h,y-h,t) \\
&+ \left(\frac{\tau}{h}c_1\right)^2[u_y(x,y+h,t) - 2u_y(x,y,t) + u_y(x,y-h,t)] + \left(\frac{\tau}{h}c_3\right)^2[w_y(x+h,y,t) \\
&- 2w_y(x,y,t) + w_y(x-h,y,t)] - 2\left(\frac{\tau}{2h}\right)^2 c_3^2[w_x(x+h,y+h,t) \\
&- w_x(x+h,y-h,t) - w_x(x-h,y+h,t) + w_x(x-h,y-h,t)] \\
&- \left(\frac{\tau}{h}c_3\right)^2\left[w_y(x,y+h,t) - 2w_y(x,y,t) + w_y(x,y-h,t)\right]
\end{aligned}
$$

$$
\begin{aligned}
w_x(x,y,t+\tau) &= w_x(x,y,t) + d_2^2\frac{\tau}{h^2}[u_x(x+h,y,t) - 2u_x(x,y,t) + u_x(x-h,y,t)] \\
&+ d_1^2\frac{\tau}{h^2}[w_x(x+h,y,t) + w_x(x-h,y,t) - 4w_x(x,y,t) + w_x(x,y+h,t) + w_x(x,y-h,t)] \\
&- 2d_2^2\frac{\tau}{(2h)^2}\left[u_y(x+h,y+h,t) - u_y(x+h,y-h,t) - u_y(x-h,y+h,t) + u_y(x-h,y-h,t)\right] \\
&- d_2^2\frac{\tau}{h^2}[u_x(x,y+h,t) - 2u_x(x,y,t) + u_x(x,y-h,t)]
\end{aligned}
$$

$$
\begin{aligned}
w_y(x,y,t+\tau) &= w_y(x,y,t) + d_2^2\frac{\tau}{h^2}\left[u_y(x+h,y,t) - 2u_y(x,y,t) + u_y(x-h,y,t)\right] \\
&+ d_1^2\frac{\tau}{h^2}\left[w_y(x+h,y,t) + w_y(x-h,y,t) - 4w_y(x,y,t) + w_y(x,y+h,t) + w_y(x,y-h,t)\right] \\
&+ 2d_2^2\frac{\tau}{(2h)^2}[u_x(x+h,y+h,t) - u_x(x+h,y-h,t) - u_x(x-h,y+h,t) + u_x(x-h,y-h,t)] \\
&- d_2^2\frac{\tau}{h^2}\left[u_y(x,y+h,t) - 2u_y(x,y,t) + u_y(x,y-h,t)\right]
\end{aligned}
\tag{10.8.1}
$$

The displacements at mesh points located at the special lines are determined by satisfying the boundary conditions, and we obtain, respectively, for points on the grid lines $x = -h/2$ and $x = L + h/2$.

$$u_x\left(\begin{smallmatrix}-\frac{h}{2}\\ L+\frac{h}{2}\end{smallmatrix},y,t\right)=u_x\left(\begin{smallmatrix}-\frac{h}{2}\\ L-\frac{h}{2}\end{smallmatrix},y,t\right)\pm\frac{1}{2}\frac{d_1^2(c_1^2-2c_2^2)+c_3^2d_2^2}{c_1^2d_1^2-c_3^2d_2^2}\begin{bmatrix}u_y\left(\begin{smallmatrix}\frac{h}{2}\\ L-\frac{h}{2}\end{smallmatrix},y+h,t\right)\\ -u_y\left(\begin{smallmatrix}\frac{h}{2}\\ L-\frac{h}{2}\end{smallmatrix},y-h,t\right)\end{bmatrix}$$
$$\pm\frac{1}{2}\frac{c_3^2(d_1^2-d_3^2)}{c_1^2d_1^2-c_3^2d_2^2}\left[w_y\left(\begin{smallmatrix}\frac{h}{2}\\ L-\frac{h}{2}\end{smallmatrix},y+h,t\right)-w_y\left(\begin{smallmatrix}\frac{h}{2}\\ L-\frac{h}{2}\end{smallmatrix},y-h,t\right)\right] \tag{10.8.2a}$$

$$w_x\left(\begin{smallmatrix}-\frac{h}{2}\\ L+\frac{h}{2}\end{smallmatrix},y,t\right)=w_x\left(\begin{smallmatrix}-\frac{h}{2}\\ L-\frac{h}{2}\end{smallmatrix},y,t\right)\pm 2\frac{d_2^2(c_1^2-2c_2^2)}{c_3^2d_2^2-c_1^2d_1^2}\left[u_y\left(\begin{smallmatrix}\frac{h}{2}\\ L-\frac{h}{2}\end{smallmatrix},y+h,t\right)-u_y\left(\begin{smallmatrix}\frac{h}{2}\\ L-\frac{h}{2}\end{smallmatrix},y-h,t\right)\right]$$
$$\pm\frac{1}{2}\frac{c_3^2d_2^2-c_1^2d_3^2}{c_3^2d_2^2-c_1^2d_1^2}\left[w_y\left(\begin{smallmatrix}\frac{h}{2}\\ L-\frac{h}{2}\end{smallmatrix},y+h,t\right)-w_y\left(\begin{smallmatrix}\frac{h}{2}\\ L-\frac{h}{2}\end{smallmatrix},y-h,t\right)\right] \tag{10.8.2b}$$

$$u_y\left(\begin{smallmatrix}-\frac{h}{2}\\ L+\frac{h}{2}\end{smallmatrix},y,t\right)=u_y\left(\begin{smallmatrix}-\frac{h}{2}\\ L-\frac{h}{2}\end{smallmatrix},y,t\right)\pm\frac{1}{2}\left[u_x\left(\begin{smallmatrix}\frac{h}{2}\\ L-\frac{h}{2}\end{smallmatrix},y+h,t\right)-u_x\left(\begin{smallmatrix}\frac{h}{2}\\ L-\frac{h}{2}\end{smallmatrix},y-h,t\right)\right]$$
$$\pm\frac{1}{2}\frac{c_3^2(d_1^2-d_3^2)}{c_2^2d_1^2-c_3^2d_2^2}\left[w_x\left(\begin{smallmatrix}\frac{h}{2}\\ L-\frac{h}{2}\end{smallmatrix},y+h,t\right)-w_x\left(\begin{smallmatrix}\frac{h}{2}\\ L-\frac{h}{2}\end{smallmatrix},y-h,t\right)\right] \tag{10.8.2c}$$

$$w_y\left(\begin{smallmatrix}-\frac{h}{2}\\ L+\frac{h}{2}\end{smallmatrix},y,t\right)=w_y\left(\begin{smallmatrix}\frac{h}{2}\\ L-\frac{h}{2}\end{smallmatrix},y,t\right)$$
$$\pm\frac{1}{2}\frac{c_3^2d_2^2-c_2^2d_3^2}{c_2^2d_1^2-c_3^2d_2^2}\left[w_x\left(\begin{smallmatrix}\frac{h}{2}\\ L-\frac{h}{2}\end{smallmatrix},y+h,t\right)-w_x\left(\begin{smallmatrix}\frac{h}{2}\\ L-\frac{h}{2}\end{smallmatrix},y-h,t\right)\right] \tag{10.8.2d}$$

where Eqs. (10.8.2a) and (10.8.2b) related to $x=-h/2$ are not valid, from the first condition of (10.6.5), at $x=0$, $u_x=0$ and $w_x=0$. To satisfy the condition, the displacements u_x and w_x at $x=-h/2$ are approximated by

$$\begin{aligned}u_x(x,-h/2,t)&=-u_x(x,h/2,t)\\ w_x(x,-h/2,t)&=-w_x(x,h/2,t)\end{aligned} \tag{10.8.3}$$

On the grid line $y=-h/2$ and $y=H+h/2$, we obtain

$$u_x\left(x,\begin{smallmatrix}-\frac{h}{2}\\ L+\frac{h}{2}\end{smallmatrix},t\right)=u_x\left(x,\begin{smallmatrix}-\frac{h}{2}\\ L-\frac{h}{2}\end{smallmatrix},t\right)\pm\frac{1}{2}\left[u_y\left(x+h,\begin{smallmatrix}\frac{h}{2}\\ L-\frac{h}{2}\end{smallmatrix},t\right)-u_y\left(x-h,\begin{smallmatrix}\frac{h}{2}\\ L-\frac{h}{2}\end{smallmatrix},t\right)\right]$$
$$\pm\frac{1}{2}\frac{c_3^2(d_1^2-d_3^2)}{c_2^2d_1^2-c_3^2d_2^2}\left[w_y\left(x+h,\begin{smallmatrix}\frac{h}{2}\\ L-\frac{h}{2}\end{smallmatrix},t\right)-w_y\left(x-h,\begin{smallmatrix}\frac{h}{2}\\ L-\frac{h}{2}\end{smallmatrix},t\right)\right] \tag{10.8.4a}$$

$$w_x\left(x,{}^{-\frac{h}{2}}_{L+\frac{h}{2}},t\right)=w_x\left(x,{}^{-\frac{h}{2}}_{L-\frac{h}{2}},t\right)\pm\frac{1}{2}\frac{c_3^2d_2^2-c_2^2d_3^2}{c_2^2d_1^2-c_3^2d_2^2}\left[w_y\left(x+h,{}^{\frac{h}{2}}_{L-\frac{h}{2}},t\right)-w_y\left(x-h,{}^{\frac{h}{2}}_{L-\frac{h}{2}},t\right)\right] \tag{10.8.4b}$$

$$u_y\left(x,{}^{-\frac{h}{2}}_{L+\frac{h}{2}},t\right)=u_y\left(x,{}^{\frac{h}{2}}_{L-\frac{h}{2}},t\right)\pm\frac{1}{2}\frac{c_3^2d_2^2+d_1^2(c_1^2-2c_2^2)}{c_1^2d_1^2-c_3^2d_2^2}\left[u_x\left(x+h,{}^{\frac{h}{2}}_{L-\frac{h}{2}},t\right)-u_x\left(x-h,{}^{\frac{h}{2}}_{L-\frac{h}{2}},t\right)\right]\pm\frac{1}{2}\frac{c_3^2(d_3^2-d_1^2)}{c_1^2d_1^2-c_3^2d_2^2}\left[w_x\left(x+h,{}^{\frac{h}{2}}_{L-\frac{h}{2}},t\right)-w_x\left(x-h,{}^{\frac{h}{2}}_{L-\frac{h}{2}},t\right)\right] \tag{10.8.4c}$$

$$w_y\left(x,{}^{-\frac{h}{2}}_{L+\frac{h}{2}},t\right)=w_y\left(x,{}^{\frac{h}{2}}_{L-\frac{h}{2}},t\right)\pm\frac{d_2^2(c_1^2-c_2^2)}{c_1^2d_1^2-c_3^2d_2^2}\left[u_x\left(x+h,{}^{\frac{h}{2}}_{L-\frac{h}{2}},t\right)-u_x\left(x-h,{}^{\frac{h}{2}}_{L-\frac{h}{2}},t\right)\right]\pm\frac{1}{2}\frac{c_1^2d_3^2-c_3^2d_2^2}{c_1^2d_1^2-c_3^2d_2^2}\left[w_x\left(x+h,{}^{\frac{h}{2}}_{L-\frac{h}{2}},t\right)-w_x\left(x-h,{}^{\frac{h}{2}}_{L-\frac{h}{2}},t\right)\right] \tag{10.8.4d}$$

in which, Eqs. (10.8.4c) and (10.8.4d) related to $y=-h/2$ are valid only along the crack surface, namely only for $x\le a-h/2$, at $y=0$, in which the crack terminates. From the last condition of (10.6.5), at $y=0$ and the ahead of the crack, $u_y=0, w_y=0$. To satisfy this condition, the displacements u_y and w_y at $y=-h/2$ are approximated by

$$\begin{aligned}u_y(x,-h/2,t)&=-u_y(x,h/2,t)\\ w_y(x,-h/2,t)&=-w_y(x,h/2,t)\end{aligned} \tag{10.8.5}$$

In constructing the approximation (10.8.2a)–(10.8.5), we follow a method proposed by Shmuely and Peretz [31] which was also successfully employed in Ref. [30] for conventional engineering materials. According to this method, derivatives perpendicular to the boundary are proposed by uncentred differences and derivatives parallel to the boundary by centred difference. The real boundary can be considered as located at a distance of half the mesh size from the grid boundaries.

The four grid corners require a special treatment. Difference methods of handling the discontinuities at such points have been proposed in the past. Here we found that satisfactory results are obtained when the displacements sought are extrapolated from those given along both sides of the corner in question. Accordingly, the components u_x, u_y, w_x, w_y at $(-h/2,-h/2)$ are given by

$$\begin{aligned}
\begin{matrix} u_x \\ u_y \end{matrix}(-h/2,-h/2,t) &= \begin{matrix} u_x \\ u_y \end{matrix}(h/2,-h/2,t) + \begin{matrix} u_x \\ u_y \end{matrix}(-h/2,h/2,t) \\
&\quad - 0.5\left[\begin{matrix} u_x \\ u_y \end{matrix}(3h/2,-h/2,t) + \begin{matrix} u_x \\ u_y \end{matrix}(-h/2,3h/2,t)\right] \\
\begin{matrix} w_x \\ w_y \end{matrix}(-h/2,-h/2,t) &= \begin{matrix} w_x \\ w_y \end{matrix}(h/2,-h/2,t) + \begin{matrix} w_x \\ w_y \end{matrix}(-h/2,h/2,t) \\
&\quad - 0.5\left[\begin{matrix} w_x \\ w_y \end{matrix}(3h/2,-h/2,t) + \begin{matrix} w_x \\ w_y \end{matrix}(-h/2,3h/2,t)\right]
\end{aligned} \tag{10.8.6}$$

Similar expressions are used for deriving the displacement components at $(-h/2, H+h/2)$, $(L+h/2, L+h/2)$ and $(L+h/2, -h/2)$.

By following relevant stability criterion of the scheme, the computation is always stable and achieves high precision. Discussions on this aspect are omitted here due to space limitation.

References

1. Lubensky T C, Ramaswamy S and Joner J, 1985, Hydrodynamics of icosahedral quasicrystals, *Phys. Rev*. B, **32**(11), 7444-7452.
2. Socolar J E S, Lubensky T C and Steinhardt P J, 1986, Phonons, phasons and dislocations in quasicrystals, *Phys. Rev*. B, **34**(5), 3345-3360.
3. Bak P, 1985, Phenomenological theory of icosahedral in commensurate (quasiperiodic)order in Mn-Al alloys, *Phys. Rev. Lett*., **54**(14), 1517-1519, 1985.
4. Bak P, 1985, Symmetry, stability and elastic properties of icosahedral in commensurate crystals, *Phys. Rev*. B, **32**(9), 5764-5772.
5. Ding D H, Yang W G, Hu C Z et al, 1993, Generalized elasticity theory of quasicrystals, *Phys. Rev*. B, **48**(10), 7003-7010.
6. Hu C Z, Wang R H and Ding D H, 2000, Symmetry groups, physical property tensors, elasticity and dislocations in quasicrystals, *Reports on Progress in Physics*, **63**(1), 1-39.
7. Fan T Y, Li X F and Sun Y F, 1999, A moving screw dislocation in one-dimensional hexagonal quasicrystal, *Acta Physica Sinica* (Overseas Edition), **8** (3), 288-295.
8. Fan T Y, 1999, A study on special heat of one-dimensional hexagonal quasicrystals, *J. Phys.: Condense. Matter*, **11**(45), L 513-L 517.
9. Fan T Y and Mai Y W, 2003, Partition function and state equation of point group 12 mm two-dimensional quasicrystals, *Euro. Phys. J*. B, **31**(1), 25-27.
10. Fan T Y and Mai Y W, 2004, Elasticity theory, fracture mechanics and some relevant thermal properties of quasicrystalline materials, *Appl. Mech. Rev*., **57**(5), 325-344.
11. Li C L and Liu Y Y, 2001, Phason-strain influences on low-temperature specific heat of the decagonal Al-Ni-Co quasicrystal, *Chin. Phys. Lett*. 18(4), 570-572.
12. Li C L and Liu Y Y, 2001, Low-temperature lattice excitation of icosahedral Al-Mn-Pd quasicrystals, *Phys. Rev*. B, **63**(6), 064203.
13. Fan T Y, Wang X F, Li W, Zhu A Y, 2009, Elasto-hydrodynamics of quasicrystals, *Phil. Mag*., **89**(6), 501-512.

14. Zhu A Y and Fan T Y, 2008, Dynamic crack propagation in a decagonal Al-Ni-Co quasicrystal, *J. Phys.: Condens. Matte*r, **20**(29), 295217.
15. Rochal S B and Lorman V L, 2000, *Phys. Rev*. B, **62**(2), 874, 2000.
16. Rochal S B and Lorman V L, 2002, Minimal model of the phonon-phason dynamics on icosahedral quasicrystals and its application for the problem of internal friction in the i-AlPdMn alloys, *Phys. Rev*. B, **66 (**14), 144204.
17. On the Eshelby's solution one can refer to Hirth J P and Lorthe J, 1982, *Theory of Dislocations*, 2nd Edition, John Wiely & Sons, New York.
18. Yoffe E H, 1951, Moving Griffith crack, *Phil. Mag*., 43(10), 739-750.
19. Li X F, 2011, A general solution of elasto-hydrodynamics of two = dimensional quasicrystals, Phil Mag Lett, 91(4), 313-320.
20. Li X F, 2013, Elastohydrodynamic problems in quasicrystal elasticity theory and wave propagation, Phil Mag, 93(13), 1500-1519.
21. Chernikov M A, Ott H R, Bianchi A et al, 1998, Elastic moduli of a single quasicrystal of decagonal Al-Ni-Co: evidence for transverse elastic isotropy, *Phys. Rev. Lett*. **80(2)**, 321-324.
22. H. C. Jeong and P. J. Steinhardt, 1993, Finite-temperature elasticity phase transition in decagonal quasicrystals, *Phys. Rev*. B **48**(13)**,** 9394-9403.
23. Walz C, 2003, Zur Hydrodynamik in Quasikristallen, Diplomarbeit, Universitaet Stuttgart.
24. Maue A W, 1954, Die entspannungswelle bei ploetzlischem Einschnitt eines gespannten elastischen Koepores, *Zeitschrift fuer angewandte Mathematik und Mechanik*, **14**(1), 1-12.
25. Murti V and Vlliappan S, 1986, The use of quarter point element in dynamic crack analysis, *Engineering Fracture Mechanics*, 23(3), 585-614.
26. Chen Y M, 1975, Numerical computation of dynamic stress intensity factor s by a Lagrangian finite-difference method (the HEMP code), *Engineering Fracture Mechanics*, **7**(8), 653-660.
27. Ebert Ph, Feuerbacher M, Tamura N et al, Evidence for a cluster-based on structure of AlPdMn single quasicrystals, 1996, *Phys. Rev. Lett*., **77**(18), 3827-3830.
28. Takeuchi S, Iwanaga H, Shibuya T, 1991, Hardness of quasicystals, Japanese J Appl Phys, 30 (3), 561-562.
29. Wang X F, Fan T Y and Zhu A Y, 2009, Dynamic behaviour of the icosahedral Al-Pd-Mn quasicrystal with a Griffith crack, Chin Phys B, 2009, 18 (2), 709-714. (in Section 10.7 a results are introduced from Zhu A Y and Fan T Y's unpublished work "Fast crack propagation in three-dimensional icosahedral Al-Pd-Mn quasicrystals", 2007 or referring to Zhu A Y: Study on analytic solutions in elasticity of three-dimensional quasicrystals and elastodynamics of two- and three-dimensional quasicrystals, Dissertation, Beijing Institute of Technology, 2009, in Chinese).
30. Shmuely M and Alterman Z S, 1973, Crack propagation analysis by finite differences, *Journal of Applied Mechanics* **40**(4), 902-908.
31. Shmuely M and Peretz D, 1976, Static and dynamic analysis of the DCB problem in fracture mechanics, *Int. J. of Solids and Structures*, **12**(1)**,** 67-67.

Chapter 11
Complex Analysis Method for Elasticity of Quasicrystals

In Chapters 7–9, we frequently used the complex analysis method to solve the problems of elasticity of quasicrystals and many exact analytic solutions were obtained by this method. In these chapters, we only provided the results, and the underling principle and details of the method could not be discussed. Considering the relative new feature and particular effect of the method, it is helpful to attempt a further discussion in depth. Of course, this may lead to a slight repletion with relevant content of Chaps. 7–9.

It is well known that the so-called complex potential method in elasticity is effective, in general, only for solving harmonic and biharmonic partial differential equations in the classical theory of elasticity, and for these equations, the solutions can be expressed by the analytic functions of single complex variable $z = x + iy$, $i = \sqrt{-1}$. In addition, in the classical elasticity, quasi-biharmonic partial differential equation can be solved by analytic functions of some different complex variables such as $z_1 = x + \alpha_1 y, z_2 = x + \alpha_2 y, \ldots$ in which $\alpha_1, \alpha_2, \ldots$ are complex constants. The study of elasticity of quasicrystals has led to discovery of some multi-harmonic and multi-quasiharmonic equations, which cover quite a wide range of partial differential equations appearing in the field to date and have been introduced in Chaps. 5–9. The discussion on the complex analysis for these equations is significant. We know that the Muskhelishvili complex analysis method for classical plane elasticity [1], which solves mainly the biharmonic equation, and the complex potential method developed by Lekhlitzkii [2] for classical anisotropic plane elasticity, which solve mainly the quasi-biharmonic equation, made great contributions for quite a wide range of fields in science and engineering. The present formulation and solutions of the complex analysis, e.g. quadruple and sextuple harmonic equations and quadruple quasiharmonic equation, are a new development of the

T.-Y. Fan, *Mathematical Theory of Elasticity of Quasicrystals and Its Applications*,
Springer Series in Materials Science 246, DOI 10.1007/978-981-10-1984-5_11

complex analysis method used for classical elasticity. Though the new method is used to solve the elasticity problems of quasicrystals at present, it may be extended into other disciplines of science and technology in future.

At first, we simply review the complex analysis method for harmonic and biharmonic equations and then focus on those for quadruple and sextuple harmonic equations and quadruple quasiharmonic equation and, with discussions in detail, presenting their new features from the angle of elasticity as well as complex potential method.

11.1 Harmonic and Biharmonic in Anti-Plane Elasticity of One-Dimensional Quasicrystals

The final governing equations of elasticity of one-dimensional quasicrystals present the following two kinds discussed in Chap. 5:

$$\begin{aligned} c_{44}\nabla^2 u_z + R_3\nabla^2 w_z &= 0 \\ R_3\nabla^2 u_z + K^2\nabla^2 w_z &= 0 \end{aligned} \tag{11.1.1}$$

$$(c_1\frac{\partial^4}{\partial x^4} + c_2\frac{\partial^4}{\partial x^3\partial y} + c_3\frac{\partial^4}{\partial x^2\partial y^2} + c_4\frac{\partial^4}{\partial x\partial y^3} + c_5\frac{\partial^4}{\partial y^4})G = 0 \tag{11.1.2}$$

in which Eq. (11.1.1) is actually two decoupled harmonic equations of u_z and w_z, whose complex variable function method was introduced in Sects. 8.1 and 8.2, and here we do not repeat any more.

Equation (11.1.2) is a quasi-biharmonic equation which describes the phonon-phason coupling elasticity field for some kinds of one-dimensional quasicrystal systems, refer to Chap. 5. As some solutions of them in terms of the complex variable function method, whose origin comes from the classical work of Lekhlitskii [2], reader can find some beneficial hints in the monograph.

11.2 Biharmonic Equations in Plane Elasticity of Point Group 12*mm* Two-Dimensional Quasicrystals

From Chap. 6, we know that in elasticity of dodecagonal quasicrystals, the phonon and phason fields are decoupled each other. For whose plane elasticity we have the final governing equations as follows:

$$\nabla^2\nabla^2 F = 0, \quad \nabla^2\nabla^2 G = 0 \tag{11.2.1}$$

The complex representation of solution of (11.2.1) is

$$\left.\begin{aligned} F(x,y) &= \mathrm{Re}[\bar{z}\varphi_1(z) + \int \psi_1(z)\mathrm{d}z] \\ G(x,y) &= \mathrm{Re}[\bar{z}\pi_1(z) + \int \chi_1(z)\mathrm{d}z] \end{aligned}\right\} \tag{11.2.2}$$

where $\phi_1(z), \psi_1(z), \pi_1(z)$ and $\chi_1(z)$ are any analytic functions of complex variable $z = x + iy$ $(i = \sqrt{-1})$. For these kind of biharmonic equations, Muskhelishvili [1] developed systematic complex variable function method, in which reader can find some details in the well-known monograph and we need not discuss those any more. The Muskhelishvili's method has some developments in China, e.g. Lu [3] and Fan [4].

11.3 The Complex Analysis of Quadruple Harmonic Equations and Applications in Two-Dimensional Quasicrystals

As it was discussed in Chaps. 6–8, for point groups $5m$ and $10mm$ or point groups 5, $\overline{5}$, and 10, $\overline{10}$ quasicrystals, either by the displacement potential formulation or by the stress potential formulation, we obtain the final governing equation is quadruple harmonic equation, whose complex variable function method is newly created by Liu and Fan [5, 6] based on the displacement potential formulation and by Li and Fan [7, 8] based on the stress potential formulation. This complex potential method that greatly develops the methodology was used in the classical elasticity. It is necessary to give some further discussions in depth. For simplicity, the following discussion is based on the stress potential formulation only, and solutions are given only for point groups 5, $\overline{5}$, and 10, $\overline{10}$ quasicrystals, because the point groups $5m$ and $10mm$ quasicrystals can be seen as a special case of the former.

11.3.1 Complex Representation of Solution of the Governing Equation

Because it is relatively simpler for the case of point groups $5m$ and $10mm$, which belong to the special case of point groups 5, $\overline{5}$ and point groups 10 and $\overline{10}$, we here discuss only the final governing equation of plane elasticity of pentagonal of point groups 5, $\overline{5}$ and decagonal quasicrystals of point groups 10, $\overline{10}$

$$\nabla^2\nabla^2\nabla^2\nabla^2 G = 0 \tag{11.3.1}$$

where $G(x, y)$ is the stress potential function. The solution of Eq. (11.3.1) is

$$G = 2\mathrm{Re}[g_1(z) + \bar{z}g_2(z) + \frac{1}{2}\bar{z}^2 g_3(z) + \frac{1}{6}\bar{z}^3 g_4(z)] \tag{11.3.2}$$

where $g_j(z)$ $(j = 1, \cdots, 4)$ are four analytic functions of a single complex variable $z \equiv x + iy = re^{i\theta}$. The bar denotes the complex conjugate hereinafter, i.e. $\bar{z} = x - iy = re^{-i\theta}$. We call these functions be the complex stress potentials, or the complex potentials in brief.

11.3.2 Complex Representation of the Stresses and Displacements

Sect. 8.4 shows that from fundamental solution (11.3.2), one can find the complex representation of the stresses as below:

$$\begin{aligned}
\sigma_{xx} &= -32c_1\mathrm{Re}(\Omega(z) - 2g_4'''(z)) \\
\sigma_{yy} &= 32c_1\mathrm{Re}(\Omega(z) + 2g_4'''(z)) \\
\sigma_{xy} &= \sigma_{yx} = 32c_1\mathrm{Im}\Omega(z) \\
H_{xx} &= 32R_1\mathrm{Re}(\Theta'(z) - \Omega(z)) - 32R_2\mathrm{Im}(\Theta'(z) - \Omega(z)) \\
H_{xy} &= -32R_1\mathrm{Im}(\Theta'(z) + \Omega(z)) - 32R_2\mathrm{Re}(\Theta'(z) + \Omega(z)) \\
H_{yx} &= -32R_1\mathrm{Im}(\Theta'(z) - \Omega(z)) - 32R_2\mathrm{Re}(\Theta'(z) - \Omega(z)) \\
H_{yy} &= -32R_1\mathrm{Re}(\Theta'(z) + \Omega(z)) + 32R_2\mathrm{Im}(\Theta'(z) + \Omega(z)
\end{aligned} \tag{11.3.3}$$

where

$$\begin{aligned}
\Theta(z) &= g_2^{(\mathrm{IV})}(z) + \bar{z}g_3^{(\mathrm{IV})}(z) + \frac{1}{2}\bar{z}^2 g_4^{(\mathrm{IV})}(z) \\
\Omega(z) &= g_3^{(\mathrm{IV})}(z) + \bar{z}g_4^{(\mathrm{IV})}(z)
\end{aligned} \tag{11.3.4}$$

in which one prime, two prime, three prime, and superscript (IV) denote the first- to fourth-order differentiation of $g_j(z)$ to variable z, in addition $\Theta'(z) = \mathrm{d}\Theta(z)/\mathrm{d}z$ and it is evident that $\Theta(z)$ and $\Omega(z)$ are not analytic functions.

By some derivation from (11.3.3), we have the complex representation of the displacements such as

$$u_x + iu_y = 32(4c_1c_2 - c_3 - c_1c_4)g_4''(z) - 32(c_1c_4 - c_3)(\overline{g_3'''(z)} + z\overline{g_4'''(z)}) \quad (11.3.5)$$

$$w_x + iw_y = \frac{32(R_1 - iR_2)}{K_1 - K_2}\overline{\Theta(z)} \quad (11.3.6)$$

with constants

$$c = M(K_1 + K_2) - 2(R_1^2 + R_2^2), c_1 = \frac{c}{K_1 - K_2} + M, c_2 = \frac{c + (L+M)(K_1 + K_2)}{4(L+M)c},$$
$$c_3 = \frac{R_1^2 + R_2^2}{c}, c_4 = \frac{K_1 + K_2}{c} \quad (11.3.7)$$

11.3.3 The Complex Representation of Boundary Conditions

In the following, we consider only the stress boundary value problem; i.e. at the boundary curve L_t, the tractions (T_x, T_y) and generalized tractions (h_x, h_y) are given, and there are the stress boundary conditions such as

$$\sigma_{xx}\cos(\mathbf{n}, x) + \sigma_{xy}\cos(\mathbf{n}, y) = T_x, \ \sigma_{xy}\cos(\mathbf{n}, x) + \sigma_{yy}\cos(\mathbf{n}, y) = T_y, \quad (x, y) \in L_t \quad (11.3.8)$$

$$H_{xx}\cos(\mathbf{n}, x) + H_{xy}\cos(\mathbf{n}, y) = h_x \ , \ H_{xy}\cos(\mathbf{n}, x) + H_{yy}\cos(\mathbf{n}, y) = h_y, \quad (x, y) \in L_t \quad (11.3.9)$$

where T_x, T_y and h_x, h_y are tractions and generalized tractions at the boundary L_t where the stresses are prescribed.

From (11.3.8) and after some derivation, the phonon stress boundary condition can be reduced to the equivalent form

$$g_4''(z) + \overline{g_3'''(z)} + z\overline{g_4'''(z)} = \frac{i}{32c_1}\int (T_x + iT_y)\mathrm{d}s, \quad z \in L_t \quad (11.3.10)$$

From Eqs. (11.3.9), (11.3.3), and (11.3.4), we have

$$(R_2 - iR_1)\Theta(z) = i\int (h_x + ih_y)\mathrm{d}s, \quad z \in L_t \quad (11.3.11)$$

11.3.4 Structure of Complex Potentials

11.3.4.1 Arbitrariness in the Definition of the Complex Potentials

For simplicity, we introduce the following new symbols

$$g_2^{(\mathrm{IV})}(z) = h_2(z), g_3'''(z) = h_3(z), g_4''(z) = h_4(z) \tag{11.3.12}$$

and then, Eq. (11.3.3) can be rewritten as follows:

$$\sigma_{xx} + \sigma_{yy} = 128c_1 \mathrm{Re}\, h_4'(z) \tag{11.3.13}$$

$$\sigma_{yy} - \sigma_{xx} + 2i\sigma_{xy} = 64c_1\Omega(z) = 64c_1[h_3'(z) + \bar{z}h_4''(z)] \tag{11.3.14}$$

$$H_{xy} - H_{yx} - i(H_{xx} + H_{yy}) = 64(iR_1 - R_2)\Omega(z) \tag{11.3.15}$$

$$(H_{xx} - H_{yy}) - i(H_{xy} + H_{yx}) = 64(R_1 + R_2)\Theta'(z) \tag{11.3.16}$$

Similar to the classical elasticity, from Eqs. (11.3.13) to (11.3.16), it is obvious that a state of phonon and phason stresses is not altered, if one replaces

$$h_4(z) \quad \text{by } h_4(z) + Diz + \gamma \tag{11.3.17}$$

$$h_3(z) \quad \text{by} \quad h_3(z) + \gamma' \tag{11.3.18}$$

$$h_2(z) \quad \text{by} \quad h_2(z) + \gamma'' \tag{11.3.19}$$

where D is a real constant and γ, γ', γ'' are arbitrary complex constants.

Now, consider how these substitutions affect the displacement components which were determined by formulas (11.3.5) and (11.3.6). Direct substitution shows that

$$\begin{aligned} u_x + iu_y = {} & 32(4c_1c_2 - c_3 - c_1c_4)h_4(z) - 32(c_1c_4 - c_3)(\overline{h_3(z)} + z\overline{h_4'(z)}) \\ & + 32(4c_1c_2 - 2c_3)Diz + [32(4c_1c_2 - c_3 - c_1c_4)\gamma - 32(c_1c_4 - c_3)\overline{\gamma'}] \end{aligned} \tag{11.3.20}$$

$$w_x + iw_y = \frac{32(R_1 - iR_2)}{K_1 - K_2}[\overline{h_2(z)} + z\overline{h_3'(z)} + \frac{1}{2}z^2\overline{h_4''(z)}] + \frac{32(R_1 - iR_2)}{K_1 - K_2}\overline{\gamma''} \tag{11.3.21}$$

Formulas (11.3.20) and (11.3.21) show that a substitution of the form (11.3.17) and (11.3.19) will affect the displacement, unless

$$D = 0,\ \gamma = \frac{c_1 c_4 - c_3}{4c_1 c_2 - c_3 - c_1 c_4}\overline{\gamma'},\ \overline{\gamma''} = 0$$

11.3.4.2 General Formulas for Finite Multi-connected Regions

Consider now the case when the region S, occupied by the quasicrystal, is multi-connected. In general, the region is bounded by several simple closed contours $s_1, s_2, \ldots, s_m, s_{m+1}$, the last of these contours is to contain all the others, depicted in Fig. 11.1, i.e. a plate with holes. We assume that the contours do not intersect themselves and have no points in common. Sometimes, we call $s_1, s_2, \ldots, s_m$ as inner boundaries and s_{m+1} as outer boundary of the region. It is evident that the points $z_1, z_2, \ldots, z_m$ are fixed points in the holes, but located out of the material.

Similar to the discussion of the classical elasticity theory (refer to [1]), we can obtained

$$h_4'(z) = \sum_{k=1}^{m} A_k \ln(z - z_k) + h_{4*}'(z) \tag{11.3.22}$$

$$h_4(z) = \sum_{k=1}^{m} A_k z \ln(z - z_k) + \sum_{k=1}^{m} \gamma_k \ln(z - z_k) + h_{4*}(z) \tag{11.3.23}$$

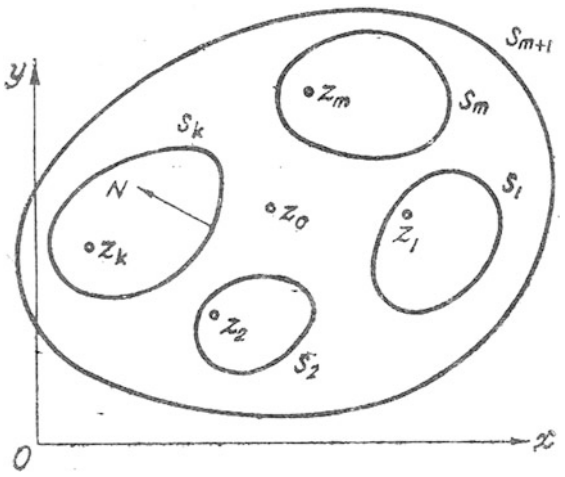

Fig. 11.1 Finite multi-connected region

$$h_3(z) = \sum_{k=1}^{m} \gamma_k' \ln(z - z_k) + h_{3*}(z) \tag{11.3.24}$$

Recalling z_k denotes the fixed points outside the region S, $h_{3*}(z), h_{4*}(z)$ are holomorphic (analytic and single-valued, refer to Major Appendix) in region S, A_k real constants, and γ_k, γ_k' complex constants.

By substituting (11.3.22)–(11.3.24) into (11.3.16), one can find that

$$h_2(z) = \sum_{k=1}^{m} \gamma_k'' \ln(z - z_k) + h_{2*}(z) \tag{11.3.25}$$

$h_{2*}(z)$ is holomorphic in S, and γ_k'' are complex constants.

Consideration will be given to the condition of single valuedness of phonon displacements. From Eq. (11.3.5), one has

$$u_x + iu_y = 32(4c_1c_2 - c_3 - c_1c_4)h_4(z) - 32(c_1c_4 - c_3)(\overline{h_3(z)} + z\overline{h_4'(z)}) \tag{11.3.26}$$

Substituting (11.3.23)–(11.3.25) into (11.3.26), it is immediately seen that

$$[u_x + iu_y]_{s_k} = 2\pi i\{[32(4c_1c_2 - c_3 - c_1c_4) + 32(c_1c_4 - c_3)]A_k z + 32(4c_1c_2 - c_3 - c_1c_4)\gamma_k + \overline{\gamma_k'(z)}\} \tag{11.3.27}$$

in which $[\,]_k$ denotes the increase undergone by the expression in brackets for one anticlockwise circuit of the contour s_k. Hence it is necessary and sufficient for the single valuedness of phonon displacements that are shown in formulas (11.3.22)–(11.3.25)

$$A_k = 0, \quad 32(4c_1c_2 - c_3 - c_1c_4)\gamma_k + \overline{\gamma_k'} = 0 \tag{11.3.28}$$

Similar to the above-mentioned discussion, by Eq. (11.3.6), one has

$$[w_x + iw_y]_{s_k} = \frac{32(R_1 - iR_2)}{K_1 - K_2}(-2\pi i)\overline{\gamma_k''} \tag{11.3.29}$$

Hence it is necessary and sufficient for the single valuedness of phason displacements is

$$\gamma_k'' = 0 \tag{11.3.30}$$

It will now be shown that the quantities $\gamma_k,\ \gamma_k'$ may be very simply expressed in terms of $X_k,\ Y_k$, where $(X_k,\ Y_k)$ denote the resultant vector of the external stresses, exerted on the contour s_k. From (11.3.10), applying it to the contour s_k, one has

$$-32c_1 i[h_4(z) + \overline{h_3(z)} + z\overline{h_4'(z)}]_{s_k} = X_k + iY_k \tag{11.3.31}$$

with

$$X_k = \int_{S_k} T_x \mathrm{d}s, Y_k = \int_{S_k} T_y \mathrm{d}s$$

In the present case, the normal vector **n** must be directed outwards with respect to the region s_k. Consequently, the contour s_k must be traversed in the clockwise direction. Taking this fact into consideration, one obtains

$$-2\pi i(\gamma_k - \overline{\gamma_k'}) = \frac{i}{32c_1}(X_k + iY_k) \tag{11.3.32}$$

By Eqs. (11.3.28), (11.3.31), and (11.3.32), one has

$$\begin{aligned} &A_k = 0 \\ &\gamma_k = d_1(X_k + iY_k),\ \gamma_k' = d_2(X_k - iY_k) \end{aligned} \tag{11.3.33}$$

where

$$d_1 = \frac{1}{64c_1\pi[32(4c_1c_2 - c_3 - c_1c_4) + 1]}, d_2 = -\frac{4c_1c_2 - c_3 - c_1c_4}{2c_1\pi[32(4c_1c_2 - c_3 - c_1c_4) + 1]} \tag{11.3.34}$$

and which are independent from the suffix k. So that

$$\begin{aligned} h_4(z) &= d_1 \sum_{k=1}^{m} (X_k + iY_k)\ln(z - z_k) + h_{4*}(z) \\ h_3(z) &= d_2 \sum_{k=1}^{m} (X_k - iY_k)\ln(z - z_k) + h_{3*}(z) \\ h_2(z) &= h_{2*}(z) \end{aligned} \tag{11.3.35}$$

We can conclude that the complex functions $h_2(z),\ h_3(z),\ h_4(z)$ must be expressed by formula (11.3.35) to assure the single valuedness of stresses and displacements, where $h_{2*}(z),\ h_{3*}(z),\ h_{4*}(z)$ are holomorphic in region S.

11.3.4.3 Case of Infinite Regions

From the point of view of application, the consideration of infinite regions is likewise of major interest. We assume that the contour s_{m+1} has entirely moved to infinity.

Because Eqs. (11.3.13) and (11.3.14) are similar to the classical elasticity theory, we have

$$\begin{aligned} h_4(z) &= d_1(X+iY)\ln z + (B+iC)z + h_4^0(z) \\ h_3(z) &= d_2(X-iY)\ln z + (B'+iC')z + h_3^0(z) \end{aligned} \tag{11.3.36}$$

where B, C, B', C' are unknown real constants to be determined and

$$X = \sum_{k=1}^{m} X_k,\ Y = \sum_{k=1}^{m} Y_k$$

$h_3^0(z)$, $h_4^0(z)$ are functions, holomorphic in region S, including the point at infinity; i.e. for sufficiently large $|z|$, they may be expanded into series of the form

$$h_4^0(z) = a_0 + \frac{a_1}{z} + \frac{a_2}{z^2} + \cdots,\ h_3^0(z) = a_0' + \frac{a_1'}{z} + \frac{a_2'}{z^2} + \cdots \tag{11.3.37}$$

On the basis of (11.3.2), the state of phonon and phason stresses will not be altered by assuming

$$a_0 = a_0' = 0$$

By the theorem of Laurent, the function $h_{2*}(z)$ may be represented in region S including point at infinity by the series

$$h_{2*}(z) = \sum_{-\infty}^{+\infty} c_n z^n \tag{11.3.38}$$

Substituting Eqs. (11.3.36) and (11.3.38) into Eq. (11.3.16), one has

$$\begin{aligned} &(H_{xx} - H_{yy}) - i(H_{xy} + H_{yx}) \\ &= 2 \times 32(R_1 + R_2)[\sum_{-\infty}^{+\infty} c_n n z^{n-1} + \bar{z}(-\frac{d_2}{z^2} + h_3^{0\prime\prime}(z)) + \frac{1}{2}\bar{z}^2(\frac{2d_1}{z^3} + h_4^{0\prime\prime\prime}(z))] \end{aligned} \tag{11.3.39}$$

and hence it follows that for the stresses to remain finite as $|z| \to \infty$, one must have

$$c_n = 0 \ (n \geq 2)$$

It is obvious that the phonon and phason stresses will be bounded, if these conditions are satisfied. Hence one has finally

$$\begin{aligned} h_4(z) &= d_1(X + iY)\ln z + (B + iC)z + h_4^0(z) \\ h_3(z) &= d_2(X - iY)\ln z + (B' + iC')z + h_3^0(z) \\ h_2(z) &= (B'' + iC'')z + h_2^0(z) \end{aligned} \tag{11.3.40}$$

where B'', C'' are unknown real constants to be determined, $h_2^0(z)$ is function, holomorphic in region S, including the point at infinity; thus, it has the form similar to that of (11.3.37):

$$h_2^0(z) = a_0'' + \frac{a_1''}{z} + \frac{a_2''}{z^2} + \cdots \tag{11.3.41}$$

We have assumed that $a_0 = a_0' = 0$ already and now further assume $a_0'' = 0$, i.e.

$$h_4^0(\infty) = h_3^0(\infty) = h_2^0(\infty) = 0.$$

Then from (11.3.40) and (11.3.13)–(11.3.16), one can determine

$$\begin{aligned} &B = \frac{\sigma_{xx}^{(\infty)} + \sigma_{yy}^{(\infty)}}{128c_1},\ B' = \frac{\sigma_{xx}^{(\infty)} - \sigma_{yy}^{(\infty)}}{64c_1},\ C' = \frac{\sigma_{xy}^{(\infty)}}{32c_1}, \\ &B'' = \frac{R_2(H_{xy}^{(\infty)} - H_{yx}^{(\infty)}) - R_1(H_{xx}^{(\infty)} + H_{yy}^{(\infty)})}{64(R_1^2 - R_2^2)},\ C'' = \frac{R_1(H_{xy}^{(\infty)} - H_{yx}^{(\infty)}) - R_2(H_{xx}^{(\infty)} + H_{yy}^{(\infty)})}{64(R_1^2 - R_2^2)} \end{aligned} \tag{11.3.42}$$

and C has no usage and we put it to be zero, in which $\sigma_{ij}^{(\infty)}$ and $H_{ij}^{(\infty)}$ represent the applied stresses at point of infinity.

11.3.5 Conformal Mapping

If we constrain our discussion only for the case of stress boundary value problems, then the problems will be solved under boundary conditions (11.3.10) and (11.3.11). For some complicated regions, solutions of the problems cannot be directly obtained in the physical plane (i.e. the z-plane). We must use a conformal mapping

$$z = \omega(\zeta) \tag{11.3.43}$$

to transform the region studied in the plane onto interior of the unit circle γ in the mapping plane (say, e.g. ζ-plane).

Substituting (11.3.43) into (11.3.40), we have

$$\begin{aligned} h_4(z) &= \Phi_4(\zeta) = d_1(X+iY)\ln\omega(\zeta) + B\omega(\zeta) + \Phi_4^0(\zeta) \\ h_3(z) &= \Phi_3(\zeta) = d_2(X-iY)\ln\omega(\zeta) + (B'+iC')\omega(\zeta) + \Phi_3^0(\zeta) \\ h_2(z) &= \Phi_2(\zeta) = (B''+iC'')\omega(\zeta) + \Phi_2^0(\zeta) \end{aligned} \tag{11.3.44}$$

where

$$\Phi_j(\zeta) = h_j[\omega(\zeta)], \Phi_j^0(\zeta) = h_j^0[\omega(\zeta)], j = 1, \ldots, 4$$

In addition,

$$h_i'(z) = \frac{\Phi_i'(\zeta)}{\omega'(\zeta)}$$

At the mapping plane, the boundary conditions (11.3.10) and (11.3.11) stand for

$$\Phi_4(\sigma) + \overline{\Phi_3(\sigma)} + \omega(\sigma)\overline{\frac{\Phi_4'(\sigma)}{\omega'(\sigma)}} = \frac{i}{32c_1}\int (T_x + iT_y)\mathrm{d}s, \tag{11.3.10'}$$

$$(R_2 - iR_1)\Theta(\sigma) = i\int (h_x + ih_y)\mathrm{d}s \tag{11.3.11'}$$

where $\sigma = \mathrm{e}^{i\varphi}$ represents the value of ζ at the unit circle (i.e. $\rho = 1$). From these boundary value equations, we can determine the unknown functions $\Phi_j(\zeta)$ $(j = 2, 3, 4)$.

11.3.6 Reduction in the Boundary Value Problem to Function Equations

Due to $\Phi_1(\zeta) = 0$, we now have three unknown functions $\Phi_i(\zeta)$ $(i = 2, 3, 4)$. Taking conjugate of (11.3.10′) yields

$$\overline{\Phi_4(\sigma)} + \Phi_3(\sigma) + \overline{\omega(\sigma)}\frac{\Phi_4'(\sigma)}{\omega'(\sigma)} = -\frac{i}{32c_1}\int (T_x - iT_y)\mathrm{d}s \tag{11.3.10''}$$

Substituting the Eq. (11.3.4) into (11.3.11′) and then multiplying $\frac{1}{2\pi i}\frac{\mathrm{d}\sigma}{\sigma-\zeta}$ on both sides of (11.3.10′), (11.3.10″), and (11.3.11′) lead to

$$\begin{aligned}
&\frac{1}{2\pi i}\int_\gamma \frac{\Phi_4(\sigma)\mathrm{d}\sigma}{\sigma-\zeta}+\frac{1}{2\pi i}\int_\gamma \frac{\overline{\Phi_3(\sigma)}\mathrm{d}\sigma}{\sigma-\zeta}+\frac{1}{2\pi i}\int_\gamma \frac{\omega(\sigma)}{\overline{\omega'(\sigma)}}\frac{\overline{\Phi_4'(\sigma)}\mathrm{d}\sigma}{\sigma-\zeta}=\frac{1}{32c_1}\frac{1}{2\pi i}\int_\gamma \frac{\mathbf{t}\mathrm{d}\sigma}{\sigma-\zeta}\\
&\frac{1}{2\pi i}\int_\gamma \frac{\overline{\Phi_4(\sigma)}\mathrm{d}\sigma}{\sigma-\zeta}+\frac{1}{2\pi i}\int_\gamma \frac{\Phi_3(\sigma)\mathrm{d}\sigma}{\sigma-\zeta}+\frac{1}{2\pi i}\int_\gamma \frac{\overline{\omega(\sigma)}}{\omega'(\sigma)}\frac{\Phi_4'(\sigma)\mathrm{d}\sigma}{\sigma-\zeta}=\frac{1}{32c_1}\frac{1}{2\pi i}\int_\gamma \frac{\bar{\mathbf{t}}\mathrm{d}\sigma}{\sigma-\zeta}\\
&\frac{1}{2\pi i}\int_\gamma \frac{\Phi_2(\sigma)\mathrm{d}\sigma}{\sigma-\zeta}+\frac{1}{2\pi i}\int_\gamma \frac{\overline{\omega(\sigma)}}{\omega'(\sigma)}\frac{\Phi_3'(\sigma)\mathrm{d}\sigma}{\sigma-\zeta}+\frac{1}{2\pi i}\Big[\int_\gamma \frac{\overline{\omega(\sigma)}^2}{[\omega'(\sigma)]^2}\frac{\Phi_4''(\sigma)\mathrm{d}\sigma}{\sigma-\zeta}\\
&\qquad -\int_\gamma \frac{\overline{\omega(\sigma)}^2\omega''(\sigma)}{[\omega'(\sigma)]^3}\frac{\Phi_4'(\sigma)\mathrm{d}\sigma}{\sigma-\zeta}\Big]=\frac{1}{R_1-iR_2}\frac{1}{2\pi i}\int_\gamma \frac{\mathbf{h}\mathrm{d}\sigma}{\sigma-\zeta}
\end{aligned}\tag{11.3.45}$$

where $\mathbf{t}=i\int(T_x+iT_y)\mathrm{d}s, \bar{\mathbf{t}}=-i\int(T_x-iT_y)\mathrm{d}s, \mathbf{h}=i\int(h_1+ih_2)\mathrm{d}s$ in Eq. (11.3.45), which are the function equations to determine the complex potentials $\Phi_i(\zeta)$, which are analytic in the interior of the unit circle γ, and satisfy the boundary value conditions (11.3.45) at the unit circle.

11.3.7 Solution of the Function Equations

According to the Cauchy's integral formula (refer to Major Appendix),

$$\frac{1}{2\pi i}\int_\gamma \frac{\Phi_i(\sigma)}{\sigma-\zeta}\mathrm{d}\sigma=\Phi_i(\zeta), \frac{1}{2\pi i}\int_\gamma \frac{\overline{\Phi_i(\sigma)}}{\sigma-\zeta}\mathrm{d}\sigma=\overline{\Phi_i(0)},\ |\zeta|<1$$

So that (11.3.45) are reduced to

$$\begin{aligned}
&\Phi_4(\zeta)+\overline{\Phi_3(0)}+\frac{1}{2\pi i}\int_\gamma \frac{\omega(\sigma)}{\overline{\omega(\sigma)}}\frac{\overline{\Phi_4'(\sigma)}\mathrm{d}\sigma}{\sigma-\zeta}=\frac{i}{32c_1}\frac{1}{2\pi i}\int_\gamma \frac{\mathbf{t}\mathrm{d}\sigma}{\sigma-\zeta}\\
&\overline{\Phi_4(0)}+\Phi_3(\zeta)+\frac{1}{2\pi i}\int_\gamma \frac{\overline{\omega(\sigma)}}{\omega(\sigma)}\frac{\Phi_4'(\sigma)\mathrm{d}\sigma}{\sigma-\zeta}=-\frac{i}{32c_1}\frac{1}{2\pi i}\int_\gamma \frac{\bar{\mathbf{t}}\mathrm{d}\sigma}{\sigma-\zeta}\\
&\Phi_2(\zeta)+\frac{1}{2\pi i}\int_\gamma \frac{\overline{\omega(\sigma)}}{\omega'(\sigma)}\frac{\Phi_3'(\sigma)\mathrm{d}\sigma}{\sigma-\zeta}+\frac{1}{2\pi i}\Big[\int_\gamma \frac{\overline{\omega(\sigma)}^2}{[\omega'(\sigma)]^2}\frac{\Phi_4''(\sigma)\mathrm{d}\sigma}{\sigma-\zeta}\\
&\qquad -\int_\gamma \frac{\overline{\omega(\sigma)}^2\omega''(\sigma)}{[\omega'(\sigma)]^3}\frac{\Phi_4'(\sigma)\mathrm{d}\sigma}{\sigma-\zeta}\Big]=\frac{i}{R_1-iR_2}\frac{1}{2\pi i}\int_\gamma \frac{\mathbf{h}\mathrm{d}\sigma}{\sigma-\zeta}
\end{aligned}\tag{11.3.46}$$

The calculation of integrals in (11.3.46) depends upon the configuration of the sample, so the mapping function is $\omega(\zeta)$ and the applied stresses are $\mathbf{t}$ and $\mathbf{h}$, respectively. In the following, we will give a concrete solution for a given configuration and applied traction.

11.3.8 Example 1 Elliptic Notch/Crack Problem and Solution

We calculate the stress and displacement field induced by an elliptic notch L: $(\frac{x^2}{a^2} + \frac{y^2}{b^2} = 1)$ in an infinite plane of decagonal quasicrystal (see Fig. 11.2), the edge of which is subjected to a uniform pressure p. Though the problem was solved in Sect. 8.4, to figure out its outline from the general formulation is meaningful.

The boundary conditions can be expressed in Eqs. (11.3.10) and (11.3.11), and for simplicity, we assume $h_x = h_y = 0$. Thus

$$\begin{aligned} &i\int (T_x + iT_y)\mathrm{d}s = i\int (-p\cos(\mathbf{n}, x) - ip\cos(\mathbf{n}, y))\mathrm{d}s = -pz = -p\omega(\sigma) \\ &i\int (h_x + ih_y)\mathrm{d}s = 0 \end{aligned} \tag{11.3.47}$$

In addition in this case in formula (11.3.44)

$$\begin{aligned} &X = Y = 0, \\ &B = 0, B' = C' = 0, B'' = C'' = 0 \end{aligned} \tag{11.3.48}$$

so $\Phi_j(\zeta) = \Phi_j^0(\zeta)$, but in the following, we omit the superscript of the functions $\Phi_i^0(\zeta)$ for simplicity.

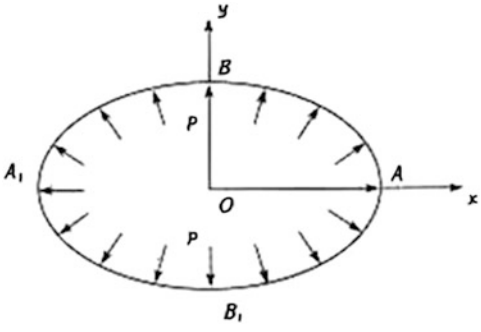

Fig. 11.2 An elliptic notch in a decagonal quasicrystal

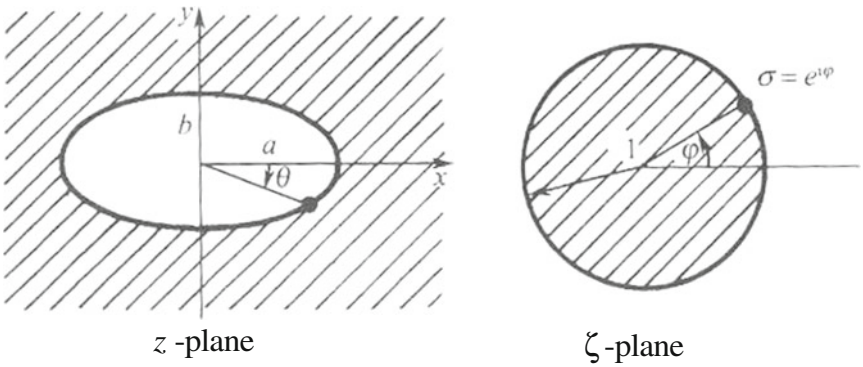

Fig. 11.3 Conformal mapping from the region at z-plane with an elliptic hole onto the interior of the unit circle at ζ-plane

The conformal mapping is

$$z = \omega(\zeta) = R_0\left(\frac{1}{\zeta} + m\zeta\right) \tag{11.3.49}$$

to transform the region containing ellipse at the z-plane onto the interior of the unit circle at the ζ-plane, refer to Fig. 11.3, where $\zeta = \xi + i\eta = \rho e^{i\varphi}$ and $R_0 = \frac{a+b}{2}$, $m = \frac{a-b}{a+b}$.

Substituting (11.3.48) and (11.3.49) into function Eq. (11.3.46), one obtains

$$\begin{aligned} \Phi_3(\zeta) &= \frac{pR_0}{32c_1}\frac{(1+m^2)\zeta}{m\zeta^2 - 1} \\ \Phi_4(\zeta) &= -\frac{pR_0}{32c_1}m\zeta \end{aligned} \tag{11.3.50}$$

$$\Phi_2(\zeta) = \frac{pR_0}{32c_1}\frac{\zeta(\zeta^2+m)[(1+m^2)(1+m\zeta^2) - (\zeta^2+m)]}{(m\zeta^2-1)^3}$$

If we take $m = 1$, from (11.3.50) we can obtain solution of the Griffith crack; in particular, the explicit solution at z-plane can be explored by taking inversion $\zeta = \omega^{-1}(z) = z/a - \sqrt{z^2/a^2 - 1}$ (as $m = 1$) into the relevant formulas.

The concrete results are given in Sect. 8.4, which are omitted here.

11.3.9 Example 2 Infinite Plane with an Elliptic Hole Subjected to a Tension at Infinity

In this case

$$X = Y = 0, T_x = T_y = 0, B = \frac{p}{64c_1}, B' = C' = 0, B'' = C'' = 0, \mathbf{t} = \bar{\mathbf{t}} = \mathbf{h} = 0 \tag{11.3.51}$$

so that from (11.3.44)

$$\begin{aligned} h_4(z) &= \Phi_4(\zeta) = B\omega(\zeta) + \Phi_4^0(\zeta) \\ h_3(z) &= \Phi_3(\zeta) = \Phi_3^0(\zeta) \\ h_2(z) &= \Phi_2(\zeta) = \Phi_2^0(\zeta) \end{aligned} \tag{11.3.51}$$

Substituting (11.3.52) into (11.3.45), we obtain the similar equations on functions $\Phi_j^0(\zeta) \quad (j = 2, 3, 4)$ bv, so the solution is similar to (11.3.50).

11.3.10 Example 3 Infinite Plane with an Elliptic Hole Subjected to a Distributed Pressure at a Part of Surface of the Hole

The problem is shown in Fig. 11.4. We here use the conformal mapping

$$z = \omega(\zeta) = R_0\left(\zeta + \frac{m}{\zeta}\right) \tag{11.3.52}$$

to transform the region at z-plane onto the exterior of the unit circle γ at ζ-plane (see Fig. 11.5).

In terms of the similar procedure, the solution we found [9] is as follows:

$$\begin{aligned} \Phi_4(\zeta) = \frac{1}{32c_1} \cdot \frac{p}{2\pi i} \cdot \left[-\frac{mR_0}{\zeta} \ln\frac{\sigma_2}{\sigma_1} + z \ln\frac{\sigma_2 - \zeta}{\sigma_1 - \zeta} + z_1 \ln(\sigma_1 - \zeta) - z_2 \ln(\sigma_2 - \zeta) \right] \\ + ip(d_1 - d_2)(z_1 - z_2) \ln \zeta \end{aligned}$$

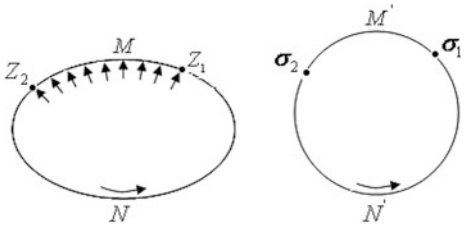

Fig. 11.4 Infinite plane with an elliptic hole subjected to a distributed pressure at a part of surface of the hole and its conformal mapping at ζ-plane

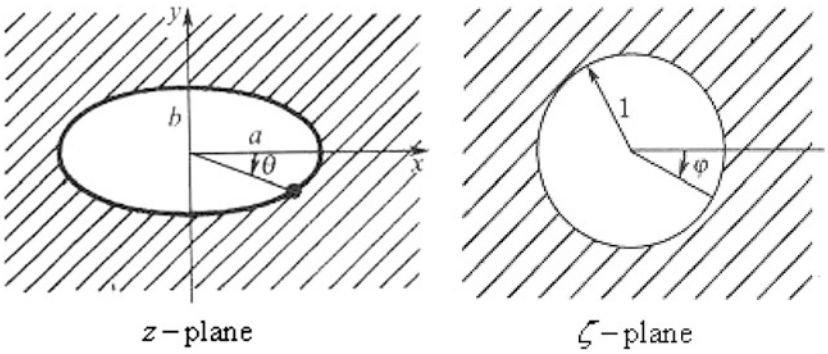

Fig. 11.5 Conformal mapping from the region at z-plane with an elliptic hole onto the exterior of the unit circle at ζ-plane

$$\Phi_3(\zeta)=\frac{1}{32c_1}\cdot\frac{p}{2\pi i}\cdot\left[-\frac{(1+m^2)R_0\zeta}{(\zeta^2-m)}\ln\frac{\sigma_2}{\sigma_1}+\frac{R_0(\sigma_1-\sigma_2)(1+m\zeta^2)}{(\zeta^2-m)}-\overline{z_2}\ln(\sigma_2-\zeta)+\overline{z_1}\ln(\sigma_1-\zeta)\right]$$
$$-ip(d_1+d_2)\cdot\left[(\overline{z_1}-\overline{z_2})\ln\zeta+(z_1-z_2)\frac{(1+m^2)}{\zeta^2-m}\right]$$

$$\Phi_2(\zeta)=\frac{1}{32c_1}\cdot\frac{pR_0}{2\pi i}\cdot\frac{(m\zeta^2+1)(\zeta^2+m)}{(\zeta^2-m)^3}(\ln\frac{\sigma_2}{\sigma_1}+\frac{\sigma_2-\sigma_1}{(\sigma_2-\zeta)(\sigma_1-\zeta)})+\frac{1}{32c_1}\cdot\frac{p}{2\pi i}\cdot\frac{(m\zeta^2+1)}{(\zeta^2-m)^2}\times$$
$$\left\{2\mathrm{Re}z_2\cdot\frac{\sigma_2-\sigma_1}{(\sigma_2-\zeta)(\sigma_1-\zeta)}+\left[z_2-R_0(\zeta-\frac{m}{\zeta})\right]\cdot\left[\frac{(\sigma_2-\zeta)(\sigma_1-\zeta)+(\sigma_2+\sigma_1-2\zeta)(\sigma_2-\sigma_1)}{(\sigma_2-\zeta)(\sigma_1-\zeta)}\right]\right\}$$
$$\frac{(m\zeta^2+1)(\zeta^2+m)}{(\zeta^2-m)^3}ip\left\{d_1(\overline{z_1}-\overline{z_2}-z_1+z_2)\frac{1}{\zeta-\sigma_1}+(d_2-d_1)(z_1-z_2)\left[\frac{1}{\zeta^2}+\frac{1}{\zeta}+\frac{1}{(\zeta-\sigma_1)^2}\right]\right\} \tag{11.3.53}$$

where

$$z_1=R_0(\sigma_1+\frac{m}{\sigma_1}),\ z_2=R_0(\sigma_2+\frac{m}{\sigma_2})$$

11.4 Complex Analysis for Sextuple Harmonic Equation and Applications to Three-Dimensional Icosahedral Quasicrystals

Plane elasticity of icosahedral quasicrystals has been reduced to a sextuple harmonic equation to solve in Chap. 9, where we have shown the solution procedure of the equation for a notch/crack problem by complex variable function method and we here provide further discussion in depth from point of complex function theory.

The aim is to develop the complex potential method for higher-order multi-harmonic equations. Though there are some similar natures in the following description with that introduced in the preceding section, the discussion here is necessary, because the governing equation and boundary conditions for icosahedral quasicrystals are quite different from those for decagonal quasicrystals.

11.4.1 The Complex Representation of Stresses and Displacements

In Sect. 9.5 by the stress potential, we obtain the final governing equation under the approximation $R^2/\mu K_1 \ll 1$

$$\nabla^2\nabla^2\nabla^2\nabla^2\nabla^2\nabla^2 G = 0 \tag{11.4.1}$$

Fundamental solution of Eq. (11.4.1) can be expressed in six analytic functions of complex variable z, i.e.

$$G(x,y) = \mathrm{Re}[g_1(z) + \bar{z}g_2(z) + \bar{z}^2 g_3(z) + \bar{z}^3 g_4(z) + \bar{z}^4 g_5(z) + \bar{z}^5 g_6(z)] \tag{11.4.2}$$

where $g_i(z)$ are arbitrary analytic functions of $z = x + iy$ and the bar denotes the complex conjugate.

From Eqs. (11.4.1), (11.4.2), (9.5.2) and (9.5.3), the stresses can be expressed as follows:

$$\begin{gathered}
\sigma_{xx} + \sigma_{yy} = 48c_2c_3R\,\mathrm{Im}\,\Gamma'(z) \quad \sigma_{yy} - \sigma_{xx} + 2i\sigma_{xy} = 8ic_2c_3R(12\overline{\Psi'(z)} - \Omega'(z)) \\
\sigma_{zy} - i\sigma_{zx} = -960c_3c_4 f_6'(z) \quad \sigma_{zz} = \frac{24\lambda R}{(\mu+\lambda)}c_2c_3\,\mathrm{Im}\,\Gamma'(z) \\
H_{xy} - H_{yx} - i(H_{xx} + H_{yy}) = -96c_2c_5\overline{\Psi'(z)} - 8c_1c_2R\Omega'(z) \\
H_{yx} + H_{xy} + i(H_{xx} - H_{yy}) = -480c_2c_5\overline{f_6'(z)} - 4c_1c_2R\Theta'(z) \\
H_{yz} + iH_{xz} = 48c_2c_6\Gamma'(z) - 4c_2R^2(2K_2 - K_1)\overline{\Omega'(z)} \\
H_{zz} = \frac{24R^2}{(\mu+\lambda)}c_2c_3\,\mathrm{Im}\,\Gamma'(z)
\end{gathered} \tag{11.4.3}$$

where

$$\begin{aligned}
\Psi(z) &= f_5(z) + 5\bar{z}f_6'(z)\\
\Gamma(z) &= f_4(z) + 4\bar{z}f_5'(z) + 10\bar{z}^2 f_6''(z)\\
\Omega(z) &= f_3(z) + 3\bar{z}f_4'(z) + 6\bar{z}^2 f_5''(z) + 10\bar{z}^3 f_6'''(z)\\
\Theta(z) &= f_2(z) + 2\bar{z}f_3'(z) + 3\bar{z}^2 f_4''(z) + 4\bar{z}^3 f_5'''(z) + 5\bar{z}^4 f_6^{(\mathrm{IV})}(z)
\end{aligned}$$

$$c_1 = \frac{R(2K_2 - K_1)(\mu K_1 + \mu K_2 - 3R^2)}{2(\mu K_1 - 2R^2)}, c_3 = \frac{1}{R}K_2(\mu K_2 - R^2) - R(2K_2 - K_1)$$

$$c_2 = \mu(K_1 - K_2) - R^2 - \frac{(\mu K_2 - R^2)^2}{\mu K_1 - 2R^2}, c_4 = c_1 R + \frac{1}{2}c_3(K_1 + \frac{\mu K_1 - 2R^2}{\lambda + \mu})$$

$$c_5 = 2c_4 - c_1 R, \quad c_6 = (2K_2 - K_1)R^2 - 4c_4\frac{\mu K_2 - R^2}{\mu K_1 - 2R^2} \tag{11.4.4}$$

In the above expressions, the function $g_1(z)$ is not used and to be assumed $g_1(z) = 0$ so $f_1(z) = 0$ for simplicity, we have introduced the following new symbols

$$\begin{aligned}
&g_2^{(9)}(z) = f_2(z), \qquad g_3^{(8)}(z) = f_3(z), \qquad g_4^{(7)}(z) = f_4(z),\\
&g_5^{(6)}(z) = f_5(z), \qquad g_6^{(5)}(z) = f_6(z)
\end{aligned} \tag{11.4.5}$$

where $g_i^{(n)}$ denote nth derivative with the argument z. Similar to the manipulation in the previous section, the complex representations of displacement components can be written as follows (here we have omitted the rigid body displacements)

$$\begin{aligned}
u_y + iu_x &= -6c_3 R(\frac{2c_2}{\mu + \lambda} + c_7)\overline{\Gamma(z)} - 2c_3 c_7 R\Omega(z)\\
u_z &= \frac{4}{\mu(K_1 + K_2) - 3R^2}(240c_{10}\mathrm{Im}f_6(z) + c_1 c_2 R^2 \mathrm{Im}(\Theta(z) - 2\Omega z) + 6\Gamma(z) - 24\Psi(z)))\\
w_y + iw_x &= -\frac{R}{c_1(\mu K_1 - 2R^2)}(24c_9\overline{\Psi(z)} - c_8\Theta(z))\\
w_z &= \frac{4(\mu K_2 - R^2)}{(K_1 - 2K_2)R(\mu(K_1 + K_2) - 3R^2)}(240c_{10}\mathrm{Im}f_6(z)) + c_1 c_2 R^2 \mathrm{Im}(\Theta(z) - 2\Omega(z)\\
&\qquad + 6\Gamma(z) - 24\Psi(z))
\end{aligned} \tag{11.4.6}$$

in which

$$c_7 = \frac{c_2K_1 + 2c_1R}{\mu K_1 - 2R^2}, \quad c_8 = c_1c_3R(\mu(K_1 - K_2) - R^2)$$
$$c_9 = c_8 + 2c_3c_4(c_2 - \frac{(\mu K_2 - R^2)^2}{\mu K_1 - 2R^2}), \quad c_{10} = c_1c_3R^2 - c_4(c_3R - c_2K_1) \tag{11.4.7}$$

11.4.2 The Complex Representation of Boundary Conditions

The boundary conditions of plane elasticity of icosahedral quasicrystals can be expressed as follows:

$$\sigma_{xx}l + \sigma_{xy}m = T_x, \quad \sigma_{yx}l + \sigma_{yy}m = T_y, \quad \sigma_{zx}l + \sigma_{zy}m = T_z \tag{11.4.8}$$

$$H_{xx}l + H_{xy}m = h_x, \quad H_{yx}l + H_{yy}m = h_y, \quad H_{zx}l + H_{zy}m = h_z \tag{11.4.9}$$

for $(x, y) \in L$ which represents the boundary of a multi-connected quasicrystalline material, and

$$l = \cos(\mathbf{n}, x) = \frac{\mathrm{d}y}{\mathrm{d}s}, \quad m = \cos(\mathbf{n}, y) = -\frac{\mathrm{d}x}{\mathrm{d}s}$$

$\mathbf{T} = (T_x, T_y, T_z)$ and $\mathbf{h} = (h_x, h_y, h_z)$ denote the surface traction vector and generalized surface traction vector, and $\mathbf{n}$ represents the outward unit normal vector of any point of the boundary, respectively.

Utilizing Eq. (11.4.3) and the first two formulas of Eq. (11.4.8), one has

$$-4c_2c_3R[3(f_4(z) + 4\bar{z}f_5'(z) + 10\bar{z}^2f_6''(z)) - (\overline{f_3(z)} + 3z\overline{f_4'(z)} + 6z^2\overline{f_5''(z)} + 10z^3\overline{f_6'''(z)})]$$
$$= i\int (T_x + iT_y)\mathrm{d}s, \quad z \in L \tag{11.4.10}$$

Taking conjugate on both sides of Eq. (11.4.10) yields

$$-4c_2c_3R[3(\overline{f_4(z)} + 4z\overline{f_5'(z)} + 10z^2\overline{f_6''(z)}) - (f_3(z) + 3\bar{z}f_4'(z) + 6z^2f_5'(z) + 10\bar{z}^3f_6'''(z)$$
$$= -i\int (T_x - iT_y)\mathrm{d}s, \ z \in L \tag{11.4.11}$$

Similarly, from Eq. (11.4.3) and the first two formulas of (11.4.9), one obtains

$$48c_2(2c_4 - c_1R)\overline{\Psi(z)} + 2c_1c_2R\Theta(z) = i\int (h_x + ih_y)\mathrm{d}s, \quad z \in L \tag{11.4.12}$$

Furthermore, we assume

$$T_z = h_z = 0 \tag{11.4.13}$$

For simplicity and by the third equations in (11.4.8) and (11.4.9) and the formulas of (11.4.3) and (11.4.13), one has

$$\begin{cases} f_6(z) + \overline{f_6(z)} = 0 \\ 4c_{11}\mathrm{Re}[f_5(z) + 5\bar{z}f_6'(z)] + (2K_2 - K_1)R\mathrm{Re}[f_4(z) + 4\bar{z}f_5'(z) + 10\bar{z}^2f_6''(z) + 20f_6(z)] = 0 \end{cases}$$

$$z \in L \tag{11.3.14}$$

in which

$$c_{11} = (2K_2 - K_1)R - \frac{4c_4(\mu K_2 - R^2)}{(\mu K_1 - 2R^2)R} \tag{11.4.15}$$

As we have shown in the previous section, complex analytic functions (i.e. the complex potentials) must be determined by boundary value equations, which are discussed below.

11.4.3 Structure of Complex Potentials

11.4.3.1 The Arbitrariness of the Complex Potentials

For explicit description, Eq. (11.4.3) can be written as follows:

$$\sigma_{zy} - i\sigma_{zx} = -960c_3c_4f_6'(z)$$

$$c_1(\sigma_{yy} - \sigma_{xx} - 2i\sigma_{xy}) + ic_2[H_{xy} - H_{yx} + i(H_{xx} + H_{yy})] = -192ic_2c_3c_4\Psi'(z)$$

$$\begin{aligned} 2c_1(H_{zy} + iH_{zx}) - R(2K_2 - K_1)[H_{xy} - H_{yx} + i(H_{xx} + H_{yy})] \\ = 96c_3cR(2K_2 - K_1)\Psi'(z) + 96c_1c_3c_6\Gamma'(z) \end{aligned}$$

$$c_5(\sigma_{yy} - \sigma_{xx} + 2i\sigma_{xy}) + ic_2R[H_{xy} - H_{yx} - i(H_{xx} + H_{yy})] = -16ic_2c_3c_4\Omega'(z)$$

$$H_{yx} + H_{xy} + i(H_{xx} - H_{yy}) = -480c_2c_5\overline{f_6'(z)} - 4c_1c_2R\Theta'(z) \tag{11.4.16}$$

Similar to the discussion of two-dimensional quasicrystals, from the equations, it is obvious that a state of phonon and phason stresses is not altered, if one replaces

$$f_i(z) \text{ by } f_i(z) + \gamma_i \qquad (i = 2, \ldots, 6) \tag{11.4.17}$$

where γ_i are the arbitrary complex constants.

Now, consider how these substitutions affect the components of the displacement vectors which were determined by the formula (11.4.6). Substituting (11.4.13) into (11.4.8)–(11.4.12) shows that if the complex constants $\gamma_i (i = 2, \ldots, 6)$ satisfy

$$\begin{aligned} &3(\frac{2c_2}{\mu+\lambda} + c_7)\overline{\gamma_4} + c_7\gamma_3 = 0 \\ &24c_9\overline{\gamma_5} - c_8\gamma_2 = 0 \\ &40c_{10}\gamma_6 - c_1c_3R^2[4(1 - \frac{c_9}{c_8})\overline{\gamma_5} - \frac{2c_2}{(\mu+\lambda)c_7}\gamma_4] = 0 \end{aligned} \tag{11.4.18}$$

then the substitution (11.4.17) will not affect the displacements.

11.4.3.2 General Formulas for Finite Multi-connected Region

Consider now the case when the region S, occupied by the body, is multi-connected (see Fig. 11.1).

Since the stress must be single-valued and Eq. (11.4.16)

$$\sigma_{zy} - i\sigma_{zx} = -960c_3c_4f_6'(z) \tag{11.4.19}$$

we know that $f_6'(z)$ is holomorphic and hence single-valued in the region inside contour s_{m+1}, so the complex function can be expressed as follows:

$$f_6(z) = \int_{z_0}^{z} f_6'(z)\mathrm{d}z + \text{constant} \tag{11.4.20}$$

where z_0 denotes fixed point. From Eq. (11.4.20), we have

$$f_6(z) = b_k \ln(z - z_k) + f_{6*}(z) \tag{11.4.21}$$

$f_{6*}(z)$ is holomorphic in the region with contour s_{m+1}.

Substituting (11.4.21) into the second formula of Eq. (11.4.16), i.e.

$$c_1(\sigma_{yy}-\sigma_{xx}-2i\sigma_{xy})+ic_2[H_{xy}-H_{yx}+i(H_{xx}+H_{yy})]=-192ic_2c_3c_4\Psi'(z),$$

shows that $f_5'(z)$ is holomorphic in the region enclosed by contour s_{m+1}, so one has

$$f_5(z)=c_k\ln(z-z_k)+f_{5*}(z) \tag{11.4.22}$$

where $f_{5*}(z)$ is holomorphic in the region of interior of contour s_{m+1}.

Similar to the above-mentioned discussion, from Eqs. (11.4.16) to (11.4.18), the complex functions $f_i(i=2,3,4)$ can be written as follows:

$$\begin{aligned} f_4(z)&=d_k\ln(z-z_k)+f_{4*}(z)\\ f_3(z)&=e_k\ln(z-z_k)+f_{3*}(z)\\ f_2(z)&=t_k\ln(z-z_k)+f_{2*}(z) \end{aligned} \tag{11.4.23}$$

where d_k, e_k and t_k are complex constants and $f_{i*}(z)$ $(i=2,3,4)$ is holomorphic in the region inside contour s_{m+1}.

By substituting (11.4.21)–(11.4.23) into the complex expressions of displacements, the condition of single valuedness of displacements will be given as follows:

$$\begin{aligned} &-3(\frac{2c_2}{\mu+\lambda}+c_7)\overline{d_k}+c_7e_k=0\\ &24c_9\overline{c_k}+c_8t_k=0\\ &240c_{10}b_k+c_1c_3R^2(t_k-2e_k+6d_k-24c_k)=0 \end{aligned} \tag{11.4.24}$$

Applying the boundary conditions given above to the contour s_k and from Eq. (11.4.24), we know that the above complex constants may be very simply expressed in terms of surface traction and generalized surface traction as

$$\begin{aligned} b_k&=\frac{c_1c_3R^2}{240c_{10}}[\frac{12c_2}{(\mu+\lambda)c_7}\overline{d_k}+24(1+\frac{c_9}{c_8})c_k]\\ c_k&=\frac{c_8}{-96\pi[c_3c_8(2c_4-c_1R)-c_1c_3R]}(h_x-ih_y)\\ t_k&=\frac{c_8}{4\pi[c_3c_8(2c_4-c_1R)-c_1c_3R]}(h_x+ih_y)\\ d_k&=\frac{(\mu+\lambda)c_7}{24\pi c_2c_3R(2c_2+(\mu+\lambda)c_7)}(T_x+iT_y)\\ e_k&=-\frac{2c_2+(\mu+\lambda)c_7}{16\pi c_2^2c_3R}(T_x-iT_y) \end{aligned} \tag{11.4.25}$$

We can easily extend the above results to the case there are m inner boundaries.

11.4.4 Case of Infinite Regions

From the point of view of application, the consideration of infinite regions is likewise of major interest. We assume that the contour s_{m+1} has entirely moved to infinity.

Similar to the discussion of two-dimensional quasicrystal, we have

$$\begin{aligned} f_6(z) &= \sum_{k=1}^{m} b_k \ln z + f_{6**}(z), \quad f_5(z) = \sum_{k=1}^{m} c_k \ln z + f_{5**}(z) \\ f_4(z) &= \sum_{k=1}^{m} d_k \ln z + f_{4**}(z), \quad f_3(z) = \sum_{k=1}^{m} e_k \ln z + f_{3**}(z) \\ f_2(z) &= \sum_{k=1}^{m} t_k \ln z + f_{2**}(z) \end{aligned} \tag{11.4.26}$$

where $f_{j**}(z) \quad (j = 2, \ldots, 6)$ are functions, holomorphic outside s_{m+1}, not including the point at infinity. By the theorem of Laurent, the function $h_{2*}(z)$ may be represented outside s_{m+1} by the series

$$f_{ji**}(z) = \sum_{-\infty}^{+\infty} a_{jn} z^n \quad (j = 2, \ldots, 6) \tag{11.4.27}$$

Substituting the first equation of (11.4.26) and (11.4.27) into the first one of Eq. (11.4.16), one has

$$\sigma_{zy} - i\sigma_{zx} = -960 c_3 c_4 \left(\sum_{k=1}^{m} b_k \frac{1}{z} + \sum_{-\infty}^{\infty} n a_{6n} z^{n-1}\right) \tag{11.4.28}$$

Hence it follows that for the stress to remain finite as $|z| \to \infty$, one must have

$$a_{6n} = 0 \ (n \geq 2) \tag{11.4.29}$$

Similarly, from Eqs. (11.4.15)–(11.4.18), to make the stresses be bounded, the following conditions are also to be satisfied

$$a_{jn} = 0 \ (n \geq 2, j = 2, \ldots, 5) \tag{11.4.30}$$

So we can obtain the expressions of the complex function $f_i(z)(i = 2, \ldots, 6)$ for the stresses to remain finite as $|z| \to \infty$, for example

$$f_6(z) = \sum_{k=1}^{m} b_k \ln z + (B + iC) z + f_6^0(z) \tag{11.4.31}$$

where B, C are unknown real constants to be determined, $f_6^0(z)$ is function, holomorphic outside s_{m+1}, including the point at infinity. The determination of unknown constants B, C is similar to that given in Sect. 11.3.4, but the details are omitted here due to the limitation of the space.

11.4.5 Conformal Mapping and Function Equations at ζ-Plane

We now have five equations of boundary value (11.4.10)–(11.4.12) and (11.3.14), from which the unknown functions $f_j(z) \quad (j = 2, \ldots, 6)$ will be determined; in addition, we have assumed that $f_1(z) = 0$, because it has no usage. For some complicated regions, the function equations cannot be directly solved at the physical plane (i.e. the z-plane), and the conformal mapping is particularly meaningful in the case.

Assume that a conformal mapping

$$z = \omega(\zeta) \tag{11.4.32}$$

is used to transform the region at z-plane onto the interior of the unit circle γ at ζ-plane. Under the mapping, the unknown functions $f_j(z)$ become

$$f_j(z) = f_j[\omega(\zeta)] = \Phi_j(\zeta) \qquad (j = 2, \ldots, 6) \tag{11.4.33}$$

Substituting (11.4.32) and (11.4.33) into the first relation of boundary conditions (11.3.14) yields

$$\frac{1}{2\pi i}\int_{\gamma} \frac{\Phi_6(\sigma)}{\sigma - \varsigma} \mathrm{d}\sigma + \frac{1}{2\pi i}\int_{\gamma} \frac{\overline{\Phi_6(\sigma)}}{\sigma - \varsigma} \mathrm{d}\sigma = 0$$

This shows

$$\Phi_6(\varsigma) = 0 \tag{11.4.34}$$

according to the Cauchy integral formula.

Substitution of (11.4.32), (11.4.33), and (11.4.34) into boundary conditions (11.4.10)–(11.4.12) and the second one of condition (11.3.14) leads to the boundary value equations to determine the unknown functions $\Phi_j(\zeta)$ $(j = 2, \ldots, 5)$ at ζ-plane, i.e.

$$\frac{3}{2\pi i}\int_{\gamma}\frac{\Phi_4(\sigma)}{\sigma-\varsigma}\mathrm{d}\sigma+\frac{4}{2\pi i}\int_{\gamma}\frac{\overline{\omega(\sigma)}}{\omega'(\sigma)}\frac{\Phi_5'(\sigma)}{\sigma-\varsigma}\mathrm{d}\sigma-\frac{1}{2\pi i}\int_{\gamma}\frac{\overline{\Phi_3(\sigma)}}{\sigma-\varsigma}\mathrm{d}\sigma$$
$$-3\frac{1}{2\pi i}\int_{\gamma}\frac{\omega(\sigma)}{\overline{\omega'(\sigma)}}\frac{\overline{\Phi_4'(\sigma)}}{\sigma-\varsigma}\mathrm{d}\sigma-6\frac{1}{2\pi i}\int_{\gamma}[\frac{[\omega(\sigma)]^2\overline{\Phi_5''(\sigma)}}{\overline{\omega'(\sigma)}^2} \tag{11.4.35}$$
$$-\frac{[\omega(\sigma)]^2\overline{\omega''(\sigma)}}{\overline{\omega'(\sigma)}^3}\overline{\Phi_5'(\sigma)}]\frac{\mathrm{d}\sigma}{\sigma-\varsigma}=\frac{1}{4c_2c_3}\frac{1}{2\pi i}\int_{\gamma}\frac{\mathbf{t}}{\sigma-\varsigma}\mathrm{d}\sigma$$

$$\frac{3}{2\pi i}\int_{\gamma}\frac{\overline{\Phi_4(\sigma)}}{\sigma-\varsigma}\mathrm{d}\sigma+\frac{4}{2\pi i}\int_{\gamma}\frac{\overline{\omega(\sigma)}}{\omega'(\sigma)}\frac{\Phi_4'(\sigma)}{\sigma-\varsigma}\mathrm{d}\sigma-\frac{1}{2\pi i}\int_{\gamma}\frac{\Phi_3(\sigma)}{\sigma-\zeta}\mathrm{d}\sigma$$
$$-3\frac{1}{2\pi i}\int_{\gamma}\frac{\overline{\omega(\sigma)}}{\omega'(\sigma)}\frac{\Phi_3(\sigma)}{\sigma-\zeta}\mathrm{d}\sigma-6\frac{1}{2\pi i}\int_{\gamma}[\frac{\overline{\omega(\sigma)}^2\Phi_5''(\sigma)}{[\omega'(\sigma)]^2} \tag{11.4.36}$$
$$-\frac{\overline{\omega(\sigma)}^2\omega''(\sigma)\Phi_5'(\sigma)}{[\omega'(\sigma)]^3}]\frac{\mathrm{d}\sigma}{\sigma-\varsigma}=\frac{1}{4c_2c_3R}\frac{1}{2\pi i}\int_{\gamma}\frac{\overline{\mathbf{t}}}{\sigma-\varsigma}\mathrm{d}\sigma$$

$$\frac{1}{2\pi i}\int_{\gamma}\frac{\Phi_2(\sigma)}{\sigma-\varsigma}\mathrm{d}\sigma+2\frac{1}{2\pi i}\int_{\gamma}\frac{\overline{\omega(\sigma)}}{\omega'(\sigma)}\frac{\Phi_3'(\sigma)}{\sigma-\varsigma}\mathrm{d}\sigma+3\frac{1}{2\pi i}\int_{\gamma}[\frac{\overline{\omega(\sigma)}^2\Phi_4''(\sigma)}{[\omega'(\sigma)]^2}$$
$$-\frac{\overline{\omega(\sigma)}^2\omega''(\sigma)\Phi_4'(\sigma)}{[\omega'(\sigma)]^3}]\frac{\mathrm{d}\sigma}{\sigma-\varsigma}+4\frac{1}{2\pi i}\int_{\gamma}[\frac{\overline{\omega(\sigma)}^2\Phi_5'''(\sigma)}{[\omega'(\sigma)]^3}-3\frac{\overline{\omega(\sigma)}^3\omega''(\sigma)\Phi_5''(\sigma)}{[\omega'(\sigma)]^4}$$
$$+3\frac{\overline{\omega(\sigma)}^3\omega''(\sigma)\Phi_5'(\sigma)}{[\omega'(\sigma)]^5}-\frac{\overline{\omega(\sigma)}^3\omega'''(\sigma)\Phi_5'(\sigma)}{[\omega'(\sigma)]^4}]\frac{\mathrm{d}\sigma}{\sigma-\varsigma}=\frac{1}{2\pi i}\int\frac{\mathbf{h}}{\sigma-\varsigma}\mathrm{d}\sigma \tag{11.4.37}$$

$$\frac{4c_{11}}{2\pi i}\int_{\gamma}\frac{\Phi_5(\sigma)}{\sigma-\varsigma}\mathrm{d}\sigma+\frac{(2K_2-K_1)R}{2\pi i}\int_{\gamma}[\frac{\Phi_4(\sigma)}{\sigma-\varsigma}+4\frac{\overline{\omega(\sigma)}}{\omega'(\sigma)}\frac{\Phi_5'(\sigma)}{\sigma-\varsigma}]\mathrm{d}\sigma=0 \tag{11.4.38}$$

in which $\mathbf{t}=i\int(T_x+iT_y)\mathrm{d}s,\overline{\mathbf{t}}=-i\int(T_x-iT_y)\mathrm{d}s,\mathbf{h}=i\int(h_1+ih_2)\mathrm{d}s$. For given configuration and applied stresses, we can obtain the solution by solving these function equations.

11.4.6 Example: Elliptic Notch Problem and Solution

We consider an icosahedral quasicrystal solid with an elliptic notch, which penetrates through the medium along the z-axis direction, the edge of the elliptic notch subjected to the uniform pressure p, similar to Fig. 11.2.

Since the measurement of generalized traction has not been reported so far, for simplicity, we assume that $h_x = 0, h_y = 0$.

However the calculation cannot be completed at the z-plane owing to the complicity, and we have to employ the conformal mapping

$$z = \omega(\zeta) = R_0(\frac{1}{\zeta} + m\zeta) \tag{11.4.38}$$

to transform the exterior of the ellipse at the z-plane onto the interior of the unit circle γ at the ζ-plane, in which

$$R_0 = (a+b)/2, \quad m = (a-b)/(a+b)$$

Let

$$f_j(z) = f_j[\omega(\zeta)] = \Phi_j(\zeta) \qquad (j = 2, \ldots, 6) \tag{11.4.39}$$

Substituting (11.4.38) into the first formula of (11.4.25), then multiplying on both sides of equations by $\mathrm{d}\sigma/[2\pi i(\sigma - \zeta)]$ (σ represents the value of at the unit circle), and integrating around the unit circle γ yield

$$\frac{1}{2\pi i}\int_{\gamma} \frac{\Phi_6(\sigma)}{\sigma - \varsigma}\mathrm{d}\sigma + \frac{1}{2\pi i}\int_{\gamma} \frac{\overline{\Phi_6(\sigma)}}{\sigma - \varsigma}\mathrm{d}\sigma = 0 \tag{11.4.40}$$

by means of Cauchy integral formula, we have

$$\Phi_6(\varsigma) = 0 \tag{11.4.41}$$

Substituting (11.4.38) and (11.4.41) into (11.4.22)–(11.4.24), then multiplying both sides of equations by $\mathrm{d}\sigma/[2\pi i(\sigma - \zeta)]$ (σ represents the value of at the unit circle), and integrating around the unit circle γ yields

$$\frac{3}{2\pi i}\int_{\gamma}\frac{\Phi_4(\sigma)}{\sigma-\varsigma}\mathrm{d}\sigma+\frac{4}{2\pi i}\int_{\gamma}\frac{\overline{\omega(\sigma)}}{\omega'(\sigma)}\frac{\Phi_5'(\sigma)}{\sigma-\varsigma}\mathrm{d}\sigma-\frac{1}{2\pi i}\int_{\gamma}\frac{\overline{\Phi_3(\sigma)}}{\sigma-\varsigma}\mathrm{d}\sigma$$
$$-3\frac{1}{2\pi i}\int_{\gamma}\frac{\omega(\sigma)}{\overline{\omega'(\sigma)}}\frac{\overline{\Phi_4'(\sigma)}}{\sigma-\varsigma}\mathrm{d}\sigma-6\frac{1}{2\pi i}\int_{\gamma}[\frac{[\omega(\sigma)]^2\overline{\Phi_5''(\sigma)}}{[\overline{\omega'(\sigma)}]^2}$$
$$-\frac{[\omega(\sigma)]^2\overline{\omega''(\sigma)}}{[\overline{\omega'(\sigma)}]^3}\overline{\Phi_5'(\sigma)}]\frac{\mathrm{d}\sigma}{\sigma-\varsigma}=\frac{p}{4c_2c_3}\int_{\gamma}\frac{\omega(\sigma)}{\sigma-\varsigma}\mathrm{d}\sigma \tag{11.4.42}$$

$$\frac{3}{2\pi i}\int_{\gamma}\frac{\overline{\Phi_4(\sigma)}}{\sigma-\varsigma}\mathrm{d}\sigma+\frac{4}{2\pi i}\int_{\gamma}\frac{\omega(\sigma)}{\overline{\omega'(\sigma)}}\frac{\Phi_5'(\sigma)}{\sigma-\varsigma}\mathrm{d}\sigma-\frac{1}{2\pi i}\int_{\gamma}\frac{\Phi_3(\sigma)}{\sigma-\zeta}\mathrm{d}\sigma$$
$$-3\frac{1}{2\pi i}\int_{\gamma}\frac{\overline{\omega(\sigma)}}{\omega'(\sigma)}\frac{\Phi_4'(\sigma)}{\sigma-\zeta}\mathrm{d}\sigma-6\frac{1}{2\pi i}\int_{\gamma}[\frac{\overline{\omega(\sigma)}^2\Phi_5''(\sigma)}{[\omega'(\sigma)]^2}$$
$$-\frac{\overline{\omega(\sigma)}^2\omega''(\sigma)\Phi_5'(\sigma)}{[\omega'(\sigma)]^3}]\frac{\mathrm{d}\sigma}{\sigma-\varsigma}=\frac{p}{4c_2c_3R}\frac{1}{2\pi i}\int_{\gamma}\frac{\overline{\omega(\sigma)}}{\sigma-\varsigma}\mathrm{d}\sigma \tag{11.4.43}$$

$$\frac{1}{2\pi i}\int_{\gamma}\frac{\Phi_2(\sigma)}{\sigma-\varsigma}\mathrm{d}\sigma+2\frac{1}{2\pi i}\int_{\gamma}\frac{\overline{\omega(\sigma)}}{\omega'(\sigma)}\frac{\Phi_3'(\sigma)}{\sigma-\varsigma}\mathrm{d}\sigma+3\frac{1}{2\pi i}\int_{\gamma}[\frac{\overline{\omega(\sigma)}^2\Phi_4''(\sigma)}{[\omega'(\sigma)]^2}$$
$$-\frac{\overline{\omega(\sigma)}^2\omega''(\sigma)\Phi_4'(\sigma)}{[\omega'(\sigma)]^3}]\frac{\mathrm{d}\sigma}{\sigma-\varsigma}+4\frac{1}{2\pi i}\int_{\gamma}[\frac{\overline{\omega(\sigma)}^3\Phi_5'''(\sigma)}{[\omega'(\sigma)]^3}-3\frac{\overline{\omega(\sigma)}^3\omega''(\sigma)\Phi_5''(\sigma)}{[\omega'(\sigma)]^4}$$
$$+3\frac{\overline{\omega(\sigma)}^3\omega''(\sigma)\Phi_5'(\sigma)}{[\omega'(\sigma)]^5}-\frac{\overline{\omega(\sigma)}^3\omega'''(\sigma)\Phi_5'(\sigma)}{[\omega'(\sigma)]^4}]\frac{\mathrm{d}\sigma}{\sigma-\varsigma}=0 \tag{11.4.44}$$

$$\frac{4c_{11}}{2\pi i}\int_{\gamma}\frac{\Phi_5(\sigma)}{\sigma-\varsigma}\mathrm{d}\sigma+\frac{(2K_2-K_1)R}{2\pi i}\int_{\gamma}[\frac{\Phi_4(\sigma)}{\sigma-\varsigma}+4\frac{\overline{\omega(\sigma)}}{\omega'(\sigma)}\frac{\Phi_5'(\sigma)}{\sigma-\varsigma}]\mathrm{d}\sigma=0 \tag{11.4.45}$$

Because

$$\frac{\overline{\omega(\sigma)}}{\omega'(\sigma)}=\sigma\frac{\sigma^2+m}{m\sigma^2-1}$$

and

$$\zeta\frac{\zeta^2+m}{m\zeta^2-1}\Phi_5'(\zeta)=\zeta\frac{\zeta^2+m}{m\zeta^2-1}(\alpha_1+2\alpha_2\zeta+3\alpha_3\zeta^2+\cdots)$$

are analytic in $|\zeta|<1$ and continuous in the unit circle γ, by means of Cauchy integral formula, from Eq. (11.4.42), we have

$$\frac{1}{2\pi i}\int_\gamma\frac{\Phi_4(\sigma)}{\sigma-\varsigma}\mathrm{d}\sigma=\Phi_4(\zeta)$$

$$\frac{1}{2\pi i}\int_\gamma\sigma\frac{\sigma^2+m}{m\sigma^2-1}\frac{\Phi_5'(\sigma)}{\sigma-\varsigma}\mathrm{d}\sigma=\zeta\frac{\zeta^2+m}{m\zeta^2-1}\Phi_5'(\zeta)$$

Substituting

$$\frac{\omega(\sigma)}{\overline{\omega'(\sigma)}}=-\frac{1}{\sigma}\frac{m\sigma^2+1}{\sigma^2-m},\quad \frac{\omega(\sigma)^2\overline{\omega''(\sigma)}}{\overline{\omega'(\sigma)}^3}=\frac{2\sigma(m\sigma^2+1)^2}{(\sigma^2-m)^3}$$

into Eq. (11.4.42), and note that

$$-\frac{1}{\zeta}\frac{m\zeta^2+1}{\zeta^2-m}\overline{\Phi_4'(\zeta)}=-\frac{1}{\zeta}\frac{m\zeta^2+1}{\zeta^2-m}(\overline{\beta_1}+2\frac{\overline{\beta_2}}{\zeta}+3\frac{\overline{\beta_3}}{\zeta^2}+\cdots)$$
$$\frac{2\zeta(m\zeta^2+1)^2}{(\zeta^2-m)^3}\overline{\Phi_5'(\zeta)}=\frac{2\zeta(m\zeta^2+1)^2}{(\zeta^2-m)^3}(\overline{\alpha_1}+2\frac{\overline{\alpha_2}}{\zeta}+3\frac{\overline{\alpha_3}}{\zeta^2}+\cdots)$$

are analytic in $|\zeta|>1$ and continuous in the unit circle γ, by means of Cauchy integral formula and analytic extension of the complex variable function theory; from Eq. (11.4.42), we obtain

$$\frac{1}{2\pi i}\int_\gamma\frac{\overline{\Phi_3(\sigma)}}{\sigma-\varsigma}\mathrm{d}\sigma=0,\quad \frac{1}{2\pi i}\int_\gamma\frac{\omega(\sigma)}{\overline{\omega'(\sigma)}}\frac{\overline{\Phi_4'(\sigma)}}{\sigma-\varsigma}\mathrm{d}\sigma=0$$
$$\frac{1}{2\pi i}\int_\gamma[\frac{\omega(\sigma)^2\overline{\Phi_5''(\sigma)}}{\overline{\omega'(\sigma)}^2}-\frac{\omega(\sigma)^2\overline{\omega''(\sigma)}}{\overline{\omega'(\sigma)}^3}\overline{\Phi_5'(\sigma)}]\frac{\mathrm{d}\sigma}{\sigma-\varsigma}=0$$

Substituting the above results into Eq. (11.4.42), with the help of Eq. (11.4.45), one has

$$\Phi_4(\zeta) = \frac{R_0}{12c_2c_3R}pm\zeta - \frac{(2K_2 - K_1)R_0}{2c_2c_3C_{11}}\frac{pm\zeta(\zeta^2 + m)}{(m\zeta^2 - 1)}$$
$$\Phi_5(\zeta) = -\frac{(2K_2 - K_1)R_0}{48c_2c_3C_{11}}pm\zeta \tag{11.4.46}$$

Similar to the above discussion, from Eqs. (11.4.43) and (11.4.44), one has

$$\Phi_2(\zeta) = -\frac{R_0}{2c_2c_3R}\frac{p\zeta(\zeta^2 + m)(m^3\zeta^2 + 1)}{(m\zeta^2 - 1)^3}$$
$$+ \frac{(2K_2 - K_1)R_0}{2c_2c_3C_{11}}\frac{pm\zeta^3(\zeta^2 + m)[m^2\zeta^6 - (m^3 + 4m)\zeta^4 + (2m^4 + 4m^2 + 5)\zeta^2 + m]}{(m\zeta^2 - 1)^5}$$
$$\Phi_3(\zeta) = -\frac{R_0}{4c_2c_3R}\frac{p\zeta(m^2 + 1)}{(m\zeta^2 - 1)} - \frac{(2K_2 - K_1)R_0}{12c_2c_3C_{11}}\frac{pm\zeta^3(\zeta^2 + m)(m\zeta^2 - m^2 - 2)}{(m\zeta^2 - 1)^3} \tag{11.4.47}$$

The elliptic notch problem is solved. The solution of the Griffith crack subjected to a uniform pressure can be obtained corresponding to the case $m = 1, R_0 = a/2$ of the above solution. The solution of crack can be expressed explicitly in the z-plane, and the concrete results refer to Sect. 9.7 in Chap. 9 for the concrete results.

11.5 Complex Analysis of Generalized Quadruple Harmonic Equation

In Chaps. 6–8, we have shown that the plane elasticity of octagonal quasicrystals is governed by the final equation

$$(\nabla^2\nabla^2\nabla^2\nabla^2 - 4\varepsilon\nabla^2\nabla^2\Lambda^2\Lambda^2 + 4\varepsilon\Lambda^2\Lambda^2\Lambda^2\Lambda^2)F = 0 \tag{11.5.1}$$

either by displacement potential or by stress potential, in which

$$\left.\begin{aligned}\nabla^2 &= \tfrac{\partial^2}{\partial x^2} + \tfrac{\partial^2}{\partial y^2}, \quad \Lambda^2 = \tfrac{\partial^2}{\partial x^2} - \tfrac{\partial^2}{\partial y^2}\\ \varepsilon &= \tfrac{R^2(L+M)(K_2+K_3)}{[M(K_1+K_2+K_3)-R^2][(L+2M)K_1-R^2]}\end{aligned}\right\} \tag{11.5.2}$$

Due to the appearance of operator Λ^2, it seems there is no any connection with complex variable functions in solving Eq. (11.5.1). But if we rewrite it as

$$[\frac{\partial^8}{\partial x^8} + 4(1 - 4\varepsilon)\frac{\partial^8}{\partial x^6\partial y^2} + 2(3 + 16\varepsilon)\frac{\partial^8}{\partial x^4\partial y^4} + 4(1 - 4\varepsilon)\frac{\partial^8}{\partial x^2\partial y^6} + \frac{\partial^8}{\partial y^8}]F = 0 \tag{11.5.3}$$

then find that this is one of typical multi-quasiharmonic partial differential equation with quadruple, and there is complex representation of solution such as

$$F(x,y) = 2\mathrm{Re}\sum_{k=1}^{4} F_k(z_k), z_k = x + \mu_k y \tag{11.5.4}$$

in which functions $F_k(z_k)$ are analytic functions of complex variable z_k $(k = 1,\ldots,4)$ and $\mu_k = \alpha_k + i\beta_k$ $(k = 1,\ldots,4)$ are complex parameters and determined by the roots of the following eigenvalue equation

$$\mu^8 + 4(1-4\varepsilon)\mu^6 + 2(3+16\varepsilon)\mu^4 + 4(1-4\varepsilon)\mu^2 + 1 = 0 \tag{11.5.5}$$

We have shown that in Chaps. 7 and 8, some solutions of dislocations (based on the displacement potential formulation) and notchs/cracks (based on the stress potential formulation) can be found in terms of this complex analysis. In the procedure, it must carry out some calculations on determinants of fourth order, so the solution expressions are quite lengthy, but which are analytic substantively.

11.6 Conclusion and Discussion

The discovery of quadruple and sextuple harmonic equations is significant for modern elasticity. This chapter gives a comprehensive discussion on the complex analysis for solving the equations, and we think the study is preliminary.

The above-mentioned complex potential approach is a new development of Muskhelishvili approach of the classical elasticity, which extends greatly the scope of the method. We believe the quadruple and sextuple harmonic equations are useful not only in quasicrystals but probably also in other disciplines of science and engineering. So the complex analysis method can be used for other studies.

Apart from the development to extend the scope of the complex potential theory and method, we also developed the Muskhelishvili method for the conformal mapping. According to the monograph [1], the conformal mapping is limited within the rational function class. But we extended it into the transcendental function class, and some exact analytic solutions for more complicated cracked configurations are achieved (see, e.g. Chap. 8).

This method is effective not only for solving elasticity problems but also for solving plasticity problem (see, e.g. Li and Fan [10] and Fan and Fan [11] and Li and Fan [12, 13]). The new summarization on the method can be found in article [14] and other references [15, 16].

11.7 Appendix of Chapter 11: Basic Formulas of Complex Analysis

It is enlightened that Muskhelishvili [1] gave extensive description in detail on complex analysis in due presentation of elasticity in his classical monograph, which is very beneficial to readers. However there is no possibility for the present book. We provide here some points only of the function theory, which were frequently cited in the text. These can be referred for readers who are advised to read books of Privalov [17] and Lavrentjev and Schabat [18] for the further details. Other knowledge has been provided in due succession of the text of Chaps. 7–9 and 11. The present contents can also be seen as a supplement in reading the material given in Chaps. 7–9 and 11 if it is needed. The importance of complex analysis is not only in deriving the solutions by the complex potential formulation but also in dealing with the solutions by integral transforms and dual integral equations to be discussed in the Appendix B of Major Appendix of this book.

11.7.1 Complex Functions, Analytic Functions

Usually, $z = x + iy$ is denoted as a complex variable in which $\sqrt{-1} = i$, or $z = re^{i\theta}$, and $r = \sqrt{x^2 + y^2}$, called the modulus of the complex number, $\theta = \arctan(\frac{y}{x})$, the argument angle of z. Assume $f(z)$ be a function of one complex variable, or complex function in abbreviation, which is denoted as

$$f(z) = P(x, y) + iQ(x, y) \tag{11.7.1}$$

in which both $P(x, y)$ and $Q(x, y)$ are functions with real variables and called the real and imaginary parts, respectively, and marked by

$$P(x, y) = \mathrm{Re} f(z), Q(x, y) = \mathrm{Im} f(z)$$

There is a sort of complex functions called analytic functions (or regular functions; single-valued analytic functions are called holomorphic functions) which have important applications in many branches of mathematics, physics, and engineering. The concepts related with this are discussed as follows.

The complex function $f(z)$ is analytic in a given region, and this means that it can be expanded in the neighbourhood of any point z_0 of the region into a non-negative integer power series (i.e. the Taylor series) of the form

$$f(z) = \sum_{n=0}^{\infty} a_n (z - z_0)^n \tag{11.7.2}$$

in which a_n is a constant (in general, a complex number). The concept are frequently used in the previous and later calculation.

Another definition of an analytic function is that if the complex function $f(z)$ is given in the region, the real part $P(x, y)$ and imaginary part $Q(x, y)$ are single-valued, have continuous partial derivatives of the first order, and satisfy Cauchy–Riemann condition such as

$$\frac{\partial P}{\partial x} = \frac{\partial Q}{\partial y}, \frac{\partial P}{\partial y} = -\frac{\partial Q}{\partial x} \tag{11.7.3}$$

in the region.

These kind of functions, P and Q, are named mutually conjugate harmonic ones. From (11.7.3), it follows that

$$\nabla^2 P = (\frac{\partial^2}{\partial x^2} + \frac{\partial^2}{\partial y^2})P = 0, \nabla^2 Q = (\frac{\partial^2}{\partial x^2} + \frac{\partial^2}{\partial y^2})Q = 0$$

This concept is also often used in the following.

An analytic function can also be defined in integral form. Assuming $f(z)$ is a complex function in a certain complex number region D, and Γ is any simple smooth closed curve (sometimes called simple curve for simplicity) in D, we can obtain that $f(z)$ is analytic in the region if

$$\int_{\Gamma} f(z)\mathrm{d}z = 0 \tag{11.7.4}$$

The result is known as the Cauchy's integral theorem (or simply called the Cauchy's theorem) which has been frequently used in the text and appendixes.

The theory of complex functions proves that the above definitions are mutually equivalent.

11.7.2 Cauchy's formula

An important result of the Cauchy's theorem is the so-called Cauchy's formula, i.e. if $f(z)$ analytic in a single-connected region D^+ bounded by a closed curve Γ and continuous in $D^+ + \Gamma$ (Fig. 11.6), then

$$\frac{1}{2\pi i}\int_{\Gamma} \frac{f(t)}{t - z}\mathrm{d}t = f(z) \tag{11.7.5}$$

in which z is an arbitrary point in D^+.

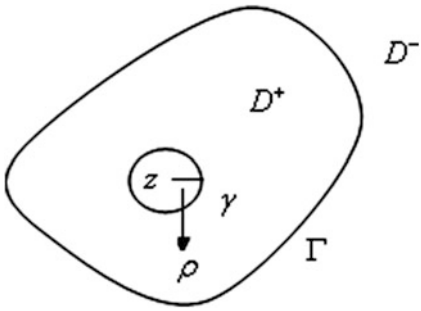

Fig. 11.6 A finite region D^+

Proof Taking z as the centre, ρ as the radius, make a small circle γ in D^+. According to Cauchy's theorem (11.7.4),

$$\int_{\Gamma} \frac{f(t)}{t-z}\mathrm{d}t = \int_{\gamma} \frac{f(t)}{t-z}\mathrm{d}t \tag{11.7.6}$$

As $f(z)$ is analytic in D^+ and continuous in $D^+ + \Gamma$, there is a small number $\varepsilon > 0$, for any point t and γ, if ρ is sufficiently small, such as

$$|f(t) - f(z)| < \varepsilon$$

and note that $|t - z| = \rho$, hence

$$\lim_{\varepsilon \to 0} \int_{\gamma} \frac{f(t)}{t-z}\mathrm{d}t = \int_{\gamma} \frac{f(z)}{t-z}\mathrm{d}t \tag{11.7.7}$$

Just as mentioned previously, $f(z)$ is analytic in D^+, and the value of the integral

$$\int_{\gamma} \frac{f(z)}{t-z}\mathrm{d}t$$

will not be changed when ρ is reducing. Therefore the limit mark in the left-hand side of (11.7.7) can be removed. In addition

$$\int_{\gamma} \frac{f(z)}{t-z}\mathrm{d}t = f(z)\int_{\gamma} \frac{\mathrm{d}t}{t-z} = f(z)\int_{0}^{2\pi} \frac{\rho e^{i\theta}}{\rho e^{i\theta}}\mathrm{d}\theta = 2\pi i f(z)$$

Based on (11.7.6) and this result, formula (11.7.5) is proved.

In formula (11.7.5), if z is taken its values in a region D^- consisting of the points lying outside Γ (see Fig. 11.6), then

$$\frac{1}{2\pi i}\int_{\Gamma}\frac{f(t)}{t-z}\mathrm{d}t = 0 \tag{11.7.8}$$

In fact, this is a direct consequence of the Cauchy's theorem, because in this case the integrand $f(z)/(\zeta - z)$ as function of ζ is analytic in region D^+, where ζ denotes the point in the region D^+.

Suppose all conditions are the same as those for (11.7.5), then

$$\frac{1}{2\pi i}\int_{\Gamma}\frac{\overline{f(t)}}{t-z}\mathrm{d}t = \overline{f(0)} \tag{11.7.9}$$

Proof For simplicity here the proof is given for the case Γ being a circle. Being analytic in the region D^+, $f(z)$ may be expanded non-negative integer power series, in which $z_0 = 0$, such that

$$f(z) = a_0 + a_1 z + a_2 z^2 + \cdots = f(0) + f'(0)z + \frac{1}{2!}f''(0)z^2 + \cdots$$

The function $\overline{f(z)}$ in formula (11.7.9) is the value of $\bar{f}(\frac{1}{z})$ at the circle Γ, and here

$$\bar{f}(\frac{1}{z}) = \overline{f(0)} + \overline{f'(0)}\frac{1}{z} + \frac{1}{2!}\overline{f''(0)}\frac{1}{z^2} + \cdots$$

is an analytic function in D^-. From the Cauchy's formula,

$$\frac{1}{2\pi i}\int_{\Gamma}\frac{\mathrm{d}t}{t^k(t-z)} = \begin{cases} 1 & k = 0 \\ 0 & k > 0 \end{cases}$$

such that (11.7.9) is proved.

In contrast to the above, current function $f(z)$ is analytic in D^- (including $z = \infty$), and then

$$\frac{1}{2\pi i}\int_{\Gamma}\frac{f(z)}{t-z}\mathrm{d}t = \begin{cases} -f(z) + f(\infty) & z \in D^- \\ f(\infty) & z \in D^+ \end{cases} \tag{11.7.10}$$

The proof of this formula can be offered in the similar manner adopted for (11.7.5), but the following points must be noted:

(i) The analytic function $f(z)$ in D^- (including $z=\infty$) may be expanded as the following series

$$f(z)=c_0+c_1\frac{1}{z}+c_2\frac{1}{z^2}+\cdots$$

(ii) $\frac{1}{2\pi i}\int_\Gamma \frac{c_0}{t-z}\mathrm{d}t=\begin{cases}0 & z\in D^-\\ c_0 & z\in D^+\end{cases}$

where $c_0=f(\infty)\neq 0$.

All conditions are the same as that for formula (11.7.10), and there exists

$$\frac{1}{2\pi i}\int_\Gamma \frac{\overline{f(t)}}{t-z}\mathrm{d}t=0 \tag{11.7.11}$$

11.7.3 Poles

Suppose a finite point in z-plane (i.e. z is not a point at infinity), and in the neighbourhood of the point, the function presents the form as follows:

$$f(z)=G(z)+f_0(z) \tag{11.7.12}$$

in which $f_0(z)$ is an analytic function in the neighbourhood of point a, and

$$G(z)=\frac{A_0}{z-a}+\frac{A_1}{(z-a)^2}+\cdots\frac{A_m}{(z-a)^m} \tag{11.7.13}$$

where $A_1,A_2,\ldots,A_m$ are constants, such that $f(z)$ is called having a pole with order m and $z=a$ is the pole.

If a is a point at infinity, $f_0(z)$ in (11.7.12) is regular at point at infinity (i.e. $f(t)=c_0+c_1z^{-1}+c_2z^{-2}+\cdots$), while at $z=\infty$

$$G(z)=A_0+A_1z+\cdots+A_mz^m \tag{11.7.14}$$

then we say that $f(z)$ has a pole of order m at $z=\infty$.

11.7.4 Residual Theorem

If the function $f(z)$ has pole a with order m, its integral may be evaluated simply by computing residual.

What is the meaning of the residual? Suppose $f(z)$ is analytic in the neighbourhood of point $z = a$, but except $z = a$, and infinite at $z = a$. In this case, the point $z = a$ is named isolated singular point. The residual of the function $f(z)$ at point $z = a$ is the value of the integral

$$\frac{1}{2\pi i}\int_{\Gamma} f(z)\mathrm{d}z$$

in which Γ represents any closed contour enclosing point $z = a$. For a residual, we will use the resignation as $\mathrm{Res}\, f(a)$.

If $z = a$ is a m-order pole of $f(z)$, its residual may be evaluated from the following formula and

$$\mathrm{Res}\, f(a) = \frac{1}{(m-1)!}\lim_{z\to a}\frac{d^{m-1}}{dz^{m-1}}\{(z-a)^m f(z)\} \tag{11.7.15}$$

Obviously, the integral is

$$\int_{\Gamma} f(z)dz = 2\pi i \mathrm{Res}\, f(a)$$

So the evaluation of integrals may be reduced to the calculation of derivatives, and it is greatly simplified. In particular, if $z = a$ is a first-order pole, then

$$\mathrm{Res}\, f(a) = \lim_{z\to a}(z-a)f(z) \tag{11.7.16}$$

in which the calculation is much simpler.

What follows the residual theorem is introduced as: let the function $f(z)$ be analytic in region D and continuous in $D+\Gamma$ except at finite isolated poles $a_1, a_2, \ldots, a_n$, then

$$\int_{\Gamma} f(z)dz = 2\pi i\sum_{k=1}^{n}\mathrm{Res}\, f(a_k) \tag{11.7.17}$$

where Γ represents the boundary of region D.

Almost all integrals in the text can be evaluated by the residual theorem.

Example Calculate the integral

$$\frac{1}{2\pi}\int_{-\infty}^{\infty}\frac{1}{-m\omega^2+k}\mathrm{e}^{-i\omega t}\mathrm{d}\omega = I \tag{11.7.18}$$

in terms of the residual theorem, where m and k are positive constants.

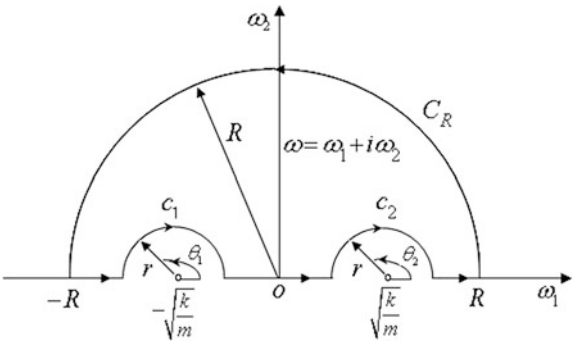

Fig. 11.7 Integration path at ω-plane

Though the integral is a real integral, it is difficult to evaluate because the integration limit is infinite and there are two singular points at the integration path, but it is easily completed by using the residual theorem. At first, we extend the real variable ω to a complex one, i.e. put $\omega = \omega_1 + i\omega_2$, where ω_1, ω_2 are real variables. At the complex plane ω, a half-circle with origin $(0, 0)$ and radius $R \to \infty$ is taken as an additional integral path, referring to Fig. 11.7. Along the real axis, the integrand of the integral has two poles $(-\sqrt{k/m}, 0)$ and $(\sqrt{m/k}, 0)$, and the value of the integral is equal to

$$\frac{1}{2\pi}\int_{-\infty}^{\infty}\frac{1}{-m\omega^2+k}\mathrm{e}^{-i\omega t}\mathrm{d}\omega = I_1 = \lim_{R\to\infty, r\to 0}\left(\int_{C_R}+\int_{1}+\int_{2}+\int_{3}+\int_{C_1}+\int_{C_2}\right) \tag{11.7.19}$$

where the first integral in the right-hand side of (11.7.19) is carried out on path of the grand half-circle, the second to fourth ones are on the path along the real axes except intervals $(-r-\sqrt{k/m}, -\sqrt{k/m}+r)$ and $(-r+\sqrt{k/m}, \sqrt{k/m}+r)$, and the fifth and sixth ones are on two small half-circle arcs C_1 and C_2 with origins $(-\sqrt{k/m}, 0)$ and $(\sqrt{k/m}, 0)$ and radius r, respectively. Because the integrand in the interior enclosing by the integration path in (11.7.19) is analytic, according to the Cauchy theorem [referring to formula (11.7.3)]

$$I_1 = 0 \tag{11.7.20}$$

Based on the behaviour of the integrand and the Jordan lemma, the first one in the right-hand side of (11.7.19) must be zero. So that

$$\lim_{R\to\infty, r\to 0}\left(\int_{1}+\int_{2}+\int_{3}+\int_{C_1}+\int_{C_2}\right) = 0$$

and

$$\lim_{R\to\infty,r\to 0}\Big(\int_1+\int_2+\int_3\Big)=I=-\lim_{r\to 0}\Big(\int_{C_1}+\int_{C_2}\Big)$$

At arc C_1: $\omega+\sqrt{k/m}=re^{i\theta_1}, d\omega=ire^{i\theta_1}d\theta_1$, and at arc C_2: $\omega-\sqrt{k/m}=re^{i\theta_2}, d\omega=ire^{i\theta_2}d\theta_2$. Substituting these into the above integrals and after some simple calculations, we obtain

$$I=\frac{\pi}{m\sqrt{k/m}}\sin\sqrt{k/m}t \tag{11.7.21}$$

In the inversion of some integral transforms and even in the solution of certain integral equations, many key calculations are completed by the similar procedure exhibited above, which will be shown in the Major Appendix B of this book.

11.7.5 Analytic Extension

A function $f_1(z)$ is analytic at region D_1, and if one can construct another function $f_2(z)$ analytic at region D_2, D_1 and D_2 are not mutually intersected regions but with common bounding Γ, furthermore

$$f_1(z)=f_2(z)\quad z\in\Gamma$$

we can say that $f_1(z)$ and $f_2(z)$ are analytic extension to each other, and we can also say that function

$$F(z)=\begin{cases}f_1(z) & as\ z\in D_1\\ f_2(z) & as\ z\in D_2\end{cases}$$

analytic at $D=D_1+D_2$ is an analytic extension of $f_1(z)$ as well as $f_2(z)$.

11.7.6 Conformal Mapping

In the text of Chaps. 7–9 and 11, by using one or several analytic functions which are also named complex potentials, we have expressed the solutions of harmonic, biharmonic, quadruple harmonic, sextuple harmonic, quasi-biharmonic, and quasi-quadruple harmonic equations, which is the complex representation of

solutions. We can see that the complex representation is only the first step for solving boundary value problems. For some problems with complicated boundaries, one must utilize the conformal mapping to transform the problem onto the mapping plane; the corresponding boundaries can be simplified to a unit circle or straight line; the calculation can be put forward; and in some cases, exact analytic solutions are available.

The so-called conformal mapping is that the complex variable $z = x + iy$ and another one $\zeta = \xi + i\eta$ can be connected by

$$z = \omega(\zeta) \tag{11.7.22}$$

in which $\omega(\zeta)$ is a single-valued analytic function of $\zeta = \xi + i\eta$ in some region. Except certain points, the inversion of mapping (11.7.22) exists. If for a certain region, the mapping is single-valued, and we say it is a single-valued conformal mapping. In general, the mapping is single-valued, but the inversion $\zeta = \omega^{-1}(z)$ is impossibly single-valued. It has the following properties:

(1) A angle at point $z = z_0$ after the mapping becomes a angle at point $\zeta = \zeta_0$, but the both angles have the same value of the argument, the rotation is either in the same direction, and this is the first kind of conformal mapping (e.g. shown in Fig. 11.5), or in counter direction, which is the second kind of conformal mapping (e.g. depicted in Fig. 11.3).
(2) If $\omega(\zeta)$ is analytic and single-valued in region Ω and transforms the region into region D, then the inversion $\zeta = \omega^{-1}(z)$ is analytic and single-valued in region D and maps D onto Ω.
(3) If D is a region and c is a simple closed curve in it, and its interior belongs to D, and if $\omega^{-1}(z)$ is analytic, and maps c onto a closed curve γ at Ω region bilaterally single-valued, then $\omega(\zeta)$ is analytic and single-valued in the region and maps D onto the interior of Ω.

In the text, we mainly used the following two kinds of conformal mapping, i.e. (1) Rational function conformal mapping, e.g.

$$\omega(\zeta) = \frac{c}{\zeta} + a_0 + a_1\zeta + \ldots + a_n\zeta^n \tag{11.7.23}$$

or

$$\omega(\zeta) = R\zeta + b_0 + b_1\frac{1}{\zeta} + \ldots + b_n\frac{1}{\zeta^n} \tag{11.7.24}$$

in which, c, a_0, a_1, …, a_n, R, b_0, b_1, …, b_n are constants. These mappings can be used in studying infinite region with a crack at physical plane onto the interior of unit circle at mapping plane. In the monograph of Muskhelishvili [1], he postulated that his method is only suitable for this kind of mapping functions. Fan [4] extended

it to transcendental mapping functions and achieved exact analytic solutions for crack problems for complicated configuration.

(2) Transcendental functions are as follows:

$$\omega(\zeta) = \frac{H}{\pi}\ln[1 + \frac{(1+\zeta)^2}{(1-\zeta)^2}] \tag{11.7.25}$$

and

$$\omega(\zeta) = \frac{2W}{\pi}\arctan\left\{\sqrt{1-\zeta^2}\tan\left(\frac{\pi a}{2W}\right)\right\} - a \tag{11.7.26}$$

which can be used to transform a finite specimen with a crack onto the interior of unit circle or upper half-plane (or lower half-plane) at mapping plane, where H, W, and a represent sample sizes and crack size.

References

1. Muskhelishvili N I, 1956, *Some Basic Problems of the Mathematical Theory of Elasticity*, P. Noordhoff, Groningen.
2. Lekhnitskii S G, 1963, *Theory of Elasticity of an Anisotropic Body*, Holden-Day, San Francisco.
3. Lu J K, 2000, Complex Variable Function Method of Plane Elasticity, Science Press, Beijing (in Chinese).
4. Fan T Y, 1990, Semi-infinite crack in a strip, Chin Phys Lett, 8(9), 401-404; 2003, Foundation of Fracture Theory, Science Press, Beijing (in Chinese).
5. Liu G T, The complex variable function method of the elastic theory of quasicrystals and defects and auxiliary equation method for solving some nonlinear evolution equations (in Chinese), Dissertation, Beijing Institute of Technology, 2004.
6. Liu G T and Fan T Y, 2003,The complex method of the plane elasticity in 2D quasicrystals point group 10 mm ten-fold rotation symmetry notch problems, *Science in China*, Series E, **46** (3), 326-336.
7. Li L H and Fan T Y, 2006, Final governing equation of plane elasticity of icosahedral quasicrystals–stress potential method, *Chin. Phys. Lett*., **24**(9) 2519-2521.
8. Li L H and Fan T Y, 2006, Complex function method for solving notch problem of point group 10 and $\overline{10}$ two-dimensional quasicrystal based on the stress potential function, *J. Phys.: Condens. Matter*, **18**(47), 10631-10641.
9. Li L H and Fan T Y, 2008, Complex function method for notch problem of plane elasticity of icosahedral quasicrystals, *Science in China*, G, **51**(6), 773-780.
10. Li W and Fan T Y, 2009, Study on elastic analysis of crack problem of two-dimensional decagonal quasicrystals of point group $10,\overline{10}$, *Int. Mod. Phys. Lett. B*, **23**(16), 1989-1999.
11. Fan T Y and Fan L, 2008, Plastic fracture of quasicrystals, *Phil. Mag*., **88**(4), 323-335.
12. Li W and Fan T Y, 2011, Plastic analysis of crack problem of two-dimensional decagonal Al-Ni-Co quasicrystalline materials of point group $10, \overline{10}$, Chin Phys B, 20(3), 036101.
13. Li W and Fan T Y, 2009, Plastic solution of crack in three-dimensional icosahedral Al-Pd-Mn quasicrystals, *Phili.Mag.*, 89(31), 2823-2832.

14. Fan T Y, Tang Z Y, Li L H and Li W, 2010, The strict theory of complex variable function method of sextuple harmonic equation and applications, *J. Math. Phys.*, 51(5), 053519.
15. Shen D W, Fan T Y, 2003, Tow collinear semi-infinite cracks in a strip, Eng Fract Mech, 70 (8), 813-822.
16. Fan T Y, Yang X C, Li H X, 1998, Complex analysis of edge crack in a finite width strip, Chin Phys Lett, 18(1), 31-34.
17. Privalov I I, 1983, Introduction to Theory of Complex Variable Functions, Science, Moscow (in Russian).
18. Lavrentjev M A, Schabat B A, 1986, Method of Complex Variable Function Theory, National Technical- Theoretical Literature Press, Moscow (in Russian).

Chapter 12
Variational Principle of Elasticity of Quasicrystals, Numerical Analysis and Applications

From Chaps. 5–11, we developed analytic theories and methods. The elasticity problems of quasicrystals were reduced to boundary value or initial-boundary value problems of some partial differential equations to solve, in which complex analysis and conformal mapping method, integral transform, integral equation method, etc. were used. For some boundary value problems, these methods are extremely powerful, even capable of obtaining exact analytic solutions. In Chap. 14 and Major Appendix, we will further develop the analytic method for studying some problems such as nonlinear deformation. The analytic solutions are very beautiful, simple and explicit, which indicate the power of the methods.

However, there are limitations themselves for these analytic methods. In general, they can only treat some problems with simple configurations and simple boundary conditions, while for more complicated problems, the methods cannot display their power.

Those solved by these analytic methods directly are partial differential equations, the solutions of which hold for the neighbourhood of any point in the region considered if the solutions are constructed. In this sense, the solutions are exact, which belong to the classical solutions in the mathematical physics, while the numerical methods are methods connected with discretization. Among them, the finite difference method displayed in Chap. 10 is one discretizing scheme. And the procedure of the finite element method is another discretizing scheme. The strict formulation of finite element method can utilize variational principle, but it is not always necessary. It has been shown that solutions obtained by these two discrete methods can approach exact solutions as the size of the discrete mesh (or element) tends to infinitesimal. By collaborating computer, the methods can solve problems with very complicated configurations, boundary conditions and material structures. This shows the power of numerical methods, which are modernized and systematized ones. In contrast to the so-called analytic (classical) solutions, modern theory

T.-Y. Fan, *Mathematical Theory of Elasticity of Quasicrystals and Its Applications*,
Springer Series in Materials Science 246, DOI 10.1007/978-981-10-1984-5_12

on partial differential equations proposed the so-called generalized (weak) solutions, and the above numerical methods are a tool to implement weak solutions. The finite difference method has been discussed in Chap. 10, and in this chapter, only the finite element method and its basis—variational principle—will be discussed. The further mathematical principle on the weak solutions will be developed in Chap. 13.

12.1 Review of Basic Relations of Elasticity of Icosahedral Quasicrystals

Because of the importance of icosahedral quasicrystals, we consider the finite element analysis only on this kind of the matter. For this purpose, we here recall the basic relations of elasticity of icosahedral quasicrystals. There are

$$\varepsilon_{ij} = \frac{1}{2}\left(\frac{\partial u_i}{\partial x_j} + \frac{\partial u_j}{\partial x_i}\right), \quad w_{ij} = \frac{\partial w_i}{\partial x_j} \tag{12.1.1}$$

In this case, the generalized Hooke's law stands for

$$\begin{aligned} \sigma_{ij} &= C_{ijkl}\varepsilon_{kl} + R_{ijkl}w_{kl} \\ H_{ij} &= K_{ijkl}w_{kl} + R_{klij}\varepsilon_{kl} \end{aligned} \tag{12.1.2}$$

where

$$C_{ijkl} = \lambda\delta_{ij}\delta_{kl} + \mu\left(\delta_{ik}\delta_{jl} + \delta_{il}\delta_{jk}\right) \tag{12.1.3}$$

$$K_{ijkl} = K_1\delta_{ik}\delta_{jl} + K_2\left(\delta_{ij}\delta_{kl} - \delta_{il}\delta_{jk}\right) \tag{12.1.4}$$

$$R_{ijkl} = R(\delta_{i1} - \delta_{i2})\left(\delta_{ij}\delta_{kl} - \delta_{ik}\delta_{jl} + \delta_{il}\delta_{jk}\right) \tag{12.1.5}$$

λ and μ are Lamé coefficients, K_1 and K_2 the phason elastic constants, and R the phonon-phason coupling elastic constant, respectively.

The stress components satisfy the equilibrium equations:

$$\frac{\partial \sigma_{ij}}{\partial x_j} + f_i = 0, \quad \frac{\partial H_{ij}}{\partial x_j} + g_i = 0 \tag{12.1.6}$$

The above formulas hold in any interior point of region Ω, and at boundary S_t, the stresses satisfy the boundary conditions:

$$\begin{aligned} &\sigma_{ij}n_j = T_i \quad (x_1, x_2, x_3) \in S_t \\ &H_{ij}n_j = h_i \end{aligned} \tag{12.1.7}$$

and at boundary S_u, the displacements satisfy the boundary conditions:

$$\begin{aligned} &u_i = \bar{u}_i \quad (x_1, x_2, x_3) \in S_u \\ &w_i = \bar{w}_i \end{aligned} \tag{12.1.8}$$

where T_i is the traction vector, h_i the generalized traction vector at boundary S_t, $\bar{u}_i$ and $\bar{w}_i$ the given displacements at boundary S_u, n_i the unit outward normal vector at any point of the boundary and $S = S_u + S_t$.

In the following, only the static problems are studied, and the initial value conditions will not be concerned. For the dynamic problems, the initial value conditions must be used, which have been discussed in Chap. 10.

12.2 General Variational Principle for Static Elasticity of Quasicrystals

The variational principle of mathematical physics is one of the basic principles, which reveals that the extreme value (or stationary value) of energy functional of a system is equivalent to the governing equations and the corresponding boundary value (or initial-boundary value) conditions of the system. Accordingly, solutions of initial-boundary value problem of the partial differential equations can be converted to determine the extreme value of the corresponding energy functional. And the latter will be implemented by a discretization procedure, and one among them is the finite element method.

We here extend the minimum potential energy principle of classical elasticity [1] to describe the elasticity of quasicrystals.

Theorem Variational principle of elasticity of quasicrystals

For sufficient smooth boundary, if all u_i and w_i satisfy the equations of deformation geometry (12.1.1) *and displacement boundary conditions* (12.1.8), *let the energy functional of quasicrystals*

$$\Pi = \int_{\Omega} F \mathrm{d}\Omega + \int_{\Omega} (f_i u_i + g_i w_i) \mathrm{d}\Omega + \int_{S_t} (T_i u_i + h_i w_i) \mathrm{d}S \tag{12.2.1}$$

to take a minimum value, then they will be the solution satisfying the equilibrium Eqs. (12.1.6) *and the stress boundary conditions* (12.1.7), *in which F is defined by*

$$
\begin{aligned}
F &= \int_0^{\varepsilon_{ij}} \sigma_{ij} \mathrm{d}\varepsilon_{ij} + \int_0^{w_{ij}} H_{ij} \mathrm{d}w_{ij} = F_u + F_w + F_{uw} \\
F_u &= \frac{1}{2} C_{ijkl} \varepsilon_{ij} \varepsilon_{kl} \\
F_w &= \frac{1}{2} K_{ijkl} w_{ij} w_{kl} \\
F_{uw} &= R_{ijkl} \varepsilon_{ij} w_{kl}
\end{aligned}
\tag{12.2.2}
$$

or by (4.4.1), Ω *the region occupied by the quasicrystal and S the boundary of* Ω. *In addition, the conditions in the theorem are sufficient and necessary.*

Proof

(i) Necessity

Assume that the functional Π takes its extreme value, i.e. $\delta\Pi = 0$. From (12.2.1)

$$
\delta\Pi = \int_\Omega \left(\frac{\partial F}{\partial \varepsilon_{ij}} \delta\varepsilon_{ij} + \frac{\partial F}{\partial w_{ij}} \delta w_{ij}\right) \mathrm{d}\Omega - \int_\Omega (f_i \delta u_i + g_i \delta w_i) \mathrm{d}\Omega - \int_{S_t} (T_i \delta u_i + h_i \delta w_i) \mathrm{d}S = 0 \tag{12.2.3}
$$

were

$$
\sigma_{ij} = \frac{\partial F}{\partial \varepsilon_{ij}}, \quad H_{ij} = \frac{\partial F}{\partial w_{ij}} \tag{12.2.4}
$$

which have been introduced in Chap. 4.

Noting that the suffixes of quantities $\frac{\partial F}{\partial \varepsilon_{ij}}$ are symmetric, therefore, we obtain

$$
\int_\Omega \frac{\partial F}{\partial \varepsilon_{ij}} \delta\varepsilon_{ij} \mathrm{d}\Omega = \int_\Omega \frac{\partial F}{\partial \varepsilon_{ij}} \delta\left(\frac{\partial u_i}{\partial x_j}\right) \mathrm{d}\Omega
$$

Making use of the Green formula to the above formula yields

$$
\begin{aligned}
\int_\Omega \frac{\partial F}{\partial \varepsilon_{ij}} \delta\varepsilon_{ij} \mathrm{d}\Omega &= \int_\Omega \frac{\partial}{\partial x_j} \left(\frac{\partial F}{\partial \varepsilon_{ij}} \delta u_i\right) \mathrm{d}\Omega - \int_\Omega \frac{\partial}{\partial x_j} \left(\frac{\partial F}{\partial \varepsilon_{ij}} \delta u_i\right) \mathrm{d}\Omega \\
&= \int_{S_u + S_t} \frac{\partial F}{\partial \varepsilon_{ij}} n_j \delta u_i \mathrm{d}S - \int_\Omega \frac{\partial}{\partial x_j} \left(\frac{\partial F}{\partial \varepsilon_{ij}}\right) \delta u_i \mathrm{d}\Omega
\end{aligned}
$$

Because the displacements are given at the boundary S_u, at which $\delta u_i = \delta \bar{u}_i = 0$, the above formula has been reduced to

$$\int_{\Omega} \frac{\partial F}{\partial \varepsilon_{ij}} \delta \varepsilon_{ij} \mathrm{d}\Omega = \int_{S_t} \frac{\partial F}{\partial \varepsilon_{ij}} n_j \delta u_i \mathrm{d}S - \int_{\Omega} \frac{\partial}{\partial x_j}\left(\frac{\partial F}{\partial \varepsilon_{ij}}\right) \delta u_i \mathrm{d}\Omega \tag{12.2.5}$$

Due to $w_{ij} = \partial w_i / \partial x_j$, a similar analysis to what adopted just above gives rise to

$$\int_{\Omega} \frac{\partial F}{\partial w_{ij}} \delta w_{ij} \mathrm{d}\Omega = \int_{\Gamma_t} \frac{\partial F}{\partial w_{ij}} n_j \delta w_i \mathrm{d}\Gamma - \int_{\Omega} \frac{\partial}{\partial x_j}\left(\frac{\partial F}{\partial w_{ij}}\right) \delta u_i \mathrm{d}\Omega \tag{12.2.6}$$

Substituting (12.2.5) and (12.2.6) into (12.2.3) leads to

$$\begin{aligned} \delta \Pi = &- \int_{\Omega} \left\{ \left[\frac{\partial}{\partial x_j}\left(\frac{\partial F}{\partial \varepsilon_{ij}}\right) + f_i \right] \delta u_i \mathrm{d}\Omega + \left[\frac{\partial}{\partial x_j}\left(\frac{\partial F}{\partial w_{ij}}\right) + g_i \right] \delta w_i \right\} \mathrm{d}\Omega \\ &+ \int_{S_t} \left\{ \left[\left(\frac{\partial F}{\partial \varepsilon_{ij}}\right) n_j - T_i \right] \delta u_i + \left[\left(\frac{\partial F}{\partial w_{ij}}\right) n_j - h_i \right] \delta w_i \right\} \mathrm{d}S = 0 \end{aligned} \tag{12.2.7}$$

Since δu_i and δw_i are of arbitrary and independent variation at region Ω and boundary S, the validity of (12.2.7) must be

$$\frac{\partial}{\partial x_j}\left(\frac{\partial F}{\partial \varepsilon_{ij}}\right) + f_i = 0, \quad \frac{\partial}{\partial x_j}\left(\frac{\partial F}{\partial w_{ij}}\right) + g_i = 0, \quad (x_1, x_2, x_3) \in \Omega$$

$$\left(\frac{\partial F}{\partial w_{ij}}\right) n_j - h_i = 0, \quad \left(\frac{\partial F}{\partial \varepsilon_{ij}}\right) n_j - T_i = 0, \quad (x_1, x_2, x_3) \in S_t$$

Substituting (12.2.4) into the above formulas yields just the equilibrium equations and stress boundary conditions. This shows that the u_i and w_i satisfying equations of deformation geometry, stress–strain relations and displacement boundary conditions and making energy functional to have minimum value should be the solution satisfying the equilibrium equations and stress boundary conditions.

(ii) Sufficiency

The sufficiency of the conditions given by the theorem means that if u_i and w_i satisfy the relations of deformation geometry and displacement boundary and make the equilibrium equations and stress boundary conditions to be satisfied, then they should do the energy functional to be minimum.

Suppose that quantities u_i, ε_{ij}, w_i and w_{ij} obey the stress–strain relations (12.1.8) and satisfy the displacement boundary conditions (12.1.13) and set

$$\begin{aligned} \varepsilon_{ij}^* &= \varepsilon_{ij} + \delta \varepsilon_{ij}, \quad u_i^* = u_i + \delta u_i \\ w_{ij}^* &= w_{ij} + \delta w_{ij}, \quad w_i^* = w_i + \delta w_i \end{aligned} \tag{12.2.8}$$

through the displacement–strain relations, what follows

$$\begin{aligned} \delta\varepsilon_{ij} &= \frac{1}{2}\left(\delta u_{i,j} - \delta u_{j,i}\right) \\ \delta w_{ij} &= \delta w_{i,j} \end{aligned} \tag{12.2.9}$$

where $u_{i,j} = \partial u_i/\partial x_j$, etc.

The free energy $F(\varepsilon_{ij}^*, w_{ij}^*)$ can be expanded into the Taylor series, as follows:

$$\begin{aligned} F(\varepsilon_{ij}^*, w_{ij}^*) = F(\varepsilon_{ij} + \delta\varepsilon_{ij}, w_{ij} + \delta w_{ij}) = F(\varepsilon_{ij}, w_{ij}) + \frac{\partial F}{\partial \varepsilon_{ij}}\delta\varepsilon_{ij} + \frac{\partial F}{\partial w_{ij}}\delta w_{ij} \\ + \frac{1}{2}\frac{\partial^2 F}{\partial\varepsilon_{ij}\partial\varepsilon_{kl}}\delta\varepsilon_{ij}\delta\varepsilon_{kl} + \frac{1}{2}\frac{\partial^2 F}{\partial w_{ij}\partial w_{kl}}\delta w_{ij}\delta w_{kl} + \frac{\partial^2 F}{\partial\varepsilon_{ij}\partial w_{kl}}\delta\varepsilon_{ij}\delta w_{kl} + \cdots \end{aligned} \tag{12.2.10}$$

If the free energy is a homogeneous quantity of strain components of second order, then the expansion of energy functional corresponding to (12.2.10) does not contain terms higher than third order, i.e.

$$\Pi^* = \Pi + \delta\Pi + \delta^2\Pi + O(\delta^3) \tag{12.2.11}$$

in which

$$\delta\Pi = \int_\Omega \left(\frac{\partial F}{\partial\varepsilon_{ij}}\delta\varepsilon_{ij} + \frac{\partial F}{\partial w_{ij}}\delta w_{ij} - f_i\delta u_i - g_i\delta w_i\right)\mathrm{d}\Omega - \int_{S_t}(T_i\delta u_i + h_i\delta w_i)\mathrm{d}S \tag{12.2.12}$$

$$\delta^2\Pi = \int_\Omega \left\{\frac{1}{2}\frac{\partial^2 F}{\partial\varepsilon_{ij}\partial\varepsilon_{kl}}\delta\varepsilon_{ij}\delta\varepsilon_{kl} + \frac{1}{2}\frac{\partial^2 F}{\partial w_{ij}\partial w_{kl}}\delta w_{ij}\delta w_{kl} + \frac{1}{2}\frac{\partial^2 F}{\partial\varepsilon_{ij}\partial w_{kl}}\delta\varepsilon_{ij}\delta w_{kl}\right\}\mathrm{d}\Omega \tag{12.2.13}$$

Applying the Green formula to (12.2.12) leads to

$$\delta\Pi = 0$$

It is because u_i and w_i (through the corresponding σ_{ij} and H_{ij}) satisfy the equilibrium equations and stress boundary conditions. This means that the energy functional takes extreme value.

According to the discussion in Ref. [2], we do some extension, i.e. $\lambda + \mu > 0$, $\mu > 0$, $K_1 > 0, K_2 > 0, \mu K_1 > R^2$, then elasticity of quasicrystals presents stability, in the case the stress-strain elastic matrix should be positive definite, so

$$\delta^2 \Pi > 0$$

This guarantees that $\delta\Pi = 0$ takes not only an extreme value, but also the minimum value of the energy functional.

But recent experimental results and some simulation show that there may be $K_2 < 0$, this does not influence the energy taking extreme value, but the extreme value may not be a minimum value.

Collaborating variational principle and theory of functional analysis, we can prove that existence, uniqueness and stability of solution of the boundary value problem (12.1.3) and (12.1.6)–(12.1.8). This is concerned not only with the numerical implementation, but also with other topics, the detailed discussion of which will be given in Chap. 13 or see Guo and Fan [2].

The variational principle can be extended to dynamic case, in which it is needed only to extend the energy functional (12.1.1) to be as follows:

$$\Pi = \int_{\Omega} F \mathrm{d}\Omega + \int_{\Omega} [(f_i - \rho \ddot{u}_i)u_i + (g_i - \kappa \dot{w}_i)w_i]\mathrm{d}\Omega + \int_{S_t} (T_i u_i + h_i w_i)\mathrm{d}S \tag{12.2.14}$$

where the meaning of ρ and κ can be found in Chap. 10. From (12.2.14), we can obtain the corresponding variational equation similar to (12.2.3), but which is equivalent to the equations of phonon-phason dynamics and related boundary and initial conditions of quasicrystals. The further discussion about this is omitted here.

12.3 Finite Element Method for Elasticity of Icosahedral Quasicrystals

Finite element method is a method discreting variational equations and region Ω. Dividing the quasicrystal body into M subregions or M elements $\Omega^{(m)}$, the superscript m denotes the number of an element, and $m = 1, \ldots, M$. For any element $\Omega^{(m)}$, the phonon and phason displacements are expressed by $u_i^{(m)}$ and $w_i^{(m)}$

$$\begin{cases} u_i^{(m)} = \sum_{\alpha=1}^{n} I_\alpha u_{i\alpha}^{(m)} \\ w_i^{(m)} = \sum_{\alpha=1}^{n} I_\alpha w_{i\alpha}^{(m)} \end{cases} \qquad (x, y, z) \in \Omega^{(m)} \tag{12.3.1}$$

in which n is the amount of mth element, subindex α the number of nodes of element m, I_α the interpolating function of node α, $u_{i\alpha}^{(m)}$ and $w_{i\alpha}^{(m)}$ the phonon and phason ith displacement components of node α. In the interior of every element, the

displacements $u_i^{(m)}$ and $w_i^{(m)}$ are continuous and single-valued, and at the interface between elements, the displacements are continuous, i.e.

$$\begin{cases} u_i^{(m)} = u_i^{(m')} \\ w_i^{(m)} = w_i^{(m')} \end{cases} \qquad (x, y, z) \in S^{(mm')} \tag{12.3.2}$$

where $S^{(mm')}$ represents the interface between elements m and m'. At the boundary S_u on which the displacements are given, the displacements satisfy the displacement boundary conditions (12.1.8).

Under satisfying these conditions, the discretization form of energy functional Π takes

$$\Pi^* = \sum_{m=1}^{M} \left[\int_{\Omega^{(m)}} \left(\frac{1}{2} C_{ijkl} \varepsilon_{ij}^{(m)} \varepsilon_{kl}^{(m)} + \frac{1}{2} K_{ijkl} w_{ij}^{(m)} w_{kl}^{(m)} + R_{ijkl} \varepsilon_{ij}^{(m)} w_{kl}^{(m)} - f_i^{(m)} u_i^{(m)} - g_i^{(m)} w_i^{(m)} \right) \mathrm{d}\Omega \right.$$
$$\left. - \int_{S_t^{(m)}} \left(T_i^{(m)} u_i^{(m)} + h_i^{(m)} w_i^{(m)} \right) \mathrm{d}S \right] \tag{12.3.3}$$

According to the following order, the strain components can be arranged as a vector:

$$\left\{ \varepsilon_{ij}, w_{ij} \right\}^{(m)\mathrm{T}} = \left\{ \varepsilon_{11}, \varepsilon_{22}, \varepsilon_{33}, \gamma_{23}, \gamma_{31}, \gamma_{12}, w_{11}, w_{22}, w_{33}, w_{23}, w_{31}, w_{12}, w_{32}, w_{13}, w_{21} \right\}^{(m)} \tag{12.3.4}$$

where $\gamma_{ij} = 2\varepsilon_{ij}$ $(i \neq j)$ and the superscript T denotes the transpose of matrix. The stresses can also be expressed as a vector:

$$\left\{ \sigma_{ij}, H_{ij} \right\}^{(m)\mathrm{T}} = \left\{ \sigma_{11}, \sigma_{22}, \sigma_{33}, \sigma_{23}, \sigma_{31}, \sigma_{12}, H_{11}, H_{22}, H_{33}, H_{23}, H_{31}, H_{12}, H_{32}, H_{13}, H_{21} \right\}^{(m)} \tag{12.3.5}$$

Utilizing (12.3.4) and (12.3.5), the relation (12.1.2) between stresses and strains stands for

$$\left\{ \sigma_{ij}, H_{ij} \right\}^{m} = [D] \left\{ \varepsilon_{ij}, w_{ij} \right\}^{m} \tag{12.3.6}$$

where $[D]$ is the elastic constant matrix, namely

$$[D] = \begin{bmatrix} [C] & [R] \\ [R]^{\mathrm{T}} & [K] \end{bmatrix} \tag{12.3.7}$$

with the submatrixes as

$$[C]=\begin{bmatrix}\lambda+2\mu & \lambda & \lambda & 0 & 0 & 0\\ \lambda & \lambda+2\mu & \lambda & 0 & 0 & 0\\ \lambda & \lambda & \lambda+2\mu & 0 & 0 & 0\\ 0 & 0 & 0 & \mu & 0 & 0\\ 0 & 0 & 0 & 0 & \mu & 0\\ 0 & 0 & 0 & 0 & 0 & \mu\end{bmatrix}$$

$$[R]=\begin{bmatrix}R & R & R & 0 & 0 & 0 & 0 & R & 0\\ -R & -R & R & 0 & 0 & 0 & 0 & -R & 0\\ 0 & 0 & -2R & 0 & 0 & 0 & 0 & 0 & 0\\ 0 & 0 & 0 & 0 & 0 & -R & R & 0 & -R\\ R & -R & 0 & 0 & R & 0 & 0 & 0 & 0\\ 0 & 0 & 0 & -R & 0 & -R & 0 & 0 & R\end{bmatrix}$$

$$[K]=\begin{bmatrix}K_1 & 0 & 0 & 0 & K_2 & 0 & 0 & K_2 & 0\\ 0 & K_1 & 0 & 0 & -K_2 & 0 & 0 & K_2 & 0\\ 0 & 0 & K_1+K_2 & 0 & 0 & 0 & 0 & 0 & 0\\ 0 & 0 & 0 & K_1-K_2 & 0 & K_2 & 0 & 0 & -K_2\\ K_2 & -K_2 & 0 & 0 & K_1-K_2 & 0 & 0 & 0 & 0\\ 0 & 0 & 0 & K_2 & 0 & K_1 & -K_2 & 0 & 0\\ 0 & 0 & 0 & 0 & 0 & -K_2 & K_1-K_2 & 0 & -K_2\\ K_2 & K_2 & 0 & 0 & 0 & 0 & 0 & K_1-K_2 & 0\\ 0 & 0 & 0 & -K_2 & 0 & 0 & -K_2 & 0 & K_1\end{bmatrix}$$

The vector representation of phonon and phason displacements can be written by

$$\left\{\bar{u}^{(m)}\right\}^{\mathrm{T}}=\{u_1,u_2,u_3,w_1,w_2,w_3\}^{(m)} \tag{12.3.8}$$

In accordance with the strain–displacement relation (12.1.1), the equation (12.3.4) can be expressed by

$$\left\{\varepsilon_{ij},w_{ij}\right\}^{(m)}=[L]\left\{\bar{u}^{(m)}\right\} \tag{12.3.9}$$

where $[L]$ represents differential operator matrix of element strain, i.e.

$$[L]^{\mathrm{T}}=\begin{bmatrix}\partial_1 & 0 & 0 & 0 & \partial_3 & \partial_2 & 0 & 0 & 0 & 0 & 0 & 0 & 0 & 0 & 0\\ 0 & \partial_2 & 0 & \partial_3 & 0 & \partial_1 & 0 & 0 & 0 & 0 & 0 & 0 & 0 & 0 & 0\\ 0 & 0 & \partial_3 & \partial_2 & \partial_1 & 0 & 0 & 0 & 0 & 0 & 0 & 0 & 0 & 0 & 0\\ 0 & 0 & 0 & 0 & 0 & 0 & \partial_1 & 0 & 0 & 0 & 0 & \partial_2 & 0 & \partial_3 & 0\\ 0 & 0 & 0 & 0 & 0 & 0 & 0 & \partial_2 & 0 & \partial_3 & 0 & 0 & 0 & 0 & \partial_1\\ 0 & 0 & 0 & 0 & 0 & 0 & 0 & 0 & \partial_3 & 0 & \partial_1 & 0 & \partial_2 & 0 & 0\end{bmatrix}. \tag{12.3.10}$$

in which $\partial_j = \frac{\partial}{\partial x_j}$ $(j = 1, 2, 3)$. Substituting (12.3.9) into (12.3.6), it follows that

$$\left\{\sigma_{ij}, H_{ij}\right\}^{(m)} = [D][L]\left\{\bar{u}^{(m)}\right\} \tag{12.3.11}$$

Inserting (12.3.8), (12.3.9) and (12.3.11) into the discreting form of the energy functional (12.3.3) yields

$$\Pi^* = \sum_{m=1}^{M}\left\{\int_{\Omega^{(m)}} \frac{1}{2}\left\{\bar{u}^{(m)}\right\}^{\mathrm{T}}[L]^{\mathrm{T}}[D][L]\left\{\bar{u}^{(m)}\right\}\mathrm{d}\Omega - \left\{\bar{u}^{(m)}\right\}^{\mathrm{T}}\left[\int_{\Omega_m}\left\{\begin{matrix} f^{(m)} \\ g^{(m)} \end{matrix}\right\}\mathrm{d}\Omega + \int_{S_t^{(m)}}\left\{\begin{matrix} T^{(m)} \\ h^{(m)} \end{matrix}\right\}\mathrm{d}S\right]\right\} \tag{12.3.12}$$

In the interior of element m, the displacement vector $\left\{\bar{u}^{(m)}\right\}$ can be expressed by the displacement vector of every node

$$\left\{\bar{u}^{(m)}\right\} = [I]\left\{\tilde{u}^{(m)}\right\} \tag{12.3.13}$$

where $[I] = [[I_1], [I_2], \ldots, [I_n]]$ is the matrix of interpolating functions:

$$[I_\alpha] = \begin{bmatrix} I_\alpha & 0 & 0 & 0 & 0 & 0 \\ 0 & I_\alpha & 0 & 0 & 0 & 0 \\ 0 & 0 & I_\alpha & 0 & 0 & 0 \\ 0 & 0 & 0 & I_\alpha & 0 & 0 \\ 0 & 0 & 0 & 0 & I_\alpha & 0 \\ 0 & 0 & 0 & 0 & 0 & I_\alpha \end{bmatrix}, \quad \alpha = 1, 2, \ldots, n \tag{12.3.14}$$

$\left\{\tilde{u}^{(m)}\right\} = \left\{\left\{\tilde{u}_1^{(m)}\right\}, \left\{\tilde{u}_2^{(m)}\right\}, \ldots, \left\{\tilde{u}_\alpha^{(m)}\right\}, \ldots, \left\{\tilde{u}_n^{(m)}\right\}\right\}$ consists of displacement vectors of every node within the element, and $\left\{\tilde{u}_\alpha^{(m)}\right\}$ the displacement vector of node α, i.e.

$$\left\{\tilde{u}_\alpha^{(m)}\right\} = \left\{u_{1\alpha}, u_{2\alpha}, u_{3\alpha}, w_{1\alpha}, w_{2\alpha}, w_{3\alpha}\right\}^{(m)} \tag{12.3.15}$$

Substituting (12.3.13) into (12.3.12), then (12.3.12) can be calculated as follows

$$\delta\Pi^* = 0 \tag{12.3.16}$$

then we have obtained the finite element scheme

$$[K]\{\tilde{u}\} = \{\mathbf{R}\} \tag{12.3.17}$$

in which

$$[K] = \sum_{m=1}^{M} \int_{\Omega^{(m)}} [B]^{\mathrm{T}}[D][B]\mathrm{d}\Omega, \quad [B_i] = [L][I_i],$$
$$\{\mathbf{R}\} = \sum_{m=1}^{M} \left(\int_{\Omega^{(m)}} [I]^{\mathrm{T}} \begin{Bmatrix} f^{(m)} \\ g^{(m)} \end{Bmatrix} \mathrm{d}\Omega + \int_{S_t^{(m)}} [I]^{\mathrm{T}} \begin{Bmatrix} T^{(m)} \\ h^{(m)} \end{Bmatrix} \mathrm{d}S \right) \tag{12.3.18}$$

$[K]$ denotes the total stiffness matrix, $\{\mathbf{R}\}$ the vector of equivalent node force, $\{\tilde{u}\} = \left\{\left\{\tilde{u}^{(1)}\right\}, \left\{\tilde{u}^{(2)}\right\}, \ldots, \left\{\tilde{u}^{(N)}\right\}\right\}$ the displacement vector of all nodes within region Ω, N the amount of nodes after discretization. From (12.3.17), one obtains the solution $\{\tilde{u}\}$ and further gets strains and stresses. The stiffness matrix $[K]$ in integral form can be evaluated by the Gauss-integrating method.

The stresses at the Gauss integral point in element m of quasicrystals can be obtained through the following expression:

$$\left\{\sigma_{ij}, H_{ij}\right\}^{(m)} = [D][B]\left\{\tilde{u}^{(m)}\right\} \tag{12.3.19}$$

12.4 Numerical Results

1. **Test example—an icosahedral Al–Pd–Mn quasicrystal bar subjected to uniaxial tension**

Consider an icosahedral Al–Pd–Mn quasicrystal bar with the height H subjected to uniaxial tensile force F as shown in Fig. 12.1. A Cartesian coordinate system (x_1, x_2, x_3) is introduced with the bottom and top surfaces lying in the planes $x_3 = 0$

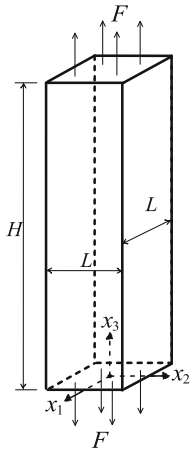

Fig. 12.1 An icosahedral quasicrystal bar subjected to uniaxial tension

and $x_3 = H$, respectively. The coordinate origin is located at the centre of the bottom of the cuboid. The area of the cross section of the cuboid is L^2.

According to the loading of bar, it is obvious that the stress components yield

$$\sigma_{33} = \frac{F}{L^2}, \quad \sigma_{11} = \sigma_{22} = \sigma_{23} = \sigma_{31} = \sigma_{12} = 0, \quad H_{ij} = 0,$$

Inserting Eq. (31) into Eq. (7) leads to the strain components in the x_3 direction:

$$\varepsilon_{11} = \varepsilon_{22} = \frac{-F\left(\lambda + \frac{2R^2}{K_1+K_2}\right)}{2L^2\left[2\mu^2 + 3\lambda\mu - \frac{R^2(9\lambda+6\mu)}{K_1+K_2}\right]}, \quad \varepsilon_{33} = \frac{F\left(\lambda + \mu - \frac{R^2}{K_1+K_2}\right)}{L^2\left[2\mu^2 + 3\lambda\mu - \frac{R^2(9\lambda+6\mu)}{K_1+K_2}\right]}$$
$$w_{33} = \frac{FR}{L^2[\mu(K_1+K_2) - 3R^2]}, \quad \text{other } \varepsilon_{ij} = w_{ij} = 0$$

The displacement boundary conditions for this problem can be written as follows:

$$u_3 = w_3 = 0, \quad \text{for } x_3 = 0;$$
$$u_1 = u_2 = w_1 = w_2 = 0, \quad \text{for } x_1 = x_2 = x_3 = 0.$$

Further, tractions in both phonon and phason are zero at all other surfaces. The displacement components are as follows:

$$u_1 = \frac{-F\left(\lambda + \frac{2R^2}{K_1+K_2}\right)x_1}{2L^2\left[2\mu^2 + 3\lambda\mu - \frac{R^2(9\lambda+6\mu)}{K_1+K_2}\right]}, \quad u_2 = \frac{-F\left(\lambda + \frac{2R^2}{K_1+K_2}\right)x_2}{2L^2\left[2\mu^2 + 3\lambda\mu - \frac{R^2(9\lambda+6\mu)}{K_1+K_2}\right]},$$
$$u_3 = \frac{F\left(\lambda + \mu - \frac{R^2}{K_1+K_2}\right)x_3}{L^2\left[2\mu^2 + 3\lambda\mu - \frac{R^2(9\lambda+6\mu)}{K_1+K_2}\right]}, \quad w_3 = \frac{FRx_3}{L^2(\mu K_1 + \mu K_2 - 3R^2)}.$$

If there is not any coupling between phonon and phason fields, i.e. $R = 0$, one can have

$$u_1 = \frac{-F\lambda x_1}{2L^2(2\mu^2 + 3\lambda\mu)}, \quad u_2 = \frac{-F\lambda x_2}{2L^2(2\mu^2 + 3\lambda\mu)},$$
$$u_3 = \frac{F(\lambda+\mu)x_3}{L^2(2\mu^2 + 3\lambda\mu)}, \quad w_3 = 0,$$

coinciding with the displacements in the classical elastic theory of crystals.

Next, the displacements calculated numerically will be compared to the analytical results. The material parameters of a 3D icosahedral Al–Pd–Mn quasicrystal are given as follows (see [3–6] or Chap. 9)

$$\lambda = 74.9 \text{ GPa}, \quad \mu = 72.4 \text{ GPa}, \quad K_1 = 72 \text{ MPa}, \quad K_2 = -37 \text{ MPa}.$$

The coupling constant R of Al–Pd–Mn has not been measured so far. In the computations, we, respectively, assume $R/\mu = 0$, 0.001, 0.002, 0.004, 0.006, 0.008 and 0.01. The height H of the cuboid is 4 cm, and the area of the cross section is $L^2 = 1$ cm^2. The tensile force F is 1 kN. Eight-node brick elements are used to mesh this model. The calculated domain is meshed by 32 0.5 cm × 0.5 cm 0.5 cm 8-node hexahedron elements.

The displacements of the point (0.5, 0.5, 4) at the top surface of the cuboid are shown in Table 12.1. The results show that the numerical and analytical solutions are the same. With increasing R/μ, the absolute values of displacements u_1, u_3 and w_3 become larger. For $R/\mu = 0.01$, the displacement w_3 is about six times u_3 demonstrating the coupling effect of this quasicrystal. Of course, the influence of R/μ on the displacements in the phonon field depends on K_1 and K_2.

The displacements along the loading axis with x_1 or x_2 as the tensile axis shown in Fig. 12.2 are briefly given as follows:

(a) When x_1 is the tensile axis, there are

$$u_1 = \frac{F\left(\lambda+\mu-\frac{R^2}{K_1+K_2}\right)x_1}{L^2\left[2\mu^2+3\lambda\mu-\frac{R^2(9\lambda+6\mu)}{K_1+K_2}\right]}, \quad w_1 = -\frac{FRx_1}{2L^2(\mu K_1+\mu K_2-3R^2)};$$

(b) When x_2 is the tensile axis, there are

$$u_2 = \frac{F\left(\lambda+\mu-\frac{R^2}{K_1+K_2}\right)x_2}{L^2\left[2\mu^2+3\lambda\mu-\frac{R^2(9\lambda+6\mu)}{K_1+K_2}\right]}, \quad w_2 = \frac{FRx_2}{2L^2(\mu K_1+\mu K_2-3R^2)}.$$

It can be seen that the phonon displacements are the same for all three kinds of tensile axes, whereas the phason displacements are different from each other. This shows the three-dimensional anisotropic characteristic of icosahedral quasicrystals.

This checks the computer program to correct and effective.

2. **Specimen of icosahedral Al–Pd–Mn quasicrystal with a crack under tension**

An icosahedral Al–Pd–Mn quasicrystal plate containing a penetrating crack subjected to a uniform load P is shown in Fig. 12.3, where a = 5 mm, H = 50 mm, L = 60 mm and $P/\mu = 0.001$. The thickness of the plate is 1 mm, which is 10 % of the crack length $2a$ and 1 % of the plate height $2H$, so the analytic solutions [6–8] can also be used in the case. The point O is the coordinate origin, and the front and

Table 12.1 Comparison of the displacements of the point (0.5, 0.5, 4)/10^{-2} cm

Displacement	R/μ	0	0.001	0.002	0.004	0.006	0.008	0.01
u_1	Analytical	−0.00070	−0.00071	−0.00073	−0.00083	−0.00103	−0.00146	−0.00258
	Numerical	−0.00070	−0.00071	−0.00073	−0.00083	−0.00103	−0.00146	−0.00258
u_3	Analytical	0.02202	0.02214	0.02249	0.02405	0.02732	0.03416	0.05215
	Numerical	0.02202	0.02214	0.02249	0.02405	0.02732	0.03416	0.05215
w_3	Analytical	0	0.11500	0.23439	0.50754	0.88298	1.51665	3.01205
	Numerical	0.00000	0.11500	0.23439	0.50754	0.88298	1.51665	3.01205

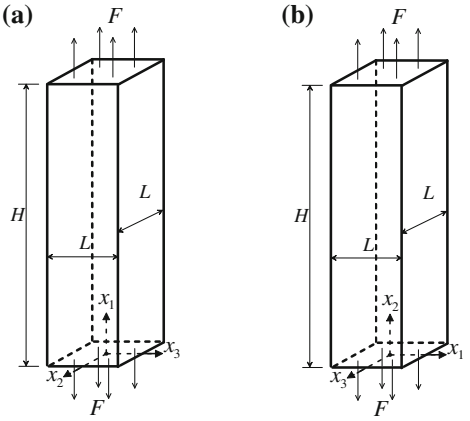

Fig. 12.2 An icosahedral quasicrystal bar subjected to uniaxial tension

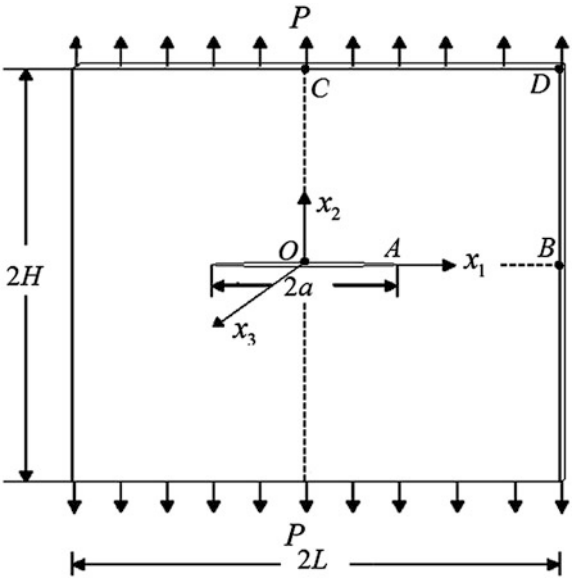

Fig. 12.3 Icosahedral quasicrystal plate with a crack under tension

back faces of the plate are lying in plane $x_3 = 0$ and $x_3 = -1$ mm. The elastic constants of the quasicrystal are the same as those in this section. We assume $R/\mu = 0.005$ for the coupled case and $R/\mu = 0$ for the decoupled case.

Due to the symmetry of the specimen, only the upper right 1/4 part $0 \leq x_1 \leq L$, $0 \leq x_2 \leq H$ has to be modelled. The following boundary conditions must be satisfied:

$$
\begin{aligned}
&a \le x_1 \le L,\ x_2 = 0: \quad u_2 = 0,\ w_2 = 0;\\
&x_1 = 0,\ 0 \le x_2 \le H: \quad u_1 = 0,\ w_1 = 0;\\
&x_3 = -0.5\ \text{mm}: \quad u_3 = 0,\ w_3 = 0;\\
&0 \le x_1 \le L,\ x_2 = H: \quad \sigma_{22} = P,\ \text{other } \sigma_{ij}n_j = 0 \text{ and } H_{ij}n_j = 0;\\
&0 \le x_1 \le a,\ x_2 = 0: \quad \sigma_{ij}n_j = 0 \text{ and } H_{ij}n_j = 0;\\
&x_1 = L,\ 0 \le x_2 \le H: \quad \sigma_{ij}n_j = 0 \text{ and } H_{ij}n_j = 0;\\
&x_3 = 0 \text{ and } -1\ \text{mm}: \quad \sigma_{ij}n_j = 0 \text{ and } H_{ij}n_j = 0.
\end{aligned}
$$

with the unit normal n_j at the boundaries. The domain $0 \le x_1 \le L$, $0 \le x_2 \le H$ is meshed by 20-node brick elements with a thickness of 1 mm along the x_3 axis. The discretization in the $x_3 = 0$ plane is shown in Fig. 12.4, and there are 766 elements and 5775 nodes. A layer of elements with 0.1 mm height is placed at the bottom of the model in order to conveniently analyse the stress intensity factor of the crack. The zone around the crack is meshed by elements with 0.1 mm height and 0.1 mm width, and the width is 2 % of the crack length a. To model the displacements and stresses near the crack tip accurately, the elements related to the crack tip are degenerated in terms of singular quarter-point brick elements [9, 10].

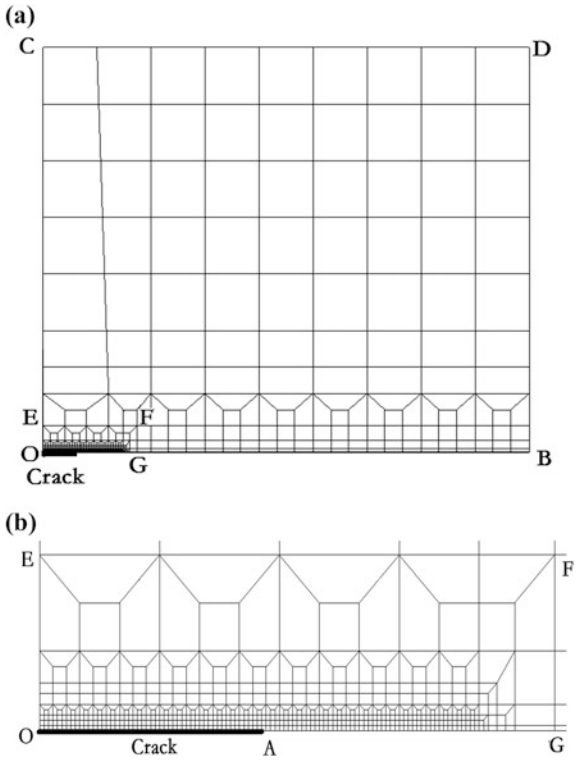

Fig. 12.4 Finite element discretization in the plane $x_3 = 0$

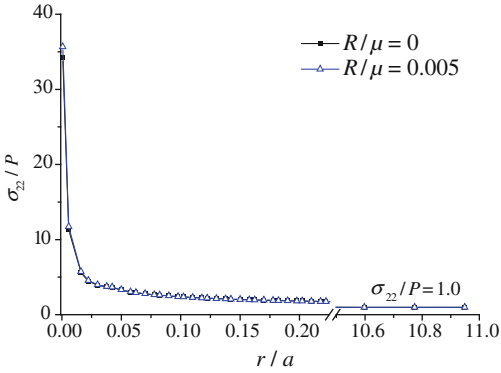

Fig. 12.5 Normal phonon stress ratio σ_{22}/P versus r/a

For the plate thickness is very small compared to the height and width of the plate, and the load P is parallel to the $x_1 - x_2$ plane, the differences of stresses in Gauss integral points of the finite element model along the x_3 direction are very small. Therefore, the stresses will be averaged along the x_3 axis.

The normal phonon stress ratio σ_{22}/P at the integration points of the element layer in the crack plane is given in Fig. 12.5, in which $r = \sqrt{(x_1 - a)^2 + x_2^2}$. The normal stress ratio at the crack tip when $R/\mu = 0.005$ is 35.667, while it is 34.187 when $R/\mu = 0$. Along with the increase in the ratio r/a, the stress ratios of the two cases are rapidly consistent with each other, finally approaching 1.0, satisfying the stress boundary condition shown according to Eq. (38).

The contours of the normal stress ratio σ_{22}/P for $R/\mu = 0.005$ are shown in Fig. 12.6. It can be seen that there is a stress concentration at the crack tip line in

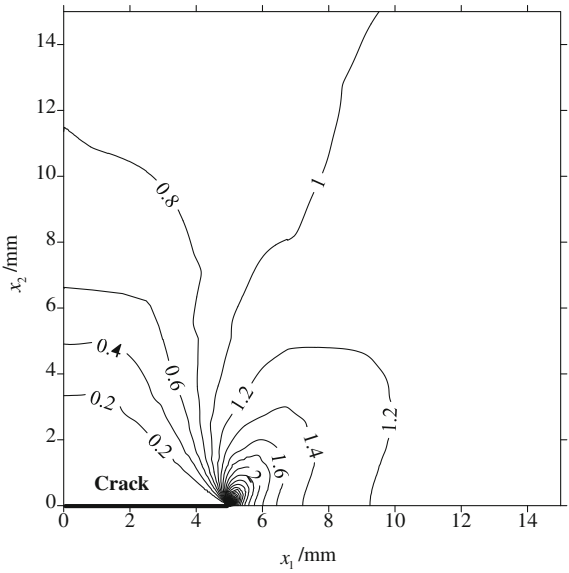

Fig. 12.6 Contours of normalized phonon stress σ_{22}/P near the crack tip for $R/\mu = 0.005$

classical elastic fracture mechanics. Far away from the crack, the stress ratio approaches 1.0, again demonstrating the consistency with the stress boundary condition according to the known analytic solutions.

To characterize crack tip loading, stress intensity factors are well-established quantities for linear fracture problems. From the well-known results the phonon stress intensity factor for a Mode I crack there is [8]

$$K^{\mid\mid} = \lim_{x_1 \to a^+} \left[\sqrt{2\pi(x_1 - a)}\sigma_{22}(x_1, 0) \right] = \sqrt{\pi a} P f(a/L, a/H),$$

with the assumption $R^2/(\mu K_1) \leq 1$, where $f(a/L, a/H)$ characterizes the geometry factor of a specimen with a finite size. In other words, for different geometries of specimens, there will be different values of $f(a/L, a/H)$ which can be determined by the present numerical computation. Because the size of the specimen is quite greater than that of the crack, $f(a/L, a/H) \approx 1$ here.

An extrapolation method based on the stresses σ_{22} at element Gauss integration points is implemented to calculate the stress intensity factors from numerical solutions. The stresses at the Gaussian points of elements in the front of the crack tip and adjacent to the crack plane are almost identical to the stresses at $x_2 = 0$. With the position x_{1s} of the corresponding normal stress $(\sigma_{22})_s$ and $r_s = x_{1s} - a$, $K_s^{\mid\mid}$ reads

$$K_s^{\mid\mid} = \sqrt{2\pi r_s}(\sigma_{22})_s$$

where the subscript s denotes the number of the Gauss points. If we choose Q Gauss points, i.e. $s = 1, \ldots, Q.$, Fig. 12.7 gives the relations of $K_s^{\mid\mid}$ and r_s for the two cases $R/\mu = 0$ and $R/\mu = 0.005$. It shows that the stress intensity factors $K_s^{\mid\mid}$ of $R/\mu = 0.005$ are almost identical to those of $R/\mu = 0$. Near the crack tip, results are inaccurate due to the singularity approaching a straight line as r_s increases.

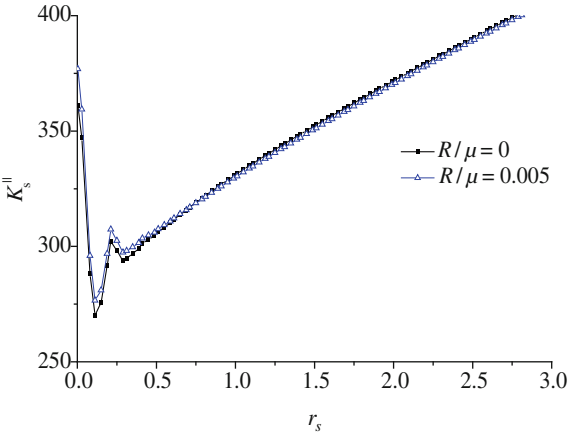

Fig. 12.7 Stress intensity factors $K_s^{\mid\mid}$ from different Gauss points versus $r_s = x_{1s} - a$

Therefore, we can apply the least-squares method to the values of the straight lines. The stress intensity factor $K^{\|}$ finally is obtained as the intersection of the straight line with the ordinate which can be calculated as follows:

$$K^{\|} \approx \frac{\sum r_s \sum r_s K_s^{\|} - \sum r_s^2 \sum K_s^{\|}}{(\sum r_s)^2 - Q \sum r_s^2}.$$

The Gauss points in the domain $0.5 < r_s < 3$ are chosen to determine the stress intensity factors $K^{\|}$ and further $Q = 76$. The intensity factors for the two cases are obtained as 290.61 and 290.21 MPa$\sqrt{\text{mm}}$, respectively, for $R/\mu = 0$ and $R/\mu = 0.005$. Substituting $a = 5$ mm and P such that $P/\mu = 0.001$ into the last term of Eq. (39), the stress intensity factor is $286.95f$ MPa$\sqrt{\text{mm}}$. The numerical solutions for geometry factors f for $R/\mu = 0$ and $R/\mu = 0.005$, respectively, are 1.013 and 1.011.

Figure 12.8 gives the opening displacement u_2 of the crack OA in the plane $x_3 = 0$. It shows that the crack opening displacement for $R/\mu = 0.005$ is larger than that for $R/\mu = 0$. At $x_1 = 0$, the opening displacement for $R/\mu = 0.005$ is 0.00441 mm, while for $R/\mu = 0$ $u_2 = 0.00402$ mm is obtained. It can be seen that the crack opening is obviously influenced by the coupling between the phonon and phason fields.

Figures 12.5, 12.7 and 12.8 show that the coupling effect between the phonon and phason fields, it has strong influence on the displacement fields, however, very weak influence on the stress fields. This phenomenon is due to the way of loading of our problem.

The finite element analysis and computation are given by Yang et al. [11].

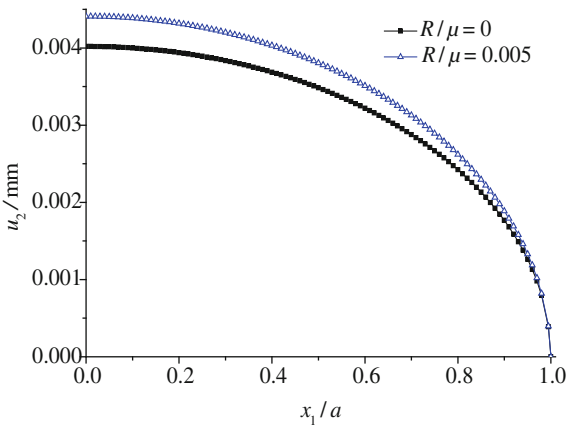

Fig. 12.8 The opening displacement u_2 of the crack at OA

12.5 Conclusion

The variational principle is set up for three-dimensional quasicrystals; in fact, it is suitable for all quasicrystals if the constitutive law to be given a slight modification. The example of cracked specimen given in Sect. 12.4 discussed a finite size body, the solution is very close to analytic solutions given by Fourier transform and complex analysis, because crack size is much smaller compared to sample size, in this sense the power of numerical method has not been fully performed, we need do more computations with practical meanings. The advantages of finite element method lie in exploring effects of complex geometry, complex boundary conditions and complex material structures.

References

1. Hu H.C., 1981, *Variational Principles of Elasticity*, Beijing, Science Press (in Chinese).
2. Guo L H and Fan T Y, 2007, Solvability of boundary value problems of elasticity theory of three-dimensional quasicrystals, *Appl Math Mech,* **28**(8), 1061–1070.
3. Newman M E, Henley C L. 1995, Phason elasticity of a three-dimensional quasicrystal: A transfer-matrix method. Phys. Rev. B, **52**: 6386–6399.
4. Capitan M J, Calvayrac Y, Quivy A, et al. 1999, X-ray diffuse scattering from icosahedral Al-Pd-Mn quasicrystals. Phys. Rev. B, **60**: 6398–6404.
5. Zhu W J, Henley CL. 1999, Phonon-phason coupling in icosahedral quasicrystals. Europhys. Lett., **46**: 748–754.
6. Zhu A Y, Fan T Y. 2009, Elastic analysis of a Griffith crack in icosahedral Al-Pd-Mn quasicrystal. Int. J. Mod. Phys.B, **23**(10):1–16.
7. Fan TY, 2003, Foundation of Fracture Theory , Science Press, Beijing (in Chinese).
8. Li L H, Fan T Y. 2008, Complex variable method for plane elasticity of icosahedral quasicrystals and elliptic notch problem. Sci. China Ser. G, 51(10): 773–780.
9. Henshell R D, Shaw K G. 1975, Crack tip finite elements are unnecessary. Int. J. Num. Meth. Eng., **9**: 495–507
10. Barsoum R S. 1976, On the use of isoparametric finite elements in linear fracture mechanics. Int. J. Num. Meth. Eng., **10**: 25–37.
11. Yang L Z, Ricoeur A, He F M and Gao Y, A finite element algorithm for static problems of icosahedral quasicrystals, Chin Phys B, 2014, 23(5), 056102

Chapter 13
Some Mathematical Principles on Solutions of Elasticity of Quasicrystals

Starting from Chap. 4, we studied several mathematical models of the elasticity of quasicrystals and gave different kinds of solutions [1]. A further discussion on some common features of solutions of mathematical physics [2] will be offered in this chapter.

13.1 Uniqueness of Solution of Elasticity of Quasicrystals

Theorem *Assume quasicrystal occupied by region* Ω *is in equilibrium under the boundary conditions*

$$\left.\begin{array}{ll} \sigma_{ij}n_j = T_i, H_{ij}n_j = h_i, & x_i \in S_t \\ u_i = \bar{u}_i, w_i = \bar{w}_i, & x_i \in S_u \end{array}\right\} \tag{13.1.1}$$

i.e., if the equations

$$\frac{\partial \sigma_{ij}}{\partial x_j} + f_i = 0, \frac{\partial H_{ij}}{\partial x_j} + g_i = 0 \quad x_i \in \Omega \tag{13.1.2}$$

coupled by

$$\begin{aligned} \sigma_{ij} &= C_{ijkl}\varepsilon_{kl} + R_{ijkl}w_{kl} \\ H_{ij} &= R_{klij}\varepsilon_{kl} + K_{ijkl}w_{kl} \end{aligned} \tag{13.1.3}$$

and

$$\varepsilon_{ij} = \frac{1}{2}\left(\frac{\partial u_i}{\partial x_j} + \frac{\partial u_j}{\partial x_i}\right), w_{ij} = \frac{\partial w_i}{\partial x_j} \tag{13.1.4}$$

T.-Y. Fan, *Mathematical Theory of Elasticity of Quasicrystals and Its Applications*, Springer Series in Materials Science 246, DOI 10.1007/978-981-10-1984-5_13

satisfying boundary conditions (13.1.1)*, then the boundary value problem* (13.1.1)–(13.1.4) *has a unique solution.*

Proof If the conclusion is not true, suppose there are two solutions of Eqs. (13.1.2)–(13.1.4) under boundary conditions (13.1.1):

$$\begin{gathered} u_i^{(1)} \oplus w_i^{(1)}, u_i^{(2)} \oplus w_i^{(2)} \\ \varepsilon_{ij}^{(1)} \oplus w_{ij}^{(1)}, \varepsilon_{ij}^{(2)} \oplus w_{ij}^{(2)} \\ \sigma_{ij}^{(1)} \oplus H_{ij}^{(1)}, \sigma_{ij}^{(2)} \oplus H_{ij}^{(2)} \end{gathered}$$

both solutions satisfy equations of deformation geometry, stress–strain relationship, equilibrium equations and boundary conditions.

According to the linear superposition principle, the difference between these two solutions

$$\begin{gathered} (u_i^{(1)} - u_i^{(2)}) \oplus (w_i^{(1)} - w_i^{(2)}) = \Delta u_i \oplus \Delta w_i \\ (\sigma_{ij}^{(1)} - \sigma_{ij}^{(2)}) \oplus (H_{ij}^{(1)} - H_{ij}^{(2)}) = \Delta\sigma_{ij} \oplus \Delta H_{ij} \end{gathered}$$

should be the solution of the problem too. The "differences" should satisfy zero boundary conditions. The work of external forces calculated by them is

$$\begin{aligned} 0 = & \int_\Omega (\Delta\mathbf{f} \oplus \Delta\mathbf{g}) \cdot (\Delta\mathbf{u} \oplus \Delta\mathbf{w}) \mathrm{d}\Omega \\ & + \int_S (\Delta\mathbf{T} \oplus \Delta\mathbf{h}) \cdot (\Delta\mathbf{u} \oplus \Delta\mathbf{w}) \mathrm{d}\Gamma = 2 \int_\Omega \Delta U \mathrm{d}\Omega \end{aligned} \tag{13.1.5}$$

where ΔU represents the strain energy density corresponding to the differences of two sets of solutions, and the derivation of the last step of (13.1.5) used the Gauss theorem.

Because ΔU is the positive definite quadratic form of $\Delta\varepsilon_{ij}$ and Δw_{ij}, there is

$$\Delta U \geq 0 \tag{13.1.6}$$

considering the left-hand side of (13.1.5) be zero, it flows that

$$\Delta U = 0 \tag{13.1.7}$$

Based on the positive definite property of ΔU, $\Delta\varepsilon_{ij}$ and Δw_{ij} must be zero, apart from only rigid displacements, so that $\varepsilon_{ij}^{(1)} = \varepsilon_{ij}^{(2)}, w_{ij}^{(1)} = w_{ij}^{(2)}$, etc.

At the same time, at boundary S_u, one has

$$\Delta\overline{u} = 0,\ \Delta\overline{w} = 0$$

This means the rigid displacements cannot exist; it must be

$$u_i^{(1)} = u_i^{(2)}, w_i^{(1)} = w_i^{(2)}$$

The uniqueness theorem is a powerful tool in the study of elasticity of quasicrystals; for example, if the solution satisfies all equations of elasticity and all boundary conditions, we confirm that the solution must be unique. All solutions offered in Chaps. 7–9 and analytic solutions given in Chap. 10 exhibited this character. But the solution of St-Venant problem in Sect. 6.9 is not unique.

13.2 Generalized Lax–Milgram Theorem

Consider a quasicrystal described by Eqs. (13.1.2)–(13.1.4) and boundary conditions (13.1.1). In the case, the displacements satisfy the following partial differential equations

$$\left.\begin{aligned} -\left[C_{ijkl}\frac{\partial^2 u_k}{\partial x_j \partial x_l} + R_{ijkl}\frac{\partial^2 w_k}{\partial x_j \partial x_l}\right] &= f_i(x,y,z) \\ -\left[R_{klij}\frac{\partial^2 u_k}{\partial x_j \partial x_l} + K_{ijkl}\frac{\partial^2 w_k}{\partial x_j \partial x_l}\right] &= g_i(x,y,z) \end{aligned}\right\} \quad (x,y,z) \in \Omega \tag{13.2.1}$$

At boundary S_u, they satisfy homogenous conditions

$$u_i|_{S_u} = 0,\ w_i|_{S_u} = 0, \tag{13.2.2}$$

And at boundary S_t, the corresponding stresses satisfy non-homogenous conditions

$$\left.\begin{aligned} \left(C_{ijkl}\frac{\partial u_k}{\partial x_l} + R_{ijkl}\frac{\partial w_k}{\partial x_l}\right)n_j|_{S_t} &= T_i(x,y,z) \\ \left(R_{klij}\frac{\partial u_k}{\partial x_l} + C_{ijkl}\frac{\partial w_k}{\partial x_l}\right)n_j|_{S_t} &= h_i(x,y,z) \end{aligned}\right\} \tag{13.2.3}$$

in which $x_1 = x, x_2 = y, x_3 = z, S = S_u + S_t$.

If $u_i, w_i \in C^2(\Omega) \cap C^1(\partial\Omega)$, and satisfy Eq. (13.2.1) and boundary conditions (13.2.2) and (13.2.3), then they will be called classical solution of boundary value problem (13.2.1)–(13.2.4), where $\partial\Omega = S = S_u + S_t$.

The boundary value problem (13.2.1)–(13.2.3) can be reduced to corresponding variational problem. For this purpose, we introduce norm

$$\left.\begin{aligned}\|u_i\|_{1,\Omega}^2 &= \int_\Omega \left[\left(\frac{\partial u_i}{\partial x}\right)^2 + \left(\frac{\partial u_i}{\partial y}\right)^2 + \left(\frac{\partial u_i}{\partial z}\right)^2\right] \mathrm{d}\Omega \\ \|w_i\|_{1,\Omega}^2 &= \int_\Omega \left[\left(\frac{\partial w_i}{\partial x}\right)^2 + \left(\frac{\partial w_i}{\partial y}\right)^2 + \left(\frac{\partial w_i}{\partial z}\right)^2\right] \mathrm{d}\Omega\end{aligned}\right\} \tag{13.2.4}$$

This norm is suitable only for case of homogeneous boundary conditions (13.2.2); otherwise, the norm will not be the present form.

After defining the norm (13.2.4), the space defining $u_i(x, y, z)$ and $w_i(x, y, z)$ is denoted as $H'(\Omega)$. If introduce inner product

$$\left.\begin{aligned}(u_i^{(1)}, u_i^{(2)}) &= \int_\Omega \left(\frac{\partial u_i^{(1)}}{\partial x}\frac{\partial u_i^{(2)}}{\partial x} + \frac{\partial u_i^{(1)}}{\partial y}\frac{\partial u_i^{(2)}}{\partial y} + \frac{\partial u_i^{(1)}}{\partial z}\frac{\partial u_i^{(2)}}{\partial z}\right) \mathrm{d}\Omega \\ (w_i^{(1)}, w_i^{(2)}) &= \int_\Omega \left(\frac{\partial w_i^{(1)}}{\partial x}\frac{\partial w_i^{(2)}}{\partial x} + \frac{\partial w_i^{(1)}}{\partial y}\frac{\partial w_i^{(2)}}{\partial y} + \frac{\partial w_i^{(1)}}{\partial z}\frac{\partial w_i^{(2)}}{\partial z}\right) \mathrm{d}\Omega\end{aligned}\right\} \tag{13.2.5}$$

then $H'(\Omega)$ is a Hilbert space, it is also named as Sobolev space.

We can define space V such as

$$V = \left\{(u_i, w_i) \in H'(\Omega), (u_i)_{S_u} = 0, (w_i)_{S_u} = 0\right\} \tag{13.2.6}$$

If defining inner product at space V by (13.2.5), then V is also a Hilbert space, and

$$V \subset H'(\Omega) \tag{13.2.7}$$

Define space

$$H = \left\{X = (u_1, u_2, u_3, w_1, w_2, w_3) \in (H'(\Omega))_1^6, (u_i)_{S_u} = 0, (w_i)_{S_u} = 0\right\} \tag{13.2.8}$$

and set up norm

$$\|X\|_{1,\Omega} = \left[\sum_{i=1}^{3}\left[\|u_i\|_{1,\Omega}^2 + \|w_i\|_{1,\Omega}^2\right)\right]^{1/2} \tag{13.2.9}$$

For any $X = (u_1, u_2, u_3, w_1, w_2, w_3) \in (H'(\Omega))_1^6$, according to strain–displacement relations

$$\varepsilon_{ij}(X) = \varepsilon_{ji}(X) = \frac{1}{2}\left(\frac{\partial u_i}{\partial x_j} + \frac{\partial u_j}{\partial x_i}\right),$$
$$w_{ij}(X) = \frac{\partial w_i}{\partial x_j}$$

and stress–strain relations of quasicrystals

$$\sigma_{ij}(X) = \sigma_{ji}(X) = C_{ijkl}\varepsilon_{kl}(X) + R_{ijkl}w_{kl}(X)$$
$$H_{ij} = R_{klij}\varepsilon_{kl}(X) + K_{ijkl}w_{kl}(X)$$

define bilinear functional

$$B(X^{(1)}, X^{(2)}) = \int_{\Omega} \left[\sigma_{ij}(X^{(1)})\varepsilon_{ij}(X^{(2)}) + H_{ij}(X^{(1)})w_{ij}(X^{(2)})\right] \mathrm{d}\Omega \tag{13.2.10}$$

in which $B(X^{(1)}, X^{(2)})$ presents symmetry, continuity and positive definite properties.

Take a linear functional

$$l(X) = \int_{\Omega} [f_i u_i + g_i w_i]\mathrm{d}\Omega + \int_{S_t} [T_i u_i + h_i w_i]\mathrm{d}S \tag{13.2.11}$$

where $(f_1, f_2, f_3, g_1, g_2, g_3) \in (L^2(\Omega))^6$, $(T_1, T_2, T_3, h_1, h_2, h_3) \in (L^2(\Omega))^6$, are given functions at Ω and S, respectively. One can prove that $l(X)$ is a continuous functional of X at region Ω, and L^2 represents the Lebesgue square integrable meaning.

There are following theorems:

Theorem 1 *Variational problem corresponding to boundary value problem* (13.2.1)–(13.2.3) *is concluded for obtaining* $X \in H$ *so that* X

$$B(X, Y) = l(Y) \quad \forall Y \in H \tag{13.2.12}$$

in which $l(Y)$ *is a linear functional defined by* (13.2.11).
(Proof is omitted)

Theorem 2 *If* $X = (u_1, u_2, u_3, w_1, w_2, w_3) \in (C^2(\Omega))^6$ *is a classical solution of boundary value problem* (13.2.1)–(13.2.3), *then* X *must be solution of variational problem* (13.2.12), *i.e.,* X *is also a generalized solution (or weak solution). Alternatively, if* X *is a solution of variational problem* (13.2.12), *and* $X \in (C^2(\Omega))^6$, *then is also a classical solution of boundary value problem* (13.2.1)–(13.2.3).
(Proof is omitted)

Theorem 3 (Generalized Lax–Milgram theorem) *Assume that* H *is the Hilbert space defined above, for elasticity of quasicrystals,* $B(X, Y)$ *is a bilinear functional at* $H \times H$, *and satisfies*

$$B(X,Y) = f(X) \quad \forall Y \in H \tag{13.2.13}$$

admits a unique solution $X \in H$, *and*

$$\|X\| \leq \frac{1}{\alpha}\|f\|_{(H)'} \tag{13.2.14}$$

where $(H)'$ *is the dual space of* H *consisting of all bounded linear functionals, and equipped with the norm*

$$\|f\|_{(H)'} = \sup_{Y \in H, Y \neq 0} \frac{f(Y)}{\|Y\|}$$

This theorem gives an extension of Lax–Milgram theorem [3, 4].
(Proof is omitted)

Theorem 4 *Assume*

$$J(X) = \frac{1}{2}B(X,X) - l(X) \tag{13.2.15}$$

and H *is the same as mentioned previously,* $B(X,Y)$ *is a bilinear functional at* $H \times H$ *defined by* (13.2.10), *then the variational problem for having* $X \in H$ *so that* $J(X)$ *being minimum*

$$J(X_0) = \min_{X \in H} J(X) \tag{13.2.16}$$

in which

(1) *Exists solution, and the number of solutions does not exceed one;*
(2) *If there is solution of problem* (13.2.16), *which must the solution of problem* (13.2.12), *and vise versa [*(13.2.12) *is called as Galerkin variational problem, and* (13.2.16) *is named as Ritz variational problem];*
(3) *If* X^* *is their solution, then*

$$J(X) - J(X^*) = \frac{1}{2}B(X - X^*, X - X^*) \quad \forall X \in H \tag{13.2.17}$$

(Proof is omitted)
The discussion of this section may provide preparedness for the following text.

13.3 Matrix Expression of Elasticity of Three-Dimensional Quasicrystals

In the previous section, the variational problem on plane elasticity of two-dimensional quasicrystals is discussed in which the concept of weak solution (generalized solution) is mentioned. In the following sections, we will deal with the weak solution of elasticity of three-dimensional icosahedral quasicrystals, for simplicity a matrix expression for the elasticity will be used. From the discussion of previous chapters, we know that the basic equations for elasticity of quasicrystals except cubic quasicrystals

$$\begin{cases} \frac{\partial \sigma_{ij}}{\partial x_j} + f_i = \rho \frac{\partial^2 u_i}{\partial^2 t}, \frac{\partial H_{ij}}{\partial x_j} + g_i = \rho \frac{\partial^2 w_i}{\partial^2 t} \left(\text{or } \kappa \frac{\partial w_i}{\partial t}\right), & (13.3.1) \\ \varepsilon_{ij} = \frac{1}{2}\left(\frac{\partial u_i}{\partial x_j} + \frac{\partial u_j}{\partial x_i}\right), w_{ij} = \frac{\partial w_i}{\partial x_j}, & (13.3.2) \\ \sigma_{ij} = C_{ijkl}\varepsilon_{kl} + R_{ijkl} w_{kl}, H_{ij} = K_{ijkl} w_{kl} + R_{klij}\varepsilon_{kl}, & (13.3.3) \end{cases} \quad x_i \in \Omega, i, j = 1, 2, 3. t > 0$$

where $u = (u_x, u_y, u_z)$ represents the phonon displacement vector, $w = (w_x, w_y, w_z)$ the phason one, ε_{ij}, w_{ij} the phonon and phason strains, σ_{ij}, H_{ij} the corresponding phonon and phason stresses, C_{ijkl}, K_{ijkl}, R_{ijkl} the elastic constants, f_i, g_i the body and generalized body force densities, ρ the mass density and $\kappa = 1/\Gamma_w$, respectively.

Denoting $\partial\Omega = (\partial\Omega)_u + (\partial\Omega)_\sigma$ to express the boundary of region occupied by the quasicrystal, there are the boundary conditions

$$x \in (\partial\Omega)_u : u_i = u_i^0,\ w_i = w_i^0 \tag{13.3.4}$$

$$x \in (\partial\Omega)_\sigma : \sigma_{ij} n_j = T_i,\ H_{ij} n_j = h_i \tag{13.3.5}$$

where u_i^0 and w_i^0 represent the known functions at boundary $(\partial\Omega)_u$, T_i and h_i the prescribed traction and generalized traction density at boundary $(\partial\Omega)_\sigma$, n_j the unit outward normal vector at any point of the boundary.

There are initial conditions for dynamic problem:

$$u_i|_{t=0} = a_i(x),\ w_i|_{t=0} = b_i(x),\ \dot{u}_i|_{t=0} = c_i(x),\ \dot{w}_i|_{t=0} = d_i(x) \tag{13.3.6}$$

(or $u_i|_{t=0} = a_i(x),\ w_i|_{t=0} = b_i(x),\ \dot{u}_i|_{t=0} = c_i(x)$) where a_i, b_i, c_i, d_i are known functions, $x = (x_1, x_2, x_3) \in \Omega$.

Putting

$$\tilde{U}^{\mathrm{T}} = (u_1\ u_2\ u_3\ w_1\ w_2\ w_3)_{1\times 6}, \tilde{F}^{\mathrm{T}} = (f_i\ g_i)_{1\times 6} = (f_1\ f_2\ f_3\ g_1\ g_2\ g_3)_{1\times 6},$$
$$\tilde{\sigma}^{\mathrm{T}} = (\sigma_{11}\ \sigma_{22}\ \sigma_{33}\ \sigma_{12}\ \sigma_{23}\ \sigma_{31}\ H_{11}\ H_{22}\ H_{33}\ H_{12}\ H_{23}\ H_{31}\ H_{13}\ H_{21}\ H_{32})_{1\times 15},$$
$$\tilde{\varepsilon}^{\mathrm{T}} = (\varepsilon_{11}\ \varepsilon_{22}\ \varepsilon_{33}\ 2\varepsilon_{12}\ 2\varepsilon_{23}\ 2\varepsilon_{31}\ w_{11}\ w_{22}\ w_{33}\ w_{12}\ w_{23}\ w_{31}\ w_{13}\ w_{21}\ w_{32})_{1\times 15},$$

$$\widetilde{\partial} = \begin{bmatrix} \widetilde{\partial}^{(1)} & 0 \\ 0 & \widetilde{\partial}^{(2)} \end{bmatrix}, \widetilde{\partial}^{(1)} = \begin{bmatrix} \partial_1 & 0 & 0 \\ 0 & \partial_2 & 0 \\ 0 & 0 & \partial_3 \\ \partial_2 & \partial_1 & 0 \\ 0 & \partial_3 & \partial_2 \\ \partial_3 & 0 & \partial_1 \end{bmatrix}, \quad \widetilde{\partial}^{(2)} = \begin{bmatrix} \partial_1 & 0 & 0 \\ 0 & \partial_2 & 0 \\ 0 & 0 & \partial_3 \\ \partial_2 & 0 & 0 \\ 0 & \partial_3 & 0 \\ 0 & 0 & \partial_1 \\ \partial_3 & 0 & 0 \\ 0 & \partial_1 & 0 \\ 0 & 0 & \partial_2 \end{bmatrix}, \quad (\partial_i = \frac{\partial}{\partial x_i})$$

$\tilde{U}^{\mathrm{T}}, \tilde{F}^{\mathrm{T}}, \partial^{\mathrm{T}}, \tilde{\sigma}^{\mathrm{T}}, \tilde{\varepsilon}^{\mathrm{T}}$ denote the transpose of $\tilde{U}, \tilde{F}, \partial, \tilde{\sigma}, \tilde{\varepsilon}$, $\sigma^i = (\sigma_{i1}, \sigma_{i2}, \sigma_{i3})$ the ith row of matrix $(\sigma_{ij})_{3\times 3}$, $H^i = (H_{i1}, H_{i2}, H_{i3})$ the ith row of matrix $(H_{ij})_{3\times 3}$.

So that, (13.3.2) can be rewritten as the matrix form:

$$\tilde{\varepsilon} = \partial \tilde{U} \tag{13.3.2′}$$

Note that $\left(\frac{\partial \sigma_{1j}}{\partial x_j} \quad \frac{\partial \sigma_{2j}}{\partial x_j} \quad \frac{\partial \sigma_{3j}}{\partial x_j} \quad \frac{\partial H_{1j}}{\partial x_j} \quad \frac{\partial H_{2j}}{\partial x_j} \quad \frac{\partial H_{3j}}{\partial x_j}\right)^{\mathrm{T}} = \partial^{\mathrm{T}} \tilde{\sigma}$, then (13.3.1) can be rewritten by

$$\partial^{\mathrm{T}} \tilde{\sigma} + F = \rho \ddot{\tilde{U}} \tag{13.3.1′}$$

Putting

$$C = \begin{bmatrix} & C_{11ij} & \\ & C_{22ij} & \\ & C_{33ij} & \\ \cdots & C_{12ij} & \cdots \\ & C_{23ij} & \\ & C_{31ij} & \end{bmatrix}_{6\times 6} = \begin{bmatrix} C_{1111} & C_{1122} & C_{1133} & C_{1112} & C_{1123} & C_{1131} \\ C_{2211} & C_{2222} & C_{2233} & C_{2212} & C_{2223} & C_{2231} \\ C_{3311} & C_{3322} & C_{3333} & C_{3312} & C_{3323} & C_{3331} \\ C_{1211} & C_{1222} & C_{1233} & C_{1212} & C_{1223} & C_{1231} \\ C_{2311} & C_{2322} & C_{2333} & C_{2312} & C_{2323} & C_{2331} \\ C_{3111} & C_{3122} & C_{3133} & C_{3112} & C_{3123} & C_{3131} \end{bmatrix}_{6\times 6}$$

$$K = \begin{bmatrix} & K_{11ij} & \\ & K_{22ij} & \\ & K_{33ij} & \\ \cdots & K_{12ij} & \cdots \\ & K_{23ij} & \\ & K_{31ij} & \\ & K_{13ij} & \\ & K_{21ij} & \\ & K_{32ij} & \end{bmatrix} = \begin{bmatrix} K_{1111} & K_{1122} & K_{1133} & K_{1112} & K_{1123} & K_{1131} & K_{1113} & K_{1121} & K_{1132} \\ K_{2211} & K_{2222} & K_{2233} & K_{2212} & K_{2223} & K_{2231} & K_{2213} & K_{2221} & K_{2232} \\ K_{3311} & K_{3322} & K_{3333} & K_{3312} & K_{3323} & K_{3331} & K_{3313} & K_{3321} & K_{3332} \\ K_{1211} & K_{1222} & K_{1233} & K_{1212} & K_{1223} & K_{1231} & K_{1213} & K_{1221} & K_{1232} \\ K_{2311} & K_{2322} & K_{2333} & K_{2312} & K_{2323} & K_{2331} & K_{2313} & K_{2321} & K_{2332} \\ K_{3111} & K_{3122} & K_{3133} & K_{3112} & K_{3123} & K_{3131} & K_{3113} & K_{3121} & K_{3132} \\ K_{1311} & K_{1322} & K_{1333} & K_{1312} & K_{1323} & K_{1331} & K_{1313} & K_{1321} & K_{1332} \\ K_{2111} & K_{2122} & K_{2133} & K_{2112} & K_{2123} & K_{2131} & K_{2113} & K_{2121} & K_{2132} \\ K_{3211} & K_{3222} & K_{3233} & K_{3212} & K_{3223} & K_{3231} & K_{3213} & K_{3221} & K_{3232} \end{bmatrix}_{9\times 9}$$

$$R=\begin{bmatrix} & R_{11ij} & \\ & R_{22ij} & \\ & R_{33ij} & \\ \cdots & R_{12ij} & \cdots \\ & R_{23ij} & \\ & R_{31ij} & \end{bmatrix}_{6\times 9}=\begin{bmatrix} R_{1111} & R_{1122} & R_{1133} & R_{1112} & R_{1123} & R_{1131} & R_{1113} & R_{1121} & R_{1132} \\ R_{2211} & R_{2222} & R_{2233} & R_{2212} & R_{2223} & R_{2231} & R_{2213} & R_{2221} & R_{2232} \\ R_{3311} & R_{3322} & R_{3333} & R_{3312} & R_{3323} & R_{3331} & R_{3313} & R_{3321} & R_{2232} \\ R_{1211} & R_{1222} & R_{1233} & R_{1212} & R_{1223} & R_{1231} & R_{1213} & R_{1221} & R_{1232} \\ R_{2311} & R_{2322} & R_{2333} & R_{2312} & R_{2323} & R_{2331} & R_{2313} & R_{2321} & R_{2332} \\ R_{3111} & R_{3122} & R_{3133} & R_{3112} & R_{3123} & R_{3131} & R_{3113} & R_{3121} & R_{3132} \end{bmatrix}_{6\times 9}$$

then

$$D=(d_{ij})_{15\times 15}=\left[\begin{array}{c|c} C & R \\ \hline R^T & K \end{array}\right]$$

Here, the order of index i,j of C is the same with those of the phonon strain tensor, the order of index i,j of K,R is the same with those of phason strain tensor, and R^{T} is the transpose of R. From the above expressions, one can find that due to the symmetry of C and K [see, e.g. (4.4.3) and (4.4.5)], the matrix D is symmetry.

The generalized Hooke's law (13.3.3) can be rewritten as

$$\tilde{\sigma}=D\tilde{\varepsilon} \tag{13.3.3′}$$

and (13.3.1′) and (13.3.2′) can be collected as below

$$\partial^{\mathrm{T}}D\partial\tilde{U}+\tilde{F}=\rho\ddot{\tilde{U}} \tag{13.3.7}$$

Put

$$A(x)=\begin{bmatrix} a_1(x) \\ a_2(x) \\ a_3(x) \\ b_1(x) \\ b_2(x) \\ b_3(x) \end{bmatrix}_{6\times 1},\quad B(x)=\begin{bmatrix} c_1(x) \\ c_2(x) \\ c_3(x) \\ d_1(x) \\ d_2(x) \\ d_3(x) \end{bmatrix}_{6\times 1},\quad \widetilde{U}^0=\begin{bmatrix} u_1^0 \\ u_2^0 \\ u_3^0 \\ w_1^0 \\ w_2^0 \\ w_3^0 \end{bmatrix}_{6\times 1},\quad \tilde{\sigma}^0=\begin{bmatrix} T_1 \\ T_2 \\ T_3 \\ h_1 \\ h_2 \\ h_3 \end{bmatrix}_{6\times 1},$$

$$\widetilde{\partial}_n=\left[\begin{array}{c|c} \widetilde{\partial}_n^{(1)} & 0 \\ \hline 0 & \widetilde{\partial}_n^{(2)} \end{array}\right]$$

$$\tilde{\partial}_n^{(1)} = \begin{bmatrix} \cos(n,x_1) & 0 & 0 \\ 0 & \cos(n,x_2) & 0 \\ 0 & 0 & \cos(n,x_3) \\ \cos(n,x_2) & \cos(n,x_1) & 0 \\ 0 & \cos(n,x_3) & \cos(n,x_2) \\ \cos(n,x_3) & 0 & \cos(n,x_1) \end{bmatrix},$$

$$\tilde{\partial}_n^{(2)} = \begin{bmatrix} \cos(n,x_1) & 0 & 0 \\ 0 & \cos(n,x_2) & 0 \\ 0 & 0 & \cos(n,x_3) \\ \cos(n,x_2) & 0 & 0 \\ 0 & \cos(n,x_3) & 0 \\ 0 & 0 & \cos(n,x_1) \\ \cos(n,x_3) & 0 & 0 \\ 0 & \cos(n,x_1) & 0 \\ 0 & 0 & \cos(n,x_2) \end{bmatrix}$$

where $\tilde{\partial}_n$, $\tilde{\partial}_n^{(1)}$, $\tilde{\partial}_n^{(2)}$ are obtained from the differential operator matrixes $\tilde{\partial}$, $\tilde{\partial}^{(1)}$, $\tilde{\partial}^{(2)}$ through a replacement ∂_i by $\cos(n,x_i)$.

Equation (13.3.4) can be rewritten as

$$\tilde{U}(x,t) = \tilde{U}^0,\ x \in (\partial\Omega)_u \tag{13.3.4′}$$

Considering the similarity of the left-hand side of (13.3.5) with the first term of (13.3.1), then (13.3.5) can be rewritten as $\tilde{\partial}_n^{\mathrm{T}}\tilde{\sigma} = \tilde{\sigma}^0,\ x \in (\partial\Omega)_\sigma$. In addition by using (13.3.2′) and (13.3.3′), there is

$$\tilde{\partial}_n^{\mathrm{T}} D\tilde{\partial}\tilde{U} = \tilde{\sigma}^0,\ x \in (\partial\Omega)_\sigma \tag{13.3.5′}$$

If the quasicrystal is in static equilibrium: $\rho\ddot{\tilde{U}} = 0$ (i.e. the inertia forces vanish), in the case it needs not the initial conditions, and the boundary value problem of quasicrystals is interpreted as follows

$$\begin{cases} -\tilde{\partial}^{\mathrm{T}} D\tilde{\partial}\tilde{U} = \tilde{F}, x \in \Omega, t > 0, \\ \tilde{U}(x,t)\big|_{(\partial\Omega)u} = \tilde{U}^0,\ \tilde{\partial}_n^{\mathrm{T}} D\tilde{\partial}\tilde{U}(x,t)\big|_{(\partial\Omega)\sigma} = \tilde{\boldsymbol{\sigma}}^0, \end{cases} \tag{13.3.8, 13.3.9}$$

where

$$\partial\Omega = (\partial\Omega)_u + (\partial\Omega)_\sigma$$

13.4 The Weak Solution of Boundary Value Problem of Elasticity of Quasicrystals

For simplicity, only the displacement boundary problem (or say the Dirichlet problem) is dealt with in the following. Suppose that $\tilde{F} \in (L^2(\Omega))^6$, if $\tilde{U}(x) \in (C^2(\tilde{\Omega}))^6$ being the solution of problem (13.3.8, 13.3.9), then for any vector function $\eta = \begin{bmatrix} \eta^1_{3\times 1} \\ \eta^2_{3\times 1} \end{bmatrix} = \begin{bmatrix} \eta^1_1 & \eta^1_2 & \eta^1_3 & \eta^2_1 & \eta^2_2 & \eta^2_3 \end{bmatrix}^{\mathrm{T}}_{1\times 6} \in (C^\infty_0(\Omega))^6$, both sides of (13.3.8, 13.3.9) are multiplying by η (by making scalar product), and then integrating along Ω, we have

$$\iiint_\Omega (-\tilde{\partial}^{\mathrm{T}} D\tilde{\partial}\tilde{U}) \cdot \eta \mathrm{d}x = \iiint_\Omega \tilde{F} \cdot \eta \mathrm{d}x \tag{13.4.1}$$

From (13.3.3) and Chap. 4 known $\sigma_{ij} = \sigma_{ji}$, in terms of Gauss formula, (13.3.2′) and (13.3.3′), there exists

$$\begin{aligned}
\iiint_\Omega (-\tilde{\partial}^T D\tilde{\partial}\tilde{U}) \cdot \eta \mathrm{d}x &= -\iiint_\Omega \left(\frac{\partial \sigma_{ij}}{\partial x_j}\eta^1_i + \frac{\partial H_{ij}}{\partial x_j}\eta^2_i \right) \mathrm{d}x \\
&= \iiint_\Omega \left[\frac{\partial}{\partial x_j}(\sigma_{ij}\eta^1_i + H_{ij}\eta^2_i) - \left(\sigma_{ij}\frac{\partial \eta^1_i}{\partial x_j} + h_{ij}\frac{\partial \eta^2_i}{\partial x_j} \right) \right] \mathrm{d}x \\
&= -\iint_{\partial\Omega} (\sigma_{ij}\eta^1_i + H_{ij}\eta^2_i) n_j \mathrm{d}S + \iiint_\Omega \left(\sigma_{ij}\frac{\partial \eta^1_i}{\partial x_j} + H_{ij}\frac{\partial \eta^2_i}{\partial x_j} \right) \mathrm{d}x \\
&= \iiint_\Omega \left(\frac{1}{2}\sigma_{ij}\frac{\partial \eta^1_i}{\partial x_j} + \frac{1}{2}\sigma_{ij}\frac{\partial \eta^1_j}{\partial x_i} + H_{ij}\frac{\partial \eta^2_i}{\partial x_j} \right) \mathrm{d}x \\
&= \iiint_\Omega [(\sigma_{ij}(\tilde{U})\varepsilon_{ij}(\eta^1) + H_{ij}(\tilde{U})w_{ij}(\eta^2)] \mathrm{d}x \\
&= \iiint_\Omega \tilde{\sigma}(\tilde{U}) \cdot \tilde{\varepsilon}(\eta) \mathrm{d}x = \iiint_\Omega (\tilde{\partial}\eta)^{\mathrm{T}} D\tilde{\partial}\tilde{U} \mathrm{d}x,
\end{aligned} \tag{13.4.2}$$

and (13.4.1) and (13.4.2) yield

$$\iiint_{\Omega} (\tilde{\partial}\eta)^{\mathrm{T}} D\tilde{\partial}\tilde{U}\mathrm{d}x = \iiint_{\Omega} \tilde{\sigma}(\tilde{U}) \cdot \tilde{\varepsilon}(\eta)\mathrm{d}x = \iiint_{\Omega} \tilde{F} \cdot \eta \mathrm{d}x \tag{13.4.3}$$

Because C_0^∞ is dense in $H_0^1(\Omega)$, (13.4.3) holds too $\forall \eta(x) \in (H_0^1(\Omega))^6$.

In contrast,if $\tilde{U}(x) \in (C^2(\bar{\Omega}))^6$, and (13.4.3) is valid $\forall \eta(x) \in (H_0^1(\Omega))^6$, we can do derivation in counter order of the above procedure and find (13.4.1) through the fundamental lemma of variational method [5]. So that we have

Definition Assume $\tilde{F} \in (L^2(\Omega))^6$, if $\tilde{U}(x) \in (H_0^1(\Omega))^6$, and (13.4.3) holds for $\forall \eta(x) \in (H_0^1(\Omega))^6$, then say $\tilde{U}(x)$ being the weak solution (or generalized solution) of the boundary value problem

$$\begin{cases} -\tilde{\partial}^{\mathrm{T}} D\tilde{\partial}\tilde{U}(x) = \tilde{F}(x), \\ \tilde{U}(x)|_{\partial\Omega} = 0 \end{cases} \tag{13.3.8′, 13.3.9′}$$

13.5 The Uniqueness of Weak Solution

Making use of $(\cdot,\cdot)$ to express inner product in $L^2(\Omega)$, the corresponding norm is $\|\cdot\| : \|\mathrm{v}\| = \left(\int_\Omega \mathrm{v}^2 \mathrm{d}x\right)^{1/2}$, for the scalar function $\mathrm{v} \in L^2(\Omega)$. And in terms of $(\cdot,\cdot)_1$ to denote the inner product in $H_0^1(\Omega)$, the corresponding norm is $\|\cdot\|_1$: $\|\mathrm{v}\|_1 = \left[\int_\Omega \mathrm{v}^2 \mathrm{d}x + \sum_{k=1}^3 \int_\Omega \left(\frac{\partial \mathrm{v}}{\partial x_k}\right)^2 \mathrm{d}x\right]^{1/2}$, and semi-norm is $|\cdot|_1$: $|\mathrm{v}|_1 = \left[\sum_{k=1}^3 \int_\Omega \left(\frac{\partial \mathrm{v}}{\partial x_k}\right)^2 \mathrm{d}x\right]^{1/2}$, for scalar function $\mathrm{v} \in L^2(\Omega)$

Note 1 Norm $\|\cdot\|_1$ is equivalent to semi-norm $|\cdot|_1$.

Note 2 The norm and semi-norm of vector function $\mathrm{v} = (\mathrm{v}_1, \mathrm{v}_2, \ldots, \mathrm{v}_n) \in (H_0^1(\Omega))^n$ (it is marked by $H_0^1(\Omega)$ some times) are denoted as $\|\cdot\|_1$ and $|\cdot|_1$ such as

$$\|\mathrm{v}\|_1^2 = \sum_{i=1}^n \|\mathrm{v}_i\|_1^2 = \sum_{i=1}^n \int_\Omega \mathrm{v}_i^2 \mathrm{d}x + \sum_{i=1}^n \sum_{k=1}^3 \int_\Omega \left(\frac{\partial \mathrm{v}_i}{\partial x_k}\right)^2 \mathrm{d}x = \int_\Omega |\mathrm{v}|^2 \mathrm{d}x + \int_\Omega |\mathrm{v}_x|^2 \mathrm{d}x$$

$$|\mathrm{v}|_1^2 = \sum_{i=1}^n \sum_{k=1}^3 \int_\Omega \left(\frac{\partial \mathrm{v}_i}{\partial x_k}\right)^2 \mathrm{d}x$$

where $|\mathrm{v}|^2 = \sum_{i=1}^n \mathrm{v}_i^2$, $|\mathrm{v}_x|^2 = \sum_{i=1}^n \sum_{k=1}^3 \left(\frac{\partial \mathrm{v}_i}{\partial x_k}\right)^2$, $\frac{\partial \mathrm{v}}{\partial x_k} = \left(\frac{\partial \mathrm{v}_1}{\partial x_k}, \frac{\partial \mathrm{v}_2}{\partial x_k}, \ldots, \frac{\partial \mathrm{v}_n}{\partial x_k}\right)$. Obviously, the Note 1 holds for vector function **v** too.

Lemma (Korn's inequality, [6–8]) *Assume* Ω *is a bounded region with boundary* $\partial\Omega$ *of sufficient smooth in* $\mathbf{R}^n$, *and* $\forall \mathrm{v} = (\mathrm{v}_1, \mathrm{v}_2, \ldots, \mathrm{v}_n) \in H_0^1(\Omega)$ *there is*

$$\sum_{i,k=1}^{n} \int_{\Omega} \left(\frac{\partial \mathrm{v}_i}{\partial x_k} + \frac{\partial \mathrm{v}_k}{\partial x_i} \right)^2 \mathrm{d}x \geq c_1 \|\mathrm{v}\|_1^2$$

in which the positive constant c_1 is dependent only with Ω.

Theorem *Suppose* Ω *is a bounded region in* $\mathbf{R}^3$ *and with sufficient smooth boundary* $\partial\Omega$, *if real symmetric matrix* $D = (d_{ij})$ *satisfies the inequality*

$$\lambda_1 \sum_{i=1}^{15} \xi_i^2 \leq \sum_{i,j=1}^{15} \xi_i d_{ij} \xi_j \leq \lambda_2 \sum_{i=1}^{15} \xi_i^2$$

where λ_1, λ_2 *are positive constants,then for any* $\tilde{F} \in (L^2(\Omega))^6$, *displacement boundary value problem* (13.3.8′, 13.3.9′) *exists unique weak solution (or generalized solution).*

Proof Put $\left\lfloor \tilde{U}, \eta \right\rfloor = \iiint_{\Omega} (\partial\eta)^{\mathrm{T}} D \partial\tilde{U} \mathrm{d}x$, then (13.4.3) can be rewritten as

$$\left\lfloor \tilde{U}, \eta \right\rfloor = (\tilde{F}, \eta), \quad \forall \eta \in (H_0^1(\Omega))^6 \tag{13.5.1}$$

At first, we prove $\lfloor \cdot, \cdot \rfloor$ is a new inner product at $(H_0^1(\Omega))^6$. For this purpose, it needs to prove: $\left\lfloor \tilde{U}, \tilde{U} \right\rfloor \geq 0$, and $\left\lfloor \tilde{U}, \tilde{U} \right\rfloor = 0 \Leftrightarrow \tilde{U} = 0$, $\forall \tilde{U} \in (H_0^1(\Omega))^6$.

In the following, we give only an outline of the proof, the detail is omitted. In addition, $\left\lfloor \tilde{U}, \eta \right\rfloor$ in (13.5.1) is positive definite bilinear functional at $H_0^1(\Omega)$, the proof can be done from the Lax–Milgram theorem (see Sect. 13.2 of this chapter).

Due to the assumption, matrix $D = (d_{ij})_{15\times 15}$ being positive definite, matrix $D = (d_{ij})_{15\times 15}$ and unit matrix I are in contract, i.e., there exists a reversible matrix $\mathbf{C}$ such that $D = \mathbf{C}^{\mathrm{T}}\mathbf{C}$ (note that here $\mathbf{C}$ is not the phonon elastic constant matrix).

Then,

$$\left\lfloor \tilde{U}, \tilde{U} \right\rfloor = \iiint_{\Omega} (\tilde{\partial}\tilde{U})^{\mathrm{T}} D \tilde{\partial}\tilde{U} \mathrm{d}x = \iiint_{\Omega} (\tilde{\partial}\tilde{U})^{\mathrm{T}} (\mathbf{C}^{\mathrm{T}}\mathbf{C}) \tilde{\partial}\tilde{U} \mathrm{d}x = \iiint_{\Omega} (\mathbf{C}\tilde{\partial}\tilde{U})^{\mathrm{T}} (\mathbf{C}\tilde{\partial}\tilde{U}) \mathrm{d}x \geq 0;$$

$$\left\lfloor \widetilde{U}, \widetilde{U} \right\rfloor = 0 \Leftrightarrow \iiint_{\Omega} (\mathbf{C}\widetilde{\partial}\widetilde{U})^{\mathrm{T}} (\mathbf{C}\widetilde{\partial}\widetilde{U}) \mathrm{d}x = 0 \Leftrightarrow \mathbf{C}\widetilde{\partial}\widetilde{U} = 0$$

Because $\mathbf{C}$ is reversible, $\widetilde{\partial}\widetilde{U} = 0$, that is,

$$\frac{\partial u_i}{\partial x_i} = 0,\ \frac{\partial u_i}{\partial x_j} + \frac{\partial u_j}{\partial x_i} = 0\ (i \neq j),\ \frac{\partial w_i}{\partial x_j} = 0, \quad i,j = 1,2,3.$$

It follows $\frac{\partial w_i}{\partial x_j} = 0$ that w_i should be constants, besides $\tilde{U}|_{\partial\Omega} = 0$, and $w_i = 0$ at the boundary. In similar analysis, we find that $u_i = 0$ at boundary. Thus, $\tilde{U} = 0$ at boundary.

In this way, we have proved $\lfloor \cdot, \cdot \rfloor$ is a new inner product at $(H_0^1(\Omega))^6$, the corresponding norm is $\left\|\widetilde{U}\right\|_{(1)} = \left\lfloor \widetilde{U}, \widetilde{U} \right\rfloor^{1/2}$.

Secondly, at $(H_0^1(\Omega))^6$ the new norm $\|\cdot\|_{(1)}$ is equivalent to the initial norm $\|\cdot\|_1$. We are going to give the proof about this.

From the Cauchy inequality, the assumption of the theorem and Note 1, there is

$$\begin{aligned}
\left\|\tilde{U}\right\|_{(1)}^2 &= \iiint_{\Omega} \sum_{i,j=1}^{15} (\tilde{\partial}\tilde{U})_i d_{ij} (\tilde{\partial}\tilde{U})_j \mathrm{d}x \le \lambda_2 \iiint_{\Omega} (\tilde{\partial}\tilde{U})^{\mathrm{T}} (\tilde{\partial}\tilde{U}) \mathrm{d}x \\
&= \lambda_2 \iiint_{\Omega} \left[\sum_{i=1}^{3} \left(\frac{\partial u_i}{\partial x_i}\right)^2 + \sum_{\substack{i,j=1 \\ i<j}}^{3} \left(\frac{\partial u_i}{\partial x_j} + \frac{\partial u_j}{\partial x_i}\right)^2 + \sum_{i,j=1}^{3} \left(\frac{\partial w_i}{\partial x_j}\right)^2 \right] \mathrm{d}x \\
&\le \lambda_2 \iiint_{\Omega} \left\{ \sum_{i=1}^{3} \left(\frac{\partial u_i}{\partial x_i}\right)^2 + 2 \sum_{\substack{i,j=1 \\ i<j}}^{3} \left[\left(\frac{\partial u_i}{\partial x_j}\right)^2 + \left(\frac{\partial u_j}{\partial x_i}\right)^2 \right] + \sum_{i,j=1}^{3} \left(\frac{\partial w_i}{\partial x_j}\right)^2 \right\} \mathrm{d}x \\
&\le 2\lambda_2 \iiint_{\Omega} \sum_{i,j=1}^{3} \left[\left(\frac{\partial u_i}{\partial x_j}\right)^2 + \left(\frac{\partial w_i}{\partial x_j}\right)^2 \right] \mathrm{d}x \\
&= 2\lambda_2 \left|\tilde{U}\right|_1^2 \le 2c \left\|\tilde{U}\right\|_1^2
\end{aligned}$$

In other hand, from the assumption of the theorem, the Korn's inequality and Note 1 there is

$$\left\|\tilde{U}\right\|_{(1)}^2 = \iiint_{\Omega} \sum_{i,j=1}^{15} (\tilde{\partial}\tilde{U})_i d_{ij} (\tilde{\partial}\tilde{U})_j \mathrm{d}x \ge \lambda_1 \iiint_{\Omega} (\tilde{\partial}\tilde{U})^{\mathrm{T}} (\tilde{\partial}\tilde{U}) \mathrm{d}x$$

Consequently, we have proved the equivalency between the new norm $\|\cdot\|_{(1)}$ and the initial norm $\|\cdot\|_1$.

Finally, for $\tilde{F} \in (L^2(\Omega))^6$, by using Schwarz inequality and the fact that the embedding $H_0^1(\Omega) \subset\!\!\rightarrow L^2(\Omega)$ is a compact embedding, we have

$$\left| \iiint_{\Omega} \tilde{F} \cdot \eta \mathrm{d}x \right| \le \left\|\tilde{F}\right\| \cdot \|\eta\| \le M \left\|\tilde{F}\right\| \cdot \|\eta\|_1 \le M_1 \left\|\tilde{F}\right\| \cdot \|\eta\|_1 \quad \forall \eta \in (H_0^1(\Omega))^6$$

that is, $\eta \mapsto \iiint_\Omega \tilde{F} \cdot \eta \mathrm{d}x \quad (\forall \eta \in (H_0^1(\Omega))^6)$ is a unique continuous linear functional at $(H_0^1(\Omega))^6$).Therefore, from Riesz theorem, there must be a unique $y_{\tilde{F}} \in (H_0^1(\Omega))^6$, so that

$$\iiint_\Omega \tilde{F} \cdot \eta \mathrm{d}x = \left\lfloor y_{\tilde{F}}, \eta \right\rfloor \quad \forall \eta \in (H_0^1(\Omega))^6$$

Thus, (13.5.1) is rewritten as

$$\left\lfloor \tilde{U}, \eta \right\rfloor = \left\lfloor y_{\tilde{F}}, \eta \right\rfloor \quad \forall \eta \in (H_0^1(\Omega))^6$$

This shows $\tilde{U} = y_{\tilde{F}}$ is the unique weak solution (generalized solution) of displacement value problem (13.3.8′, 13.3.9′).

In the above proof, using Korn's inequality is crucial (the second Korn's inequality will be used for the stress boundary value problem, but this discussion is not included here).

13.6 Conclusion and Discussion

In some extent, the discussion Sects. 13.3–13.5 is a development of Sect. 13.2. These discussions provide a basis for the numerical methods developed in Chaps. 10 and 12 from point of view of weak solution. Of course for the stress boundary value problems and dynamic problems, the discussion needs to do some extensions of the previous discussions. Due to the limitation of space, the additional extensions are not be given any more.

It is evident that the discussion in Sects. 13.3–13.5 is valid for any systems of one-, two- and three-dimensional quasicrystals, except cubic quasicrystals, for which $w_{ij} = \partial w_i / \partial x_j$ should be replaced by $w_{ij} = (\partial w_i / \partial x_j + \partial w_j / \partial x_i)/2$ in the Eq. (13.3.2) only. The difference of the formulation for different quasicrystal systems lies in the elastic constant matrix D, one can directly use the above formulation for any quasicrystal systems only by substituting the concrete matrix D into the relevant formulas.

References

1. Fan T Y, Mai Y W, 2004, Elasticity theory, fracture mechanics and some relevant thermal properties of quasicrystalline materials. *Appl. Mech. Rev.*, **57**(5), 325-344.
2. Courant R and Hilbert D, 1955, *Methods of Mathematical Physics*, Interscience Publisher Inc., New York.
3. Ying L A, 1998, Theory of Finite Element, Klower, Amsterdan.

4. Jiang L S, 1984, Finite Element Foundation, High Education Press, Beijing (in Chinese).
5. Guo L H and Fan T Y, 2007, Solvability on boundary-value problems of elasticity of three-dimensional quasicrystals, *Applied Mathematics and Mechanics*, **28**(8), 1061-1070.
6. Fikera G., 1974, *Existence Theorems of Elasticity Theory*. World Press, Moscow (in Russian).
7. Kondrat'eb W A, Oleinik O A, 1988, Korn Inequality of Boundary Value Problems for Systems of Theory of Elasticity in Boundless Region. UMN Press, Moscow (in Russian).
8. Kondrat'eb W A, Oleinik O A, 1988, Boundary-value problems for the systems of elasticity in unbounded domains, Korn's inequalities, Russian Math Surveys, 43(5):65-119.

Chapter 14
Nonlinear Behaviour of Quasicrystals

From Chaps. 4 to 13, we mainly discussed the elasticity and relevant properties of quasicrystals, which belong to linear regime both physically and mathematically. Their mathematical treatment is relatively easy though the calculations are quite complex.

The current chapter is to give a simple description on deformation and fracture of quasicrystals with nonlinear behaviour, considering the great difficulty in this topic. For the conventional engineering materials including crystalline material, the nonlinear behaviour means mainly the plasticity. In the study on the classical plasticity, there are two different theories: one is the macroscopic plasticity theory, which is based on some assumptions concluded from certain experimental data, and the other is the so-called crystal plasticity theory, which is based on the mechanism of motion of dislocation, to some extent, can be seen as a "microscopic" theory. The difficulty for quasicrystal plasticity lies in the lack of both enough macro- and micro-data. At present, the macroscopic experiments have not, as yet, been properly undertaken. Although there is some work on the mechanism in microscopy of the plasticity, the data are very limited. This leads to the constitutive law of quasicrystals being essentially unknown. Due to this reason, the systematic mathematical analysis on deformation and fracture for the material is not available so far.

In spite of these difficulties, study on plasticity of quasicrystals has aroused a great deal of attention among researchers [1–8]. But the analytic quantitative work may be at an infant stage. Considering the readers' interest and the development level, it is beneficial to give brief discussion on some simple problems of nonlinear behaviour of the material with some simple models and by extending results in the study of linear regime. Of course, these discussions are not complete, which may provide some hints for further development of the area.

This chapter is structured as follows. First, we discuss some experimental results on the nonlinear deformation behaviour of quasicrystals and then describe a possible plastic constitutive relation of the material, in view of the difficulty for setting up the equations we turn to introduce nonlinear elastic constitutive equations of quasicrystals which are available at present though not equivalent to the plastic

T.-Y. Fan, *Mathematical Theory of Elasticity of Quasicrystals and Its Applications*,
Springer Series in Materials Science 246, DOI 10.1007/978-981-10-1984-5_14

constitutive equations. Sections 14.4 and 14.5 may be seen as applications of the macro-constitutive law in which some nonlinear solutions on quasicrystals are offered. In Sect. 14.6, another version of the study based on the dislocation model or "microscopic model" is exhibited; it achieves the same results those given in Sects. 14.4 and 14.5.

14.1 Macroscopic Behaviour of Plastic Deformation of Quasicrystals

At medium and low temperature, quasicrystals exhibit brittleness, but they present plasticity ductility at high temperature. In addition, near the high stress concentration zone, e.g. around dislocation core or crack tip, plastic flow appears also. It was observed in experiments that plastic deformation of quasicrystals is induced by motion of dislocations in the material. This reveals the important connection between plasticity and the structural defects in quasicrystals. To some extent there are similarities between the phenomena of crystals and quasicrystals. But latter presents salient structural features, fundamentally differing from those of conventional crystals. The plasticity of quasicrystals must be studied in a quite different way from that for studying the classical plasticity.

The fundamental step in studying plasticity of quasicrystals is, of course, experimental observation.

As in the previous discussion, this chapter is mainly dealt with icosahedral and decagonal quasicrystals.

Recently there are many experimental data for Al–Mn–Pd icosahedral quasicrystals, which are the most intensively studied and possess a very high brittle-ductile transition temperature. At strain rate of $10^{-5}/\mathrm{s}$, the ductile range sets in at about 690 °C corresponding to a homologous temperature (i.e. the absolute temperature scaled by the absolute melting temperature) of about 0.82. At lower strain rates of $10^{-6}/\mathrm{s}$ and below limited ductility temperatures down to about 480 °C can be observed. Figure 14.1 shows the stress–strain curves of the quasicrystal in the high-temperature range 730–800 °C at strain rate of $10^{-5}/\mathrm{s}$.

As another class of icosahedral quasicrystals, icosahedral Zn–Mg–Dy, the stress–strain curves measured by experiments are similar to those given by Fig. 14.1.

Feuerbacher and Urban [9], Guyot and Canova [10], Feuerbacher et al. [11], etc., discussed the constitutive equation based on the experimental data on dislocation density and dislocation velocity, e.g. the plastic strain rate and the applied stress in a power law form

$$\dot{\varepsilon}_{\mathrm{p}} = B(\sigma/\hat{\sigma})^{m} \tag{14.1.1}$$

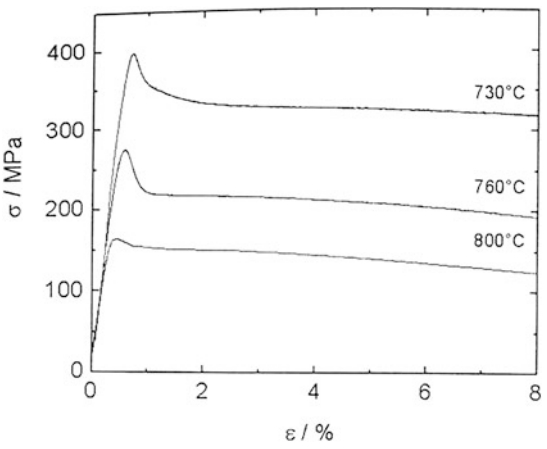

Fig. 14.1 Stress–strain curves of icosahedral Al–Mn–Pd icosahedral single quasicrystals at strain rate of $10^{-5}/s$ [9]

in which B and m are temperature-dependent parameters and $\hat{\sigma}$ is the internal variable that can be regarded as a reference stress representing the current microstructural state of the material and is used to accommodate the model to the description of different materials or hardening mechanism [12]. Combining relevant information, Formula (14.1.1) can be used to well predict the experimental curves, e.g. recorded by Fig. 14.1. It is needed to point out, although there are some similar formulas to (14.1.1) in the form in the classical plasticity, they are quite different substantively. For example, the current parameters B, m and $\hat{\sigma}$ are different from those appearing in relevant formulas in the classical plasticity. Those parameters in the classical plasticity were measured from pure macroscopic approach rather than dislocation model; some detail about the latter can be found in Refs [9–12], which, from the angle of methodology, are different from those adopted in the classical plasticity. Unfortunately, there is a lack of the comprehensive macroscopic experimental data (e.g. the data arising from multi-axial loading condition) for quasicrystal plasticity so far.

Decagonal quasicrystal is an interesting topic for plastic deformation studies since the phase possesses quasiperiodic as well as periodic lattice directions. Therefore, the influences of periodicity and quasiperiodicity on the plastic deformation can be directly revealed on one material by investigating the plastic properties in different deformation geometries—an anisotropic behaviour is expected.

In Ref. [9], the experimental data for stress–strain curves for Al–Ni–Co decagonal quasicrystals are depicted in Fig. 14.2 (note that: the results obtained for the basic cobalt (b-Co) modification of decagonal Al–Ni–Co); it presents plastic properties different from those of icosahedral quasicrystals. The reason for this is the distinguishing nature of quasicrystalline lattice between the two phases. It is different from icosahedral phase, and decagonal phase possesses quasiperiodic as

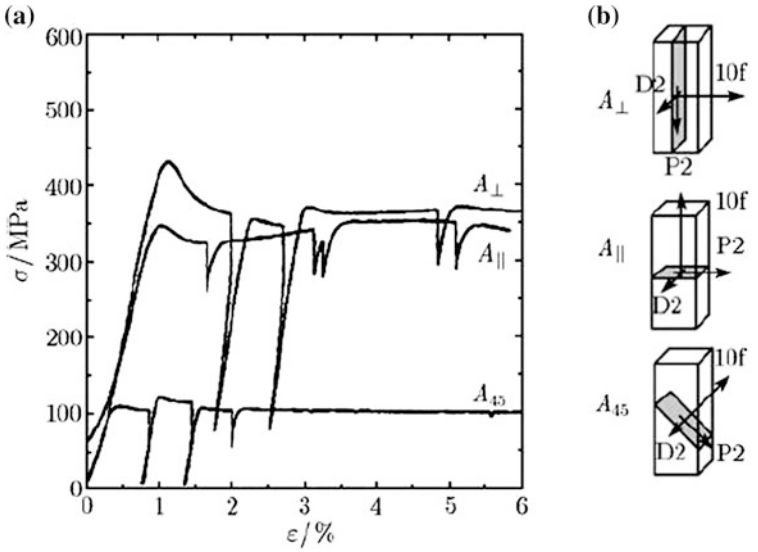

Fig. 14.2 **a** Stress–strain curves of decagonal b–Co decagonal Al–Ni–Co single quasicrystals for different specimen orientations at strain rate of 10^{-5}/s, **b** definition of the specimen orientations $A_\perp$, $A_\parallel$ and A_{45} [9]

well as periodic lattice directions. Therefore, the influences of periodicity and quasiperiodicity on the plastic deformation lead to an anisotropic behaviour. To reveal this feature, Fig. 14.2 gives the data to those orientations as $A_\parallel$, $A_\perp$ and A_{45}, respectively. It is obvious the effect of anisotropy is important.

The experimental data are worth for theoretical study.

14.2 Possible Scheme of Plastic Constitutive Equations

The Formula (14.1.1) calibrated from experimental data with the help of dislocation model assists in studying plastic constitutive equations of quasicrystals.

From the point of view macroscopically, the result is obtained for "uniaxial loading" condition as, at present, there is a lack of data under multi-axial loading condition. We assume that, if sufficient experimental data are available on yield surface/loading surface for some quasicrystals, then we can obtain an equation for yield surface such as

$$\Phi = \sigma_{\text{eff}} - Y = 0 \tag{14.2.1}$$

where $\sigma_{\text{eff}} = \sigma_e + f(H_{ij})$ denotes a generalized effective stress in which σ_e represents the classical effective stress of phonon stresses σ_{ij} and $f(H_{ij})$ the part coming from phason stresses H_{ij}. If

$$Y = \sigma_{\text{Y}} = \text{const} \tag{14.2.2}$$

in which σ_{Y} is the uniaxial yield limit of the material, then(14.2.1) represents the initial yield surface. On the other hand, if

$$Y = Y(h) \tag{14.2.3}$$

where h is related to deformation history, then (14.2.1) describes the evolution law of material deformation. When we have the yield surface/loading surface like (14.2.1), one can construct the following plastic constitutive equation as

$$\begin{aligned} \dot{\varepsilon}_{ij} &= \frac{1}{H(\sigma_{\text{eff}})}\dot{\sigma}_{\text{eff}}\frac{\partial \Phi}{\partial \sigma_{ij}} \\ \dot{w}_{ij} &= \frac{1}{H(\sigma_{\text{eff}})}\dot{\sigma}_{\text{eff}}\frac{\partial \Phi}{\partial H_{ij}} \end{aligned} \tag{14.2.4}$$

provided the flow rule of the isotropic hardening is taken, where Φ is the above-mentioned yield surface/loading surface function. The dot over physical quantities denotes the variation rate of the quantities, and $H(\sigma_{\text{eff}})$ the hardening modulus of the material can be calibrated by a test of a simple stress–strain state, e.g. given by (14.1.1). Then adding the elastic constitutive relationship to (14.2.4), the elastic–plastic constitutive equation will be set up. The elastic constitutive law was fully discussed in the previous chapters.

The expected constitutive law shown in Eq. (14.2.4) which are incremental plastic equations can describe effect of deformation history including loading/unloading state within the deformation process. This may be a complete constitutive equation. There is a possible and relative simpler constitutive law belonging to total plasticity theory or deformation plasticity theory. That is if defining the effective stress σ_{eff} and effective strain ε_{eff}, in which the former was introduced above, and the latter has a similar definition and consists of phonon strains ε_{ij} as well as phason strains w_{ij}, and then between the strains and stresses, there are relations

$$\begin{aligned} \varepsilon_{ij} - \frac{1}{3}\varepsilon_{kk}\delta_{ij} &= \frac{3\varepsilon_{\text{eff}}}{2\sigma_{\text{eff}}}\left(\sigma_{ij} - \frac{1}{3}\sigma_{kk}\delta_{ij}\right) \\ w_{ij} - \frac{1}{3}w_{kk}\delta_{ij} &= \frac{3\varepsilon_{\text{eff}}}{2\sigma_{\text{eff}}}\left(H_{ij} - \frac{1}{3}H_{kk}\delta_{ij}\right) \end{aligned} \tag{14.2.5}$$

in which

$$\varepsilon_{kk} = \varepsilon_{xx} + \varepsilon_{yy} + \varepsilon_{zz}, \quad w_{kk} = w_{xx} + w_{yy} + w_{zz},$$
$$\sigma_{kk} = \sigma_{xx} + \sigma_{yy} + \sigma_{zz}, \quad H_{kk} = H_{xx} + H_{yy} + H_{zz}$$

and we assume that

$$\varepsilon_{\text{eff}} = \begin{cases} \varepsilon_{\text{eff}}^{(e)}, & \sigma_{\text{eff}} < \sigma_0 \\ A(\sigma_{\text{eff}})^n, & \sigma_{\text{eff}} > \sigma_0 \end{cases} \tag{14.2.6}$$

where σ_0, A and n are material constants of the quasicrystals can be measured through a uniaxial test, $\varepsilon_{\text{eff}}^{(e)}$ represents the quantity at elastic deformation stage, and σ_0 the uniaxial tensile yield stress.

In contrast to (14.2.4), Eq. (14.2.5) cannot describe deformation history, as they are substantively nonlinear elastic constitutive equations rather than plastic constitutive equations related to quasicrystalline materials. However, they can describe plastic deformation in the case of proportional loading and no unloading. It is evident that either (14.2.4) or (14.2.5) belongs to a supposed incremental plastic constitutive law or total plastic constitutive law for quasicrystals. One cannot say whether they are correct or not due to the lack of enough experimental data.

If one has the constitutive Eqs. (14.2.4) or (14.2.5), then by coupling the equations of deformation geometry

$$\varepsilon_{ij} = \frac{1}{2}\left(\frac{\partial u_i}{\partial x_j} + \frac{\partial u_j}{\partial x_i}\right), \quad w_{ij} = \frac{\partial w_i}{\partial x_j} \tag{14.2.7}$$

and the equilibrium equations

$$\frac{\partial \sigma_{ij}}{\partial x_j} = 0, \quad \frac{\partial H_{ij}}{\partial x_j} = 0 \tag{14.2.8}$$

the basic framework of the theory of macro-plasticity, in the sense of incremental or total deformation, of quasicrystals can be set up.

At present, there is a lack of such data, so Eqs. (14.2.1), (14.2.2) and (14.2.4) have not been set up yet. With the same reason, Eq. (14.2.5) has not been set up either. This is the major difficulty of macro-plasticity theory currently. It is evident the possible theory is nonlinear, because the material parameters are not constants any more, and the mechanical behaviour is dependent with the history of deformation process in general. The solution is of course more difficult than that for elastic deformation.

Due to relative simplicity of Eq. (14.2.5), for some simple configurations, e.g. anti-plane elasticity of one-dimensional hexagonal, three-dimensional cubic and three-dimensional icosahedral quasicrystals, one can make some probes for plastic analysis by using the constitutive equations.

14.3 Nonlinear Elasticity and Its Formulation

As pointed out in the previous section due to the lack of constitutive equations of plasticity of quasicrystals up to now, analysis of plastic deformation for the material is not available. By this reason, we can perform some simpler nonlinear elastic analysis first, though the mechanisms of nonlinear elastic deformation and plastic deformation are quite different. Furthermore, there are some differences between the following nonlinear elasticity and the total plasticity introduced by Eq. (14.2.5). We here do not constrain the concrete form of relationship between stresses and strains. The results obtained in the following may provide some useful hints for further plastic analysis.

Consider the following nonlinear elastic constitutive relations such as define the free energy (or strain energy density)

$$F(\varepsilon_{ij}, w_{ij}) = \int_0^{\varepsilon_{ij}} \sigma_{ij} \mathrm{d}\varepsilon_{ij} + \int_0^{w_{ij}} H_{ij} \mathrm{d}w_{ij}; \tag{14.3.1}$$

then there is

$$\sigma_{ij} = \frac{\partial F}{\partial \varepsilon_{ij}}, \quad H_{ij} = \frac{\partial F}{\partial w_{ij}} \tag{14.3.2}$$

So the formulas (14.3.1) and (14.3.2) can be seen as constitutive law for linear as well as nonlinear elasticity of quasicrystals, which, in general, cannot describe plastic deformation. If there is proportional loading and no unloading the relationship can give appropriate description of the plastic deformation.

In above formulas, ε_{ij} and w_{ij} are phonon and phason strain tensors given by

$$\varepsilon_{ij} = \frac{1}{2}\left(\frac{\partial u_i}{\partial x_j} + \frac{\partial u_j}{\partial x_i}\right), \quad w_{ij} = \frac{\partial w_i}{\partial x_j} \tag{14.3.3}$$

where u_i and w_i denote the phonon and phason displacement vectors, and σ_{ij} and H_{ij} the phonon and phason stress tensors, respectively, which satisfy the equilibrium equations (if the body forces and generalized body forces are omitted)

$$\frac{\partial \sigma_{ij}}{\partial x_j} = 0, \quad \frac{\partial H_{ij}}{\partial x_j} = 0 \tag{14.3.4}$$

Equations (14.3.1)–(14.3.4) are basic equations describing nonlinear elastic deformation of a quasicrystal. In Sect. 14.5 of this chapter, we will give some applications of formulation (14.3.1)–(14.3.4), and we can show that it constitutes the basis of those nonlinear analyses given Sect. 14.4.

14.4 Nonlinear Solutions Based on Some Simple Models

In this section, we give some nonlinear solutions based on some simple models which substantively are extended from the framework of Eshelby work [13]; the classical Eshelby hypothesis was set up for linear elasticity, which can be extended into nonlinear elasticity even total plasticity (or deformation plasticity). Fan and Fan [14] carried out the investigation.

14.4.1 Generalized Dugdale–Barenblatt Model for Anti-plane Elasticity for Some Quasicrystals

The crack problem of nonlinear deformation of quasicrystals is very interesting. For solving this problem, one of the available models is the generalized Dugdale–Barenblatt model (or generalized DB model for simplicity) [15, 16] originated from the classical nonlinear fracture theory which was used for conventional structural materials including crystalline material.

The linear solutions for a crack for anti-plane for some quasicrystals have been discussed in Chaps. 8 and 9. We now discuss only the nonlinear solution.

Assume that there is an atomic cohesive force zone at the crack tip with length d shown in Fig. 14.3, the value of which is unknown at moment to be determined. In continuum theory of quasicrystals, the atomic cohesive force zone is the plastic zone macroscopically, and the distribution of atomic cohesive force must be evaluated by experimental observation. Due to lack of the data of the new material, if we assume that the atomic cohesive is a constant τ_c, the shear yield limit (or shear yield strength) of the material, within the zone, then the problem is simplified. In this version, the nonlinear boundary value problem is linearized already. So the previous formulation exhibited, e.g. in Chap. 8, can be used to solve the present problem. The most effective method in solving the problem is the complex variable function method, but the formulation and calculation are quite complicated and lengthy, more complex than those given in the previous chapters. The details are omitted, and we here list only the final results:

$$\begin{aligned} F_1(\zeta) &= \frac{2i}{C_{44}}\left(\frac{2\theta_1}{\pi\zeta^2}\tau_c - \tau_1\right)\frac{\zeta^2}{\zeta^2-1} + \frac{1}{2\pi i}\frac{2i}{C_{44}}\tau_c \ln\frac{e^{2i\theta_1}-\zeta^2}{e^{-2i\theta_1}-\zeta^2} \\ F_2(\zeta) &= 0 \end{aligned} \tag{14.4.1}$$

in which

$$\begin{aligned} F_1(\zeta) &= \phi'(\zeta) + \frac{R_3}{C_{44}}\psi'(\zeta) \\ F_2(\zeta) &= \psi'(\zeta) + \frac{R_3}{K_2}\phi'(\zeta) \end{aligned}$$

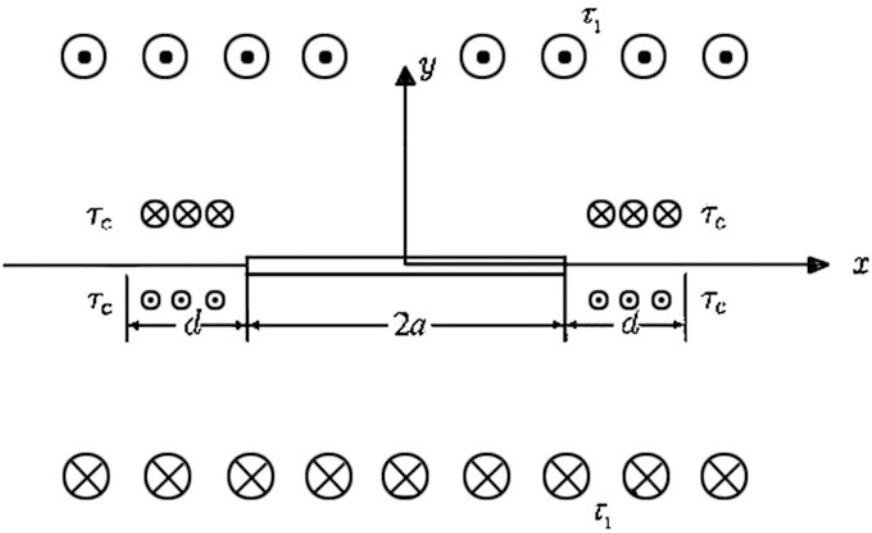

Fig. 14.3 Atomic cohesive force zone near the crack tip for anti-plane elasticity for some quasicrystals

and

$$\phi(\zeta) = \phi_1(t) = \phi_1(\omega'(\zeta)), \psi(\zeta) = \psi_1(t) = \psi_1(\omega'(\zeta))$$

where

$$t = \omega'(\zeta) = \frac{a+d}{2}(\zeta + \zeta^{-1})$$

represents the conformal mapping from t-plane (xy-plane) onto ζ-plane, under the mapping the region of xy-plane is transformed onto the interior of the unit circle at ζ-plane, and $\phi'(\zeta)$ and $\psi'(\zeta)$ are the derivatives of the functions to the new complex variable ζ, and θ_1 is the angle of point at the unit circle corresponding to the crack tip (i.e. $y = 0, x = a$, and there is relation $\cos\theta_1 = a/(a+d)$ between the corresponding points at t-plane and ζ-plane).

From the solution, the size of plastic zone d is determined as

$$d = a\left[\sec\left(\frac{\pi\tau_1}{2\tau_c}\right) - 1\right] \tag{14.4.2}$$

i.e. $\theta_1 = \frac{\pi\tau_1}{2\tau_c}$, and the crack tip opening displacement is

$$\delta_{III} = \frac{4K_2\tau_c a}{\pi(C_{44}K_2 - R_3^2)}\left[\ln \sec\left(\frac{\pi\tau_1}{2\tau_c}\right)\right] \tag{14.4.3}$$

It is obvious that the results are very simple and explicit, and the effects of phason to plastic deformation and fracture are explored. If taking the opening displacement as a nonlinear fracture parameter, then a fracture criterion for one-dimensional hexagonal quasicrystal

$$\delta_{III} = \delta_{IIIc} \tag{14.4.4}$$

is suggested in which δ_{IIIc} is the critical value of the crack tip opening displacement, measured by experiment, a material constant.

In the low stress level case, i.e. $\tau_1/\tau_c \ll 1$, in which

$$\sec\left(\frac{\pi\tau_1}{2\tau_c}\right) = 1 + \frac{1}{2}\left(\frac{\pi\tau_1}{2\tau_c}\right)^2 + \cdots$$

if we remain the first two terms and substituting it into (14.4.2)

$$d = \frac{\pi}{8}\left(\frac{K_{III}^{\|}}{\tau_c}\right)^2 \ll a$$

in which $K_{III}^{\|} = \sqrt{\pi a}\tau_1$ (refer to Sect. 8.2). The result is very close to the plastic size based on the "small-scale yield modification" of classical fracture theory. Furthermore,

$$\ln \sec\left(\frac{\pi\tau_1}{2\tau_c}\right) = \frac{1}{2}\left(\frac{\pi\tau_1}{2\tau_c}\right)^2 + \frac{1}{12}\left(\frac{\pi\tau_1}{2\tau_c}\right)^4 + \cdots$$

If we take only the first two terms, then substituting it to (14.4.3) so

$$\delta_{III} = \frac{G_{III}}{\tau_c} \tag{14.4.5}$$

in which $G_{III} = \frac{K_2 K_{III}^{\|2}}{C_{44}K_2 - R_3^2}$ represents the energy release rate in linear elastic case (refer to Sect. 8.2). This shows that parameter δ_{III} is equivalent to energy release rate G_{III} in the linear elastic case or "small-scale-yielding "plasticity.

The above results are given for one-dimensional hexagonal quasicrystals, which hold for three-dimensional icosahedral quasicrystals, if the material constants C_{44}, K_2 and R_3 are replaced by $\mu, K_1 - K_2$ and R, which hold for three-dimensional cubic quasicrystals too, if the constants are replaced by C_{44}, K_{44} and R_{44}, respectively.

14.4.2 Generalized Dugdale–Barenblatt Model for Plane Elasticity of Two-Dimensional Point Groups 5 m, 10 mm and $5, \bar{5}$, 10, $\overline{10}$ Quasicrystals

The linear analysis for a crack in plane elasticity in point groups 5 m and 10 mm as well as in point groups $5, \bar{5}$ and $10, \overline{10}$ of two-dimensional quasicrystals is given in Sects. 8.3 and 8.4 of Chapter 8 in terms of the Fourier method and complex analysis method, respectively, where we pointed out that if taking $R_1 = R, R_2 = 0$ then the solution on point groups $5, \bar{5}$ and $10, \overline{10}$ will exactly reduce to that on point groups 5 m and 10 mm. In the following, we discuss the nonlinear solution only based on the complex analysis method.

For two-dimensional quasicrystals, a similar generalized Dugdale–Barenblatt model to that given in the Sect. 14.4.1 is suggested as below, refer to Fig. 14.4. That is, there is the so-called atomic cohesive force zone, or the plastic zone macroscopically, with length d, temporarily unknown and to be determined. If we suppose that the distribution of the atomic cohesive force distribution and magnitude of the atomic cohesive force $\sigma_c = \sigma_c(x)$ are known, furthermore $\sigma_c =$ constant within the zone, then the nonlinear problem is linearized already, in which σ_c represents the macro-tensile yield strength of the quasicrystal. Therefore, the formulation introduced above can be used to solve the present problem. The powerful method for the problem is the complex variable function-conformal mapping method, which was displayed briefly in Sect. 14.4.1. But the calculation is much more complicated and lengthy than those listed in the previous subsection. The detail of complex variable function-conformal mapping method is given in

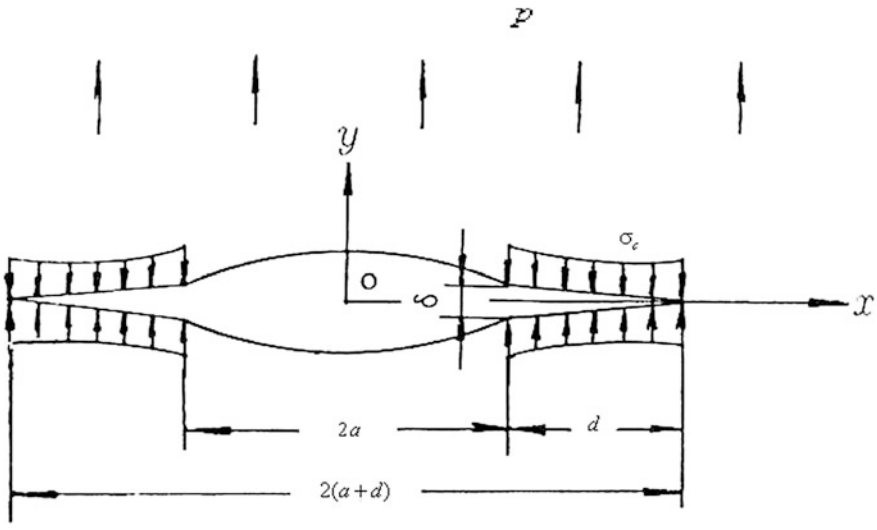

Fig. 14.4 Generalized DB model for two-dimensional decagonal quasicrystal

Sect. 11.3.10 of Chapter 11 and Sect. A.3 of Major Appendix, and here we list the final plastic solution only as follows.

The size of the plastic zone is determined as

$$d = a\left[\sec\left(\frac{\pi p}{2\sigma_c}\right) - 1\right] \tag{14.4.6}$$

which is similar to that given by (14.4.2), but the meaning is different. And the crack tip opening displacement is for point groups 5 m and 10 mm quasicrystals

$$\delta_I = \frac{2\sigma_c a}{\pi}\left[\frac{1}{L+M} + \frac{K_1}{MK_1 - R^2}\right]\left[\ln\ \sec\left(\frac{\pi p}{2\sigma_c}\right)\right] \tag{14.4.7a}$$

and for point group $10, \overline{10}$

$$\delta_I = \frac{2\sigma_c a}{\pi}\left[\frac{1}{L+M} + \frac{K_1}{MK_1 - (R_1^2 + R_2^2)}\right]\left[\ln\ \sec\left(\frac{\pi p}{2\sigma_c}\right)\right] \tag{14.4.7b}$$

which is also similar to that obtained by (14.4.3) in which $L = C_{12}, M = (C_{11} - C_{12})/2$ are phonon elastic constants, K_1 the phason elastic constant and R the phonon-phason coupling constant, respectively. It is very interesting that the solution (14.4.7a), (14.4.7b) exactly covers the solutions of crystals and conventional structural materials, as $K_1 = R = 0$, e.g. for classical conventional materials

$$\delta_I = \mathrm{CTOD} = \begin{cases} \frac{(1+\kappa)\sigma_c a}{\pi\mu}\ln\ \sec\left(\frac{\pi}{2}\frac{p}{\sigma_c}\right) = \frac{4(1-\nu)\sigma_c a}{\pi\mu}\ln\ \sec\left(\frac{\pi}{2}\frac{p}{\sigma_c}\right), & \text{plane strain state} \\ \frac{(1+\kappa')\sigma_c a}{\pi\mu}\ln\ \sec\left(\frac{\pi}{2}\frac{p}{\sigma_c}\right) = \frac{4\sigma_s a}{(1+\nu)\pi\mu}\ln\ \sec\left(\frac{\pi}{2}\frac{p}{\sigma_c}\right), & \text{plane stress state} \end{cases}$$

where $\kappa = 3 - 4\nu$ for plane strain, and $\kappa' = \frac{3-\nu}{1+\nu}$ for plane stress, and ν is the Poisson's ratio of the materials. So the solutions of crystals and conventional structural materials are the specific cases of our solution of quasicrystals. Figure 14.5 shows the normalized crack tip opening displacement δ_I/a versus normalized stress p/σ_c and gives the comparison between quasicrystals and crystals as well as the comparison between point groups 10 mm and $10, \overline{10}$ quasicrystals. The detail of solution including point group $10, \overline{10}$ is given in Section A.3 of Major Appendix.

Based on the parameter δ_I given by (14.4.7a) and (14.4.7b), we can suggest the nonlinear fracture criterion for pentagonal and/or decagonal quasicrystals for the Mode I loading as

$$\delta_I = \delta_{Ic} \tag{14.4.8}$$

in which δ_{Ic} denotes critical value of the crack opening displacement, measured by experiment, a material constant.

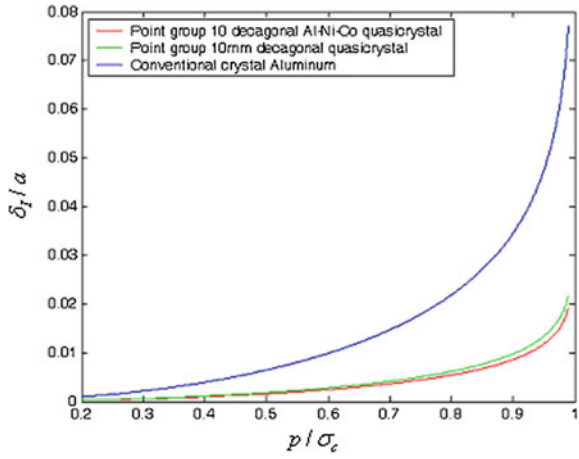

Fig. 14.5 Normalized crack tip opening displacement versus normalized stress and comparison [27]

In linear elastic case, i.e. $p/\sigma_c \ll 1$, through a similar analysis like in previous the crack tip opening displacement reduces to

$$\delta_I = \frac{G_I}{\sigma_c} \tag{14.4.9}$$

where G_I is defined by (8.3.19), and this gives the simple connection between these two parameters, so the criterion (14.4.8) can be reduced to the energy release rate criterion for linear elastic deformation of the quasicrystals discussed in Chap. 8.

14.4.3 Generalized Dugdale–Barenblatt Model for Plane Elasticity of Three-Dimensional Icosahedral Quasicrystals

The schematic figure of the model for icosahedral quasicrystals is similar to Fig. 14.4, the plastic zone is the same given by (14.4.6), and the crack tip opening displacement is as follows:

$$\delta_I = \lim_{x \to l} 2u_y(x,0) = \lim_{\varphi \to \varphi_2} 2u_y(x,0) = 2\left(\frac{1}{\lambda+\mu} + \frac{c_4}{c_2}\right) \cdot \frac{\sigma_s a}{\pi} \cdot \ln \sec\left(\frac{\pi}{2}\frac{p}{\sigma_s}\right) \tag{14.4.10}$$

in which

$$c_2 = \mu(K_1 - K_2) - R^2 - \frac{(\mu K_2 - R^2)^2}{\mu K_1 - 2R^2}, \quad c_4 = c_1 R + \frac{1}{2} c_2 \left(K_1 + \frac{\mu K_1 - 2R^2}{\lambda + \mu}\right) \tag{14.4.11}$$

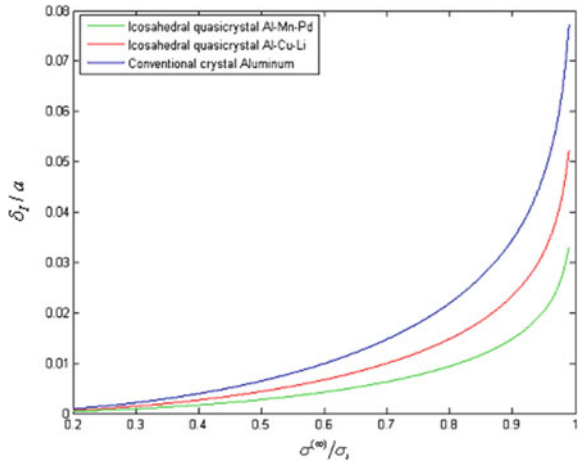

Fig. 14.6 Normalized crack tip opening displacement of icosahedral quasicrystals versus normalized applied stress [27]

with $c_1 = \frac{R(2K_2-K_1)(\mu K_1+\mu K_2-3R^2)}{2(\mu K_1-2R^2)}$.

The variation of normalized crack tip opening displacement versus normalized applies stress is shown in Fig. 14.6.

14.5 Nonlinear Analysis Based on the Generalized Eshelby Theory

In the previous section, we obtained some nonlinear solutions for one-, two- and three-dimensional quasicrystals by using some simple physical models. We will show that those solutions have some inherent relations to the generalized Eshelby theory originated from the classical reference [13] for crystals. Fan and Fan [14] did some work to extend the classical Eshelby model for crystals to that for quasicrystals

14.5.1 Generalized Eshelby Energy-Momentum Tensor and Generalized Eshelby Integral

Fan and Fan [14] (can also refer to Refs. [17, 18]) defined the generalized Eshelby energy-momentum tensor as

$$G = Fn_1 - \sigma_{ij}n_j\frac{\partial u_i}{\partial x_1} - H_{ij}n_j\frac{\partial w_j}{\partial x_1} \tag{14.5.1}$$

where F is defined by (14.3.1) and n_i the unit vector of outward normal at any point of an arc in a quasicrystal, and at which there are:

$$\sigma_{ij}n_j = T_i, \quad H_{ij}n_j = h_i$$

where T_i denotes the traction vector, and h_i the generalized traction vector, shown in Fig. 14.7.

Furthermore, we define an integral such as

$$E = \int_{\Gamma} G\mathrm{d}\Gamma \tag{14.5.2}$$

in which Γ is an integration path enclosing a crack tip in the material. To memorize Eshelby, the integral is named generalized Eshelby integral. The integral exhibits path-independency. In Sect. 14.8, i.e. Appendix of Chapter 14, the proof on the path-independency of the integral is given.

Because the integral presents this important character, it has some applications in fracture analysis of quasicrystals.

Another important character is the value of the integral is equal to the energy release rate G_{III} (under Mode III loading), or G_{II} (under Mode II loading), or G_{I} (under Mode I loading) of one-, two- and three-dimensional quasicrystals when the material is in linear elastic deformation state. The mathematical proof about this is provided in Sect. 14.8, i.e. Appendix of Chapter 14.

The features of the generalized Eshelby integral (14.5.2) exhibited above imply that it may be significant for the analysis of nonlinear fracture of quasicrystals. In the following, an application for this purpose is discussed.

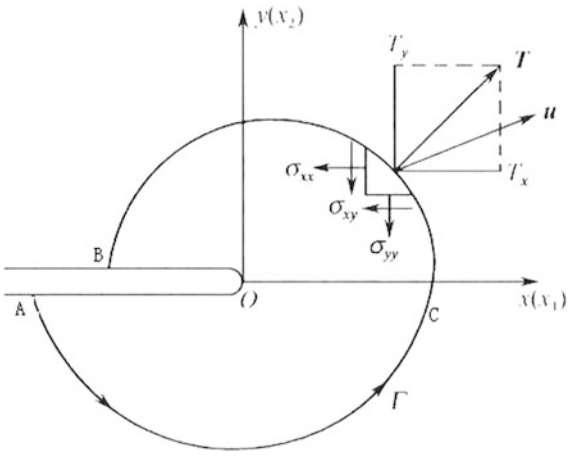

Fig. 14.7 Path of the generalized Eshelby integral

14.5.2 Relation Between Crack Tip Opening Displacement and the Generalized Eshelby Integral

By using the path-independency of E-integral (14.5.2), we take the integration path Γ as given by red colour and shown in Fig. 14.8 and let the path closing to the surface of the plastic zone as near as possible. Now the integration path is $\int_{ACB}$, and along segment AB and BC, i.e.

$$dy = 0, \quad T_1 = 0, \quad T_2 = \sigma_c, \quad h_1 = 0, \quad h_2 = H_c$$

so that

$$\begin{aligned} E &= \int_{\Gamma} G\mathrm{d}\Gamma = \int_{ACB} G\mathrm{d}\Gamma = \int_{A}^{B} \left(\sigma_c \frac{\partial u_y}{\partial x}\mathrm{d}x + H_c \frac{\partial w_y}{\partial x}\mathrm{d}x \right) \\ &= \sigma_c[(u_y)_B - (u_y)_A] + H_c[(w_y)_B - (w_y)_A] \approx \sigma_c[(u_y)_B - (u_y)_A] = \sigma_c \delta_I \end{aligned} \tag{14.5.3}$$

This proves the relation between the generalized Eshelby integral and crack tip opening displacement, and it shows the E-integral presents an equivalency to the crack tip opening displacement, where σ_c is the atomic cohesive force (or the plastic yield strength in macroscopic sense). In general, σ_c can be understood the cohesive force of phonon field; similarly, we can introduce H_c as the "generalized atomic cohesive force" of the phason field of quasicrystal material. In microscopy, the

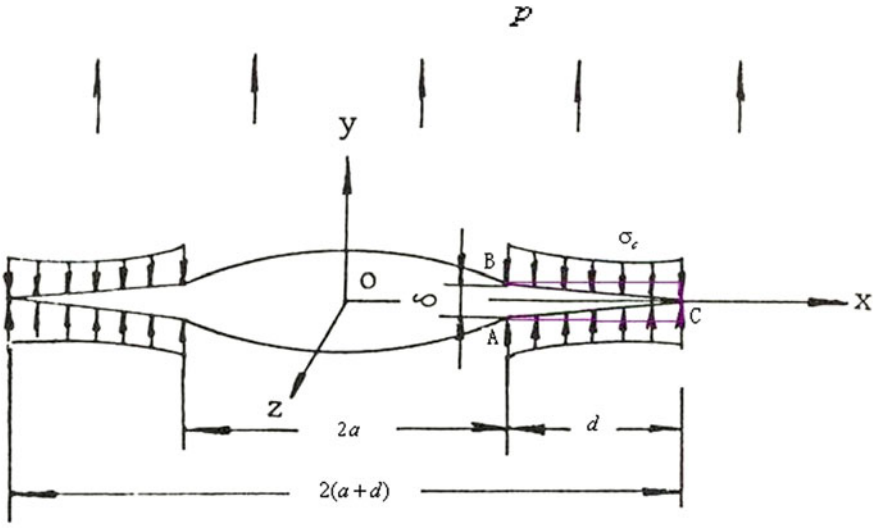

Fig. 14.8 Integration path for evaluating crack tip opening displacement

quantity H_c is meaningful, but it has not been measured macroscopically at present; the effects of which are omitted in formula (14.5.3) for this reason.

For Mode II and Mode III crack the proof is similar.

Since by generalized BCS model (refer to the next section) and generalized DB model, one can obtain the same result on crack tip opening displacement, which is also a direct result of generalized Eshelby integral for quasicrystals, and we realize that the generalized Eshelby energy-momentum tensor theory is the uniform physical basis of the two models.

14.5.3 Some Further Interpretation on Application of E-Integral to the Nonlinear Fracture Analysis of Quasicrystals

The above subsections and the appendixes exhibit the generalized Eshelby integral can be as a uniform basis of generalized BCS model as well as generalized DB model for nonlinear fracture analysis of some one-, two- and three-dimensional quasicrystals. We suggest taking the E-integral as a fracture parameter, and

$$E = E_c \tag{14.5.4}$$

as fracture criterion, where E_c is the critical value of the integral, a material constant, which can be measured through some conventional specimens, and the discussion will be given in Sect. 14.8—Appendix of Chapter 14.

Though the measurement of the critical value of generalized Eshelby integral may be easier, the evaluation of values of E-integral for plastic deformation of quasicrystals is very difficult. Therefore, the implementation of the criterion (14.5.4) is not so convenient in practice. Instead, people can use the fracture criterion of crack tip opening displacement considering the equivalency between the crack tip opening displacement $\delta(\delta_I, \delta_{II}, \delta_{III})$ and E-integral. Elastoplastic crack solutions for some one-, two- and three-dimensional quasicrystals have been found based on the generalized Dugdale–Barenblatt model, refer to Refs. [14, 18, 27], in which the size of the plastic zone and crack tip opening displacement are determined, with these data an equivalent plastic fracture criterion is suggested in the previous section as

$$\delta = \delta_c \tag{14.5.5}$$

in which δ_c represents the critical value of the crack tip opening displacement, a material constant. The evaluation of crack tip opening displacement has been exactly completed for large plates with central crack and narrow plastic zone and introduced in Sect. 14.4 or refer to Refs. [14, 18, 27], and some approximate solution for other configuration may be obtained by complex variable function method (an outline of the method was interpreted in Refs. [14, 18, 27]) and other methods (mainly the approximate methods and numerical methods). The

shortcoming of this procedure lies in some difficulties of the determination of δ_c, but which can be obtained through relation

$$\delta_c = \frac{E_c}{\sigma_c} \tag{14.5.6}$$

and the Sect. 14.8 shows the measurement of E_c be easier. So the collaboration of criterions (14.5.4) and (14.5.5) makes the nonlinear fracture analysis for quasicrystals being available. Some details are given in the Appendix of this chapter (i.e. Sect. 14.8).

14.6 Nonlinear Analysis Based on the Dislocation Model

We pointed out at the beginning in this chapter that in the study on the classical plasticity there are two different theories: one is the macroscopic plasticity theory and the other is the so-called crystal plasticity theory; to some extent, the latter can be seen as a "microscopic" theory which is based on the mechanism of motion of dislocation. We discussed quite more dislocation solutions in Chap. 7 for one- and two-dimensional quasicrystals and in Chap. 9 for three-dimensional quasicrystals; those results are helpful to explore the plastic deformation and fracture of the material. Because this analysis need not rely on nonlinear macroscopic constitutive law, it reduces a great difficulty in mathematical treatment. With some results of dislocation solutions, here we focus on the discussion concerning plastic flow around crack tip for some one-, two- and three-dimensional quasicrystals, respectively.

14.6.1 Screw Dislocation Pile-Up for Hexagonal or Icosahedral or Cubic Quasicrystals

For the topic the basis is the generalized BCS model developed by Fan and co-workers [8], which is stated as below.

Assume there is a Griffith crack with length $2\ l$ along the direction of z-axis in a one- or three-dimensional quasicrystal, subjected to a shear stress $\tau^{(\infty)}$ at infinity see Fig. 14.9. Around the crack tip, there is a dislocation pile-up with size d which is unknown so far to be determined. Within the zone of dislocation pile-up, the material presents plastic flow, and the stress σ_{yz} is equal to the critic shear stress τ_c, the atomic cohesive force, or the so-called flow limit of the material macroscopically. For simplicity, the external applied stress at the infinity can be removed; instead, it is applied at the crack surface. The latter is equivalent to former from point of view of fracture behaviour for any studied systems. This is the generalized

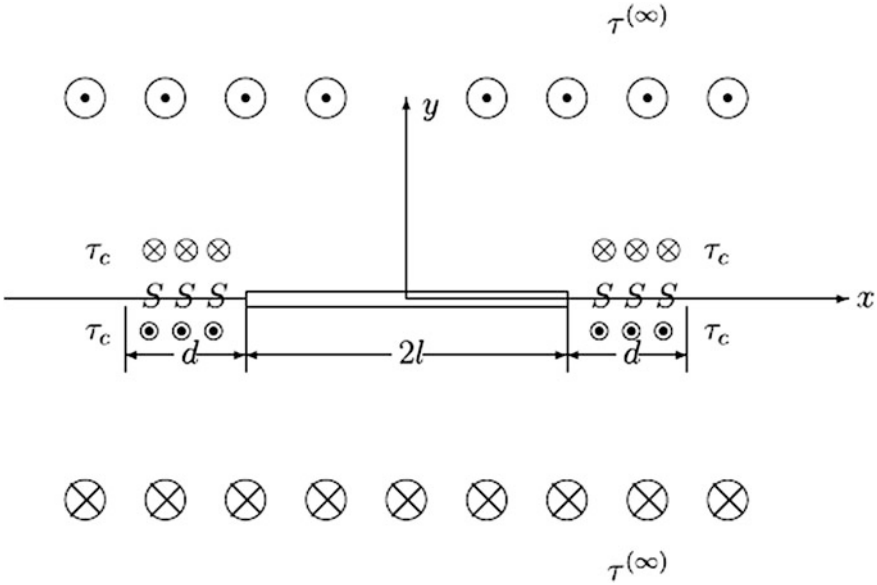

Fig. 14.9 Schematic picture of a crew dislocation pile-up coupled with a crack in anti-plane elasticity of quasicrystals

BCS model for quasicrystals. The origin of the model was given by Bilby et al. [20, 21] for crystals. The Ref. [8] developed model to the study for some one- and two-dimensional quasicrystals. The model can be formulated by the following boundary conditions for anti-plane elasticity:

$$\begin{aligned} &(x^2+y^2)^{1/2}\to\infty: \quad \sigma_{ij}=0, \quad H_{ij}=0 \\ &y=0, \quad |x|<l: \quad \sigma_{yz}=-\tau^{(\infty)}, \quad H_{yz}=0 \\ &y=0, \quad l<|x|<l+d: \quad \sigma_{yz}=-\tau^{(\infty)}+\tau_c=0, \quad H_{yz}=0 \end{aligned} \tag{14.6.1}$$

For some detailed statements about the formalism, readers can refer to Ref. [18].The boundary conditions (14.6.1) have been shown that the nonlinear (plastic deformation) problem is linearized mathematically. So it has been transformed into a linear problem (or an "equivalent" elasticity problem) described by the final governing equations

$$\nabla^2 u_z=0, \quad \nabla^2 w_z=0 \tag{14.6.2}$$

The boundary value problem (14.6.1), (14.6.2) is the problem solved in Sect. 14.4, where the complex variable function method-conformal mapping method was used, but there is a simpler procedure to solve it if we need only some plastic deformation parameters around crack tip and if we have a dislocation solution, the latter is given

by Sect. 7.1. For this purpose, we first introduce a dislocation density function $f(\xi)$; then, problems (14.6.1) and (14.6.2) can be transformed into the following singular integral equation problem such as

$$\int_L \frac{f(\xi)\mathrm{d}\xi}{\xi - x} = \frac{\tau(x)}{A} \tag{14.6.3}$$

in which ξ denotes the dislocation source point coordinate, x the field point coordinate at the real axis and L represents interval $(l, l+d)$. From the dislocation solution given in Sect. 7.1, the constant A is defined by

$$A = -\frac{(C_{44}K_2 - R^2)b_3^{\|}}{2\pi K_2} \tag{14.6.4}$$

and the shear stress distribution is

$$\tau(x) = \begin{cases} -\tau^{(\infty)}, & |x| < l \\ -\tau^{(\infty)} + \tau_c, & l < |x| < l+d \end{cases}$$

which comes from the boundary condition (14.6.1).

In terms of the Muskhelishvili [26] theory, Fan et al. [8] solved the integral Eqs. (14.6.3) under condition (14.6.4), the solution is

$$\begin{aligned} f(x) &= -\frac{1}{\pi^2 A}\sqrt{\frac{x+(l+d)}{x-(l+d)}}\int_L \sqrt{\frac{\xi-(l+d)}{\xi+(L+d)}}\tau(\xi)\frac{\mathrm{d}\xi}{\xi - x} \\ &= -\frac{1}{\pi^2 A}\sqrt{\frac{x+(l+d)}{x-(l+d)}}\left\{ i\left[2\tau_c \cos^{-1}\left(\frac{l}{l+d}\right) - \tau^{(\infty)}\pi\right]\right\} \\ &\quad + \frac{\tau_c}{\pi^2 A}\left[\cosh^{-1}\left|\frac{(l+d)^2 - lx}{(l+d)(l-x)}\right| - \cosh^{-1}\left|\frac{(l+d)^2 + lx}{(l+d)(l+x)}\right|\right] \end{aligned} \tag{14.6.5}$$

Because the $f(x)$ should be a real number, the factor multiplying the imaginary number i must be zero in the first term of right-hand side of (14.6.5); this leads to

$$2\tau_c \cos^{-1}\left(\frac{l}{l+d}\right) - \tau^{(\infty)}\pi = 0$$

i.e.

$$d = l\left[\sec\left(\frac{\pi\tau^{(\infty)}}{2\tau_c}\right) - 1\right] \tag{14.6.6}$$

This is the same of (14.4.2) if l is replaced by a.

From solution (14.6.5), we evaluate amount of dislocations $N(x)$ such as

$$N(x) = \int_0^x f(\xi)\mathrm{d}\xi \tag{14.6.7}$$

Substituting (16.6.5) [coupled with (14.6.6)] into (14.6.7), we can get $N(l+d)$ and $N(l)$, so the amount of dislocation motion is

$$\delta_{\mathrm{III}} = b_3^{\|}[N(l+d) - N(l)] = \frac{2b_3^{\|}l\tau_{\mathrm{c}}}{\pi^2 A}\left(\ln\frac{l+d}{l}\right) = \frac{4K_2\tau_{\mathrm{c}}l}{\pi(C_{44}K_2 - R^2)}\ln\ \sec\left(\frac{\pi\tau^{(\infty)}}{2\tau_{\mathrm{c}}}\right) \tag{14.6.8}$$

This is the same of (14.4.3) apart from difference of some notations.

14.6.2 Edge Dislocation Pile-Up for Pentagonal or Decagonal Two-Dimensional Quasicrystals

For plane elasticity, the corresponding problem is "edge" dislocation pile-up problem shown in Fig. 14.10; here we consider the pile-up in the pentagonal or decagonal two-dimensional quasicrystals. There are the boundary conditions

$$\begin{aligned}
&(x^2+y^2)^{1/2} \to \infty: \quad \sigma_{ij} = 0, \quad H_{ij} = 0\\
&y = 0, \quad |x| < l: \quad \sigma_{yx} = -\tau^{(\infty)}, \quad H_{yx} = 0, \quad \sigma_{yz} = 0, \quad H_{yz} = 0\\
&y = 0, \quad l < |x| < l+d: \quad \sigma_{yx} = -\tau^{(\infty)} + \tau_{\mathrm{c}}, \quad H_{yx} = 0, \quad \sigma_{yz} = 0, \quad H_{yz} = 0
\end{aligned} \tag{14.6.9}$$

and the governing equation

$$\nabla^2\nabla^2\nabla^2\nabla^2 F(x,y) = 0 \tag{14.6.10}$$

Instead of solving the boundary value problem (14.6.9) and (14.6.10), one can determine a dislocation density which satisfies the Eq. (14.6.3) if the relevant quantity A is known beforehand.

In the singular integral equation, the shear stress distribution function $\tau(x)$ is the same as previous subsection, but here A is replaced by

$$A = \frac{b_1^{\|}}{\pi}\frac{(L+M)(MK_1 - R^2)}{(L+M)K_1 + (MK_1 - R^2)} \tag{14.6.11}$$

which has been found in solution of Sect. 7.2 for point groups 5 m and 10 mm quasicrystals.

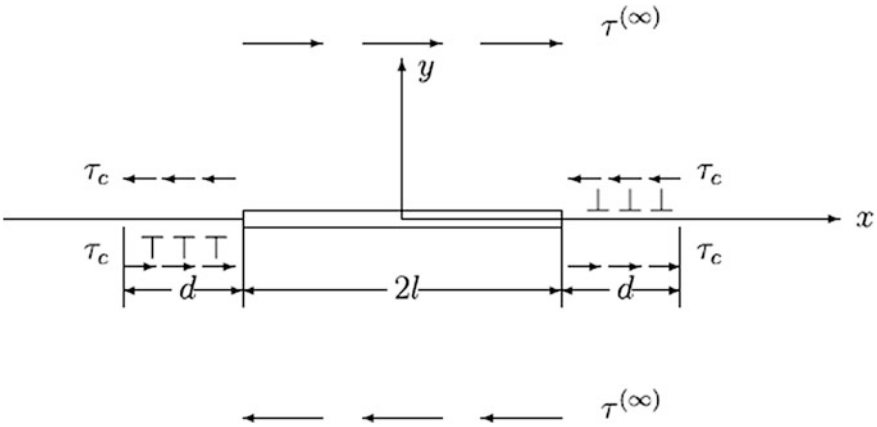

Fig. 14.10 Schematic picture of an "edge" dislocation pile-up coupled with a crack in plane elasticity of quasicrystals

According to the condition concerning factor multiplying the imaginary i to be zero in (14.6.5), the plastic zone size is determined by (14.6.6); this is similar to (14.4.6), but there are some differences in physical meaning.

A similar calculation on amount of dislocation motion we can obtain the slip of the crack tip such as

$$\delta_{\mathrm{II}} = \frac{2b_1^{\parallel} l}{\pi^2 A} \ln \sec\left(\frac{2\tau^{(\infty)}}{\pi\tau_c}\right) = \frac{2\tau_c l}{\pi}\left(\frac{1}{M+K_1} + \frac{K_1}{MK_1 - R^2}\right) \ln \sec\left(\frac{2\tau^{(\infty)}}{\pi\tau_c}\right) \tag{14.6.12}$$

It is evident the result of (14.6.12) is similar to that of (14.4.7a), (14.4.7b), but the physical meaning is different. According to the macroscopic fracture mechanics, the crack tip slips corresponding to the Mode II crack tip displacement (i.e. the crack tip sliding displacement) δ_{II}. But for the Mode I crack tip opening displacement (14.4.7a), (14.4.7b), there is no physical basis of dislocation model, though the similar mathematical treatment can be easily given, which is omitted here.

The dislocation model provides a powerful support to the generalized cohesive force model and generalized Eshelby model presented in the previous sections; even if there is a difficulty physically, we are unable to derive δ_{I} directly from the model and results in a slight faulty aspect of the procedure.

14.6.3 Edge Dislocation Pile-Up for Three-Dimensional Icosahedral Quasicrystals

For three-dimensional icosahedral quasicrystals, the relevant dislocation pile-up problems can be formulated as

$$(x^2+y^2)^{1/2}\to\infty:\quad \sigma_{ij}=0,\quad H_{ij}=0$$
$$y=0,\quad |x|<l:\quad \sigma_{yx}=-\tau^{(\infty)},\quad H_{yx}=0,\quad \sigma_{yz}=0,\quad H_{yz}=0,\quad \sigma_{yy}=0,\quad H_{yy}=0,$$
$$y=0,\quad l<|x|<l+d:\quad \sigma_{yx}=-\tau^{(\infty)}+\tau_c,\quad H_{yx}=0,\quad \sigma_{yz}=0,\quad H_{yz}=0,\quad \sigma_{yy}=0,\quad H_{yy}=0,$$
$$\nabla^2\nabla^2\nabla^2\nabla^2\nabla^2\nabla^2F(x,y)=0$$

The solution through the dislocation density method can be offered similar to above. Because the formulas are too lengthy (please refer to Sect. 9.6 for the dislocation solution that is the basis of the present method), the discussion is omitted.

14.7 Conclusion and Discussion

This chapter discussed the deformation and fracture exhibiting nonlinear behaviour of quasicrystals, and this is a topic which has not been well studied so far. The discussion in the chapter shows that the nonlinear elastic constitutive equation possesses some meaning for the investigation due to lack of plastic constitutive equation at present. The generalized Eshelby principle based on the nonlinear elastic constitutive law plays an important role in revealing the fracture behaviour of quasicrystals under nonlinear deformation which may be a basis of generalized DB model to some extent. We realize that the generalized Eshelby principle and generalized DB model are based on the macro-nonlinear continuous mechanics of quasicrystals. The generalized BCS model developed in Sect. 14.6 emphasizes dislocation mechanism for the plastic deformation, which is a "microscopic" model and different from those of the generalized DB hypothesis as well as the generalized Eshelby principle at physical basis and methodology. The attractiveness is that results derived from these quite different hypothesizes are in exact agreement with the study.

The reader can find that even if there is a lack of plastic constitutive equations for quasicrystals so far, the nonlinear analysis explored in this chapter (including the text and appendixes) with considerable achievements and meaningful description encourage us to furthermore explore the physical nature and mathematical solution in the field.

14.8 Appendix of Chapter 14: Some Mathematical Details

14.8.1 Proof on Path-Independency of E-Integral

Consider a single-connected region D with a closed boundary C. From the Green formula, the first, second and third terms of the left-hand side of the integral (14.5.2) will be

$$\int_C Fn_1 \mathrm{d}\Gamma = \int_C F\mathrm{d}x_2 = \iint_D \frac{\partial F}{\partial x_1}\mathrm{d}x_1\mathrm{d}x_2$$

$$\int_C \left(\sigma_{ij}n_j\frac{\partial u_i}{\partial x_1} + H_{ij}n_j\frac{\partial w_i}{\partial x_1}\right)\mathrm{d}\Gamma = \iint_D \frac{\partial}{\partial x_j}\left(\sigma_{ij}\frac{\partial u_i}{\partial x_1} + H_{ij}\frac{\partial w_i}{\partial x_1}\right)\mathrm{d}x_1\mathrm{d}x_2$$

So that

$$\int_C G\mathrm{d}\Gamma = \iint_D \left[\frac{\partial F}{\partial x_1} - \frac{\partial}{\partial x_j}\left(\sigma_{ij}\frac{\partial u_i}{\partial x_1} + H_{ij}\frac{\partial w_i}{\partial x_1}\right)\right]\mathrm{d}x_1\mathrm{d}x_2 \tag{14.8.1}$$

Meantime, (14.3.2) provides that

$$\begin{aligned}\frac{\partial F}{\partial x_1} &= \frac{\partial F}{\partial \varepsilon_{ij}}\frac{\partial \varepsilon_{ij}}{\partial x_1} + \frac{\partial F}{\partial w_{ij}}\frac{\partial w_{ij}}{\partial x_1} = \sigma_{ij}\frac{\partial \varepsilon_{ij}}{\partial x_1} + H_{ij}\frac{\partial w_{ij}}{\partial x_1} \\ &= \sigma_{ij}\frac{\partial}{\partial x_1}\left[\frac{1}{2}\left(\frac{\partial u_i}{\partial x_j} + \frac{\partial u_j}{\partial x_i}\right)\right] + H_{ij}\frac{\partial}{\partial x_1}\left(\frac{\partial w_i}{\partial x_j}\right) \\ &= \sigma_{ij}\frac{\partial}{\partial x_1}\left(\frac{\partial u_i}{\partial x_j}\right) + H_{ij}\frac{\partial}{\partial x_1}\left(\frac{\partial w_i}{\partial x_j}\right)\end{aligned}$$

here the symmetry of tensor ε_{ij} [given by the first equation of (14.3.3)] is used. The above result can be rewritten as

$$\begin{aligned}\frac{\partial F}{\partial x_1} &= \frac{\partial}{\partial x_j}\left(\sigma_{ij}\frac{\partial u_i}{\partial x_1}\right) - \frac{\partial \sigma_{ij}}{\partial x_j}\frac{\partial u_i}{\partial x_1} + \frac{\partial}{\partial x_j}\left(H_{ij}\frac{\partial w_i}{\partial x_1}\right) - \frac{\partial H_{ij}}{\partial x_j}\frac{\partial w_i}{\partial x_1} \\ &= \frac{\partial}{\partial x_j}\left(\sigma_{ij}\frac{\partial u_i}{\partial x_1} + H_{ij}\frac{\partial w_i}{\partial x_1}\right)\end{aligned} \tag{14.8.2}$$

in the last step in driving (14.8.2), the equilibrium Eq. (14.3.4) is used.

Substituting (14.8.2) into (14.8.1), we have

$$\int_C G\mathrm{d}\Gamma = 0$$

If taking $C = \Gamma + BB' - \Gamma' + A'A$ in which Γ' is a path similar to Γ, and these two curves intersect the upper face of the crack at points B and B', and the lower face at points A and A', respectively. Due to

$$\mathrm{d}x_2 = \mathrm{d}y = 0, \quad T_i = 0, \quad h_i = 0$$

at the segments BB' and $A'A$, there are

$$\int_{BB'+A'A} G\mathrm{d}\Gamma = 0, \quad \int_{\Gamma} G\mathrm{d}\Gamma = \int_{\Gamma'} G\mathrm{d}\Gamma$$

Because Γ and Γ' are arbitrary paths satisfying the requirements of E-integral definition, the last equality proves its path-independency.

14.8.2 Proof on the Equivalency of E-Integral to Energy Release Rate Under Linear Elastic Case for Quasicrystals

In the text of this chapter, we argue that the E-integral is equivalent to the energy release rate when the quasicrystals are in linear elastic deformation state; the mathematical proof about this is given here. The proof can be done for one-, two- and three-dimensional quasicrystals and for Mode I, Mode II and Mode III cracks. For simplicity, here we only discuss Mode III crack for one-dimensional hexagonal quasicrystals, but it is valid for other quasicrystals as well.

At linear elastic case, the generalized Hooke's law

$$\begin{aligned} \sigma_{ij} &= C_{ijkl}\varepsilon_{kl} + R_{ijkl}w_{kl} \\ H_{ij} &= K_{ijkl}w_{kl} + R_{klij}\varepsilon_{kl} \end{aligned}$$

is reduced to

$$\begin{aligned} \sigma_{yz} &= \sigma_{yz} = 2C_{44}\varepsilon_{yz} + R_3 w_{zy} \\ \sigma_{zx} &= \sigma_{xz} = 2C_{44}\varepsilon_{zx} + R_3 w_{zx} \\ H_{zy} &= K_2 w_{zy} + 2R_3\varepsilon_{zy} \\ H_{zx} &= K_2 w_{zx} + 2R_3\varepsilon_{zx} \end{aligned}$$

for the phonon-phason coupling anti-plane shearing (or longitudinal shearing) state in elasticity of one-dimensional hexagonal quasicrystals; one finds the free energy density (or strain energy density) as

$$F = C_{44}(\varepsilon_{xz}^2 + \varepsilon_{yz}^2) + \frac{1}{2}K_2(w_{zx}^2 + w_{zy}^2) + R_3(\varepsilon_{zx}w_{zx} + \varepsilon_{yz}w_{zy}) \tag{14.8.3}$$

Substituting the crack solution given in Chap. 8 into (14.8.3), we have

$$F = \frac{1}{4(C_{44}K_2 - R_3^2)}\left\{C_{44}\left[K_2K_{\mathrm{III}}^{\parallel} - R_3K_{\mathrm{III}}^{\perp}\right]^2 + 2K_2\left[C_{44}K_{\mathrm{III}}^{\perp} - R_3K_{\mathrm{III}}^{\parallel}\right]^2 + 2R_3\left[K_2K_{\mathrm{III}}^{\parallel} - R_3K_{\mathrm{III}}^{\perp}\right]\left[C_{44}K_{\mathrm{III}}^{\perp} - R_3K_{\mathrm{III}}^{\parallel}\right]\right\} \tag{14.8.4}$$

where $K_{\mathrm{III}}^{\parallel} = \sqrt{\pi a}\tau_1$ and $K_{\mathrm{III}}^{\perp} = \sqrt{\pi a}\tau_2$ are stress intensity factors associated with phonon and phason fields, respectively.

Integrating the quantity given by (14.8.4) along a path enclosing the crack tip, one can obtain the first term of the *E*-integral. Because of the path-independency of the integral, we can take a half-circle with the crack tip as its origin and with radius r, so that

$$\int_{\pi}^{-\pi} F\mathrm{d}y = \int_{\pi}^{-\pi} Fr\cos\theta\mathrm{d}\theta = 0 \tag{14.8.5}$$

where (r, θ) denote the crack tip coordinates.

Now we calculate the second and third terms of the integral.

According to the definition of Sect. 14.3, it is known that between the traction, generalized traction and the phonon, phason stresses there are

$$T_z = \sigma_{zx}n_x + \sigma_{zy}n_y = \sigma_{zx}\cos\theta + \sigma_{zy}\sin\theta$$
$$h_z = H_{zx}n_x + H_{zy}n_y = H_{zx}\cos\theta + H_{zy}\sin\theta$$

by substituting the crack solution given in Sect. 8.1 into the above formulae we find

$$T_z = \frac{1}{\sqrt{2\pi r}}K_{\mathrm{III}}^{\parallel}\sin\frac{1}{2}\theta, \quad h_z = \frac{1}{\sqrt{2\pi r}}K_{\mathrm{III}}^{\perp}\sin\frac{1}{2}\theta \tag{14.8.6}$$

Based on the crack solution given in Sect. 8.1, there are

$$u_z = \frac{K_2\tau_1 - R_3\tau_2}{C_{44}K_2 - R_3^2}\sqrt{2ar}\sin\frac{1}{2}\theta$$
$$w_z = \frac{C_{44}\tau_2 - R_3\tau_1}{C_{44}K_2 - R_3^2}\sqrt{2ar}\sin\frac{1}{2}\theta \tag{14.8.7}$$

In addition

$$\frac{\partial}{\partial x} = \frac{\partial}{\partial r}\frac{\partial r}{\partial x} + \frac{\partial}{\partial\theta}\frac{\partial\theta}{\partial x} = \cos\theta\frac{\partial}{\partial r} - \sin\theta\frac{\partial}{\partial\theta}$$

Substituting these results and relations into the second and third terms of the integral, we obtain

$$-\int_{\pi}^{-\pi}\left(\sigma_{ij}n_j\frac{\partial u_i}{\partial x_1}+H_{ij}n_j\frac{\partial w_i}{\partial x_1}\right)\mathrm{d}\Gamma=\frac{K_2(K_{\mathrm{III}}^{\parallel})^2+C_{44}(K_{\mathrm{III}}^{\perp})^2-2R_3K_{\mathrm{III}}^{\parallel}K_{\mathrm{III}}^{\perp}}{C_{44}K_2-R_3^2} \quad (14.8.8)$$

From (14.8.5) and (14.8.8), we find that

$$E_{\mathrm{III}}=\frac{K_2(K_{\mathrm{III}}^{\parallel})^2+C_{44}(K_{\mathrm{III}}^{\perp})^2-2R_3K_{\mathrm{III}}^{\parallel}K_{\mathrm{III}}^{\perp}}{C_{44}K_2-R_3^2}=G_{\mathrm{III}} \quad (14.8.9)$$

which is just (8.1.25) given by Chap. 8.

Similarly

$$E_{\mathrm{I}}=G_{\mathrm{I}} \quad (14.8.10)$$

and

$$E_{\mathrm{II}}=G_{\mathrm{II}} \quad (14.8.11)$$

where the suffixes mean the Mode I, Mode II and Mode III of the cracks. The above demonstration indicates that the generalized Eshelby integral is equivalent to energy release rate of crack in linear elasticity of quasicrystals.

Under plastic deformation of quasicrystals, in general, the generalized Eshelby integral does not represent energy release rate; the reason of this is the unloading can appear due to crack extension, and stress–strain relations described by (14.3.1) and (14.3.2) do not remain one to one correspondence, and the physical background of the *E*-integral will be broken down. But if we define the potential energy per unit thickness for a plane (i.e. a two-dimensional) region Ω occupied by a quasicrystal and denote the boundary of which by Γ

$$V=\int_{\Omega}F\mathrm{d}x\mathrm{d}y-\int_{\Gamma}(T_iu_i+h_iw_i)\mathrm{d}\Gamma \quad (14.8.12)$$

then the total potential energy is

$$\Pi=BV \quad (14.8.13)$$

where B denotes the thickness of the specimen, and there is relation

$$E=-\frac{\delta\Pi}{\delta A}=-\frac{1}{B}\frac{\delta\Pi}{\delta a} \quad (14.8.14)$$

where E-integral can be expressed only by the "difference quotient" rather than the "differential quotient". The difference quotient is not energy release rate, and it only represents the ratio between individual difference of the energy over difference of crack length for the same configuration specimen but with different initial crack lengths. Considering the situation, the physical meaning of (14.8.14) is left for further discussion. Even if there is the faulty aspect, (14.8.14) provides useful application for calibrating the measurement data of the integral in experiments. The relevant discussion will be done in the next subsection.

14.8.3 On the Evaluation of the Critic Value of E-Integral

The E-integral provides not only the theoretical basis for generalized BCS model as well as generalized DB model, but also an effective tool for measuring the material constants E_c and δ_c. We mentioned that the measurement of δ_c is difficult, whereas the measurement of E_c is easier. Due to the connection between these two quantities, the value of the former can be obtained from that of the latter.

At low and conventional temperatures, quasicrystals present brittle behaviour, and the fracture belongs to linear elastic fracture, and the measurement of fracture toughness can be carried out by indentation technique, see, e.g. Mong et al. [19]. At high temperature, the materials present large plastic deformation and the measurement can be done by bending experiment, in which the three-point bending specimen, see Fig. 14.11, is one of the most useful specimens. There are two procedures either by multi-specimens testing or by single specimen testing.

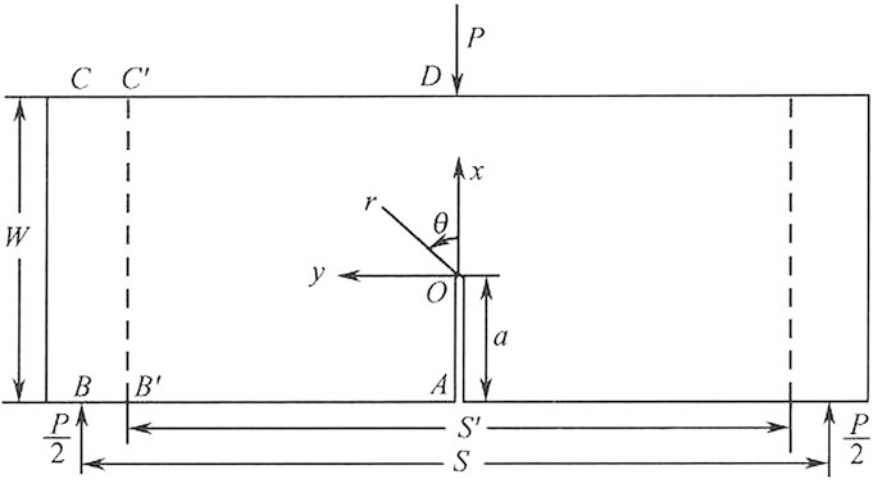

Fig. 14.11 Three-point bending specimen

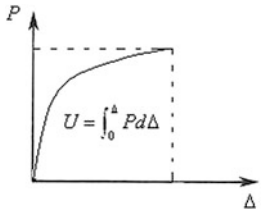

Fig. 14.12 Depiction of the specimen deformation energy

For simplicity, we here discuss the procedure by single specimen testing only. For the three-point bending specimen shown in Fig. 14.11, based on formula (14.8.14), the value of E-integral is approximately

$$E = \frac{2U}{B(W-a)} \tag{14.8.15}$$

where W represents the width, B the thickness of the specimen and U the area under $P-\Delta$ curve (shown by Fig. 14.12), i.e.

$$U = \int P\mathrm{d}\Delta \tag{14.8.16}$$

in which P is the load (force per unit thickness) at loading point, and Δ the displacement of the same point. When one observes the initiation of crack growth, the value of E-integral is marked as the fracture toughness of the quasicrystal.

If the phason field is absent, the material is reduced to conventional structural material including crystals. In this case, the E-integral is reduced to conventional Eshelby integral or J-integral; the latter was introduced by Rice [22] and Cherepanov [23] after 11 years compared with the Eshelby early publication [13], but the work of Rice has been systematically developed, especially Begley and Landes [24, 25] put forward the experimental study on J-integral, further promotes the development of nonlinear fracture theory and its applications for conventional engineering materials, these experiences would be helpful for the experimental study of nonlinear fracture of quasicrystalline materials.

References

1. Messerschmidt U, 2010, Dislocation Dynamics during Plastic Deformation, Springer-Verlag, Heidelberg.
2. Geyer B, Bartisch M, Feuerbacher M et al, 2000, Plastic deformation of icosahedral Al-Pd-Mn single quasicrystals, I. Experimental results, *Phil. Mag.* **A**, **80**(**7**), 1151-1164.
3. Messerschmidt U, Bartisch M, Geyer B et al, 2000, Plastic deformation of icosahedral Al-Pd-Mn single quasicrystals, II, Interpretation of experimental results, *Phil. Mag.* **A**, **80**(7), 1165-1181.

4. Urban K and Wollgarten M, 1994, Dislocation and plasticity of quasicrystals, *Materials Sci. Forum*, **150-151**(2), 315-322.
5. Wollgarten M et al, 1995, In-situ observation of dislocation motion in icosahedral Al-Pd-Mn single quasicrystals, *Phil. Mag. Lett.*, **71**(1), 99-105.
6. Feuerbacher M, Bartsch B, Grushk B et al, 1997, Plastic deformation of decagonal Al-Ni-Co quasicrystals, *Phil. Mag. Lett*., **76**(4), 396-375.
7. Messerschmidt U, Bartsch M, Feuerbacher M, et al, Friction mechanism of dislocation motion in icosahedral Al-Pd-Mn single quasicrystals, *Phil. Mag*. **A**, **79**(11), 2123-2135.
8. Fan T Y, Trebin H-R, Messerschmidt U and Mai Y W, 2004, Plastic flow coupled with a Griffith crack in some one- and two-dimensional quasicrystals, *J. Phys.: Condens. Matter*, **16**(47), 5229-5240..
9. Feuerbacher M and Urban K, 2003, Platic behaviour of quasicrystalline materials, in : *Quasicrystals*, ed. by Trebin H R, Wiley Press, Berlin.
10. Guyot P and Canova G, 1999, The plasticity of icosahedral quasicrystals, *Phil. Mag*. A, **79**(11), 2815-2822.
11. Feuerbacher M, Schall P, Estrin Y et al, 2001, A constitutive model for quasicrystal plasticity, *Phil. Mag.Lett*, **81**(7), 473-482 .
12. Estrin Y, 1996, in: *Unified Constitutive Laws of Plastic Deformation*, ed. by Krausz A and Krausz K, Academic Press, New York.
13. Eshelby J D, 1956, The continuum theory of dislocations in crystals, *Solid State Physics* (Ed. by Seits F et al), Vol. 3, New York: Academic Press.
14. Fan T Y and Fan L, 2008, Plastic fracture of quasicrystals, *Phil. Mag.*, **88**(4), 523-535.
15. Dugdale D S, 1960, Yielding of steel sheets containing slits, *J. Mech. Phys. Solids*, **32**(2), 105-108.
16. Barenblatt G I, 1962, The mathematical theory of equilibrium of crack in brittle fracture, *Advances in Applied Mechanics,* Vol. **7**, 55-129.
17. Fan T Y and Mai Y W, 2004, Elasticity theory, fracture mechanics and some relevant thermal properties of quasicrystalline materials, *Appl. Mech. Rev*., **57**(5), 325-344.
18. Fan T Y and Fan L, 2011, Relation between Eshelby integral and generalized BCS and generalized DB models for some one- and two-dimensional quasicrystals, *Chin. Phys. B,* 20(4),036102.
19. Mong X M, Tong B Y and Wu Y K, 1994, Mechanical properties of quasicrystals $Al_{65}Cu_{20}Co_{15}$, *Acta Metallurgica Sinica*, **A**, **30**(3), 61-64. (in Chinese).
20. Bilby B A, Cottrell A H and Swinden K H, 1963, The spread of plastic yield from a notch, *Proc. R. Soc.* A, **272** (2), 304-314.
21. Bilby B A, Cottrell A H, Smith E et al, 1964, Plastic yielding from sharp notches, ibid, **279** (1), 1-9.
22. Rice J R, 1968, A path independent integral and approximate analysis of strain concentration by notches and cracks, *J. Appl. Mech*., **35**(4), 379-386.
23. Cherepanov G P, 1969, On crack propagation in solids, *Int. J. Solids and Structures*, **5**(8), 863-871.
24. Begley G T and Landes J D, 1972, The J-integral as a fracture criterion, *Fracture Toughness*, ASTM STP 514, American Society for Testing and Materials, Philadelphia, 1-20.
25. Landes J D and Begley G T, 1972, The effect of specimen geometry on J_{IC}, *Fracture Toughness*, ASTM STP 514, American Society for Testing and Materials, Philadelphia, 24-29.
26. Muskhelishvili N I, 1956, *Singular Integral Equations*, English translation by Radok J R M, Noordhoff, Groningen.
27. Li W and Fan T Y, 2009, Study on plastic analysis of crack problem of three-dimensional quasicrystalline materials, Phil. Mag, 89(31), 2823-2831.

Chapter 15
Fracture Theory of Solid Quasicrystals

Solid quasicrystals are brittle, and the study on fracture behaviour of the material is significant. In the previous chapters, many of crack problems are investigated, and the exact analytic, approximate and numerical solutions are constructed; this provides a basis for discussing the fracture theory. The exact solutions of crack problem of quasicrystals present particular importance, which reveal the essential nature describing fracture behaviour of this kind material. The first exact analytic solution on a Griffith crack in decagonal quasicrystals was given by Li and Fan [1] in 1999. Afterwards, the author and co-workers in Refs. [1–3] developed the idea of linear elastic fracture mechanics of quasicrystals based on the common feature of crack solutions obtained in that date. Trebin et al. [4] discussed the relevant topic from the other point of view. Recently, Fan and Guo [5], Zhu and Fan [6] and Li and Fan [7] observed the analytic solutions of cracks in three-dimensional icosahedral quasicrystals, Fan and Fan [8, 9] and Li and Fan [15] and Fan et al. [16] found the plastic analytic solutions of cracks and Zhu and Fan [10] and Wang et al. [11] carried out the numerical analysis on dynamic crack of quasicrystals, respectively. And the measurement of fracture toughness of the material is also reported [12]. The quite fruit information mentioned above suggests to be needed to give a summary on the fracture study of quasicrystals. This chapter undertakes a task and may put forward some pointers for the fracture theory of quasicrystals.

15.1 Linear Fracture Theory of Quasicrystals

The descriptions on crack solutions in different chapters reveal some common nature of stress field and displacement field around crack tip. For all exact solutions of cracks of one-, two- and three-dimensional quasicrystals in linear elasticity regime, the resulting expressions of stress and displacement components hold with respect to arbitrary variables x and y. In addition, we found a quite lot of solutions of cracks of dynamic state and nonlinear behaviour of quasicrystals, and some

T.-Y. Fan, *Mathematical Theory of Elasticity of Quasicrystals and Its Applications*,
Springer Series in Materials Science 246, DOI 10.1007/978-981-10-1984-5_15

common features are also exhibited. At first, we analyse the linear elastic solutions. As indicted in Sect. 8.1, within the framework of linear elasticity and infinite-sharp crack model, stress near crack tip, i.e.

$$r_1/a \ll 1, \tag{15.1.1}$$

stresses for phonons as well as for phasons appear singular in order of $r_1^{-1/2}$ $(r_1 \to 0)$, and other terms can be ignored when compared to this term. Although stress singularity is implausible, it is the result of idealized mathematical model. Quite a few researchers indicated its severe weakness in theory and the paradox of its methodology [1, 2]. However, prior to the actual establishment of more reasonable fracture theory, we still continue using this theory in expectable near future.

If temporarily accepting this theory, we focus on the field variables near crack tip. If in (8.3.14) only keeping the term in order of $(r_1/a)^{-1/2}$, we have

$$\sigma_{xx} = \frac{K_{\mathrm{I}}^{\|}}{\sqrt{2\pi r_1}}\cos\frac{1}{2}\theta_1\left(1 - \sin\frac{1}{2}\theta_1 \sin\frac{3}{2}\theta_1\right)$$

$$\sigma_{yy} = \frac{K_{\mathrm{I}}^{\|}}{\sqrt{2\pi r_1}}\cos\frac{1}{2}\theta_1\left(1 + \sin\frac{1}{2}\theta_1 \sin\frac{3}{2}\theta_1\right)$$

$$\sigma_{xy} = \sigma_{yx} = \frac{K_{\mathrm{I}}^{\|}}{\sqrt{2\pi r_1}}\cos\frac{1}{2}\theta_1 \cos\frac{3}{2}\theta_1$$

$$H_{xx} = -\frac{d_{21}K_{\mathrm{I}}^{\|}}{\sqrt{2\pi r_1}}\sin\theta_1\left(2\sin\frac{3}{2}\theta_1 + \frac{3}{2}\sin\theta_1\cos\frac{5}{2}\theta_1\right)$$

$$H_{yy} = \frac{d_{21}K_{\mathrm{I}}^{\|}}{\sqrt{2\pi r_1}}\frac{3}{2}\sin^2\theta_1\cos\frac{5}{2}\theta_1$$

$$H_{xy} = -\frac{d_{21}K_{\mathrm{I}}^{\|}}{\sqrt{2\pi r_1}}\frac{3}{2}\sin^2\theta_1\sin\frac{5}{2}\theta_1$$

$$H_{yx} = \frac{d_{21}K_{\mathrm{I}}^{\|}}{\sqrt{2\pi r_1}}\sin\theta_1\left(2\cos\frac{3}{2}\theta_1 - \frac{3}{2}\sin\theta_1\sin\frac{5}{2}\theta_1\right) \tag{15.1.2}$$

where $d_{21} = R(K_1 - K_2)/4(MK_1 - R^2)$ given in Sect. 8.3 and

$$K_{\mathrm{I}}^{\|} = \lim_{x\to a^+}\sqrt{2\pi(x-a)}\sigma_{yy}(x,0) = \sqrt{\pi a}p, \tag{15.1.3}$$

in which

$$\sigma_{yy}(x,0)=\begin{cases} p\left(\frac{x}{\sqrt{x^2-a^2}}-1\right) & |x|>a \\ -p & |x|<a \end{cases} \tag{15.1.4}$$

it is one of results of Sects. 8.3 and 8.4, and (15.1.3) represents a physical parameter describing the fracture behaviour of quasicrystals under Mode I loading condition.

The physical meaning of the generalized surface forces $h_i = H_{ij}n_j$ is clear, but have not been measured so far, and we do not consider h_i at the physical boundary (simply assume zero). Therefore, we only obtain the $K_{\mathrm{I}}^{\|}$, but the stress intensity factor for phason field still exits if we do not assume the generalized tractions h_i to be zero. Can we use the stress intensity factor $K_{\mathrm{I}}^{\|}$ in the parallel space (physical space) as the physical parameter to control the crack stability (instability) in quasicrystals? This only depends upon tests.

It can be found that $K_{\mathrm{I}}^{\|}$ given by (15.1.3) is not directly related to the material constants of quasicrystals in the case for any self-equilibrium applied stress state (this is similar to that for conventional fracture mechanics for structural materials). Nevertheless, it does not mean that it cannot be used as the physical parameter to govern the crack stability/instability in quasicrystals. Further study is needed in this topic.

But the displacement field concerning crack is strongly related to material constants (this is also similar to that of conventional fracture mechanics for structural materials), and we must distinguish the results for different quasicrystal systems.

For point groups 5-m and 10-mm quasicrystals, it can be found from (8.3.17) that

$$u_y(x,0)=\begin{cases} 0 & |x|>a \\ \frac{p}{2}\left(\frac{K_1}{MK_1-R^2}+\frac{1}{L+M}\right)\sqrt{a^2-x^2} & |x|<a \end{cases} \tag{15.1.5}$$

$$w_{\mathrm{y}}(x,0)=0, \quad |x|<\infty.$$

The strain energy of the system due to the existence of crack is

$$\begin{aligned} W_{\mathrm{I}} &= 2\int_0^a (\sigma_{yy}(x,0)\oplus H_{yy}(x,0))(u_y(x,0)\oplus w_y(x,0))\mathrm{d}x \\ &= 2\int_0^a \sigma_{yy}(x,0)u_y(x,0)\mathrm{d}x \\ &= \frac{\pi a^2 p^2}{4}\left(\frac{1}{L+M}+\frac{K_1}{MK_1-R^2}\right) \end{aligned} \tag{15.1.6}$$

which is called crack strain energy with the suffix "I" to indicate the Mode I crack.

It can be found from solution in Sects. 8.3 and 8.4 that under the assumption of generalized surface traction $h_i = H_{ij}n_j$ being free, the crack strain energy is still relevant to both the elastic constant K_1 of the phason field and the phonon-phason coupling elasticity constant R apart from relevant to the phonon elastic constants $L = C_{12}$, $M = (C_{11} - C_{12})/2$.

Similar to Sect. 8.1, we define the strain energy release rate (crack growth force) for point groups 5 m and 10 mm

$$\begin{aligned} G_{\mathrm{I}} &= \frac{1}{2}\frac{\partial W_1}{\partial a} = \frac{\pi a p^2}{4}\left(\frac{1}{L+M} + \frac{K_1}{MK_1 - R^2}\right) \\ &= \frac{1}{4}\left(\frac{1}{L+M} + \frac{K_1}{MK_1 - R}\right)(K_{\mathrm{I}}^{\parallel})^2 \end{aligned} \tag{15.1.7}$$

for point groups $5, \overline{5}$ and $10, \overline{10}$ quasicrystals

$$G_{\mathrm{I}} = \frac{L(K_1 + K_2) + 2(R_1^2 + R_2^2)}{8(L+M)c}(K_{\mathrm{I}}^{\parallel})^2. \tag{15.1.8}$$

$$c = M(K_1 + K_2) - 2(R_1^2 + R_2^2)$$

and for icosahedral quasicrystals

$$G_{\mathrm{I}}^{\parallel} = \frac{1}{2}\left(\frac{1}{\mu + \lambda} + \frac{c_7}{c_3}\right)(K_{\mathrm{I}}^{\parallel})^2 \tag{15.1.9}$$

$$c_1 = \frac{R(2K_2 - K_1)(\mu K_1 + \mu K_2 - 3R^2)}{2(\mu K_1 - 2R^2)}$$

$$c_3 = \mu(K_1 - K_2) - R^2 - \frac{(\mu K_2 - R^2)^2}{\mu K_1 - 2R^2},$$

$$c_7 = \frac{c_3 K_1 + 2c_1 R}{\mu K_1 - 2R^2}$$

which also indicate that the strain energy release rate relating is not only the phonon elasticity constants $L = C_{12}$, $M = (C_{11} - C_{12})/2$, but also the phason elasticity constant K_1, K_2 and phonon-phason coupling constants R_1 and R_2.

In the above relations, for point groups 5 m and 10 mm, due to $L + M > 0$, $MK_1 - R^2 > 0$, $M + L > 0$ and crack energy W_{I} and crack energy release rate G_{I} are all positive, meaningful in physical sense. For point groups $5, \overline{5}$ and $10, \overline{10}$, there are icosahedral and other quasicrystals too.

Considering the obvious physical meaning of G_{I}, we recommend

$$G_{\mathrm{I}} = G_{\mathrm{IC}} \tag{15.1.10}$$

as the crack initiation criterion, where G_{IC} is the critical value, a material constant determined experimentally. With the availability of explicit expression G_{I}, the measurement of G_{IC} is convenient, to be discussed in the next section. The above results have been documented in Chaps. 8 and 9 and the relevant references.

With these common features of cracks in quasicrystalline materials, the fundamental of fracture theory for the material can be set up.

15.2 Crack Extension Force Expressions of Standard Quasicrystal Samples and Related Testing Strategy for Determining Critical Value G_{IC}

Mong et al. [12] measured the fracture toughness for $Al_{65}Cu_{20}Co_{15}$ decagonal quasicrystal by using nonstandard specimen, because in that time, there were lack of expressions on stress intensity factors and energy release rate for quasicrystalline material. In addition, the measurement of fracture toughness used nonstandard approach, e.g. indentation approach.

During the characterization of mechanical properties of quasicrystals, similar to conventional structural materials, standard samples are expected to use, such as cracked samples. Here, we recommend three-point bending specimen shown by Fig. 14.11 in Appendix of Chap. 14 and compact tension specimen shown in Fig. 15.1 for determining G_{IC}. The corresponding G_{I} expressions are obtained by extending the formula (15.1.7) and others.

15.2.1 Characterization of G_{I} and G_{IC} of Three-Point Bending Quasicrystal Samples

Due to $K_{\mathrm{I}}^{\parallel}$ independent of material constants, according to fracture mechanics, the stress intensity factor corresponding to the three-point bending specimen as shown in Fig. 14.11 in Appendix of Chap. 14 is

$$K_{\mathrm{I}}^{\parallel} = \frac{PS}{BW^{3/2}}\left[29\left(\frac{a}{W}\right)^{1/2} - 4.6\left(\frac{a}{W}\right)^{3/2} + 21.8\left(\frac{a}{W}\right)^{5/2} - 37.6\left(\frac{a}{W}\right)^{7/2} + 38.7\left(\frac{a}{W}\right)^{9/2}\right] \tag{15.2.1}$$

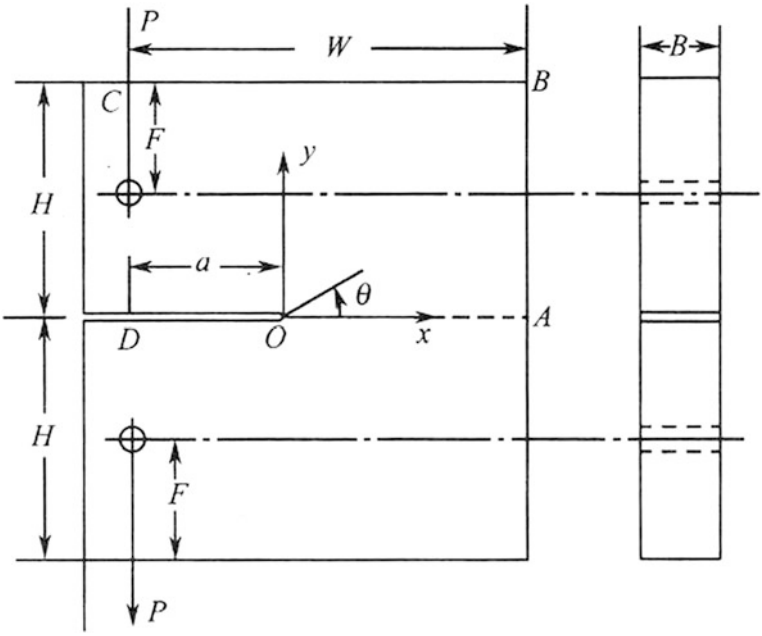

Fig. 15.1 Compact tension specimen for measuring fracture toughness of quasicrystalline material

Therefore, extension of (15.1.7) leads to

$$G_{\mathrm{I}} = \frac{1}{4}\left(\frac{1}{L+M} + \frac{K_1}{MK_1 - R^2}\right)\frac{PS}{BW^{3/2}}\left[29\left(\frac{a}{W}\right)^{1/2} - 4.6\left(\frac{a}{W}\right)^{3/2} + 21.8\left(\frac{a}{W}\right)^{5/2} - 37.6\left(\frac{a}{W}\right)^{7/2} + 38.7\left(\frac{a}{W}\right)^{9/2}\right] \tag{15.2.2}$$

for point groups 5-m and 10-mm quasicrystals, where S is the sample span, B the sample thickness, W the sample width, a the crack length plus the size of the machined notch and P is the external force (per unit length). Finally, the G_{IC} value can be determined by measuring the critical external force P_{C}. For other quasicrystal systems, there are similar results.

15.2.2 *Characterization of G_{I} and G_{IC} of Compact Tension Quasicrystal Sample*

It can be found in fracture mechanics that the stress intensity factor of the compact tension specimen as shown in Fig. 15.1 is

$$K_{\mathrm{I}}^{\|} = \frac{PS}{BW^{3/2}}\left[29.6\left(\frac{a}{W}\right)^{1/2} - 185.5\left(\frac{a}{W}\right)^{3/2} + 655.7\left(\frac{a}{W}\right)^{5/2} - 1017.0\left(\frac{a}{W}\right)^{7/2} + 638.9\left(\frac{a}{W}\right)^{9/2}\right] \tag{15.2.3}$$

Therefore, for point groups 5-m and 10-mm quasicrystals.

$$G_{\mathrm{I}} = \frac{1}{4}\left(\frac{1}{L+M} + \frac{K_1}{MK_1 - R^2}\right)\frac{P}{BW^{3/2}}\left[29.6\left(\frac{a}{W}\right)^{1/2} - 185.5\left(\frac{a}{W}\right)^{3/2} + 655.7\left(\frac{a}{W}\right)^{5/2} - 1017.0\left(\frac{a}{W}\right)^{7/2} + 638.9\left(\frac{a}{W}\right)^{9/2}\right], \tag{15.2.4}$$

where B, W, a and P have the same meanings above. The G_{IC} value can be determined by measuring the critical external force P_{C}. For other quasicrystal systems, there are similar results.

15.3 Nonlinear Fracture Mechanics

In the regime for nonlinear deformation of quasicrystals, the stress intensity factor and energy release rate cannot be used as a fracture parameter, and we must carry out elasto-plastic analysis, and the exact solutions of the crack problems have not been obtained except a few of special cases. Fortunately, this difficult topic has been discussed in Chap. 14 in detail, and now, it is needed listing some key points only.

Instead of stress intensity factor and energy release rate, the crack tip opening displacement or Eshelby integral may be a parameter characterizing the mechanical behaviour of crack tip under nonlinear deformation of quasicrystals. These quantities are strongly related to material constants, so the discussion must be done for distinguishing quasicrystal systems.

For one-dimensional hexagonal quasicrystals, we have obtained the crack tip sliding displacement for Mode III crack as

$$\delta_{\mathrm{III}} = \frac{4K_2\tau_{\mathrm{c}}a}{\pi(C_{44}K_2 - R_3^2)}\left[\ln\ \sec\left(\frac{\pi\tau_1}{2\tau_{\mathrm{c}}}\right)\right] \tag{15.3.1}$$

and for two-dimensional quasicrystals with point groups 5 m and 10 mm, the crack tip opening displacement for Mode I crack is

$$\delta_{\mathrm{I}} = \frac{2\sigma_{\mathrm{c}}a}{\pi}\left[\frac{1}{L+M} + \frac{K_1}{MK_1 - R^2}\right]\left[\ln\ \sec\left(\frac{\pi p}{2\sigma_{\mathrm{c}}}\right)\right] \tag{15.3.2}$$

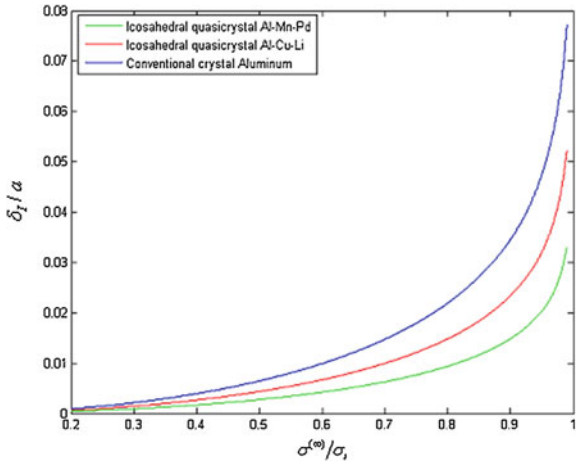

Fig. 15.2 Crack tip opening displacement of icosahedral quasicrystals versus applied stress

For icosahedral quasicrystal, the crack tip opening displacement is

$$\delta_{\mathrm{I}} = \lim_{x \to l} 2u_y(x,0) = \lim_{\varphi \to \varphi_2} 2u_y(x,0) = 2\left(\frac{1}{\lambda+\mu} + \frac{c_4}{c_2}\right) \cdot \frac{\sigma_s a}{\pi} \cdot \ln \sec\left(\frac{\pi}{2}\frac{p}{\sigma_s}\right) \tag{15.3.3}$$

in which

$$c_2 = \mu(K_1 - K_2) - R^2 - \frac{(\mu K_2 - R^2)^2}{\mu K_1 - 2R^2}, \quad c_4 = c_1 R + \frac{1}{2} c_2 \left(K_1 + \frac{\mu K_1 - 2R^2}{\lambda+\mu}\right) \tag{15.3.4}$$

with $c_1 = \frac{R(2K_2 - K_1)(\mu K_1 + \mu K_2 - 3R^2)}{2(\mu K_1 - 2R^2)}$.

Fig. 15.2 shows the crack tip opening displacement versus applied stress.

And the size of plastic zone around the crack tip is

$$d = a\left[\sec\left(\frac{\pi\tau_1}{2\tau_c}\right) - 1\right]$$

for one-dimensional hexagonal quasicrystals and

$$d = a\left[\sec\left(\frac{\pi p}{2\sigma_c}\right) - 1\right]$$

for two-dimensional quasicrystals with point groups 5 m and 10 mm.

And we have fracture criterion for Mode I crack

$$\delta_{\mathrm{I}} = \delta_{\mathrm{Ic}} \tag{15.3.5}$$

For Mode II and Mode III crack, there are similar criteria, which have been discussed in Chap. 14.

As pointed out in Chap. 14, the Eshelby integral can also be as a fracture parameter, and based on which one can set up a fracture criterion, the full discussion can be found there.

The experimental measurement of nonlinear fracture toughness of quasicrystals has been introduced in Appendix of Chap. 14, and it does not mention any more.

15.4 Dynamic Fracture

As we have known from Chap. 10, the study on dynamics for quasicrystals presents difficult situation, so the study for dynamic fracture.

Nevertheless, Chap. 10 provides some beneficial data for us.

By taking the so-called phonon-phason dynamic equation system for quasicrystals, the dynamic crack initiation problem can be solved by the finite difference method. In linear case, the crack dynamic initiation can be described by dynamic stress intensity factor, and for some samples, the results are listed in Chap. 10, which are sensitive functions of loading type, loading rate and sample geometry, including crack geometry. One of results can be seen in Fig. 15.3.

With the results, we can propose the fracture criterion for dynamic crack initiation

$$K_{\mathrm{I}}(t) = K_{\mathrm{Id}}(\dot{\sigma}) \tag{15.4.1}$$

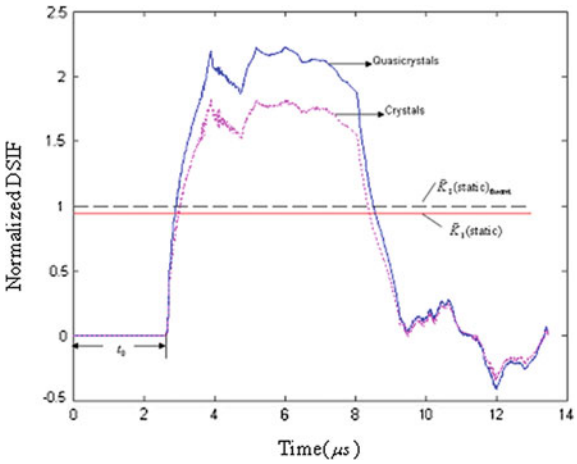

Fig. 15.3 Normalized dynamic stress intensity factor of central stationary crack specimen under Heaviside impact loading (for decagonal Al–Ni–Co quasicrystals)

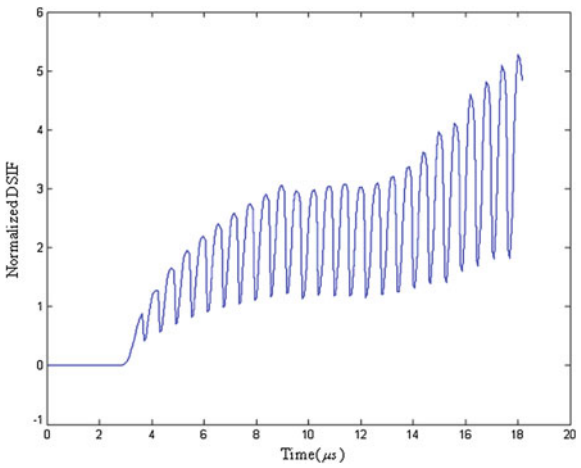

Fig. 15.4 Normalized dynamic stress intensity factor of propagating crack with the constant crack speed of central crack specimen (for icosahedral Al–Pd–Mn quasicrystals)

in which $K_{\mathrm{I}}(t)$ is the dynamic stress intensity factor evaluated by different approaches, and $K_{\mathrm{Id}}(\dot{\sigma})$ represents the dynamic fracture toughness for the initiation of crack growth of the material and is measured by test, a material constant, but is function of loading rate $\dot{\sigma}$. While for fast crack propagation/crack arrest problems we have results, e.g. shown in Fig. 15.4 for central crack specimen, there is fracture criterion such as

$$K_{\mathrm{I}}(t) \leq K_{\mathrm{ID}}(V) \tag{15.4.2}$$

where $K_{\mathrm{I}}(t)$ is also the dynamic stress intensity factor, a computational quantity, while $K_{\mathrm{ID}}(V)$ denotes the fracture toughness for fast propagating crack and must be measured by test, a material constant, but is the function of crack speed $V = \mathrm{d}a/\mathrm{d}t$. In (15.4.2), the equality sign represents crack propagation condition, and the inequality sign marks the crack arrest condition.

15.5 Measurement of Fracture Toughness and Relevant Mechanical Parameters of Quasicrystalline Material

Reference [12] reported the measurement of fracture toughness of two-dimensional decagonal quasicrystal $Al_{65}Cu_{20}Co_{15}$ as well as three-dimensional icosahedral Al–Li–Cu quasicrystal, and the authors used the indentation approach.

15.5.1 Fracture Toughness

The material is locally pressed, the crack around the indentation will appear as the compressible stress reaches a certain value and this describes the ability of fracture of the material along the direction of the compressible stress. When the crack length $2a$ is greater than the 2.5 times of length $2c$ of diagonal of the indentation, then the fracture toughness can be evaluated by

$$K_{\mathrm{IC}} = 0.203\ \mathrm{HV}\sqrt{c}\left(\sqrt[3]{\frac{c}{a}}\right) \tag{15.5.1}$$

in which HV denotes hardness of the material.

Their results of measurement for decagonal Al–Ni–Co quasicrystal are

$$K_{\mathrm{IC}} = 1.0{-}1.2\,\mathrm{MPa}\sqrt{m} \tag{15.5.2}$$

with HV $= 11.0{-}11.5$ GPa and for icosahedral Al–Li–Cu quasicrystal are

$$K_{\mathrm{IC}} = 0.94\,\mathrm{MPa}\sqrt{m} \tag{15.5.3}$$

in which HV $= 4.10$ GPa.

The values of fracture toughness for general alloys for black metals measured by Ma et al. [13] are much greater than the above data, those for aluminium alloys and other coloured metals are also, e.g. for aluminium is $33\,\mathrm{MPa}\sqrt{m}$ refer to Fan [14]. So one finds that quasicrystals are very brittle.

The author of the book minds the indirect measurement for fracture toughness of quasicrystals though indentation probably is not so exact, because formula (15.5.1) is empirical, the exact measurement should be using the stress intensity factor formula. Due to the high brittleness of the material, maybe it is easy by taking the indentation approach.

15.5.2 Tension Strength

The tensile strength σ_{c} is measured through the formula

$$\sigma_{\mathrm{c}} = 0.187\ P/a^2 \tag{15.5.4}$$

Meng et al. [12] obtained

$$\sigma_{\mathrm{c}} = 450\,\mathrm{MPa} \tag{15.5.5}$$

before annealing and

$$\sigma_c = 550\,\text{MPa} \tag{15.5.6}$$

after annealing for decagonal Al–Ni–Co quasicrystal.

Figure 15.5 shows the SEM morphology of grain interior containing large hole, Fig. 15.6 shows diagram of indentation crack under applied load 100 g before annealing and after annealing and Fig. 15.7 shows the SEM fractograph and fracture feature for decagonal $Al_{65}Cu_{20}Co_{15}$ quasicrystal.

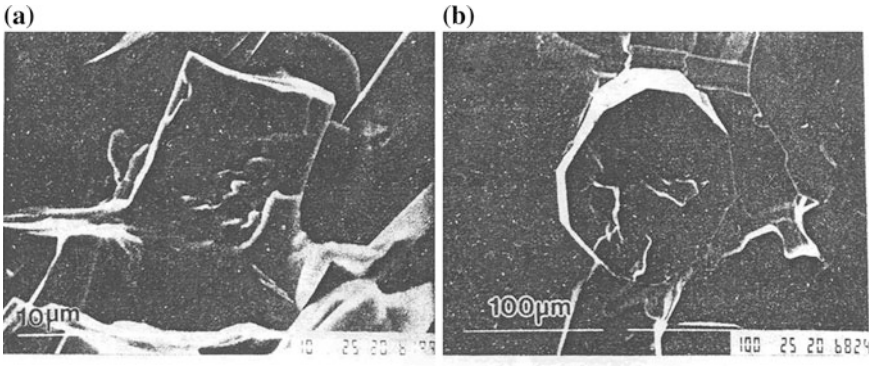

Fig. 15.5 SEM morphology of grain interior hole **a** prismatic grain with perfect basic plane, **b** grain with prefect prismatic plane

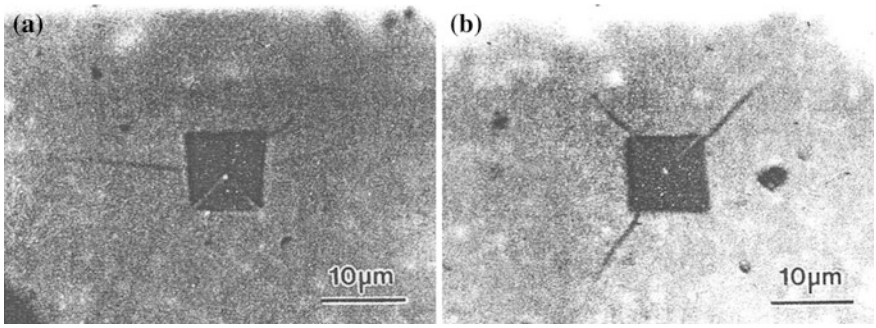

Fig. 15.6 Morphology of cracks near impression under 100 g load **a** before annealing, **b** after 850 °C, 36 h annealing

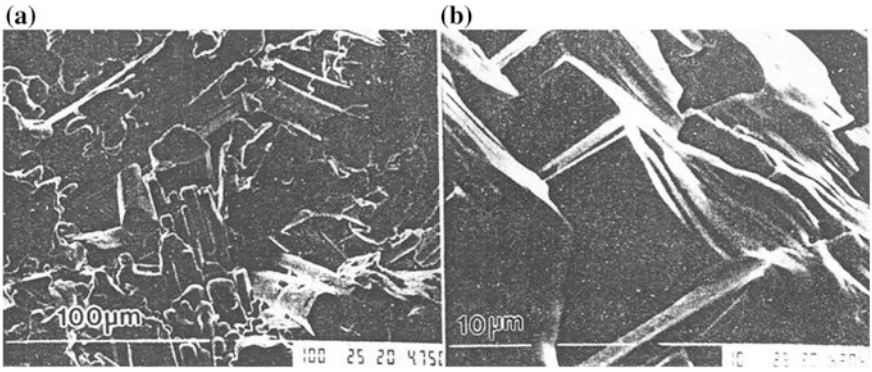

Fig. 15.7 **a** SEM fractograph, fracture feature of decagonal $Al_{65}Cu_{20}Co_{15}$ quasicrystal grain without plastic deformation, **b** magnification

References

1. Li X F, The defect problems and their analytic solutions in elasticity of quasicrystals, Dissertation, Beijing Institute of Technology, Beijing 1999; Li X F, Fan T Y and Sun Y F, 1999, A decagonal quasicrystal with a Griffith crack, *Phil. Mag.* A, **79**(8), 1943-1952.
2. Fan T Y, 2000, Mathematical theory of elasticity and defects of quasicrystals, *Advances of Mechanics*, **30**(2), 161-174 (in Chinese).
3. Fan T Y and Mai Y W, 2004, Theory of elasticity, fracture mechanics and some relevant thermal properties of quasicrystalline materials, *Appl. Mech. Rev.*, **57**(5), 235-244.
4. Rudhart C, Gumsch and Trebin H R, 2003, Crack propagation in quasicrystals, *Quasicrystals*, ed by Trebin H R, Berlin: Wiely Press.
5. Fan T Y and Guo L H, 2005, The final governing equation of plane elasticity of icosahedral quasicrystals, *Phys. Ltte*. A, **341**(5), 235-239.
6. Zhu A Y and Fan T Y, 2007, Elastic analysis of Mode II Griffith crack in an icosahedral quasicrystal, *Chinese Physics*, **16**(4), 1111-1118.
7. Li L H and Fan T Y, 2008, Complex variable method for plane elasticity of icosahedral quasicrystals and elliptic notch problem, *Science in China*, G, **51**(6), 1-8.
8. Fan T Y and Fan L, 2008, Plastic fracture of quasicrystals, *Phil. Mag*., **88**(4), 323-335.
9. Fan T Y and Fan L, 2008, The relation between generalized Eshelby energy-momentum tensor and generalized BCS and DB models, *Chinese Physics*, to be published.
10. Zhu A Y and Fan T Y, 2008, Dynamic crack propagation of decagonal $Al-Ni-Co$ decagonal quasicrystals, *J. Phys.: Condens. Matter*, 20(29), 295217.
11. Wang X F, Fan T Y and Zhu A Y, 2009, Dynamic behaviour of the icosahedral Al-Pd-Mn quasicrystals with a Griffith crack, Chin. Phys. B, 18(2), 709-714.
12. Meng X M, Tong B Y and Wu Y K, 1994, Mechanical behaviour of $Al_{65}Cu_{20}Co_{15}$ quasicrystal, *Acta Metallurgy Sinica* (in Chinese), 30(1), 61-64.
13. Ma D L (ed), 1994, *Handbook for Parameters of Fracture Mechanics Behaviour of General Black Metals*, Beijing: Industrial Press (in Chinese).
14. Fan T Y, 2003, *Foundation of Fracture Theory*, Beijing: Science Press (in Chinese).
15. Li W and Fan T Y, 2009, Study on plastic analysis of crack problem decagonal Al-Ni-Co quasicrystals of point group 10, $\overline{10}$, *Int. Mod. Phys. Lett. B,* 23(16), 1989-1999.
16. Fan T Y, Tang Z Y and Chen W Q, 2012, Theory of linear, nonlinear and dynamic fracture of quasicrystalline materials, Eng Fract Mech, 82(2), 185-194.

Chapter 16
Hydrodynamics of Solid Quasicrystals

Generalized hydrodynamics is one of the important branches on study of solid quasicrystals, refer to Lubensky et al. [1, 2]. Though the discussion on phonon-phason dynamics in Chap. 10, suggested by Rochal and Norman [3] and Fan et al. [4], is concerned somewhat with generalized hydrodynamics, the description there is too simple and too simplified, some nature of hydrodynamics of quasicrystals have not been touched. We here intend to give a detailed introduction on hydrodynamics of solid quasicrystals of Lubensky et al. The theory is concerned with many aspects of physics and mathematics, which are listed in Appendix C of Major Appendix.

Before the discovery of quasicrystals, hydrodynamics of solid (crystals) has been developed, see e.g. the work of Martin et al. [5], Fleming and Cohen [6], which is related to viscosity of solid. Considering the viscosity, the numbers of field variables and field equations are enlarged. The nature is connected to symmetry-breaking. At first we introduce some basic concepts of viscosity of solid, which are beneficial to understand hydrodynamics of quasicrystals.

16.1 Viscosity of Solid

The elasticity discussed in the first 13 chapters is reversible, and the plasticity studied in Chap. 14 is one of the irreversible deformations. The irreversibility of plasticity lies in existence of dissipation. The viscosity of solid is another kind of dissipation. To study viscosity of solid one can take a method similar to that in fluid dynamics [7]. Introducing velocity of mass point $\mathbf{V} = \left(V_x, V_y, V_z\right)$ and tensor of deformation velocity

$$\dot{\xi}_{ij} = \frac{1}{2}\left(\frac{\partial V_i}{\partial x_j} + \frac{\partial V_j}{\partial x_i}\right) \tag{16.1.1}$$

T.-Y. Fan, *Mathematical Theory of Elasticity of Quasicrystals and Its Applications*,
Springer Series in Materials Science 246, DOI 10.1007/978-981-10-1984-5_16

then viscosity stress tensor is defined by

$$\sigma'_{ij} = 2\eta\left(\dot{\xi}_{ij} - \frac{1}{3}\dot{\xi}_{kk}\delta_{ij}\right) + \zeta\dot{\xi}_{kk}\delta_{ij} \tag{16.1.2}$$

here is considered only the isotropic viscosity, and denote η the bulk viscosity constant, ζ the shear one. Equation (16.1.2) is the constitutive law of viscosity of isotropic solid.

The general constitutive law of viscosity of solid is

$$\sigma'_{ij} = \eta_{ijkl}\dot{\xi}_{kl} \tag{16.1.3}$$

in which η_{ijkl} represents viscosity coefficient tensor of anisotropic viscosity of solid.

A description of viscosity of solid can also be introduced by a dissipation function R such as

$$R = \frac{1}{2}\eta_{ijkl}\dot{\xi}_{ij}\dot{\xi}_{kl} \tag{16.1.4}$$

so that we have

$$\sigma'_{ij} = \frac{\partial R}{\partial \dot{\xi}_{ij}} \tag{16.1.5}$$

which is similar to the relation between stress and density of strain energy in the elasticity in form. For the icosahedral quasicrystals, the viscosity coefficients can be expressed as

$$\eta_{ijkl} = \zeta\delta_{ij}\delta_{kl} + \eta\left(\delta_{ik}\delta_{jl} + \delta_{il}\delta_{jk} - \frac{2}{3}\delta_{ij}\delta_{kl}\right) \tag{16.1.6}$$

For simplicity, in the following we consider only the simplest case, i.e., $\sigma'_{ij} = 2\eta\left(\dot{\xi}_{ij} - \frac{1}{3}\dot{\xi}_{kk}\delta ij\right)$, only one viscosity constant η (the bulk or longitudinal viscosity constant) is used. The detailed description about viscosity of solid physically, refer to Ref [1].

16.2 Generalized Hydrodynamics of Solid Quasicrystals

Considering both elasticity and viscosity of solid quasicrystals lead to a **generalized hydrodynamics that is developed by** Lubensky et al. [1, 2], they derived the governing equations of the hydrodynamics by using Poisson bracket method. Here, there are 4 systems of equations: mass conservation equation, momentum conservation equations, equations of motion of phonons due to symmetry breaking and

phason dissipation equations, if the energy conservation equation does not considered. The mass conservation equation is

$$\frac{\partial \rho\,(\mathrm{r},t)}{\partial t} = -\nabla_i(\mathrm{r})\,(\rho V_i) \tag{16.2.1}$$

and the momentum conservation law is

$$\begin{aligned}\frac{\partial g_i(\mathrm{r},t)}{\partial t} &= -\nabla_k(\mathrm{r})(V_k g_i) + \nabla_j(\mathrm{r})\left(\eta_{ijkl}\nabla_k(\mathrm{r})g_l\right)\\ &\quad - \left(\delta_{ij} - \nabla_i(\mathrm{r})u_j\right)\frac{\delta H}{\delta u_j} + \left(\nabla_i(r)w_j\right)\frac{\delta H}{\delta w_j} - \rho\nabla_i(\mathrm{r})\frac{\delta H}{\delta \rho},\\ g_j &= \rho V_j\end{aligned} \tag{16.2.2}$$

At meantime one has equations of motion of phonons due to symmetry breaking

$$\frac{\partial u_i(\mathrm{r},t)}{\partial t} = -V_j\nabla_j(\mathrm{r})u_i - \Gamma_{\mathrm{u}}\frac{\delta H}{\delta u_i} + V_i \tag{16.2.3}$$

and phason dissipation equations

$$\frac{\partial w_i(\mathrm{r},t)}{\partial t} = -V_j\nabla_j(\mathrm{r})w_i - \Gamma_{\mathbf{w}}\frac{\delta H}{\delta w_i} \tag{16.2.4}$$

The detailed discussions on the equations can be found in Appendix C, in which the Hamiltonian H is defined by:

$$\begin{cases} H = \int\left[\frac{\mathrm{g}^2}{2\rho} + \frac{1}{2}A\left(\frac{\delta\rho}{\rho_0}\right)^2 + B\left(\frac{\delta\rho}{\rho_0}\right)\nabla\cdot\mathrm{u}\right]d^d\mathrm{r} + F_{\mathrm{u}} + F_{\mathrm{w}} + F_{\mathrm{uw}},\\ \mathrm{g} = \rho\mathrm{V}\end{cases} \tag{16.2.5}$$

where the integral in (16.2.5) describes the contributions of momentum and variation of mass density, the last three terms of (16.2.5) denote the contributions of phonon, phason and phonon-phason coupling, and A, B are new constants of materials describing the effect due to variation of mass density, respectively, the superscript of volume element of integral represents dimension. Equations (16.2.1)–(16.2.4) are the equations of motion of hydrodynamics for solid quasicrystals, and the field variables include mass density ρ, velocity V_i (or momentum $\rho\, V_i$), phonon displacement u_i and phason displacement w_i. In order to write the Hamiltonian H (16.2.5), one must give constitutive law of quasicrystals, in which the elastic constitutive equations are discussed in detail in the first 13 chapters.

Above listed equations are derived by Lubensky et al. [1] in 1985, but there was no detail of derivation which are supplemented in Appendix C. Some arguments on the equations can be found in Refs. [3, 8, 9]. The amount of the filed equations including deformation geometry and constitutive law is 52 and belongs to differential-variational equations; the solving of the initial-boundary value problems of these equations is difficult.

16.3 Simplification of Plane Field Equations in Two-Dimensional 5- and 10-Fold Symmetrical Solid Quasicrystals

The equations of Lubensky et al. are derived for icosahedral quasicrystals, but can be used for other solid quasicrystals observed so far. We here discuss point group $5, \overline{5}$ pentagonal and point group $10, \overline{10}$ decagonal quasicrystals, and only for plane field, i.e. the motion of the medium is in xy-plane if the z-axis is taken as 5- or 10-fold symmetry axis. In this case, the governing equations are the same for both point group $5, \overline{5}$ pentagonal and point group $10, \overline{10}$ decagonal quasicrystals. All field variables depend only on variables x, y and t, and those of z-components are vanished. If terms $\left(\nabla_i(\mathrm{r})u_j\right)\frac{\delta H}{\delta u_j}\left(\nabla_i(\mathrm{r})\mathrm{w}_j\right)\frac{\delta H}{\delta w_j}$ were omitted in Eq. (16.2.2), the governing Eqs. (16.2.1)–(16.2.4) would reduce to (16.3.1), i.e.

$$
\begin{aligned}
&\frac{\partial \rho}{\partial t}+\nabla\cdot(\rho\mathbf{V})=0\\
&\frac{\partial(\rho V_x)}{\partial t}+\frac{\partial(V_x\rho V_x)}{\partial x}+\frac{\partial(V_y\rho V_x)}{\partial y}=\eta\nabla^2(\rho V_x)+\tfrac{1}{3}\eta\frac{\partial}{\partial x}\nabla\cdot\mathbf{V}+M\nabla^2u_x+\\
&(L+M-B)\frac{\partial}{\partial x}\nabla\cdot\mathbf{u}+R_1\left(\frac{\partial^2w_x}{\partial x^2}+2\frac{\partial^2w_y}{\partial x\partial y}-\frac{\partial^2w_x}{\partial y^2}\right)-R_2\left(\frac{\partial^2w_y}{\partial x^2}-2\frac{\partial^2w_x}{\partial x\partial y}-\frac{\partial^2w_y}{\partial y^2}\right)\\
&-(A-B)\frac{1}{\rho_0}\frac{\partial\delta\rho}{\partial x}\\
&\frac{\partial(\rho V_y)}{\partial t}+\frac{\partial(V_x\rho V_y)}{\partial x}+\frac{\partial(V_y\rho V_y)}{\partial y}=\eta\nabla^2(\rho V_y)+\tfrac{1}{3}\eta\frac{\partial}{\partial y}\nabla\cdot\mathbf{V}+M\nabla^2u_y+(L+M-B)\frac{\partial}{\partial y}\nabla\cdot\mathbf{u}\\
&+R_1\left(\frac{\partial^2w_y}{\partial x^2}-2\frac{\partial^2w_x}{\partial x\partial y}-\frac{\partial^2w_y}{\partial y^2}\right)+R_2\left(\frac{\partial^2w_x}{\partial x^2}+2\frac{\partial^2w_y}{\partial x\partial y}-\frac{\partial^2w_x}{\partial y^2}\right)-(A-B)\frac{1}{\rho_0}\frac{\partial\delta\rho}{\partial y}\\
&\frac{\partial u_x}{\partial t}+V_x\frac{\partial u_x}{\partial x}+V_y\frac{\partial u_x}{\partial y}=V_x+\Gamma_{\mathbf{u}}[M\nabla^2u_x+(L+M)\frac{\partial}{\partial x}\nabla\cdot\mathbf{u}+\\
&R_1\left(\frac{\partial^2w_x}{\partial x^2}+2\frac{\partial^2w_y}{\partial x\partial y}-\frac{\partial w_y}{\partial y^2}\right)-R_2\left(\frac{\partial^2w_y}{\partial x^2}-2\frac{\partial^2w_x}{\partial x\partial y}-\frac{\partial^2w_y}{\partial y^2}\right)]\\
&\frac{\partial u_y}{\partial t}+V_x\frac{\partial u_y}{\partial x}+V_y\frac{\partial u_y}{\partial y}=V_y+\Gamma_{\mathbf{u}}[M\nabla^2u_y+(L+M)\frac{\partial}{\partial y}\nabla\cdot\mathbf{u}+\\
&R_1\left(\frac{\partial^2w_y}{\partial x^2}-2\frac{\partial^2w_x}{\partial x\partial y}-\frac{\partial^2w_y}{\partial y^2}\right)+R_2\left(\frac{\partial^2w_x}{\partial x^2}+2\frac{\partial^2w_y}{\partial x\partial y}-\frac{\partial^2w_x}{\partial y^2}\right)]\\
&\qquad\frac{\partial w_x}{\partial t}+V_x\frac{\partial w_x}{\partial x}+V_y\frac{\partial w_x}{\partial y}=\Gamma_{\mathbf{w}}[K_1\nabla^2w_x+\\
&\qquad R_1\left(\frac{\partial^2u_x}{\partial x^2}-2\frac{\partial^2u_y}{\partial x\partial y}-\frac{\partial^2u_x}{\partial y^2}\right)+R_2\left(\frac{\partial^2u_y}{\partial x^2}+2\frac{\partial^2u_x}{\partial x\partial y}-\frac{\partial^2u_y}{\partial y^2}\right)]\\
&\qquad\frac{\partial w_y}{\partial t}+V_x\frac{\partial w_y}{\partial x}+V_y\frac{\partial w_y}{\partial y}=\Gamma_{\mathbf{w}}[K_1\nabla^2w_y+\\
&\qquad R_1\left(\frac{\partial^2u_y}{\partial x^2}+2\frac{\partial^2u_x}{\partial x\partial y}-\frac{\partial^2u_y}{\partial y^2}\right)-R_2\left(\frac{\partial^2u_x}{\partial x^2}-2\frac{\partial^2u_y}{\partial x\partial y}-\frac{\partial^2u_x}{\partial y^2}\right)]
\end{aligned}
\tag{16.3.1}
$$

in which $\nabla\cdot=\mathbf{i}\frac{\partial}{\partial x}+\mathbf{j}\frac{\partial}{\partial y}$, $\mathbf{V}=\mathbf{i}V_x+\mathbf{j}V_y$, $\mathbf{u}=\mathbf{i}u_x+\mathbf{j}u_y$.

16.4 Numerical Solution

The deformation, motion, dynamic behaviour and structure including structure reconstruction of solid quasicrystals are often needed to solve the equations such as (16.3.1), and the solving must be under appropriate initial and boundary conditions.

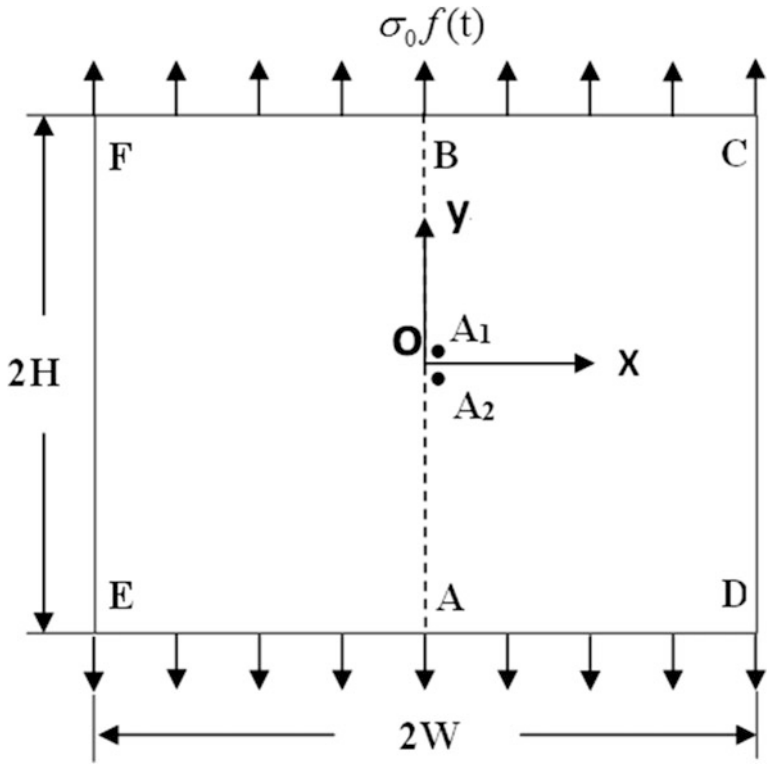

Fig. 16.1 Specimen of quasicrystal under impact loading

To solve the Eqs. (16.3.1) at physical time-space domain, the corresponding initial and boundary conditions must be given simultaneously. The more general discussion on the initial and boundary conditions of hydrodynamics of solid quasicrystals here has not been undertaken. We take a specimen shown by Fig. 16.1 and list the relevant conditions for the specimen, in which the computational points A_1 and A_2 and their coordinates are as follows

$$A_1(10^{-4}\ \text{m},\ 10^{-4}\ \text{m})\ \text{and}\ A_2(10^{-4}\ \text{m}, -10^{-4}\ \text{m})$$

We assume the specimen at initial time is in rest, so there are initial conditions

$$t = 0 : u_x = u_y = 0, w_x = w_y = 0, V_x = V_y = 0, \rho = \rho_0. \tag{16.4.1}$$

At the surface of the specimen, there are the following boundary conditions

$$\begin{aligned} &y = \pm H, |x| < W : \sigma_{yy} = \sigma_0 f(t), \sigma_{yx} = 0, H_{yy} = H_{yx} = 0, V_x = V_y = 0; \\ &x = \pm W, |y| < H : \sigma_{xx} = \sigma_{xy} = 0, H_{xx} = H_{xy} = 0, V_x = V_y = 0. \end{aligned} \tag{16.4.2}$$

in which σ_0 is a constant with the stress dimension, $f(t)$ the function of time, we here take it as Heaviside function, i.e. $f(t) = H(t)$, of course this loading is an idealized case. The boundary conditions designed belong to the simplest one for both numerical computation and further experimental measurement, in which the non-homogeneous boundary condition is only for phonon stress, and the boundary conditions for phason field and viscosity flow field are zero. As an example, we calculate a decagonal Al–Ni–Co quasicrystal, with the experimentally measured material data $\rho_0 = 4.1868 \times 10^{-3}$ g/mm^3, viscosity coefficient $\eta = 1$ cm^2/s (note that here η in fact is corresponding to η/ρ refer to Ref [1]) approximately [1] and elastic moduli $C_{11} = 2.3430$, $C_{12} = 0.5741$ (10^{12} dyn/cm^2), which are obtained by resonant ultrasound spectroscopy; we have also chosen $K_1 = 1.22$ and $K_2 = 0.24$ (10^{12} dyn/cm^2) estimated by Monte Carlo simulation, $\Gamma_u = 4.8 \times 10^{-8}$, $\Gamma_w = 4.8 \times 10^{-10}$ (cm^{3}μs/g), refer to Chap. 10, $A = B = 10^{10}$ dyn/cm^2 by an estimation. The coupling constants R_1, R_2 have not been measured so far. In computation, we take $R_1/M = 0.001$ and $R_2/M = 0.002$, where $M = (C_{11} - C_{12})/2$, $\sigma_0 = 5$ MPa, $H = 20$ mm and $W = 10$ mm.

The specimen shown in Fig. 16.1 is a simplest specimen for exploring the hydrodynamic behaviour of the quasicrystal through computational analysis. The upper and lower surfaces of the specimen are subjected to impact external stress $\sigma_{yy} = \sigma_0 H(t)$, where the loading function is taken to be the Heaviside function

$$H(t) = \begin{cases} 0, & t = 0 \\ 1, & t > 0 \end{cases}$$

Of course this is an extreme case (at $t = 0$, the loading rate is infinite).

What Eqs. (16.3.1) under initial and boundary value conditions (16.4.1) and (16.4.2) is named initial-boundary value problem (16.3.1)–(16.4.1), (16.4.2), this is a nonlinear initial-boundary value problem, because the partial differential equation set is nonlinear. We solve the initial-boundary value problem by a finite difference method. The numerical solutions with high stability are obtained.

The impact loading at the upper and lower surfaces of the specimen is the disturbance source, if the initial propagating rate of the disturbance source is denoted by v_0, which can be evaluated by $v_0 = \frac{H}{t_0}$, where t_0 the time of propagation of the disturbance source to the central transverse section, and our computational point is very close to the location. The computation for time t_0 is very easy to obtain which can directly check our computation.

In Fig. 16.2, the variation of mass density versus time is illustrated, which explicitly explores the wave propagation character of the physical process under the given boundary conditions of the specimen. Before arriving of the wave emanated from the upper surface in the computational point A_1 whose distance to upper surface is almost equal to H (completely similar to the wave emanated from lower surface arriving in the computational point A_2), the mass density maintains its initial value ρ_0, the "propagation time" is equal to $t_0 = 2.545$ μs, which is evaluated by

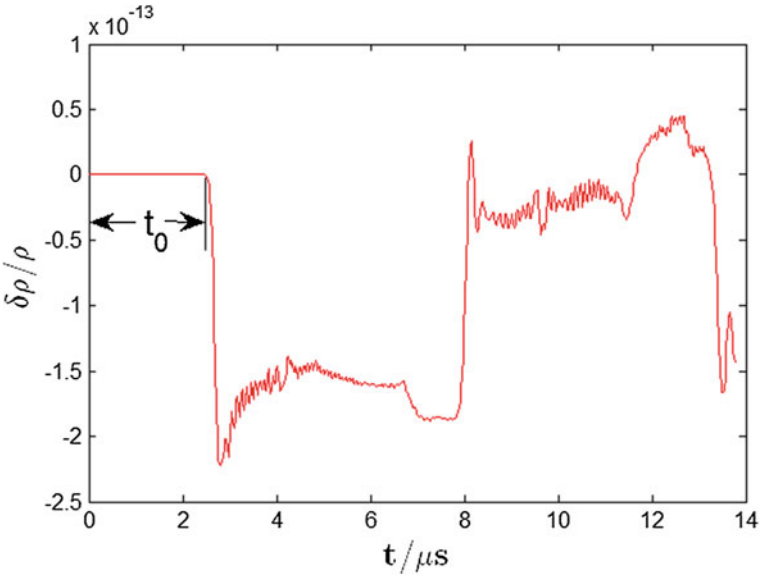

Fig. 16.2 Variation of mass density of the computational point A_1 (or A_2) of specimen versus time

$t_0 = \frac{H}{v_0}$ and $v_0 = \frac{H}{t_0} = 7.8585$ km/s and which is very close to the value of the longitudinal wave speed $c_L = \sqrt{(L+2M+A-2B)/\rho_0} = 7.4807$ km/s (The formula of the longitudinal wave, refer to Lubensky et al. [1]). This is a direct check to the computation physically, though there is a smaller difference between the values of v_0 and c_L. It is understandable, because the longitudinal wave speed formula is a linear elastic result, and the present case is nonlinear medium; the disturbance source propagating speed v_0 from upper surface to the computational point is not exactly equal to linear longitudinal wave rate, but these two values are very close to each other. This shows that the mathematical formulation of the initial-boundary value problem (16.3.1)–(16.4.1), (16.4.2) is correct physically, the solving method is effective and solution presents satisfactory precise.

The phenomenon indicates that for the complex system of wave propagation and diffusion coupling, the phonon wave propagation plays a dominating role. At the moment that the wave arrives at the central, because the dynamic load is an impacting force which produces a tensile wave, the value of mass density at central section decreases steeply to the minimum.

After the longitudinal waves emanated from upper and lower surfaces confluent each other at the central section, and the arrival of succeeded transverse wave and

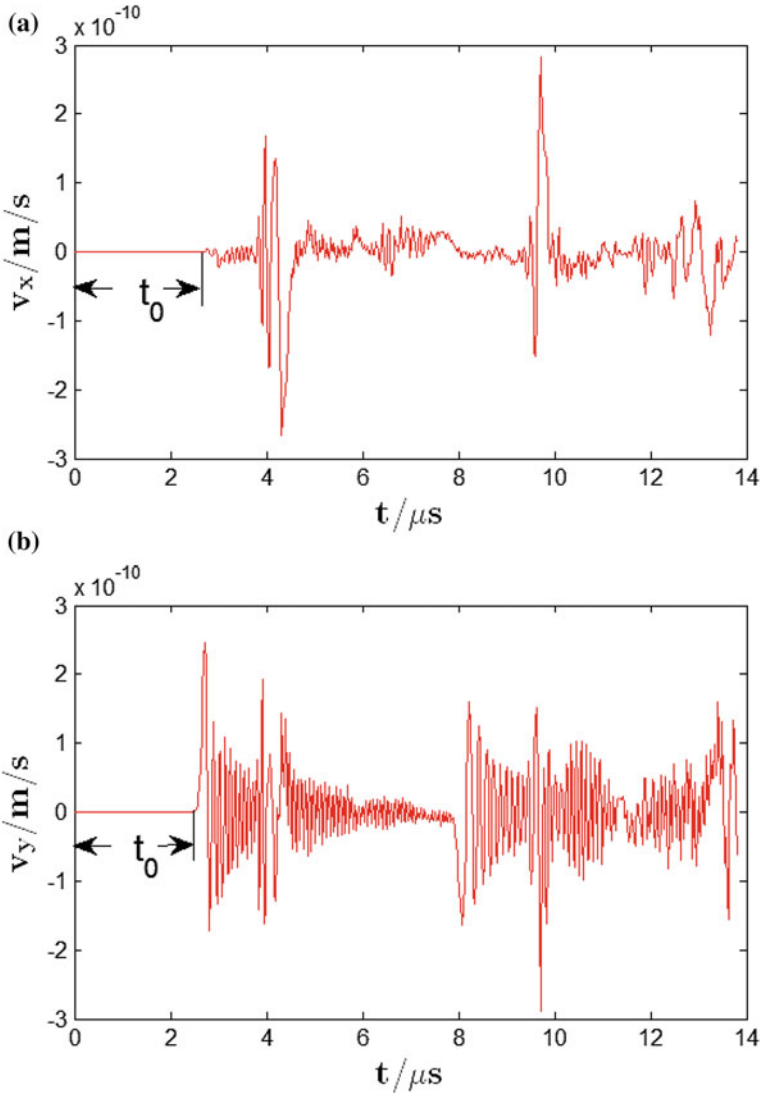

Fig. 16.3 Velocity fields at the computational point A_1 of specimen versus time: **a** V_x and **b** V_y

the reflected waves by lateral surfaces of the specimen, the material at the location is compressible, the value of $\delta\rho/\rho_0$ will be increasing, and then grows into a maximum value 2.527×10^{-14} at times 8.149 μs indicates that ρ beyond the initial value ρ_0 of mass density.

Fig. 16.3 gives the time variation of velocities (the velocities of mass point to the coordinates) at point A_1 in x- and y-directions, respectively, in which the wave behaviour is still exhibited before the "propagation time" t_0, and the values of

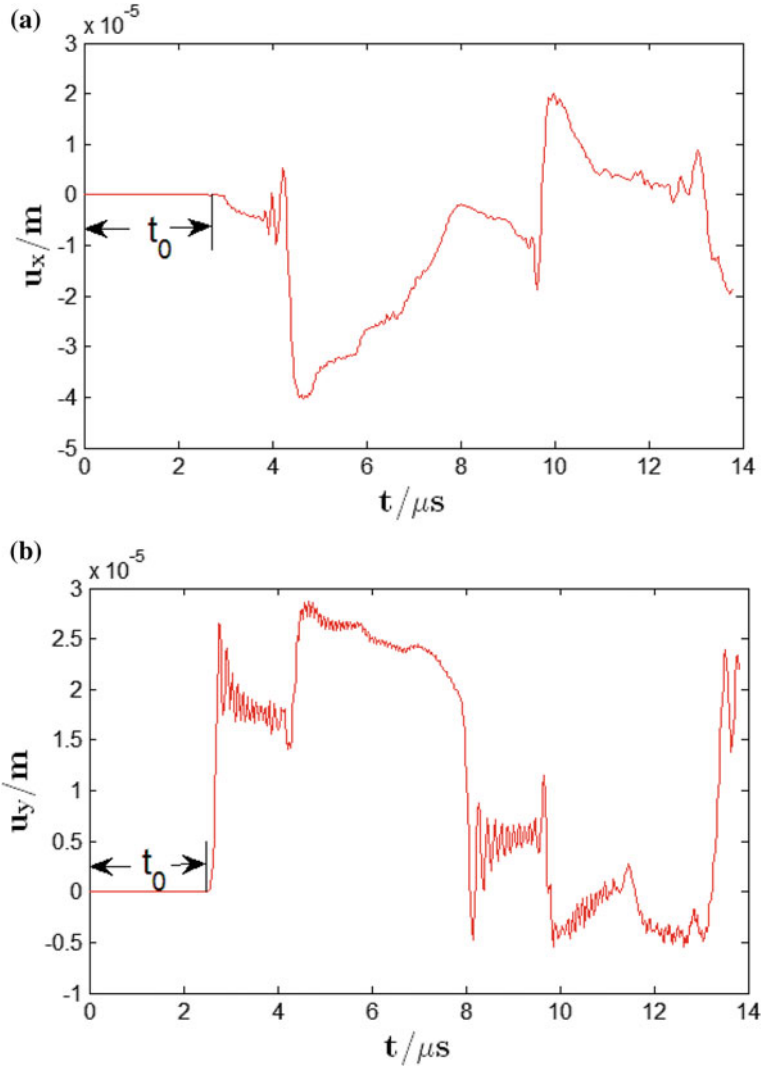

Fig. 16.4 Phonon displacement fields at the computational point A_1 versus time: **a** u_x and **b** u_y

velocities are zero. The order of their magnitude is 10^{-10} m/s for the material, this quantitatively explores the hydrodynamic character of the motion pointed out by Lubensky et al. Though one knows the motion should be very slow, but beforehand we did not know the realistic order of magnitude of the rate, and naturally there was no possibility to know the exact values of the rate, in that time the analysis was only qualitative.

Figure 16.4 illustrated the time variation of phonon displacements at point A_1 in directions x and y, respectively. The results show the wave propagation behaviour

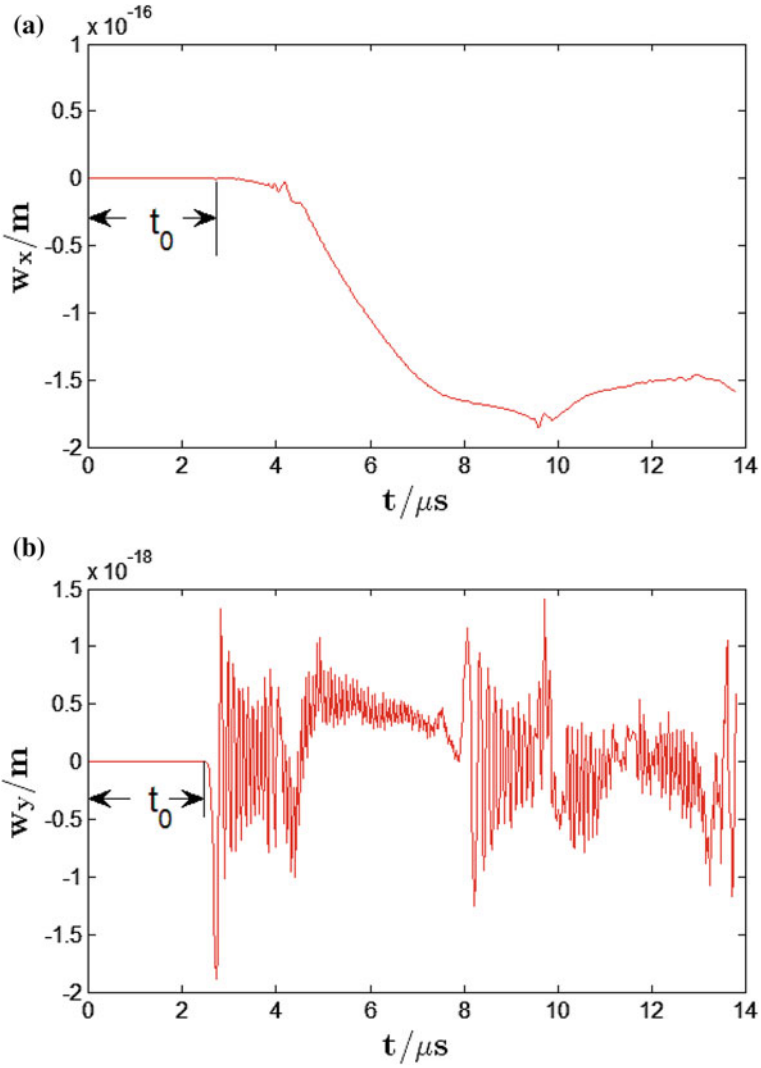

Fig. 16.5 Phason displacement fields at the computational point A_1 of specimen versus time: **a** w_x and **b** w_y

of the field variables, which is evident. Of course, the performance of u_x and u_y is different from each other, which is resulted from the boundary conditions and specimen configuration.

The results on phason displacements w_x and w_y are plotted by Fig. 16.5, and their order of magnitude is very smaller than that of phonons; this is understandable, because the external disturbance source comes from the phonon stress only, and the corresponding phason boundary conditions are homogeneous (the zero

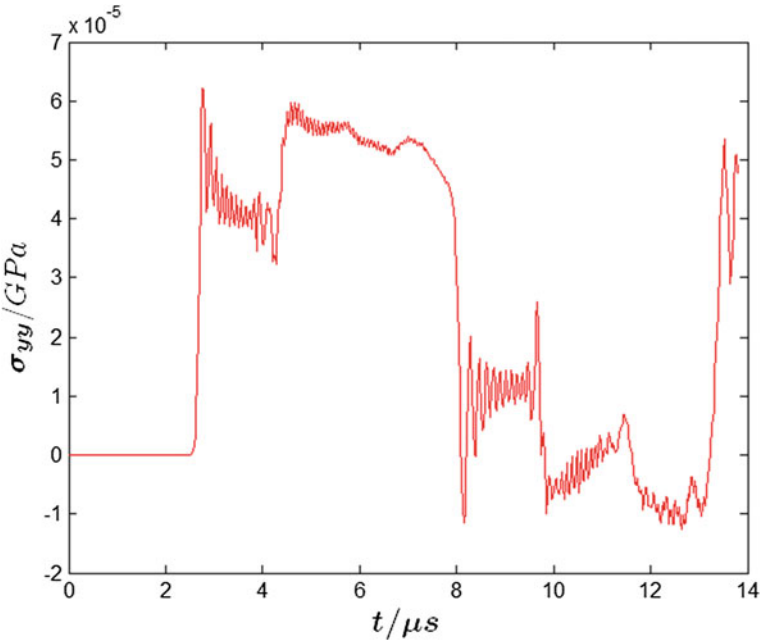

Fig. 16.6 Elastic normal stress at the computational point A_1 (or A_2) of specimen versus time

boundary conditions). If we take the phonon stress boundary conditions are homogeneous and phason stress boundary conditions are nonhomogeneous, then the order of magnitude of solutions of phasons is much greater than that of the present results. In addition, the phason displacement field represents diffusion rather than wave propagation in physical nature, but the profile of the figures of w_x and w_y does not exhibit pure diffusion feature which exhibited for solutions of simple diffusion equation due to the strong coupling of wave equations and the controlling of the mixed boundary conditions.

Figs. 16.6, 16.7 and 16.8 show the time variation of phonon, phason and viscosity normal stresses at the computational point, and it is evident that phonon stress is greater by two orders of magnitude than phason one; the phonon and phason stresses are much greater than viscosity one. The outline of phason stress describes certain diffusive behaviour so is evident different from that of phonon one, while the outline of phonon and viscosity ones exhibit typical wave propagation character and present strong oscillation.

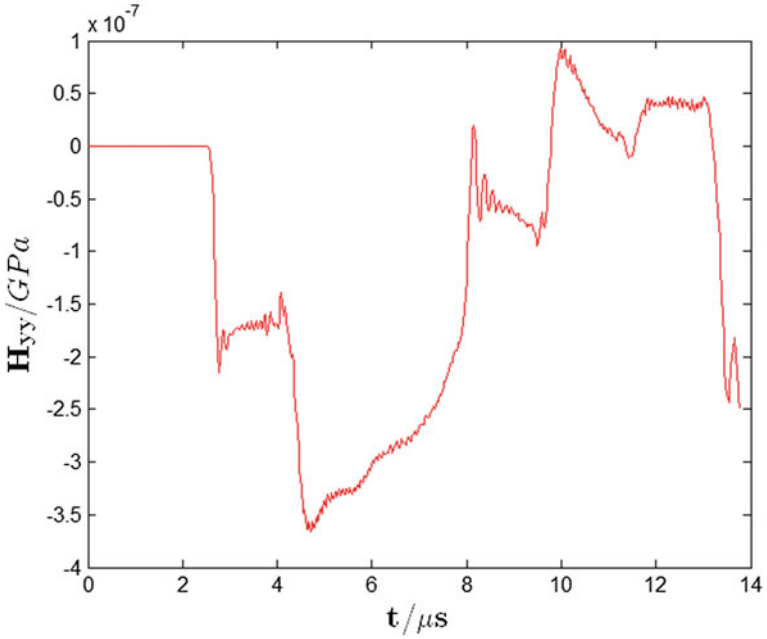

Fig. 16.7 Phason normal stress at the computational point A_1 (or A_2) of specimen versus time

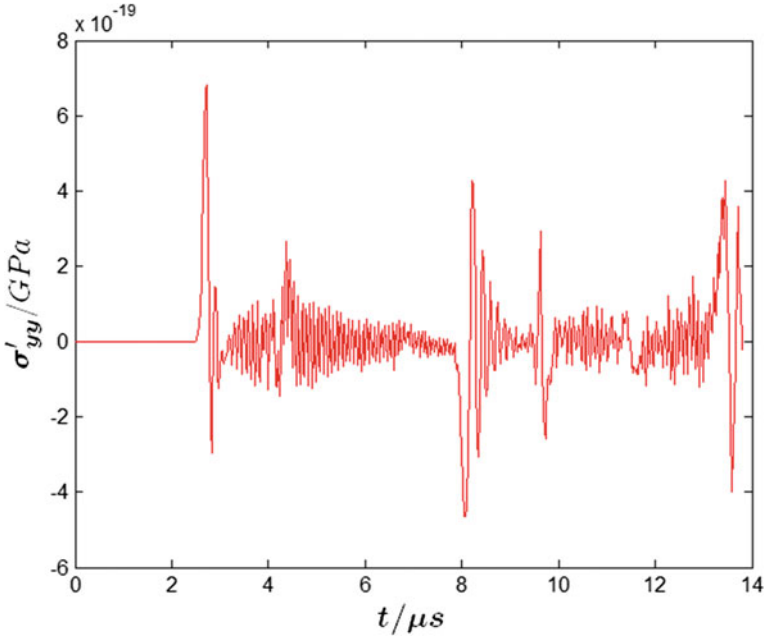

Fig. 16.8 Viscosity normal stress at the computational point A_1 (or A_2) of specimen versus time

16.5 Conclusion and Discussion

This chapter gives an introduction on hydrodynamics of solid quasicrystals of Lubensky et al., which was the development of one of the crystals given by Martin et al. [5] and Fleming and Cohen [6]. The numerical computation verifies the solvability of equations of Lubensky et al. [1]. The numerical computation verifies the correctness of the formulation developed here too. However it is carried out through only a simple specimen, describes only one of dynamic processes of solid quasicrystals, results are limited for a local computational point and a short time duration, conveys limited information. Nevertheless, the numerical solving and computer implementation for such a complex substantive system are significant, the obtained stable and physically meaningful results are also significant.

The computational results reveal the phonon and phonon-phason coupling dominate the deformation and motion of the matter, which is undoubted for most quasicrystals. The computational results show the variation of mass density is small, and the viscosity stresses are small for the present computed specimen, these do not mean the common response for all dynamic processes of the matter. Even if the weakness of effects of compressibility and viscosity at the computed specimen, they may present significance in other dynamic processes. We know, the similar phenomena appear often in physics, for example, the gravitation due to curved space-time is very weak in general, but it is important for some special cases, for example, the gravitational waves observed recently.[1]

So far the solutions in time-space domain of hydrodynamics of Lubensky et al. are very few, and developing the computation is significant. This work can be referenced to that carried out for solid quasicrystals [10] and soft-matter quasicrystals, e.g. [11], which show the importance of hydrodynamics applied in soft-matter quasicrystals. In principle, the hydrodynamics of Lubensky et al will be valid for soft-matter quasicrystals apart from some modification and supplementation, the discussion about this can be referred to Appendix D.

The work of hydrodynamics study may help us enhance the understanding to the deformation and motion of solid quasicrysals. Of course, the analysis of hydrodynamics here is a preliminary attempt; it is needed further development of both aspects in the theory and computation.

References

1. Lubensky T C, Ramaswamy S and Toner J, 1985, Hydrodynamics of icosahedral quasicrystals, *Phys. Rev*. B, 32(11), pp. 7444-7452.
2. Lubensky T C, 1988, Symmetry, elasticity and hydrodynamics of quasistructures, in Ed. V M Jaric, Introduction to Quasicrystals, Boston, Academic Press, 1988, pp. 199-280.

[1]Abbott B P et al, 2016, Phys Rev Lett, 116, 061102.

3. Rochal S B and Norman V L, 2002, Minimal model of the phonon-phason dynamics of quasicrystals, *Phys Rev* B, 66, pp. 144204.
4. Fan TY, Wang X F, Li W and Zhu A Y, 2009, Elasto-hydrodynamics of quasicrystals, Phil. Mag, 89(6), pp. 501-512.
5. Martin P C, Parodi O and Pershan P S, 1972, United hydrodynamic theory for crystals, liquid crystals and normal fluids, *Phys Rev* A, 6(6), pp. 2401-2420.
6. Fleming P D and Cohen C, 1976, Hydrodynamics of solids, *Phys Rev B*, 13(2), pp. 500-516.
7. Landau L D and Lifshitz E M, 1988, Theory of Elasticity, Oxford, Pergamon Press.
8. Khannanov S K, 2002, Dynamics of elastic and phason field in quasicrystals, Phys Met Metallogr. (USSR), 93, pp. 397-403.
9. Coddens G, 2006, On the problem of the relation between phason elasticity and phason dynamics in quasicrystals, *Eur. Phys. J.* B, 54(1), pp. 37-65.
10. Cheng H, Fan T Y, Sun J J and Wei H, Time-space solutions for hydrodynamics of pentagonal/decagonal quasicrystals, Appl Math Mech, 37(10), in press. .
11. Chen H, Fan T Y and Wei H, 2016, Complete solution of possible soft-matter quasicrystals with 5- and 10-fold symmetries, submitted.

Chapter 17
Remarkable Conclusion

The discussion mainly on elasticity and a few of on plasticity and hydrodynamics of quasicrystals is ended up to Chap. 16.

Elasticity is one of the important branches of the natural science since the time of Hooke, Euler, Bernoulli, Navier, Cauchy, and St Venant, among others. So that it is emphasized by great theoretical physicists e.g. Sommerfeld [1] and Landau and Lifshitz [2] and presented in their famous theoretical physics courses. However, those they discussed belongs to the classical elasticity or crystal elasticity in scope of continuum mechanics, which presents important meaning for engineering as well as science including modern physics, e.g. one application of the theory combining the Planck's quantization by Debye [3] and Born [4] to specific heat of crystals at low temperature (refer to [1] for the detail) leads to phonon concept and the appearance of lattice dynamics, which is an important basis of modern solid state physics.

Elasticity of quasicrystals is a branch of condensed matter physics rather than classical mechanics. Landau and Anderson did a great contribution to the condensed matter physics, the symmetry breaking principle sets up the paradigm of the branch of physics. The basis of the elasticity is phonon, phason and phonon-phason coupling, which are originated from Landau elementary excitation principle, the concept is a quantum mechanics description on collective excitation of massive atoms, this shows the elasticity of quasicrystals is connected essentially with quantization, the idea is beyond classical mechanics.

Apart from quantization, the symmetry and phase are also the basis of elasticity of quasicrystals. The quantization, symmetry and phase belong to the main theme of 20th century physics. Anderson [5] revealed the nature of phonon from the phase of Landau's order parameter in three-dimensional reciprocal space. The pioneering researchers Bak, Lubensky et al. [6–9] of study of elasticity of quasicrystals extended the Anderson's argument in six-dimensional reciprocal space and explained the nature of phason. If limited only to the intuitive idea of classical mechanics, then the phason cannot be understood, although the phason concept was drawn from incommensurate phase physics at beginning. These discussions may

T.-Y. Fan, *Mathematical Theory of Elasticity of Quasicrystals and Its Applications*,
Springer Series in Materials Science 246, DOI 10.1007/978-981-10-1984-5_17

help us to deep our understanding elasticity of quasicrystals which were introduced in Chaps. 1 and 4, respectively.

Based on the concepts and principles, fundamentals of the theory of elasticity of solid quasicrystals have been developed, and quite fruitful achievements are obtained, which are partly introduced in the first 15 chapters.

Although the quasicrystal elasticity is different from classical elasticity in nature, there are some connections in methodology between these two disciplines, the development of theory of quasicrystal elasticity is helped from the crystal elasticity [10–12], it also gets the help from the crystal plasticity [13–16], crystal dislocation [17, 18] and classical crack theories [19, 20]. Besides, there are much inherent connections between quasicrystal elasticity and group theory [21, 22], partial differential equations [23–25], Fourier analysis [18, 23, 26], complex analysis [27], integral equations [19, 20, 26] and computational mathematics [28], without the help of these powerful mathematics branches, the development of elasticity of quasicrystals is impossible. These problems are also introduced in the text of first 15 chapters and Major Appendix, some among them are quite detailed, and explored physics-mathematics compatibility and consistence and shown the power, excellence and beauty of analytic mathematics.

Hydrodynamics, according to the summarization by Dzyaloshinskii and Volovick [29], covers a quite wide range of disciplines from conventional fluid, superfluid to spin waves in magnets, spin glasses, liquid crystals, and so on. The hydrodynamics of solid quasicrystals was created by Lubensky et al. [8], constitutes another important field of solid quasicrystals; the theory is much more complex than that of elasticity and beyond the scope of the first 15 chapters and has not been discussed in detail. The observation of soft-matter quasicrystals is a dramatic event [30–34] in Twenty-first-century chemistry and aroused a great deal of attention of researchers. The study of the soft-matter quasicrystals must deal with hydrodynamics [35, 36] but is beyond the scope of the present book, we give only a very simple introduction in the major appendix of the book. Due to the enlarging of scope of quasicrystals, the concepts concerning the study are extended recently too, e.g. the first and second phason elementary excitations are suggested [35]. There is no possibility to discuss the relevant topics in text as well as in appendix, but we particularly list some quantities in Notations to readers for their referring.

References

1. Sommerfeld A, 1952, Vorlesungen ueber theoretische Physik, Band II: Mechanik der deformirbaren Medien, Diederich Verlag, Wiesbaden.
2. Landau L D and Lifshitz E M, 1986, Theoretical Physics, Vol. VII: Theory of Elasticity, Pergamon Press, Oxford.
3. Debye P, 1912. Eigentuemlichkeit der spezifischen Waermen bei tiefen Temperaturen, Arch de Genéve, **33**(7), 256-258.

4. Born M and von Kármán Th, Zur Theorie der spezifischen Waermen, Physikalische Zeitschrift, **14**(1), 15-19, 1913; Born M and Huang K, 1954, Dynamic Theory of Crystal Lattices, Clarendon Press, Oxford.
5. Anderson P W, 1984, Basic Notation of Condensed Matter Physics, Menlo Park: Benjamin-Cummings.
6. Bak P, 1985, Symmetry, stability and elastic properties of icosahedral incommensurate crystals, *Phys. Rev.* B, **32**(9), 5764-5772.
7. Horn P M, Malzfeldt W, DiVincenzo D P, Toner J et al, 1986, Systematics of Disorder in Quasiperiodic Material, *Phys. Rev. Lett*., **57**(12), 1444-1447.
8. Lubensky T C, Ramaswamy S and Toner J, 1985, Hydrodynamics of icosahedral quasicrystals, *Phys. Rev*. B, **32**(11), 7444-7452.
9. Lubensky T C, 1988, Introduction to Quasicrystals, ed by Jaric M V, Boston: Academic Press.
10. De P, Pelcovits R A, 1987, Linear elasticity theory of pentagonal quasicrystals, Phys Rev B, 35(16), 8609-8620.
11. Ding D H, Yang W G, Hu C Z, Wang R H, 1993, Generalized elasticity theory of quasicrystals, Phys Rev B, 48(10), 7003-7010.
12. Li X F, Fan T Y, 1998, New method for solving elasticity problems of some planar quasicrystals and solution, Chin Phys Lett, 15(4), 278-280.
13. Feurbacher M and Urban K, 2003, Plastic behaviour of quasicrystalline materials, Quasicrystals (ed. Trebin H), Wiley Press, Berlin.
14. Messerschmidt U, 2010, Dislocation Dynamics during Plastic Deformation, Springer-Verlag, Heidelberg.
15. Fan T Y and Fan L, 2008, Plastic deformation of quasicrystals, Phil Mag, 88(4), 323-335.
16. Fan T Y and Fan L, 2011, Relation between generalized Eshelby integral and generalized BCS and generalized DB models for some one- and two-dimensional quasicrystals, Chin Phys B,20(4), 036102.
17. Yang S H, Ding D H, 1998, Crystal Dislocation Theory, Vol.2, Beijing, Science Press (in Chinese).
18. Li X F, Duan X Y, Fan T Y, Sun Y F, 1999, Elastic field for a straight dislocation in a decagonal quasicrystal, J Phys Condens Matter, 11(3), 703-711.
19. Fan T Y, Trebin H-R, Messerschmidt U, Mai Y W, 2004, Plastic flow coupled with a Griffith crack in some one- and two-dimensional quasicrystals, J Phys Condens Matter, 16 (27),5229-5240.
20. Li X F, Fan T Y, Sun Y F, 1999, A decagonal quasicrystals with a Griffith crack, Phil Mag A, 79(8), 1943-1952.
21. Janssen T, 1992, The symmetry operations for n-dimensional periodic and quasi-periodic structures, Zeitschrift fuer Kristallographie, 198(1-2), 17-32.
22. Hu C Z, Wang R H, Ding D H, 2000, Symmetry groups, physical property tensors, elasticity and dislocations in quasicrystals, *Rep. Prog. Phys*., **63**(1), 1-39.
23. Ding D H, Wang R H, Yang W G, Hu C Z, 1995, Elasticity theory of straight dislocation in quasicrystals, Phil Mag Lett, 72(5), 353-359.
24. Fan T Y, Guo L H, 2005, Final governing equation of plane elasticity of icosahedral quasicrystals, Phys Lett A, 341(5), 235-239.
25. Guo L H, Fan T Y, 2007, Solvability on boundary-value problems of elasticity of three-dimensional quasicrystals, Appl Math Mech, 28(8), 1061-1070.
26. Zhou W M and Fan T Y, 2000, Axisymmetric elasticity problem of cubic quasicrystals, Chin Phys, 9(4), 294-303.
27. Fan T Y, Tang Z Y, Li L H, Li W, 2010, The strict theory of complex variable function method of sextuple harmonic equation and applications, J Math Phys, 51(5), 053519.
28. Zhu A Y, Fan T Y, 2008, Dynamic crack propagation in a decagonal Al-Ni-Co quasicrystal, J Phys Condens Matter, 20(29), 295217.
29. Dzyaloshinskii I E, Volovick G E, . Poisson brackets in condensed matter physics. Ann Phys (NY), 1980, 125(1): 67-97.
30. Zeng X ,Ungar G, Liu Y, Percec V, Dulcey A E and Hobbs J K, 2004, Supramolecular dendritic liquid quasicrystals, Nature, **428**, 157-159.

31. Takano K, 2005, A mesoscopic Archimedian tiling having a complexity in polymeric stars, J Polym Sci Pol Phys, 43, 2427-2432.
32. Hayashida K, Dotera T, Takano A, Matsushita Y, 2007, Polymeric quasicrystal : mesoscopic quasicrystalline tiling in ABC starpolymmers, Phys Rev Lett, **98**, 195502 .
33. Talapin V D, Shevechenko E V, Bodnarchuk M I, Ye X C, Chen J and Murray C B, 2009, Quasicrystalline order in self-assembled binary nanoparticle superlattices, Nature, **461**, 964-967.
34. Fischer S, Exner A, Zielske K, Perlich J, Deloudi S, Steuer W, Linder P and Foestor S, 2011, Colloidal quasicrystals with 12-fold and 18-fold diffraction symmetry, Proc Nat Ac Sci, **108**, 1810-1814.
35. Fan T Y, 2016, Equation system of generalized hydrodynamics of soft-matter quasicrystals, Appl Math Mech, 37(4), 331-344.
36. Cheng H, Fan T Y, Sun J J, Wei H, 2015, Possible soft-matter quasicrystals of 5- and 10-fold symmetries and hydrodynamics, Computational Materials Science, 205(7), 47-54.

Major Appendix: On Some Mathematical Additional Materials

Mathematical solutions for individual boundary value problems are given in the previous chapters. Due to the complexity of boundary conditions for realistic problems of physics, we must develop some special techniques, in which the complex function method collaborating conformal mapping and Fourier analysis collaborating dual integral equations are powerful procedures. The use of the procedures has been exhibited in the previous chapters. Though some appendixes in relevant chapters were given in the text for discussing some special problems, we list some necessary additional materials on complex analysis and dual integral equations in separate two parts in Appendices A and B (including Appendix of Chap. 11). It is interesting, in particular, between these two parts, there are some close inherent connections. Probably these materials are not necessary for readers majoring applied mathematics, but which may be helpful for young scholars and postgraduate students who are not majoring applied mathematics.

The discussion of hydrodynamics concerns Poisson bracket method in condensed matter physics, and the Appendix C gives some relevant materials and detailed derivation of equations of motion of hydrodynamics of solid quasicrystals, which are beneficial to learn hydrodynamics of soft-matter quasicrystals as well.

Appendix A: Additional Calculations Related to Complex Analysis

A.1 Additional Derivation of Solution (8.2.19)

In Chap. 8, we emphasized the importance of complex analysis (see [1–3]) and pointed out that the Muskhelishvili's [1] method limited the conformal mapping to be rational functions. However our practice breaks the limitation, e.g. [4, 5]; the calculation is handled as below.

Formula (8.2.19) is obtained from the integral of (8.2.6) in which the conformal mapping $\omega(\zeta)$ is given by (8.2.17). The difficulty of the calculation lies in the

T.-Y. Fan, *Mathematical Theory of Elasticity of Quasicrystals and Its Applications*,
Springer Series in Materials Science 246, DOI 10.1007/978-981-10-1984-5

integral path which is a part of circle rather than whole circle. Substituting (8.2.17) into the right-hand side of (8.2.6) yields

$$F(\zeta) = -\frac{p}{2\pi i}\int_{-1}^{1}\frac{\omega(\sigma)}{(\sigma-\zeta)^2}\mathrm{d}\sigma = -\frac{p}{2\pi i}\int_{-1}^{1}\frac{\omega'(\sigma)}{\sigma-\zeta}\mathrm{d}\sigma$$

where

$$\omega'(\sigma) = -\frac{4H\alpha(1-\beta)}{\pi}\frac{1-\sigma}{1+\sigma}\frac{(1+\sigma)^2}{\left[(1+\sigma)^2+\alpha(1-\sigma^2)^2\right]\left[(1+\sigma)^2+\beta\alpha(1-\sigma)^2\right]}$$

Substituting $\mathrm{e}^{\mathrm{i}\varphi}$ by $(1+ix)/(1-ix)$ yields

$$\frac{1-\sigma}{1+\sigma} = -2x, \quad \mathrm{d}\sigma = \frac{2i}{(1-ix)^2}\mathrm{d}x, \quad (1+\sigma)^2 = \frac{4}{(1-ix)^2},$$
$$\frac{1}{\sigma-\zeta} = \frac{1-ix}{1-\zeta+ix(1+\zeta)} = \frac{(1-ix)[1-\zeta-ix(1+\zeta)]}{(1-\zeta)^2+x^2(1+\zeta)^2} - \frac{1-\zeta-x^2(1+\zeta)-2ix}{(1-\zeta)^2+x^2(1+\zeta)^2}$$

So that

$$\begin{aligned}
F(\zeta) &= -\frac{pH\alpha(1-\beta)}{\pi^2}\int_{-1}^{1}\frac{ix[1-\zeta-x^2(1+\zeta)-2ix]}{(1-\alpha x^2)(1-\beta\alpha x^2)\left[(1-\zeta)^2+x^2(1+\zeta)^2\right]}\mathrm{d}x \\
&= -\frac{4pH\alpha(1-\beta)}{\pi^2}\int_{0}^{1}\frac{x^2}{(1-\alpha x^2)(1-\beta\alpha x^2)\left[(1-\zeta)^2+x^2(1+\zeta)^2\right]}\mathrm{d}x \\
&= \frac{2pH}{\pi^2}\frac{\alpha(1-\beta)(1-\zeta^2)}{\left[\alpha(1-\zeta)^2+(1+\zeta)^2\right]\left[\beta\alpha(1-\zeta)^2+(1+\zeta)^2\right]} \\
&\quad\times\left[\arctan\left(\frac{1+\zeta}{1-\zeta}\right)-\arctan\left(\frac{1+\zeta}{-1-\zeta}\right)\right] - \frac{4pH}{\pi^2}\frac{\sqrt{\alpha}\arctan h\sqrt{\alpha}}{\alpha(1-\zeta)^2+(1+\zeta)^2} \\
&\quad -\frac{\sqrt{\beta\alpha}\arctan h\sqrt{\alpha}}{\beta\alpha(1-\zeta)^2+(1+\zeta)^2}]
\end{aligned} \tag{A.1.1}$$

In the last step, the evaluation is used the ***Mathematica3.0*** [6].
By considering

$$A = \ln\frac{1+\sqrt{\alpha}}{1-\sqrt{\alpha}} = 2\arctan h\sqrt{\alpha},$$
$$M = \ln\frac{1+\sqrt{\gamma\alpha}}{1-\sqrt{\gamma\alpha}} = 2\arctan h\sqrt{\gamma\alpha},$$
$$\arctan\left(\frac{1+\zeta}{-1+\zeta}\right) = -2\arctan\left(\frac{1+\zeta}{1-\zeta}\right) = \frac{i}{2}\ln\left(\frac{i-\zeta}{1-i\zeta}\right)$$

then (A.1.1) is just the formula (8.2.19).

In the calculation, if let $L \to 0$, then the integral (8.2.7) can be obtained.

A.2 Additional Derivation of Solution (11.3.53)

In example 3 of Section 11.3, the calculation is quite lengthy, and here, we provide some details on the evaluation. As an example, we can show the derivation on function $\Phi_4(\zeta)$, which is

$$\Phi_4(\zeta) = d_1(X+iY)\ln\zeta + B\omega(\zeta) + \Phi_4^*(\zeta)$$

in which the first two terms are known (see the text), and the single-valued analytic function $\Phi_4^*(\zeta)$ satisfies the following boundary condition

$$\Phi_4^*(\sigma) + \overline{\Phi_3^*(\sigma)} + \frac{\omega(\sigma)}{\overline{\omega'(\sigma)}}\cdot\overline{\Phi_4^{*\prime}(\sigma)} = f_0$$

where

$$f_0 = \frac{i}{32c_1}\int (T_x+iT_y)\mathrm{d}s - (d_1-d_2)(X+iY)\ln\sigma - \frac{\omega(\sigma)}{\overline{\omega'(\sigma)}}\cdot d_1(X-iY)\cdot\sigma - 2B\omega(\sigma) - (B'-iC')\overline{\omega(\sigma)} \tag{A.1.2}$$

and (referring to Fig. 11.4 of Chap. 11)

$T_x = -p\cos(n,x), T_y = -p\cos(n,y)$ at $\overset{\frown}{z_1Mz_2}$

$$(T_x+iT_y)\mathrm{d}s = \begin{cases} ip\mathrm{d}z & \overset{\frown}{z_1Mz_2} \\ 0 & \overset{\frown}{z_2Nz_1} \end{cases} \tag{A.1.3}$$

$$X+iY = \int (T_x+iT_y)\mathrm{d}s = ip(z_1-z_2)$$

Multiplying both sides of the above boundary equation by $\frac{1}{2\pi i}\frac{\mathrm{d}\sigma}{\sigma-\zeta}$ and integrating along the unit circle, we have

$$\frac{1}{2\pi i}\int_{\gamma}\frac{\Phi_4^*(\sigma)}{\sigma-\zeta}\mathrm{d}\sigma+\frac{1}{2\pi i}\int_{\gamma}\frac{\omega(\sigma)}{\overline{\omega'(\sigma)}}\frac{\overline{\Phi_4^{*\prime}(\sigma)}}{\sigma-\zeta}\mathrm{d}\sigma+\frac{1}{2\pi i}\int_{\gamma}\frac{\overline{\Phi_3^*(\sigma)}}{\sigma-\zeta}\mathrm{d}\sigma=\frac{1}{2\pi i}\int_{\gamma}\frac{f_0}{\sigma-\zeta}\mathrm{d}\sigma\ (\mathrm{a})$$

in which according to the Cauchy's integral formula (referring to formula (11.7.5) in Appendix of Chap. 11), there is

$$\frac{1}{2\pi i}\int_{\gamma}\frac{\Phi_4^*(\sigma)}{\sigma-\zeta}\mathrm{d}\sigma=\Phi_4^*(\zeta)$$

and in terms of analytic extension principle and the Cauchy theorem (referring to Appendix of Chap. 11)

$$\frac{1}{2\pi i}\int_{\gamma}\frac{\omega(\sigma)}{\overline{\omega'(\sigma)}}\frac{\overline{\Phi_4^{*\prime}(\sigma)}}{\sigma-\zeta}=0$$

and according to formula (11.7.9)

$$\frac{1}{2\pi i}\int_{\gamma}\frac{\overline{\Phi_3^*(\sigma)}}{\sigma-\zeta}\mathrm{d}\sigma=\mathrm{const}$$

So that (a) reduces to

$$\Phi_4^*(\zeta)=\frac{1}{2\pi i}\int_{\gamma}\frac{f_0}{\sigma-\zeta}\mathrm{d}\sigma+\mathrm{const}$$

And substituting (A.1.1) into the right-hand side yields

$$\frac{1}{2\pi i}\int_{\gamma}\frac{f_0}{\sigma-\zeta}\mathrm{d}\sigma=\frac{pR_0}{2\pi ic_1}\int_{\sigma_1}^{\sigma_2}\left(\sigma+\frac{m}{\sigma}\right))\frac{\mathrm{d}\sigma}{\sigma-\zeta}+\frac{pz_2}{2\pi i}\int_{\sigma_1}^{\sigma_2}\frac{\mathrm{d}\sigma}{\sigma-\zeta}+\frac{p(z_1-z_2)}{2\pi i}\frac{1}{2\pi i}\int_{\gamma}\frac{\ln\sigma}{\sigma-\zeta}\mathrm{d}\sigma$$

$$-\frac{p(\overline{z_1}-\overline{z_2})}{2\pi i}\frac{1}{2\pi i}\int_{\gamma}\frac{\sigma^2+m}{1-m\sigma^2}\frac{\mathrm{d}\sigma}{\sigma-\zeta}$$

in which

$$\int_{\sigma_1}^{\sigma_2}\left(\sigma+\frac{m}{\sigma}\right)\frac{\mathrm{d}\sigma}{\sigma-\zeta}=\sigma_2-\sigma_1-\frac{m}{\zeta}\ln\frac{\sigma_2}{\sigma_1}+\left(\zeta+\frac{m}{\zeta}\right)\ln\frac{\sigma_2-\zeta}{\sigma_1-\zeta}$$

$$\int_{\sigma_1}^{\sigma_2}\frac{\mathrm{d}\sigma}{\sigma-\zeta}=\ln\frac{\sigma_1-\zeta}{\sigma_2-\zeta}$$

In accordance with the Cauchy's theorem (referring to formula (11.7.4)), we have

$$\frac{1}{2\pi i}\int_{\gamma}\frac{\sigma^2+m}{1-m\sigma^2}\frac{d\sigma}{\sigma-\zeta}=0$$

because the integrand is single-valued analytic function in the region outside the unit circle γ.

The remaining term is

$$I(\zeta)=\frac{1}{2\pi i}\int_{\gamma}\frac{\ln\sigma}{\sigma-\zeta}\mathrm{d}\sigma$$

For calculating it, we consider

$$\begin{aligned}\frac{\mathrm{d}I}{\mathrm{d}\zeta}&=\frac{1}{2\pi i}\int_{\gamma}\frac{\ln\sigma}{(\sigma-\zeta)^2}\mathrm{d}\sigma=-\frac{1}{2\pi i}\int_{\gamma}\ln\sigma\mathrm{d}\frac{1}{\sigma-\zeta}\\&=-\frac{1}{2\pi i}\left[\frac{\ln\sigma}{\sigma-\zeta}\right]_{\sigma=\exp(i\varphi_1)}^{\sigma=\exp i(\varphi_1+2\pi)}+\frac{1}{2\pi i}\int_{\gamma}\frac{\mathrm{d}\sigma}{\sigma(\sigma-\zeta)}\\&=-\frac{1}{2\pi i}\frac{1}{\sigma_1-\zeta}\ln\frac{\exp i(\varphi_1+2\pi)}{\exp(i\varphi_1)}-\frac{1}{\zeta}=-\frac{1}{\sigma_1-\zeta}-\frac{1}{\zeta}\end{aligned}$$

So that

$$I(\zeta)=\ln(\sigma_1-\zeta)-\ln\zeta+\mathrm{const}$$

Hence function $\Phi_4^*(\zeta)$ is determined so the function $\Phi_4(\zeta)$in which the constant term is omitted:

$$\begin{aligned}\Phi_4(\zeta)=&\frac{1}{32c_1}\cdot\frac{p}{2\pi i}\cdot\left[-\frac{mR_0}{\zeta}\ln\frac{\sigma_2}{\sigma_1}+z\ln\frac{\sigma_2-\zeta}{\sigma_1-\zeta}+z_1\ln(\sigma_1-\zeta)-z_2\ln(\sigma_2-\zeta)\right]\\&+ip(d_1-d_2)(z_1-z_2)\ln\zeta\end{aligned}$$

which is just the first formula of (11.3.53), where d_1 and d_2 were given by (11.3.34) in the text. The others can be similarly derived. In the derivation, the classical work of Muskhelishvili [1] is referred.

A.3 Detail of Complex Analysis of Solution (14.4.7) of Generalized Cohesive Force Model for Plane Plasticity of Two-Dimensional Point Groups 5m, 10mm and $10, \overline{10}$ Quasicrystals

The elasticity solution (11.3.53) based on complex analysis can be used to solve the present problem.

The generalized Dugdale-Barenblatt model or generalized cohesive model for decagonal quasicrystals makes the plastic problem to be linearized, so the final governing equation is reduced to solve the equation

$$\nabla^2\nabla^2\nabla^2\nabla^2 G = 0 \tag{A.1.4}$$

under boundary conditions

$$\begin{cases} \sigma_{yy} = p, \sigma_{xx} = \sigma_{xy} = 0, H_{xx} = H_{yy} = H_{xy} = H_{yx} = 0 & \sqrt{x^2+y^2} \to \infty \\ \sigma_{yy} = \sigma_{xy} = 0, H_{yy} = H_{yx} = 0 & y = 0, |x| < a \\ \sigma_{yy} = \sigma_c, \sigma_{xy} = 0, H_{yy} = H_{yx} = 0 & y = 0, a < |x| < a + d \end{cases} \tag{A.1.5}$$

which can decomposed into two cases, among them one is

$$\begin{cases} \sigma_{xx} = \sigma_{xy} = \sigma_{yy} = 0, H_{xx} = H_{yy} = H_{xy} = H_{yx} = 0 & \sqrt{x^2+y^2} \to \infty \\ \sigma_{yy} = \sigma_{xy} = 0, H_{yy} = H_{yx} = 0 & y = 0, |x| < a \\ \sigma_{yy} = \sigma_c, \sigma_{xy} = 0, H_{yy} = H_{yx} = 0 & a < |x| < a + d \end{cases} \tag{A.1.6}$$

and another

$$\begin{cases} \sigma_{yy} = p, \sigma_{xx} = \sigma_{xy} = 0, H_{xx} = H_{yy} = H_{xy} = H_{yx} = 0 & \sqrt{x^2+y^2} \to \infty \\ \sigma_{yy} = \sigma_{xy} = 0, H_{yy} = H_{yx} = 0 & y = 0, |x| < a + d \end{cases} \tag{A.1.7}$$

The solution of problems (A.1.4) and (A.1.7) can be obtained from (11.3.53); i.e. if we put $m = 1, R_0 = (a+d)/2$, then the elliptic hole reduced to a Griffith crack with half-length $(a + d)$. In Fig. 11.3.3 let $z_1 = (a+d, +0), z_2 = (a, +0)$; from

(11.3.53), we can obtain a solution, similarly put $z_1 = (a+d, -0), z_2 = (a, -0)$, $z_1 = (-a-d, +0), z_2 = (-a, +0)$, and $z_1 = (-a-d, -0), z_2 = (-a, -0)$, respectively; and from (11.3.53), one can find other corresponding three solutions, by superposing which one can obtain solution

$$\begin{cases} \Phi_4^{(1)}(\zeta) = \frac{1}{32c_1} \cdot \frac{\sigma_c(a+d)\varphi_2}{\pi} \cdot \frac{1}{\zeta} - \frac{1}{32c_1} \cdot \frac{\sigma_c}{2\pi i} \left[z\left(\ln \frac{\sigma_2 - \zeta}{\overline{\sigma_2} - \zeta} + \ln \frac{\sigma_2 + \zeta}{\overline{\sigma_2} + \zeta} \right) - l \ln \frac{(\zeta - \sigma_2)(\zeta + \overline{\sigma_2})}{(\zeta + \sigma_2)(\zeta - \overline{\sigma_2})} \right] \\ \Phi_3^{(1)}(\zeta) = \frac{1}{32c_1} \cdot \frac{\sigma_c(a+d)\varphi_2}{\pi} \cdot \frac{2\zeta}{\zeta^2 - 1} - \frac{1}{32c_1} \cdot \frac{\sigma_c a}{2\pi i} \ln \frac{(\zeta - \sigma_2)(\zeta + \overline{\sigma_2})}{(\zeta + \sigma_2)(\zeta - \overline{\sigma_2})} \end{cases} \tag{A.1.8}$$

where $\sigma = e^{i\varphi}$ represents the value of ζ at the unit circle in the mapping plane, and $\sigma_2 = e^{i\varphi_2}$, $a = (a+d)\cos\varphi_2$.

And the solution of problems (A.1.4) and (A.1.7), as the solution of Griffith crack problem, is known, i.e.

$$\begin{cases} \Phi_4^{(2)}(\zeta) = -\frac{1}{32c_1} \frac{p}{2} (a+d) \frac{1}{\zeta} \\ \Phi_3^{(2)}(\zeta) = -\frac{p}{32c_1} (a+d) \left[\frac{\zeta}{(\zeta^2 - 1)} \right] \end{cases} \tag{A.1.9}$$

The superposition of (A.1.8) and (A.1.9) gives the total solution for $\Phi_4(\zeta) = \Phi_4^{(1)}(\zeta) + \Phi_4^{(2)}(\zeta), \Phi_3(\zeta) = \Phi_3^{(1)}(\zeta) + \Phi_3^{(2)}(\zeta)$; for example, the first term of $\Phi_4(\zeta)$ is

$$-\frac{1}{32c_1} \frac{p}{2} (a+d) \frac{1}{\zeta} + \frac{1}{32c_1} \cdot \frac{\sigma_c(a+d)\varphi_2}{\pi} \cdot \frac{1}{\zeta} \tag{A.1.10}$$

and $\Phi_2(\zeta)$ has not been listed here because it is too lengthy, so the stresses and displacements are determined already. In addition, we know that

$$\sigma_{ij}, H_{ij} \sim \Phi'(\zeta)/\omega'(\zeta) \tag{A.1.11}$$

here $\Phi(\zeta)$ means $\Phi_4(\zeta)$ or $\Phi_3(\zeta)$, and $\omega'(\zeta) \sim 1/(1-\zeta^2)$.

From Sect. 14.4 in the text, we know that there is no stress singularity at the generalized Dugdale-Barrenblatt crack tip, and this fact and conjunct with (A.1.10) and (A.1.11) require that the value of formula (A.1.10) must be zero, which leads to (14.4.6) in the text. Considering this the final version of $\Phi_4(\zeta)$ is

$$\Phi_4(\zeta) = -\frac{1}{32c_1} \cdot \frac{\sigma_c}{2\pi i} \left[z\left(\ln \frac{\sigma_2 - \zeta}{\overline{\sigma_2} - \zeta} + \ln \frac{\sigma_2 + \zeta}{\overline{\sigma_2} + \zeta} \right) - a \ln \frac{(\zeta - \sigma_2)(\zeta + \overline{\sigma_2})}{(\zeta + \sigma_2)(\zeta - \overline{\sigma_2})} \right] \tag{A.1.12}$$

And the displacement at the crack surface presents the form

$$u_y(x,0) = (128c_1c_2 - 64c_3)\mathrm{Im}(\Phi_4(\zeta))_{\zeta=\sigma} \tag{A.1.13}$$

After some calculation, we find that

$$u_y(x,0) = \frac{(4c_1c_2 - 2c_3)}{c_1} \cdot \frac{\sigma_c(a+d)}{2\pi} \cdot \left[\cos\varphi \ln\frac{\sin(\varphi_2 - \varphi)}{\sin(\varphi_2 + \varphi)} - \cos\varphi_2 \ln\frac{(\sin\varphi_2 - \sin\varphi)}{(\sin\varphi_2 + \sin\varphi)}\right] \tag{A.1.14}$$

so the crack tip opening displacement is

$$\delta_t = \mathrm{CTOD} = \lim_{x\to l} 2u_y(x,0) = \lim_{\varphi\to\varphi_2} 2u_y(x,0) = \frac{(8c_1c_2 - 4c_3)\sigma_s a}{c_1\pi} \ln\sec\left(\frac{\pi}{2}\frac{\sigma^{(\infty)}}{\sigma_s}\right) \tag{A.1.15}$$

in which the constants c_1, c_2, c_3 are defined in Sect. 11.3, so the solution holds for point groups 5 m and 10 mm as well as point groups $5, \bar{5}, 10, \overline{10}$ quasicrystals. When we assume $R_1 = R$, $R_2 = 0$ in Eq. (A.1.15), δ_t will be the corresponding solution of point groups 5 m and 10 mm quasicrystals, i.e.

$$\delta_t = \mathrm{CTOD} = \frac{2\sigma_s a}{\pi}\left[\frac{1}{L+M} + \frac{K_1}{MK_1 - R^2}\right] \ln\sec\left(\frac{\pi}{2}\frac{\sigma^{(\infty)}}{\sigma_s}\right),$$

which is just the (14.4.7). If let $K_1 = R = 0, L = \lambda, M = \mu$ in above formula, then it exactly reduces to the classical Dugdale-Barenblatt solution holding for engineering material (or structural material) including crystalline material (referring to Sect. 14.4).

The more details can be found in article given by Fan and Fan [7].

A.4 On the Calculation of Integral (9.2.14)

In formula (9.2.14), $y > 0$ results in the integrals being convergent. We let ξ to extend to complex number $\xi = \xi_1 + i\xi_2$, take integration path at complex $\xi-$plane similar to Fig. 11.7; by physical consideration $k(K_1 - K_2) > 0$, $\mu(K_1 - K_2) - R^2 > 0$, and $k = \mu^{(c)}/h$; then we can find the integrand of (9.2.14) in the interior of the region enclosing by the integration path is analytic except poles

$$\xi_1^{(1)} = \frac{k(K_1 - K_2)}{R^2 - \mu(K_1 - K_2)} < 0, \quad \xi_1^{(2)} = -\frac{k(K_1 - K_2)}{R^2 - \mu(K_1 - K_2)} > 0 \tag{A.1.16}$$

at real axis ξ_1; and by a generalized Jordan lemma, the integral along the big half-circle is zero.

If in Fig. 11.7 of Chap. 11 put $\omega = \xi, \omega_1 = \xi_1, \omega_2 = \xi_2, \sqrt{k/m} = \xi_1^{(1)}, -\sqrt{k/m} = \xi_1^{(2)}$according to the additional integration path at complex ξ-plane, through the similar manner for evaluating integral (11.7.18), then we can obtain results (9.2.15) and (9.2.16), respectively where$\xi_1^{(1)}, \xi_1^{(2)}$ are defined by (A.1.16).

A.5 On the Calculation of Integral (8.8.9)

$$\begin{aligned}\phi'(\zeta) &= \frac{p}{2\pi i}\int_{-1}^{1}\frac{2w}{\pi}\cdot\left(\frac{-\sigma\tan\left(\frac{\pi a}{2w}\right)}{\left[1+(1-\sigma^2)\tan^2\left(\frac{\pi a}{2w}\right)\right]\sqrt{1-\sigma^2}}\right)\cdot\frac{1}{\sigma-\zeta}\mathrm{d}\sigma \\ &= -\frac{pw}{\pi^2 i}\tan(\frac{\pi a}{2w})\int_{-1}^{1}\left(\frac{\sigma}{\left[1+(1-\sigma^2)\tan^2(\frac{\pi a}{2w})\right]\sqrt{1-\sigma^2}}\right)\cdot\frac{1}{\sigma-\zeta}\mathrm{d}\sigma\end{aligned} \tag{A.1.17}$$

Put $m = \tan\left(\frac{\pi a}{2w}\right)$, so $m^2 = \tan^2\left(\frac{\pi a}{2w}\right)$
We calculate

$$\begin{aligned}I(\zeta) &= \int_{-1}^{1}\left(\frac{\sigma}{\left[1+(1-\sigma^2)\tan^2\left(\frac{\pi a}{2w}\right)\right]\sqrt{1-\sigma^2}}\right)\cdot\frac{1}{\sigma-\zeta}\mathrm{d}\sigma \\ &= \int_{-1}^{1}\left(\frac{1}{[1+(1-\sigma^2)m^2]\sqrt{1-\sigma^2}}\right)\mathrm{d}\sigma + \int_{-1}^{1}\left(\frac{\zeta}{[1+(1-\sigma^2)m^2]\sqrt{1-\sigma^2}(\sigma-\zeta)}\right)\mathrm{d}\sigma \\ &= I_1 + I_2\end{aligned} \tag{A.1.18}$$

The calculation of the first integral is easy, and we now calculate the second one. Put $\zeta = b, \sigma = x$, such that

$$I_2 = \int_{-1}^{1}\left(\frac{b}{[1+(1-x^2)m^2]\sqrt{1-x^2}(x-b)}\right)\mathrm{d}\sigma$$

Denote $x = \sin t, t \in \left[-\frac{\pi}{2}, \frac{\pi}{2}\right], \mathrm{d}x = \cos t\mathrm{d}t$ where $\begin{cases} t = -\dfrac{\pi}{2}\ as\ x = -1 \\ t = \dfrac{\pi}{2}\ as\ x = 1 \end{cases}$

$$
\begin{aligned}
I_2 &= \int_{-\pi/2}^{\pi/2} \frac{b}{[1+m^2\cos t]\cdot(\sin t - b)\cdot\cos t}\cdot\cos t \mathrm{d}\sigma \\
&= \int_{-\pi/2}^{\pi/2} \frac{b}{[1+m^2\cos^2 t](\sin t - b)}\mathrm{d}t \\
&= \int_{0}^{\pi/2} \frac{b}{[1+m^2\cos^2 t](\sin t - b)}\mathrm{d}t + \int_{-\pi/2}^{0} \frac{b}{[1+m^2\cos^2 t](\sin t - b)}\mathrm{d}t
\end{aligned}
\tag{A.1.19}
$$

For the second integral of A.1.19, put $t=-x, \mathrm{d}t=-\mathrm{d}x, t=-\frac{\pi}{2}$ as $x=\frac{\pi}{2}; t=0$ as $x=0$

$$
\int_{-\pi/2}^{0} \frac{b}{[1+m^2\cos^2 t](\sin t - b)}\mathrm{d}t = -\int_{0}^{\pi/2} \frac{b}{[1+m^2\cos^2 x](\sin x + b)}\mathrm{d}x.
$$

So that

$$
\begin{aligned}
\int_{-\pi/2}^{\pi/2} \frac{b}{[1+m^2\cos^2 t](\sin t - b)}\mathrm{d}t &= \int_{0}^{\pi/2} \frac{b}{[1+m^2\cos^2 t](\sin t - b)}\mathrm{d}t \\
&\quad - \int_{0}^{\pi/2} \frac{b}{[1+m^2\cos^2 t](\sin t + b)}\mathrm{d}t \\
&= \int_{0}^{\pi/2} \frac{2b^2}{[1+m^2\cos^2 t](\sin^2 t - b^2)}\mathrm{d}t \\
&= A\cdot\int_{0}^{\pi/2} \frac{1}{[1+m^2\cos^2 t]}\mathrm{d}t + B\cdot\int_{0}^{\pi/2} \frac{1}{(\sin^2 t - b^2)}\mathrm{d}t
\end{aligned}
\tag{A.1.20}
$$

The constants A and B can be determined by

$$
\begin{aligned}
A &= \frac{2m^2b^2}{[m^2(1-b^2)+1]} \\
B &= \frac{2b^2}{[m^2(1-b^2)+1]}
\end{aligned}
$$

Therefore

$$A \cdot \int_0^{\pi/2} \frac{1}{[1+m^2\cos^2 t]} \mathrm{d}t = A \cdot \frac{\pi}{2} \cdot \cos\left(\frac{\pi a}{2w}\right)$$

$$B \cdot \int_0^{\pi/2} \frac{1}{(\sin^2 t - b^2)} \mathrm{d}t = B \cdot \int_0^{\pi/2} \frac{1/2b}{(\sin t - b)} \mathrm{d}t - B \cdot \int_0^{\pi/2} \frac{1/2b}{(\sin t + b)} \mathrm{d}t$$

$$= B \cdot 1/2b \left[\int_0^{\pi/2} \frac{1}{(\sin t - b)} \mathrm{d}t - \int_0^{\pi/2} \frac{1}{(\sin t + b)} \mathrm{d}t \right]$$

From the integral table, one can find

$$B \cdot \int_0^{\pi/2} \frac{1}{(\sin^2 t - b^2)} \mathrm{d}t = \frac{B}{2b\sqrt{1-b^2}} \left\{ \ln \left| \frac{-b+1-\sqrt{1-b^2}}{-b+1+\sqrt{1-b^2}} \right| - \ln \left| \frac{1-\sqrt{1-b^2}}{1+\sqrt{1-b^2}} \right| \right.$$

$$\left. - \ln \left| \frac{b+1-\sqrt{1-b^2}}{b+1+\sqrt{1-b^2}} \right| + \ln \left| \frac{1-\sqrt{1-b^2}}{1+\sqrt{1-b^2}} \right| \right.$$

$$= \frac{B}{2b\sqrt{1-b^2}} \left\{ \ln \left| \frac{-b+1-\sqrt{1-b^2}}{-b+1+\sqrt{1-b^2}} \right| \left| \frac{b+1+\sqrt{1-b^2}}{b+1-\sqrt{1-b^2}} \right| \right\}$$

$$= \frac{B}{2b\sqrt{1-b^2}} \left\{ \ln \left| \frac{\left(-2b\sqrt{1-b^2}\right)^2}{4b^2(b^2-1)} \right| \right\} = \frac{B}{2b\sqrt{1-b^2}} \ln \left| \frac{1}{b} \right|$$

Therefore

$$\phi'(\zeta) = -\frac{pw}{\pi i} \sin\left(\frac{\pi a}{2w}\right) - \frac{pw}{\pi i} \sin\left(\frac{\pi a}{2w}\right) \frac{\zeta^2 \tan^2\left(\frac{\pi a}{2w}\right)}{\left[1+(1-\zeta^{2s})\tan^2\left(\frac{\pi a}{2w}\right)\right]}$$

$$+ \frac{pw}{\pi^2 i} \tan\left(\frac{\pi a}{2w}\right) \frac{\ln|\zeta|}{\left[1+(1-\zeta^2)\tan^2\left(\frac{\pi a}{2w}\right)\right]} \cdot \frac{\zeta}{\sqrt{1-\zeta^2}} \mathrm{d}\sigma \qquad \text{(A.1.21)}$$

It is easily found that $\phi'(0) = -\frac{pw}{\pi i} \sin\left(\frac{\pi a}{2w}\right)$.

References

1. Muskhelishvili N I, 1953, *Some Basic Problems of the Mathematical Theory of Elasticity,* Noordhoff Ltd, Groningen.
2. Privalov I I, 1984, *Introduction to Complex Variable Functions Theory*, Science, Moscow (in Russian).

3. Lavrentjev M A and Schabat B V, 1986, *Methods of Complex Variable Functions Theory,* 6th Edition, National Technical- Theoretical Literature Press, Moscow (in Russian).
4. Fan T Y, 1990, Semi-infinite crack in a strip, *Chin. Phys. Lett.*, **8**(9), 401-404.
5. Shen D W and Fan T Y, 2003, Two collinear semi-infinite cracks in a strip, *Eng. Fract. Mech.*, **70**(8), 813-822.
6. Wolfran St., 1996, *The Mathematica Book*, 3rd, ed by Wolfran St, Cambridge University Press, Cambridge.
7. Fan T Y and Fan L, 2011, Relation between Eshelby integral and generalized BCS and generalized DB models for some one- and two-dimensional quasicrystals, Chin. Phys B., **20**(4), 036102 .
8. Fan T Y, Yang X C and Li H X, 1998, Complex analysis of edge crack in a finite width strip, Chin Phys Lett, **18**(1), 31-34.
9. Li W, 2011, Analytic solutions of a finite width strip with a single edge crack of two-dimensional quasicrystals, Chin Phys B, **20**(11), 116201.

Appendix B: Dual Integral Equations and Some Additional Calculations

B.1 Dual Integral Equations

It is well known that the Fourier transform or Hankel transform is very useful tool in solving partial differential equations which have been shown in Chaps. 7–9 though the introduction is very limited. For non-harmonic and non-multi-harmonic equations, the complex potential method is not effective, and we have to use the Fourier transform, Hankel transform, Mellin transform, or others. After the transform, the boundary value problems of the dislocations are reduced to some algebraic equations to solve (this is relatively simpler), while those of the cracks are concluded for solving the following dual integral equations

$$\left.\begin{aligned} \int_0^\infty y^\alpha f(y) J_v(xy)\mathrm{d}y = g(x), \quad & 0<x<1 \\ \int_0^\infty f(y) J_v(xy)\mathrm{d}y = 0, \quad & x>1 \end{aligned}\right\} \tag{B.1.1}$$

or

$$\left.\begin{aligned} \int_0^\infty y^{\alpha_j} \sum_{k=1}^{n} a'_{jk} f_j(y) J_{v_j}(xy)\mathrm{d}y = g_j(x), \quad & 0<x<1 \\ \int_0^\infty \sum_{k=1}^{n} a_{jk} f_j(y) J_{v_j}(xy)\mathrm{d}y = 0, \quad & x>1 \\ (j=1,2,\ldots,n) & \end{aligned}\right\} \tag{B.1.2}$$

or

$$\left.\begin{aligned}&\int_0^\infty\int_0^\infty g_1(\xi_1,\xi_2,s,x_1,x_2)f(\xi_1,\xi_2,s)J_\alpha(\xi_1x_1)J_\beta(\xi_2x_2)d\xi_1d\xi_2=h(x_1,x_2,s),\quad (x_1,x_2)\in\Omega_1\\&\int_0^\infty\int_0^\infty g_2(\xi_1,\xi_2,s,x_1,x_2)f(\xi_1,\xi_2,s)J_\alpha(\xi_1x_1)J_\beta(\xi_2x_2)d\xi_1d\xi_2=0,\quad (x_1,x_2)\in\Omega_2\end{aligned}\right\}\tag{B.1.3}$$

Among them, Eqs. (B.1.1) are the simplest ones, which will be discussed in the following only. Eqs. (B.1.2) deal with multi-unknown functions and (B.1.3) are the two-dimensional dual integral equations, and these two kinds of dual integral equations are more complicated.

In Eqs. (B.1.1), $f(x)$ is a unknown function to be determined, $g(x)$ is known one, αv are constants, and $J_v(xy)$ is the first kind Bessel function of v order. Titchmarsh [1] and Busbridge [2] gave the analytic solution of the equations. Various authors [3–11] discussed the solutions with different methods. Here only the procedure of Refs. [1, 2] is introduced. Titchmarsh [1] gave formal solution for the case $\alpha > 0$. Busbridge [2] extended the discussion to the case $\alpha > -2$ and gave proof for the existence of the solution. The solution is given through a complex integral as follows:

$$f(x)=\frac{1}{2\pi i}\int_{k-i\infty}^{k+i\infty}2^{s-\alpha}\frac{\Gamma\left(\frac{1}{2}+\frac{1}{2}v+\frac{1}{2}s\right)}{\Gamma\left(\frac{1}{2}+\frac{1}{2}v+\frac{1}{2}\alpha-\frac{1}{2}s\right)}\psi(s)x^{-s}\mathrm{d}s\tag{B.1.4}$$

in which $s=\sigma+i\tau$ and

$$\psi(s)=\frac{1}{2\pi i}\int_{C-i\infty}^{C+i\infty}\frac{\Gamma\left(\frac{1}{2}+\frac{1}{2}v-\frac{1}{2}\alpha+\frac{1}{2}w\right)}{\Gamma\left(\frac{1}{2}+\frac{1}{2}v+\frac{1}{2}w\right)}\cdot\frac{\overline{g}(\alpha+1-w)}{w-s}\mathrm{d}w\tag{B.1.5}$$

where $w=u+i\upsilon$ (in which υ represents the imaginary part of complex variable w, do not confuse with v—the suffix of the Bessel function, which represents the order of the Bessel function) $\sigma<u$ and

$$\overline{g}(\alpha+1-w)=\int_0^1 g(x)x^{\alpha-w}\mathrm{d}x$$

in above formulas $\Gamma(x)$ represent Euler gamma function. The solution of (B.1.4) holds for both $\alpha>0$ and $\alpha>-2$.

For $\alpha>0$, the solution can be expressed by real integral as

$$f(x)=\frac{(2x)^{1-\alpha/2}}{\Gamma(\alpha/2)}\int_0^1 \mu^{1+\alpha/2}J_{\nu+\alpha/2}(\mu x)\mathrm{d}\mu\int_0^1 g(\rho\mu)\rho^{\nu+1}(1-\rho^2)^{\alpha/2-1}\mathrm{d}\rho \quad \text{(B.1.4}')$$

and for $\alpha > -2$, which is in form

$$\begin{aligned} f(x)=\frac{2^{-\alpha/2}x^{-\alpha}}{\Gamma(1+\alpha/2)}\Bigg[&x^{1+\alpha/2}J_{\nu+\alpha/2}(x)\int_0^1 y^{\nu+1}(1-y^2)^{\alpha/2}g(y)\mathrm{d}y \\ &+\int_0^1 y^{\alpha+1}(1-y^2)^{\alpha/2}dy\int_0^1 (xu)^{2+\alpha/2}g(yu)J_{\nu+1+\alpha/2}(xu)\mathrm{d}u\Bigg] \end{aligned} \quad \text{(B.1.4}'')$$

Theorem *If* $\alpha > -2$, $-\nu-1<\alpha-\frac{1}{2}<\nu+1$, *the Mellin transforms of* $g(x)$ *and* $f(x)$ *exist, the latter is analytic in the strip region* $-\nu<\mathrm{Re}s=\sigma<\alpha$ *and has the order* $O(|t|^{\sigma-\alpha+\varepsilon})$ $(\varepsilon>0, t\to\infty)$, *where* $s=\sigma+i\tau$*the Mellin transform parameter, then Eq.* (B.1.1) *have one and only one solution* (B.1.4).

Proof Because the strict proof given by Busbridge [2] is very lengthy, we cannot quote its all details here; instead, only a rough outline of the proof is figured out in the following. One can find that in the proof, a quite lot of complex variable function knowledge is used, and this seems that the theory on dual integral equations presents the inherent connection with complex analysis. So the appendix of Chap. 11 is helpful for the present discussion too.

At first, assume that $0<\alpha<2, -\nu-1<\alpha-\frac{1}{2}<\nu+1$, and the Mellin transform of $f(x)$

$$\overline{f}(s)=\int_0^\infty f(x)x^{s-1}\mathrm{d}x \quad s=\sigma+i\tau$$

is analytic in region $-\nu<\sigma<\alpha$, and assuming as $\varepsilon>0$ and as $t\to\infty$, it has order $O(|t|^{-\alpha+\varepsilon})$ (in fact this is a lemma, but we omit the proof for simplicity).

According to the definition, the Mellin transform of function $y^\alpha J_\nu(xy)$ is

$$\overline{J}_\alpha(s)\equiv\int_0^\infty [y^\alpha J_\nu(xy)]y^{s-1}\mathrm{d}y=\frac{2^{\alpha+s-1}}{x^{\alpha+s}}\frac{\Gamma\left(\frac{1}{2}\alpha+\frac{1}{2}\nu+\frac{1}{2}s\right)}{\Gamma\left(1-\frac{1}{2}\alpha+\frac{1}{2}\nu-\frac{1}{2}s\right)} \quad \text{(B.1.6)}$$

Recall that $s=\sigma+i\tau$. By using the notation of relevant Mellin transforms, the left-hand side of the first and second equations in (B.1.1) becomes

$$\int_0^\infty y^\alpha f(y)J_\nu(xy)\mathrm{d}y=\frac{1}{2\pi i}\int_{C-i\infty}^{C+i\infty}\overline{f}(s)\overline{J}_\alpha(1-s)\mathrm{d}s$$

$$\int_0^\infty f(y)J_v(xy)\mathrm{d}y = \frac{1}{2\pi i}\int_{C-i\infty}^{C+i\infty} \overline{f}(s)\overline{J}_0(1-s)\mathrm{d}s$$

and substituting (B.1.6) into the above formulas yields

$$\frac{1}{2\pi i}\int_{C-i\infty}^{C+i\infty} \frac{2^{\alpha-s}}{x^{1-s}}\frac{\Gamma\left(\frac{1}{2}+\frac{1}{2}\alpha+\frac{1}{2}v-\frac{1}{2}s\right)}{\Gamma\left(\frac{1}{2}-\frac{1}{2}\alpha+\frac{1}{2}v+\frac{1}{2}s\right)}\overline{f}(s)\mathrm{d}s = g(x) \quad 0<x<1$$

$$\frac{1}{2\pi i}\int_{C-i\infty}^{C+i\infty} \frac{2^{\alpha-s}\Gamma\left(\frac{1}{2}+\frac{1}{2}v-\frac{1}{2}s\right)}{\Gamma\left(\frac{1}{2}+\frac{1}{2}v+\frac{1}{2}s\right)}\overline{f}(s)\mathrm{d}s = 0 \quad x>1$$

Put

$$\overline{f}(s) = \frac{2^{\alpha-s}\Gamma\left(\frac{1}{2}+\frac{1}{2}v+\frac{1}{2}s\right)}{\Gamma\left(\frac{1}{2}+\frac{1}{2}\alpha+\frac{1}{2}v-\frac{1}{2}s\right)}\psi(s) \tag{B.1.7}$$

Then the above equations reduce to

$$\left.\begin{array}{ll} \frac{1}{2\pi i}\int_{C-i\infty}^{C+i\infty} \frac{\Gamma\left(\frac{1}{2}+\frac{1}{2}v+\frac{1}{2}s\right)}{\Gamma\left(\frac{1}{2}+\frac{1}{2}v-\frac{1}{2}\alpha+\frac{1}{2}s\right)}\psi(s)x^{s-1-\alpha}\mathrm{d}s = g(x), & 0<x<1 \\ \frac{1}{2\pi i}\int_{C-i\infty}^{C+i\infty} \frac{\Gamma\left(\frac{1}{2}+\frac{1}{2}v-\frac{1}{2}s\right)}{\Gamma\left(\frac{1}{2}+\frac{1}{2}v+\frac{1}{2}\alpha-\frac{1}{2}s\right)}\psi(s)x^{s-1}\mathrm{d}s = 0, & x>1 \end{array}\right\} \tag{B.1.8}$$

Multiply $x^{\alpha-w}$to the first one of (B.1.8), where $w = u+iv$ and $\sigma - u > 0$, and then integrate over $(0,1)$ to x and

$$\frac{1}{2\pi i}\int_{C-i\infty}^{C+i\infty} \frac{\Gamma\left(\frac{1}{2}+\frac{1}{2}v+\frac{1}{2}s\right)}{\Gamma\left(\frac{1}{2}+\frac{1}{2}v-\frac{1}{2}\alpha+\frac{1}{2}s\right)}\psi(s)\frac{\mathrm{d}s}{s-w} = \overline{g}(\alpha-w+1) \tag{B.1.9}$$

where $u<C$, and

$$\overline{g}(\alpha-w+1) = \int_0^1 g(x)x^{\alpha-w}\mathrm{d}x$$

The left-hand side of Eq. (B.1.9) is analytic everywhere in the strip zone

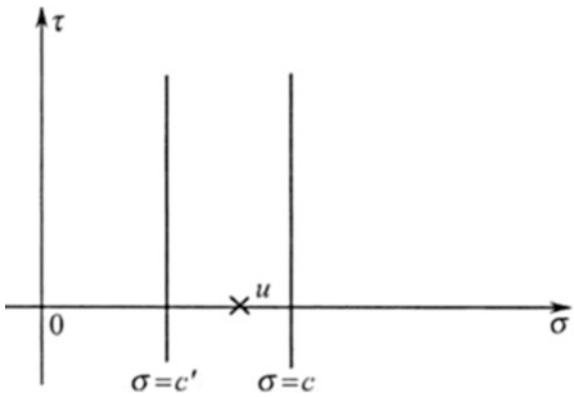

Fig. B.1 The integration path in $s = \sigma + i\tau$-plane

$$-v < \sigma < \alpha$$

except the simple pole $s = w$ and behaves order $O(|t|^{-\alpha+\varepsilon})$. If we move the integration path from $\sigma = C$ to $\sigma = C' < u$, see Fig. B.1, based on the Cauchy's integral formula [referring to formula (11.7.5)].

$$\frac{1}{2\pi i}\int_{C'-i\infty}^{C'+i\infty} \frac{\Gamma\left(\frac{1}{2}+\frac{1}{2}v+\frac{1}{2}s\right)}{\Gamma\left(\frac{1}{2}+\frac{1}{2}v-\frac{1}{2}\alpha+\frac{1}{2}s\right)}\psi(s)\frac{\mathrm{d}s}{s-w}$$
$$= \overline{g}(\alpha - w + 1) - \frac{\Gamma\left(\frac{1}{2}+\frac{1}{2}v+\frac{1}{2}w\right)}{\Gamma\left(\frac{1}{2}+\frac{1}{2}v-\frac{1}{2}\alpha+\frac{1}{2}w\right)}\psi(w)$$

This translation of the integration line corresponds to form a closed region, and the value of the integral around the closed region is just equal to the second term of the above formula including the sign of the term. The left-hand side is analytic as $u > C'$, so is the right-hand side. In addition,

$$\psi(w) - \frac{\Gamma\left(\frac{1}{2}+\frac{1}{2}v-\frac{1}{2}\alpha+\frac{1}{2}w\right)}{\Gamma\left(\frac{1}{2}+\frac{1}{2}v+\frac{1}{2}\alpha\right)}\overline{g}(\alpha - w + 1) \tag{B.1.10}$$

is analytic for the case

$$\frac{1}{2}+\frac{1}{2}v-\frac{1}{2}\alpha+\frac{1}{2}w \neq 0, -1, -2\cdots$$

Integrate function (B.1.10) along a big rectangle whose corners are the points

$$C-iT, C+iT, -T+iT, -T-iT \quad (T>|\upsilon|).$$

One can find the absolute values of the integrals

$$\left|\int_{C-iT}^{-T+iT}\right|, \quad \left|\int_{-T+iT}^{-T-iT}\right|, \quad \left|\int_{-T-iT}^{C-iT}\right|$$

have order $O(|T|^{-\alpha/2+\varepsilon})$, and the value of ε can be always taken less than $\alpha/2$, and then they can tend to zero as $T\to\infty$. According to the Cauchy's integral theorem (referring to formula (11.7.4) of Chap. 11),

$$\frac{1}{2\pi i}\int_{C-i\infty}^{C+i\infty}\left\{\psi(s)-\frac{\Gamma\left(\frac{1}{2}+\frac{1}{2}v-\frac{1}{2}\alpha+\frac{1}{2}w\right)}{\Gamma\left(\frac{1}{2}+\frac{1}{2}v+\frac{1}{2}s\right)}\overline{g}(\alpha-s+1)\right\}\frac{ds}{s-w}=0 \quad (u<C) \tag{B.1.11}$$

Similarly, multiply $x^{-w}$to the second one of equations (B.1.8), where $\sigma-w<0$ and then integrate to x over $(1,\infty)$

$$\frac{1}{2\pi i}\int_{C'-i\infty}^{C'+i\infty}\frac{\Gamma\left(\frac{1}{2}+\frac{1}{2}v-\frac{1}{2}s\right)}{\Gamma\left(\frac{1}{2}+\frac{1}{2}v+\frac{1}{2}\alpha-\frac{1}{2}s\right)}\psi(s)\frac{ds}{s-w}=0 \quad (u>C')$$

Move the integration path and find that

$$\psi(w)=\frac{1}{2\pi i}\int_{C-i\infty}^{C+i\infty}\psi(s)\frac{\mathrm{d}s}{s-w} \quad (u<C) \tag{B.1.12}$$

Comparing (B.1.11) and (B.1.12), we can find (B.1.5), so the solution (B.1.4), in which

$$\overline{g}(\alpha-s+1)=\int_0^1 g(\xi)\xi^{\alpha-s}\mathrm{d}\xi$$

The theorem is proved.

Furthermore the form of real integral of the solution can be obtained as below. In fact

$$\frac{1}{s-w}=\int_0^1 \eta^{s-w-1}\mathrm{d}\eta$$

If we exchange the integration order, then (B.1.5) may be rewritten as

$$\psi(w)=\int_0^1 g(\xi)\xi^{\alpha}\mathrm{d}\xi\int_0^1 \eta^{-w-1}\mathrm{d}\eta\times\frac{1}{2\pi i}\int_{C-i\infty}^{C+i\infty}\frac{\Gamma\left(\frac{1}{2}+\frac{1}{2}v-\frac{1}{2}\alpha+\frac{1}{2}s\right)}{\Gamma\left(\frac{1}{2}+\frac{1}{2}v+\frac{1}{2}s\right)}\left(\frac{\xi}{\eta}\right)^{-s}\mathrm{d}s$$

in which the integration is [12, 13]

$$\begin{aligned}&\frac{1}{2\pi i}\int_{C-i\infty}^{C+i\infty}\frac{\Gamma\left(\frac{1}{2}+\frac{1}{2}v-\frac{1}{2}\alpha+\frac{1}{2}s\right)}{\Gamma\left(\frac{1}{2}+\frac{1}{2}v+\frac{1}{2}s\right)}\left(\frac{\xi}{\eta}\right)^{-s}\mathrm{d}s\\&=\begin{cases}\frac{2}{\Gamma\left(\frac{1}{2}\alpha\right)}\xi^{1+v-\alpha}(\eta^2-\xi^2)^{\alpha/2-1}\eta^{1-v}, & \eta\geq\xi\\ 0, & 0<\eta<\xi\end{cases}\end{aligned}$$

So that

$$\psi(w)=\frac{2}{\Gamma(\alpha/2)}\int_0^1 g(\xi)\xi^{1+v}\mathrm{d}\xi\int_{\xi}^1 \eta^{-w-v}(\eta^2-\xi^2)^{\alpha/2-1}\mathrm{d}\eta$$

By exchanging the integration order, we may find that

$$\begin{aligned}\psi(w)&=\frac{2}{\Gamma(\alpha/2)}\int_0^1 \eta^{-w-v}\mathrm{d}\eta\int_0^1 g(\xi)\xi^{1+v}(\eta^2-\xi^2)^{\alpha/2-1}\mathrm{d}\xi\\&=\frac{2}{\Gamma(\alpha/2)}\int_0^1 \eta^{\alpha-\omega}\mathrm{d}\eta\int_0^1 g(\xi)\xi^{1+v}(1-\xi^2)^{\alpha/2-1}\mathrm{d}\xi\end{aligned}$$

Substituting it into (B.1.4) yields

$$\begin{aligned}f(x)=&\frac{2}{\Gamma(\alpha/2)}\int_0^1 \eta^{\alpha}\mathrm{d}\eta\int_0^1 g(\eta\zeta)\zeta^{1+v}(1-\zeta^2)^{\alpha/2-1}\mathrm{d}\zeta\\&\times\frac{1}{2\pi i}\int_{C-i\infty}^{C+i\infty}2^{s-\alpha}(x\eta)^{-s}\frac{\Gamma\left(\frac{1}{2}+\frac{1}{2}v+\frac{1}{2}s\right)}{\Gamma\left(\frac{1}{2}+\frac{1}{2}v+\frac{1}{2}\alpha-\frac{1}{2}s\right)}\mathrm{d}s\end{aligned}$$

By utilizing the inversion of the Mellin transform [12, 13],

$$\frac{1}{2\pi i}\int_{C-i\infty}^{C+i\infty} 2^{s-\alpha}\frac{\Gamma\left(\frac{1}{2}+\frac{1}{2}\nu+\frac{1}{2}s\right)}{\Gamma\left(\frac{1}{2}+\frac{1}{2}\nu+\frac{1}{2}\alpha-\frac{1}{2}s\right)}(\mathrm{at})^{-s}\mathrm{d}s = 2^{-\alpha/2}(\mathrm{at})^{1-\alpha/2}J_{\nu+\alpha/2}(\mathrm{at})$$

Then one finds (B.1.4').

For the case $\alpha > -2$, the derivation is similar. For some details reader can refer to Busbridge [2].

In the following, some examples are discussed in detail, which are the dual integral equations appeared in Chaps. 8 and 9 respectively, where only the solutions were listed without derivation detail.

B.2 Additional Derivation on the Solution of Dual Integral Equations (8.3.8) and (9.7.4)

Equations (8.3.8) in the text are

$$\left.\begin{aligned}
&\tfrac{2}{d_{11}}\int_0^\infty [C(\xi)\xi - 6D(\xi)]\cos(\xi x)\mathrm{d}\xi = -p, && 0<x<a\\
&\int_0^\infty \xi^{-1}[C(\xi)\xi - 6D(\xi)]\cos(\xi x)\mathrm{d}\xi = 0, && x>a\\
&\tfrac{2}{d_{12}}\int_0^\infty D(\xi)\cos(\xi x)\mathrm{d}\xi = 0, && 0<x<a\\
&\int_0^\infty \xi^{-1}D(\xi)\cos(\xi x)\mathrm{d}\xi = 0, && x>a
\end{aligned}\right\} \tag{B.1.13}$$

It is evident that the second pair of dual integral equations (B.1.13) has the zero solution, i.e. $D(\xi) = 0$, and we only consider the first pair in the equations, which is

$$\left.\begin{aligned}
&\tfrac{2}{d_{11}}\int_0^\infty C(\xi)\xi\cos(\xi x)\mathrm{d}\xi = -p, && 0<x<a\\
&\int_0^\infty C(\xi)\cos(\xi x)\mathrm{d}\xi = 0, && x>a
\end{aligned}\right\} \tag{B.1.14}$$

and is similar to that of (9.7.4) in Chap. 9. Because of

$$\cos(\xi x) = \left(\frac{\pi\xi x}{2}\right)^{1/2} J_{-1/2}(\xi x)$$

and denoting

$$\xi^{1/2}C(\xi)=f(\xi),\quad \eta=a\xi,\quad \rho=\frac{x}{a},\quad g(\rho)=a\left(\frac{\pi a d_{11}}{2\rho}\right)^{1/2}p$$

then (B.1.14) is reduced to

$$\left.\begin{aligned}&\frac{2}{d_{11}}\int_0^\infty \eta f(\eta)J_{-1/2}(\eta\rho)d\eta=g(\rho),0<\rho<1\\&\int_0^\infty f(\eta)J_{-1/2}(\eta\rho)d\eta=0,\rho>1\end{aligned}\right\}\tag{B.1.14′}$$

which becomes one of the standard dual integral equations shown in (B.1.1) with

$$\alpha=1,\quad v=-1/2,\quad g(\rho)=g_0\rho^{-1/2},\quad g_0=\text{const}=a(\pi a d_{11})^{1/2}p$$

In this case, it is very easy to calculate the solution of dual integral equations (B.1.14) (or B.1.14′) by formulas (B.1.4) and (B.1.5), but the key step is the choosing integration path. In the previous introduction on Titchmarsh–Busbridge solution, we mentioned that it must require that $-v>k>\alpha, -v<C<\alpha$ and $k<C$. At present case, $v=-1/2,\alpha=1$ such that $1/2<k<1$ and $1/2<C<1$. The concrete calculation is:

$$\overline{g}(\alpha+1-t)=\int_0^1 g(\rho)\rho^{\alpha-t}\mathrm{d}\rho=g_0\int_0^1\rho^{-1/2}\rho^{1-t}\mathrm{d}\rho=\frac{g_0}{\frac{3}{2}-t}$$

where $t=t_1+it_2$ represents a complex variable, and requires that $t_1<3/2$. Substituting the relevant data and the above result into (B.1.5), we have

$$\psi(s)=g_0\frac{1}{2\pi i}\int_{C-i\infty}^{C+i\infty}\frac{\Gamma\left(-\frac{1}{4}+\frac{t}{2}\right)}{\Gamma\left(\frac{1}{4}+\frac{t}{2}\right)}\frac{1}{t-s}\frac{1}{\frac{3}{2}-t}\mathrm{d}t$$

The integration path is shown in Fig. B.2. In this case, the integrand has only one pole at point $t=3/2$ of first order. According to the formula for evaluating (11.7.15), the above integral is very easily obtained as

$$\psi(s)=g_0\frac{\Gamma\left(\frac{1}{2}\right)}{\Gamma(1)}\frac{1}{\frac{3}{2}-s}=g_0\frac{\sqrt{\pi}}{\frac{3}{2}-s}\tag{B.1.15}$$

whereas $\Gamma(1)=1,\Gamma\left(\frac{1}{2}\right)=\sqrt{\pi}$. Substituting the result into formula (B.1.4) leads to

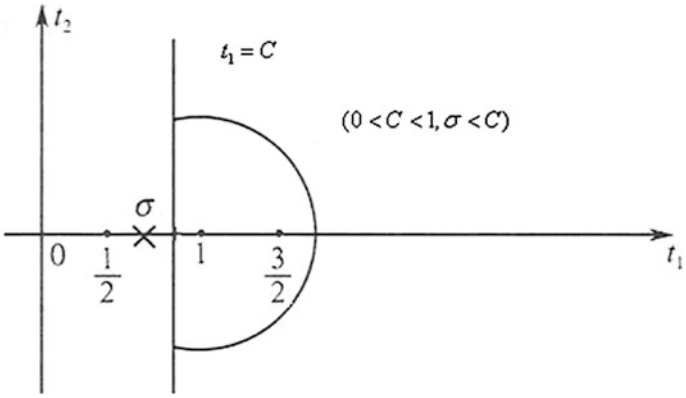

Fig. B.2 The integration path in $t = t_1 + it_2$-plane

$$f(\eta) = g_0\sqrt{\pi}\frac{1}{2\pi i}\int_{k-i\infty}^{k+i\infty}\frac{2^{s-\alpha}\Gamma\left(\frac{1}{4}+\frac{s}{2}\right)}{\Gamma\left(\frac{1}{4}-\frac{s}{2}\right)}\eta^{-s}\mathrm{d}s \tag{B.1.16}$$

In terms of the inversion of the Mellin transform [13],

$$\begin{aligned}&\frac{1}{2\pi i}\int_{k-i\infty}^{k+i\infty}2^{s-\lambda}\frac{\Gamma\left(\frac{1}{2}+\frac{1}{2}\mu+\frac{1}{2}s\right)}{\Gamma\left(\frac{1}{2}+\frac{1}{2}\mu+\frac{1}{2}\lambda-\frac{1}{2}s\right)}(\beta\eta)^{-s}\mathrm{d}s\\&\quad=2^{-\lambda/2}(\beta\eta)^{1-\lambda/2}J_{\mu+\lambda/2}(\beta\eta)\end{aligned} \tag{B.1.17}$$

In formula (B.1.16), $\mu = -1/2, \lambda = 3, \beta = 1$, so that

$$f(\eta) = g_0\left(\frac{\pi}{2\eta}\right)^{1/2}J_1(\eta)$$

and

$$C(\xi) = \xi^{-1/2}f(\xi) = \frac{\pi a d_{11}}{2}\xi^{-1}J_1(a\xi)$$

This is just the result given by (8.3.10) and (9.7.8), and the difference between them lies in a constant factor.

The calculation through (B.1.4′) and (B.1.4″) yields the same result, so the correctness of the result is demonstrated.

B.3 Additional Derivation on the Solution of Dual Integral Equations (9.9.8)

In Sect. 9.9 in the text of Chap. 9, the dual integral equations

$$\begin{aligned}\int_0^\infty \xi A_i(\xi) J_0(\xi r) d\xi &= M_i p_0, \quad 0 < r < a \\ \int_0^\infty A_i(\xi) J_0(\xi r) d\xi &= 0, \quad r > a\end{aligned} \tag{B.1.18}$$

are solved and obtained the solution (9.9.8). We here give the detail for the derivation.

According to the standard type of the equations here $\alpha = 1, v = 0$, $g(\rho) = g_0 = \text{const}$, put $\rho = r/a$, so

$$\overline{g}(\alpha + 1 - t) = \int_0^1 g(\rho)\rho^{\alpha - t} \mathrm{d}\rho = \frac{g_0}{2 - t} \quad (\mathrm{Re} t = t_1 < 2)$$

$$\psi(s) = g_0 \frac{1}{2\pi i} \int_{C - i\infty}^{C + i\infty} \frac{\Gamma\left(\frac{1}{2}\right)}{\Gamma\left(\frac{1}{2} + \frac{t}{2}\right)} \frac{1}{t - s} \frac{1}{2 - t} \mathrm{d}t = g_0 \frac{2}{\sqrt{\pi}} \frac{1}{2 - s}$$

in which $s = \sigma + i\tau$, and the integral is evaluated through the residual of pole $t = 2$ and the integration path is shown in Fig. B.3.

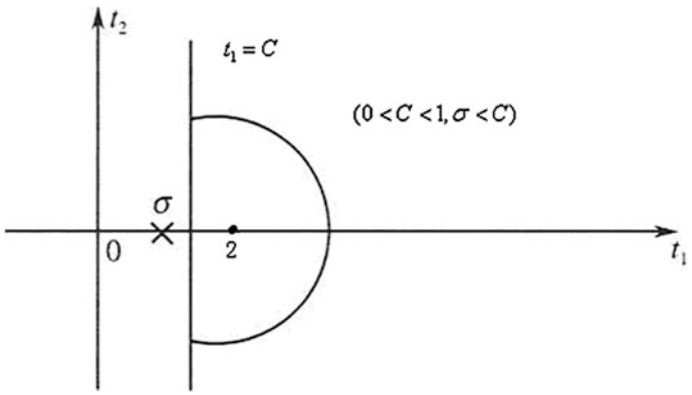

Fig. B.3 Integration path at the $t = t_1 + it_2$-plane

Substituting the result into (B.1.4) yields

$$A_i(\xi) = f(\xi) = g_0 \frac{2}{\sqrt{\pi}} \frac{1}{2\pi i} \int_{k-i\infty}^{k+i\infty} \frac{2^s \Gamma\left(\frac{1}{2} + \frac{s}{2}\right)}{\Gamma\left(2 - \frac{s}{2}\right)} \xi^{-s} \mathrm{d}s = \frac{2g_0}{\sqrt{2\pi}} \xi^{-1/2} J_{3/2}(\xi)$$

which is just the solution (9.9.8), a little bit difference with that lies where we used the normalized coordinate $\rho = r/a$. In the last step of the calculation, the inversion of the Mellin transform (B.1.17) was used.

The evaluation through formulas (B.1.4′) and (B.1.4″) finds the same result, and this checks the correctness of the above calculation.

The above two subsections demonstrate the effect and simplicity of complex variable function method in evaluating solutions of Titchmarsh–Busbridge dual integral equations.

The system of dual integral equations (B.1.2) and its applications are discussed by Fan [14], and the two-dimensional dual integral equations (B.1.3) are solved approximately by Fan and Sun [15], in which some applications are also given.

Application of integral transforms in elasticity of quasicrystals may be effective and more widely used than that of complex variable function method and has got much analytic solutions, see, e.g. Li [16], Zhou and Fan [17], Zhou [18], and Zhu and Fan [19, 20], and due to the limitation of the space, much results have not been quoted. The application of the method to crack problems often leads to some dual integral equations, so it is helpful for a discussion about this.

References

1. Titchmarsh B C, 1937, *Introduction to the Fourier Integrals*, Clarenden Press, Oxford.
2. Busbridge I W, 1938, Dual integral equations, *Math. Soc. Proc.,* **44**(2), 115-129.
3. Weber H, 1873, Ueber die Besselschen Functionen und ihre Anwendung auf die Theorie der electrischen Stroeme, *J. fuer reihe und angewandte Mathematik*, **75**(1), 5-105.
4. McDonald H M, 1895, The electrical distribution induced on a disk placed in any fluid of force, *Phil. Mag.,* **26**(1), 257-260.
5. King L V, 1935, On the acoustic radiation pressure on circular disk, *Roy. Soc. London Proc.* Ser A, **153**(1), 1-16.
6. Copson E T, 1947, On the problem of the electric disk, *Edinburg Math. Soc. Proc.*, **8**(1), 5-14.
7. Tranter C J, 1951, On some dual integral equations, *Quar. J. Math.* Ser 2, **2**(1), 60-66.
8. Sneddon I N, 1951, *Fourier Transforms*, McGraw-Hill, New York.
9. Gordon A N, 1954, Dual integral equations, *London Math .Soc. J.*, **29**(5), 360-369.
10. Noble B, 1955, On some dual integral equations, *Quar. J. Math.* Ser 2, **6**(2), 61-67.
11. Noble B, 1963, The solutions of Bessel function dual integral equations by a multiplying factor method, *Cambridge Phil. Soc. Proceeding*, **59**(4), 351-362.
12. Watson G N, 1955, *A Treatise on the Theory of Bessel Functions*, Amazon Com, New York.
13. Erdelyi A, 1953, *Higher Transcendental Functions*, Vol.2, McGraw-Hill, New York.
14. Fan T Y, 1979, Dual integral equations and system of dual integral equations and their applications in solid mechanics and fluid mechanics, *Mathematica Applicata Sinica*, **2**(3), 212-230 (in Chinese).

15. Fan T Y and Sun Z F, 2007, A class of two-dimensional dual integral equations and applications, *Appl. Math. Mech.*, **28**(2), 247-252..
16. Li X F, 1999, Defects and their analytic solution in elasticity of quasicrystals, Dissertation, Beijing Institute of Technology.
17. Zhou W M and Fan T Y, 2001, Plane elasticity problem of two-dimensional octagonal quasicrystal and crack problem, *Chin. Phys*., **10**(8), 743-747.
18. Zhou W M, 2000, Mathematical analysis of elasticity and defects of two- and three-dimensional quasicrystals (in Chinese), Dissertation, Beijing Institute of Technology, Beijing.
19. Zhu A Y and Fan T Y, 2007, Elastic analysis of a mode II crack in an icosahedral quasicrystal, *Chin. Phys.*, **16**(5), 1111-1119.
20. Zhu A Y and Fan T Y, 2009, Elastic analysis of a Griffith crack in an icosahedral Al-Pd-Mn quasicrystal, *Int. J. Modern Phys. B*, **23**(10), 1-16.

Appendix C: Poisson Brackets in Condensed Matter Physics, Concept of Lie Group and Lie Algebra and Their Applications

In Chap. 16, the equations of motion of solid quasicrystals as a source of those of soft-matter quasicrystals, the latter are put forward as an extension of the former, and the detail of derivation of the equations of solid quasicrystals has not been given in the text, which needs a tool—Poisson brackets in condensed matter physics. In this appendix, we first introduce the method and then give the derivation of those equations.

C.1 Poisson Brackets in Condensed Matter Physics

Due to symmetry breaking, the derivation of some equations of motion of hydrodynamics of some substantive systems cannot be obtained directly by conventional conservations laws. The Poisson brackets in condensed matter physics become a useful method for the derivation, which simplifies the calculation. The method is originated from the Landau and his school in former Soviet Union and Russia (see [1–6]). The physicists Martin et al. [7], and Fleming and Cohen [8] in USA developed the method to hydrodynamics of crystals and liquid crystals, but their derivations were still lengthy. Lubensky et al. [9] further developed the approach in deriving the hydrodynamic equations of quasicrystals, simplified the derivation, and made it arrives in systematization.

Poisson brackets come from the classical analytic mechanics, i.e., for two mechanical quantities f, g and there is the following relation

$$\{f,g\}=\sum_i\left(\frac{\partial f}{\partial q_i}\frac{\partial g}{\partial p_i}-\frac{\partial f}{\partial p_i}\frac{\partial g}{\partial q_i}\right) \tag{C.1.1}$$

which is the Poisson bracket, where p_i, q_i denote the canonic momentum and canonic coordinate.

According to the terminology of physics, (C.1.1) is named classical Poisson bracket hereafter.

Relative to the classical Poisson bracket (C.1.1), there is a quantum Poisson bracket, which is related to the commutation relation in quantum mechanics

$$\left[\hat{A},\hat{B}\right]=\hat{A}\hat{B}-\hat{B}\hat{A} \tag{C.1.2}$$

in which $\hat{A},\hat{B}$ represent two operators; e.g. $\hat{A}$ represents coordinate operator x_α and $\hat{B}$ the momentum operator p_β, and then

$$\left[x_\alpha,p_\beta\right]=i\hbar\delta_{\alpha\beta},\left[x_\alpha,x_\beta\right]=0,\left[p_\alpha,p_\beta\right]=0 \tag{C.1.3}$$

where $i=\sqrt{-1},\hbar=h/2\pi,h$ the Planck constant, $\delta_{\alpha\beta}$ unit tensor. Equation (C.1.3) is named quantum Poisson bracket. In the quantum mechanics, mechanics quantities represent operators. Equation (C.1.3) holds for any operators, in general.

There is inherent connection between the quantum Poisson bracket and classical Poisson bracket, i.e.

$$\lim_{\hbar\to 0}\frac{i\left[\hat{A}\hat{B}-\hat{B}\hat{A}\right]}{\hbar}=\{A,B\} \tag{C.1.4}$$

This is well-known result in the quantum mechanics.

Landau [4] introduced the limit passing over (C.1.4) from quantum Poisson bracket to the classical Poisson bracket in deriving the hydrodynamic equations of superfluid. He takes the expansion of mass density and momentum such as:

$$\hat{\rho}(r)=\sum_\alpha m_\alpha\delta(r_\alpha-r) \tag{C.1.5}$$

$$\hat{g}_k(r)=\sum_\alpha\hat{p}_k^\alpha\delta(r_\alpha-r) \tag{C.1.6}$$

whose quantum Poisson brackets are

$$\begin{aligned}&[\hat{\rho}(r_1),\hat{\rho}(r_2)]=0\\&[\hat{p}_k(r_1),\hat{\rho}(r_2)]=i\hbar\hat{\rho}(r_1)\nabla_k(r_1)\delta(r_1-r_2)\\&[\hat{p}_k(r_1),\hat{p}_l(r_2)]=i\hbar(\hat{p}_l(r_1)\nabla_k(r_1)-\hat{p}_k(r_2)\nabla_k(r_2))\delta(r_1-r_2)\end{aligned} \tag{C.1.7}$$

where $\nabla_k(r_1)$ represents derivative carrying out on coordinate r_1 and $\nabla_l(r_2)$ on coordinate r_2.

By using the limit passing over (C.1.4) from the quantum Poisson to the classical Poisson bracket, from (C.1.7) one can obtain the corresponding classical Poisson brackets:

$$\begin{aligned}\{p_k(r_1), \rho(r_2)\} &= \rho(r_1)\nabla_k(r_1)\delta(r_1 - r_2)\\ \{p_k(r_1), p_l(r_2)\} &= (p_l(r_1)\nabla_k(r_1) - p_k(r_2)\nabla_k(r_2))\delta(r_1 - r_2)\end{aligned} \tag{C.1.8}$$

Lubensky et al. [9] extended the discussion to solid quasicrystals, and they introduced the Landau expansion to phonon field u_i and phason field w_i as below

$$u_k(r) = \sum_{\alpha} u_k^{\alpha}\delta(r_{\alpha} - r) \tag{C.1.9}$$

$$w_k(r) = \sum_{\alpha} w_k^{\alpha}\delta(r_{\alpha} - r) \tag{C.1.10}$$

By using the limit passing over (C.1.4) from the quantum Poisson to the classical Poisson bracket, from (C.1.9) and (C.1.10) one can find whose corresponding classical Poisson brackets as follows:

$$\{u_k(r_1), g_l(r_2)\} = (-\delta_{kl} + \nabla_l(r_1)u_k)\delta(r_1 - r_2) \tag{C.1.11}$$

$$\{w_k(r_1), g_l(r_2)\} = (\nabla_l(r_1)w_k)\delta(r_1 - r_2) \tag{C.1.12}$$

It is evident that (C.1.12) is quite different from (C.1.11), and this leads to the dissipation equations of phasons given in the subsequent discussion which are quite different from those of phonons. The relevant derivations are carried out by Lubensky et al. [9].

C.2 Generalized Langevin Equation and Coarse Graining

Apart from Poisson brackets, it is needed some other basis in the derivation of hydrodynamic equations of quasicrystals, which is related to the Langevin equation or generalized Langevin equation.

It is well known that the conventional Langevin equation stands for

$$\frac{\partial\psi(r,t)}{\partial t} = -\Gamma\psi(r,t) + F_s \tag{C.2.1}$$

in which $\psi(r,t)$ is a mechanics quantity, Γ represents a resistant force, and F_s a stochastic force. The equation describes a stochastic process. Ginzburg and Landau extended it to the case of multi-variables

$$\frac{\partial \psi_\alpha(r,t)}{\partial t} = -\Gamma_{\alpha\beta}\frac{\delta H}{\delta \psi_\beta(r,t)} + (F_s)_\alpha \tag{C.2.2}$$

in which the summation convention is used like that in the previous presentation of this book, where $H = H[\psi(r,t)]$ denotes a energy functional, which can also be named Hamiltonian, $\frac{\delta H}{\delta \psi_\beta(r,t)}$ represents a variation of $H = H[\psi(r,t)]$ to $\psi_\beta(r,t)$, $\Gamma_{\alpha\beta}$ are the elements of resistant matrix (or dissipation kinetic coefficient matrix), and the meanings of definitions of other quantities are the same as before. Equation (C.2.2) is a kind of generalized Langevin equation, which can also be extended in more wide sense. If the macroscopic quantity $\psi_\alpha(r,t)$ may be seen as thermodynamic average of microscopic quantity $\psi^\mu_\alpha(r,\{q^\alpha\},\{p^\alpha\})$, i.e.

$$\psi_\alpha(r,t) = \left\langle \psi^\mu_\alpha(r,\{q^\alpha\},\{p^\alpha\})\right\rangle \tag{C.2.3}$$

this treatment is called coarse graining, in which p^α, q^α are the canonic momentum and canonic coordinate, and the micro-quantities obey the microscopic Liouville equation

$$\frac{\partial \psi^\mu_\alpha}{\partial t} = \left\{H^\mu, \psi^\mu_\alpha\right\} \tag{C.2.4}$$

where $H^\mu(\{q^\alpha\},\{p^\alpha\})$ denote the microscopic Hamiltonian.

In d-dimensional space, the partial derivative of macro-quantity $\psi_\alpha(r,t)$ to time

$$\frac{\partial \psi_\alpha(r,t)}{\partial t}$$

consists of various terms, one among them is

$$-\int\left(\left\{\psi_\beta(r'),\psi_\alpha(r)\right\}\frac{\delta H}{\delta \psi_\beta(r',t)}\right)\mathrm{d}^d r' \tag{C.2.5}$$

and the other is

$$\int\left(\frac{\delta\left\{\psi_\beta(r'),\psi_\alpha(r)\right\}}{\delta \psi_\beta(r',t)}\right)\mathrm{d}^d r' \tag{C.2.6}$$

Combining (C.2.5), (C.2.6), then (C.2.2) is generalized as

$$\frac{\partial \psi_\alpha(r,t)}{\partial t} = -\int \left(\{\psi_\beta(r'), \psi_\alpha(r)\} \frac{\delta H}{\delta \psi_\beta(r',t)} \right) \mathrm{d}^d r' + \int \left(\frac{\delta \{\psi_\beta(r'), \psi_\alpha(r)\}}{\delta \psi_\beta(r',t)} \right) \mathrm{d}^d r' - \mathbf{\Gamma}_{\alpha\beta} \frac{\delta H}{\delta \psi_\beta(r,t)} + (F_s)_\alpha \tag{C.2.7}$$

where $\mathrm{d}^d r' = \mathrm{d}V$ represents volume element of the integral. Based on formulas (C.1.8), (C.1.11) and (C.1.12), Lubensky et al. [9] utilized Eq. (C.2.7) to derive the hydrodynamic equations of quasicrystals. This will be given in the next subsection. In the derivation, the last term in (C.2.7) is omitted.

C.3 Derivation of Hydrodynamic Equations of Solid Quasicrystals

The derivation of equation of mass conservation is very simple, which is the same with that in the conventional fluid, and is omitted here.

At first, consider the derivation of phonon dissipation equations:

Putting $\psi_\alpha(r,t) = u_i(r,t), \psi_\beta(r',t) = g_j(r',t)$ in (C.2.7) and omitting the second and fourth terms in the right-hand side of the equation, then

$$\frac{\partial u_i(r,t)}{\partial t} = -\int \left(\{u_i(r'), g_j(r)\} \frac{\delta H}{\delta g_j(r',t)} \right) \mathrm{d}^d r' - \Gamma_{\mathbf{u}} \frac{\delta H}{\delta u_i(r,t)}$$

Substituting bracket (C.1.11) into the integral of right-hand side yields

$$\begin{aligned} \frac{\partial u_i(r,t)}{\partial t} &= \int \left(-\delta_{ij} + \nabla_j(r) u_i\right) \delta(r-r') \frac{g_j(r')}{\rho(r')} d^d r' + \Gamma_u \frac{\delta H}{\delta u_i(r,t)} \\ &= -V_j \nabla_j(r) u_i - \Gamma_u \frac{\delta H}{\delta u_i(r,t)} + V_i \end{aligned} \tag{C.3.1}$$

where Γ_u enotes the phonon dissipation kinematic coefficient, and the Hamiltonian is defined by

$$\begin{aligned} H &= H[\psi(r,t)] = \int \frac{\mathrm{g}^2}{2\rho} \mathrm{d}^d r + \int \left[\frac{1}{2} A \left(\frac{\delta \rho}{\rho_0} \right)^2 + B \left(\frac{\delta \rho}{\rho_0} \right) \nabla \cdot \mathrm{u} \right] \mathrm{d}^d r + F_{\mathrm{el}} \\ &= H_{\mathrm{kin}} + H_{\mathrm{density}} + F_{\mathrm{el}} \\ F_{\mathrm{el}} &= F_u + F_w + F_{uw}, \quad g = \rho V \end{aligned} \tag{C.3.2}$$

and A, B are the constants describe density variation, and the last term of (C.2.7) represents elastic energies, which consist of phonons, phasons and phonon-phason coupling parts, respectively:

$$\begin{aligned} F_{\mathrm{u}} &= \int \frac{1}{2} C_{ijkl}\varepsilon_{ij}\varepsilon_{kl}\mathrm{d}^d r \\ F_{\mathrm{w}} &= \int \frac{1}{2} K_{ijkl}w_{ij}w_{kl}\mathrm{d}^d r \\ F_{\mathrm{uw}} &= \int \left(R_{ijkl}\varepsilon_{ij}w_{kl} + R_{klij}w_{ij}\varepsilon_{kl}\right)\mathrm{d}^d r \end{aligned} \tag{C.3.3}$$

C_{ijkl} the phonon elastic constants, K_{ijkl} the phason elastic constants, and R_{ijkl}, R_{klij} the phonon-phason coupling elastic constants, and the strain tensors ε_{ij}, w_{ij} are defined by

$$\varepsilon_{ij} = \frac{1}{2}\left(\frac{\partial u_i}{\partial x_j} + \frac{\partial u_j}{\partial x_i}\right), \quad w_{ij} = \frac{\partial w_i}{\partial x_j} \tag{C.3.4}$$

The associated stress tensors are related through the generalized Hooke's law

$$\left.\begin{aligned} \sigma_{ij} &= \frac{\partial F}{\partial \varepsilon_{ij}} = C_{ijkl}\varepsilon_{kl} + R_{ijkl}w_{kl} \\ H_{ij} &= \frac{\partial F}{\partial w_{ij}} = K_{ijkl}w_{kl} + R_{klij}\varepsilon_{kl} \end{aligned}\right\} \tag{C.3.5}$$

Equation (C.3.1) is just Eq. (16.5.14) in the text of Chap. 16.

Now, consider the derivation of phason dissipation equations.

In (C.2.7), put $\psi_\alpha(r,t) = w_i(r,t), \psi_\beta(r',t) = g_j(r',t)$, neglecting the second and fourth terms in the right-hand side, and then substituting the Poisson bracket (C.2.7) into it leads to

$$\frac{\partial w_i(r,t)}{\partial t} = -\int \left(\left\{w_i(r'), g_j(r)\right\}\frac{\delta H}{\delta g_j(r',t)}\right)\mathrm{d}^d r' - \Gamma_w \frac{\delta H}{\delta w_i(r,t)}$$

Then

$$\begin{aligned} \frac{\partial w_i(r,t)}{\partial t} &= \int \left(\nabla_j(r)w_i\right)\delta(r-r')\frac{g_j(r')}{\rho(r')}\mathrm{d}^d r' - \Gamma_w \frac{\delta H}{\delta w_i(r,t)} \\ &= -V_j\nabla_j(r)w_i - \Gamma_w \frac{\delta H}{\delta w_i(r,t)} \end{aligned} \tag{C.3.6}$$

which is just Eq. (16.5.16) in the text of Chap. 16, and Γ_w denotes the phason dissipation coefficient, and Hamiltonian is defined by (C.3.2).

By comparing (C.2.7) and (C.2.7), it is found that the physical meanings of phonon and phason in hydrodynamic sense are quite different. According to the explanation of Lubensky et al. [9], the phonon represents wave propagation, while phason represents diffusion.

Of course the other difference between phonon and phason is that they belong to the different irreducible representations of point groups, which has been discussed in Chap. 4.

The derivation of momentum Eq. (16.5.3) is somehow lengthy. The calculation is related with momentum $g_j = \rho V_j$, mass density ρ, phonon u_i and phason w_i, and this means that the integrands in the right-hand side of (C.2.7) need to use simultaneously the Poisson brackets listed in (C.1.8), (C.1.11) and (C.1.12), i.e.

$$\begin{aligned}\frac{\partial g_i(r,t)}{\partial t} = &-\int\left(\{g_i(r),\rho(r')\}\frac{\delta H}{\delta\rho(r',t)}\right)\mathrm{d}^d r' - \int\left(\{g_i(r),g_j(r')\}\frac{\delta H}{\delta g_j(r',t)}\right)\mathrm{d}^d r' \\ &-\int\left(\{g_i(r),u_j(r')\}\frac{\delta H}{\delta u_j(r\prime,t)}\right)\mathrm{d}^d r' - \int\left(\{g_i(r),w_j(r')\}\frac{\delta H}{\delta w_j(r',t)}\right)\mathrm{d}^d r' \\ &\int\left(\frac{\delta\{g_i(r),\psi_\beta(r')\}}{\delta\psi_\beta(r',t)}\right)\mathrm{d}^d r' + \Gamma_g\frac{\delta H}{\delta g_i(r,t)}, \Gamma_g = \eta_{ijkl}\end{aligned} \tag{C.3.7}$$

in which the first integral of the right-hand side can be evaluated as

$$\begin{aligned}\int\left(\{g_i(r),\rho(r')\}\frac{\delta H}{\delta\rho(r',t)}\right)\mathrm{d}^d r' &= \int\left(\rho(r)\nabla_i\delta(r-r')\frac{\delta(H_{\mathrm{kin}}+H_{\mathrm{density}})}{\delta\rho(r',t)}\right)\mathrm{d}^d r' \\ &= \rho(r)\nabla_i\int\left(\delta(r-r')\frac{\delta(H_{\mathrm{kin}}+H_{\mathrm{density}})}{\delta\rho(r',t)}\right)\mathrm{d}^d r' \\ &= \rho(r)\nabla_i\left(\frac{\delta H_{\mathrm{density}}}{\delta\rho}\right)+\rho(r)\nabla_i\left(-\frac{g^2}{2\rho^2}\right) \\ &= \rho(r)\nabla_i\left(\frac{\delta H_{\mathrm{density}}}{\delta\rho}\right)-g_j\nabla_i V_j\end{aligned}$$

Similarly, the second to fifth integrals are evaluated, and the fifth integral is

$$\begin{aligned}\int\left(\frac{\delta\{g_i(r,t),\psi_\beta(r',t)\}}{\delta\psi_\beta(r',t)}\right)\mathrm{d}^d r' = &\int\left(\frac{\delta\{g_i(r,t),\rho(r',t)\}}{\delta\rho(r',t)}\right)\mathrm{d}^d r' + \int\left(\frac{\delta\{g_i(r,t),g_j(r',t)\}}{\delta g_j(r',t)}\right)\mathrm{d}^d r' \\ &+\int\left(\frac{\delta\{g_i(r,t),u_j(r',t)\}}{\delta u_j(r',t)}\right)\mathrm{d}^d r' + \int\left(\frac{\delta\{g_i(r,t),w_j(r',t)\}}{\delta w_j(r',t)}\right)\mathrm{d}^d r'\end{aligned}$$

The right-hand side consists of four terms, and the third one among them results in after some calculation

$$\int \left(\frac{\delta\{g_i(r,t),u_j(r',t)\}}{\delta u_j(r',t)}\right)\mathrm{d}^d r' = \int \left(\frac{\delta\{\delta_{ij}-\nabla_i(r')u_j(r',t)\}}{\delta u_j(r',t)}\delta(r'-r)\right)\mathrm{d}^d r'$$
$$= \int \left(\nabla_i(r')\frac{\delta u_j(r',t)}{\delta u_j(r',t)}\delta(r'-r)\right)d^d r'$$
$$= \int ((\nabla_i(r')1)\delta(r'-r))d^d r' = 0$$

Similarly, the fourth term can be evaluated. The sum of the first and second terms is zero. Then making some algebraic manipulations yields

$$\frac{\partial g_i(r,t)}{\partial t} = -\nabla_k(r)(V_k g_i) + \nabla_j(r)\left(\eta_{ijkl}\nabla_k(r)V_l\right) - \left(\delta_{ij}-\nabla_i u_j\right)\frac{\delta H}{\delta u_j(r,t)} + \left(\nabla_i w_j\right)\frac{\delta H}{\delta w_j(r,t)} - \rho\nabla_i(r)\frac{\delta H}{\delta\rho(r,t)}, \quad g_j = \rho V_j \tag{C.3.8}$$

in which η_{ijkl} denotes the viscosity coefficient tensor of solid, and the viscous stress tensor is

$$\sigma'_{ij} = \eta_{ijkl}\dot{\xi}_{kl} \tag{C.3.9}$$

with the deformation rate tensor

$$\dot{\xi}_{kl} = \frac{1}{2}\left(\frac{\partial V_k}{\partial x_l} + \frac{\partial V_l}{\partial x_k}\right) \tag{C.3.10}$$

Equations (C.3.1), (C.3.6) and (C.3.8) and mass density conservation equation

$$\frac{\partial\rho}{\partial t} + \nabla_k(\rho V_k) = 0 \tag{C.3.11}$$

are the equations of hydrodynamic equations of icosahedral quaiscrystals, which are obtained by Lubensky et al. [9], in which there are field variables' mass density ρ, velocities V_i (or momentums $g_i = \rho V_i$), phonon displacements u_i and phason displacements w_i.

After the publication of the work since 1985, which are cited by many authors, at meantime there are some discussions [11–13], in which the Ref. [11] suggested some simplifications to the equations, e.g.

$$\frac{\partial\rho}{\partial t} + \nabla_k(\rho V_k) = 0 \tag{C.3.13}$$

$$\frac{\partial g_i(r,t)}{\partial t} = \nabla_j(r)\left(\eta_{ijkl}\nabla_k(r)V_l\right) - \frac{\delta H}{\delta u_i(r,t)} - \rho\nabla_i(r)\frac{\delta H}{\delta \rho(r,t)}, \quad g_j = \rho V_j \tag{C.3.12}$$

$$\frac{\partial u_i(r,t)}{\partial t} = -\Gamma_u \frac{\delta H}{\delta u_i(r,t)} + V_i \tag{C.3.14}$$

$$\frac{\partial w_i(r,t)}{\partial t} = -\Gamma_w \frac{\delta H}{\delta w_i(r,t)} \tag{C.3.15}$$

C.4 Concept of Lie Group and Derivation on Some Formulas

The above derivation indicates that the Poisson brackets (C.1.8), (C.1.11) and (C.1.12) are fundamental, which can also be derived based on the concept of Lie group. In this section, we give an introduction in brief on the derivation.

Lie group is a group like the point groups discussed in the first 15 chapters, which satisfy the axioms of groups, referring to the Appendix of Chap. 1. However there is difference between point group and Lie group which is a kind of continuous group. The momentum operator mentioned previously is a generator of movement group, spin operator is a generator of rotation group in spin space, and the quantum Poisson brackets are connected inherent to the Lie group, so that Ref. [3] suggests the concept of "group Poisson bracket".

Assuming g be an element of group G, it has relation to the m real continuous parameters α_i, i.e.

$$g(\alpha_i) \in G, \quad \alpha_i \in \mathbb{R}, \quad i = 1, 2, \ldots, m \tag{C.4.1}$$

$\mathbb{R}$ denotes a real space.

Notion "$\cdot$" connects two elements, $a(\alpha_i)$ and $b(\beta_i)$, and gives another element $c(\gamma_i) \in G$:

$$c(\gamma_i) = a(\alpha_i) \cdot b(\beta_i), \quad i = 1, 2, \ldots, m \tag{C.4.2}$$

For the continuous parameters, there is

$$\gamma_i = \varphi_i(\alpha_1, \alpha_2, \ldots, \alpha_m, \beta_1, \beta_2, \ldots, \beta_m) \tag{C.4.3}$$

If φ_i is an single-valued analytic function of $\alpha_1, \alpha_2, \ldots, \alpha_m, \beta_1, \beta_2, \ldots, \beta_m$, this group is Lie group. The concept on single-valued analytic function can be found in the appendix of Chap. 11 of this book.

People usually take a parameter α_i and identical element E (the concept of identical element E referring to the Appendix of Chap. 1), then $\alpha_i(E) = 0$. The generator of Lie group is taken to be L_i, which can be expressed by the following partial differential

$$L_i = i\frac{\partial a(\ldots, \alpha_i, \ldots)}{\partial \alpha_i}|_{\alpha_i=0} \tag{C.4.4}$$

Group element a can be expressed by the following expansion

$$a(\ldots, \alpha_i, \ldots) = E(\ldots, 0, \ldots) + \alpha_i L_i + O(\alpha_i^2) \tag{C.4.5}$$

The infinitesimal element in the Lie group presents important sense in this kind of groups. Assume matrix $D(A)$ be the representation matrix of element A of Lie group. The parameter α_i of infinitesimal element $A(\alpha)$is an infinitesimal quantity. The matrix $D(A)$ can be expanded as below:

$$D(A) = 1 - i\sum_{j=1}^{N} \alpha_j I_j \tag{C.4.6}$$

and

$$I_j = i\frac{\partial D(A)}{\partial \alpha_j}\bigg|_{\alpha_j=0} \tag{C.4.7}$$

in which N I_j are named generators of representation matrix, and Lie algebra is constituted through the commutation relation between generators

$$[L_i, L_j] = C_{ij}^k L_k, \quad i, j, k = 1, 2, \ldots, m \tag{C.4.7}$$

where C_{ij}^k is called the structure constant. The asymmetry, linearity and Jacobi identity of Lie algebra are as follows:

$$[L_i, L_j] = -[L_j, L_i] \tag{C.4.8}$$

$$\big[\alpha L_i + \beta L_j, L_k\big] = \alpha[L_i, L_k] + \beta\big[L_j, L_k\big], \quad \alpha, \beta \in \mathbb{R} \tag{C.4.9}$$

$$\big[L_i, [L_j, L_k]\big] + \big[L_k, [L_i, L_j]\big] + \big[L_j, [L_k, L_i]\big] = 0 \tag{C.4.10}$$

respectively. In classical continuum mechanics, the coordinate transformation

$$x^k \to x^k + u^k(r) \tag{C.4.11}$$

is often used, which is called translation group or movement group, or infinitesimal movement group. It is interesting that in particular, $u^k(r)$ presents evident physical meaning and represent displacement, or phonon. Note that x^k here is the contravariant vector, while x_i is the covariant vector. We recall that the physical quantities mentioned previously present very close connection to the group algebra, because momentum operator is the generator of movement group, spin operator is the generator of rotation group in spin space, etc. Some correlation between physical quantities $a, b, c, \ldots$ and elements of transformation group $A, B, C, \ldots$

$$\{a, b, c, \ldots\} \to \{A, B, C, \ldots\} \tag{C.4.12}$$

may be set up. The linear combination of group element$A$ can be given by the following linear expression

$$A = \sum_{g \in G} A(g)g, \quad A(g) \in \mathbb{R} \tag{C.4.13}$$

where $A(g)$can be understood the coefficients of the expansion, but the series is for discrete group only, it should be replaced by integral for continuous group, and in the case, the group elements vary **continuously**.

Assume A can be transformed according to the following version

$$A \to gAg^{-1} \tag{C.4.14}$$

Suppose δg be an infinitesimal transformation, if $g = 1 + \delta g$, then the linear approximation is

$$A \to A + \delta A \tag{C.4.15}$$

and

$$\delta A = [\delta g, A] \tag{C.4.16}$$

The infinitesimal transformation δg is of the form

$$\delta g = \frac{i}{\hbar} \int \alpha^k(r) L^k(r) \mathrm{d}^d r \tag{C.4.17}$$

in which $\alpha^k(r)$ is the local infinitesimal "angular", $L^k(r)$ is the generators of local transformation group, $i = \sqrt{-1}, \hbar = h/2\pi$, and h is the Planck constant.

For the movement group, take $\alpha^k(r) = u^k(r)$, and the generator is the momentum, and then from (C.4.15) and (C.4.17),

$$\delta A(r) = \frac{i}{\hbar}\int \alpha^k(r')\left[L^k(r'), A(r)\right]\mathrm{d}^d r' \tag{C.4.18}$$

This equation shows that δA is the linear functional of "angular" $\alpha^k(r)$ of infinitesimal local transformation, and the corresponding variation is

$$\frac{\delta A(r)}{\delta \alpha^k(r')} = \frac{i}{\hbar}\left[L^k(r'), A(r)\right] \tag{C.4.19}$$

The limit passing over from quantum mechanics to classical mechanics is

$$\frac{\delta \hat{A}}{\delta \alpha} = \frac{i}{\hbar}\left[\hat{L}, \hat{A}\right] \to \frac{\delta A}{\delta \alpha} = \{L, A\} \tag{C.4.20}$$

Recall again that $\hat{L}, \hat{A}$ represent operators in quantum mechanics and L, A the field variables in classical mechanics, so that the right-hand side of (C.4.19) may be written as

$$\frac{\delta a}{\delta \alpha} = \{l, a\} \tag{C.4.21}$$

in which a can represent any field variables $a, b, c, \ldots$ of hydrodynamics and l the generator $l^k(r)$ corresponding to the group, so that from (C.4.21)

$$\frac{\delta a(r)}{\delta \alpha^k(r')} = \left\{l^k(r'), a(r)\right\} \tag{C.4.22}$$

Furthermore

$$\frac{\delta l^m(r)}{\delta \alpha^k(r')} = \left\{l^k(r'), l^m(r)\right\}, \{a, a\} = \{a, b\} = \{b, b\} = 0 \tag{C.4.23}$$

At the finite temperature, the Hamiltonian can be expressed by

$$H = \int \varepsilon(\mathrm{p}, \rho, s)\mathrm{d}^d r$$
$$\mathrm{d}\varepsilon = V^k \mathrm{d}p_k + \mu \mathrm{d}\rho + T\mathrm{d}s$$

where ε denotes the energy density, the others are the same before, $\mathrm{p} = (p_x, p_y, p_z)$ and ρ the momentum and mass density, s the entropy, $\mathrm{V} = (V_x, V_y, V_z)$ the velocity, μ the chemical potential, T the absolute temperature, respectively, so

$$\begin{aligned}\delta p_k &= -u^l \nabla_l p_k - p_k \nabla_l u^l - p_k \nabla_l u^l \\ \delta \rho &= -u^l \nabla_l \rho - \rho \nabla_k u^k \\ \delta s &= -u^l \nabla_l s - s \nabla_k u^k\end{aligned} \tag{C.4.24}$$

From (C.4.23) and (C.4.24), one obtains

$$\begin{aligned}\{p_k(r_1), \rho(r_2)\} &= \rho(r_1)\nabla_k(r_1)\delta(r_1 - r_2) \\ \{p_k(r_1), p_l(r_2)\} &= (p_l(r_1)\nabla_k(r_1) - p_k(r_2)\nabla_k(r_2))\delta(r_1 - r_2)\end{aligned} \tag{C.4.25}$$

This is identical to (C.1.8) given by Poisson bracket method of condensed matter physics, which is the result of Ref. [2, 4].

Applying the above results into quasicrystals, there are

$$\{u_k(r_1), g_l(r_2)\} = (-\delta_{kl} + \nabla_l(r_1)u_k)\delta(r_1 - r_2) \tag{C.4.26}$$

$$\{w_k(r_1), g_l(r_2)\} = (\nabla_l(r_1)w_k)\delta(r_1 - r_2) \tag{C.4.27}$$

These are identical to (C.4.23) and (C.4.24) given by Lubensky et al. [9], and they derived directly using the Poisson bracket method.

This description shows the power of Lie group method. Ref. [4] shows further that if introducing the Liouville equation, equations of motion for some complex systems can be obtained, which are identical to those derived Sect. C.3.

Some detailed derivations are given by Fan [14].

References

1. Landau L D, Lifshitz M E, 1998, Fluid Mechanics, Theory of Elasticity, Oxford: Pergamon.
2. Landau L D, 1941, The theory of superfluidity of heilium II, Zh. Eksp.Teor. Fiz, II, 592, J Phys USSR, **5**, 71-90.
3. Landau L D, Lifshitz E M, 1935, Zur Theorie der Dispersion der magnetische Permeabilität der ferromagnetische Körpern., Physik Zeitschrift fuer Sowjetunion, **8**(2): 158-164.
4. Dzyaloshinskii I E, Volovick G E, 1980, Poisson brackets in condensed matter physics. Ann Phys (NY), **125**(1): 67-97.
5. Dzyaloshinskii I E, Volovick G E, 1978, On the concept of local invariance in spin glass theory, J de Phys, **39**(6), 693-700.
6. Volovick G E, 1978, Additional localized degrees of freedom in spin glasses, Zh Eksp Teor Fiz, **75**(7), 1102-1109.
7. Martin P C, Paron O, Pershan P S, 1972, Unified hydrodynamic theory for crystals, liquid crystals, and normal fluids. Phys Rev A, **6**(6): 2401-2420.
8. Fleming P D and Cohen C, 1976, Hydrodynamics of solids, Phys Rev B, **13**(2), 500-516.
9. Lubensky T C, Ramaswamy S, Toner J, 1985, Hydrodynamics of icosahedral quasicrystals, Phys Rev B, **32**(11), 7444-7411.
10. Lubensky T C, 1988, Symmetry, elasticity and hydrodynamics of quasiperioic structures, in ed M V Jaric, Aperiodic Crystals, Vol. I, Academic Press, Boston, pp.199-280.

11. Rochal S B, Lorman VL, 2002, Minimal model of the phonon-phason dynamics in icosahedral quasicrystals and its application to the problem of internal friction in the i-AlPdMn alloy. Physical Review B, **66**(14), 144204.
12. Khannanov S K, 2002, Dynamics of elastic and phason fields in quasicrystals. The Physics of Metals and Metallography, **93**(5): 397-403.
13. Coddens G, 2006, On the problem of the relation between phason elasticity and phason dynamics in quasicrystals. The European Physical Journal B, **54**(1): 37-65.
14. Fan T Y, 2013, Poisson bracket method and its applications to quasicrystals, liquid quasicrystals and a kind of soft matter, Chinese Journal of Theoretical and Applied Mechanics, **45**(4), 548-559 (in Chinese).

Appendix D: Some Preliminary Introductions on Soft-Matter Quasicrystals

The previous discussions in the text have dealt with solid quasicrystals, including binary and ternary metal alloy quasicrystals and natural quasicrystals observed so far, and focused mainly on their elasticity. Since 2004, the quasicrystals with 12-fold symmetry have been observed in liquid crystals, colloids and polymers. In particular, 18-fold symmetry quasicrystals in colloids were discovered in 2011. These kinds of quasicrystals can be called as soft-matter quasicrystals, which present very interesting and attractive features and have aroused a great deal of attention of researchers in physics and chemistry.

D.1 Soft-Matter Quasicrystals with 12- and 18-Fold Symmetries

D.1.1 The Discovery of Soft-Matter Quasicrystals with 12- and 18-Fold Symmetries

During 2004, Zeng et al. [1] observed the quasicrystals with 12-fold symmetry in liquid crystals. Almost at the same time, in 2005 Takano [2], in 2007 Hayashida et al. [3] discovered the similar structure in polymers. The quasicrystals of 12-fold symmetry were observed also in chalcogenides and organic dendrons.

In 2009, Talapin et al. [4] found the quasicrystals of 12-fold symmetry in complex of binary nanoparticles.

Figure D.1 shows the diffraction pattern of soft-matter quasicrystals with 12-fold symmetry.

More recently, the 12- and 18-fold symmetry quasicrystals are discovered in colloids by Fischer et al. [5], and they observed the structures in PI_{30}-PEO_{120} of one of poly (isoprene-*b*-ethylene oxide) (PI_n-PEO_m) at room temperature, by using X-ray scattering and neutron scattering. The 18-fold symmetry quasicrystal is the

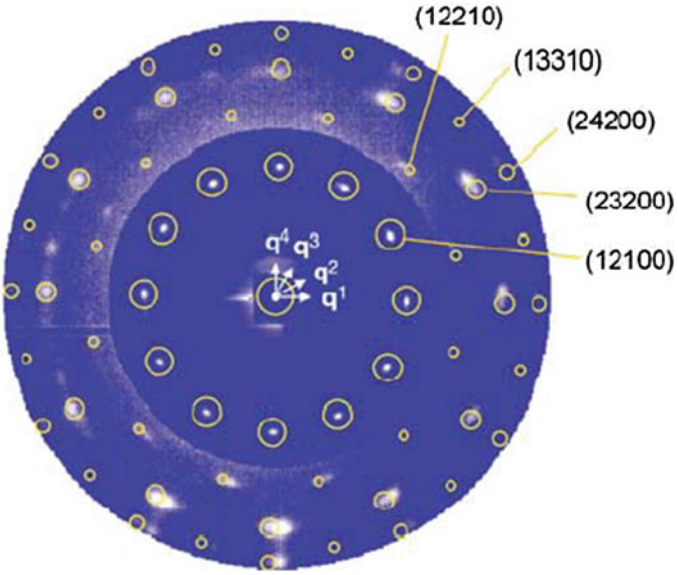

Fig. D.1 Diffraction pattern of 12-fold symmetry quasicrystals in soft matter

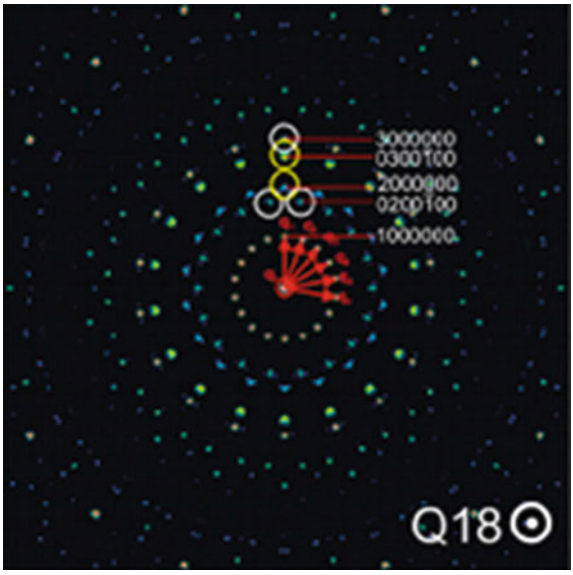

Fig. D.2 Diffraction pattern of soft-matter quasicrystals with 18-fold symmetry

first observed since 1982 in solid and soft-matter quasicrystals, whose diffraction pattern and Penrose tiling are shown in Figs. D.2 and D.3, respectively.

Though the 12-fold symmetry quasicrystals in solids were discussed in Chaps. 6–8, the 18-fold symmetry quasicrystals are studied for the first time to us, which have not

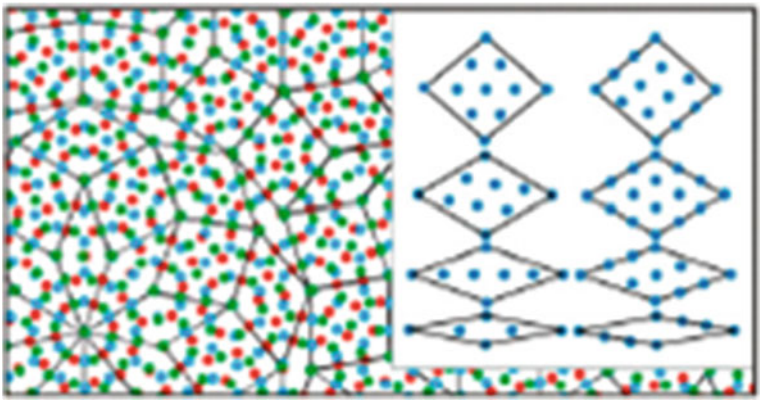

Fig. D.3 The Penrose tiling of quasicrystals with 18-fold symmetry in soft matter

been known previously. This is very new and interesting topics. The 12-fold symmetry quasicrystals in solid are discussed in Chaps. 6–8, but the 18-fold symmetry quasicrystals are total newly phase to the researchers, which have not been discussed in the previous chapters, and we have only very few of understanding for the structure and properties.

These discoveries present highly importance. At first, under certain temperature and density, quasicrystal state in soft matter is stable and this promotes us to understand quasicrystals theoretically. It is well known that quasicrystal state in metallic alloys is formed under rapid cooling condition, which is quite different from that of soft-matter quasicrystals, because these two cases are in quite different thermodynamic environments. The discovery of 18-fold symmetry quasicrystals leads to appearance of new point groups and space groups and promotes the development of symmetry theory and group theory. Of course, the appearance of these new quasicrystals enlarges the scope of the quasicrystal study. Finally, soft-matter quasicrystals may be a class of photon band grasp material, present application meaning. In addition, the self-assembly technique developing in the study is meaningful.

D.1.2 Characters of Soft-Matter Quasicrystals

Based on the experimental results, the soft-matter quasicrystals observed in different kinds of soft matter and their forms and structures are quite different to each other. It is here unable specially and in detail to study soft matter. Our object is only to study the soft-matter quasicrystals, and for this purpose, we have to understand a preliminary and necessary knowledge on soft matter. The nature of soft matter is an intermediate phase between ideal solid and simple fluid, or call is as a complex fluid or structured fluid, which is one of soft condensed matter.

The soft-matter quasicrystals observed so far are two-dimensional. During the process of their formation, it accomplished chemical reactions, and some phase transitions, such as crystal–quasicrystal transition and liquid crystal–quasicrystal transition. In the formation process of quasicrystals coming from colloids, there is connection with electricity, because the particles in colloids have charges. Our understanding to these complex physical–chemical effects is very limited.

The discussion on quasicrystals in soft matter is only an introduction of the subject. The same as we have done in the first 15 chapters for solid quasicrystals, and the main attention here is on mechanical behaviour and continuous mechanics of soft-matter quasicrystals. For example, under action of impact tension with stress amplitude $\sigma_0 = 5$ MPa, the variation of mass density $\delta\rho/\rho_0$ is 10^{-14} for solid quasicrystals, while under action of impact tension with stress amplitude $\sigma_0 = 0.01$ MPa, the variation of mass density $\delta\rho/\rho_0$ is 10^{-3} for soft-matter quasicrystals; the viscosity stress $\sigma'_{yy} = 10^{-19}$ GPa for solid quasicrystals under action of impact tension with stress amplitude $\sigma_0 = 5$ MPa, while the fluid stress $\sigma'_{yy} = 10^{-3}$ GPa for soft-matter quasicrystals under action of impact tension with stress amplitude $\sigma_0 = 0.01$ MPa These show the huge differences of mechanical properties between solid quasicrystals and soft-matter quasicrystals. Of course, for the computation for soft-matter quasicrystals, the equation of state was used, which is needed to be verified by experiments.

The related thermodynamics of soft-matter quasicrystals was done by Lifshitz et al. [7, 8], and they attended the stability of the new phase, which is a very important problem, of course. For studying hydrodynamics of soft-matter quasicrystals, an equation of state is necessary, and Fan and co-workers [9, 10] gave some preliminary discussions, but the model needs experimental verification.

D.2 Mathematical Model of Hydrodynamics of Soft-Matter Quasicrystals

However, the work on the deformation and motion of the new phase has not well been carried out due to the lack of fundamental experimental data to date. In addition, the scope of topic goes beyond elasticity. Hence, one should undertake the research on the relevant hydrodynamics. It is well known that the hydrodynamics in solid quasicrystals is a very difficult subject. Chapter 16, thus, only gave a very brief introduction. Readers might be found that many problems and questions there were left. There are much more principle difficulties in studying hydrodynamics for the new phase in physics and mathematics. At first, some mechanisms of deformation and motion of the matter have not been sufficiently explored owing to the lack of experimental data. Secondly, there is the lack of effective equation of state $p = f(\rho)$ or $\rho = g(p)$ for soft matter, where p denotes fluid pressure and ρ the mass density, respectively. This is a difficulty arising from thermodynamic study of soft matter. The thermodynamics is a more fundamental theory than the hydrodynamics.

The work on thermodynamics of soft-matter quasicrystals has been given by some researchers, as mentioned previously, but has not been well developed. Furthermore, no experimental verification has been made for some proposed models. It is an evident that the study of hydrodynamics for soft-matter quasicrystals is more difficult than that for solid quasicrystals.

In spite of this, the probe on hydrodynamic study of soft-matter quasicrystals is available and significant. The hydrodynamics of solid quasicrystals initiated by Lubensky et al. [6] over the past three decades has accumulated fruit achievements and experience. This is worthwhile providing a mode to develop hydrodynamics of soft-matter quasicrystals by drawing from that of solid quasicrystals.

After the careful consideration and preliminary practice, one can find that the common fundamentals for hydrodynamics, for example the generalized Langevin equation and Poisson bracket method of condensed matter physics, are valid for both solid quasicrystals and soft-matter quasicrystals (a rough address can be referred to Appendix C). In addition, the Hamiltonians in both solid and soft-matter quasicrystals are similar. This fact indicates that the theoretical framework for soft-matter quasicrystals focusing on hydrodynamics may be set up. For simplicity, the study on soft matters here should be confined to the case of small deformations such that the phonon and phason stresses and strains yield the generalized linear Hooke's law, and the fluid stresses and deformation rates follow the generalized linear Newton's law. Under these assumptions, the corresponding hydrodynamic equation system can be deduced. The equations provide a basis for computation at least, which lead to some information and data on displacement, velocity and stress fields in physical time-spatial domain. They can also provide possible comparisons with experiments hereafter. This enables one to explore the physical nature of deformation and motion of soft-matter quasicrystals. Some results are reported in [11–14].

This discussion on soft-matter quasicrystals and their hydrodynamics is beyond the scope of this book, and the relevant contents are given in works [15, 16].

References

1. Zeng X, Ungar G, Liu Y, Percec V, Dulcey A E, Hobbs J K, 2004, Supramolecular dendritic liquid quasicrystals, Nature, **428**, 157-159.
2. Takano K, 2005, A mesoscopic Archimedian tiling having a complexity in polymeric stars, J Polym Sci Pol Phys, 43, 2427-2432.
3. Hayashida K, Dotera T, Takano A, Matsushita Y, 2007, Polymeric quasicrystal : mesoscopic quasicrystalline tiling in ABC starpolymmers, Phys Rev Lett, **98**, 195502 .
4. Talapin V D, Shevechenko E V, Bodnarchuk M I, Ye X C, Chen J and Murray C B, 2009, Quasicrystalline order in self-assembled binary nanoparticle superlattices, Nature, **461**, 964-967.
5. Fischer S, Exner A, Zielske K, Perlich J, Deloudi S, Steuer W, Linder P and Foestor S, 2011, Colloidal quasicrystals with 12-fold and 18-fold diffraction symmetry, Proc Nat Ac Sci, **108**, 1810-1814.

6. Lubensky T C, Ramaswamy S, Toner J, 1985, Hydrodynamics of icosahedral quasicrystals, Phys. Rev. B, **32**(11), 7444-7452.
7. Lifshitz R and Diamant H,2007, Soft quasicrystals—Why are they stable? Phil Mag, 87 (18), 3021-3030.
8. Barkan K, Diamant H and Lifshitz R, 2011, Stability of quasicrystals composed of soft isotropic particles, Phys Rev B, 83, 172201.
9. Fan T Y and Sun J J, 2014, Four phonon model for studying thermodynamics of soft-matter quasicrystals, Phil Mag Lett, 94(2), 112-117.
10. Fan T Y and Fan L, 2016, Equation of state of some structures in soft matter.
11. Cheng H, Fan T Y, Sun J J and Wei H, 2015, Possible soft-matter quasicrystals with 5- and 10-fold symmetries and hydrodynamics, Computational Materials Science, **105**(7), 47-54.
12. Cheng H, Fan T Y and Wei H, 2016, Complete solution of possible soft-matter quasicrystals with 5- and 10-fold symmetries and hydrodynamics, submitted.
13. Fan T Y, 2016, Equation system of generalized hydrodynamics of soft-matter quasicrystals, Appl Math Mech, 37(4), 331-347.
14. Fan T Y, 2016, Stokes-Oseen flow in soft-matter quasicrystals, Appl Math Mech, in reviewing.
15. Fan T Y, 2016, Generalized dynamics of Soft-Matter Quasicrysals: Mathematical Models and Solutions, Beijing Institute of Technology Press, Beijing/Springer-Verlag, Heidelberg 2016, to be published.
16. Li X F and Fan T Y, 2016, Dislocations in the second kind two-dimensional quasicrystals of soft matter, Physica B, 52, 175-180.